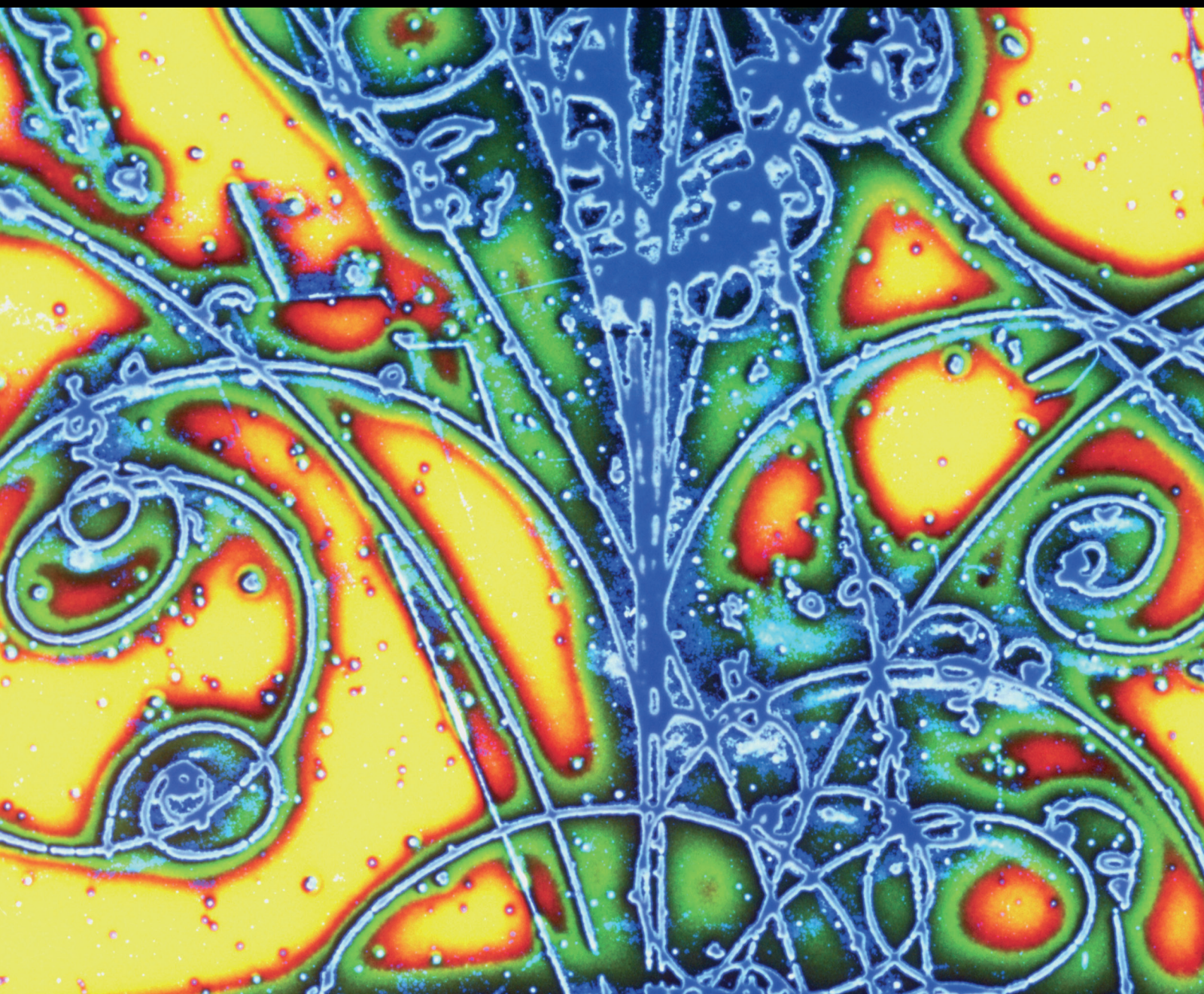


Advances in High Energy Physics

Classical and Quantum Approaches to Black Holes

Lead Guest Editor: Irina Radinschi

Guest Editors: Farook Rahaman, Theophanes Grammenos, Saibal Ray,
and I-Ching Yang





Classical and Quantum Approaches to Black Holes

Advances in High Energy Physics

Classical and Quantum Approaches to Black Holes

Lead Guest Editor: Irina Radinschi

Guest Editors: Farook Rahaman, Theophanes Grammenos,
Saibal Ray, and I-Ching Yang



Copyright © 2019 Hindawi. All rights reserved.

This is a special issue published in “Advances in High Energy Physics.” All articles are open access articles distributed under the Creative Commons Attribution License, which permits unrestricted use, distribution, and reproduction in any medium, provided the original work is properly cited.

Editorial Board

Antonio J. Accioly, Brazil
Giovanni Amelino-Camelia, Italy
Luis A. Anchordoqui, USA
Michele Arzano, Italy
T. Asselmeyer-Maluga, Germany
Alessandro Baldini, Italy
Marco Battaglia, Switzerland
Lorenzo Bianchini, Switzerland
Roelof Bijker, Mexico
Burak Bilki, USA
Rong-Gen Cai, China
Anna Cimmino, France
Osvaldo Civitarese, Argentina
Andrea Coccaro, Italy
Shi-Hai Dong, Mexico
Lorenzo Fortunato, Italy
Mariana Frank, Canada
Ricardo G. Felipe, Portugal

Chao-Qiang Geng, Taiwan
Philippe Gras, France
Xiaochun He, USA
Luis Herrera, Spain
Filipe R. Joaquim, Portugal
Aurelio Juste, Spain
Theocharis Kosmas, Greece
Ming Liu, USA
Enrico Lunghi, USA
Salvatore Mignemi, Italy
Omar G. Miranda, Mexico
Grégory Moreau, France
Piero Nicolini, Germany
Carlos Pajares, Spain
Sergio Palomares-Ruiz, Spain
Giovanni Pauletta, Italy
Yvonne Peters, UK
Anastasios Petkou, Greece



Alexey A. Petrov, USA
Thomas Rössler, Sweden
Diego Saez-Chillon Gomez, Spain
Takao Sakaguchi, USA
Juan José Sanz-Cillero, Spain
Edward Sarkisyan-Grinbaum, USA
Sally Seidel, USA
George Siopsis, USA
Luca Stanco, Italy
Jouni Suhonen, Finland
Mariam Tórtola, Spain
Smarajit Triambak, South Africa
Jose M. Udías, Spain
Elias C. Vagenas, Kuwait
Sunny Vagnozzi, Sweden
Yau W. Wah, USA

Contents

Classical and Quantum Approaches to Black Holes

Irina Radinschi , Farook Rahaman , Theophanes Grammenos, Saibal Ray , and I-Ching Yang 
Editorial (4 pages), Article ID 5726836, Volume 2019 (2019)

Perfect Fluid Dark Matter Influence on Thermodynamics and Phase Transition for a Reissner-Nordstrom-Anti-de Sitter Black Hole

Zhaoyi Xu , Xian Hou , Jiancheng Wang, and Yi Liao 
Research Article (6 pages), Article ID 2434390, Volume 2019 (2019)

Anti-de-Sitter-Maxwell-Yang-Mills Black Holes Thermodynamics from Nonlocal Observables Point of View

H. El Moumni 
Research Article (13 pages), Article ID 6870793, Volume 2019 (2019)

New Phase Transition Related to the Black Hole's Topological Charge

Shan-Quan Lan , Gu-Qiang Li, Jie-Xiong Mo, and Xiao-Bao Xu
Research Article (8 pages), Article ID 8270265, Volume 2019 (2019)


A Covariant Canonical Quantization of General Relativity

Stuart Marongwe 
Research Article (7 pages), Article ID 4537058, Volume 2018 (2019)




Thermodynamics of Charged AdS Black Holes in Rainbow Gravity

Ping Li, Miao He, Jia-Cheng Ding, Xian-Ru Hu, and Jian-Bo Deng 
Research Article (6 pages), Article ID 1043639, Volume 2018 (2019)


Nonlocal Black Hole Evaporation and Quantum Metric Fluctuations via Inhomogeneous Vacuum Density

Alexander Y. Yosifov  and Lachezar G. Filipov
Research Article (9 pages), Article ID 3131728, Volume 2018 (2019)

Localization of Energy-Momentum for a Black Hole Spacetime Geometry with Constant Topological Euler Density

Irina Radinschi , Theophanes Grammenos, Farook Rahaman , Andromahi Spanou, Marius Mihai Cazacu, Surajit Chattopadhyay, and Antonio Pasqua 
Research Article (7 pages), Article ID 5212696, Volume 2018 (2019)

Revisiting the Black Hole Entropy and the Information Paradox

Ovidiu Cristinel Stoica 
Research Article (16 pages), Article ID 4130417, Volume 2018 (2019)

Hawking Radiation of a Single-Partition Black Hole

Youngsub Yoon 
Research Article (5 pages), Article ID 3601489, Volume 2018 (2019)

Classical Polymerization of the Schwarzschild Metric

Babak Vakili 

Research Article (10 pages), Article ID 3610543, Volume 2018 (2019)

Particle Motion around Charged Black Holes in Generalized Dilaton-Axion Gravity

Susmita Sarkar, Farook Rahaman , Irina Radinschi , Theophanes Grammenos, and Joydeep Chakraborty

Research Article (8 pages), Article ID 5427158, Volume 2018 (2019)

An Alternative Approach to the Static Spherically Symmetric, Vacuum Global Solution to the Einstein Equations

Luis Herrera  and Louis Witten

Research Article (5 pages), Article ID 3839103, Volume 2018 (2019)

λ Phase Transition in Horava Gravity

Wei Xu 

Research Article (14 pages), Article ID 2175818, Volume 2018 (2019)

Tunneling Glashow-Weinberg-Salam Model Particles from Black Hole Solutions in Rastall Theory

Ali Övgün , Wajiha Javed, and Riasat Ali

Research Article (11 pages), Article ID 3131620, Volume 2018 (2019)

Spectroscopy of $z = 0$ Lifshitz Black Hole

Gulnihal Tokgoz  and Izzet Sakalli 

Research Article (7 pages), Article ID 3270790, Volume 2018 (2019)

Thermodynamic Volume Product in Spherically Symmetric and Axisymmetric Spacetime

Parthapratim Pradhan 

Research Article (15 pages), Article ID 5816826, Volume 2018 (2019)

Interactions in an Acoustic World: Dumb Hole

Ion Simaciu , Gheorghe Dumitrescu, Zoltan Borsos, and Mariana Brădac

Research Article (6 pages), Article ID 7265362, Volume 2018 (2019)

Rainbow Gravity Corrections to the Entropic Force

Zhong-Wen Feng  and Shu-Zheng Yang

Research Article (8 pages), Article ID 5968284, Volume 2018 (2019)

Editorial

Classical and Quantum Approaches to Black Holes

Irina Radinschi ¹, Farook Rahaman ², Theophanes Grammenos,³
Saibal Ray ⁴ and I-Ching Yang ⁵

¹“Gheorghe Asachi” Technical University, Iasi, Romania

²Jadavpur University, India

³University of Thessaly, Greece

⁴Government College of Engineering and Ceramic Technology, India

⁵National Taitung University, Taiwan

Correspondence should be addressed to Irina Radinschi; radinschi@yahoo.com

Received 6 March 2019; Accepted 6 March 2019; Published 1 April 2019

Copyright © 2019 Irina Radinschi et al. This is an open access article distributed under the Creative Commons Attribution License, which permits unrestricted use, distribution, and reproduction in any medium, provided the original work is properly cited.

This special issue aims to investigate both classical and quantum approaches to black holes. The result is a collection of eighteen original research articles submitted by authors representing fifteen countries across Asia, Europe, North America, and South America.

In their article “An Alternative Approach to the Static Spherically Symmetric, Vacuum Global Solution to the Einstein Equations”, L. Herrera and L. Witten propose an alternative description of the Schwarzschild black hole solution by extending the solution outside the horizon to its interior. Indeed, based on the requirement that the solution is static not only outside but also inside the horizon, the authors consider the entire space-time resulting from the union of two static 4-manifolds, one for $0 < R < 2m$ with signature $(+ - - -)$ and one for $2m < R < \infty$ with signature $(- + + +)$ with the horizon as a common boundary. In this way, the entire space-time is described by a complete 4-manifold for the interior and a complete 4-manifold for the exterior, and a global static solution is obtained representing a “phase transition” on the horizon with a different symmetry on both sides of the latter. The horizon surface $R = 2m$ is excluded from both manifolds which meet there only for $\theta = 0$. As a result, within the horizon the time independence is kept but the spatial symmetry is changed. Then, by examining test particles, it is concluded that the complete picture of their motion near the horizon cannot be fully understood by use of Einstein’s field equations alone and the need of a quantum theory approach is stressed.

When sound perturbations are trapped in a supersonic fluid flow system, they behave similarly to trapped photons in black holes and the system considered is a black hole analogue called acoustic (or sonic) black hole or simply *dumb hole*. The border at which the fluid speed changes from greater to lesser than the local speed of sound is the event horizon of the acoustic black hole. The article “Interactions in an Acoustic World: Dumb Hole”, by I. Simaciu et al., is a follow-up to earlier published work on the so-called “acoustic world”, the latter being defined as the finite volume of a fluid or of a solid containing the fluid, together with the processes occurring within this volume. By assuming that the acoustic processes are similar to the processes occurring in vacuum, the authors examine interactions between inhomogeneities of an acoustic medium that are produced by acoustic perturbations travelling in this medium. In this context, the inhomogeneities induced by a wave or a wave packet are studied and the dumb hole corresponding to the acoustic wave packet is examined.

The *polymer quantization* procedure was developed in background independent approaches to quantum field theory and its name relied on the fact that the basic quantum excitations of gravity and gauge field theories are one-dimensional, polymer-like excitations. In loop quantum gravity space-time exhibits a granular structure, thus supporting the existence of a fundamental length in the theory. Polymer quantization comes forward as an *effective theory* that uses a minimal length scale and, in fact, one is led to polymer quantization

in mini-superspace models of quantum cosmology. Now, the polymeric length (that shows the scale of the segments of granular space-time) plays the role of the minimal length of the theory and labels the granular properties of space entering, as an additional quantum parameter, the Hamiltonian of the system deforming it into the *polymeric Hamiltonian*. In the article “Classical Polymerization of the Schwarzschild Metric”, B. Vakili studies how the Schwarzschild black hole metric is modified by applying the classical polymerization procedure. The energy-momentum tensor of the matter field corresponding to the new polymerized metric and some of its thermodynamic properties are examined, while radial null as well as time-like geodesics are also examined and some interesting conclusions are drawn showing that the polymerized metric still describes a black hole space-time.

In their paper “Localization of Energy-Momentum for a Black Hole Spacetime Geometry with Constant Topological Euler Density”, I. Radinschi et al. address the topic of energy-momentum localization in General Relativity by using various energy-momentum complexes. They calculate the energy and momentum of a four-dimensional black hole space-time geometry with constant topological Euler density with the aid of the Einstein and Møller prescriptions. The energy obtained depends on the mass M and the charge q of the black hole, the cosmological constant λ , and the radial coordinate r , while in both prescriptions all the momenta vanish. Some limiting and particular cases are analyzed and discussed, illustrating the rather extraordinary character of the space-time geometry studied. The conclusion is that the Einstein and Møller prescriptions may provide an instructive tool for the energy-momentum localization.

In recent years, two issues of great interest that are extensively studied are the black hole information paradox and the black hole entropy. In his article “Revisiting the Black Hole Entropy and the Information Paradox”, O. C. Stoica revisited some paradoxes and also the black hole complementarity and the firewall proposals, with an emphasis on the less obvious assumptions. In order to carry out this study, arguments used in the literature are reviewed, and also some new counter-arguments are presented. Furthermore, some less considered less radical possibilities are examined, and the subject of an interesting discussion is a conservative solution, which is more consistent with the principle of equivalence from General Relativity and also with the unitarity from quantum theory.

In their article “Nonlocal Black Hole Evaporation and Quantum Metric Fluctuations via Inhomogeneous Vacuum Density”, A. Y. Yosifov and L. G. Filipov examine the back-reaction of a Schwarzschild black hole to the highly inhomogeneous vacuum density. Also, the authors argue that the fluctuations lead to deviations from General Relativity in the near-horizon region. It has been found that vacuum fluctuations onto the horizon trigger an adiabatic release of quantum information. In the vicinity of the horizon vacuum fluctuations produce potentially observable metric fluctuations of the order of the Schwarzschild radius. The authors propose a form of strong nonviolent nonlocality in which

it is possible to obtain simultaneously a nonlocal release of quantum information and observable metric fluctuations.

In the paper “Tunneling Glashow-Weinberg-Salam Model Particles from Black Hole Solutions in Rastall Theory”, A. Övgün et al. solve an equation of motion for the Glashow-Weinberg-Salam model with the aid of the semiclassical WKB approximation and the Hamilton-Jacobi method. This is especially useful for understanding the unified gauge-theory of weak and electromagnetic interactions. In this light, the tunneling rate of the massive charged W -bosons in the background of an electromagnetic field has been calculated, in order to study the Hawking temperature in the case of black holes surrounded by a perfect fluid in Rastall theory. Further, the quantum gravity effects on the generalized Proca equation with generalized uncertainty principle (GUP) on this background have been examined. It is demonstrated that quantum gravity effects leave their remnants on the Hawking temperature. Also, it is proved that the Hawking radiation becomes nonthermal.

In the letter “Thermodynamic Volume Product in Spherically Symmetric and Axisymmetric Spacetime”, P. Pradhan investigates the thermodynamic volume products for spherically symmetric and axisymmetric space-time in the framework of extended phase space. These volume products are expressed in terms of the outer and inner horizons of black holes and, together with other thermodynamic expressions like volume sum, volume minus, and volume division, are useful in the case of different spherically symmetric space-times and axisymmetric space-times. The thermodynamic volume products for the outer horizon and for the inner horizon of several classes of spherically symmetric and axisymmetric black holes including the AdS black hole metric are calculated. In these cases, it is found that the simple volume product of H^\pm is not mass independent, but more complicated volume functional relations are mass independent.

Due to its multifunctional properties the entropic force attracts a lot of interest. In their paper “Rainbow Gravity Corrections to the Entropic Force”, Z.-W. Feng and S.-Z. Yang, employing the new kind of rainbow gravity model of Magueijo and Smolin, investigate the quantum gravity corrections to the entropic force. In order to make this study, they derive the modified thermodynamics of a rainbow black hole via its surface gravity, and after this the quantum corrections to the entropic force are obtained according to Verlinde’s theory. The conclusion is that the modified entropic force is related to both the properties of the black hole and the Planck length l_p and the rainbow parameter γ . Also, modified Einstein’s field equations and the modified Friedmann equation are obtained based on the rainbow gravity corrected entropic force.

In their paper “Perfect Fluid Dark Matter Influence on Thermodynamics and Phase Transition for a Reissner-Nordstrom-Anti-de Sitter Black Hole”, Z. Xu et al. have studied the thermodynamics and phase transition by extending the phase space defined by the charge square and the conjugate quantity, with the latter being a function of the horizon radius. They found that the thermodynamics

systems are similar to van der Waals systems and can be explained by mean field theory. The Ruppeiner thermodynamic geometry feature and the connection with microscopic structure have also been studied. The authors found that in extended phase space there are singularity points of Ruppeiner curvature and these points could be explained as phase transitions.

In their paper “New Phase Transition Related to the Black Hole’s Topological Charge”, the authors S.-Q. Lan et al. performed a study about a new phase transition related to the topological charge in Einstein-Maxwell theory. They derived the explicit solutions corresponding to the divergence of specific heat in order to determine the phase transition critical point. Furthermore, the curves $T-r$ and $T-S$ are investigated and found to exhibit an interesting van der Waals system’s behavior. Also, a van der Waals system’s swallow tail behavior is observed when the topological charge is greater than the corresponding value in the critical point in the $F-T$ graph. The analytic phase transition coexistence lines have been obtained by using the Maxwell equal area law and free energy analysis, the results of which are consistent with each other.

In his paper “A Covariant Canonical Quantization of General Relativity” S. Marongwe presents a Hamiltonian formulation of General Relativity within the context of the Nexus Paradigm of quantum gravity. He demonstrates that the Ricci flow in a compact matter free manifold serves as the Hamiltonian density of the vacuum as well as a time evolution operator for the vacuum energy density. An interpretation of General Relativity in terms of the fundamental concepts of quantum mechanics has been possible in the condition of the metric tensor of General Relativity expressed in terms of the Bloch energy eigenstate functions of the quantum vacuum.

In the work “ λ Phase Transition in Horava Gravity” the author W. Xu has presented a superfluid black hole containing a λ phase transition in the context of Horava gravity. After studying the extended thermodynamics of general dimensional Horava-Lifshitz AdS black holes, it is found that only the one with a spherical horizon in four and five dimensions has a λ phase transition, which is a line of (continuous) second-order phase transitions and was famous in the discussion of the superfluidity of liquid ^4He . The “superfluid” black hole phase and the “normal” black hole phase are also distinguished. Particularly, six-dimensional Horava-Lifshitz AdS black holes exhibit infinitely many critical points in $P - \nu$ plane and the divergent points for specific heat, for which they only contain the “normal” black hole phase while the “superfluid” black hole phase disappears due to the physical temperature constraint and therefore there is no similar phase transition. In this context, the author has shown that, in more than six dimensions, there is no $P - \nu$ critical behavior. After choosing the appropriate ordering field, the author studied the critical phenomena in different planes of thermodynamical phase space along with a calculation of the critical exponents, which are the same as for the van der Waals fluid.

In the investigation “Anti-de-Sitter-Maxwell-Yang-Mills Black Holes Thermodynamics from Nonlocal Observables

Point of View”, H. El Mounni analyzes the thermodynamic properties of the Anti-de-Sitter black hole in the Einstein-Maxwell-Yang-Mills- (EMYM-) AdS gravity via many approaches and for different thermodynamical ensembles (canonical/grand canonical). First, the author gives a concise overview of this phase structure in the entropy-thermal diagram for fixed charges and then he investigates this thermodynamical structure for the fixed potentials ensemble. The next relevant step is recalling the nonlocal observables such as holographic entanglement entropy and two-point correlation function to show that both observables exhibit a van der Waals-like behavior in numerical accuracy and just near the critical line as the case of the thermal entropy for fixed charges by checking Maxwell’s equal area law and the critical exponent. In the light of the grand canonical ensemble, the author also finds a new phase structure for such a black hole where the critical behavior disappears in the thermal picture as well as in the holographic one.

The thermodynamic property of a charged AdS black hole is studied in rainbow gravity. In their article entitled “Thermodynamics of Charged AdS Black Holes in Rainbow Gravity”, P. Li et al. got a deformed temperature in a charged AdS black hole using no-zero mass of a test particle. Their result shows that the phase structure has a relationship to an AdS radius l . In particular, an analogy between the charged AdS black hole in the rainbow gravity and the liquid-gas system is discussed. Finally, the Gibbs free energy has been examined and a characteristic “swallow tail” has been obtained that can be the explanation of a first-order phase transition.

In the work “Particle Motion around Charged Black Holes in Generalized Dilaton-Axion Gravity”, the authors S. Sarkar et al. have studied the behavior of massive and massless test particles around asymptotically and spherically symmetric, charged black holes in the context of generalized dilaton-axion gravity in four dimensions. The motion of a massive and charged test particle in the gravitational field of a charged black hole in generalized dilaton-axion gravity has been examined by exploiting the Hamilton-Jacobi equation.

In mid 2010’s, full discreteness of the Hawking radiation spectrum and the Maxwell-Boltzmann nature of the Hawking radiation spectrum were found. So, a new area spectrum is presented. In his paper entitled “Hawking Radiation of a Single-Partition Black Hole”, Y. Yoon showed what the thermodynamics of a single-partition black hole implies about the degeneracy of the area spectrum. As a consequence, the decay time of a single-partition black hole is roughly constant.

In the article “Spectroscopy of $z = 0$ Lifshitz Black Hole” G. Tokgoz and I. Sakalli have studied the thermodynamics and spectroscopy of a 4-dimensional, $z = 0$ Lifshitz black hole. The entropy/area spectra of the $z = 0$ Lifshitz black hole are computed. The quantum spectra of the $z = 0$ Lifshitz black hole were studied using the Maggiore method, which is based on the adiabatic invariant quantity. Their finding is in agreement with Bekenstein’s conjecture, and the equispacing of the entropy/area spectra of the $z = 0$ Lifshitz black hole supports Kothawala et al.’s hypothesis.

Conflicts of Interest

The editors declare that they have no conflicts of interest regarding the publication of this special issue.

Irina Radinschi
Farook Rahaman
Theophanes Grammenos
Saibal Ray
I-Ching Yang

Research Article

Perfect Fluid Dark Matter Influence on Thermodynamics and Phase Transition for a Reissner-Nordstrom-Anti-de Sitter Black Hole

Zhaoyi Xu ^{1,2,3,4} Xian Hou ^{1,3,4} Jiancheng Wang,^{1,2,3,4} and Yi Liao ^{5,6}

¹Yunnan Observatories, Chinese Academy of Sciences, 396 Yangfangwang, Guandu District, Kunming, 650216, China

²University of Chinese Academy of Sciences, Beijing, 100049, China

³Key Laboratory for the Structure and Evolution of Celestial Objects, Chinese Academy of Sciences, 396 Yangfangwang, Guandu District, Kunming, 650216, China

⁴Center for Astronomical Mega-Science, Chinese Academy of Sciences, 20A Datun Road, Chaoyang District, Beijing, 100012, China

⁵Department of Physics, National University of Defense Technology, Changsha, 410073, China

⁶Interdisciplinary Center for Quantum Information, National University of Defense Technology, Changsha, 410073, China

Correspondence should be addressed to Zhaoyi Xu; zyxu88@ynao.ac.cn, Xian Hou; xianhou.astro@gmail.com, and Yi Liao; liaoityianyi@gmail.com

Received 5 June 2018; Accepted 23 December 2018; Published 23 January 2019

Guest Editor: Farook Rahaman

Copyright © 2019 Zhaoyi Xu et al. This is an open access article distributed under the Creative Commons Attribution License, which permits unrestricted use, distribution, and reproduction in any medium, provided the original work is properly cited. The publication of this article was funded by SCOAP³.

Based on Reissner-Nordstrom-anti-de Sitter(RN-AdS) black hole surrounded by perfect fluid dark matter, we study the thermodynamics and phase transition by extending the phase space defined by the charge square Q^2 and the conjugate quantity ψ , where ψ is a function of horizon radius. The first law of thermodynamics and the equation of state are derived in the form $Q^2 = Q^2(T, \psi)$. By investigating the critical behaviour of perfect fluid dark matter around Reissner-Nordstrom-anti-de Sitter black hole, we find that these thermodynamics system are similar to Van der Waals system and can be explained by mean field theory. We also explore the Ruppeiner thermodynamic geometry feature and their connection with microscopic structure. We find that in extended phase space there are existence singularity points of Ruppeiner curvature and they could explained as phase transitions.

1. Introduction

Black hole thermodynamics are one of the most important topics in modern physics research and have been widely studied in recent years. The laws of black hole dynamics and thermodynamics were analyzed by Bekenstein and Hawking [1–5]. The four laws of black hole thermodynamics have been discussed [6]. Since the Hawking-Page phase transition was discovered, phase transitions have become a important topic in the black hole area. There are lots of work on the phase transition of different black holes, such as Reissner-Nordstrom black hole, Kerr black hole, and Kerr-Newman black hole [7–10]. These works have also been generalized to other black holes or applied to general situations [11–16]. Recently, several studies have considered the cosmological

constant as a dynamical variable which is similar to thermodynamical pressure [17]. Utilizing this method, some works have obtained the phase transition in AdS-black hole, in which the analogy between the critical behaviours of the Van der Waals gas and the RN-AdS black hole have been found [18–22].

From recent observations, we know that our universe is dominated by Dark Energy and Dark Matter [23, 24]. The dark energy makes the universe to be in accelerated expansion, and its state of equation is very close to the cosmological constant or the vacuum energy [25]. But the dynamics of dark energy are more like quintessence or other dynamical dark energy in behaviour [26]. The dark energy with quintessence could affect the black hole spacetime [27]. For the Schwarzschild black hole in quintessence field, the

modified black hole metric has been obtained by Kiselev [28, 29]. Recently the rotational quintessence black hole and Kerr-Newman-AdS black hole solutions have also been obtained [30, 31]. For the Schwarzschild black hole surrounded by quintessence matter, the thermodynamics and phase transition have been discussed in Tharanath et al. [32]; Ghaderi & Malakolkalami [33, 34]. For rotational black hole surrounded by quintessence case, the thermodynamics and phase transition have been studied recently by Xu & Wang [35]. The Reissner-Nordstrom black hole and Reissner-Nordstrom-dS black hole have been studied by Ghaderi & Malakolkalami [34]; Wei & Chu [36]; Wei & Ren [37]; Thomas et al. [38]; Mandal & Biswas [39]; Ma et al. [40]; the thermodynamics [41, 42] and phase transition through holography framework for Reissner-Nordstrom-AdS black hole have been investigated [43]. Following these works, the cold dark matter around black hole in phantom field background have been obtained by Li & Yang [44], and references therein. In this paper, we study the thermodynamics and phase transition of Reissner-Nordstrom-AdS black hole surround by perfect fluid dark matter.

This paper focuses on the study of the influence of perfect fluid dark matters on thermodynamics and phase transition for Reissner-Nordstrom-anti-de Sitter black hole. In Section 2, we introduce the Reissner-Nordstrom-anti-de Sitter black hole with perfect fluid dark matter background. In Section 3, we study the thermodynamical features, the equation of state in (Q^2, ψ) space, and the critical behaviour. In Section 4, we study the Ruppeiner thermodynamic geometry and their connection with microscopic structure for these black hole systems. We summarize our results in Section 5.

2. The Spacetime of Perfect Fluid Dark Matter around Reissner-Nordstrom-AdS Black Hole

We consider the dark matter field minimally coupled to gravity, electromagnetic field, and cosmological constant [28, 29, 44, 45]:

$$S = \int d^4x \sqrt{-g} \left(\frac{1}{16\pi G} R - \frac{1}{8\pi G} \Lambda + \frac{1}{4} F^{\mu\nu} F_{\mu\nu} + \mathcal{L}_{DM} \right), \quad (1)$$

where G is the Newton gravity constant, Λ is the cosmological constant, $F_{\mu\nu}$ is the Faraday tensor of electromagnetic field, \mathcal{L}_{DM} is the dark matter Lagrangian density, and this dark matter can be any dark matter model. By variation, we obtain the field equation from action principle as

$$\begin{aligned} R_{\mu\nu} - \frac{1}{2} g_{\mu\nu} R + \Lambda g_{\mu\nu} &= -8\pi G (\overline{T}_{\mu\nu} + T_{\mu\nu}(DM)) \\ &= -8\pi G T_{\mu\nu}, \end{aligned} \quad (2)$$

$$F^{\mu\nu}{}_{;\nu} = 0,$$

$$F^{\mu\nu;\alpha} + F^{\gamma\alpha;\mu} + F^{\alpha\mu;\gamma} = 0$$

where $\overline{T}_{\mu\nu}$ is the energy-momentum tensors of ordinary matter and $T_{\mu\nu}(DM)$ is the energy-momentum tensors of

dark matter. In the case of black holes surrounded by dark matter, we assume that dark matter is perfect fluid. The energy-momentum tensors can be written as $T^t_t = -\rho$, $T^r_r = T^\theta_\theta = T^\phi_\phi = p$ (where $T^\mu_\mu = g^{\mu\nu} T_{\mu\nu}$). In addition, for the simplest case, we assume $T^r_r = T^\theta_\theta = T^\phi_\phi = T^t_t(1 - \delta)$, where δ is a constant. We refer to such dark matter as the “perfect fluid dark matter” in this work.

For the Reissner-Nordstrom-AdS spacetime metric in perfect fluid DM, the black hole solution is as follows [28, 29, 44]:

$$ds^2 = -f(r) dt^2 + f^{-1}(r) dr^2 + r^2 (d\theta^2 + \sin^2\theta d\phi^2), \quad (3)$$

where

$$f(r) = 1 - \frac{2M}{r} + \frac{Q^2}{r^2} + \frac{1}{3}\Lambda r^2 + \frac{\alpha}{r} \ln\left(\frac{r}{|\alpha|}\right), \quad (4)$$

where α is a parameter describing the intensity of the perfect fluid DM, M is the black hole mass, and Q is the charge of black hole. This solution corresponds to a specific case of the general solution in Kiselev [28, 29] and Li & Yang [44]. It is interesting to note that this black hole solution implies that the rotational velocity is asymptotically flat in the equatorial plane, which could explain the observed rotation curves in spiral galaxies [28, 29, 44].

3. Thermodynamics of Dark Matter around Reissner-Nordstrom-AdS Black Hole

In Section 2, we have obtained the metric of spherically symmetric Reissner-Nordstrom-AdS black hole in perfect fluid dark matter. These black holes have three horizons which are Cauchy horizon r_- , event horizon r_+ , and cosmological horizon r_Λ . In this work, we always use event horizon r_+ . The black hole mass M can be expressed in event horizon r_+ as

$$M = \frac{r_+}{2} + \frac{Q^2}{2r_+} + \frac{1}{6}\Lambda r_+^3 + \frac{\alpha}{2} \ln\left(\frac{r_+}{|\alpha|}\right). \quad (5)$$

The semi-hawking temperature and the entropy are given by

$$\begin{aligned} T &= \frac{1}{4\pi} \left. \frac{df(r)}{dr} \right|_{r=r_+} \\ &= \frac{r_+ (2M + \alpha (1 - \ln(r_+/|\alpha|)) + (2/3)\Lambda r_+^3) - 2Q^2}{4\pi r_+^3} \end{aligned} \quad (6)$$

$$= \frac{r_+ (\alpha + r_+ + \Lambda r_+^3) - Q^2}{4\pi r_+^3},$$

$$S = \int_0^{r_+} \frac{1}{T} \left(\frac{\partial M}{\partial r_+} \right) dr_+ = \pi r_+^2. \quad (7)$$

Now we study the thermodynamical properties of the black hole with perfect fluid dark matter by extending to new phase space. This phase space is constructed by the entropy S , the perfect fluid dark matter density α , the charge square Q^2 , and the pressure $P = -\Lambda/8\pi$ corresponding to the

cosmological constant Λ . Therefore the black hole mass can be expressed as

$$M(S, Q^2, P, \alpha) = \frac{1}{2} \sqrt{\frac{S}{\pi}} + \frac{Q^2}{2} \sqrt{\frac{\pi}{S}} - \frac{4}{3} PS \sqrt{\frac{S}{\pi}} + \frac{\alpha}{2} \ln \left(\frac{1}{|\alpha|} \sqrt{\frac{S}{\pi}} \right). \quad (8)$$

The intensive parameters are defined by

$$\begin{aligned} T &= \left. \frac{\partial M}{\partial S} \right|_{P, Q^2, \alpha}, \\ \psi &= \left. \frac{\partial M}{\partial Q^2} \right|_{S, P, \alpha}, \\ V &= \left. \frac{\partial M}{\partial P} \right|_{S, Q^2, \alpha}, \\ \Pi &= \left. \frac{\partial M}{\partial \alpha} \right|_{S, Q^2, P}, \end{aligned} \quad (9)$$

where T denotes the temperature and the new physical quantity ψ is related to the specific volume as $\psi = 1/\nu$, where $\nu = 2r_+$. In thermodynamical space, the volume is $V = 4\pi r_+^3/3$ and the quantity $\Pi = (1/2) \ln(r_+/|\alpha|)$. The generalized first law of black hole thermodynamics in this extended phase space is expressed by

$$dM = TdS + \psi dQ^2 + VdP + \Pi d\alpha, \quad (10)$$

and the generalized Smarr formula is given by

$$M = 2TS + \psi Q^2 - 2VP + \Pi\alpha. \quad (11)$$

For the first law of black hole thermodynamics, the term ψdQ becomes ψdQ^2 in this phase space, where ψ represents the electric potential. This change leads to the interesting behaviour with $dM = SdT + \psi dQ$ in formal phase space. When the perfect fluid dark matter is around black hole, the phase transition of black hole occurs in (P, ν) plane. We can discuss this phase transition in (Q^2, ψ) plane, including the critical point, Gibbs free energy, and critical exponents under the effect of perfect fluid dark matter. Through calculations, we obtain the state equation $Q^2(T, \psi)$ as

$$\begin{aligned} Q^2 &= r_+ \left(\alpha + r_+ + \Lambda r_+^3 - 4\pi r_+^2 T \right) \\ &= \frac{1}{2\psi} \left[\alpha + \frac{1}{2\psi} + \frac{3}{8\psi^3 l^2} - \frac{\pi}{\psi^2} T \right], \end{aligned} \quad (12)$$

where $l^2 = 3/\Lambda$. The above equation describes the behaviours of Q^2 for different T, ψ and α .

Q^2 and ψ also satisfy the Maxwell equal area theorem given by Spallucci & Smailagic [46]:

$$\oint \psi dQ^2 = 0. \quad (13)$$

For $T > T_c$, where T_c critical temperature, there is an inflection point which is similar to the Van der Waals system. From general method, the coordinates of the critical point are determined by the following:

$$\begin{aligned} \left. \frac{\partial^2 Q^2}{\partial \psi^2} \right|_{T_c} &= 0, \\ \left. \frac{\partial Q^2}{\partial \psi} \right|_{T_c} &= 0. \end{aligned} \quad (14)$$

We then obtain the following equations:

$$\begin{aligned} \frac{15}{4\psi_c^3 l^2} + \alpha + \frac{3}{2\psi_c} - \frac{6\pi}{\psi_c^2} T_c &= 0, \\ -\frac{3}{2\psi_c^3 l^2} - \alpha - \frac{1}{\psi_c} + \frac{3\pi}{\psi_c^2} T_c &= 0. \end{aligned} \quad (15)$$

We then get the equation of critical ψ_c and T_c as

$$\begin{aligned} \alpha \psi_c^3 + \frac{1}{2} \psi_c^2 - \frac{3}{4l^2} &= 0, \\ T_c &= \frac{\psi_c^2}{3\pi} \left(\frac{3}{2\psi_c^3 l^2} + \alpha + \frac{1}{\psi_c} \right). \end{aligned} \quad (16)$$

The universal number is

$$\begin{aligned} \rho_c &= Q_c^2 T_c \psi_c \\ &= \frac{\psi_c^2}{3\pi} \left(\alpha + \frac{1}{4} + \frac{3}{2\psi_c^3 l^2} \right) \left(\frac{\alpha}{3} + \frac{1}{12\psi_c} - \frac{1}{16\psi_c^3 l^2} \right), \end{aligned} \quad (17)$$

where $0 < \alpha < 2$ for perfect fluid dark matter. When $\alpha = 0$, we have the following values:

$$\begin{aligned} T_c &= \frac{\sqrt{6}}{3\pi l}, \\ Q_c^2 &= \frac{l^2}{36}, \\ \psi_c &= \sqrt{\frac{3}{2l^2}}, \end{aligned} \quad (18)$$

which have been obtained by Dehyadegari et al. [47].

Now we study the critical behaviour near the phase transition with perfect fluid dark matter in new phase space. We first define $\psi_r = \psi/\psi_c$, $Q_r^2 = Q^2/Q_c^2$, and $T_r = T/T_c$; we then get $\psi_r = 1 + \chi$, $Q_r^2 = 1 + \varrho$, and $T_r = 1 + t$, where χ, ϱ and t represent the deviations away from critical points. The thermodynamics quantities are defined as

$$\begin{aligned} C_\psi &= |t|^{-a}, \\ \eta &= |t|^b, \\ \kappa_T &= |t|^{-c} \end{aligned} \quad (19)$$

$$|Q^2 - Q_c^2| = |\psi - \psi_c|^d$$

where a, b, c and d are the critical exponents. The critical exponent a is derived by fixing potential ψ for heat capacity as

$$C_\psi = T \left. \frac{\partial S}{\partial T} \right|_\psi = 0, \quad (20)$$

$$a = 0.$$

The critical exponent b is derived from Q^2 as

$$Q_r^2 = \frac{1}{2Q_c^2 \psi_c \psi_r} \left(\alpha + \frac{1}{2\psi_r \psi_c} + \frac{3}{8l^2 \psi_r^3 \psi_c^3} - \frac{\pi T_c}{\psi_r^2 \psi_c^2} T_r \right) \quad (21)$$

$$= \frac{F_1(\psi_c)}{\psi_r} + \frac{F_2(\psi_c)}{\psi_r^2} + \frac{F_3(\psi_c)}{\psi_r^3} + \frac{F_4(\psi_c)}{\psi_r^4} T_r,$$

where $F_1(\psi_c) = \alpha/(2Q_c^2 \psi_c)$, $F_2(\psi_c) = 1/(4Q_c^2 \psi_c^2)$, $F_3(\psi_c) = 3/(16Q_c^2 \psi_c^4 l^2)$, $F_4(\psi_c) = -\pi T_c/(2Q_c^2 \psi_c^3)$, and the critical points ψ_c, Q_c^2, T_c are functions of α, l^2 . In order to obtain critical exponent, we expand the equation near the critical point using $\psi_r = 1 + \chi$, $T_r = 1 + t$ and $Q_r^2 = 1 + \varrho$, and obtain

$$\varrho = F_4(\psi_c) t - 4F_4(\psi_c) t \chi$$

$$- (F_1(\psi_c) + 4F_2(\psi_c) + 4F_3(\psi_c) + 50F_4(\psi_c)) \chi^3 \quad (22)$$

$$+ \text{high order term}.$$

Through differentiating (22) with respect to χ and χ , and using (13), we obtain $\chi_s = -\chi_l = \sqrt{-4F_4(\psi_c) t / (F_1(\psi_c) + 4F_2(\psi_c) + 4F_3(\psi_c) + 50F_4(\psi_c))}$, where l and s represent large and small black hole phase, respectively. We then find that

$$|\chi_s - \chi_l| = 2\chi_s$$

$$= \sqrt{\frac{-16F_4(\psi_c)}{F_1(\psi_c) + 4F_2(\psi_c) + 4F_3(\psi_c) + 50F_4(\psi_c)}} t^{1/2}, \quad (23)$$

$$b = \frac{1}{2}.$$

The critical exponent c is derived from isothermal compressibility coefficient κ_T as

$$\kappa_T = \left. \frac{\partial \psi}{\partial Q^2} \right|_T \propto \frac{\psi_c}{-4F_4(\psi_c) Q_c^2 t}, \quad c = 1, \quad (24)$$

The critical exponent d is obtained from (22) as

$$\varrho|_{t=0}$$

$$= - (F_1(\psi_c) + 4F_2(\psi_c) + 4F_3(\psi_c) + 50F_4(\psi_c)) \chi^3, \quad (25)$$

$$d = 3.$$

From the above analysis, we find that these critical exponents resemble those in Van der Waals system, implying that the critical phenomenon can be explained by mean

field theory [17]. These critical exponents satisfy the scale symmetry given by

$$a + 2b + c = 2,$$

$$a + b(d + 1) = 2,$$

$$c(d + 1) = (2 - a)(d - 1), \quad (26)$$

$$c = b(d - 1).$$

The perfect fluid dark matters around black holes could explain the formation of supermassive black holes in approximate stationary situation. In the past decades, some high redshift quasars have been discovered and the centre supermassive black hole with the mass beyond 10 billion of solar masses. Usually such black hole is difficult to form in the Universe less than one billion years old. Because perfect fluid dark matter black holes satisfy the first law of thermodynamics, the perfect fluid dark matter could accelerate the formation of supermassive black holes.

4. Geothermodynamics of Dark Matter around Reissner-Nordstrom-AdS Black Hole

In the black hole thermodynamics, the thermodynamic geometry method is a usual tool to understand the property of black hole thermodynamics system. In the work, we use the Ruppeiner metric to study the thermodynamical effect of the perfect fluid dark matter on the microscopical structure of Reissner-Nordstrom-AdS black hole [48]. We define the metric on (M, Q^2) space given by

$$g_{\mu\nu}(R) = \frac{1}{T} \frac{\partial^2 M}{\partial X^\mu \partial X^\nu} = \begin{pmatrix} \frac{1}{T} \frac{\partial^2 M}{\partial S^2} & \frac{1}{T} \frac{\partial^2 M}{\partial S \partial Q^2} \\ \frac{1}{T} \frac{\partial^2 M}{\partial S \partial Q^2} & \frac{1}{T} \frac{\partial^2 M}{\partial Q^4} \end{pmatrix} \quad (27)$$

where $X^\mu = (S, Q^2)$.

From (5) and (6), we find that $M(S, Q^2)$ and $T(S, Q^2)$ in (M, Q^2) space are given by

$$M(S, Q^2) = \frac{1}{2} \sqrt{\frac{S}{\pi}} + \frac{Q^2}{2} \sqrt{\frac{\pi}{S}} + \frac{1}{2l^2 \pi} S \sqrt{\frac{S}{\pi}} \quad (28)$$

$$+ \frac{\alpha}{2} \ln \left(\frac{1}{|\alpha|} \sqrt{\frac{S}{\pi}} \right),$$

$$T(S, Q^2) = \frac{\alpha}{4S} + \frac{3}{4\pi l^2} \sqrt{\frac{S}{\pi}} + \frac{1}{4\pi} \sqrt{\frac{\pi}{S}} - \frac{Q^2}{4S} \sqrt{\frac{\pi}{S}}. \quad (29)$$

From geometry, the Ricci scalar can be calculated for perfect fluid dark matter around Reissner-Nordstrom-AdS black holes by

$$\begin{aligned}
R(RN - AdSDM) &= R^{\mu\nu\rho\sigma} R_{\mu\nu\rho\sigma} \\
&= \frac{H^2}{(-l^2\pi^2Q^2 - 2\alpha l^2\sqrt{\pi^3S} + l^2\pi S + 3S^2)^2} \\
&= \frac{H^2}{\left(-l^2\pi^2Q^2 - \frac{\alpha l^2\pi^2}{\psi} + \frac{l^2\pi^3}{4\psi^2} + \frac{3\pi^2}{16\psi^4}\right)^2},
\end{aligned} \tag{30}$$

where H are function of α, l^2, Q^2 and S . From above equation, we find that the phase transition occurs when the following condition is satisfied:

$$-l^2\pi^2Q^2 - \frac{\alpha l^2\pi^2}{\psi} + \frac{l^2\pi^3}{4\psi^2} + \frac{3\pi^2}{16\psi^4} = 0. \tag{31}$$

We know that the sign of the Ricci scalar R can be explained by intermolecular interaction in thermodynamical system. The positive sign refers to the repulsive interaction between the constituents of the thermodynamical system, while the negative sign refers to the attractive interaction between the constituents of the thermodynamical system ([42] and references therein). For perfect fluid dark matter around Reissner-Nordstrom-AdS black hole, the interactions are absent in the thermodynamical system for a null Ricci scalar R , which is similar to that in classical ideal gas [49].

5. Summary

In the paper, we study the perfect fluid dark matter influence on thermodynamics and phase transition of Reissner-Nordstrom-AdS black hole by extending phase space defined by the charge square Q^2 and conjugate quantity ψ . The first law of thermodynamics and the equation of state are derived in the form of $Q^2 = Q^2(T, \psi)$. We analyze the critical behaviour of dark matter around Reissner-Nordstrom-AdS black hole and find that these thermodynamics system resemble the Van der Waals system which can be explained by mean field theory. We also find that the critical exponents satisfy the scale law of thermodynamical system. Using Ruppeiner thermodynamic geometry, we study the geometric property of perfect fluid dark matter around black holes. We find that, in extended phase space, some singular points appear on the Ruppeiner curvature, which can be explained as the critical points of phase transitions.

The Reissner-Nordstrom-AdS black hole surrounded by dark matters could appear in the Universe. In the future work we plan to study the observed effects of perfect fluid dark matter on black holes and the influence of perfect fluid dark matter on gravitational lensing and the evolution of dark matter in the universe.

Data Availability

No data were used to support this study.

Conflicts of Interest

The authors declare that they have no conflicts of interest.

Acknowledgments

The authors acknowledge the financial support from the National Natural Science Foundation of China, 11573060 and 11661161010.

References

- [1] J. D. Bekenstein, "Black holes and the second law," *Lettere Al Nuovo Cimento Series 2*, vol. 4, no. 15, pp. 737–740, 1972.
- [2] J. D. Bekenstein, "Generalized second law of thermodynamics in black-hole physics," *Physical Review D: Particles, Fields, Gravitation and Cosmology*, vol. 9, no. 12, pp. 3292–3300, 1974.
- [3] J. D. Bekenstein, "Black holes and entropy," *Physical Review D: Particles, Fields, Gravitation and Cosmology*, vol. 7, pp. 2333–2346, 1973.
- [4] S. W. Hawking, "Gravitational radiation from colliding black holes," *Physical Review Letters*, vol. 26, no. 21, pp. 1344–1346, 1971.
- [5] S. W. Hawking, "Black hole explosions?" *Nature*, vol. 284, no. 5443, pp. 30–31, 1974.
- [6] J. M. Bardeen, B. Carter, and S. W. Hawking, "The four laws of black hole mechanics," *Communications in Mathematical Physics*, vol. 31, pp. 161–170, 1973.
- [7] M. M. Caldarelli, G. Cognola, and D. Klemm, "Thermodynamics of Kerr-Newman-AdS black holes and conformal field theories," *Classical and Quantum Gravity*, vol. 17, no. 2, pp. 399–420, 2000.
- [8] P. C. Davies, "Thermodynamic phase transitions of Kerr-Newman black holes in de Sitter space," *Classical and Quantum Gravity*, vol. 6, no. 12, pp. 1909–1914, 1989.
- [9] P. C. W. Davies, "Thermodynamics of black holes," *Reports on Progress in Physics*, vol. 41, no. 8, pp. 1313–1355, 1978.
- [10] P. C. W. Davies, "The Thermodynamic Theory of Black Holes," *Proceedings of the Royal Society of London Series A*, vol. 353, pp. 499–521, 1977.
- [11] S. W. Hawking and D. N. Page, "Thermodynamics of black holes in anti-de Sitter space," *Communications in Mathematical Physics*, vol. 87, no. 4, pp. 577–588, 1983.
- [12] P. Hut, "Charged black holes and phase transitions," *Monthly Notices of the Royal Astronomical Society*, vol. 180, pp. 379–389, 1977.
- [13] X.-B. Gong, Y. Liao, and Z.-Y. Xu, "A mathematical form of force-free magnetosphere equation around Kerr black holes and its application to Meissner effect," *Physics Letters B*, vol. 760, pp. 112–116, 2016.
- [14] Y. Liao, X.-B. Gong, and J.-S. Wu, "Phase-transition Theory of Kerr Black Holes in the Electromagnetic Field," *The Astrophysical Journal*, vol. 835, no. 2, p. 247, 2017.
- [15] A. Mandal, S. Samanta, and B. Ranjan Majhi, "Phase transition and critical phenomena of black holes: A general approach," *Physical Review D*, vol. 94, Article ID 064069, 2016.
- [16] B. Ranjan Majhi and S. Samanta, "P-V criticality of AdS black holes in a general framework," *Physics Letters B*, vol. 773, pp. 203–207, 2017.
- [17] D. Kubiznák and R. B. Mann, "P – V criticality of charged AdS black holes," *Journal of High Energy Physics*, vol. 7, p. 33, 2012.
- [18] A. Belhaj, M. Chabab, H. El Moumni, K. Masmar, and M. B. Sedra, "On thermodynamics of AdS black holes in M-theory," *The European Physical Journal C*, vol. 76, no. 73, 2016.

- [19] A. Belhaj, M. Chabab, H. El Moumni, K. Masmar, and M. B. Sedra, "Maxwell's equal-area law for Gauss–Bonnet–Anti-de Sitter black holes," *The European Physical Journal C*, vol. 75, article 71, 2015.
- [20] A. Belhaj, M. Chabab, H. E. Moumni, and M. B. Sedra, "On thermodynamics of AdS black holes in arbitrary dimensions," *Chinese Physics Letters*, vol. 29, no. 10, Article ID 100401, 2012.
- [21] A. Belhaj, M. Chabab, H. El Moumni, L. Medari, and M. B. Sedra, "The Thermodynamical Behaviors of Kerr–Newman AdS Black Holes," *Chinese Physics Letters*, vol. 30, Article ID 090402, 2013.
- [22] M. Chabab, H. El Moumni, and K. Masmar, "On thermodynamics of charged AdS black holes in extended phases space via M2-branes background," *The European Physical Journal C*, vol. 76, p. 304, 2016.
- [23] E. Komatsu, K. M. Smith, J. Dunkley et al., "Seven-year wilkinson microwave anisotropy probe (WMAP*) observations: cosmological interpretation," *The Astrophysical Journal*, vol. 192, no. 2, p. 18, 2011.
- [24] A. G. Riess, L.-G. Strolger, J. Tonry et al., "Type Ia Supernova Discoveries at $z > 1$ from the Hubble Space Telescope: Evidence for Past Deceleration and Constraints on Dark Energy Evolution," *The Astrophysical Journal*, vol. 607, p. 665, 2004.
- [25] P. J. E. Peebles and B. Ratra, "The cosmological constant and dark energy," *Reviews of Modern Physics*, vol. 75, no. 2, pp. 559–606, 2003.
- [26] E. J. Copeland, M. Sami, and S. Tsujikawa, "Dynamics of dark energy," *International Journal of Modern Physics D*, vol. 15, no. 11, pp. 1753–1935, 2006.
- [27] Z. Stuchlík, "Influence of the RELICT Cosmological Constant on Accretion Discs," *Modern Physics Letters A*, vol. 20, no. 8, pp. 561–575, 2005.
- [28] V. V. Kiselev, "Quintessence and black holes," *Classical and Quantum Gravity*, vol. 20, no. 6, pp. 1187–1197, 2003.
- [29] V. V. Kiselev, "Quintessential solution of dark matter rotation curves and its simulation by extra dimensions," *High Energy Physics*, 11 pages, 2003.
- [30] B. Toshmatov, Z. Stuchlík, and B. Ahmedov, "Rotating black hole solutions with quintessential energy," 2015, <https://arxiv.org/abs/1512.01498v1>.
- [31] Z. Xu and J. Wang, "Kerr–Newman–AdS black hole in quintessential dark energy," *Physical Review D: Particles, Fields, Gravitation and Cosmology*, vol. 95, Article ID 06415, 2017.
- [32] R. Tharanath, N. Varghese, and V. C. Kuriakose, "Phase transition, quasinormal modes and Hawking radiation of Schwarzschild black hole in quintessence field," *Modern Physics Letters A*, vol. 29, Article ID 1450057, 2014.
- [33] K. Ghaderi and B. Malakolkalami, "Effects of quintessence on thermodynamics of the black holes," *Astrophysics and Space Science*, vol. 361, p. 161, 2016.
- [34] K. Ghaderi and B. Malakolkalami, "Thermodynamics of the Schwarzschild and the Reissner–Nordström black holes with quintessence," *Nuclear Physics B*, vol. 903, pp. 10–18, 2016.
- [35] Z. Xu and J. Wang, "Thermodynamics and Phase Transition in Rotational Kiselev Black Hole," 2016, <https://arxiv.org/abs/1610.00376>.
- [36] Y.-H. Wei and Z.-H. Chu, "Thermodynamic Properties of a Reissner–Nordström Quintessence Black Hole," *Chinese Physics Letters*, vol. 28, Article ID 100403, 2011.
- [37] Y.-H. Wei and J. Ren, "Thermodynamic properties of Reissner–Nordström–de Sitter quintessence black holes," *Chinese Physics B*, vol. 22, Article ID 030402, 2013.
- [38] B. B. Thomas, M. Saleh, and T. C. Kofane, "Thermodynamics and phase transition of the Reissner–Nordström black hole surrounded by quintessence," *General Relativity and Gravitation*, vol. 44, no. 9, pp. 2181–2189, 2012.
- [39] A. Mandal and R. Biswas, "Effects of cosmic acceleration on black hole thermodynamics," *Astrophysics and Space Science*, vol. 357, p. 8, 2015.
- [40] M.-S. Ma, R. Zhao, and Y.-Q. Ma, "Thermodynamic stability of black holes surrounded by quintessence," *General Relativity and Gravitation*, vol. 49, p. 79, 2017.
- [41] P. Pradhan, "Thermodynamic Products in Extended Phase Space," *International Journal of Modern Physics D*, vol. 26, no. 2, 2017.
- [42] M. Chabab, H. El Moumni, S. Iraoui, K. Masmar, and S. Zhizeh, "More insight into microscopic properties of RN–AdS black hole surrounded by quintessence via an alternative extended phase space," *International Journal of Geometric Methods in Modern Physics*, vol. 15, no. 10, 2018.
- [43] X.-X. Zeng and L.-F. Li, "Van der Waals phase transition in the framework of holography," *Physics Letters B*, vol. 764, pp. 100–108, 2017.
- [44] M.-H. Li and K.-C. Yang, "Galactic dark matter in the phantom field," *Physical Review D: Particles, Fields, Gravitation and Cosmology*, vol. 86, Article ID 123015, 2012.
- [45] V. V. Kiselev, "Vector field and rotational curves in dark galactic halos," *Classical and Quantum Gravity*, vol. 22, no. 3, pp. 541–557, 2005.
- [46] E. Spallucci and A. Smailagic, "Maxwell's equal area law and the Hawking–Page phase transition," 2013, <https://arxiv.org/abs/1310.2186v1>.
- [47] A. Dehyadegari, A. Sheykhi, and A. Montakhab, "Critical behavior and microscopic structure of charged AdS black holes via an alternative phase space," *Physics Letters B*, vol. 768, pp. 235–240, 2017.
- [48] A. Sahay, T. Sarkar, and G. Sengupta, "Thermodynamic geometry and phase transitions in Kerr–Newman–AdS black holes," *Journal of High Energy Physics*, vol. 7, p. 82, 2010.
- [49] G. Ruppeiner, "Thermodynamics: a Riemannian geometric model," *Physical Review A: Atomic, Molecular and Optical Physics*, vol. 20, no. 4, pp. 1608–1613, 1979.

Research Article

Anti-de-Sitter-Maxwell-Yang-Mills Black Holes Thermodynamics from Nonlocal Observables Point of View

H. El Moumni ^{1,2}

¹*EPTHE, Physics Department, Faculty of Sciences, Ibn Zohr University, Agadir, Morocco*

²*High Energy Physics and Astrophysics Laboratory, Faculty of Science Semlalia, Cadi Ayyad University, 40000 Marrakesh, Morocco*

Correspondence should be addressed to H. El Moumni; hasan.elmoumni@edu.uca.ma

Received 29 June 2018; Revised 28 October 2018; Accepted 23 December 2018; Published 20 January 2019

Guest Editor: Saibal Ray

Copyright © 2019 H. El Moumni. This is an open access article distributed under the Creative Commons Attribution License, which permits unrestricted use, distribution, and reproduction in any medium, provided the original work is properly cited. The publication of this article was funded by SCOAP³.

In this paper we analyze the thermodynamic properties of the Anti-de-Sitter black hole in the Einstein-Maxwell-Yang-Mills-AdS gravity (EMYM) via many approaches and in different thermodynamical ensembles (canonical/grand canonical). First, we give a concise overview of this phase structure in the entropy-thermal diagram for fixed charges and then we investigate this thermodynamical structure in fixed potentials ensemble. The next relevant step is recalling the nonlocal observables such as holographic entanglement entropy and two-point correlation function to show that both observables exhibit a Van der Waals-like behavior in our numerical accuracy and just near the critical line as the case of the thermal entropy for fixed charges by checking Maxwell's equal area law and the critical exponent. In the light of the grand canonical ensemble, we also find a newly phase structure for such a black hole where the critical behavior disappears in the thermal picture as well as in the holographic one.

1. Introduction

Over the last years, a great emphasis has been put on the application of the Anti-de-Sitter/conformal field theory correspondence [1, 2] which plays a pivotal role in recent developments of many physical themes [3–5]; in this particular context the thermodynamics of Anti-de-Sitter black holes become more attractive for investigation [6].

In general, black hole thermodynamics has emerged as a fascinating laboratory for testing the predictions of candidate theories of quantum gravity. It has been figured that black holes are associated thermodynamically with a entropy and a temperature [7] and a pressure [8]. This association has led to a rich structure of phase picture and a remarkable critical behavior similar to van der Waals liquid/gas phase transition [9–19]. Another confirmation of this similarity appears when we employ nonlocal observables such as entanglement entropy, Wilson loop, two-point correlation function, and the complexity growth rate [20–33]. Meanwhile, these tools are used extensively in quantum information and to characterize phases and thermodynamical behavior [21, 23, 34–41].

The black hole charge finds a deep interpretation in the context of the AdS/CFT correspondence linked to condensed matter physics; the charged black hole introduces a charge density/chemical potential and temperature in the quantum field theory defined on the boundary [42]. In this background, the charged black hole can be viewed as an uncondensed unstable phase which develops a scalar hair at low temperature and breaks $U(1)$ symmetry near the black hole horizon reminiscing the second-order phase transition between conductor and superconductor phases [43]; this situation is called the "s-wave" holographic superconductor. It has also been shown that "p-wave" holographic superconductor corresponds to vector hair models [44, 45]. The simplest example of p-wave holographic superconductors may be provided by an Einstein-Yang-Mills theory with $SU(2)$ gauge group and no scalar fields, where the electromagnetic gauge symmetry is identified with an $U(1)$ subgroup of $SU(2)$. The other components of the $SU(2)$ gauge field play the role of charged fields dual to some vector operators that break the $U(1)$ symmetry, leading to a phase transition in the dual field theory.

Motivated by all the ideas described above, although the Yang-Mills fields are confined to acting inside nuclei while the Maxwell field dominates outside, the consideration of such theory where the two kinds of field live is encouraged by the existence of exotic and highly dense matter in our universe. In this work, we try to contribute to this rich area by revisiting the phase transition of Anti-de-Sitter black holes in Einstein-Maxwell-Yang-Mills (EYM) gravity. More especially, we investigate the first- and second-order phase transition by different approaches including the holographic one and in different canonical ensembles.

This work is organized as follow: First, we present some thermodynamic properties and phase structure of the EYM-AdS black holes in (temperature, entropy)-plane in canonical and grand canonical ensemble. Next, we show in Section 3 that the holographic approach exhibits the same behavior; in other words we recall the entanglement entropy and two-point correlation function to check the Maxwell's equal area law and calculate the critical exponent of the specific heat capacity which is consistent with that of the mean field theory of the Van der Waals in the canonical ensemble near the critical point. In the grand canonical one, a new phase structure arises where the critical behavior disappears in the thermal as well as the holographic framework. The last section is devoted to a conclusion.

2. Critical Behavior of Einstein-Maxwell-Yang-Mills-AdS Black Holes in Thermal Picture

2.1. Canonical Ensemble. We start this section by writing the N -dimensional for Einstein-Maxwell-Yang-Mills gravity with a cosmological constant Λ described by the following action [46, 47]

$$\mathcal{I} = \frac{1}{2} \int_{\mathcal{M}} dx^N \sqrt{-g} \left(R - \frac{(N-1)(N-2)}{3} \Lambda - \mathcal{F}_M - \mathcal{F}_{YM} \right), \quad (1)$$

where R is the Ricci scalar while Λ is the cosmological constant. Also $\mathcal{F}_M = F_{\mu\nu}F^{\mu\nu}$ and $\mathcal{F}_{YM} = \text{Tr}(F_{\mu\nu}^{(a)}F^{(a)\mu\nu})$ are the Maxwell invariant and the Yang-Mills invariant, respectively; the trace element stands for $\text{Tr}(\cdot) = \sum_{a=1}^{(N-1)(N-2)/2} (\cdot)$. Varying the action (1) with respect to the metric tensor $g_{\mu\nu}$, the Faraday tensor $F_{\mu\nu}$, and the YM tensor $F_{\mu\nu}^{(a)}$, one can obtain the following field equations

$$G_{\mu\nu} + \Lambda g_{\mu\nu} = T_{\mu\nu}^M + T_{\mu\nu}^{YM} \quad (2)$$

$$\nabla F^{\mu\nu} = 0 \quad (3)$$

$$\widehat{D}_\mu F_{\mu\nu}^{(a)} = \nabla_\mu F^{(a)\mu\nu} + \frac{1}{\Theta} \varepsilon_{(b)(c)}^{(a)} A_\mu^{(b)} F^{(c)\mu\nu} = 0 \quad (4)$$

where $G_{\mu\nu}$ is the Einstein tensor, the quantity $\varepsilon_{(b)(c)}^{(a)}$'s stands for the structure constants of the $((N-1)(N-2)/2)$ -parameters Lie group G , Θ is coupling constant, and $A_\mu^{(a)}$ denotes the $SO(N-1)$ gauge group YM potential. We also note that the

internal indices $\{a, b, c, \dots\}$ do not differ whether in covariant or contravariant form. In addition, $T_{\mu\nu}^M$ and $T_{\mu\nu}^{YM}$ are the energy momentum tensor of Maxwell and YM fields with the following formula

$$T_{\mu\nu}^M = -\frac{1}{2} g_{\mu\nu} F_{\rho\sigma} F^{\rho\sigma} + 2F_{\mu\lambda} F_\nu^\lambda \quad (5)$$

$$T_{\mu\nu}^{YM} = \sum_{a=1}^{(N-1)(N-2)/2} \left[-\frac{1}{2} g_{\mu\nu} F_{\rho\sigma}^{(a)} F^{(a)\rho\sigma} + 2F_{\mu\lambda}^{(a)} F_\nu^{(a)\lambda} \right] \quad (6)$$

$$F_{\mu\nu}^{(a)} = \partial_\mu A_\nu^{(a)} - \partial_\nu A_\mu^{(a)} + \frac{1}{2\Theta} \varepsilon_{(b)(c)}^{(a)} A_\mu^{(b)} A_\nu^{(c)}, \quad (7)$$

$$F_{\mu\nu} = \partial_\mu A_\nu - \partial_\nu A_\mu. \quad (8)$$

where A_μ is the usual Maxwell potential. The metric for such N dimensional spherical black hole may be chosen to be [47]

$$ds^2 = -f(r) dt^2 + \frac{1}{f(r)} dr^2 + r^2 d\Omega_n^2 \quad (9)$$

in which $d\Omega_n^2$ represents the volume of the unit n -sphere which can be expressed in the standard spherical form

$$d\Omega_{N-2}^2 = d\theta_1^2 + \sum_{i=2}^{N-3} \Pi_{j=1}^{i-1} \sin^2 \theta_j d\theta_i^2 \quad (10)$$

where $0 \leq \theta_1 \leq \pi$, $0 \leq \theta_i \leq 2\pi$.

In order to find the electromagnetic field, we recall the following radial gauge potential ansatz $A_\mu = h(r)\delta_\mu^0$ which obeys the Maxwell field equations (3) with the following solution

$$\frac{dh(r)}{dr} = \frac{c}{r^{N-2}} \quad (11)$$

where c is an integration constant related to electric charge C of the solutions. To solve the YM field, (4), we use the magnetic Wu-Yang ansatz of the gauge potential [48, 49] given by

$$\begin{aligned} A^{(a)} &= \frac{Q}{r^2} (x_i dx_j - x_j dx_i) \\ 2 \leq i \leq N-1, \\ 1 \leq j \leq i-1 \\ 1 \leq (a) \leq \frac{(N-1)(N-2)}{2} \end{aligned} \quad (12)$$

where we imply (to have a systematic process) that the super indices a are chosen according to the values of i and j in order. For instance, we present some of them

$$\begin{aligned}
 A^{(1)} &= \frac{Q}{r^2} (x_2 dx_1 - x_1 dx_2) \\
 A^{(2)} &= \frac{Q}{r^2} (x_3 dx_1 - x_1 dx_3) \\
 A^{(3)} &= \frac{Q}{r^2} (x_3 dx_2 - x_2 dx_3) \\
 A^{(4)} &= \frac{Q}{r^2} (x_4 dx_1 - x_1 dx_4) \\
 A^{(5)} &= \frac{Q}{r^2} (x_4 dx_2 - x_2 dx_4) \\
 A^{(6)} &= \frac{Q}{r^2} (x_4 dx_3 - x_3 dx_4) \\
 A^{(7)} &= \frac{Q}{r^2} (x_5 dx_1 - x_1 dx_5) \\
 A^{(8)} &= \frac{Q}{r^2} (x_5 dx_2 - x_2 dx_5) \\
 A^{(9)} &= \frac{Q}{r^2} (x_5 dx_3 - x_3 dx_5) \\
 A^{(10)} &= \frac{Q}{r^2} (x_5 dx_4 - x_4 dx_5) \\
 &\dots
 \end{aligned} \tag{13}$$

in which $r^2 = \sum_{i=1}^{N-1} x_i^2$. The YM field 2-forms are defined by the expression

$$F^{(a)} = dA^{(a)} + \frac{1}{2Q} \varepsilon_{(b)(c)}^{(a)} A^{(b)} \wedge A^{(c)}. \tag{14}$$

In general for N we must have $(N-1)(N-2)/2$ gauge potentials. The integrability conditions

$$dF^{(a)} + \frac{1}{Q} \varepsilon_{(b)(c)}^{(a)} A^{(b)} \wedge F^{(c)} = 0 \tag{15}$$

are easily satisfied by using (28). The YM equations

$$d * F^{(a)} + \frac{1}{Q} \varepsilon_{(b)(c)}^{(a)} A^{(b)} \wedge * F^{(c)} = 0 \tag{16}$$

also are all satisfied. The energy-momentum tensor (4) becomes after

$$\sum_{a=1}^{(N-1)(N-2)/2} [F_{\lambda\sigma}^{(a)} F^{(a)\lambda\sigma}] = \frac{(N-3)(N-2)Q^2}{r^4} \tag{17}$$

with the nonzero components

$$\begin{aligned}
 T_{00} &= \frac{(N-3)(N-2)Q^2 f(r)}{2r^4} \\
 T_{11} &= -\frac{(N-3)(N-2)Q^2}{2r^4 f(r)} \\
 T_{22} &= -\frac{(N-3)(N-6)Q^2}{2r^2} \\
 T_{AA} &= -\frac{(N-3)(N-6)Q^2}{2r^2} \Pi_{i=1}^{A-2} \sin^2 \theta_i \\
 2 &< A \leq N-1.
 \end{aligned} \tag{18}$$

Using (2) and after some simplifications, one can find that the metric function $f(r)$ has the following form given by

$$f(r) = 1 - \frac{2m}{r^{n-1}} - \frac{\Lambda}{3} r^2 + \frac{2(n-1)C^2}{nr^{2n-2}} - \frac{(n-1)Q^2}{(n-3)r^2}, \tag{19}$$

where $N = n + 2$; one can note in the particular case for $n = 3$ that the last term of (19) diverges, involving an unusual logarithmic term in Yang-Mills charge [46]. For this gravity background the parameter m is related to the mass of such black hole, while C and Q are the charges of Maxwell field and Yang-Mills field, respectively. Following previous literature [8, 9], one can find a close connection between the cosmological constant and pressure as $P = -\Lambda/8\pi$, leading to the following expressions of Hawking temperature, mass, and entropy of such black hole in terms of the horizon radius r_+

$$\begin{aligned}
 T &= \frac{f'(r_+)}{4\pi} = \frac{n-1}{4\pi r_+} + \frac{2(n+1)P}{3} r_+ - \frac{(n-1)Q^2}{4\pi r_+^3} \\
 &\quad - \frac{(n-1)^2 C^2}{2\pi n r_+^{2n-1}},
 \end{aligned} \tag{20}$$

$$\begin{aligned}
 M &= \frac{n\omega_n}{48\pi} \left(8\pi P r_+^{n+1} + \frac{3(n-1)Q^2 r_+^{n-3}}{3-n} + 3r_+^{n-1} \right. \\
 &\quad \left. + \frac{6(n-1)C^2}{nr_+^{n-1}} \right),
 \end{aligned} \tag{21}$$

$$S = \frac{\omega_n r_+^n}{4}, \tag{22}$$

The Yang-Mills potential Φ_Q and the electromagnetic one Φ_C can be written as

$$\Phi_Q = \left(\frac{\partial M}{\partial Q} \right)_{C,P,r_+} = \frac{\omega_n (n-1) n Q}{8\pi (3-n)} r_+^{n-3}, \tag{23}$$

$$\Phi_C = \left(\frac{\partial M}{\partial C} \right)_{Q,P,r_+} = \frac{\omega_n (n-1) C}{4\pi r_+^{n-1}}, \tag{24}$$

where $\omega_n = 2\pi^{(n+1)/2}/\Gamma((n+1)/2)$ is the volume of the unit n -sphere. In fact, according to the interpretation of the black

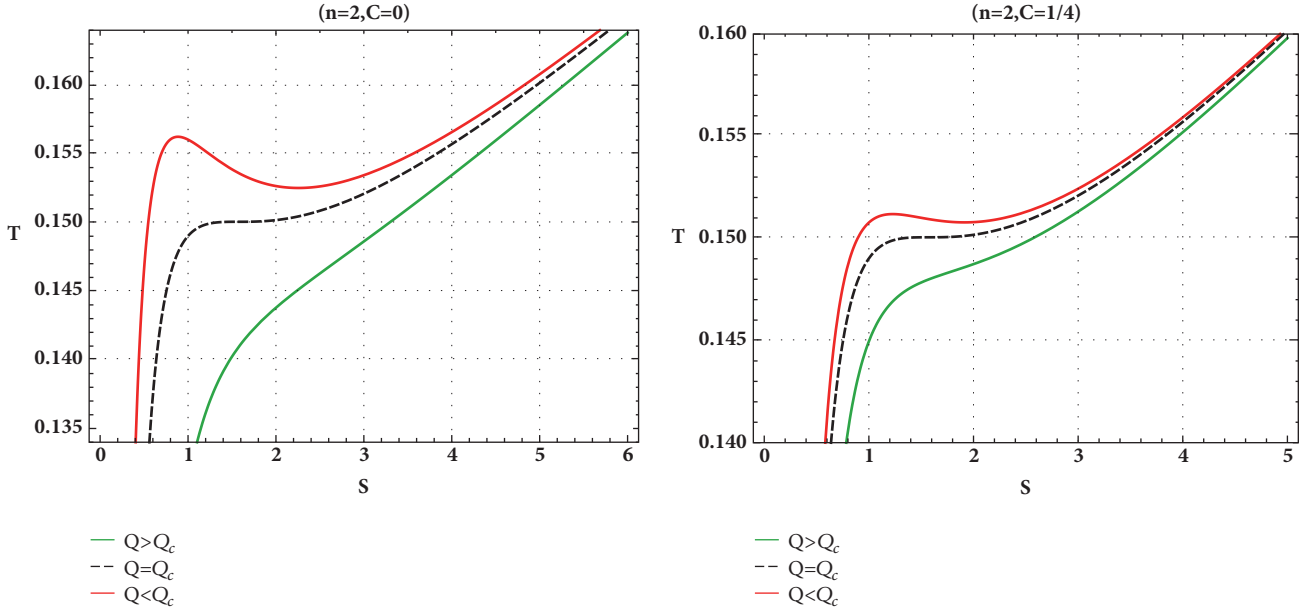


FIGURE 1: The temperature as a function of the entropy for different values of charge C . **(Left)** $C = 0$. **(Right)** $C \neq 0$.

hole mass M as an enthalpy [8] in the extended phase space context, the free energy \mathcal{F} of black hole can be written as

$$\mathcal{F} = M - T \cdot S \quad (25)$$

and the heat capacity is given by

$$C_Q = T \left. \frac{\partial S}{\partial T} \right|_Q \quad (26)$$

It is straightforward to show that obtained quantities (20), (21), and (22) obey the first law of black hole thermodynamics in the extended phase space

$$dM = TdS + \Phi_Q dQ + \Phi_C dC + VdP, \quad (27)$$

where V is the Legendre transform of the pressure, which denotes the thermodynamic volume with

$$V = \left(\frac{\partial M}{\partial P} \right)_{S, \Phi_Q, \Phi_C} = \frac{n\omega_n \pi}{3} r^{n+1}. \quad (28)$$

In addition to this, using scaling argument, the corresponding Smarr formula is

$$M = \frac{n}{n-1} TS + \Phi_C C + \frac{1}{(n-1)} \Phi_Q Q - \frac{2}{n-1} VP. \quad (29)$$

Without loss of generality, inserting (22) into (20), we can get the entropy Hawking temperature relation of such black hole, namely,

$$\begin{aligned} T = \frac{1}{12\pi n} & \left[6C(n-1)^2 \left(4^{1/n} \left(\frac{S}{\omega_n} \right)^{1/n} \right)^{1-2n} \right. \\ & + \pi 2^{2/n+3} n(n+1) P \left(\frac{S}{\omega_n} \right)^{1/n} \\ & - 3(n-1)nQ^2 4^{-3/n} \left(\frac{S}{\omega_n} \right)^{-3/n} \\ & \left. + 3 \cdot 4^{-1/n} (n-1)n \left(\frac{S}{\omega_n} \right)^{-1/n} \right] \end{aligned} \quad (30)$$

This relation is depicted in Figure 1; indeed it has been shown that there is a Van der Waals-like phase transition; furthermore a direct confirmation comes from the solution of the following system

$$\left(\frac{\partial T}{\partial S} \right)_Q = \left(\frac{\partial^2 T}{\partial S^2} \right)_Q = 0. \quad (31)$$

which reveal the existence of a critical point. The critical charge, entropy, and temperature are given in Table 1; for the rest of the paper we keep $n = 2$.

An important remark that can be observed here is that both quantities T_c and S_c are insensitive with the charge C . The behavior of the free energy \mathcal{F} with respect to the temperature may be investigated by plotting in Figure 2 the graph $\mathcal{F} - T$ for a fixed value of charge Q under the critical one. From

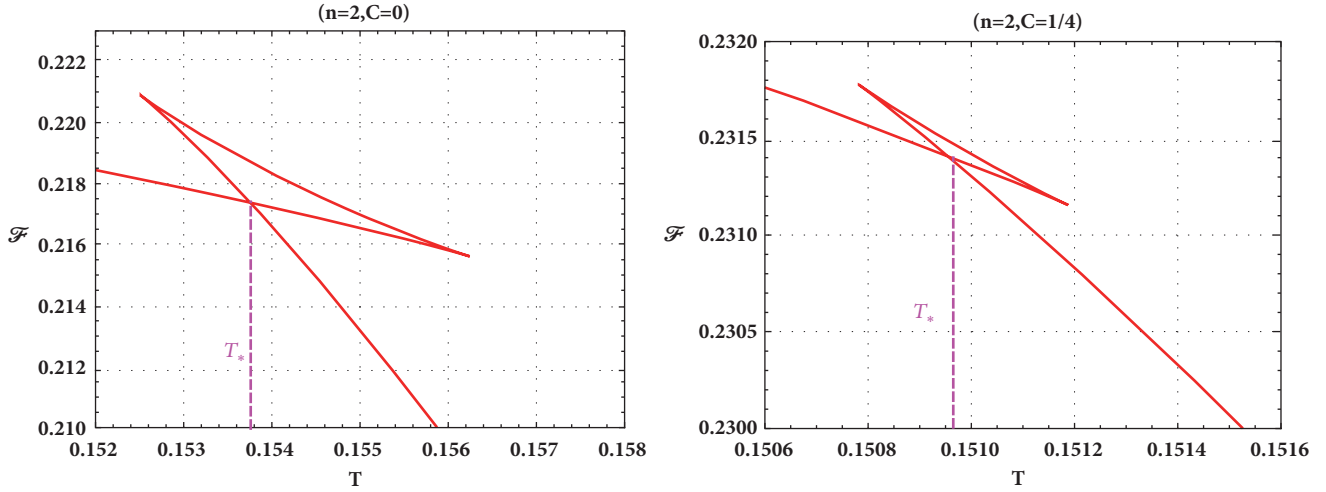


FIGURE 2: The Helmholtz free energy in function of the entropy for EYM-AdS black holes for different values of the charge C . **(Left)** $C = 0$. **(Right)** $C \neq 0$.

TABLE 1: Coordinates of the critical points for different values of C in (T, S) -diagram.

	Q_c	S_c	T_c
$C = 0$	$\frac{1}{2\sqrt{3}}$	$\frac{\pi}{2}$	$\frac{\sqrt{2}}{3\pi}$
$C \neq 0$	$\frac{1}{6}\sqrt{3 - 36C^2}$	$\frac{\pi}{2}$	$\frac{\sqrt{2}}{3\pi}$

TABLE 2: Check of the equal area law in the $T - S$ plane for different C .

C	T_*	S_1	S_2	S_3	A_1	A_2
0	0.15376	0.638237	1.52994	3.13241	0.383499	0.38350
$\frac{1}{4}$	150965	1.05043	11.54616	2.25932	00.18248	0.1825

this plot, we can observe the characteristic swallow-tail which guarantees the existence of the Van der Waals-like phase transition.

Using Figure 2, we can derive numerically the coexistence temperature T_* needed in the Maxwell's equal area law construction

$$\begin{aligned}
 A_1 &\equiv \int_{S_1}^{S_2} T(S) dS - T_*(S_2 - S_1) \\
 &= T_*(S_3 - S_2) - \int_{S_2}^{S_3} T(S) dS \equiv A_2,
 \end{aligned}
 \tag{32}$$

where S_3 , S_2 , and S_1 are the solutions of $T(S) = T_*$ in descending order, in addition to the numerical values of these points, and we report in Table 2 the areas A_1 and A_2 in Maxwell's law (32)

Obviously, the area A_1 equals area A_2 for different C , so the equal area law does not break. For the second phase transition, we know that, near the critical point, there is always a linear relation with slope equal to 3 [47, 50]

$$\log |T - T_c| = 3 \log |S - S_c| + \text{constant} \tag{33}$$

in this context, the heat capacity behaves like

$$C_Q \sim (T - T_c)^{-2/3} \tag{34}$$

where the critical exponent of the second-order phase is $-2/3$, which is consistent with the mean field theory.

2.2. Grand Canonical Ensemble. Having described the thermodynamical behavior of the EYM-AdS black hole with a fixed charge, by showing the occurrence of the first and second phase transition, we will focus this section on the phase structure when the potentials are kept fixed.

To facilitate the calculation of relevant quantities, it is convenient to reexpress the Hawking temperature as a function of entropy, Yang-Mills, and electromagnetic potentials, inserting (23) and (24) into (30); one can write

$$T = \frac{1}{3\pi 2^{2(n+1)/n}} \left(\frac{S}{\omega_n} \right)^{-1/n} \times \left[\frac{96\pi^2 \left(-2^{(n+8)/n} (n-3)^2 \Phi_Q^2 \left(4^{1/n} (S/\omega_n)^{1/n} \right)^{-2n} (S/\omega_n)^{4/n} / (n-1) - n\Phi_c^2 \right)}{n^2 \omega_n^2} \right. \\ \left. - 16^{1/n} \Lambda (n+1) \left(\frac{S}{\omega_n} \right)^{2/n} + 3(n-1) \right] \quad (35)$$

In our assumptions, where $n = 2$ and $\Lambda = -1$, (35) reduces to

$$T = \frac{S - \pi (\Phi_c^2 + \Phi_Q^2 - 1)}{4\pi^{3/2} \sqrt{S}} \quad (36)$$

which is in agreement with the result of [51, 52] if we set $\Phi_Q = 0$. Now we are able to write easily

$$\left(\frac{\partial T}{\partial S} \right)_{\Phi_Q, \Phi_c} = \frac{-S - 3\pi (\Phi_c^2 + \Phi_Q^2 - 1)}{16\pi^{3/2} S^{5/2}} \quad (37)$$

$$\left(\frac{\partial^2 T}{\partial S^2} \right)_{\Phi_Q, \Phi_c} = \frac{S + \pi (\Phi_c^2 + \Phi_Q^2 - 1)}{8\pi^{3/2} S^{3/2}} \quad (38)$$

The solution of $(\partial T / \partial S)_{\Phi_Q, \Phi_c} = 0$ can be derived as

$$S_1 = -\pi (\Phi_c^2 + \Phi_Q^2 - 1) \quad (39)$$

where the condition $\Phi_c^2 + \Phi_Q^2 < 1$ should be verified to ensure that the entropy in (39) is positive. In the other case $\Phi_c^2 + \Phi_Q^2 > 1$, one cannot find meaningful root of the equation $(\partial T / \partial S)_{\Phi_Q, \Phi_c} = 0$. Substituting (39) into (38) we obtain the following constraint

$$\left(\frac{\partial^2 T}{\partial S^2} \right)_{\Phi_Q, \Phi_c} \Big|_{S=S_1} = \frac{1}{8\pi^3 (-\Phi_c^2 - \Phi_Q^2 + 1)^{3/2}} > 0 \quad (40)$$

implying that no critical point is observed in the $T - S$ diagram. This observation differs from the result in the previous section where the charges are kept fixed, consolidating the assertion that the thermodynamics in the grand canonical ensemble is quite different from that in the canonical one. In Figure 3, we depict the Hawking temperature for both the cases $\Phi_c^2 + \Phi_Q^2 < 1$ and $\Phi_c^2 + \Phi_Q^2 > 1$ and one can see that there exists minimum temperature for the left panel. Substituting (39) into (36), the minimum temperature can be obtained as

$$T_{min} = \frac{\sqrt{-\Phi_c^2 - \Phi_Q^2 + 1}}{2\pi}. \quad (41)$$

However, the Hawking temperature increases monotonically in the right panel.

Having obtained the phase picture of the thermal entropy of the AdS-Maxwell-Yang-Mills black hole, the canonical/grand canonical ensemble, we will now revisit the phase

structure of the entanglement entropy and two-point correlation function to see whether they have similar phase structure in each thermodynamical ensemble.

3. Phase Transitions of Einstein-Maxwell-Yang-Mills-AdS Black Holes in Holographic Picture

3.1. Holographic Entanglement Entropy. First, let us provide a concise review of some generalities about the holographic entanglement entropy. For a given quantum field theory described by a density matrix ρ , with A being some region of a Cauchy surface of spacetime and A^c standing for its complement, the von Neumann entropy traduces the entanglement between these two regions

$$S_A = -\text{Tr}_A (\rho_A \log \rho_A), \quad (42)$$

with ρ_A being the reduced density matrix of given by A $\rho_A = \text{Tr}_{A^c}(\rho)$. Ryu and Takayanagi propose a simple geometric way to evaluate the entanglement entropy as [53, 54]

$$S_A = \frac{\text{Area}(\Gamma_A)}{4G_N}, \quad (43)$$

in which Γ_A denotes a codimension-2 minimal surface with boundary condition $\partial \Gamma_A = \partial A$ and G_N stands for the gravitational Newton's constant. In our black hole model we choose the region A to be a spherical cap on the boundary delimited by $\theta \leq \theta_0$, and the minimal surface can be parametrized by the function $r(\theta)$. According to definition of the area and (9) and (43), one can show that the holographic entanglement entropy is governed by

$$S_A = \frac{\omega_{n-2}}{4} \int_0^{\theta_0} r^{n-2} \sin^{n-2} \theta \sqrt{\frac{(r')^2}{f(r)} + r^2} d\theta, \quad (44)$$

where the notation prime denotes the derivative with respect to θ ; e.g., $r' \equiv dr/d\theta$. Treat (44) as a Lagrangian and solve the equation of motion given by

$$r'(\theta)^2 [\sin \theta r(\theta)^2 f'(r) - 2 \cos \theta r'(\theta)] - 2r(\theta) f(r) \\ \cdot [r(\theta) (\sin \theta r''(\theta) + \cos \theta r'(\theta)) - 3 \sin \theta r'(\theta)^2] \\ + 4 \sin(\theta) r(\theta)^3 f(r)^2 = 0. \quad (45)$$

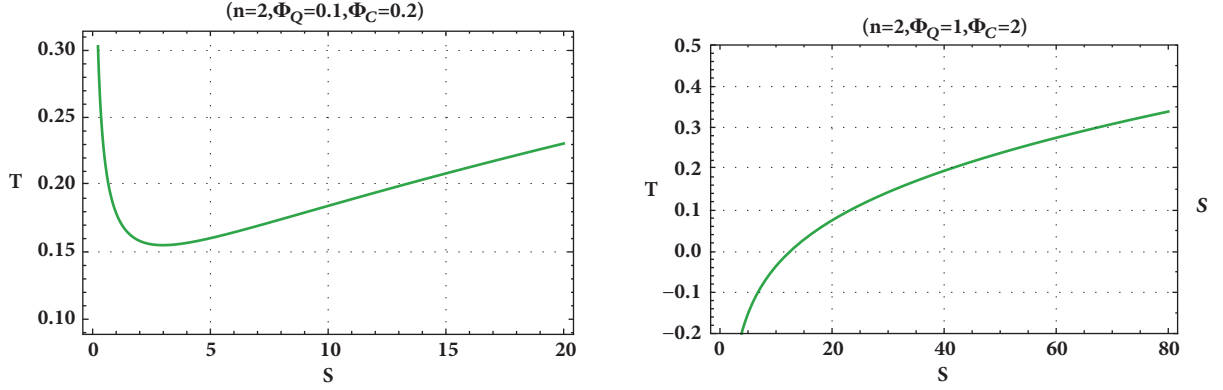


FIGURE 3: The temperature as a function of the entropy for different potentials. **(Left)** $\Phi_c^2 + \Phi_Q^2 < 1$. **(Right)** $\Phi_c^2 + \Phi_Q^2 > 1$.

Due to the difficulty to find an analytical form of the solution $r(\theta)$, we will perform a numerical calculation with adopting the following boundary conditions

$$\begin{aligned} r'(\theta) &= 0, \\ r(0) &= r_0. \end{aligned} \quad (46)$$

Knowing that the entanglement entropy is divergent at the boundary, we regularized it by subtracting the area of the minimal surface in pure AdS whose boundary is also $\theta = \theta_0$ with

$$r_{AdS}(\theta) = L \left(\left(\frac{\cos \theta}{\cos \theta_0} \right)^2 - 1 \right)^{-1/2}. \quad (47)$$

We label the regularized entanglement entropy by ΔS_A and for our numerical calculation we choose $\theta_0 = 0.2$ and 0.3 while Ultra Violet cutoff is chosen to be $\theta_c = 0.199$ and 0.299 , respectively. To compare with the phase structure in the thermal picture, we will study the relation between the entanglement entropy and the Hawking temperature representing the temperature of the dual field theory; this relation is depicted in Figure 4 for different values of Maxwell's charge with a fixed Yang-Mills one near the critical point and the chosen θ_0 .

For each panel, the red lines are associated with a charge less than the critical one while the ones equal to the critical charge are depicted in black dashed lines and green lines correspond to a charge upper than the critical one. Particularly, the first-order phase transition temperature T_* and second-order phase transition temperature T_c are plotted by magenta and orange dashed line, respectively. As can be seen in all these plots, the Van der Waals-like phase structure can also be observed in the $T - \Delta S_A$ diagram. Particularly, the coexistence temperature T_* and second-order phase transition temperature T_c are exactly the same as those in the thermal entropy structure.

Adopting the same steps as in the thermal picture, we will also check numerically whether Maxwell's equal area law holds

$$A_1 = \int_{\Delta S_A^{(1)}}^{\Delta S_A^{(2)}} T(\Delta S_A, Q) d\Delta S_A - T_* (\Delta S_A^{(2)} - \Delta S_A^{(1)}) \quad (48)$$

$$A_2 = T_* (\Delta S_A^{(3)} - \Delta S_A^{(2)}) - \int_{\Delta S_A^{(2)}}^{\Delta S_A^{(3)}} T(\Delta S_A, Q) d\Delta S_A \quad (49)$$

with the quantities $\Delta S_A^{(1)}$, $\Delta S_A^{(2)}$, and $\Delta S_A^{(3)}$ being roots of the equation $T_* = T(\Delta S_A, Q)$ in ascending order. The Maxwell's equal area law stipulates that

$$A_1 = A_2. \quad (50)$$

We tabulate in Table 3 the values of the both areas A_1 and A_2 for the chosen θ_0 and the charge C as well as the relative error between A_1 and A_2 taken to be the difference between A_1 and A_2 divided by their average.

Based on Table 3, we can see that, as the pressure approaches the critical one, the relative error which translates the disagreement between Maxwell's areas decreases. We can claim that the first-order phase transition of the holographic entanglement entropy obeys Maxwell's equal area law just near the critical point and within our numerical accuracy.

The next obvious step in our investigation is the check of the critical exponent of the second-order phase transition by analyzing the slope of the relation between $\log |T - T_c|$ and $\log |\Delta S_A - \Delta S_{A_c}|$, where ΔS_{A_c} is the critical entanglement entropy found numerically by an equation $T(\Delta S_A) = T_c$. We also introduce the definition of an analog to heat capacity by writing

$$\mathcal{C}_Q = T \left. \frac{\partial (\Delta S_A)}{\partial T} \right|_Q. \quad (51)$$

Taking $\theta_0 = 0.2$ and for different charge C , we plot the relationship between $\log |T - T_c|$ and $\log |\Delta S_A - \Delta S_{A_c}|$ in Figure 5, and the analytical relation can be fitted as

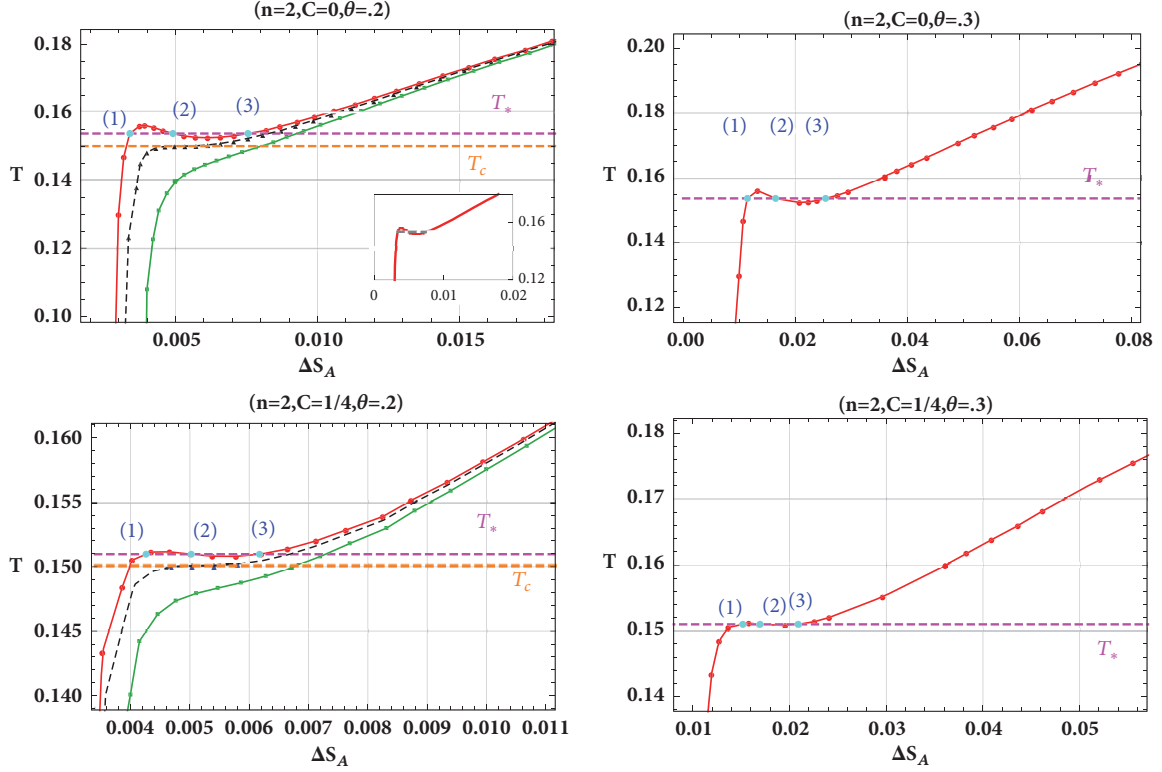


FIGURE 4: Plot of isocharges on the $(T, \Delta S_A)$ -plan, for different values of θ_0 , C . For all panels: the values of the charge are $Q = .9Q_c$ (red), $Q = Q_c$ (dashed black), and $Q = 2Q_c$ (green). The coexistence phase isotherm T_* (dashed magenta line) is obtained from the free energy (Figure 2) and the critical temperature (dashed orange line). For all curves, we also show the data points which are used to create the interpolation.

TABLE 3: Comparison of A_1 and A_2 for the EMPYM-AdS black hole using entanglement entropy.

C	$\frac{Q}{Q_c}$	θ_0	$\Delta S_A^{(1)}$	$\Delta S_A^{(2)}$	$\Delta S_A^{(3)}$	A_1	A_2	Relative error
0	0.9	0.2	0.00339417	0.00490769	0.00755095	2.271×10^{-6}	2.218×10^{-6}	2.36 %
		0.3	0.011477	0.0164978	0.0254236	6.563×10^{-6}	6.407×10^{-6}	2.4%
	0.5	0.2	0.00161291	0.0042458	0.0130777	0.00007432	0.00005560	28.81%
$\frac{1}{4}$	0.9	0.2	0.00425941	0.00502275	0.00617356	9.961×10^{-8}	1.023×10^{-7}	2.66%
		0.3	0.0151665	0.0169359	0.0208834	1.601×10^{-7}	1.631×10^{-7}	1.85%
	0.5	0.2	0.00339968	0.00496717	0.00743883	2.12718×10^{-6}	1.76781×10^{-6}	18.44%

$$\log |T - T_c| = \begin{cases} 14.2558 + 3.09904 \log |\Delta S_A - \Delta S_{A_c}| & (C = 0) \\ 2.9293 + 3.031061 \log |\Delta S_A - \Delta S_{A_c}| & \left(C = \frac{1}{4}\right) \end{cases} \quad (52)$$

The slope of (52) is around 3 indicating that the critical exponent is $-2/3$ in total concordance with that in (33); therefore the critical exponent for second-order phase transition of the holographic entanglement entropy agrees with that of the thermal entropy in the canonical ensemble [47, 50].

Now, we turn our attention to the grand canonical ensemble; we adopt the same analysis and the chosen values of the previous subsection, by writing (19) and (45) as a function of the potentials Φ_Q and Φ_c ; taking the same boundary

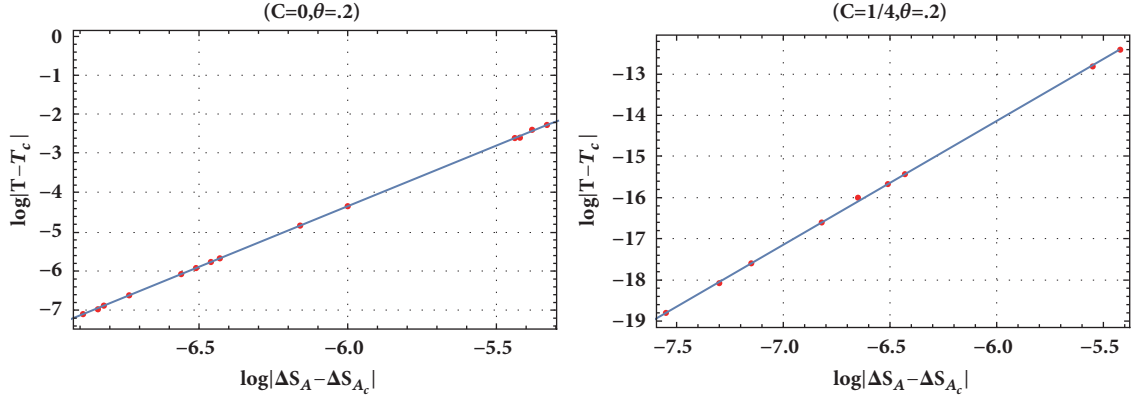
conditions (46), we perform the numerical calculations used in the plot of Hawking temperature as a function of the holographic entanglement entropy with fixed potentials in Figure 6.

Comparing Figure 3 with Figure 6, one may find that the thermal picture shares the same behavior of the holographic entanglement entropy; we can also observe the same minimum value of the temperature $T_{min} = 0.155125$. Then the holographic framework reproduces the same attitude of the $T - S$ diagram in the grand canonical ensemble.

Now, after showing that the holographic entanglement entropy shears the same phase picture as that of the thermal entropy for grand canonical and just near the critical point for the canonical ensemble since the relative disagreement between Maxwell's areas can become significantly large at low

TABLE 4: Comparison of A_1 and A_2 for the EYM-AdS black hole using two-point correlation function.

C	$\frac{Q}{Q_c}$	θ_0	$\Delta L_A^{(1)}$	$\Delta L_A^{(2)}$	$\Delta L_A^{(3)}$	A_1	A_2	relative error
0	0.9	0.2	1.34978	1.34987	1.35003	0.000287	0.000300	4.42%
		0.3	0.881705	0.881911	0.882274	0.000197	0.000208	5.43%
	0.4	0.2	1.34967	1.34983	1.35043	0.001431	0.001812	23.49%
$\frac{1}{4}$	0.9	0.2	1.34983	1.34988	1.34995	0.000142	0.000138	2.85%
		0.3	0.881822	0.881926	0.882085	0.000209	0.000216	3.29%
	0.4	0.2	1.34978	1.34987	1.35003	0.0003907	0.0004653	17.42%

FIGURE 5: The relation between $\log|T - T_c|$ and $\log|\Delta S_A - \Delta S_{A_c}|$ for different C . (Left) $C = 0$. (Right) $C \neq 0$.

pressure, we attempt in the next section to explore whether the two-point correlation function has similar behavior to that of the entanglement entropy.

3.2. Two-Point Correlation Function. According to the Anti-de-Sitter/conformal fields theory correspondence, the time two-point correlation function can be written under the saddle-point assumption and in the large limit of Δ as [55]

$$\langle \mathcal{O}(t_0, x_i) \mathcal{O}(t_0, x_j) \rangle \approx e^{-\Delta L}, \quad (53)$$

where Δ is the conformal dimension of the scalar operator \mathcal{O} in the dual field theory and the quantity L stands for the length of the bulk geodesic between the points (t_0, x_i) and (t_0, x_j) on the AdS boundary. Taking into account the symmetry of the considered black hole spacetime, we can simply use $x_i = \theta$ with the boundary θ_0 and employ it to parameterize the trajectory. In this case, the proper length can be expressed as

$$L = \int_0^{\theta_0} \mathcal{L}(r(\theta), \theta) d\theta, \quad (54)$$

$$\mathcal{L} = \sqrt{\frac{(r'(\theta))^2}{f(r(\theta))} + r(\theta)^2}, \quad \text{where } r' = \frac{dr}{d\theta}$$

Treating \mathcal{L} as Lagrangian and θ as time, one can write the equation of motion for $r(\theta)$ as

$$r'(\theta)^2 f'(r(\theta)) - 2f(r(\theta)) r''(\theta) + 2r(\theta) f(r(\theta))^2 = 0. \quad (55)$$

Recalling the boundary conditions of (46) we attempt to solve this equation by choosing the same background of the previous section, in other words the same values of the parameter θ_0 with the same UV cutoff values in the dual field theory. The regularized two-point correlation function is labeled as $\Delta L_A = L - L_0$, where L_0 denotes the geodesic length in pure AdS under the same boundary region. In Figure 7 we depict the behavior of the temperature T in function of ΔL_A ; all plots show the Van der Waals-like phase transition as in the case of the thermal and the holographic entanglement entropy portrait.

As in the case of the holographic entanglement entropy, the relevant calculated results are listed in Table 4 which are the θ_0 values, the $\Delta \mathcal{L}_{A_{1,2,3}}$, and the areas A_1 and A_2 .

The results of Table 4 tell us that under our numerical accuracy and just near the critical point Maxwell's equal area law still is verified implying that A_1 and A_2 are equal in the proximity to the critical pressure. These remarks consolidate the behavior of all panels of Figure 7. At this point, one can conclude that, like the entanglement entropy, the two-point correlation function also exhibits apparently a first-order phase transition as that of the thermal entropy. However, exploring broader ranges of the pressure has revealed the fact that the equal area law does not also hold.

For the second phase transition, we will be interested in the quantities $\log|T - T_c|$ and $\log|\Delta L_A - \Delta L_{A_c}|$ in which ΔL_{A_c} is obtained numerically by the equation $T(\Delta L_A) = T_c$. The

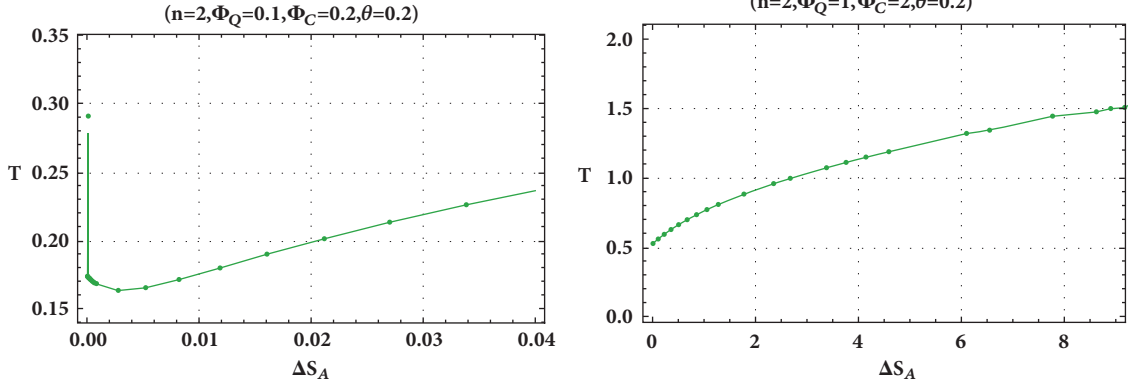


FIGURE 6: The relation between $\log |T - T_c|$ and $\log |\Delta S_A - \Delta S_{A_c}|$ for different C . (Left) ($\Phi_c = 0.1, \Phi_Q = 0.2$). (Right) ($\Phi_c = 1, \Phi_Q = 2$).

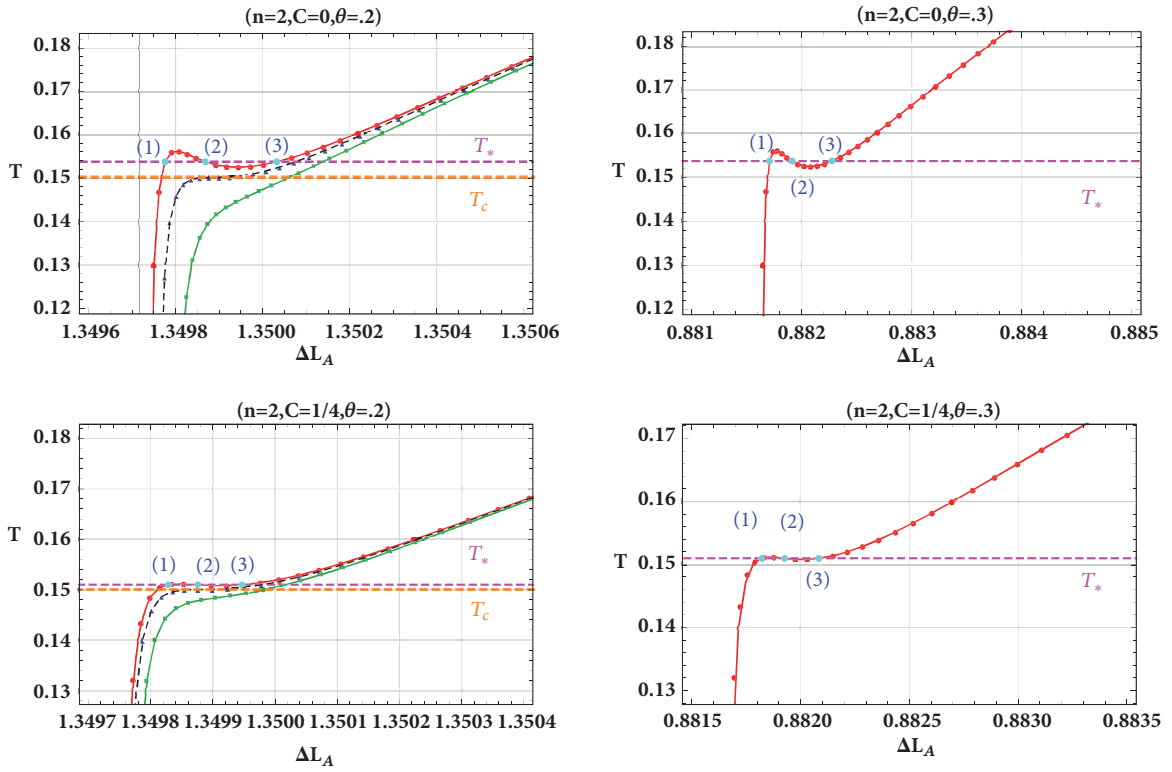


FIGURE 7: Plot of isocharges on the $(T, \Delta L_A)$ -plan, for $C = 0$ (left) and $C \neq 0$ (right). For all panels: the values of the charge are $Q = 0.9Q_c$ (red), $Q = Q_c$ (dashed black), and $Q = 2Q_c$ (green).

relations between the logarithms of $|T - T_c|$ and $|\Delta L_A - \Delta L_{A_c}|$ are shown in Figure 8

The straight blue line in each panel of Figure 8 is fitted following the linear equations

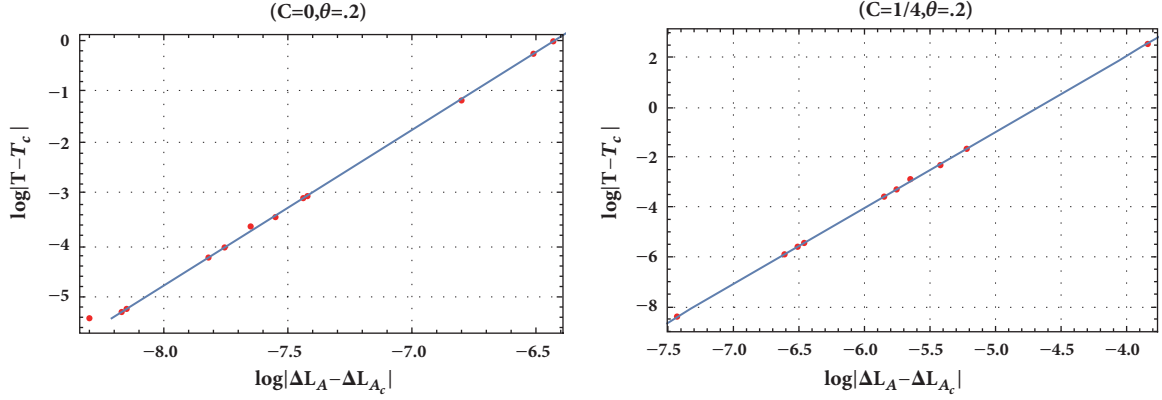
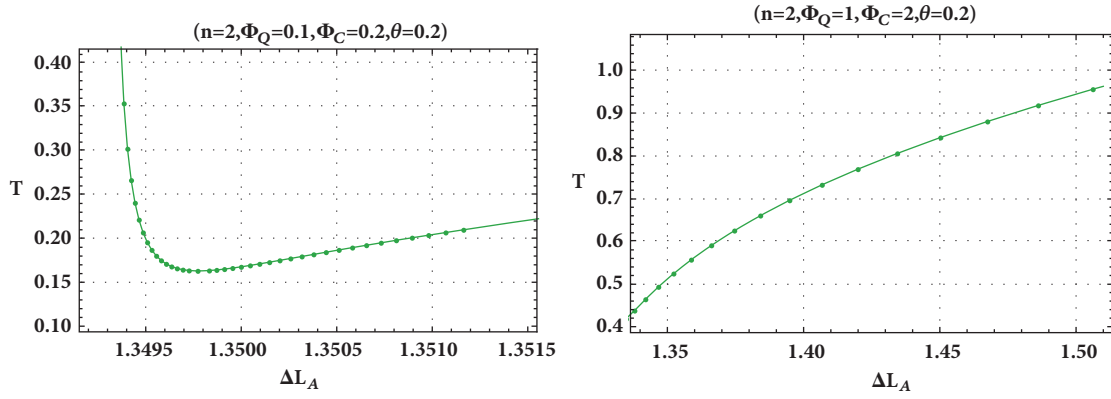
$$\log |T - T_c| = \begin{cases} 19.056 + 3.03594 \log |\Delta L_A - \Delta L_{A_c}| & (C = 0) \\ 14.25487 + 3.04967 \log |\Delta L_A - \Delta L_{A_c}| & \left(C = \frac{1}{4}\right) \end{cases} \quad (56)$$

Again, we found a slope around 3; then the critical exponent of the specific heat capacity is consistent with that of

the mean field theory of the Van der Waals as in the thermal and entanglement entropy portraits [47, 50]. Therefore, we conclude that the two-point correlation function of the Anti-de Sitter-Maxwell-Yang-Mills black hole exists in a second-order phase transition at the critical temperature T_c .

For the grand canonical ensemble, we also plot the temperature T in function of ΔL_A in Figure 9, from which we can see that thermodynamical behavior is held as the thermal and the holographic entanglement entropy frameworks.

At this level we remark that radical rupture appears when we change the thermodynamical ensemble (canonical/grand canonical). The complete comprehension of such different

FIGURE 8: The relation between $\log|T - T_c|$ and $\log|\Delta L_A - \Delta L_{A_c}|$ for different charge C .FIGURE 9: The relation between $\log|T - T_c|$ and $\log|\Delta S_A - \Delta S_{A_c}|$ for different C . (Left) $(\Phi_c = 0.1, \Phi_Q = 0.2)$. (Right) $(\Phi_c = 1, \Phi_Q = 2)$.

behaviors is not yet completely understood. We believe that it is typical of such system [41].

4. Conclusion

In this work We have investigated the phase transition of Anti-de-Sitter black hole in the Einstein-Maxwell-Yang-Mills gravity considering the canonical and the grand canonical ensemble. We first studied the phase structure of the thermal entropy in the (T, S) -plane for fixed charges and found that the phase structure agrees with the study made in [47] when the electrodynamics is linear. The authors consider the thermodynamics of such black hole in the (P, V) -plane, notably the critical behavior and the analogy with the Van der Waals gas. We also have shown that this behavior disappears in the grand canonical ensemble where the potentials Φ_Q and Φ_c are kept fixed.

Then, we found that this phase structure of the EYM-AdS black hole can be probed by the two-point correlation function and holographic entanglement entropy in each thermodynamical ensemble, which reproduce the same thermodynamical behavior of the thermal portrait just for a range of the pressure near the critical one where the equal area law holds within our numerical accuracy; for broader ranges the disagreement between Maxwell's areas becomes significant.

These remarks remain open questions while this approach provides a new step in our understanding of the black hole phase structure from the point of view of holography. Considering the high dimensional solutions or additional hairs by adding Yang-Mills fields and taking into account their confinement can be the object of a future publication.

Data Availability

The data used to support the findings of this study are available from the corresponding author upon request.

Conflicts of Interest

The author declares that they have no conflicts of interest.

References

- [1] J. Maldacena, "The large N limit of superconformal field theories and supergravity," *International Journal of Theoretical Physics*, vol. 38, no. 2, Article ID 1113, 1999, [Advances in Theoretical and Mathematical Physics, vol. 2, p. 231, 1998].
- [2] O. Aharony, S. S. Gubser, J. Maldacena, H. Ooguri, and Y. Oz, "Large N field theories, string theory and gravity," *Physics Reports*, vol. 323, no. 3-4, pp. 183–386, 2000.

- [3] A. Hashimoto and N. Itzhaki, "Non-commutative Yang-Mills and the AdS/CFT correspondence," *Physics Letters. B. Particle Physics, Nuclear Physics and Cosmology*, vol. 465, no. 1-4, pp. 142–147, 1999.
- [4] M. Faizal, A. F. Ali, and A. Nassar, "AdS/CFT correspondence beyond its supergravity approximation," *International Journal of Modern Physics A*, vol. 30, no. 30, p. 1550183, 2015.
- [5] S. A. Hartnoll, "Lectures on holographic methods for condensed matter physics," *Classical and Quantum Gravity*, vol. 26, no. 22, 224002, 61 pages, 2009.
- [6] A. Chamblin, R. Emparan, C. V. Johnson, and R. C. Myers, "Charged AdS black holes and catastrophic holography," *Physical Review D: Particles, Fields, Gravitation and Cosmology*, vol. 60, no. 6, Article ID 064018, 1999.
- [7] S. W. Hawking and D. N. Page, "Thermodynamics of black holes in anti-de Sitter space," *Communications in Mathematical Physics*, vol. 87, no. 4, pp. 577–588, 1982/83.
- [8] D. Kastor, S. Ray, and J. Traschen, "Enthalpy and the mechanics of AdS black holes," *Classical and Quantum Gravity*, vol. 26, no. 19, Article ID 195011, 16 pages, 2009.
- [9] D. Kubiznak and R. B. Mann, "P-V criticality of charged AdS black holes," *Journal of High Energy Physics*, vol. 2012, no. 7, article 033, 2012.
- [10] A. Belhaj, M. Chabab, H. E. Moumni, and M. B. Sedra, "On thermodynamics of AdS black holes in arbitrary dimensions," *Chinese Physics Letters*, vol. 29, no. 10, Article ID 100401, 2012.
- [11] A. Belhaj, M. Chabab, H. El Moumni, K. Masmar, M. B. Sedra, and A. Segui, "On heat properties of AdS black holes in higher dimensions," *Journal of High Energy Physics*, vol. 2015, no. 5, Article ID 149, 2015.
- [12] M. Chabab, H. El Moumni, and K. Masmar, "On thermodynamics of charged AdS black holes in extended phases space via M2-branes background," *The European Physical Journal C*, vol. 76, no. 6, Article ID 304, 2016.
- [13] M. Chabab, H. El Moumni, S. Iraoui, K. Masmar, and S. Zhizeh, "Chaos in charged AdS black hole extended phase space," *Physics Letters B*, vol. 781, pp. 316–321, 2018.
- [14] G.-M. Deng, J. Fan, X. Li, and Y.-C. Huang, "Thermodynamics and phase transition of charged AdS black holes with a global monopole," *International Journal of Modern Physics A*, vol. 33, no. 3, Article ID 1850022, 2018.
- [15] S. H. Hendi, A. Sheykhi, and M. H. Dehghani, "Thermodynamics of higher dimensional topological charged AdS black branes in dilaton gravity," *The European Physical Journal C*, vol. 70, no. 3, pp. 703–712, 2010.
- [16] Al Övgün I, " $P - v$ criticality of a specific black hole in $f(R)$ gravity coupled with Yang-Mills field," *Advances in High Energy Physics*, vol. 2018, Article ID 8153721, 7 pages, 2018.
- [17] J.-X. Mo, G.-Q. Li, and X.-B. Xu, "Combined effects of $f(R)$ gravity and conformally invariant Maxwell field on the extended phase space thermodynamics of higher-dimensional black holes," *The European Physical Journal C*, vol. 76, no. 10, article no. 545, 2016.
- [18] S. H. Hendi, S. Panahiyan, and B. Eslam Panah, "Extended phase space of black holes in Lovelock gravity with nonlinear electrodynamics," *PTEP. Progress of Theoretical and Experimental Physics*, no. 10, 103E01, 17 pages, 2015.
- [19] M. H. Dehghani, S. H. Hendi, A. Sheykhi, and H. R. Sedehi, "Thermodynamics of rotating black branes in $(n+1)$ -dimensional Einstein-Born-Infeld-dilaton gravity," *Journal of Cosmology and Astroparticle Physics*, vol. 2007, no. 2, article 020, 2007.
- [20] H. E. Moumni, "Phase Transition of AdS Black Holes with Non Linear Source in the Holographic Framework," *International Journal of Theoretical Physics*, vol. 56, no. 2, pp. 554–565, 2017.
- [21] H.-L. Li, S.-Z. Yang, and X.-T. Zu, "Holographic research on phase transitions for a five dimensional AdS black hole with conformally coupled scalar hair," *Physics Letters B*, vol. 764, pp. 310–317, 2017.
- [22] Y. Sun, H. Xu, and L. Zhao, "Thermodynamics and holographic entanglement entropy for spherical black holes in 5D Gauss-Bonnet gravity," *Journal of High Energy Physics*, vol. 2016, no. 9, Article ID 060, 2016.
- [23] S. He, L. F. Li, and X. X. Zeng, "Holographic van der waals-like phase transition in the Gauss–Bonnet gravity," *Nuclear Physics B*, vol. 915, pp. 243–261, 2017.
- [24] J.-X. Mo, G.-Q. Li, Z.-T. Lin, and X.-X. Zeng, "Revisiting van der Waals like behavior of $f(R)$ AdS black holes via the two point correlation function," *Nuclear Physics. B. Theoretical, Phenomenological, and Experimental High Energy Physics. Quantum Field Theory and Statistical Systems*, vol. 918, pp. 11–22, 2017.
- [25] C. V. Johnson, "Large N phase transitions, finite volume, and entanglement entropy," *Journal of High Energy Physics*, vol. 2014, article 47, 2014.
- [26] E. Caceres, P. H. Nguyen, and J. F. Pedraza, "Holographic entanglement entropy and the extended phase structure of STU black holes," *Journal of High Energy Physics*, vol. 2015, no. 9, article no. 184, 2015.
- [27] P. H. Nguyen, "An equal area law for holographic entanglement entropy of the AdS-RN black hole," *Journal of High Energy Physics*, vol. 2015, article 139, 2015.
- [28] X. X. Zeng and L. F. Li, "Van der waals phase transition in the framework of holography," *Physics Letters B*, vol. 764, pp. 100–108, 2017.
- [29] J. X. Mo, G. Q. Li, Z. T. Lin, and X. X. Zeng, "Van der Waals like behavior and equal area law of two point correlation function of $f(R)$ AdS black holes," *Nuclear Physics B*, vol. 918, pp. 11–22, 2017.
- [30] S. Kundu and J. F. Pedraza, "Aspects of holographic entanglement at finite temperature and chemical potential," *Journal of High Energy Physics*, vol. 2008, no. 8, Article ID 177, 2016.
- [31] H. El Moumni, "Revisiting the phase transition of AdS-Maxwell-power-YangMills black holes via AdS/CFT tools," *Physics Letters B*, vol. 776, p. 124, 2018.
- [32] E. Yaraie, H. Ghaffarnejad, and M. Farsam, "Complexity growth and shock wave geometry in AdS-Maxwell-power-Yang–Mills theory," *The European Physical Journal C*, vol. 78, no. 11, 2018.
- [33] X. X. Zeng, H. Zhang, and L. F. Li, "Phase transition of holographic entanglement entropy in massive gravity," *Physics Letters B*, vol. 756, p. 170, 2016.
- [34] J. X. Mo, "An alternative perspective to observe the critical phenomena of dilaton AdS black holes," *The European Physical Journal C*, vol. 77, p. 529, 2017.
- [35] D. Kubiznak, R. B. Mann, and M. Teo, "Black hole chemistry: thermodynamics with λ ," *Classical and Quantum Gravity*, vol. 34, no. 6, Article ID 063001, 2017.
- [36] X.-X. Zeng and L.-F. Li, "Holographic Phase Transition Probed by Nonlocal Observables," *Advances in High Energy Physics*, vol. 2016, Article ID 6153435, 13 pages, 2016.
- [37] J. Couch, W. Fischler, and P. H. Nguyen, "Noether charge, black hole volume, and complexity," *Journal of High Energy Physics*, vol. 2017, no. 3, Article ID 119, 2017.

- [38] X.-X. Zeng and Y.-W. Han, “Holographic van der Waals Phase Transition for a Hairy Black Hole,” *Advances in High Energy Physics*, vol. 2017, Article ID 2356174, 8 pages, 2017.
- [39] A. Dey, S. Mahapatra, and T. Sarkar, “Thermodynamics and entanglement entropy with Weyl corrections,” *Physical Review D: Particles, Fields, Gravitation and Cosmology*, vol. 94, no. 2, Article ID 026006, 2016.
- [40] D. Dudal and S. Mahapatra, “Interplay between the holographic QCD phase diagram and entanglement entropy,” *Journal of High Energy Physics*, vol. 2018, no. 7, Article ID 1807, 2018.
- [41] A. Belhaj and H. El Moumni, “Entanglement entropy and phase portrait of $f(R)$ -AdS black holes in the grand canonical ensemble,” *Nuclear Physics. B. Theoretical, Phenomenological, and Experimental High Energy Physics. Quantum Field Theory and Statistical Systems*, vol. 938, pp. 200–211, 2019.
- [42] G. L. Giordano and A. R. Lugo, “Holographic phase transitions from higgsed, non abelian charged black holes,” *Journal of High Energy Physics*, vol. 2015, no. 7, Article ID 172, 172 pages, 2015.
- [43] S. S. Gubser, “Breaking an Abelian gauge symmetry near a black hole horizon,” *Physical Review D: Particles, Fields, Gravitation and Cosmology*, vol. 78, no. 6, Article ID 065034, 2008.
- [44] S. S. Gubser, “Colorful horizons with charge in anti-de Sitter space,” *Physical Review Letters*, vol. 101, no. 19, 191601, 4 pages, 2008.
- [45] S. Gangopadhyay and D. Roychowdhury, “Analytic study of properties of holographic p-wave superconductors,” *Journal of High Energy Physics*, vol. 2012, no. 8, Article ID 1208, 2012.
- [46] S. Habib Mazharimousavi and M. Halilsoy, “Black Holes in Einstein-Maxwell-Yang-Mills Theory and their Gauss-Bonnet Extensions,” *Journal of Cosmology and Astroparticle Physics*, vol. 2008, no. 12, Article ID 005, 2008.
- [47] M. Zhang, Z.-Y. Yang, D.-C. Zou, W. Xu, and R.-H. Yue, “P-V criticality of AdS black hole in the Einstein-Maxwell-power-Yang-Mills gravity,” *General Relativity and Gravitation*, vol. 47, no. 2, Article ID 14, 2015.
- [48] A. B. Balakin, J. P. Lemos, and A. E. Zayats, “Regular nonminimal magnetic black holes in spacetimes with a cosmological constant,” *Physical Review D: Particles, Fields, Gravitation and Cosmology*, vol. 93, no. 2, Article ID 024008, 2016.
- [49] A. B. Balakin and A. E. Zayats, “Non-minimal Wu-Yang monopole,” *Physics Letters. B. Particle Physics, Nuclear Physics and Cosmology*, vol. 644, no. 5-6, pp. 294–298, 2007.
- [50] K. Bhattacharya, B. R. Majhi, and S. Samanta, “van der Waals criticality in AdS black holes: a phenomenological study,” *Physical Review D: Particles, Fields, Gravitation and Cosmology*, vol. 96, no. 8, 084037, 8 pages, 2017.
- [51] R. Banerjee, S. K. Modak, and D. Roychowdhury, “A unified picture of phase transition: from liquid-vapour systems to AdS black holes,” *Journal of High Energy Physics (JHEP)*, vol. 1210, p. 125, 2012.
- [52] R. Banerjee, S. Ghosh, and D. Roychowdhury, “New type of phase transition in Reissner Nordström-AdS black hole and its thermodynamic geometry,” *Physics Letters B*, vol. 696, no. 1-2, pp. 156–162, 2011.
- [53] S. Ryu and T. Takayanagi, “Holographic derivation of entanglement entropy from AdS/CFT,” *Physical Review Letters*, vol. 96, Article ID 181602, 2006.
- [54] S. Ryu and T. Takayanagi, “Aspects of holographic entanglement entropy,” *Journal of High Energy Physics*, vol. 2006, no. 8, article 045, 2006.
- [55] V. Balasubramanian and S. F. Ross, “Holographic particle detection,” *Physical Review D: Particles, Fields, Gravitation and Cosmology*, vol. 61, no. 4, Article ID 044007, 2000.

Research Article

New Phase Transition Related to the Black Hole's Topological Charge

Shan-Quan Lan , Gu-Qiang Li, Jie-Xiong Mo, and Xiao-Bao Xu

Department of Physics, Lingnan Normal University, Zhanjiang, Guangdong 524048, China

Correspondence should be addressed to Shan-Quan Lan; shanquanlan@126.com

Received 23 May 2018; Accepted 13 December 2018; Published 2 January 2019

Guest Editor: Farook Rahaman

Copyright © 2019 Shan-Quan Lan et al. This is an open access article distributed under the Creative Commons Attribution License, which permits unrestricted use, distribution, and reproduction in any medium, provided the original work is properly cited. The publication of this article was funded by SCOAP³.

The topological charge ϵ of AdS black hole is introduced by Tian et al. in their papers, where a complete thermodynamic first law is obtained. In this paper, we investigate a new phase transition related to the topological charge in Einstein-Maxwell theory. Firstly, we derive the explicit solutions corresponding to the divergence of specific heat C_ϵ and determine the phase transition critical point. Secondly, the $T - r$ curve and $T - S$ curve are investigated and they exhibit an interesting van der Waals system's behavior. Critical physical quantities are also obtained which are consistent with those derived from the specific heat analysis. Thirdly, a van der Waals system's swallow tail behavior is observed when $\epsilon > \epsilon_c$ in the $F - T$ graph. What is more, the analytic phase transition coexistence lines are obtained by using the Maxwell equal area law and free energy analysis, the results of which are consistent with each other.

1. Introduction

Black hole is a complicated object; there are Hawking radiation, entropy, phase transition, etc. Although black hole's microscopic mechanism is still not clear, its thermodynamic properties can be systematically studied as it is a thermodynamic system which is described by only few physical quantities, such as mass, charge, angular momentum, temperature, and entropy. Since the establishing of the four laws of black hole by Bardeen, Carter, and Hawking [1], black hole thermodynamics has become an exciting and extensively studied topic. Especially, in the anti-de Sitter space, there exists Hawking-Page phase transition [2] which is explained as the confinement/deconfinement phase transition of a gauge field [3] due to the AdS/CFT duality [4–6] and phase transition between small and large charged black holes which is reminiscent to the liquid-gas phase transition of van der Waals system [7]. This close relation between AdS black holes and van der Waals liquid-gas system has been further enhanced by the seminal work of Kubiznak and Mann in [8] where the cosmological constant is identified as thermodynamic pressure and the mass of the black hole is identified as the enthalpy [9]. The $P - V$ curves and the Gibbs free energy graphs in this extended phase space are shown

to exhibit an interesting van der Waals systems behavior. For a review on this topic, one can refer to [10] and the references therein. However, in this paper, we will treat the cosmological constant as a constant, leaving the other case for future investigation [11].

Generally, the thermodynamic quantities are described on the horizon and they are related by the first law. However, they can be generalised on surface out of the horizon [12–14]. This has gotten new attention with the development of AdS/CFT, since the black hole thermodynamics on holographic screen has acquired a new and interesting interpretation as a duality of the correspondence field theory [15]. In [16, 17], a maximally symmetric black hole thermodynamics on holographic screen are studied in Einstein-Maxwell's gravity and Lovelock-Maxwell theory. The author found a topological charge naturally arisen in holography. Together with all other known charges (electric charge, mass, and entropy [18]), they satisfy an extended first law and the Gibbs-Duhem-like relation as a completeness. Based on the extended first law in Einstein-Maxwell's gravity, we will investigate the black hole's possible phase transition phenomenon related to the topological charge. Actually, we found that the $T - S$ curves and the free energy graphs also exhibit an interesting van der Waals systems behavior as the extended phase space case

does. This result is unexpected, noting that the cosmological constant is not treated as thermodynamic pressure here.

This paper is organized as follows. In Section 2 we will briefly review how the extended first law is obtained in [17]. In Section 3, by analysing the specific heat, the phase transition of AdS black hole in 4-dimensional space-time is studied and the critical point is determined. Then the van der Waals like behavior of temperature is observed in both $T - r$ graph and $T - S$ graph in Section 4. In Section 5 we use the Maxwell equal area law and free energy to have obtained a consistent phase transition coexistence line. Conclusions are drawn in Section 6.

2. Review of the Topologically Charged AdS Black Holes

A d -dimensional space-time AdS black hole solution with the extra topological charge in the Einstein-Maxwell theory was investigated in [16, 17]. The metric reads

$$ds^2 = \frac{dr^2}{f(r)} - f(r) dt^2 + r^2 d\Omega_{d-2}^{(k)2}, \quad (1)$$

where

$$f(r) = k + \frac{r^2}{l^2} - \frac{m}{r^{d-3}} + \frac{q^2}{r^{2d-6}}, \quad (2)$$

$$d\Omega_{d-2}^{(k)2} = \tilde{g}_{ij}^{(k)}(x) dx^i dx^j,$$

$$A = -\frac{\sqrt{d-2}q}{\sqrt{2(d-3)r^{d-3}}} dt.$$

m, q, l are related to the ADM mass M , electric charge Q , and cosmological constant Λ by

$$M = \frac{(d-2)\Omega_{d-2}^{(k)}}{16\pi} m, \quad (3)$$

$$Q = \sqrt{2(d-2)(d-3)} \left(\frac{\Omega_{d-2}^{(k)}}{8\pi} \right) q,$$

$$\Lambda = -\frac{(d-1)(d-2)}{2l^2},$$

and $\Omega_{d-2}^{(k)}$ is the volume of the “unit” sphere, plane, or hyperbola and k stands for the spatial curvature of the black hole. Under suitable compactifications for $k \leq 0$, we assume that the volume of the unit space is a constant $\Omega_{d-2} = \Omega_{d-2}^{(k=1)}$ hereafter [16, 17].

Following [17], the first law can be obtained. Considering an equipotential surface $f(r) = c$ with fixed c , which can be rewritten as

$$f(r, k, m, q) - c = k + \frac{r^2}{l^2} - \frac{m}{r^{d-3}} + \frac{q^2}{r^{2d-6}} - c, \quad (4)$$

defining $K \equiv k - c$, we have

$$df(r, k, m, q) = \frac{\partial f}{\partial r} dr + \frac{\partial f}{\partial K} dK + \frac{\partial f}{\partial m} dm + \frac{\partial f}{\partial q} dq \quad (5)$$

$$= 0.$$

Noting

$$\begin{aligned} \partial_r f &= 4\pi T, \\ \partial_K f &= 1, \\ \partial_m f &= -\frac{1}{r^{d-3}}, \\ \partial_q f &= \frac{2q}{r^{2d-6}}, \end{aligned} \quad (6)$$

we obtain

$$dm = \frac{4\pi T}{d-2} dr^{d-2} + r^{d-3} dK + \frac{2q}{r^{d-3}} dq. \quad (7)$$

Multiplying both sides with a constant factor $(d-2)\Omega_{d-2}/16\pi$, the above equation becomes

$$dM = TdS + \frac{(d-2)\Omega_{d-2}}{16\pi} r^{d-3} dK + \Phi dq, \quad (8)$$

where $T = \partial_r f/4\pi$ is the Unruh-Verlinde temperature [12, 19], $S = (\Omega_{d-2}/4)r^{d-2}$ is the Wald-Padmanabhan entropy [18, 20], and $\Phi = \sqrt{(d-2)/2(d-3)}(q/r^{d-3})$ is the electric potential. If we introduce a new “charge” as in [16, 17]

$$\epsilon = \Omega_{d-2} K^{(d-2)/2}, \quad (9)$$

and denote its conjugate potential as $\omega = (1/8\pi)K^{(4-d)/2}r^{d-3}$, then the generalized first law is

$$dM = TdS + \omega d\epsilon + \Phi dq. \quad (10)$$

This new charge ϵ is called the last (lost) charge of a black hole, and it together with all other known charges satisfies the Gibbs-Duhem-like relation as a completeness relation [17].

3. A New Phase Transition of AdS Black Hole

From the generalized first law, we see there is a topological charge ϵ . In this section, we will investigate the phase transition of AdS black hole in $d = 4$ dimensional space-time in canonical ensemble related to the topological charge rather than the electric charge. To do so, one can observe the behavior of the specific heat at constant topological charge [21].

The Unruh-Verlinde temperature is

$$\begin{aligned} T &= \frac{f'(r)}{4\pi} = \frac{1}{4\pi r} \left(K - \frac{q^2}{r^2} + \frac{3r^2}{l^2} \right) \\ &= \frac{S\epsilon - 4\pi^2 Q^2 + 12S^2/l^2}{8\pi\Omega_2^{1/2}S^{3/2}} \end{aligned} \quad (11)$$

Setting $l = 1, Q = 1, \Omega_2 = 4\pi$ hereafter, the corresponding specific heat with topological charge ϵ fixed can be calculated as

$$\begin{aligned} C_\epsilon &= T \left(\frac{\partial S}{\partial T} \right)_\epsilon = \frac{24S^3 + 2\epsilon S^2 - 8\pi^2 S}{12S^2 - \epsilon S + 12\pi^2} \\ &= \frac{2\pi r^2 (12\pi r^4 + \epsilon r^2 - 4\pi)}{12\pi r^4 - \epsilon r^2 + 12\pi} \end{aligned} \quad (12)$$

From the denominator, we can conclude the following.

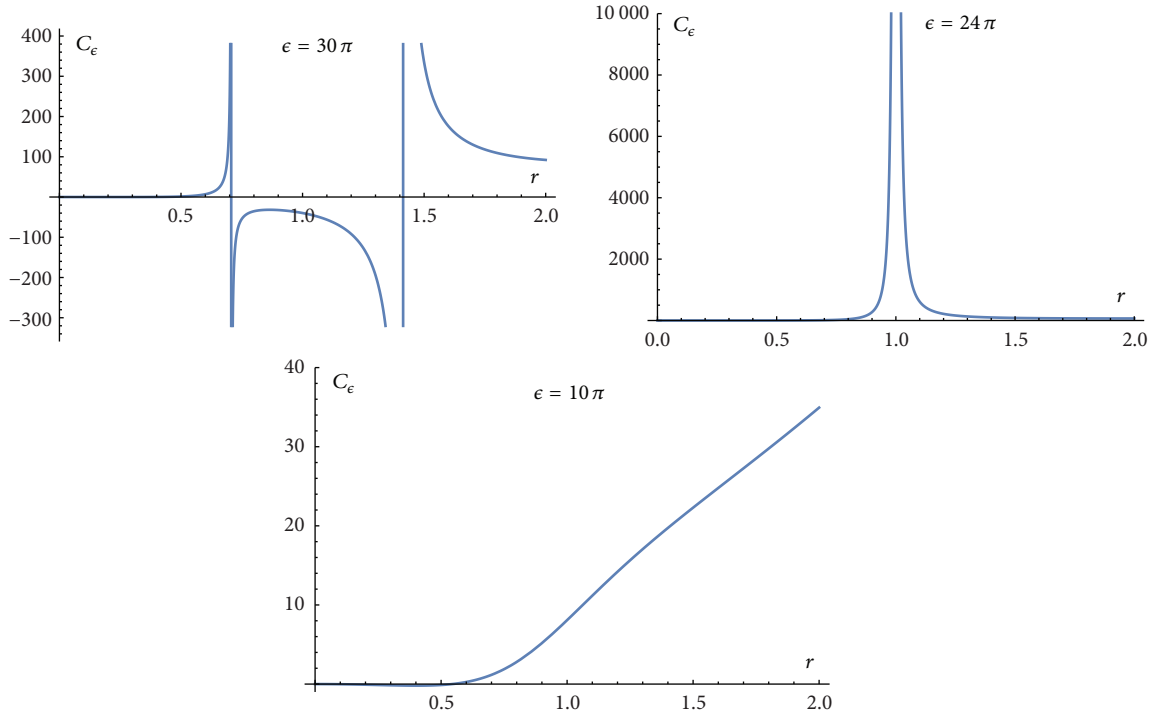


FIGURE 1: The specific heat C_ϵ versus r for $\epsilon = 30\pi > \epsilon_c$ which has two divergent points, $\epsilon = 24\pi = \epsilon_c$ which has only one divergent point, and $\epsilon = 10\pi < \epsilon_c$ which has no divergent point.

(1) When $\epsilon > 24\pi$, C_ϵ has two divergent points at

$$S_\pm = \frac{\epsilon \pm \sqrt{\epsilon^2 - (24\pi)^2}}{24}, \quad (13)$$

which corresponds to

$$r_\pm = \sqrt{\frac{\epsilon \pm \sqrt{\epsilon^2 - (24\pi)^2}}{24\pi}}. \quad (14)$$

(2) When $\epsilon = \epsilon_c = 24\pi$, C_ϵ has only one divergent point at

$$S = S_c = \pi, \quad (15)$$

which corresponds to

$$r = r_c = 1. \quad (16)$$

The temperature is $T_c = 2/\pi$.

(3) When $\epsilon < 24\pi$, $C_\epsilon > 0$.

Figure 1 shows the behavior of specific heat for the cases $\epsilon > \epsilon_c$, $\epsilon = \epsilon_c$, $\epsilon < \epsilon_c$. For $\epsilon > \epsilon_c$, there are two divergent points on the specific heat curve; they divide the region into three parts: the large radius region, the medium radius region, and the small radius region. With positive specific heat, both the large radius region and the small radius region are thermodynamically stable. While with negative specific heat, the medium radius region is unstable. So there is a phase transition taking place between small black hole and large black hole. For $\epsilon = \epsilon_c$, the curve of specific heat has only one divergent point and is always positive which denote that ϵ_c

is the phase transition critical point. While, for $\epsilon < \epsilon_c$, the curve of specific heat has no divergent point and is always positive, which denote that the black holes are stable and no phase transition will take place.

4. Van der Waals Like Behavior of Temperature

It was shown in [8] that when the cosmological constant is identified as thermodynamic pressure [9], P - v graph exhibits van der Waals like behavior. Since this pioneering work, this universal property is discovered in various black holes [22–45]. Here, we find that, for different topological charges, temperature of AdS black holes also possess the interesting van der Waals like property.

In $T - r$ curve, the possible critical point can be obtained by

$$\begin{aligned} \left(\frac{\partial T}{\partial r} \right)_{\epsilon=\epsilon_c, r=r_c} &= 0, \\ \left(\frac{\partial^2 T}{\partial r^2} \right)_{\epsilon=\epsilon_c, r=r_c} &= 0. \end{aligned} \quad (17)$$

Solving the above equations, one can obtain

$$\begin{aligned} \epsilon_c &= 24\pi, \\ r_c &= 1, \end{aligned} \quad (18)$$

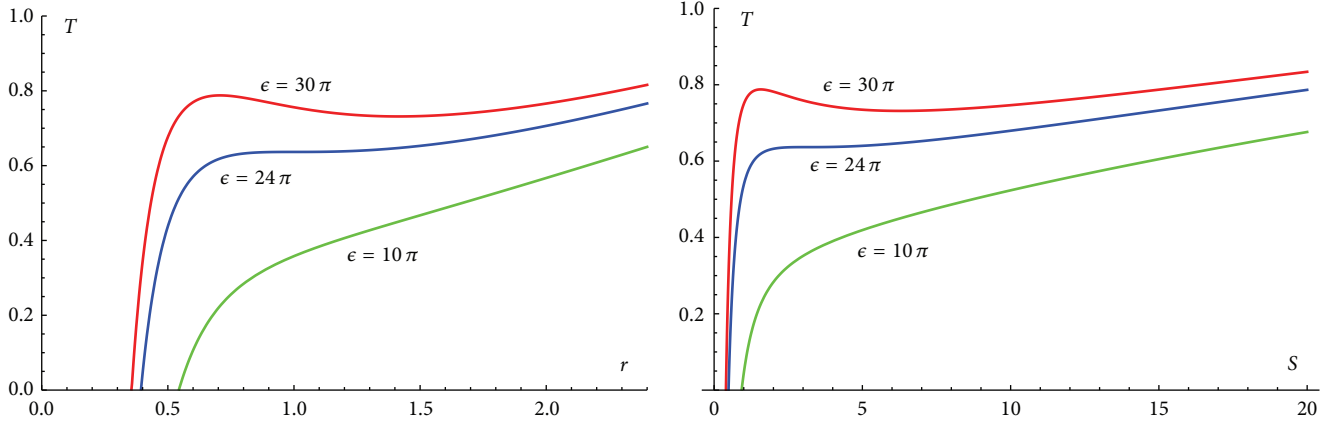


FIGURE 2: T versus r (left graph) and T versus S (right graph) for different topological charge ϵ . There is an oscillating behavior when $\epsilon > \epsilon_c = 24\pi$ for both $T(r)$ and $T(S)$ which is reminiscent of the van der Waals phase transition behavior.

which are exactly the same critical point we obtained by analysing the divergent behavior of specific heat.

In $T - S$ curve, the possible critical point can be obtained by

$$\begin{aligned} \left(\frac{\partial T}{\partial S} \right)_{\epsilon=\epsilon_c, S=S_c} &= 0, \\ \left(\frac{\partial^2 T}{\partial S^2} \right)_{\epsilon=\epsilon_c, S=S_c} &= 0. \end{aligned} \quad (19)$$

Solving the above equations, one can obtain

$$\begin{aligned} \epsilon_c &= 24\pi, \\ S_c &= \pi, \end{aligned} \quad (20)$$

which are also exactly the same critical point we obtained by analysing the divergent behavior of specific heat. As the entropy S is proportional to r^2 , the $T - r$ behavior will be similar to the $T - S$ behavior. However r and S are different physical quantities, so we show the $T - r$ graph and $T - S$ graph in the same figure to demonstrate their minor differences.

Figure 2 shows the temperature behavior as a function of r or S for different values of topological charge ϵ . When $\epsilon > \epsilon_c$, the curve can be divided into three branches. The slopes of the large radius branch and the small radius branch are both positive, while the slope of the medium radius branch is negative. When $\epsilon < \epsilon_c$, the temperature increases monotonically as r or S increases. This phenomenon is analogous to that of the van der Waals liquid-gas system.

From above, one can find that, by analysing the specific heat curves, the $T - r$ curves, and the $T - S$ curves, the critical points are obtained and they are consistent with each other. In the above section, we have shown that both the large radius branch and the small radius branch are stable with positive specific heat, while the medium radius branch is unstable with negative specific heat. As argued in [25], one can use the Maxwell equal area law to remove the unstable branch in $T - S$ curve with a bar vertical to the temperature axis $T = T^*$ and obtain the phase transition point (T^*, ϵ) . In the next

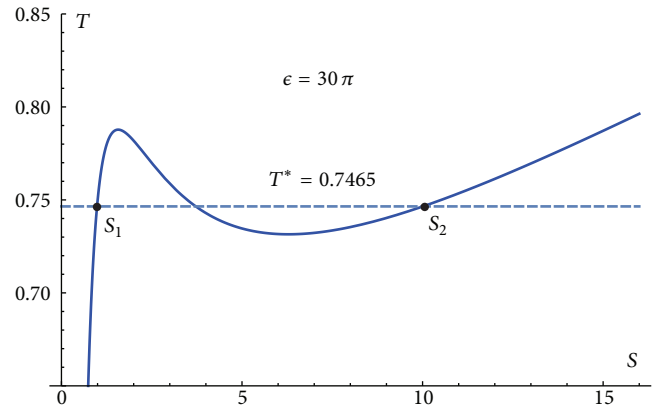


FIGURE 3: T versus S at $\epsilon = 30\pi > \epsilon_c$. The dashed line $T = 0.7465$ equally separates the oscillating part. According to the Maxwell's equal area law, the phase transition point is $(T = 0.7465, \epsilon = 30\pi)$.

section, we will use the Maxwell equal area law and analyse the free energy to determine the phase transition coexistence line.

5. Maxwell Equal Area Law, Free Energy, and Phase Diagram

In Figure 3, for fixed topological charge $\epsilon > \epsilon_c$, temperature $T(S, \epsilon)$ curve shows an oscillating behavior which denotes a phase transition. The oscillating part needs to be replaced by an isobar (denote as T^*) such that the areas above and below it are equal to each other. This treatment is called Maxwell's equal area law. In what follows, we will analytically determine this isobar T^* for fixed ϵ [25, 26].

Maxwell's equal area law is manifested as

$$\begin{aligned} T^* (S_2 - S_1) &= \int_{S_1}^{S_2} T(S, \epsilon) dS = \frac{1}{8\pi^{3/2}} (4S_2^{3/2} + \epsilon S_2^{1/2} \\ &\quad + 4\pi^2 S_2^{-1/2} - 4S_1^{3/2} - \epsilon S_1^{1/2} + 4\pi^2 S_1^{-1/2}). \end{aligned} \quad (21)$$

At points (S_1, T^*) , (S_2, T^*) , we have two equations:

$$T^* = T(S_1, \epsilon)$$

$$= \frac{1}{16\pi^{3/2}} (12S_1^{1/2} + \epsilon S_1^{-1/2} - 4\pi^2 S_1^{-3/2}),$$

$$T^* = T(S_2, \epsilon)$$

$$= \frac{1}{16\pi^{3/2}} (12S_2^{1/2} + \epsilon S_2^{-1/2} - 4\pi^2 S_2^{-3/2}).$$

(22)

The above three equations can be solved as

$$S_1 = \frac{\epsilon - 16\pi - \sqrt{(\epsilon - 16\pi)^2 - 64\pi^2}}{8},$$

$$S_2 = \frac{\epsilon - 16\pi + \sqrt{(\epsilon - 16\pi)^2 - 64\pi^2}}{8},$$

(23)

$$T^* = \frac{\epsilon^2 - \epsilon\sqrt{\epsilon^2 - 32\pi\epsilon + 192\pi^2} - 28\pi\epsilon + 12\pi\sqrt{\epsilon^2 - 32\pi\epsilon + 192\pi^2} + 160\pi^2}{\sqrt{2}\pi^{3/2}(\epsilon - 16\pi - \sqrt{\epsilon^2 - 32\pi\epsilon + 192\pi^2})^{3/2}}.$$

The last equation $T^*(\epsilon)$ is the phase transition curve we are looking for.

To double-check the phase transition curve obtained by Maxwell's equal area law, we will probe the behavior of free energy, which is derived as

$$F = M - TS = \frac{12\pi^2 + \epsilon S - 4S^2}{16\pi^{3/2}\sqrt{S}}. \quad (24)$$

Since temperature is also a function of S and ϵ , we can plot F versus T in Figure 4. When $\epsilon > 24\pi = \epsilon_c$, $F - T$ curve shows a swallow tail behavior which is reminiscent of $G - T$ curve for the van der Waals system. In this sense, the free energy here should be regarded as Gibbs free energy, and the inner energy M should be regarded as enthalpy. Anyway, the cross point is determined by the equations below.

$$T^* = T(S_1, \epsilon) = T(S_2, \epsilon),$$

$$F^* = F(S_1, \epsilon) = F(S_2, \epsilon).$$

(25)

The right side equations can be rewritten as

$$\frac{1}{16\pi^{3/2}} (12S_1^{1/2} + \epsilon S_1^{-1/2} - 4\pi^2 S_1^{-3/2})$$

$$= \frac{1}{16\pi^{3/2}} (12S_2^{1/2} + \epsilon S_2^{-1/2} - 4\pi^2 S_2^{-3/2}),$$

(26)

$$\frac{1}{16\pi^{3/2}} (12\pi^2 S_1^{-1/2} + \epsilon S_1^{1/2} - 4S_1^{3/2})$$

$$= \frac{1}{16\pi^{3/2}} (12\pi^2 S_2^{-1/2} + \epsilon S_2^{1/2} - 4S_2^{3/2}).$$

These equations can be solved as

$$S_1 = \frac{\epsilon - 16\pi - \sqrt{(\epsilon - 16\pi)^2 - 64\pi^2}}{8},$$

$$S_2 = \frac{\epsilon - 16\pi + \sqrt{(\epsilon - 16\pi)^2 - 64\pi^2}}{8},$$

(27)

$$F^* = \frac{\epsilon - \sqrt{\epsilon^2 - 32\pi\epsilon + 192\pi^2} - 8\pi}{2\sqrt{2}\pi\sqrt{\epsilon - 16\pi - \sqrt{\epsilon^2 - 32\pi\epsilon + 192\pi^2}}},$$

$$T^* = \frac{\epsilon^2 - \epsilon\sqrt{\epsilon^2 - 32\pi\epsilon + 192\pi^2} - 28\pi\epsilon + 12\pi\sqrt{\epsilon^2 - 32\pi\epsilon + 192\pi^2} + 160\pi^2}{\sqrt{2}\pi^{3/2}(\epsilon - 16\pi - \sqrt{\epsilon^2 - 32\pi\epsilon + 192\pi^2})^{3/2}}.$$

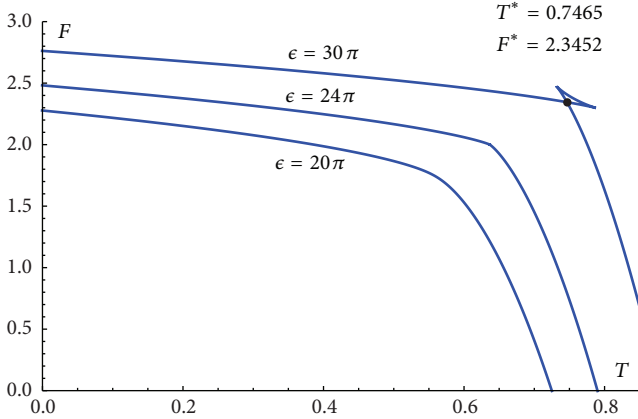


FIGURE 4: F versus T for different topological charge ϵ . When $\epsilon > 24\pi = \epsilon_c$, the curve shows a swallow tail behavior.

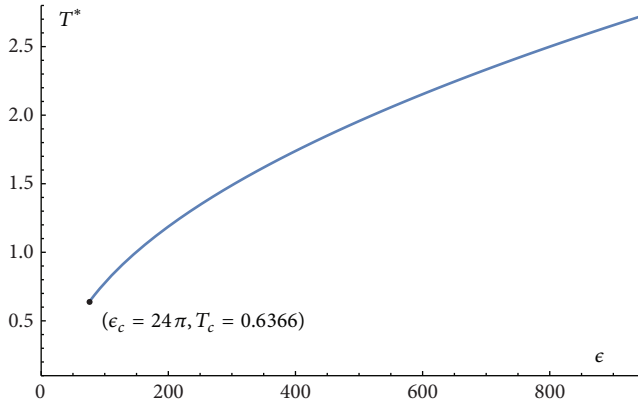


FIGURE 5: The phase transition coexistence line $T^* - \epsilon$ for fixed electric charge $Q = 1$ and AdS radius $l = 1$.

They are consistent with the results obtained by Maxwell's equal area law.

Finally, we can show the phase transition coexistence line in Figure 5 for fixed electric charge Q and AdS radius l . This kind of phase transition is special, as the critical point is at the small value of (T^*, ϵ) in phase diagram.

6. Conclusion

In this paper, the phase transition phenomenon of Reissner-Nordström AdS black holes relating to the topological charge ϵ in canonical ensemble in 4-dimensional space-time are studied. As we are interested in the effects of the topological charge, so the electric charge is fixed $Q = 1$. Firstly, the black hole's specific heat C_ϵ is calculated and the corresponding divergence solutions are derived. The two solutions merge into one denoting the critical point where $\epsilon_c = 24\pi$, $r_c = 1$. When $\epsilon > \epsilon_c$, the curve of specific heat has two divergent points and is divided into three regions. The specific heat is positive for both the large radius region and the small radius region which are thermodynamically stable, while it is negative for the medium radius region which is unstable.

When $\epsilon < \epsilon_c$, the specific heat is always positive implying the black holes are stable and no phase transition will take place.

Secondly, the behavior of temperature in both the $T - r$ graph and $T - S$ graph is studied. They exhibit the interesting van de Waals gas-liquid system's behavior. The critical points correspond to the inflection points of $T - r$ curve and $T - S$ curve, and they are consistent with that derived from the specific heat analysis. When $\epsilon > \epsilon_c$, the curves can be divided into three regions. The slopes of the large radius regions and the small radius regions are positive while those of the medium radius region are negative. When $\epsilon < \epsilon_c$, the temperature increase monotonically.

Thirdly, a van der Waals system's swallow tail behavior is observed when $\epsilon > \epsilon_c$ in the $F - T$ graph. What is more, by using the Maxwell's equal area law and analysing the free energy, the analytic phase transition coexistence lines are obtained, and they are consistent with each other.

From the above detailed study, one can find that this van der Waals like system exhibits phase transition of special property. The phase transition take place at large topological charge $\epsilon > \epsilon_c$ and high temperature which can be clearly seen from the phase transition coexistence line in Figure 5. Whether this phase transition property is universal in other gravity theories (such as the Lovelock, Gauss-Bonnet theory) and different dimensional space-time is unknown.

There are some other interesting topics that are worth investigating, such as the holographic duality in the field theory of this kind of phase transition; the cases of space-time dimension $d > 4$, as the topological charge's conjugate potential $\omega = (1/8\pi)K^{(4-d)/2}r^{d-3}$ decayed to $1/8\pi r$ which is irrelevant to K at $d = 4$ dimensional space-time, the black hole thermodynamics in the extended phase space where the cosmological constant is identified as thermodynamic pressure and the spatial curvature of black hole is treated as topological charge.

Data Availability

No data were used to support this study.

Conflicts of Interest

The authors declare that they have no conflicts of interest.

Acknowledgments

This research is in part supported by National Natural Science Foundation of China (Grant nos. 11605082, 11747017), Natural Science Foundation of Guangdong Province, China (Grant nos. 2016A030310363, 2016A030307051, and 2015A030313789), and Department of Education of Guangdong Province, China (Grant nos. 2017KQNCX124, 2017KZDXM056).

References

- [1] J. M. Bardeen, B. Carter, and S. W. Hawking, "The four laws of black hole mechanics," *Communications in Mathematical Physics*, vol. 31, pp. 161–170, 1973.

- [2] S. W. Hawking and D. N. Page, "Thermodynamics of black holes in anti-de Sitter space," *Communications in Mathematical Physics*, vol. 87, no. 4, pp. 577–588, 1982/83.
- [3] E. Witten, "Anti-de Sitter space, thermal phase transition, and confinement in gauge theories," *Advances in Theoretical and Mathematical Physics*, vol. 2, no. 3, pp. 505–532, 1998.
- [4] J. Maldacena, "The large N limit of superconformal field theories and supergravity," *Advances in Theoretical and Mathematical Physics*, vol. 2, no. 2, pp. 231–252, 1998.
- [5] S. S. Gubser, I. R. Klebanov, and A. M. Polyakov, "Gauge theory correlators from non-critical string theory," *Physics Letters B*, vol. 428, no. 1-2, pp. 105–114, 1998.
- [6] E. Witten, "Anti de Sitter space and holography," *Advances in Theoretical and Mathematical Physics*, vol. 2, no. 2, pp. 253–291, 1998.
- [7] A. Chamblin, R. Emparan, C. V. Johnson, and R. C. Myers, "Holography, thermodynamics, and fluctuations of charged AdS black holes," *Physical Review D: Particles, Fields, Gravitation and Cosmology*, vol. 60, no. 10, Article ID 104026, 1999.
- [8] D. Kubiznak and R. B. Mann, "P-V criticality of charged AdS black holes," *Journal of High Energy Physics*, vol. 2012, no. 7, article 033, 2012.
- [9] D. Kastor, S. Ray, and J. Traschen, "Enthalpy and the mechanics of AdS black holes," *Classical and Quantum Gravity*, vol. 26, no. 19, Article ID 195011, 16 pages, 2009.
- [10] D. Kubiznak, R. B. Mann, and M. Teo, "Black hole chemistry: thermodynamics with λ ," *Classical and Quantum Gravity*, vol. 34, no. 6, Article ID 063001, 2017.
- [11] S. Lan, "Phase Transition of RN-AdS Black Hole with Fixed Electric Charge and Topological Charge," *Advances in High Energy Physics*, vol. 2018, Article ID 4350287, 10 pages, 2018.
- [12] Y.-X. Chen and J.-L. Li, "First law of thermodynamics on holographic screens in entropic force frame," *Physics Letters. B. Particle Physics, Nuclear Physics and Cosmology*, vol. 700, no. 5, pp. 380–384, 2011.
- [13] J. D. Brown and J. W. York Jr., "Quasilocal energy and conserved charges derived from the gravitational action," *Physical Review D: Particles, Fields, Gravitation and Cosmology*, vol. 47, no. 4, pp. 1407–1419, 1993.
- [14] J. D. Brown and J. York, "Microcanonical functional integral for the gravitational field," *Physical Review D: Particles, Fields, Gravitation and Cosmology*, vol. 47, no. 4, pp. 1420–1431, 1993.
- [15] I. Bredberg, C. Keeler, V. Lysov, and A. Strominger, "From Navier-Stokes to Einstein," *Journal of High Energy Physics*, vol. 7, article 146, 2012.
- [16] Y. Tian, X.-N. Wu, and H. Zhang, "Holographic entropy production," *Journal of High Energy Physics*, no. 10, article no. 170, 2014.
- [17] Y. Tian, "The last (lost) charge of a black hole," 2018, <https://arxiv.org/abs/1804.00249>.
- [18] R. M. Wald, "Black hole entropy is the Noether charge," *Physical Review D: Particles, Fields, Gravitation and Cosmology*, vol. 48, no. 8, pp. R3427–R3431, 1993.
- [19] Y. Tian and X. Wu, "Dynamics of gravity as thermodynamics on the spherical holographic screen," *Physical Review D: Particles, Fields, Gravitation and Cosmology*, vol. 83, no. 2, Article ID 021501, 2011.
- [20] T. Padmanabhan, "Surface density of spacetime degrees of freedom from equipartition law in theories of gravity," *Physical Review D: Particles, Fields, Gravitation and Cosmology*, vol. 81, no. 12, Article ID 124040, 2010.
- [21] J.-X. Mo, G.-Q. Li, and Y.-C. Wu, "A consistent and unified picture for critical phenomena of $f(R)$ AdS black holes," *Journal of Cosmology and Astroparticle Physics*, vol. 1604, article 045, 2016.
- [22] S. H. Hendi, R. B. Mann, S. Panahiyan, and B. Eslam Panah, "Van der Waals like behavior of topological AdS black holes in massive gravity," *Physical Review D: Particles, Fields, Gravitation and Cosmology*, vol. 95, no. 2, Article ID 021501, 2017.
- [23] S. H. Hendi, B. Eslam Panah, and S. Panahiyan, "Topological charged black holes in massive gravity's rainbow and their thermodynamical analysis through various approaches," *Physics Letters B*, vol. 769, pp. 191–201, 2017.
- [24] S. H. Hendi, S. Panahiyan, and B. Eslam Panah, "Extended phase space of black holes in Lovelock gravity with nonlinear electrodynamics," *PTEP. Progress of Theoretical and Experimental Physics*, no. 10, 103E01, 17 pages, 2015.
- [25] E. Spallucci and A. Smailagic, "Maxwell's equal-area law for charged Anti-de Sitter black holes," *Physics Letters B*, vol. 723, no. 4-5, pp. 436–441, 2013.
- [26] S.-Q. Lan, J.-X. Mo, and W.-B. Liu, "A note on Maxwell's equal area law for black hole phase transition," *The European Physical Journal C*, vol. 75, no. 9, article 419, 2015.
- [27] M.-S. Ma and R.-H. Wang, "Peculiar P-V criticality of topological Horava-Lifshitz black holes," *Physical Review D: Particles, Fields, Gravitation and Cosmology*, vol. 96, no. 2, article no. 024052, 2017.
- [28] S. W. Wei, B. Liang, and Y. Liu, "Critical phenomena and chemical potential of a charged AdS black hole," *Physical Review D: Particles, Fields, Gravitation and Cosmology*, vol. 96, no. 12, article no. 124018, 2017.
- [29] K. Bhattacharya and B. R. Majhi, "Thermogeometric description of the van der Waals like phase transition in AdS black holes," *Physical Review D: Particles, Fields, Gravitation and Cosmology*, vol. 95, no. 10, article no. 104024, 2017.
- [30] S. H. Hendi, B. E. Panah, S. Panahiyan, and M. S. Talezadeh, "Geometrical thermodynamics and P-V criticality of the black holes with power-law Maxwell field," *The European Physical Journal C*, vol. 77, no. 2, article no. 133, 2017.
- [31] X. Kuang and O. Miskovic, "Thermal phase transitions of dimensionally continued AdS black holes," *Physical Review D: Particles, Fields, Gravitation and Cosmology*, vol. 95, no. 4, Article ID 046009, 2017.
- [32] S. Fernando, "P-V criticality in AdS black holes of massive gravity," *Physical Review D: Particles, Fields, Gravitation and Cosmology*, vol. 94, no. 12, Article ID 124049, 2016.
- [33] B. R. Majhi and S. Samanta, "P-V criticality of AdS black holes in a general framework," *Physics Letters. B. Particle Physics, Nuclear Physics and Cosmology*, vol. 773, pp. 203–207, 2017.
- [34] S. He, L. F. Li, and X. X. Zeng, "Holographic Van der Waals-like phase transition in the Gauss-Bonnet gravity," *Nuclear Physics B*, vol. 915, pp. 243–261, 2017.
- [35] J. Sadeghi, B. Pourhassan, and M. Rostami, "P-V criticality of logarithm-corrected dyonic charged AdS black holes," *Physical Review D: Particles, Fields, Gravitation and Cosmology*, vol. 94, no. 6, Article ID 064006, 2016.
- [36] X. X. Zeng and L. F. Li, "Van der waals phase transition in the framework of holography," *Physics Letters B*, vol. 764, pp. 100–108, 2017.
- [37] P. H. Nguyen, "An equal area law for holographic entanglement entropy of the AdS-RN black hole," *Journal of High Energy Physics*, vol. 2015, article 139, 2015.

- [38] J. Xu, L.-M. Cao, and Y.-P. Hu, "P-V criticality in the extended phase space of black holes in massive gravity," *Physical Review D: Particles, Fields, Gravitation and Cosmology*, vol. 91, no. 12, Article ID 124033, 2015.
- [39] Z.-Y. Nie and H. Zeng, "P-T phase diagram of a holographic s+p model from Gauss-Bonnet gravity," *Journal of High Energy Physics*, no. 10, article no. 047, 2015.
- [40] L. C. Zhang, H. H. Zhao, R. Zhao, and M. S. Ma, "Equal Area Laws and Latent Heat for d-Dimensional RN-AdS Black Hole," *Advances in High Energy Physics*, vol. 2014, Article ID 816728, 7 pages, 2014.
- [41] A. Belhaj, M. Chabab, H. El Moumni, K. Masmar, and M. B. Sedra, "Maxwell's equal-area law for Gauss-Bonnet-Anti-de Sitter black holes," *The European Physical Journal C*, vol. 75, article 71, 2015.
- [42] M. H. Dehghani, S. Kamrani, and A. Sheykhi, "P-V criticality of charged dilatonic black holes," *Physical Review D: Particles, Fields, Gravitation and Cosmology*, vol. 90, no. 10, Article ID 104020, 2014.
- [43] J.-X. Mo and W.-B. Liu, "Ehrenfest scheme for P - V criticality in the extended phase space of black holes," *Physics Letters B*, vol. 727, no. 1-3, pp. 336-339, 2013.
- [44] R.-G. Cai, L.-M. Cao, L. Li, and R.-Q. Yang, "P-V criticality in the extended phase space of Gauss-Bonnet black holes in AdS space," *Journal of High Energy Physics*, vol. 2013, no. 9, article 5, 2013.
- [45] S. Chen, X. Liu, C. Liu, and J. Jing, "P-V criticality of AdS black hole in $f(R)$ gravity," *Chinese Physics Letters*, vol. 30, no. 6, Article ID 060401, 2013.

Research Article

A Covariant Canonical Quantization of General Relativity

Stuart Marongwe 

Department of Physics and Astronomy, Botswana International University of Science and Technology, P. Bag 16, Palapye, Botswana

Correspondence should be addressed to Stuart Marongwe; stuartmarongwe@gmail.com

Received 13 June 2018; Accepted 8 November 2018; Published 19 December 2018

Guest Editor: Farook Rahaman

Copyright © 2018 Stuart Marongwe. This is an open access article distributed under the Creative Commons Attribution License, which permits unrestricted use, distribution, and reproduction in any medium, provided the original work is properly cited. The publication of this article was funded by SCOAP³.

A Hamiltonian formulation of General Relativity within the context of the Nexus Paradigm of quantum gravity is presented. We show that the Ricci flow in a compact matter free manifold serves as the Hamiltonian density of the vacuum as well as a time evolution operator for the vacuum energy density. The metric tensor of GR is expressed in terms of the Bloch energy eigenstate functions of the quantum vacuum allowing an interpretation of GR in terms of the fundamental concepts of quantum mechanics.

1. Introduction

The gravitational field which is elegantly described by Einstein's field equations has so far eluded a quantum description. Much effort has been placed into formulating General Relativity (GR) in terms of Hamilton's equations since a Hamiltonian formulation of a classical field theory leads naturally to its quantization. The earliest such attempt is the ADM formalism [1], named for its authors Richard Arnowitt, Stanley Deser, and Charles W. Misner first published in 1959. This formalism starts from the assumption that space is foliated into a family of time slices Σ_t , labeled by their time coordinate t and with space coordinates on each slice given by x^k . The dynamic variables of this theory are then taken to be the metric tensor of three-dimensional spatial slices $\gamma_{ij}(t, x^k)$ and their conjugate momenta $\pi^{ij}(t, x^k)$. Using these variables it is possible to define a Hamiltonian and thereby write the equations of motion for GR in Hamilton's form. The time slices are then welded together using four Lagrange multipliers and components of a shift vector field. An extensive review of this formalism can be found in the literature notably in [2–5].

The ADM formalism was first applied by Bryce De Witt in 1967 [6] to quantize gravity which resulted in the Wheeler–De Witt equation of quantum gravity. It is a functional differential equation in which the three-dimensional spatial metrics have the form of an operator acting on a wave function. This wave function contains all of the information about

the geometry and matter content of the universe of each time slice. However, the Hamiltonian no longer determines the evolution of the system and leads to the problem of timelessness [7, 8]. Hawking rightly points out that the very act of splitting space-time into space and time destroys the spirit of GR (general covariance) and therefore not much can be gained from this approach to quantization of gravity. Perturbative covariant approaches to the problem of quantum gravity have an inherent weakness in that they depend on a fine classical background. It is therefore difficult to obtain a self-consistent quantum theory of gravity with a classical background space-time. Steven Carlip [9, 10] and Claus Kiefer [11, 12] have made excellent and extensive reviews of the problems faced by current approaches to the problem of quantum gravity. Carlip [9] in particular singles out the lack of a firm conceptual understanding of the foundational concepts of quantum gravity as the source of much of the difficulty in understanding quantum gravity. These deep conceptual issues result in technical problems in the attempt to develop a consistent quantum theory of gravity.

In this paper we report a successful covariant canonical quantization of the gravitational field which preserves the success of GR while simultaneously explaining Dark Energy (DE) and Dark Matter (DM). This approach to quantization takes place in 4-space of metric signature $(-1,1,1,1)$ in which the quanta are excitations of the quantum vacuum called Nexus gravitons. Though the Nexus Paradigm has been introduced in the following papers [13–15], the aim of this

study is to explicitly express the Hamiltonian formulation of the theory using the Bloch eigenstate functions of the quantum vacuum. These wave functions contain information about the energy state of the quantum vacuum which in turn dictates the geometry of space-time.

2. Methods

Our first step towards a covariant canonical quantization begins with defining a quantized space-time and its quanta. We then modify Einstein's vacuum equations to be consistent with the quantized space-time followed by the defining of Hamilton's equations of the quantized space-time. This step is then followed by the Poisson brackets which provide the bridge between classical and quantum mechanics (QM). The covariant canonical quantization procedure is carried out within the context of the Nexus Paradigm of quantum gravity.

2.1. Quantization of 4-Space and the Nexus Graviton. The primary objective of physics is the study of functional relationships amongst measurable physical quantities. In particular, a unifying paradigm of physical phenomena should reveal the functional relationship between the fundamental physical quantities of 4-space and 4-momentum. Currently GR and QM offer the best predictions of the results of measurement of physical phenomena in their respective domains using different languages. GR describes gravitation in the language of geometry and thus far, it has been difficult to apply the the language of wave functions used in QM to give it a QM description. The problem of quantum gravity is therefore to interpret GR in terms of the wavefunctions of QM. Translating the language of measurement of GR into that of QM becomes the primary objective of this present attempt to resolve the problem of quantum gravity.

Measurements in GR take place in a local patch of a Riemannian manifold. This local patch can be considered as a flat Minkowski space. The line element in Minkowski space which is the subject of measurement can be computed through the inner product of the local coordinates as

$$\begin{aligned}\Delta x^\mu \Delta x_\mu &= \Delta x^2 + \Delta y^2 + \Delta z^2 - c^2 \Delta t^2 \\ &= (A\Delta x + B\Delta y + C\Delta z + iDc\Delta t) \\ &\quad \cdot (A\Delta x + B\Delta y + C\Delta z + iDc\Delta t)\end{aligned}\quad (1)$$

On multiplying the right hand side we see that to get all the cross terms such as $\Delta x \Delta y$ to cancel out we must assume

$$\begin{aligned}AB + BA &= 0 \\ A^2 = B^2 &= \dots = 1\end{aligned}\quad (2)$$

The above conditions therefore imply that the coefficients (A, B, C, D) generate a Clifford algebra and therefore must be matrices. We rewrite these coefficients in the 4-tuple form as $(\gamma^1, \gamma^2, \gamma^3, \gamma^0)$ which may be summarized using the Minkowski metric on space-time as follows:

$$\{\gamma^\mu, \gamma^\nu\} = 2\eta^{\mu\nu} \quad (3)$$

The gammas are of course the Dirac matrices. Thus in order to satisfy (1) we can express a displacement 4-vector as

$$\Delta x^\mu = a\gamma^\mu \quad (4)$$

where a is the amplitude of a displacement vector in Minkowski space. If we consider the Hubble diameter as the maximum dimension of the local patch of space then $a = r_{HS}$ where r_{HS} is the Hubble radius. This choice of a maximum amplitude is justified from the fact that we cannot physically interact with objects beyond the Hubble 4-radius. It is important to note that the line element is the square of the amplitude of the displacement 4-vector. Thus if we are to express GR in terms of the language of QM we must make the radical assumption that the displacement vectors in Minkowski space are pulses of 4-space which can be expressed in terms of Fourier functions as follows:

$$\begin{aligned}\Delta x_n^\mu &= \frac{2r_{HS}}{n\pi} \gamma^\mu \int_{-\infty}^{\infty} \text{sinc}(kx) e^{ikx} dk \\ &= \gamma^\mu \int_{-\infty}^{\infty} a_{nk} \varphi_{(nkx)} dk\end{aligned}\quad (5)$$

$$\text{Where } \frac{2r_{HS}}{n\pi} = \sum_{k=-\infty}^{k=+\infty} a_{nk} \quad (6)$$

Here $\varphi_{(nkx)} = \text{sinc}(kx)e^{ikx}$ are Bloch energy eigenstate functions. The Bloch functions can only allow the four wave vector to assume the following quantized values:

$$k^\mu = \frac{n\pi}{r_{HS}} \quad n = \pm 1, \pm 2 \dots 10^{60} \quad (7)$$

The minimum 4-radius in Minkowski space is the Planck 4-length since it is impossible to measure this length without forming a black hole. The 10^{60} states arise from the ratio of Hubble 4-radius to the Planck 4-length. The displacement 4-vectors in each eigenstate of space-time generate an infinite Bravais 4-lattice. Also, condition (7) transforms (5) to

$$\Delta x_n^\mu = \gamma^\mu \int_{-nk_1}^{nk_1} a_{nk} \varphi_{(n,k,x)} dk \quad (8)$$

The second assumption we make is that each displacement 4-vector is associated with a conjugate pulse of four-momentum which can also be expressed as a Fourier integral

$$\begin{aligned}\Delta p_{(n)\mu} &= \frac{2np_1}{\pi} \gamma_\mu \int_{-nk_1}^{nk_1} \varphi_{(n,k,x)} dk \\ &= \gamma_\mu \int_{-nk_1}^{nk_1} c_{nk} \varphi_{(n,k,x)} dk\end{aligned}\quad (9)$$

where $p_{(1)\mu}$ is the four-momentum of the ground state.

A displacement 4-vector and its conjugate 4-momentum satisfy the Heisenberg uncertainty relation

$$\Delta x_n \Delta p_n \geq \frac{\hbar}{2} \quad (10)$$

The Uncertainty Principle plays the important role of generating a vector bundle, out of the total uncertainty space E of trivial displacement 4-vectors from which a closed compact manifold X is formed, i.e., $(\pi : E \rightarrow X)$. Each point on the manifold is associated with a vector which is along a normal to the manifold.

The wave packet described by (8) is essentially a particle of four-space. The spin of this particle can be determined from the fact that each component of the four-displacement vector transforms according to the law

$$\Delta x'^{\mu}_n = \exp\left(\frac{1}{8}\omega_{\mu\nu} [\gamma_{\mu}, \gamma_{\nu}]\right) \Delta x^{\mu}_n \quad (11)$$

where $\omega_{\mu\nu}$ is an antisymmetric 4x4 matrix parameterizing the transformation.

Therefore, each component of the 4-vector has a spin half. A summation of all the four half spins yields a total spin of 2. We give the name the Nexus graviton to this particle of 4-space since the primary objective of quantum gravity is to find the nexus between the concepts of GR and QM.

From (7) the norm squared of the 4-momentum of the n -th state graviton is

$$(\hbar)^2 k^{\mu} k_{\mu} = \frac{E_n^2}{c^2} - \frac{3(nhH_0)^2}{c^2} = 0 \quad (12)$$

where H_0 is the Hubble constant ($2.2 \times 10^{-18} \text{ s}^{-1}$) and can be expressed in terms of the cosmological constant, Λ , as

$$\Lambda_n = \frac{E_n^2}{(hc)^2} = \frac{3k_n^2}{(2\pi)^2} = n^2 \Lambda \quad (13)$$

We infer from (13) that the Nexus graviton (or displacement 4-vector) in the n -th quantum state forms a trivial vector bundle via the Uncertainty Principle which generates a compact Riemannian manifold of positive Ricci curvature that can be expressed in the form

$$G_{(nk)\mu\nu} = n^2 \Lambda g_{(n,k)\mu\nu} \quad (14)$$

where $G_{(nk)\mu\nu}$ is the Einstein tensor of space-time in the n -th state. Equation (14) depicts a contracting geodesic ball and as explained in [13–15] this is DM which is an intrinsic compactification of the elements space-time in the n -th quantum state. This compactification is a result of the superposition of several plane waves as described by (8) to form an increasingly localized wave packet as more waves are added. Similarly the converse is also true. The loss of harmonic waves expands the elements of space-time which gives rise to DE. Thus the DE arises from the emission of a ground state graviton such that (14) becomes

$$G_{(nk)\mu\nu} = (n^2 - 1) \Lambda g_{(n,k)\mu\nu} \quad (15)$$

These are Einstein's vacuum field equations in the quantized space-time. If the graviton field is perturbed by the presence of baryonic matter then (15) becomes

$$\begin{aligned} G_{(nk)\mu\nu} &= kT_{\mu\nu} + (n^2 - 1) \Lambda g_{(n,k)\mu\nu} \\ &= kT_{\mu\nu} + (n^2 - 1) k\rho_{DE} g_{(n,k)\mu\nu} \end{aligned} \quad (16)$$

where ρ_{DE} is the density of DE.

From [14] the static solution to (14) for a spherically symmetric Nexus graviton is computed as

$$ds^2 = -\left(1 - \left(\frac{2}{n^2}\right)\right) c^2 dt^2 + \left(1 - \left(\frac{2}{n^2}\right)\right)^{-1} dr^2 + r^2 (d\theta^2 + \sin^2 \theta d\phi^2) \quad (17)$$

There are no singularities in (17). At high energies, characterized by microcosmic scale wavelengths of the Nexus graviton and high values of n , space-time is flat and highly compact. This implies a continuous length contraction of the local coordinates via the addition of more waves resulting in an increase in localization. Also, from a world line perspective of a test particle, it implies that the deviation from a rectilinear trajectory due to uncertainties in its location in 4-space is small. Thus at microcosmic scales, in the realm of subatomic particles space-time is extremely flat. The world line begins to substantially deviate from a well defined rectilinear path at low energies as the uncertainties in its location are increased. That is, at low values of n , the world line becomes degenerate allowing a multiplicity of trajectories which in GR are averaged by the Ricci curvature tensor. Thus gravity is a low energy phenomenon which vanishes asymptotically at high energies.

The gravitational effects of the Nexus graviton manifest at large scales and for galaxies, these effects begin to manifest when the density of DE is equal to the density of baryonic matter as described by (16) or when the acceleration due to baryonic matter is equal and opposite to the acceleration due to the emission of the ground state graviton as described in [14]. A solution to eqn (16) from [14] in the weak field at galactic scale radii is

$$\frac{d^2 r}{dt^2} = \frac{GM(r)}{r^2} + H_0 v_n - H_0 c \quad (18)$$

Here c is the speed of light.

The first term on the right is the Newtonian gravitational acceleration, the second term is a radial acceleration due to space-time in the n -th quantum state, and the final term is acceleration due to DE. The dynamics becomes strongly non-Newtonian when

$$\frac{GM(r)}{r^2} = H_0 c = \frac{v_n^2}{r} \quad (19)$$

These are conditions in which the acceleration due to baryonic matter is annulled by that due to the DE. Under such conditions

$$r = \frac{v_n^2}{H_0 c} \quad (20)$$

Substituting for r in (19) yields

$$v_n^4 = GM(r) H_0 c \quad (21)$$

This is the Baryonic Tully–Fisher relation. The conditions permitting the DE to cancel out the acceleration due to baryonic matter leave quantum gravity as the unique source of gravity. Thus condition (19) reduces (18) to

$$\frac{d^2 r}{dt^2} = \frac{dv_n}{dt} = H_0 v_n \quad (22)$$

from which we obtain the following equations of galactic and cosmic evolution:

$$r_n = \frac{1}{H_0} e^{(H_0 t)} (GM(r) H_0 c)^{1/4} \quad (23)$$

$$v_n = e^{(H_0 t)} (GM(r) H_0 c)^{1/4} \quad (24)$$

$$a_n = H_0 e^{(H_0 t)} (GM(r) H_0 c)^{1/4} \quad (25)$$

Here r_n is the radius of curvature of space-time in the n -th quantum state (which is also the radius of the n -th state nexus graviton), v_n the radial velocity of objects embedded in that space-time, and a_n their radial acceleration within it. The amplification of the radius of curvature with time explains the existence of ultra-diffuse galaxies and the spiral shapes of most galaxies. The increase in radial velocity with time explains why early type galaxies composed of population II stars are fast rotators. Equation (25) explains late time cosmic acceleration which began once condition (19) was satisfied or equivalently from (16), when the density of baryonic matter was at the same value as that of DE. Thus condition (19) also explains the Coincidence Problem.

2.2. Canonical Transformations in the Nexus Paradigm. In classical mechanics, a system is described by n independent coordinates (q_1, q_2, \dots, q_n) together with their conjugate momenta (p_1, p_2, \dots, p_n) . In the Nexus Paradigm, the labeling q_n refers to a creation of a Nexus graviton in the n -th quantum state associated with a conjugate momentum p_n . The Hamiltonian equation

$$\dot{q}_n = \frac{\partial H}{\partial p_n} \quad (26)$$

refers to the rate of expansion or contraction of space-time generated by the addition or emission of harmonic waves to the Nexus graviton and

$$\dot{p}_n = -\frac{\partial H}{\partial q_n} \quad (27)$$

refers to the force field associated with the addition or emission of harmonic waves to the Nexus graviton. It is important to note that this force field generates an isotropic expansion or contraction of space-time within the spatiotemporal dimensions of the graviton.

We can also rewrite the Hamiltonian equations in terms of Poisson brackets which are invariant under canonical transformations as

$$\begin{aligned} \dot{q}_n &= \{q_n, H\}, \\ \dot{p}_n &= \{p_n, H\} \end{aligned} \quad (28)$$

The Poisson brackets provide the bridge between classical and QM and in QM, these brackets are written as

$$\begin{aligned} \dot{\hat{q}}_n &= [\hat{q}_n, \hat{H}], \\ \dot{\hat{p}}_n &= [\hat{p}_n, \hat{H}] \end{aligned} \quad (29)$$

and obey the following commutation rules

$$\begin{aligned} [\hat{q}_n, \hat{q}_s] &= 0, \\ [\hat{p}_n, \hat{p}_s] &= 0, \\ [\hat{q}_n, \hat{p}_s] &= \delta_{ns} \end{aligned} \quad (30)$$

2.3. The Hamiltonian Formulation for the Quantum Vacuum. The Nexus graviton is a pulse of 4-space which can only

expand or contract and does not execute translational motion implying that the Hamiltonian density of the system is equal to the Lagrangian density.

$$H = L \quad (31)$$

GR is a metric field in which the energy density in four-space determines its value. Since the Bloch energy eigenstate functions determine the energy of space-time, we must seek to express the metric in terms of the Bloch wave functions. To this end we shall express the eigenstate four-space components of the Nexus graviton in the k -th band as

$$\Delta x_{n,k}^\mu = z_{n,k}^\mu = a_{nk} \gamma^\mu \text{sinc}(kx) e^{ikx} \quad (32)$$

such that an infinitesimal four-radius within the k -th band is computed as

$$dr_{n,k} = \frac{\partial z_{n,k}^\mu}{\partial k^\mu} dk^\mu = i x a_{nk} \gamma^\mu \text{sinc}(kx) e^{ikx} dk \quad (33)$$

In (33) the first-order derivative of the periodic sinc function is equal to zero for all integral values of n . The interval within the band is then computed as

$$\begin{aligned} ds^2 &= dr_{n,k}^2 = \frac{\partial z_{n,k}^\mu}{\partial k^\mu} \frac{\partial z_{n,k}^\nu}{\partial k^\nu} dk^\mu dk^\nu \\ &= \alpha \beta \gamma^\mu \gamma^\nu \varphi_{(n,k,x)} \varphi_{(n,k,x)} dk^\mu dk^\nu \end{aligned} \quad (34)$$

Here the interval is described in terms of the reciprocal lattice with $\alpha = i x_\mu a_{nk}$ and $\beta = i x_\nu a_{nk}$. The metric tensor of four-space in the k -th band is therefore associated with the Bloch energy eigenstate functions of the quantum vacuum as follows:

$$g_{(n,k)}^{\mu\nu} = \gamma^\mu \gamma^\nu \varphi_{(n,k,x)} \varphi_{(n,k,x)} = \eta^{\mu\nu} \varphi_{(n,k,x)} \varphi_{(n,k,x)} \quad (35)$$

Equation (35) translates the geometric language of GR into the wave function language of QM.

We initiate the translation procedure of GR into QM by first finding the Lagrange density for the quantized vacuum from (15) which following Einstein and Hilbert is found to be

$$L_{EH} = k (R - 2(n^2 - 1)\Lambda) \quad (36)$$

Given that the Einstein tensor in a compact manifold is equal to the Ricci flow

$$-\partial_t g_{\mu\nu} = \Delta g_{\mu\nu} = R_{\mu\nu} - \frac{1}{2} R g_{\mu\nu} = G_{\mu\nu} \quad (37)$$

therefore the equations of motion of the quantum vacuum obtained from (36) yield the following quantized field equations:

$$\begin{aligned} -\partial_t (\gamma^\mu \varphi_{(n,k,x)} \gamma^\nu \varphi_{(n,k,x)}) \\ = (n^2 - 1) \Lambda \gamma^\mu \varphi_{(n,k,x)} \gamma^\nu \varphi_{(n,k,x)} \end{aligned} \quad (38)$$

which can be written as

$$\begin{aligned} \partial_t (\gamma^\mu \varphi_{(n-1,k,x)} \gamma^\nu \varphi_{(n+1,k,x)}) \\ = \frac{-i^2}{(2\pi)^2} \nabla_\mu \nabla_\nu \gamma^\mu \varphi_{(n-1,k,x)} \gamma^\nu \varphi_{(n+1,k,x)} \\ = \frac{1}{4\pi^2} \nabla_\mu \nabla_\nu \gamma^\mu \varphi_{(n-1,k,x)} \gamma^\nu \varphi_{(n+1,k,x)} \end{aligned} \quad (39)$$

where

$$\varphi_{(n-1,k,x)} = \text{sinc}((n-1)k_1 x) e^{i(n-1)k_1 x} \quad (40)$$

$$\varphi_{(n+1,k,x)} = \text{sinc}((n+1)k_1 x) e^{i(n+1)k_1 x} \quad (41)$$

$$\frac{3k_1^2}{(2\pi)^2} = \Lambda \quad (42)$$

For large values of n the Bloch functions satisfy the condition

$$\varphi_{(n-1,k,x)} \approx \varphi_{(n,k,x)} \approx \varphi_{(n+1,k,x)} \quad (43)$$

The quantum vacuum can therefore be interpreted as a system in which there are a constant annihilation and creation of quanta as implied by (40) and (41) which causes the Nexus graviton to either expand or contract.

2.4. The Hamiltonian Formulation in the Presence of Matter Fields. We now seek to introduce matter fields into the quantum vacuum. If we compare the quantized metric of (17) describing the gravity within a Nexus graviton with the Schwarzschild metric describing the gravitational field around baryonic matter, we notice that we can describe the gravitational field around baryonic matter in terms of the quantum state of space-time through the relation

$$\frac{2}{n^2} = \frac{2GM}{c^2 r} \quad (44)$$

This yields a relationship between the quantum state of space-time and the amount of baryonic matter embedded within it as follows:

$$n^2 = \frac{c^2 r}{GM} = \frac{c^2}{v^2} \quad (45)$$

Equation (45) reveals a family of concentric stable circular orbits $r_n = n^2 GM/c^2$ with corresponding orbital speeds of $v_n = c/n$. Thus in the Nexus Paradigm, unlike in GR, the innermost stable circular orbit occurs at $n = 1$ or at half the Schwarzschild radius which implies that the event horizon predicted by the Nexus Paradigm is half the size predicted in GR. Also (45) reveals how the Nexus graviton in the n -th quantum state imitates DM if M is considered as the apparent mass of the DM. Through this comparison, we can also deduce that the deflection of light through gravitational lensing by space-time in the n -th quantum state is

$$\alpha = \frac{4}{n^2} \quad (46)$$

Thus gravitational lensing can be used to constrain the value of the quantum state n of space-time within a lensing system.

Having obtained the relationship between the quantum state of space-time and the amount of baryonic matter embedded within it, the result of (45) is then added to (39) to yield the time evolution of the quantum vacuum in the presence of baryonic matter as

$$\begin{aligned} \partial_t (\gamma^\mu \varphi_{(n-1,n,k,x)} \gamma^\nu \varphi_{(n+1,n,k,x)}) \\ = \frac{1}{4\pi^2} \nabla_\mu \nabla_\nu \gamma^\mu \varphi_{(n-1,k,x)} \gamma^\nu \varphi_{(n+1,k,x)} \\ - n^2 \Lambda \gamma^\mu \varphi_{(n,k,x)} \gamma^\nu \varphi_{(n,k,x)} \end{aligned} \quad (47)$$

Thus the time evolution of the quantum vacuum in the presence of matter resembles thermal flow in the presence of

a heat sink. The second term on the R.H.S. of (47) is an 8-cell or 4-cube that operates as a sinc filter with a four-wave cut-off of

$$k_c = nk_1 = 2\pi \sqrt{\frac{\Lambda}{3} \cdot \frac{c^2 r}{GM}} \quad (48)$$

The filtration of high frequencies from the vacuum lowers the quantum vacuum state and generates a gravitational field in much the same way as the Casimir Effect is generated. The physical process of filtration occurs as follows: A 4-cube with baryonic matter embedded with in it acquires inertia. The inertia gives the cell inductive impedance and becomes less responsive to high frequency vibrations of the quantum vacuum. Thus the heavier the cell, the lower the cut-off frequency. Equation (48) shows that when the radius of the cell is equal to half the Schwarzschild radius, the only permitted frequency is that of the ground state. Thus the inside of a black hole is in the ground state having a negative metric signature.

We now introduce a test particle of mass m , into the quantum vacuum perturbed by matter fields. The particle will flow along with the Ricci flow and the Hamiltonian of the system becomes

$$\begin{aligned} \hat{H} (\gamma^\mu \varphi_{(n-1,n,k,x)} \gamma^\nu \varphi_{(n+1,n,k,x)}) \\ = \frac{\hat{P}_\mu \hat{P}_\nu}{2m} (\gamma^\mu \varphi_{(n-1,k,x)} \gamma^\nu \varphi_{(n+1,k,x)}) \\ - V (\gamma^\mu \varphi_{(n,k,x)} \gamma^\nu \varphi_{(n,k,x)}) \end{aligned} \quad (49)$$

Here

$$V = n^2 \frac{\hbar^2}{2m} \Lambda = \frac{rc^2}{GM} \cdot \frac{3\hbar^2 k_1^2}{2m} \quad (50)$$

$$\hat{P}_\mu = -i\hbar \nabla_\mu \quad (51)$$

$$\hat{H} = -i\hbar \partial_t \quad (52)$$

Equation (49) is equivalent to (31) in which the Hamiltonian is equal to the Lagrangian.

$$\begin{aligned} \hat{H} (\gamma^\mu \varphi_{(n-1,n,k,x)} \gamma^\nu \varphi_{(n+1,n,k,x)}) \\ = L (\gamma^\mu \varphi_{(n-1,n,k,x)} \gamma^\nu \varphi_{(n+1,n,k,x)}) \end{aligned} \quad (53)$$

The Lagrangian is not relativistic because the energy reference frames or space-time states involved in the transition dynamics $n-1$, n , and $n+1$ are separated by a small energy gap, $E = \sqrt{3} \cdot \hbar H_0$. The exchanged quantum of energy between states is responsible for “welding” them together.

Equation (50) is the gravitational interaction in reciprocal space-time. The weakness of the gravitational interaction is due to the small value of the cosmological constant.

3. Line Elements and Information in K-Space

A close inspection of (34) reveals the relationship between a line element in 4-space and its conjugate line in K-space

$$ds^2 = \alpha \beta d\kappa^2 \quad (54)$$

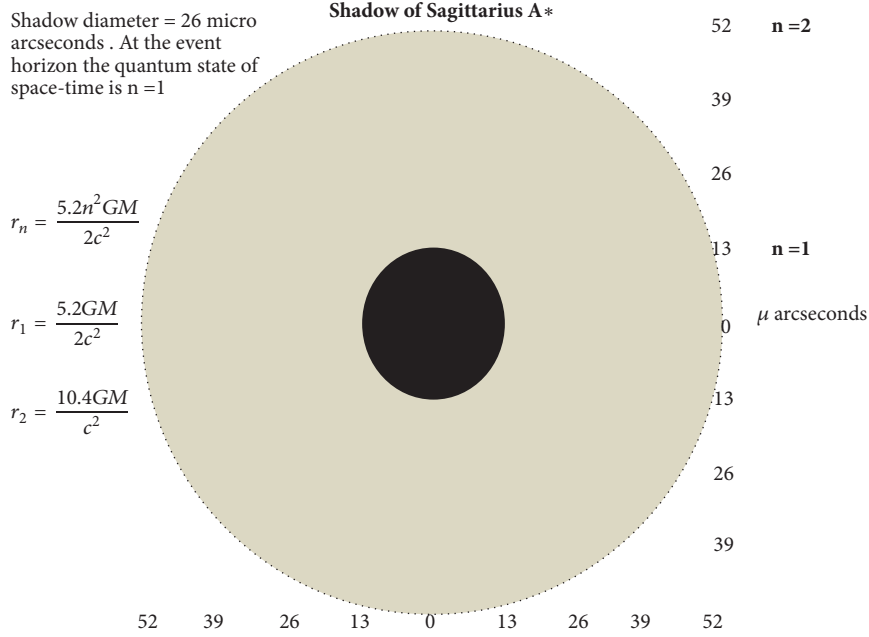


FIGURE 1: Shadow of Sagittarius A*.

where

$$d\kappa^2 = \gamma^\mu \varphi_{(n,k,x)} \gamma^\nu \varphi_{(n,k,x)} dk^\mu dk^\nu \quad (55)$$

The term $\gamma^\mu \varphi_{(n,k,x)} \gamma^\nu \varphi_{(n,k,x)}$ refers to the normalized information flux density passing through an elementary surface $dk^\mu dk^\nu$ in K-space. The gradient of the flux density yields the baseband bandwidth $k_{(n)\mu}$.

$$\partial_\mu \gamma^\mu \varphi_{(n,k,x)} \gamma^\nu \varphi_{(n,k,x)} = k_{(n)\mu} \gamma^\mu \varphi_{(n,k,x)} \gamma^\nu \varphi_{(n,k,x)} \quad (56)$$

This gradient is also a measure of the acutance or sharpness of the information. A large bandwidth provides detailed information while a small bandwidth provides diffuse information. Equation (49) describes the diffusion of information as it flows into a gravitational well. Unitarity is preserved if the flux is summed over the total diffusion surface.

$$\iint_0^\Sigma \gamma^\mu \varphi_{(n,k,x)} \gamma^\nu \varphi_{(n,k,x)} dk_\mu dk_\nu = 1 \quad (57)$$

Here the integral implies that one bit of information is found on a surface $\Sigma = k_n^2$ in K-space which corresponds to an area $A_n = 4\pi^2/k_n^2$ in 4-space. The k_1 bandwidth permitted within a black hole generates the smallest elementary surface or pixel in K-space of k_1^2 suggesting that information inside a blackhole is diluted to one bit per area equivalent to the square of the Hubble 4-radius in 4-space or from (48) the information surface density is $k_1^2 = 4\pi^2\Lambda/3$. Thus the cosmological constant can also be interpreted as a unit of information surface density. The ratio of the Planck surface in K-space to the smallest elementary surface in K-space yields 10^{120} . This huge number represents the maximum number of pixels that can fit on the largest surface in K-space. Hence the expression $W = k_p^2/k_n^2$ represents the number of empty

pixel slots available in the n-th quantum state or the number of degenerate energy levels.

$$|\varphi\rangle_n = c_1 |\psi_1\rangle_n + c_2 |\psi_2\rangle_n \dots c_W |\psi_W\rangle_n. \quad (58)$$

The entropy of the n-state therefore becomes

$$S = k_B \ln W = k_B \ln \frac{k_p^2}{k_n^2} = k_B \ln \frac{A_n}{l_p^2} = k_B \ln \frac{c^3 A_n}{G\hbar} \quad (59)$$

Here we observe that objects fall into a gravitational field because it leads to an increase in entropy. In strong fields the information is delocalized. A black hole does not annihilate information; it simply diffuses or dilutes it by increasing the entropy. It can also be interpreted as a low pass filter that permits one bit of information to pass per Hubble time. Since information is delocalized close to a black hole, then we do not expect the Event Horizon Telescope to observe a silhouette surrounded by a well defined accretion disc but a circular silhouette surrounded by a cloud of degenerate (delocalized) matter (grey area) as depicted in Figure 1.

The radii are calculated from (45) and the magnification factor, 5.2/2, arises from gravitational lensing. The silhouette is half the size predicted in GR.

4. Discussion

A successful covariant canonical quantization of the gravitational field has been presented in which we find that gravity is akin to a thermal flow of space-time and that space-time can also be described in terms of a reciprocal lattice. The presence of matter creates an impure lattice and a potential well arises in the region of perturbation through filtration of high frequencies from the quantum vacuum. A test particle flows along with the quantum vacuum and the presence of

a potential well will cause it to flow towards the sink. This formulation will find important applications in high energy lattice gauge field theories where it may help expand the standard model of particle physics by eliminating divergent terms in the current theory and predicting hitherto unknown phenomena.

Data Availability

The results of this theoretical research will be confirmed by data from the Event Horizon Collaboration on the size and shape of the shadow of Sgr A*.

Conflicts of Interest

The author declares no conflicts of interest.

Acknowledgments

The author gratefully appreciates the funding and support from the Department of Physics and Astronomy at the Botswana International University of Science and Technology (BIUST).

References

- [1] R. Arnowitt, S. Deser, and C. W. Misner, "Dynamical structure and definition of energy in general relativity," *Physical Review A: Atomic, Molecular and Optical Physics*, vol. 116, no. 5, pp. 1322–1330, 1959.
- [2] Y. Sendouda, N. Deruelle, M. Sasaki, and D. Yamauchi, "Higher curvature theories of gravity in the adm canonical formalism," *International Journal of Modern Physics: Conference Series*, vol. 01, pp. 297–302, 2011.
- [3] E.ourgoulhon, "3+1 formalism and bases for numerical relativity," 2007, <https://arxiv.org/abs/gr-qc/0703035>.
- [4] N. Kiriushcheva and S. Kuzmin, "The Hamiltonian formulation of general relativity: myths and reality," *Open Physics*, vol. 9, no. 3, pp. 576–615, 2011.
- [5] E. Anderson, "Problem of time in quantum gravity," *Annalen der Physik*, vol. 524, no. 12, pp. 757–786, 2012.
- [6] B. S. DeWitt, "Quantum theory of gravity. I. The canonical theory," *Physical Review A: Atomic, Molecular and Optical Physics*, vol. 160, article 1113, 1967.
- [7] M. Bojowald and P. A. Hohn, "An Effective approach to the problem of time," *Classical and Quantum Gravity*, vol. 28, no. 3, Article ID 035006, 2011.
- [8] C. Kiefer, "Does time exist in Quantum Gravity?" in *Towards a Theory of Spacetime Theories. Einstein Studies*, D. Lehmkuhl, G. Schiemamm, and E. Scholz, Eds., vol. 13, pp. 287–295, Birkhauser, New York, NY, USA, 2017.
- [9] S. Carlip, "Quantum gravity: a progress report," *Reports on Progress in Physics*, vol. 64, no. 8, pp. 885–942, 2001.
- [10] S. Carlip, D.-W. Chiou, W.-T. Ni, and R. Woodard, "Quantum gravity: a brief history of ideas and some prospects," *International Journal of Modern Physics D: Gravitation, Astrophysics, Cosmology*, vol. 24, no. 11, Article ID 1530028, 23 pages, 2015.
- [11] C. Kiefer, "Quantum gravity: general introduction and recent developments," *Annalen der Physik*, vol. 15, no. 1-2, pp. 129–148, 2006.
- [12] C. Kiefer, "Conceptual problems in quantum gravity and quantum cosmology," *ISRN Mathematical Physics*, vol. 2013, Article ID 509316, 17 pages, 2013.
- [13] S. Marongwe, "The Nexus graviton: A quantum of Dark Energy and Dark Matter," *International Journal of Geometric Methods in Modern Physics*, vol. 11, no. 06, Article ID 1450059, 2014.
- [14] S. Marongwe, "The Schwarzschild solution to the Nexus graviton field," *International Journal of Geometric Methods in Modern Physics*, vol. 12, no. 4, Article ID 1550042, 10 pages, 2015.
- [15] S. Marongwe, "The electromagnetic signature of gravitational wave interaction with the quantum vacuum," *International Journal of Modern Physics D: Gravitation, Astrophysics, Cosmology*, vol. 26, no. 3, Article ID 1750020, 15 pages, 2017.

Research Article

Thermodynamics of Charged AdS Black Holes in Rainbow Gravity

Ping Li, Miao He, Jia-Cheng Ding, Xian-Ru Hu, and Jian-Bo Deng 

Institute of Theoretical Physics, Lanzhou University, Lanzhou 730000, China

Correspondence should be addressed to Jian-Bo Deng; dengjb@lzu.edu.cn

Received 4 June 2018; Accepted 5 December 2018; Published 18 December 2018

Guest Editor: Farook Rahaman

Copyright © 2018 Ping Li et al. This is an open access article distributed under the Creative Commons Attribution License, which permits unrestricted use, distribution, and reproduction in any medium, provided the original work is properly cited. The publication of this article was funded by SCOAP³.

In this paper, the thermodynamic property of charged AdS black holes is studied in rainbow gravity. By the Heisenberg Uncertainty Principle and the modified dispersion relation, we obtain deformed temperature. Moreover, in rainbow gravity we calculate the heat capacity in a fixed charge and discuss the thermal stability. We also obtain a similar behaviour with the liquid-gas system in extending phase space (including P and r) and study its critical behavior with the pressure given by the cosmological constant and with a fixed black hole charge Q . Furthermore, we study the Gibbs function and find its characteristic swallow tail behavior, which indicates the phase transition. We also find that there is a special value about the mass of test particle which would lead the black hole to zero temperature and a diverging heat capacity with a fixed charge.

1. Introduction

It is known Lorentz symmetry which is one of most important symmetries in nature; however, some researches indicate that the Lorentz symmetry might be violated in the ultraviolet limit [1–5]. Since the standard energy-momentum dispersion relation relates to the Lorentz symmetry, the deformation of Lorentz symmetry would lead to the modification of energy-momentum dispersion relation. In fact, some calculations in loop quantum gravity have showed the dispersion relations may be deformed. Meanwhile, based on the deformed energy-momentum dispersion relation the double special relativity has arisen [6, 7]. In this theory, in addition to the velocity of light being the maximum velocity attainable there is another constant for maximum energy scale in nature which is the Planck energy E_p . It gives different picture for the special relativity in microcosmic physics. The theory has been generalized to curved spacetime by Joao Magueijo and Lee Smolin, called gravity's rainbow [8]. In their theory, the geometry of spacetime depends on the energy of the test particle and observers of different energy would see different geometry of spacetime. Hence, a family of energy-dependent metrics named rainbow metrics will describe the geometry of spacetime, which is different from

general gravity theory. Based on the nonlinear of Lorentz transformation, the energy-momentum dispersion relation can be rewritten as

$$E^2 f^2 \left(\frac{E}{E_p} \right) - p^2 g^2 \left(\frac{E}{E_p} \right) = m^2, \quad (1)$$

where E_p is the Planck energy. The rainbow functions $f(E/E_p)$ and $g(E/E_p)$ are required to satisfy

$$\begin{aligned} \lim_{E/E_p \rightarrow 0} f \left(\frac{E}{E_p} \right) &= 1, \\ \lim_{E/E_p \rightarrow 0} g \left(\frac{E}{E_p} \right) &= 1. \end{aligned} \quad (2)$$

In this case, the deformed energy-momentum dispersion relation equation (1) will go back to classical one when the energy of the test particle is much lower than E_p . Due to this energy-dependent modification to the dispersion relation, the metric $h(E)$ in gravity's rainbow could be rewritten as [9]

$$h(E) = \eta^{ab} e_a(E) \otimes e_b(E), \quad (3)$$

where the energy dependence of the frame fields is

$$\begin{aligned} e_0(E) &= \frac{1}{f(E/E_P)} \tilde{e}_0, \\ e_i(E) &= \frac{1}{g(E/E_P)} \tilde{e}_i, \end{aligned} \quad (4)$$

and here the tilde quantities refer to the energy-independent frame fields. This leads to a one-parameter Einstein equation

$$\begin{aligned} G_{\mu\nu} \left(\frac{E}{E_P} \right) + \Lambda \left(\frac{E}{E_P} \right) g_{\mu\nu} \left(\frac{E}{E_P} \right) \\ = 8\pi G \left(\frac{E}{E_P} \right) T_{\mu\nu} \left(\frac{E}{E_P} \right), \end{aligned} \quad (5)$$

where $G_{\mu\nu}(E/E_P)$ and $T_{\mu\nu}(E/E_P)$ are energy-dependent Einstein tensor and energy-momentum tensor and $\Lambda(E/E_P)$ and $G(E/E_P)$ are energy-dependent cosmological constant and Newton constant. Generally, many forms of rainbow functions have been discussed in literatures; in this paper we will mainly employ the following rainbow functions:

$$\begin{aligned} f \left(\frac{E}{E_P} \right) &= 1, \\ g \left(\frac{E}{E_P} \right) &= \sqrt{1 - \eta \left(\frac{E}{E_P} \right)^n}, \end{aligned} \quad (6)$$

which has been widely used in [10–18].

Recently, Schwarzschild black holes, Schwarzschild AdS black holes, and Reissner-Nordstrom black holes in rainbow gravity [19–21] have been studied. Ahmed Farag Alia, Mir Faizald, and Mohammed M. Khalile [15] studied the deformed temperature about charged AdS black holes in rainbow gravity based on Heisenberg Uncertainty Principle (HUP), $E = \Delta p \sim 1/r_+$. In this paper, we study the thermodynamical property about the charged AdS black holes in rainbow gravity based on the usual HUP, $p = \Delta p \sim 1/r_+$. Moreover, we study how the mass of test particle influences thermodynamical property for charged AdS black holes.

The paper is organized as follows. In the next section, by using the HUP and the modified dispersion relation, we obtain deformed temperature, and we also calculate heat capacity with a fixed charge and discuss the thermal stability. In Section 3, we find the charged AdS black holes have similar behaviour with the liquid-gas system with the pressure given by the cosmological constant while we treat the black holes charge Q as a fixed external parameter, not a thermodynamic variable. We also calculate the Gibbs free energy and find characteristic swallow tail behavior. Finally, the conclusion and discussion will be offered in Section 4.

2. The Thermal Stability

In rainbow gravity the line element of the modified charged AdS black holes can be described as [15]

$$ds^2 = -\frac{N}{f^2} dt^2 + \frac{1}{Ng^2} dr^2 + \frac{r^2}{g^2} d\Omega^2, \quad (7)$$

where

$$N = 1 - \frac{2M}{r} + \frac{Q^2}{r^2} + \frac{r^2}{l^2}. \quad (8)$$

Generally, $-3/l^2 = \Lambda$ which is cosmological constant. Because all energy dependence in the energy-independent coordinates must be in the rainbow functions f and g , N is independent on the energy of test particle [8]. In gravity's rainbow, the deformed temperature related to the standard temperature T_0 was [15]

$$T = -\frac{1}{4\pi} \lim_{r \rightarrow r_+} \sqrt{\frac{-g^{11}(g^{00})'}{g^{00}g^{00}}} = \frac{g(E/E_P)}{f(E/E_P)} T_0, \quad (9)$$

where r_+ is horizon radius.

In gravity's rainbow, although the metric depends on the energy of test particle, the usual HUP can be still used [19]. For simplicity we take $n = 2$ in the following discussion, by combining (1) with (6) we can get

$$g = \sqrt{1 - \eta G_0 m^2} \sqrt{\frac{r_+^2}{r_+^2 + \eta G_0}}, \quad (10)$$

where $G_0 = 1/E_P^2$, m is the mass of test particle, and η is a constant parameter.

Generally, the standard temperature was given by [22]

$$T_0 = \frac{1}{4\pi} \left(\frac{1}{r_+} + \frac{3r_+}{l^2} - \frac{Q^2}{r_+^3} \right). \quad (11)$$

When using (6) and (10), we can get the temperature of charged AdS black holes in rainbow gravity

$$T = gT_0 = \frac{1}{4\pi k} \sqrt{\frac{r_+^2}{r_+^2 + \eta G_0}} \left(\frac{1}{r_+} + \frac{3r_+}{l^2} - \frac{Q^2}{r_+^3} \right), \quad (12)$$

where $k = 1/\sqrt{1 - \eta G_0 m^2}$. It is easy to find $T = T_0$ when $\eta = 0$. Equation (12) shows that there are two solutions when $T = 0$, one corresponds to extreme black hole and the other to $m^2 = 1/\eta G$. The second solution indicates the temperature of black holes completely depends on the mass of test particle when the black holes keep with fixed mass, charge, and anti-de Sitter radius. The bigger the mass of test particle is, the smaller the temperature of black holes is. When $m^2 = 1/\eta G$, the temperature keeps zero. Generally, due to gravity's rainbow, a minimum radius with respect to the black hole is given and is related to a radius of black hole remnant when the temperature tends to zero [15]. However, our paper shows all black holes can keep zero temperature when the test particle mass approaches a value, such as $m^2 = 1/\eta G$. But due to $m \ll M_P$ in general condition, it may be difficult to test the phenomenon with zero temperature about black holes.

In general, the thermal stability can be determined by the heat capacity, which is also used to the systems of black holes [17, 23–25]. In other words, the positive heat capacity corresponds to a stable state and the negative heat capacity corresponds to unstable state. In following discussions, we

will focus on the heat capacity to discuss the stability of black holes. When $N = 0$, the mass of charged AdS black holes can be calculated as

$$M = \frac{1}{2} \left(r_+ + \frac{Q^2}{r_+} + \frac{r_+^3}{l^2} \right). \quad (13)$$

Based on the first law $dM = TdS$ with the deformed temperature [20], the modified entropy can be computed

$$S = \int \frac{dM}{T} \quad (14)$$

$$= \pi k r_+ \sqrt{r_+^2 + \eta G_0} + \pi k \eta G_0 \ln \left(r_+ + \sqrt{r_+^2 + \eta G_0} \right).$$

Note that the next leading order is logarithmic as $S \approx \pi r_+^2 + (1/2)\pi\eta G_0 \ln(4r_+^2)$, which is similar to the quantum correction in [26–31]. With $A = 4\pi r_+^2$ we can get $S \approx A/4 + (1/2)\pi\eta G_0 \ln(A/\pi)$. We can find the result is in agreement with the standard entropy $S = A/4$ when $\eta = 0$, which is standard condition.

The heat capacity with a fixed charge can be calculated as

$$C_Q = T \frac{dS}{dT} = \left(\frac{\partial M / \partial r_+}{\partial T / \partial r_+} \right) \quad (15)$$

$$= 2\pi k \frac{(-Q^2 l^2 r_+^2 + l^2 r_+^4 + 3r_+^6)(r_+^2 + \eta G_0)^{3/2}}{3r_+^7 + (6\eta G_0 - l^2)r_+^5 + 3Q^2 l^2 r_+^3 + 2\eta G_0 Q^2 l^2 r_+},$$

which shows that C_Q reduces to standard condition [22] with $\eta = 0$. Obviously, the heat capacity is diverging when $m^2 = 1/\eta G$. Generally, when the temperature vanishes, the heat capacity also tends to zero. However, our paper shows a different and anomalous phenomenon. Fortunately, the phenomenon is just an observation effect; the result gives us a way to test the theory of rainbow gravity. Some of the conditions above indicate that the mass of test particle does not influence the forms of temperature, entropy, and heat capacity but only changes their amplitudes.

The numerical methods indicate there are three situations corresponding to zero, one, and two diverging points of heat capacity respectively, which have been described in Figures 1, 2, and 3. Figure 1 shows a continuous phase and does not appear phase transition with $l < l_c$. In Figure 2, there are one diverging point and two stable phases for $C_Q > 0$ with $l = l_c$, phase 1 and phase 2, which individually represent a phase of large black hole (LBH) and a small black hole (SBH). In Figure 3, one can find there are three phases and two diverging points with $l > l_c$. Phase 1 experiences a continuous process from a unstable phase $C_Q < 0$ to a stable phase $C_Q > 0$; phase 2 is a pure unstable phase with $C_Q < 0$; phase 3 is a stable phase with $C_Q > 0$. It is easy to see phase 1 represents the phase of SBH and phase 3 represents the phase of LBH. However, there is a special unstable phase 2 between phase 1 and phase 3. This indicates when the system evolves from phase 3 to phase 1, the system must experience a medium unstable state which could be explained as an exotic quark-gluon plasma with negative heat capacity [32, 33].

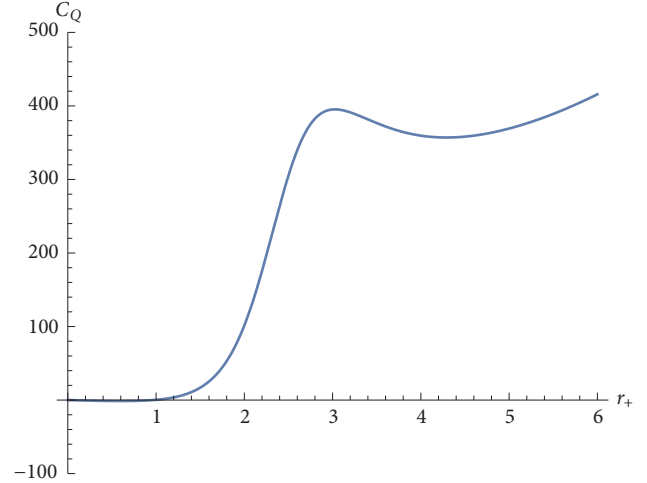


FIGURE 1: C_Q - r_+ diagram of charged AdS black holes in the rainbow gravity. It corresponds to $l = 6$. We have set $Q = 1, \eta = 1, m = 0$.

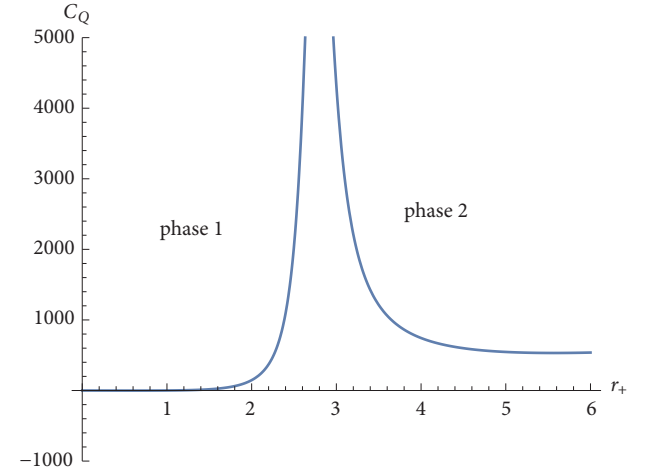


FIGURE 2: C_Q - r_+ diagram of charged AdS black holes in the rainbow gravity. It corresponds to $l = 7.05$. We have set $Q = 1, \eta = 1, m = 0$.

3. The Phase Transition of Charged AdS Black Holes in Extending Phase Space

Surprisingly, although rainbow functions modify the $\Lambda(E/E_P)$ term, they do not affect thermodynamical pressure related to the cosmological constant [17, 34]. So we can take the following relation:

$$P = -\frac{\Lambda(0)}{8\pi} = \frac{3}{8\pi l^2}. \quad (16)$$

Since David Kubiznak and Robert B. Mann have showed the critical behaviour of charged AdS black holes and completed the analogy of this system with the liquid-gas system [22], in what follows we will study whether the critical behavior of the charged AdS black holes system in rainbow

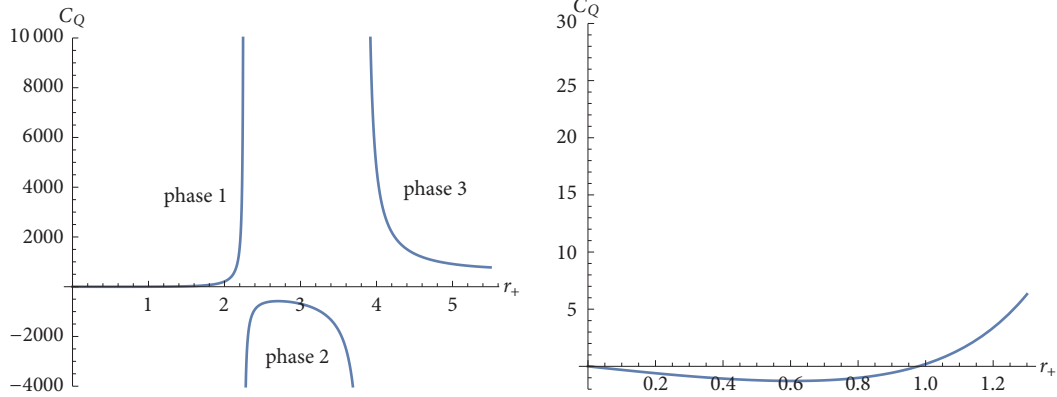


FIGURE 3: $C_Q - r_+$ diagram of charged AdS black holes in the rainbow gravity. It corresponds to $l = 8$, right one corresponds to an extending part of near $r_+ = 1$. We have set $\eta = 1$, $Q = 1$, $m = 0$.

gravity is kept. Using (12) and (16) in extended phase space, we can get

$$P = \frac{k}{2} \sqrt{\frac{r_+^2 + \eta G_0}{r_+^4}} T - \frac{1}{8\pi} \frac{1}{r_+^2} + \frac{1}{8\pi} \frac{Q^2}{r_+^4}. \quad (17)$$

Similarly with [17], the critical point is obtained from

$$\begin{aligned} \frac{\partial P}{\partial r_+} &= 0, \\ \frac{\partial^2 P}{\partial r_+^2} &= 0, \end{aligned} \quad (18)$$

which leads to

$$\begin{aligned} r_c &= \sqrt{\frac{2^{4/3} \eta G_0 Q^2 + 2^{4/3} Q^4 + 2Q^2 (x + y)^{1/3} + 2^{2/3} (x + y)^{2/3}}{(x + y)^{1/3}}}, \\ T_c &= \frac{1}{2\pi k} \frac{r_c^2 - 2Q^2}{r_c^4 + 2\eta G_0 r_c^2} \sqrt{r_c^2 + \eta G_0}, \end{aligned} \quad (19)$$

$$P_c = \frac{r_c^4 - 3Q^2 r_c^2 - 2\eta G_0 Q^2}{8\pi r_c^4 (r_c^2 + 2\eta G_0)},$$

where $x = \eta G_0 Q^2 (\eta G_0 + Q^2)$ and $y = Q^2 (\eta G_0 + Q^2) (\eta G_0 + 2Q^2)$. We can obtain

$$\frac{P_c r_c}{T_c} = k \frac{r_c^4 - 3Q^2 r_c^2 - 2\eta G_0 Q^2}{4r_c (r_c^2 - 2Q^2) \sqrt{r_c^2 + \eta G_0}}, \quad (20)$$

which shows the critical ratio is deformed due to the existence of rainbow gravity. It is notable that (20) will back to the usual ratio with $\eta = 0$. Generally, for charged AdS black holes, the pressure and temperature are demanded as positive real value. From (19), when $P_c > 0$ and $T_c > 0$, we have

$$\begin{aligned} r_c^4 - 3Q^2 r_c^2 - 2\eta G_0 Q^2 &> 0, \\ r_c &> \sqrt{2}Q, \end{aligned} \quad (21)$$

which indicates a restriction between Q and η . The $P - r_+$ diagram has been described in Figure 4. From Figure 4, we can find that charged AdS black holes in rainbow gravity have an analogy with the Van-der-Waals system and have a first-order phase transition with $T < T_c$. Namely, when considering rainbow gravity with the form of (6), the behavior like Van-der-Waals system can also be obtained.

Based on [14, 35] the black hole mass is identified with the enthalpy, rather than the internal energy, so the Gibbs free energy for fixed charge in the rainbow gravity will be

$$\begin{aligned} G &= H - TS \\ &= \frac{1}{2} \left(r_+ + \frac{Q^2}{r_+} + \frac{r_+^3}{l^2} \right) - kT (\pi r_+ \sqrt{r_+^2 + \eta G_0} \\ &\quad + \pi \eta G_0 \ln (r_+ + \sqrt{r_+^2 + \eta G_0})), \end{aligned} \quad (22)$$

which has been showed in Figure 5. Because the picture of G demonstrates the characteristic swallow tail behaviour, there is a first-order transition in the system.

4. Conclusion

In this paper, we have studied the thermodynamic behavior of charged AdS black holes in rainbow gravity. By the modified dispersion relation and HUP, we got deformed temperature in charged AdS black holes using no-zero mass of test particle. We have discussed the divergence about the heat capacity with a fixed charge. Our result shows that the phase structure has a relationship with AdS radius l . When $l = l_c$, there is only one diverging point about heat capacity; when $l > l_c$, we have found there are two diverging points and three phases including two stable phases and one unstable phase. In particular, an analogy between the charged AdS black holes in the rainbow gravity and the liquid-gas system is discussed. We have also showed $P - r_+$ critical behavior about the charged AdS black holes in the rainbow gravity. The consequence shows there is the Van-der-Waals like behavior in the rainbow gravity when η and Q coincide with (21). The rainbow functions deform the forms of critical pressure,

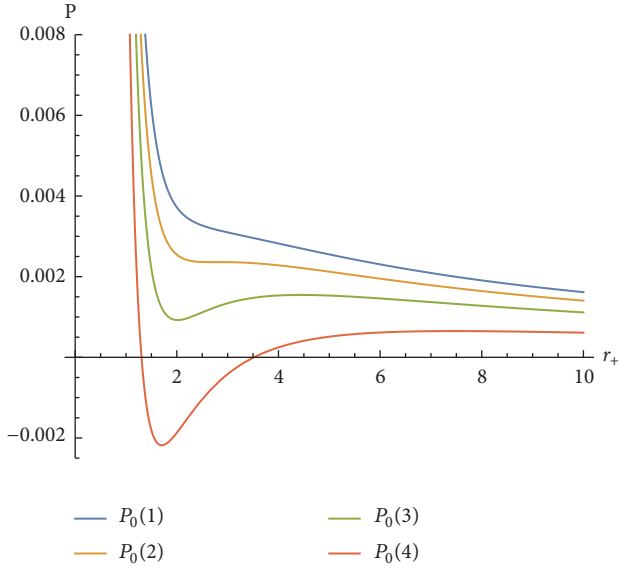


FIGURE 4: $P-r_+$ diagram of charged AdS black holes in the rainbow gravity. The temperature of isotherms decreases from top to bottom. The $P_0(1)$ line corresponds to one-phase for $T > T_c$. The critical state, $T_c = 0.0358$, is denoted by the $P_0(2)$ line. The lowest two lines correspond to the smaller temperature than the critical temperature. We have set $Q = 1$, $\eta = 1$, $m = 0$.

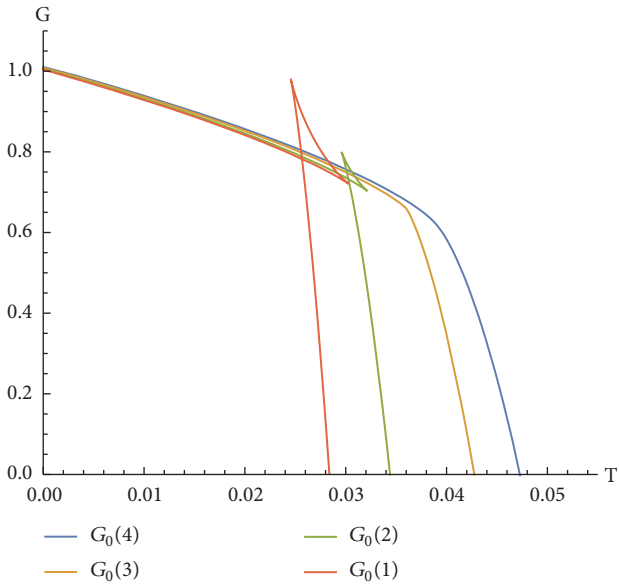


FIGURE 5: Gibbs free energy of charged AdS black holes in rainbow gravity. The blue line $G_0(3)$ corresponds to the critical pressure $P_c \approx 0.0024$, the line $G_0(4)$ corresponds to pressure $P > P_c$, and the others corresponds to pressure $P < P_c$. We have set $Q = 1$, $\eta = 1$, $m = 0$.

temperature, and radius. At last, we have discussed the Gibbs free energy and have obtained characteristic “swallow tail” behaviour which can be the explanation of first-order phase transition.

We find the mass of test particle does not influence the forms of temperature, entropy, and heat capacity but only

changes their amplitudes. Moreover, there is a special value about the mass of test particle encountered $m^2 = 1/\eta G$, which would lead to zero temperature and diverging heat capacity for charged AdS black holes in rainbow gravity.

Data Availability

No data were used to support this study.

Conflicts of Interest

The authors declare that there are no conflicts of interest regarding the publication of this paper.

Acknowledgments

We would like to thank the National Natural Science Foundation of China (Grant no. 11571342) for supporting us on this work.

References

- [1] R. Iengo, J. G. Russo, and M. Serone, “Renormalization group in Lifshitz-type theories,” *Journal of High Energy Physics*, vol. 2009, no. 11, 2009.
- [2] A. Adams, N. Arkani-Hamed, S. Dubovsky, A. Nicolis, and R. Rattazzi, “Causality, analyticity and an IR obstruction to UV completion,” *Journal of High Energy Physics*, vol. 2006, no. 10, 2006.
- [3] B. M. Gripaios, “Modified gravity via spontaneous symmetry breaking,” *Journal of High Energy Physics*, vol. 2004, no. 10, 2004.
- [4] J. Alfaro, P. González, and Á. Ricardo, “Electroweak standard model with very special relativity,” *Physical Review D*, vol. 91, no. 10, Article ID 105007, 2015.
- [5] H. Belich and K. Bakke, “Geometric quantum phases from Lorentz symmetry breaking effects in the cosmic string space-time,” *Physical Review D: Particles, Fields, Gravitation and Cosmology*, vol. 90, no. 2, 2014.
- [6] J. Magueijo and L. Smolin, “String theories with deformed energy-momentum relations, and a possible nontachyonic bosonic string,” *Physical Review D: Particles, Fields, Gravitation and Cosmology*, vol. 71, Article ID 026010, 2005.
- [7] J. Magueijo and L. Smolin, “Generalized Lorentz invariance with an invariant energy scale,” *Physical Review D: Particles, Fields, Gravitation and Cosmology*, vol. 67, Article ID 044017, 2003.
- [8] J. Magueijo and L. Smolin, “Gravity’s rainbow,” *Classical and Quantum Gravity*, vol. 21, pp. 1725–1736, 2004.
- [9] J.-J. Peng and S.-Q. Wu, “Covariant anomaly and Hawking radiation from the modified black hole in the rainbow gravity theory,” *General Relativity and Gravitation*, vol. 40, no. 12, pp. 2619–2626, 2008.
- [10] G. Amelino-Camelia, J. Ellis, N. E. Mavromatos, and D. V. Nanopoulos, “Distance measurement and wave dispersion in a Liouville-string approach to quantum gravity,” *International Journal of Modern Physics A*, vol. 12, no. 3, pp. 607–623, 1997.
- [11] U. Jacob, F. Mercati, G. Amelino-Camelia, and T. Piran, “Modifications to Lorentz invariant dispersion in relatively boosted frames,” *Physical Review D: Particles, Fields, Gravitation and Cosmology*, vol. 82, no. 8, Article ID 084021, 2010.

- [12] G. Amelino-Camelia, "Quantum-spacetime phenomenology," *Living Reviews in Relativity*, vol. 16, no. 1, p. 5, 2013.
- [13] A. F. Ali, "Black hole remnant from gravity's rainbow," *Physical Review D: Particles, Fields, Gravitation and Cosmology*, vol. 89, no. 10, Article ID 104040, 2014.
- [14] A. F. Ali, M. Faizal, and M. M. Khalil, "Absence of black holes at LHC due to gravity's rainbow," *Physics Letters. B. Particle Physics, Nuclear Physics and Cosmology*, vol. 743, pp. 295–300, 2015.
- [15] A. F. Ali, M. Faizal, and M. M. Khalil, "Remnant for all black objects due to gravity's rainbow," *Nuclear Physics B*, vol. 894, pp. 341–360, 2015.
- [16] S. H. Hendi and M. Faizal, "Black holes in Gauss-Bonnet gravity's rainbow," *Physical Review D: Particles, Fields, Gravitation and Cosmology*, vol. 92, no. 4, Article ID 044027, 2015.
- [17] S. H. Hendi, B. Eslam Panah, and S. Panahiyan, "Three-dimensional dilatonic gravity's rainbow: exact solutions," *PTEP. Progress of Theoretical and Experimental Physics*, vol. 76, no. 5, pp. 1–15, 2016.
- [18] S. Gangopadhyay and A. Dutta, "Constraints on rainbow gravity functions from black-hole thermodynamics," *EPL (Europhysics Letters)*, vol. 115, no. 5, 2016.
- [19] Y. Gim and W. Kim, "Thermodynamic phase transition in the rainbow Schwarzschild black hole," *Journal of Cosmology and Astroparticle Physics*, vol. 2014, no. 10, 2014.
- [20] Y.-W. Kim, S. K. Kim, and Y.-J. Park, "Thermodynamic stability of modified Schwarzschild–AdS black hole in rainbow gravity," *The European Physical Journal C*, vol. 76, no. 10, p. 557, 2016.
- [21] C. Liu, "Charged Particle's Tunneling in a Modified Reissner-Nordstrom Black Hole," *International Journal of Theoretical Physics*, vol. 53, no. 1, pp. 60–71, 2014.
- [22] D. Kubiznak and R. B. Mann, "P-V criticality of charged AdS black holes," *Journal of High Energy Physics*, vol. 2012, no. 7, pp. 1–25, 2012.
- [23] G.-M. Deng, J. Fan, X. Li, and Y.-C. Huang, "Thermodynamics and phase transition of charged AdS black holes with a global monopole," *International Journal of Modern Physics A*, vol. 33, no. 3, Article ID 1850022, 2018.
- [24] G. Deng and Y. Huang, "Q- Φ criticality and microstructure of charged AdS black holes in $f(R)$ gravity," *International Journal of Modern Physics A*, vol. 32, no. 35, Article ID 1750204, 2017.
- [25] S. H. Hendi and M. Momennia, "AdS charged black holes in Einstein–Yang–Mills gravity's rainbow: Thermal stability and p-v criticality," *Physics Letters B*, vol. 777, pp. 222–234, 2018.
- [26] D. V. Fursaev, "Temperature and entropy of a quantum black hole and conformal anomaly," *Physical Review D: Particles, Fields, Gravitation and Cosmology*, vol. 51, no. 10, Article ID R5352, 1995.
- [27] R. K. Kaul and P. Majumdar, "Logarithmic correction to the Bekenstein-Hawking entropy," *Physical Review Letters*, vol. 84, no. 23, pp. 5255–5257, 2000.
- [28] S. Das, P. Majumdar, and R. K. Bhaduri, "General logarithmic corrections to black-hole entropy," *Classical and Quantum Gravity*, vol. 19, no. 9, pp. 2355–2367, 2002.
- [29] A. Chatterjee and P. Majumdar, "Universal canonical black hole entropy," *Physical Review Letters*, vol. 92, no. 14, Article ID 141301, 2004.
- [30] F. J. Wang, Y. X. Gui, and C. R. Ma, "Entropy corrections for Schwarzschild black holes," *Physics Letters. B. Particle Physics, Nuclear Physics and Cosmology*, vol. 660, no. 3, pp. 144–146, 2008.
- [31] B. Eslam Panah, "Effects of energy dependent spacetime on geometrical thermodynamics and heat engine of black holes: Gravity's rainbow," *Physics Letters. B. Particle Physics, Nuclear Physics and Cosmology*, vol. 787, pp. 45–55, 2018.
- [32] P. Burikham and T. Chullaphan, "Comments on holographic star and the dual QGP," *Journal of High Energy Physics*, vol. 2014, no. 5, 2014.
- [33] P. Burikham and C. Promsiri, "The Mixed Phase of Charged AdS Black Holes," *Advances in High Energy Physics*, vol. 2016, 2016.
- [34] S. H. Hendi, S. Panahiyan, B. Eslam Panah, M. Faizal, and M. Momennia, "Critical behavior of charged black holes in Gauss-Bonnet gravity's rainbow," *Physical Review D: Particles, Fields, Gravitation and Cosmology*, vol. 94, no. 2, Article ID 024028, 2016.
- [35] D. Kastor, S. Ray, and J. Traschen, "Enthalpy and the mechanics of AdS black holes," *Classical and Quantum Gravity*, vol. 26, no. 19, Article ID 195011, 16 pages, 2009.

Research Article

Nonlocal Black Hole Evaporation and Quantum Metric Fluctuations via Inhomogeneous Vacuum Density

Alexander Y. Yosifov¹ and Lachezar G. Filipov²

¹Department of Physics and Astronomy, Shumen University, Bulgaria

²Space Research and Technology Institute, Bulgarian Academy of Sciences, Bulgaria

Correspondence should be addressed to Alexander Y. Yosifov; alexanderyosifov@gmail.com

Received 18 June 2018; Accepted 21 October 2018; Published 8 November 2018

Guest Editor: Farook Rahaman

Copyright © 2018 Alexander Y. Yosifov and Lachezar G. Filipov. This is an open access article distributed under the Creative Commons Attribution License, which permits unrestricted use, distribution, and reproduction in any medium, provided the original work is properly cited. The publication of this article was funded by SCOAP³.

Inhomogeneity of the *actual* value of the vacuum energy density is considered in a black hole background. We examine the back-reaction of a Schwarzschild black hole to the highly inhomogeneous vacuum density and argue the fluctuations lead to deviations from general relativity in the near-horizon region. In particular, we found that vacuum fluctuations *onto* the horizon trigger adiabatic release of quantum information, while vacuum fluctuations in the vicinity of the horizon produce potentially observable metric fluctuations of order of the Schwarzschild radius. Consequently, we propose a form of strong nonviolent nonlocality in which we simultaneously get nonlocal release of quantum information and observable metric fluctuations.

1. Introduction

Recently, Unruh et al. argued (see [1]) the observed small nonnegative cosmological constant can be achieved without introducing new degrees of freedom, *e.g.*, negative-pressure scalar field. Instead, they address the cosmological constant problem by embracing the diverging value of the vacuum energy density as predicted by quantum field theory, without applying any renormalization procedures. Interestingly, by studying the gravitational effects of the constantly fluctuating vacuum, they found its local energy density to be highly inhomogeneous. As a result of this inhomogeneity, the spatial distance between a pair of neighboring points undergoes constant phase transitions in the form of rapid changes between expansion and contraction. Also, the singular expectation value of the local energy density of the vacuum was argued to be harmless at the energy levels of effective field theory since the fluctuations lead to huge cancellations on cosmological scales and ultimately to the observed accelerating expansion of the universe.

In a separate work [2], we studied the back-reaction of a Schwarzschild black hole geometry to quantum vacuum fluctuations. We examined how the black hole metric back-reacts to vacuum fluctuations in two regions, *onto* the horizon,

and in the vicinity of the black hole. We considered vacuum fluctuations with local energy density *below* and *above* a certain threshold ζ . We found that “*strong*” quantum fluctuations (considered *onto* the horizon) lead to brief nonviolent departures from classicality, which allow for adiabatic leakage of low-temperature Hawking quanta at the necessary rate. In addition, we argued that quantum information can begin leaking out of the black hole as early as $r_s \log r_s$ after the initial collapse. The “*weak*” quantum fluctuations (considered in the vicinity of the black hole) were argued to be the microscopic source, which on scales of order of the Schwarzschild radius $\mathcal{O}(r_s)$ accumulates and produces metric fluctuations [2, 3].

The current model questions the classical black hole picture of local quantum field theory on a semiclassical geometry. In this work we apply the Unruh et al. model to Schwarzschild geometry; namely, we rewrite the equations of [1] in that background and study the gravitational effects of the inhomogeneous vacuum density. As a result, we propose a form of strong nonviolent nonlocality which yields significant modifications to the well-known general relativistic picture of black holes. The conjectured deviations from classicality lead simultaneously to nonlocal release of Hawking particles and quantum metric fluctuations. In fact, the present work may be

thought of as the microscopic origin of the initially proposed by Giddings nonviolent nonlocality model [4–6].

The paper is organized as follows. In Section 2 we summarize the relevant work. In Section 3 we rewrite the equations of [1] in Schwarzschild black hole background and show that we can derive nontrivial modifications to general relativity in the near-horizon region.

2. Summary of Related Work

To make the paper self-contained, we begin by making a brief review of the main results of [1, 2]. Note the Unruh et al. model will serve as a basis for the scenario we will present later in Section 3. In Section 2.1 we demonstrate the physical interpretation of the conjectured in [1] inhomogeneous microscopically diverging vacuum energy density, and its effects on cosmological scales. Then, in Section 2.2, we review [2] to show how we initially derived the “soft” but nontrivial modifications to general relativity in the near-horizon region.

2.1. Accelerating Expansion via Inhomogeneous Quantum Vacuum Density. In the generic Λ CDM model of the universe the vacuum energy density is considered to be constant and homogeneous throughout space. As it was pointed out in [1], however, this basic assumption is only true for the expectation value of the vacuum energy density. Its *actual* value, *i.e.*, the one obtained by performing repeated measurements at a particular spatial point, constantly fluctuates. Consequently, we get a picture, where although the expectation value is effectively constant and homogeneous on cosmological scales, the actual value is rapidly changing in both time, as well as from point to point. Physically, this inhomogeneity of the vacuum density implies the spatial distance between any pair of nearby points constantly changes between phases of expansion and contraction. As we show in greater detail later, this leads to very important results in a black hole background.

Taking the constantly fluctuating inhomogeneous vacuum density as a starting point, we now briefly demonstrate its effects in a general spacetime [1]. Note that in Section 3 we apply those results to Schwarzschild black hole geometry.

Suppose the local energy density $\rho_{x,x'}$ between a pair of neighboring spatial points x and x' in some general metric $g_{\mu\nu}$ is [1]

$$\rho_{x,x'} = \frac{\text{cov}(T_{00}(x), T_{00}(x'))}{\sigma_x \sigma_{x'}} \quad (1)$$

where

$$\sigma_x = \sqrt{\langle (T_{00}(x) - \langle T_{00}(x) \rangle)^2 \rangle} \quad (2)$$

Here, $T_{00}(x)$ and $T_{00}(x')$ are the local vacuum densities defined at the spatial points x and x' , respectively.

Evidently from (1), the value of $\rho_{x,x'}$ is determined by the covariant vacuum densities, defined at the neighboring spatial coordinates, namely, $T_{00}(x)$ and $T_{00}(x')$. Effectively, one can think of $\rho_{x,x'}$ as a 2-point correlation function. That is, in order for $\rho_{x,x'}$ to have a nontrivial value, it

must always be evaluated between close spacetime points. Otherwise, $\rho_{x,x'} \rightarrow 0$ as the separation between x and x' becomes large, in which case $T_{00}(x)$ and $T_{00}(x')$ are no longer correlated and thus evolve independently. The requirement that x and x' are close comes from the limited domain of dependence of individual vacuum fluctuations, that is, their high momentum/short wavelength.

Assuming $\rho_{x,x'}$ is nonvanishing, then in order for it to be positive/negative, both $T_{00}(x)$ and $T_{00}(x')$ need to be, respectively, above/below the zero threshold of $\langle T_{00} \rangle$ [1]

$$\rho_{x,x'} = \begin{cases} > 0 & \text{if } T_{00}(x), T_{00}(x') > 0 \\ < 0 & \text{if } T_{00}(x), T_{00}(x') < 0 \end{cases} \quad (3)$$

Therefore, the coefficient $\rho_{x,x'}$ shows the correlation between vacuum densities defined between a pair of nearby points x and x' . One should note that since in this model we do not apply any renormalization procedures, we cannot use the generic stress-energy tensor as a source in the Einstein field equations. Instead, we must slightly modify the stress tensor in order to account for the diverging expectation value of the vacuum fluctuations.

Studying the gravitational effects of the inhomogeneous vacuum density requires inhomogeneity of the underlying metric as well. So in this scenario, the scale factor has to have an extra stochastic component which would allow it to account for that inhomogeneity. Therefore, following (1), the generic scale factor of the standard Friedmann-Robertson-Walker metric is modified as

$$ds^2 = -dt^2 + a^2(t, x)(dx^2 + dy^2 + dz^2) \quad (4)$$

As a result of the vacuum inhomogeneity, the scale factor $a(t, x)$ now has additional degrees of freedom in the form of a space-dependent coupling term. That is, when the local scale factor is evaluated at a given spacetime point, its dynamics is dictated (sourced) by the stochastically varying vacuum fluctuations at that point. This richer structure of the scale factor allows for a pair of nearby points to be expanding or contracting, depending on the sign of $\rho_{x,x'}$, (3). In particular, for $\rho_{x,x'} > 0$ the spatial separation between the pair of points increases, while for $\rho_{x,x'} < 0$, the spatial separation decreases.

It was then shown in [1] that one could consider a local Hubble rate term and evaluate it between the neighboring x and x'

$$\nabla H = -4\pi G J \quad (5)$$

where $H \equiv \dot{a}/a$ is the Hubble parameter and J denotes the energy flux of the vacuum, which accumulates over a given region of space. Hence J can be thought of as a functional of the local energy density in that neighborhood $\langle J(x, x') \rangle \sim \int_x^{x'} \rho_{x,x'}$.

Interestingly enough, following the extra degrees of freedom of $a(t, x)$, ∇H was found to be *constantly* fluctuating with energy, sourced by the accumulation of the vacuum density.

The general solution of (5) reads

$$H(t, x) = H(t, x_0) - 4\pi G \int_x^{x'} J(t, x') (dx', dy', dz') \quad (6)$$

As (6) shows, the local Hubble rate depends on the spatial accumulation of J in the region between x and x' . To be more precise, we expect there may be some dissipation of the accumulated energy to nearby coordinates. For simplicity, however, throughout the paper we ignore all such effects and focus solely on individual 2-point functions.

Using this more complex spacetime dynamics induced by the inhomogeneous vacuum density, it was proposed that the equation of motion of ∇H goes as

$$\ddot{a} + \Omega^2(t, x) a = 0 \quad (7)$$

where

$$\Omega^2(t, x) = \frac{4\pi G}{3} \left(\rho + \sum_{i=1}^3 P_i \right), \quad \rho = T_{00}, \quad P_i = \frac{T_{ii}}{a^2} \quad (8)$$

In this case, (7) simply states that ∇H has the behavior of a harmonic oscillator. That is, it constantly fluctuates around its equilibrium point. Of course, every crossing of the equilibrium point is associated with a change of sign.

Let us briefly summarize the spacetime back-reaction to the conjectured in [1] constantly fluctuating inhomogeneous vacuum density. Physically, (5) and (7) describe a picture where the separation between a pair of neighboring points, $\Delta x \equiv |x - x'|$, is constantly fluctuating between phases of expansion and contraction. In fact, when Δx (herein defined as the proper distance) is expanding in some region, a neighboring region must be contracting, and vice versa. When a vacuum fluctuation with local energy density *above* its equilibrium point is considered between x and x' , Δx (i.e., the proper distance) grows. On the other hand, if the local energy density is *below* the equilibrium point, the proper distance Δx decreases. This enhanced spacetime dynamics is characterized by constant local phase transitions between expansion and contraction which happen as the local energy density of the vacuum goes through its equilibrium point and changes sign as it does so. Those constant phase changes accumulate and lead to massive cancellations on cosmological scales. However, assuming a slight *positive* excess, we get the observed cosmological expansion. Although the microscopic values of ρ may be huge, their infrared effects are small, i.e., the wild fluctuations do not lead to $\mathcal{O}(1)$ corrections in weak gravitational regimes. Besides, (8) tell us that the scale factor $a(t, x)$, in a given neighborhood, depends on the time-dependent frequency $\Omega(t, x)$ which exhibits quasiperiodic dynamics.

2.2. Unitary Black Hole Evolution and Horizon Fluctuations via Quantum Vacuum Fluctuations. In [2] we argued that treating gravity in the near-horizon region of Schwarzschild black hole as a field theory and considering its coupling to the matter fields in this region $\int \phi^{\mu\nu} T_{\mu\nu}$ produce fluctuations which modify the general relativistic description. We considered fluctuations with local energy density *below* and *above* ζ , where ζ is an arbitrary threshold. We then studied how the black hole geometry back-reacts to those fluctuations in two distinct regions, i.e., *onto* the horizon and just outside the black hole.

More precisely, we studied how the horizon geometry back-reacts to “strong” quantum fluctuations and how the near-horizon region back-reacts to “weak” fluctuations. The analysis was carried out under the assumptions that (i) black holes are fast scramblers [7], (ii) quantum information is found in the emitted Hawking particles, and (iii) the scrambled infallen information *need not* be embedded uniformly across the horizon.

Let us now precisely define what we mean by “strong” and “weak” quantum fluctuations.

(A) In a broader sense, we take a fluctuation to be *strong* if, when considered at asymptotic infinity, its local energy density leads to a localized particle production

$$a_i^\dagger |0\rangle = |x\rangle \quad (9)$$

Therefore, if we had a measuring apparatus counting the strong fluctuations in a given spacetime region Σ at asymptotic infinity, its results would be consistent with the expectation value of the number operator $\langle N \rangle$ in that region

$$\langle N \rangle = \sum_i^{\mathcal{N}} \int_{\Sigma} \varphi_i^{strong} \quad (10)$$

More specifically, in a black hole background, we argue a “strong” quantum fluctuation *onto* the horizon yields brief departure from local quantum field theory.

(B) A quantum fluctuation is taken as *weak* if its local energy density is below the threshold ζ . Because of the small local energy density, we assume the back-reaction of the background metric would be negligible if we considered weak fluctuations in a relatively small part of the near-horizon region. That is why we are interested in how the near-horizon metric back-reacts when the weak fluctuations are taken on scale $\mathcal{O}(r_S)$.

We argue that weak fluctuations on scale $\mathcal{O}(r_S)$ lead to nonperturbative effects which manifest in potentially observable metric fluctuations that can play an important role in observer complementarity and in gravitational wave astronomy in the form of detectable “echoes” and deviations from general relativity close to the horizon. We assume that away from a black hole the weak fluctuations do not lead to perturbations and leave the geodesic equation invariant. One should keep in mind that, although effectively negligible at infinity, when examined locally, the weak fluctuations still cause a pair of points to rapidly change phases between expansion and contraction.

To demonstrate how we define the weak fluctuations in the vicinity of the horizon we adopted the following analogy. Suppose we interpret individual fluctuations as harmonic oscillators, denoted by χ_i . Imagine we place the harmonic oscillators on a string in the vicinity of the horizon, Figure 1. Using an arbitrary normalized spacing ϵ , we can generally describe the string as

$$\sum_{i=1}^N \int_{S_2} d\varphi(n_i \varphi_i) \quad (11)$$

where φ_i is the oscillation frequency of the different harmonic oscillators.

In this picture we get an ensemble of fluctuations which, as we will argue later, yield coherent Schwarzschild-scale metric fluctuations. We assume separate harmonic oscillators *need not* have the same frequency. In fact, due to their limited domain of dependence (of order of the wavelength of the fluctuation), even neighboring harmonic oscillators have different frequencies. Thus an evolution equation for a particular spacetime region can be given in terms of a linear combination of the harmonic oscillators in that region. Like we mentioned earlier, despite the arbitrarily high (diverging) oscillating frequency a single harmonic oscillator may have microscopically, its effect in an infrared cut-off is negligible, and we do not expect $\mathcal{O}(1)$ corrections to the background metric.

Our analysis in [2] lead us to the following two main results.

First, we found that “strong” fluctuations, considered onto the horizon, lead to nonlocal release of quantum information via substantial deviations from classicality (for similar results [4–6]). We also demonstrated the model achieves Page-like evaporation spectrum [8, 9] and predicts black holes begin emitting Hawking particles in time, logarithmic in the entropy, *i.e.*, $t_* \sim \mathcal{O}(r_S \log r_S)$, where $t_* \ll M^3$.

Second, we found that “weak” quantum fluctuations, considered in the vicinity of the horizon, produce metric fluctuations which, although locally negligible, were shown to accumulate and on scale of order of the Schwarzschild radius lead to significant modifications to general relativity. Physically, the horizon periodically shifts (with frequency ω) radially outward with an amplitude δ , where $l_p \ll \delta < M$. In Schwarzschild coordinates the metric fluctuations translate to shift of the horizon from $r = 2M$ to $r = 2M + \delta$. One can think of the weak fluctuations as exerting a drag-like force on the black hole which produces observable macroscopic quantum gravity effects. Schematically

$$\omega \sim M_{BH}^{-1} \quad (12)$$

where ω is the frequency of the metric fluctuations.

The inverse proportionality between the frequency of the metric fluctuations and the mass of the black hole was argued to lead to thermodynamic instability at late times. Imagine a freely evaporating Schwarzschild black hole with no perturbations being introduced to it. Given $M_{BH} = 1/T$, we expect T to monotonically increase as the black hole evaporates. As we can see, (12) dictates that, as the black hole loses mass, ω steadily increases. Tracing that evolution to the final stages of the evaporation we assume the black hole becomes thermodynamically unstable as $M_{BH} \rightarrow m_P$, where m_P is the Planck mass. At that point, the black hole was conjectured to explode [10]. Here, late-time black hole evolution is in agreement with the thermodynamic instability first proposed in [10].

Recently, the authors of [11] numerically solved the Einstein equations modified with metric fluctuations. Similar to the current work, they showed that the proposed metric fluctuations lead to major deviations from the traditional general relativistic black hole description. In agreement with our results (in particular (12)), their analysis shows there is

an inverse proportionality between the frequency of the fluctuations, and black hole’s mass, where for a black hole binary merger, the overlap between the classical and the modified pictures of the waveform of the emitted gravitational waves decreases as the mass of the binary gets smaller. That is, as the frequency of the metric fluctuations increases, the near-horizon region deviates from general relativity even more significantly.

3. The Quantum Vacuum Origin of Metric Fluctuations and Nonlocal Evaporation

In the current section we adopt the Unruh et al. model and study its effects in Schwarzschild background. Consequently, we propose a dynamical mechanism for a form of strong nonviolent nonlocality which significantly modifies the traditional field theory picture in the near-horizon region. Specifically, we demonstrate how the conjectured in [1] inhomogeneous vacuum density leads simultaneously to quantum metric fluctuations [2, 4–6, 11–13] and nonlocal release of quantum information. One should note we do not attempt to quantize gravity in the current paper. Although the considered vacuum fluctuations may not be normalized, which modifies the stress-energy tensor and makes it nongeneric, they still contribute to its expectation value.

We aim to make the transition from cosmological scales to a black hole case more consistent. That is why we would like to first expand more on the implications of (1) for black hole backgrounds.

So let us now focus in more detail on how a pair of neighboring spacetime points x and x' is affected by the suggested extremely inhomogeneous vacuum density. Consider the following [1]:

$$\Delta \rho^2(\Delta x) = \frac{\left\langle \left\{ T_{00}(t, x) - T_{00}(t, x') \right\}^2 \right\rangle}{(4/3) \langle T_{00}(t, x) \rangle^2} \quad (13)$$

where $T_{00}(x)$ is the vacuum density at x and $\Delta x \equiv |x - x'|$ denotes the separation between x and x' .

Recall our earlier discussion about the evolution of the local energy density. Specifically, $\rho \rightarrow 0$ as Δx gets large, in which case $T_{00}(x)$ and $T_{00}(x')$ evolve independently.

Keeping that in mind, suppose a classical Schwarzschild solution

$$ds^2 = -\left(1 - \frac{2M}{r}\right) dt^2 + \left(1 - \frac{2M}{r}\right)^{-1} dr^2 + r^2 d\Omega^2 \quad (14)$$

where $d\Omega^2 = (d\theta^2 + \sin^2\theta d\phi^2)$.

Particularly, we are interested in rewriting (13) in Schwarzschild geometry. Working in a black hole background requires us to take into account the large gradient with respect to the horizon

$$\rho = \partial_r (\partial_r \phi)^2 \quad (15)$$

where ρ is the local energy density and ϕ is the gravitational potential. Thus near a matter source (15) is very sensitive to changes in the radial coordinate.

Therefore, by taking into account (15), we can rewrite (13) in Schwarzschild background as

$$\int_R \int_x^{x'} J^2 = \int_R \int_x^{x'} \frac{\langle \{ \partial_r J(t, x) - \partial_r J(t, x') \}^2 \rangle}{(4/3) \langle \partial_r J(t, x) \rangle^2} \quad (16)$$

where R denotes the near-horizon region and J is the vacuum accumulation term.

Notice that since we no longer work on cosmological scales, (15) becomes relevant, and so we substituted the vacuum energy density terms, defined on particular spacetime points, with J . Both terms $J(x)$ and $J(x')$ are calculated with respect to the horizon. Here, J is very sensitive to radial changes because of (15). In case x and x' both lie on the same $r = \text{const}$ surface, the expectation value of J between them varies stochastically.

Because J is of particular importance in the near-horizon neighborhood, let us now focus on its general properties.

Since the local energy density in a spacetime region which includes a black hole exhibits Gaussian-like distribution (15), we assume that as $r \rightarrow \infty$, $\langle J \rangle \rightarrow 0$. Although this may be true for the expectation value of J , its *actual* value must still constantly fluctuate due to the extremely inhomogeneous vacuum density. Clearly, we can see that, in the near-horizon region, J has a nonzero expectation value $\int_R \langle J \rangle \gg 0$. Therefore, the strongly radial-dependent behavior of J in the near-horizon region is trivially given as

$$\int_R \frac{\partial \langle J \rangle}{\partial r} \quad (17)$$

Where depending on r with respect to the horizon, the general solutions to (17) are

$$\int_R \frac{\partial \langle J \rangle}{\partial r} = \begin{cases} 0 & \text{for } r > r_S \\ > 0 & \text{for } 2M < r < r_S \end{cases} \quad (18)$$

Lastly, we can easily extend (17) to include an arbitrary number of gauge fields as

$$\int_R \langle T_{\mu\nu} \rangle + \frac{\partial \lambda}{\partial r} \quad (19)$$

where λ is the vacuum and $T_{\mu\nu}$ is the stress-energy tensor.

Note that, at constant r from the horizon, the energy density of the vacuum fluctuations depends on the internal degrees of freedom of the black hole and varies stochastically.

3.1. Metric Fluctuations: Weak Quantum Fluctuations = Local Phase Transitions. In this subsection we demonstrate how the proposed inhomogeneous vacuum density can modify the classical near-horizon physics and thus yield metric fluctuations. Specifically, by embracing the harmonic-oscillator-like constant phase transitions of ∇H , we rewrite (5) in Schwarzschild background and study how the metric back-reacts. Hence, we show that in this scenario one can obtain the conjectured quantum corrections to general relativity in the region just outside the black hole. Like we saw earlier, the

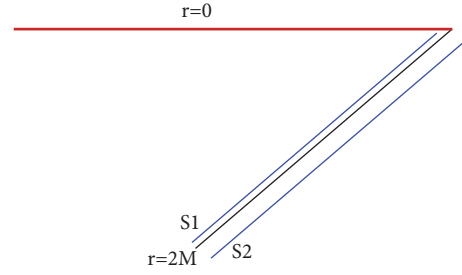


FIGURE 1: The bold red line is the singularity, and the bold black line, $r = 2M$, is the horizon. Imagine that S1 coincides with the horizon, and thus modes located on S1 are spacelike separated from an observer outside the black hole. Further, imagine that S2 is placed in the vicinity of the horizon.

microscopically extremely inhomogeneous vacuum density gives freedom to the scale factor to be locally expanding or contracting. Recall that in (5) we defined a local Hubble rate term ∇H and argued that, due to the inhomogeneous vacuum density, it has the dynamics of a harmonic oscillator (7). Namely, it constantly changes between phases of expansion and contraction.

For the sake of completeness we will examine coarse-grained and fine-grained version of the argument.

3.1.1. Coarse-Grained. In the particular case we neglect contributions coming from individual degrees of freedom and instead only focus on the effective (macroscopic) back-reaction on scale of order of the Schwarzschild radius.

Keeping in mind the large field-strength radial dependence in this region (15), we can rewrite (5) as

$$\int_{S1}^{S2} \nabla H = -4\pi G \int_{S1}^{S2} \partial_t \langle J \rangle \quad (20)$$

Unlike earlier, where we considered ∇H between the neighboring points x and x' , we now evaluate it in the region between S2 and S1 (the horizon), Figure 1.

To better demonstrate the back-reaction of the near-horizon geometry (20), consider the following *gedanken* experiment. Imagine S2 is a timelike hypersurface the size of the Schwarzschild radius just outside the black hole, coupled to the horizon degrees of freedom. Suppose we wish to evaluate the constant ∇H phase transitions in the region between the hypersurface and the horizon. We assume this region constantly undergoes uniform phase transitions with characteristic oscillation cycle time T , where by “uniform” we mean that, once every T , a phase change of ∇H in that region takes place. Unlike the cosmological case [1], here we assume that on every T the phase transitions average out to a small *negative* value. Here, T is given as

$$T = \frac{2\pi}{\Omega} \quad (21)$$

where Ω is time-dependent frequency which depends on $\langle T_{00} \rangle$.

That constant change between phases of expansion and contraction just outside the black hole (assuming a slight

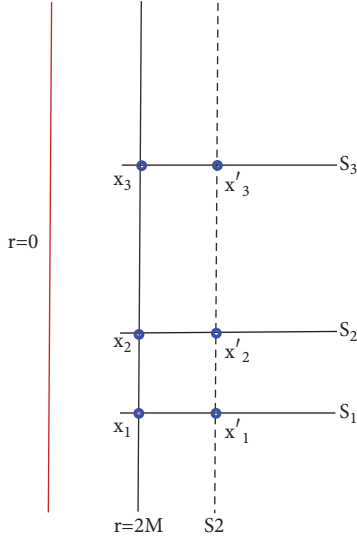


FIGURE 2: Similar to Figure 1, imagine S_1 coincides with the horizon. The dotted line, S_2 , is an artificial (nonphysical) timelike hypersurface in the vicinity of the horizon. Note that the blue dots x_i and x'_i are pairs of corresponding points, where $x_i \in S_1$, $x'_i \in S_2$, and $x_i, x'_i \in S_i$. Also, $\sum_i x_i \equiv S_1$ and $\sum_i x'_i \equiv S_2$.

negative excess every T) yields the dragging-like effect on the horizon. For simplicity, one can imagine the conjectured dynamics outside the black hole as the back-reaction of the horizon to a vector field coupled to matter fields in Rindler space, where we consider only contributions from modes very close to the horizon.

Physically, the back-reaction of the near-horizon region manifests as a slight outward shift of the horizon from $r = 2M$ to $r = 2M + \delta$ in Schwarzschild coordinates.

Imagine a far-away observer who cannot probe the region near the horizon. As far as she is concerned, she may effectively interpret those metric fluctuations as a Planck scale structure just outside the horizon (similar to the stretched horizon in observer complementarity or gravitational wave “echoes”). Different proposals have recently been made regarding the possibility of observing such quantum gravity effects (see [11–13]).

In conclusion, we can see that by rewriting (5) in a Schwarzschild black hole background we can effectively derive the proposed in [2–6, 11–13] metric fluctuations.

3.1.2. Fine-Grained. In this case we focus on contributions coming from individual degrees of freedom, *i.e.*, phase transitions of ∇H between a pair of corresponding points (say, x and x'), where both lie on the same spacelike hypersurface S_i in the near-horizon region. Namely, $x \in S_1$, $x' \in S_2$, and $x, x' \in S_i$, Figure 2.

Suppose we foliate the black hole spacetime into $t = \text{const}$ spacelike hypersurfaces. The particular foliation \mathcal{F} forms a family of extrinsically flat slicing. The slicing is generic and compatible with the Killing symmetries of the spherically symmetric spacetime. Thus \mathcal{F} preserves the spherical symmetry of the horizon geometry. The foliation can be

intuitively identified with a family of observers that only have time and radial components. We have chosen this more trivial geometry-preserving foliation as we aim to make the study of the back-reaction of the metric to individual 2-point functions easier.

Considering the particular foliation, we can straightforwardly rewrite (20) as

$$\sum_{i=1}^{\mathcal{N}} \nabla H_i = -4\pi G \sum_{i=1}^{\mathcal{N}} \langle J(x_i, x'_i) \rangle \quad (22)$$

where x and x' lie on the same spacelike hypersurface S_i and also $\sum_i x_i \equiv S_1$ and $\sum_i x'_i \equiv S_2$. We think of S_2 as an artificial (nonphysical) $r = \text{const}$ timelike hypersurface, and we assume it respects the same foliation as the horizon, Figure 2.

Evidently from (22), and in agreement with what we have argued earlier (5), the phase transitions of ∇H between a pair of neighboring points depend on the vacuum accumulation term J between them. Note that, due to the stochastic nature of the inhomogeneous vacuum density, the r.h.s. of (22) fluctuates constantly with field strength of order of the expectation value of the vacuum density in the region $\langle J(x, x') \rangle \approx \int_x^{x'} \langle T_{00} \rangle$.

However, (22) does not suffice for a complete description of the near-horizon dynamics. In addition, we also need to examine the evolution of the local scale factor. The equation of motion of $a(t, x)$ away from matter source is given as [1]

$$\tan \Theta_x = \frac{\Omega(0, x)}{\Omega(0, x')} \tan \Theta_x + \frac{4\pi G}{\Omega(0, x')} \int_x^{x'} J(0, x') dl' \quad (23)$$

where Θ_x is the initial phase of $a(t, x)$ at some arbitrary x .

Similar to what we did with (22), we now wish to express the equation of motion of $a(t, x)$ in the vicinity of the horizon. We do that in terms of the vacuum accumulation between a pair of corresponding points both of which lie on the same spacelike hypersurface. Neglecting the initial phase of $a(t, x)$ because of its constant fluctuations, we get

$$\tan \Theta_{x,x'} = \int_x^{x'} \frac{\Omega(x)}{\Omega(x')} \tan \Theta_{x,x'} + \frac{4\pi G}{\Omega(x')} \langle J(x, x') \rangle \quad (24)$$

where $\langle J(x, x') \rangle \approx \int_x^{x'} \langle T_{00} \rangle$. One should recall we focus on the small negative excess of the fluctuations every T .

The back-reaction of the near black hole geometry to the fluctuations between a pair of points on a single slice (22) is negligible, regardless of their microscopically singular expectation value. However, the spatial separation between the pair, Δx , is constantly fluctuating in a harmonic-oscillator-like manner between phases of expansion and contraction due to the inhomogeneous vacuum density. Consequently, by considering the constant fluctuations of Δx on all hypersurfaces of order of the Schwarzschild radius and assuming a

subtle *negative* excess on each slice every $T = 2\pi/\Omega$, the back-reaction accumulates and leads to deviations from general relativity which manifest in metric fluctuations.

In case $M_{BH} = \text{const}$, then $\langle J(x, x') \rangle$ depends on the dimensionality of the internal Hilbert space of the black hole and thus fluctuates stochastically

$$\langle J(x, x') \rangle \sim \int_x^{x'} \langle T_{00} \rangle \sim \dim(\mathcal{H}_{int}) \quad (25)$$

Therefore, following (15) and considering the microscopic back-reaction of the metric to the constantly fluctuating inhomogeneous vacuum density, the action for the near-horizon region reads

$$I_{near} = \int_R \int dx \int dt \left[\partial_r \lambda + T_{00}(x, x') \partial_r(x, x') \partial_t \lambda \right] \quad (26)$$

where the radial-dependent term of the vacuum $\partial_r \lambda$ is given by (15). The time-dependent vacuum term $\partial_t \lambda$ is taken on a $r = \text{const}$ surface with respect to the horizon and varies with the change in the mass of the black hole. The action is given in terms of couplings between the inhomogeneous constantly fluctuating and radially dependent vacuum term λ and the local energy density.

In summary, we demonstrated that when we consider the accumulated back-reaction of the background metric to the weak quantum vacuum fluctuations (*i.e.*, constant phase transitions of ∇H on different hypersurfaces) across the whole horizon area, $\mathcal{O}(r_s)$, we effectively get the proposed quantum metric fluctuations. The current derivation of these “soft” quantum modifications to the effective black hole geometry may be thought of as the microscopic origin of the metric fluctuations proposed by Giddings [4–6].

3.2. Nonlocal Black Hole Evaporation via Strong Quantum Vacuum Fluctuations. In this subsection we continue the study of the back-reaction of a Schwarzschild black hole to the constantly fluctuating inhomogeneous vacuum density. More precisely, we examine what effects the conjectured in [2] strong quantum vacuum fluctuations have, when they are considered *onto* the horizon. Specifically, we focus on how the locality constraint of local quantum field theory is modified due to the back-reaction of the metric to those fluctuations. As a result, we argue the horizon geometry *need not* always respect locality.

Given the fundamental degrees of freedom are not continuously distributed, we assume the semiclassical geometry to be just an effective field theory. Thus we expect the local quantum field theory evolution to only be approximately correct. As a result, deviations from it should be present in high energy regimes. For instance, black holes are one such place where we expect nonlocal corrections to manifest. That is the case since due to the large field-strength radial dependence in the near-horizon region, $\langle T_{00}(x) \rangle \gg \langle T_{00}(y) \rangle$, where $2M \leq x \leq R$ and $y > R$.

The particular strong vacuum fluctuations are assumed to have high enough local energy density as to yield “soft” (*i.e.*, brief and highly localized) nonlocal corrections to

local quantum field theory. Similar to [1], we assume these soft corrections manifest in the form of local singularity points.

Because in [1] the local scale factor $a(t, x)$, defined at each spacetime point, was argued to have a harmonic-oscillator-like behavior, as it changes phases, $a(t, x)$ must inevitably go through zero, *i.e.*, yield a local singularity point. However, this was shown to not be physically problematic. Since we interpret the local scale factor as a harmonic oscillator, $a(t, x) = 0$ is just a generic part of the oscillation cycle which takes place every T . Namely, a harmonic oscillator cannot change sign (phase) without passing through zero. Therefore, in a generic oscillation cycle a singularity point disappears almost immediately.

Similarly here, because we interpret individual strong vacuum fluctuations *onto* the horizon as harmonic oscillators, the microscopically singular expectation value (as predicted by quantum field theory) of a single strong fluctuation at a given point on the horizon should not be problematic. Likewise, we assume the local singularity point disappears almost immediately.

Physically, a strong vacuum fluctuation on the horizon briefly violates the generic locality constraint of local quantum field theory in that small region. As a result, this deviation from classicality allows quantum information to escape to asymptotic infinity at the necessary rate. Due to the small domain of dependence and brief lifespan of the local singularity points, their effects on a freely falling observer are negligible. These nonlocal corrections to the semiclassical geometry, although “soft,” have significant effect on the black hole over periods compared to its lifetime. That being said, we assume that, since the inhomogeneous vacuum density is constantly fluctuating, it will carry out quantum information at a rate of $\mathcal{O}(1)$ per light-crossing time as to restore unitary quantum mechanics. Such local quantum field theory modifications allow evaporation of information-carrying Hawking particles to begin as early as the scrambling time.

Let us clarify what we mean when we characterize the nonlocal corrections as “soft.” The local quantum field theory deviations (*i.e.*, local singularity points) are “brief” in the sense that they have very short lifespan of order of the lifetime of the fluctuation. Furthermore, the deviations are considered to be “highly localized” (*i.e.*, short wavelength/high momentum) since they manifest on scales of order of the wavelength of the fluctuation. Thus a strong vacuum fluctuation has a limited domain of dependence, and cannot lead to $\mathcal{O}(1)$ corrections to the background metric of a solar mass black hole.

Let us now point out an important distinction between the local singularity points on cosmological scales (away from a black hole) [1] and onto the horizon. We claim there is an intrinsic difference in the stage of the oscillation cycle during which a singularity point is produced. More precisely, a strong vacuum fluctuation (onto the horizon) produces a local singularity when, during an oscillation cycle T , it reaches the maximum of its local energy density, which also happens to be above a certain threshold ζ . On the other hand, the local scale factor $a(t, x)$ (away from a black hole) produces

a singularity point when it reaches zero during its oscillation cycle.

Moreover, the local singularity points, although similar, should not be mistaken with spacetime defects (see [14, 15]). For instance, (i) at a local singularity point/spacetime defect the curvature is divergent, and (ii) particle passing through (near) a spacetime defect/local singularity will be scattered off, *i.e.*, experience a local Lorentz boost.

4. Casimir Stress Interpretation

In [1] the Casimir effect was used as a tool for illustrating the effects of vacuum fluctuations. In the current Section we present a toy model in which we restate the conjectured quantum metric fluctuations in terms of the Casimir effect in the near-horizon region. Specifically, we present the metric fluctuations in the language of the Casimir effect just outside the black hole (between $S1$ and $S2$, Figure 1).

Likewise, we will examine two distinct cases: coarse-grained and fine-grained.

In its general form, the Casimir stress equation is given as [1]

$$S(t, x, y) = T_{zz}^{\text{inside}} - T_{zz}^{\text{outside}} \quad (27)$$

In this picture, imagine the role of the pair of conducting plates is played by $S1$ and $S2$, Figure 1.

4.1. Coarse-Grained. Similar to Section 3, we are only interested in the effective (macroscopic) dynamics and thus neglect contributions from individual degrees of freedom.

We can straightforwardly expand (27) in the near-horizon region as

$$\int_{S1}^{S2} S(t, x, y) = \int_{S1}^{S2} \langle \partial_r \rho_{in} \rangle - \int_{S2}^{\infty} \langle \partial_r \rho_{out} \rangle \quad (28)$$

where, as we showed earlier, the expectation value of the radially dependent local energy density $\langle \partial_r \rho_{in} \rangle$ is of order of the vacuum accumulation term in that region

$$\int_{S1}^{S2} \langle \partial_r \rho_{in} \rangle \sim \int_{S1}^{S2} \partial_r \langle J \rangle \quad (29)$$

Following (18), we expect $\int_R \langle J \rangle \gg 0$ and $\int_{\infty} \langle J \rangle = 0$. That is, the second term on the r.h.s. of (28) vanishes at the asymptotic limit; namely $\langle \rho_{out} \rangle \rightarrow 0$ as $r \rightarrow \infty$.

Therefore, we generally get

$$\langle T_{zz}^{\text{inside}} \rangle \gg \langle T_{zz}^{\text{outside}} \rangle \quad (30)$$

One should keep in mind that, regardless of whether $\langle J \rangle$ vanishes or not, it constantly fluctuates due to the inhomogeneous vacuum density.

Notice that (30) is in agreement with the general construction of the Casimir effect (27).

Considering the microscopic back-reaction of the spherically symmetric background metric that we discussed earlier and the greater energy density in the vicinity of the horizon (30), one can easily see how the proposed quantum metric fluctuations of order of the Schwarzschild radius emerge in this setting.

4.2. Fine-Grained. Similar to our approach in Section 3.1.2, we begin by foliating the horizon region into individual spacelike hypersurfaces. As a result, we can now express the l.h.s. of (28) as

$$\int_R S(t, x, y) = \sum_{i=1}^{\mathcal{N}} \langle J(x_i, x'_i) \rangle \quad (31)$$

Evidently, the nonvanishing l.h.s. of (28) can straightforwardly be rewritten as a linear combination of vacuum accumulation terms, defined on individual slices.

Due to the inhomogeneous vacuum density, Δx on any given slice constantly fluctuates between phases of expansion and contraction. Moreover, because of the strong field gradient (15) and considering (30), we assume that in the large \mathcal{N} limit (*i.e.*, of order of the Schwarzschild radius) the accumulated back-reaction is positive. Thus, an observer at asymptotic infinity sees oscillations of the horizon as a back-reaction of the underlying black hole metric.

In summary, we see that with minimal assumptions one can restate our earlier argument about quantum metric fluctuations in terms of the Casimir effect in a near black hole region.

5. Conclusions

In the current work we studied how a Schwarzschild black hole back-reacts to the constantly fluctuating inhomogeneous vacuum density proposed in [1]. More precisely, embracing the microscopically singular expectation value of the local energy density of the inhomogeneous vacuum fluctuations (predicted by quantum field theory), we examined how a black hole metric back-reacts in two distinct regions: the vicinity of the black hole and onto the horizon. As a result, we demonstrated that vacuum fluctuations above a given threshold, considered onto the horizon, cause deviations from local quantum field theory. Meanwhile, fluctuations below that threshold, considered in the vicinity of the horizon, lead to potentially observable metric fluctuations of order of the Schwarzschild radius.

Physically, the conjectured modifications of local quantum field theory, induced by the strong vacuum fluctuations onto the horizon, were argued to lead to nonlocal release of information-carrying Hawking particles. In fact, we argued that in this scenario a black hole can begin radiating quantum information to infinity as early as the scrambling time [2].

On the other hand, we argued that weak fluctuations in the near-horizon region yield observable macroscopic quantum gravity effects in the form of metric fluctuations of order of the Schwarzschild radius, that is, constant oscillations of the horizon between $r = 2M$ and $r = 2M + \delta$. As far as a distant observer is concerned, we assume she may interpret the conjectured metric fluctuations as a physical membrane just outside the horizon. Thus the proposed metric fluctuations may serve as the microscopic origin of the stretched horizon in observer complementarity [16]. Also, we assume the proposed metric fluctuations play a significant role in binary black hole mergers. In particular, they may

produce observable postmerger gravitational wave “echoes” similar to [17].

The recent advances in gravitational wave astronomy have opened new possibilities for experimentally testing models, similar to this one, which predict deviations from general relativity in the near-horizon region. In addition, the current scenario could also be approached from an accretion disk perspective as we believe the metric fluctuations may have measurable effects on accretion disk flows around a black hole.

Data Availability

No data were used to support this study.

Conflicts of Interest

The authors declare that they have no conflicts of interest.

Acknowledgments

This research is supported in part by project RD-08-112/2018 of Shumen University.

References

- [1] Q. Wang, Z. Zhu, and W. G. Unruh, “How the huge energy of quantum vacuum gravitates to drive the slow accelerating expansion of the Universe,” *Physical Review D: Particles, Fields, Gravitation and Cosmology*, vol. 95, no. 10, Article ID 103504, 2017.
- [2] A. Y. Yosifov and L. G. Filipov, “Entropic entanglement: information prison break,” *Advances in High Energy Physics*, vol. 2017, Article ID 8621513, 7 pages, 2017.
- [3] A. Y. Yosifov and L. G. Filipov, “Oscillations for Equivalence Preservation and Information Retrieval from Young Black Holes,” *Electronic Journal of Theoretical Physics*, vol. 36, pp. 183–198, 2016.
- [4] S. B. Giddings, “Models for unitary black hole disintegration,” *Physical Review D: Particles, Fields, Gravitation and Cosmology*, vol. 85, no. 4, Article ID 044038, 2012.
- [5] S. B. Giddings, “Nonviolent information transfer from black holes: a field theory parametrization,” *Physical Review D*, vol. 88, no. 2, Article ID 024018, 2013.
- [6] S. B. Giddings, “Modulated Hawking radiation and a nonviolent channel for information release,” *Physics Letters B*, vol. 738, pp. 92–96, 2014.
- [7] P. Hayden and J. Preskill, “Black holes as mirrors: quantum information in random subsystems,” *Journal of High Energy Physics*, vol. 2007, no. 9, article 120, 2007.
- [8] D. N. Page, “Information in black hole radiation,” *Physical Review Letters*, vol. 71, no. 23, pp. 3743–3746, 1993.
- [9] D. N. Page, “Black hole information,” in *Proceedings of the 5th Canadian Conference on General Relativity and Relativistic Astrophysics*, R. B. Mann and R. G. McLenaghan, Eds., pp. 13–15, University of Waterloo, Singapore, 1993.
- [10] S. W. Hawking, “Black hole explosions?” *Nature*, vol. 248, no. 5443, pp. 30–31, 1974.
- [11] S. L. Liebling, M. Lippert, and M. Kavic, “Probing near-horizon fluctuations with black hole binary mergers,” *Journal of High Energy Physics*, vol. 2018, no. 3, 2018.
- [12] S. B. Giddings, “Possible observational windows for quantum effects from black holes,” *Physical Review D: Particles, Fields, Gravitation and Cosmology*, vol. 90, no. 12, 2014.
- [13] S. B. Giddings, “Gravitational wave tests of quantum modifications to black hole structure – with post-GW150914 update,” *Classical and Quantum Gravity*, vol. 33, p. 235010, 2016.
- [14] S. Hossenfelder, “Phenomenology of Space-time Imperfection I: Nonlocal Defects,” *Physical Review*, vol. 88, p. 124030, 2013.
- [15] S. Hossenfelder and R. G. Torromé, “General relativity with space-time defects,” *Classical and Quantum Gravity*, vol. 35, 2018.
- [16] L. Susskind, L. Thorlacius, and J. Uglum, “The stretched horizon and black hole complementarity,” *Physical Review D: Particles, Fields, Gravitation and Cosmology*, vol. 48, no. 8, pp. 3743–3761, 1993.
- [17] J. Abedi and N. Afshordi, “Echoes from the Abyss: A highly spinning black hole remnant for the binary neutron star merger GW170817,” <https://arxiv.org/abs/1803.10454>.

Research Article

Localization of Energy-Momentum for a Black Hole Spacetime Geometry with Constant Topological Euler Density

Irina Radinschi ¹, Theophanes Grammenos,² Farook Rahaman ³, Andromahi Spanou,⁴ Marius Mihai Cazacu,¹ Surajit Chattopadhyay,⁵ and Antonio Pasqua ⁶

¹Department of Physics “Gh. Asachi” Technical University, Iasi 700050, Romania

²Department of Civil Engineering, University of Thessaly, 383 34 Volos, Greece

³Department of Mathematics, Jadavpur University, Kolkata 700 032, West Bengal, India

⁴School of Applied Mathematics and Physical Sciences, National Technical University of Athens, 157 80 Athens, Greece

⁵Department of Mathematics, Amity University, Kolkata 700135, India

⁶Department of Physics, University of Trieste, 34127 Trieste, Italy

Correspondence should be addressed to Irina Radinschi; radinschi@yahoo.com

Received 5 July 2018; Revised 1 October 2018; Accepted 16 October 2018; Published 25 October 2018

Academic Editor: Elias C. Vagenas

Copyright © 2018 Irina Radinschi et al. This is an open access article distributed under the Creative Commons Attribution License, which permits unrestricted use, distribution, and reproduction in any medium, provided the original work is properly cited. The publication of this article was funded by SCOAP³.

The evaluation of the energy-momentum distribution for a new four-dimensional, spherically symmetric, static and charged black hole spacetime geometry with constant nonzero topological Euler density is performed by using the energy-momentum complexes of Einstein and Møller. This black hole solution was recently developed in the context of the coupled Einstein–nonlinear electrodynamics of the Born-Infeld type. The energy is found to depend on the mass M and the charge q of the black hole, the cosmological constant Λ , and the radial coordinate r , while in both prescriptions all the momenta vanish. Some limiting and particular cases are analyzed and discussed, illustrating the rather extraordinary character of the spacetime geometry considered.

1. Introduction

The issue of energy-momentum localization systematised researchers' work in a special way. Looking deeply into the problem, it was clear that the main difficulty consists in the lack of a proper definition for the energy density of gravitational backgrounds. In this light, much research work has been done over the last years concerning the best tools used for the energy-momentum localization. A brief survey points out the leading role played notably by super-energy tensors [1–4], quasi-local expressions [5–10], and the famous energy-momentum complexes of Einstein [11, 12], Landau-Lifshitz [13], Papapetrou [14], Bergmann-Thomson [15], Møller [16], and Weinberg [17]. Among the aforementioned computational tools, the energy-momentum complexes have been proven to be interesting and useful as well due to the diverse and numerous reasonable expressions that can be obtained by their application. Some observations

are in order here. First, according to their underlying mathematical mechanism, their construction involves the use of two parts, one for the matter and the other for the gravitational field. Second, despite the fact that the energy-momentum complexes allow one to obtain many interesting and physically meaningful results for different space-time geometries, their construction is connected to an inherent central problem, namely, their coordinate dependence. As it is well-known from the relevant literature, this problem has found a solution in the case of the Møller energy-momentum complex. Indeed, the calculations for the energy-momentum of a given gravitational background in the Møller prescription enable the use of any coordinates such that the energy density component transforms as a four-vector density under purely spatial coordinate transformations for metrics with a line element of the form $ds^2 = g_{00}dt^2 - g_{ij}dx^i dx^j$. As for the other energy-momentum complexes, the Schwarzschild Cartesian coordinates and the Kerr-Schild

Cartesian coordinates have to be utilised for the calculations providing physically reasonable results for the cases of space-time geometries in $(3+1)$, $(2+1)$, and $(1+1)$ dimensions (see, e.g., [18–34] and references therein). At this point it should be noticed that, in order to avoid the coordinate dependence, an alternative method for the computation of the energy and momentum distributions is provided by the teleparallel equivalent of general relativity and certain modified versions of the teleparallel theory (see, e.g., [35–40] and references therein).

Regarding the Einstein, Landau-Lifshitz, Papapetrou, Bergmann-Thomson, Weinberg, and Møller energy-momentum complexes there is an agreement with the definition of the quasi-local mass introduced by Penrose [41] and developed by Tod [42] for some gravitational backgrounds. We point out that some rather recent works show that several energy-momentum complexes “provide the same results” for any metric of the Kerr-Schild class and indeed even for solutions that are more general than those of the Kerr-Schild class (see, e.g., [43, 44] and the interesting article [45] on the subject). Further, the entire historical development of the energy-momentum complexes that started with the formulation of their definitions also includes the attempts made for their rehabilitation [46–49]. In this sense, perhaps the most interesting issue was the fact that different energy-momentum complexes yield the same results for the energy-momentum distribution in the case of various gravitating systems.

The present paper has the following structure: in Section 2 we describe the new class of four-dimensional spherically symmetric, static, and charged black hole solutions with constant nonzero topological Euler density which we will consider. Section 3 focuses on the presentation of the Einstein and Møller prescriptions used for performing the calculations. In Section 4 we present the calculations and the results obtained for the energy and momentum distributions. Finally, in the discussion provided in Section 5, we give a brief description of the results obtained as well as some limiting and particular cases. Throughout we use geometrized units ($c = G = 1$) and the signature chosen is $(+, -, -, -)$. Further, the calculations are performed by using the Schwarzschild Cartesian coordinates $\{t, x, y, z\}$ for the Einstein energy-momentum complex and the Schwarzschild coordinates $\{t, r, \theta, \varphi\}$ for the Møller energy-momentum complex. Finally, Greek indices run from 0 to 3, while Latin indices range from 1 to 3.

2. Description of the New Black Hole Solution with Constant Topological Euler Density

This section deals with the presentation of the new four-dimensional spherically symmetric, static, and charged black hole solution with constant topological Euler density [50] examined in the present study. Connecting geometry with topology, from the generalised Gauss-Bonnet theorem (see, e.g., [51]) applied to four dimensions the Euler-Poincaré characteristic is obtained by the integral of the Euler density

$$\mathcal{G} = \frac{1}{32\pi^2} (R^{\kappa\lambda\mu\nu} R_{\kappa\lambda\mu\nu} - 4R^{\kappa\lambda} R_{\kappa\lambda} + R^2), \quad (1)$$

where $R_{\kappa\lambda\mu\nu}$ is the Riemann curvature tensor, $R_{\kappa\lambda}$ is the Ricci tensor, and R is the Ricci scalar (often the topological Euler density is given without the factor $1/32\pi^2$ (see, e.g., [52])). In fact, the terms in the parenthesis constitute the so-called “quadratic Gauss-Bonnet term” in the Lovelock gravity Lagrangian). For a general, spherically symmetric and static geometry described by the line element

$$ds^2 = f(r) dt^2 - f(r)^{-1} dr^2 - r^2 (d\theta^2 + \sin^2\theta d\varphi^2) \quad (2)$$

(1) becomes

$$\mathcal{G} = \frac{4}{r^2} \{f'(r)^2 + [f(r) - 1] f''(r)\}, \quad (3)$$

where the constant $32\pi^2$ has been absorbed in \mathcal{G} . For constant topological density $\mathcal{G} = \alpha \neq 0$, (3) gives for the metric function

$$f(r) = 1 \pm \left(1 - 2A + Br + \frac{\alpha r^4}{24}\right)^{1/2}, \quad (4)$$

with A, B arbitrary constants. In what follows, we will keep only the negative sign of (4), as it is the one leading to black hole solutions.

The new solution derived in [50] is based on the coupling of gravity to nonlinear electromagnetic fields as described by the nonlinear generalisation of Maxwell’s electrodynamics according to the Born-Infeld theory. Thus, in the chosen case of electrovacuum, the radial electric field,

$$E(r) = \frac{r^2}{4q} (4R^{\mu\nu} R_{\mu\nu} - R^2)^{1/2} \quad (5)$$

where q is the electric charge, solves the Einstein-nonlinear electrodynamics coupled system with the Ricci tensor $R_{\mu\nu}$ and the Ricci scalar R calculated by using the line element (2) and the metric function (4). In fact, with the values $A = 1/2 + q^2\Lambda/3$, $B = 4M\Lambda/3$, and $\alpha = 8\Lambda^2/3$, with Λ being the cosmological constant and M being the mass of the black hole, the line element (2) with the metric function (4) becomes

$$ds^2 = \left[1 - \sqrt{\frac{4M\Lambda r}{3} + \frac{\Lambda^2 r^4}{9} - \frac{2q^2\Lambda}{3}}\right] dt^2 - \left[1 - \sqrt{\frac{4M\Lambda r}{3} + \frac{\Lambda^2 r^4}{9} - \frac{2q^2\Lambda}{3}}\right]^{-1} dr^2 - r^2 (d\theta^2 + \sin^2\theta d\varphi^2), \quad (6)$$

describing a Reissner-Nordström-de Sitter black hole space-time geometry.

Now one can distinguish between two different cases, namely, the massive case ($M \neq 0$) and the massless case ($M = 0$). In the first case, (6), when $q = 0$ and $\Lambda > 0$, shows that the geometry is regular everywhere except at the origin $r = 0$. However, this case has no particular interest

from the electrodynamic viewpoint. Black hole solutions with zero mass were proposed as a conjecture by A. Strominger [53] in order to explain conifold singularities in the context of string theory. In particular, the ten-dimensional IIA (resp., IIB) string theory admits black D2- (resp., D3-) brane solutions with a mass proportional to their area. After applying a Calabi-Yau compactification these solutions may wrap around minimal 2-surfaces (resp., 3-surfaces) in the Calabi-Yau space and they appear as four-dimensional black holes. As the area of the surface around which they wrap is let to go to zero, the corresponding extremal black holes become massless, topologically stable, structures. In fact, the existence of stable black hole solutions with zero ADM mass was shown in [54] although their relation to the massless solutions suggested in [53] is still not clarified. Indeed, since then there has been an increasing interest in massless black hole solutions (see, e.g., [55, 56] and references therein). Recently, massless black hole solutions were obtained from the dyonic black hole solution of the Einstein–Maxwell–dilaton theory [57]. Although the black hole solution examined here does not originate from string theory we will proceed to the consideration of the massless ($M = 0$) case despite its physically dubious character.

Thus for $M = 0$, the line element (6) becomes

$$ds^2 = \left[1 - \sqrt{\frac{\Lambda^2 r^4}{9} - \frac{2q^2 \Lambda}{3}} \right] dt^2 - \left[1 - \sqrt{\frac{\Lambda^2 r^4}{9} - \frac{2q^2 \Lambda}{3}} \right]^{-1} dr^2 - r^2 (d\theta^2 + \sin^2 \theta d\varphi^2). \quad (7)$$

Here, when $q = 0$ and $\Lambda \neq 0$ the de Sitter solution is obtained, while for $q \neq 0$ but $\Lambda = 0$ one gets the Minkowski solution. In the case $q \neq 0$ and $\Lambda < 0$, an event horizon exists and the spacetime is singular at the origin $r = 0$, while the electric field is everywhere regularisable. An overall detailed study of the black hole's behavior in the massive as well as in the massless case is presented in [50].

3. Einstein and Møller Energy-Momentum Complexes

In this section we outline the definitions of the Einstein and Møller energy-momentum complexes.

The expression for the Einstein energy-momentum complex [11] in the case of a (3+1)-dimensional gravitational background was later found to be given by

$$\theta_\nu^\mu = \frac{1}{16\pi} h_\nu^{\mu\lambda}. \quad (8)$$

The Freud superpotentials $h_\nu^{\mu\lambda}$ in (8) are calculated by the compact formula (found by Landau and Lifshitz)

$$h_\nu^{\mu\lambda} = \frac{1}{\sqrt{-g}} g_{\nu\sigma} \left[-g \left(g^{\mu\sigma} g^{\lambda\kappa} - g^{\lambda\sigma} g^{\mu\kappa} \right) \right]_{,\kappa} \quad (9)$$

and satisfy the antisymmetric property

$$h_\nu^{\mu\lambda} = -h_\nu^{\lambda\mu}. \quad (10)$$

We notice that in the Einstein prescription the local conservation law is respected:

$$\theta_{\nu,\mu}^\mu = 0. \quad (11)$$

Consequently, the energy and momentum can be calculated in Einstein's prescription by

$$P_\nu = \iiint \theta_\nu^0 dx^1 dx^2 dx^3. \quad (12)$$

Here, θ_0^0 and θ_i^0 represent the energy and momentum density components, respectively.

Applying Gauss' theorem, the energy-momentum reads

$$P_\mu = \frac{1}{16\pi} \iint h_\mu^{0i} n_i dS, \quad (13)$$

with n_i being the outward unit normal vector over the surface dS . In (13) the component P_0 represents the energy.

According to [16], the Møller energy-momentum complex is

$$\mathcal{F}_\nu^\mu = \frac{1}{8\pi} M_\nu^{\mu\lambda}, \quad (14)$$

with the Møller superpotentials $M_\nu^{\mu\lambda}$ given by

$$M_\nu^{\mu\lambda} = \sqrt{-g} \left(\frac{\partial g_{\nu\sigma}}{\partial x^\kappa} - \frac{\partial g_{\nu\kappa}}{\partial x^\sigma} \right) g^{\mu\kappa} g^{\lambda\sigma}. \quad (15)$$

The Møller superpotentials $M_\nu^{\mu\lambda}$ satisfy the antisymmetric property

$$M_\nu^{\mu\lambda} = -M_\nu^{\lambda\mu}. \quad (16)$$

As in the case of the Einstein prescription, in the Møller prescription the local conservation law is also satisfied:

$$\frac{\partial \mathcal{F}_\nu^\mu}{\partial x^\mu} = 0. \quad (17)$$

In (17) the component \mathcal{F}_0^0 represents the energy density and \mathcal{F}_i^0 gives the momentum density components.

For the Møller energy-momentum complex, the energy-momentum distributions are given by

$$P_\nu = \iiint \mathcal{F}_\nu^0 dx^1 dx^2 dx^3. \quad (18)$$

In particular, the energy distribution can be computed by

$$E = \iiint \mathcal{F}_0^0 dx^1 dx^2 dx^3. \quad (19)$$

Using Gauss' theorem one gets

$$P_\nu = \frac{1}{8\pi} \iint M_\nu^{0i} n_i dS, \quad (20)$$

where, again, n_i is the outward unit normal vector over the surface dS .

4. Energy and Momentum Distribution for the Black Hole Solution with Constant Topological Euler Density

To compute the energy and momenta with the Einstein energy-momentum complex, we have to transform the metric given by the line element (6) in Schwarzschild Cartesian coordinates by using the coordinate transformation $x = r \sin \theta \cos \varphi$, $y = r \sin \theta \sin \varphi$, $z = r \cos \theta$. Thus, we obtain a new form for the line element:

$$ds^2 = f(r) dt^2 - (dx^2 + dy^2 + dz^2) - \frac{f^{-1}(r) - 1}{r^2} (xdx + ydy + zdz)^2. \quad (21)$$

In Schwarzschild Cartesian coordinates for $\nu = 0, 1, 2, 3$ and $i = 1, 2, 3$ we find the following vanishing components of the superpotentials h_ν^{0i} :

$$\begin{aligned} h_1^{01} &= h_1^{02} = h_1^{03} = 0, \\ h_2^{01} &= h_2^{02} = h_2^{03} = 0, \\ h_3^{01} &= h_3^{02} = h_3^{03} = 0. \end{aligned} \quad (22)$$

In order to compute the nonvanishing components of the superpotentials in the Einstein prescription we use (9) and we obtain the following expressions:

$$h_0^{01} = \frac{2x}{r^2} \sqrt{\frac{4M\Lambda r}{3} + \frac{\Lambda^2 r^4}{9} - \frac{2q^2 \Lambda}{3}}, \quad (23)$$

$$h_0^{02} = \frac{2y}{r^2} \sqrt{\frac{4M\Lambda r}{3} + \frac{\Lambda^2 r^4}{9} - \frac{2q^2 \Lambda}{3}}, \quad (24)$$

$$h_0^{03} = \frac{2z}{r^2} \sqrt{\frac{4M\Lambda r}{3} + \frac{\Lambda^2 r^4}{9} - \frac{2q^2 \Lambda}{3}}. \quad (25)$$

With the aid of the line element (21), the expression for the energy given by (13), and the expressions (23)-(25) for the superpotentials, we get the energy distribution for the examined black hole in the Einstein prescription:

$$E_E = \frac{r}{2} \sqrt{\frac{4M\Lambda r}{3} + \frac{\Lambda^2 r^4}{9} - \frac{2q^2 \Lambda}{3}}. \quad (26)$$

In order to calculate the momentum components we employ (13) and (22) and performing the calculations we find that all the momenta vanish:

$$P_x = P_y = P_z = 0. \quad (27)$$

In the Møller prescription we perform the calculations in Schwarzschild coordinates $\{t, r, \theta, \varphi\}$ with the aid of the line element (6) and we find only one nonvanishing superpotential:

$$M_0^{01} = -\frac{1}{6} \frac{12M\Lambda + 4\Lambda^2 r^3}{\sqrt{12M\Lambda r + \Lambda^2 r^4 - 6q^2 \Lambda}} r^2 \sin \theta. \quad (28)$$

TABLE 1: Limiting behavior of the energy of the massive ($M \neq 0$) black hole solution in the Einstein and Møller prescriptions.

Energy	$r \rightarrow \infty$	$q = 0$
E_E	∞	$\frac{r}{2} \sqrt{\frac{4M\Lambda r}{3} + \frac{\Lambda^2 r^4}{9}}$
E_M	$-\infty$	$-\frac{r^2}{12} \frac{12M\Lambda + 4\Lambda^2 r^3}{\sqrt{12M\Lambda r + \Lambda^2 r^4}}$

Using the above expression for the superpotential and the expression for the energy obtained from (20), we get the energy in the Møller prescription:

$$E_M = -\frac{r^2}{12} \frac{12M\Lambda + 4\Lambda^2 r^3}{\sqrt{12M\Lambda r + \Lambda^2 r^4 - 6q^2 \Lambda}}. \quad (29)$$

Finally, all the momenta are found to be zero:

$$P_r = P_\theta = P_\varphi = 0. \quad (30)$$

5. Discussion

Our paper focuses on the analysis of the energy-momentum localization for a new four-dimensional, spherically symmetric, static, and charged black hole spacetime geometry with constant nonzero topological Euler density, given by the line element (6). The solution describes a Reissner–Nordström–de Sitter spacetime geometry as the result of the coupling of Einstein gravity with nonlinear electrodynamics of the Born–Infeld type. For $q = 0$ the solution has a near-de Sitter behavior, while for $\Lambda > 0$ the solution is regular everywhere except at the origin $r = 0$. To perform our study we use the Einstein and Møller energy-momentum complexes. The calculations provide the well-defined expressions (26) and (29) for the energy distribution in both prescriptions. These energy distributions depend on the mass M and the charge q of the black hole, the cosmological constant Λ , and the radial coordinate r , while in both energy-momentum complexes all the momenta vanish.

In order to study the limiting behavior of the energy distributions obtained by the Einstein and Møller prescriptions, we consider the energy for $r \rightarrow \infty$ in the uncharged case $q = 0$ for the massive ($M \neq 0$) black hole and for $r \rightarrow \infty$, $\Lambda = 0$, and $q = 0$ for the massless ($M = 0$) black hole.

Starting with the massive black hole ($M \neq 0$) the results for the limiting cases $r \rightarrow \infty$ and $q = 0$ are presented in Table 1.

For the charged ($q \neq 0$) black hole without cosmological constant ($\Lambda = 0$), the spacetime geometry becomes the Minkowski geometry. If the black hole is uncharged ($q = 0$) and the cosmological constant is nonzero ($\Lambda > 0$), then the spacetime is regular everywhere except at the origin $r = 0$, as it is inferred from the calculation of the curvature invariants (Kretschmann and Ricci) in [50]. Indeed, the fact that, despite the regular behavior of the metric, the energy diverges at infinity in both prescriptions can possibly be attributed to the de Sitter like asymptotic behavior of the solution. The

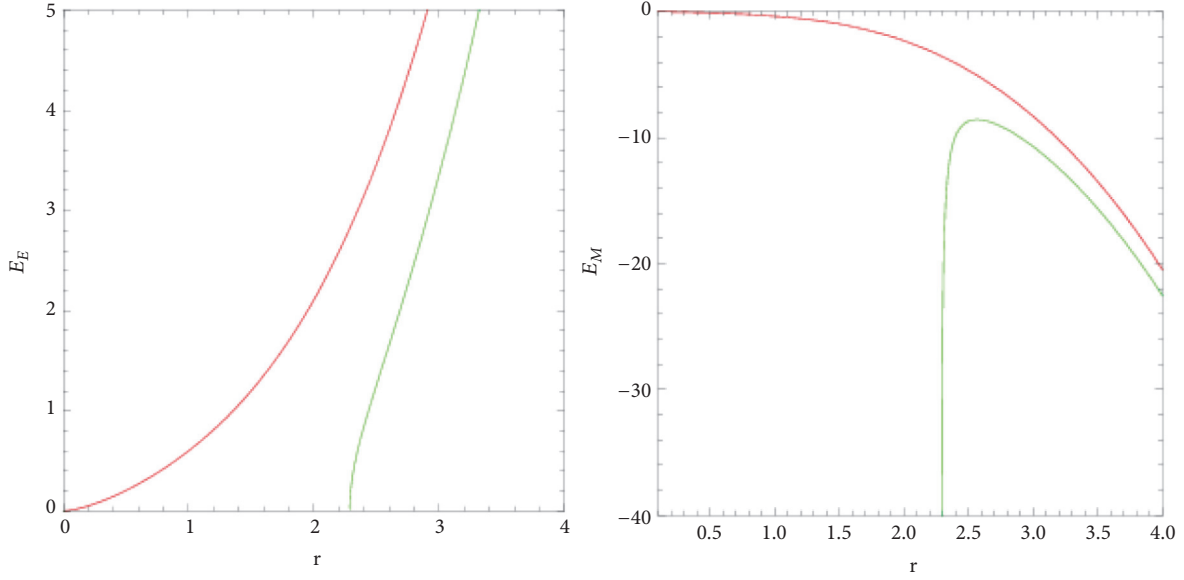


FIGURE 1: Evolution of the Einstein energy E_E (left) and of the Møller energy E_M (right) with respect to the r coordinate for the massive and charged black hole. In both cases we have chosen $M = 1$ and $q = 1$, while the red line and the green line correspond to $\Lambda = 1$ and $\Lambda = -1$, respectively.

evolution of the Einstein energy and of the Møller energy with respect to the r coordinate, as given by (26) and (29), is presented for $\Lambda > 0$ and $\Lambda < 0$ in Figure 1. In fact, the Møller energy given by (29) is negative for a large range of values for r and the parameters M , Λ , and q . The observed negativity of the energy might sound a note of warning regarding the physical interpretation of this result and, consequently, the merits of the Møller complex despite the physically acceptable results obtained by the latter in many other cases. Furthermore, if one considers the behavior of the energy regarding r , one concludes that the fourth-degree polynomial $12M\Lambda r + \Lambda^2 r^4 - 6q^2\Lambda$ in the denominator of (29) vanishes for several sets of values for the parameters M , Λ , and q with its roots consisting in two real and two complex conjugate solutions. As a result, at finite distances from the black hole the Einstein energy, given by (26), vanishes, while the Møller energy, given by (29), diverges. Equally interesting is the vanishing of the third-degree polynomial $12M\Lambda + 4\Lambda^2 r^3$ in the nominator of (29). In this case, one real and two complex conjugate solutions are obtained for every finite value of the mass parameter M and $\Lambda < 0$. As a result, the Møller energy vanishes at finite distances from the black hole. We have not found any plausible explanation for this rather pathological behavior of the energy in the two prescriptions, beside the fact that the black hole solution considered is quite peculiar. Some more light could be shed on this strange state of things through the comparison of the present results with the energy calculated, for example, by the Landau-Lifshitz and the Weinberg energy-momentum complexes for the metric considered, a task left for future work.

In the massless case ($M = 0$), when the black hole is charged ($q \neq 0$) and the cosmological constant is nonzero ($\Lambda \neq 0$), the spacetime geometry is described by the line element (7). In fact, an event horizon appears at $r_{\text{eh}} = [9/\Lambda^2 +$

TABLE 2: Energy of the massless ($M = 0$) black hole solution in the Einstein and Møller prescriptions.

Energy	$q \neq 0, \Lambda \neq 0$	$q = 0, \Lambda \neq 0$
E_E	$\frac{r}{2} \sqrt{\frac{\Lambda^2 r^4}{9} - \frac{2q^2 \Lambda}{3}}$	$\frac{r}{2} \sqrt{\frac{\Lambda^2 r^4}{9}}$
E_M	$-\frac{1}{3} \frac{\Lambda^2 r^5}{\sqrt{\Lambda^2 r^4 - 6q^2 \Lambda}}$	$-\frac{1}{3} \frac{\Lambda^2 r^5}{\sqrt{\Lambda^2 r^4}}$

$6q^2/\Lambda]^{1/4}$ for a negative cosmological constant $\Lambda < -3/(2q^2)$. Further, when $\Lambda > 0$, at the position $r_s = (6q^2/\Lambda)^{1/4}$ a singularity appears, while, when $\Lambda < 0$, this singularity can be avoided but there appears another singularity at $r = 0$ (see [50]). If this massless black hole has no charge ($q = 0$) but the cosmological constant is nonzero ($\Lambda \neq 0$), then a de Sitter spacetime geometry is obtained:

$$ds^2 = \left(1 - \sqrt{\frac{\Lambda^2 r^4}{9}}\right) dt^2 - \left(1 - \sqrt{\frac{\Lambda^2 r^4}{9}}\right)^{-1} dr^2 - r^2 (d\theta^2 + \sin^2 \theta d\varphi^2), \quad (31)$$

with a cosmological horizon appearing at $r_{\text{ch}} = \sqrt{3/\Lambda}$. The energy of the massless black hole for the charged and the uncharged case, computed in the Einstein and Møller prescriptions, is presented in Table 2.

In Table 3 we present the limiting behavior of the Einstein energy and the Møller energy for the charged and the uncharged massless ($M = 0$) black hole as $r \rightarrow \infty$. In both cases the cosmological constant is nonzero.

TABLE 3: Limiting behavior of the energy of the massless black hole solution in the Einstein and Møller prescriptions.

Energy	$q \neq 0, \Lambda \neq 0, r \rightarrow \infty$	$q = 0, \Lambda \neq 0, r \rightarrow \infty$
E_E	∞	∞
E_M	$-\infty$	$-\infty$

According to the obtained results, we come to the conclusion that the Einstein and Møller energy-momentum complexes may provide an instructive tool for the study of the energy-momentum localization of gravitating systems, although in this work we cannot reach a definite answer to the problem of localization. That being said, the investigation of the problem of the energy-momentum localization in the context of the black hole solution considered here, by applying other energy-momentum complexes as well as the teleparallel equivalent of general relativity (TEGR), is planned as a future perspective.

Data Availability

No data were used to support this study.

Conflicts of Interest

The authors declare that they have no conflicts of interest.

Acknowledgments

Farook Rahaman and Surajit Chattopadhyay are grateful to the Inter-University Centre for Astronomy and Astrophysics (IUCAA), India, for providing the Associateship Programme. Farook Rahaman is thankful to DST, Govt. of India, for providing financial support under the SERB programme. Irina Radinschi is indebted to Prof. Rodica Tudorache and Prof. Dorel Fetcu from the Department of Mathematics and Informatics of the “Gheorghe Asachi” Technical University, Iasi, Romania, for their invaluable assistance.

References

- [1] L. Bel, “Définition d’une densité d’énergie et d’un état de radiation totale généralisée,” *Comptes Rendus de l’Académie des Sciences*, vol. 246, pp. 3015–3018, 1958.
- [2] I. Robinson, “On the Bel–Robinson tensor,” *Classical and Quantum Gravity*, vol. 14, no. 1A, pp. A331–A333, 1997.
- [3] M. A. G. Bonilla and J. M. M. Senovilla, “Some properties of the BEL and BEL–Robinson tensors,” *General Relativity and Gravitation*, vol. 29, no. 1, pp. 91–116, 1997.
- [4] J. M. Senovilla, “Super-energy tensors,” *Classical and Quantum Gravity*, vol. 17, no. 14, pp. 2799–2841, 2000.
- [5] J. D. Brown and J. W. York Jr., “Quasilocal energy and conserved charges derived from the gravitational action,” *Physical Review D: Particles, Fields, Gravitation and Cosmology*, vol. 47, no. 4, pp. 1407–1419, 1993.
- [6] S. A. Hayward, “Quasilocal gravitational energy,” *Physical Review D: Particles, Fields, Gravitation and Cosmology*, vol. 49, no. 2, pp. 831–839, 1994.
- [7] C.-M. Chen and J. M. Nester, “Quasilocal quantities for general relativity and other gravity theories,” *Classical and Quantum Gravity*, vol. 16, no. 4, pp. 1279–1304, 1999.
- [8] C.-C. M. Liu and S.-T. Yau, “Positivity of quasilocal mass,” *Physical Review Letters*, vol. 90, no. 23, Article ID 231102, 2003.
- [9] L. Balart, “Quasilocal energy, Komar charge and horizon for regular black holes,” *Physics Letters B*, vol. 687, no. 4-5, pp. 280–285, 2010.
- [10] L. B. Szabados, “Quasi-local energy-momentum and angular momentum in general relativity,” *Living Reviews in Relativity*, vol. 12, article 4, 2009.
- [11] A. Einstein, “On the general theory of relativity,” *Sitzungsberichte der Königlich Preussischen Akademie der Wissenschaften*, vol. 47, pp. 778–786, 1915, Addendum: Sitzungsberichte der Königlich Preussischen Akademie der Wissenschaften., vol. 47, p. 799, 1915.
- [12] A. Trautman, “Conservation Laws in General Relativity,” in *Gravitation: An Introduction to Current Research*, L. Witten, Ed., pp. 169–198, John Wiley & Sons, New York, NY, USA, 1962.
- [13] L. D. Landau and E. M. Lifshitz, *The Classical Theory of Fields*, Addison-Wesley, Reading, Mass, USA, 1951.
- [14] A. Papapetrou, “Einstein’s theory of gravitation and flat space,” *Proceedings of the Royal Irish Academy*, vol. 52, pp. 11–23, 1948.
- [15] P. G. Bergmann and R. Thomson, “Spin and angular momentum in general relativity,” *Physical Review A: Atomic, Molecular and Optical Physics*, vol. 89, no. 2, pp. 400–407, 1953.
- [16] C. Møller, “On the localization of the energy of a physical system in the general theory of relativity,” *Annals of Physics*, vol. 4, no. 4, pp. 347–371, 1958.
- [17] S. Weinberg, *Gravitation and Cosmology: Principles and Applications of General Theory of Relativity*, John Wiley & Sons, New York, NY, USA, 1972.
- [18] A. K. Sinha, G. K. Pandey, A. K. Bhaskar et al., “Effective gravitational mass of the Ayón-Beato and García metric,” *Modern Physics Letters A*, vol. 30, no. 25, 1550120, 12 pages, 2015.
- [19] S. K. Tripathy, B. Mishra, G. K. Pandey, A. K. Singh, T. Kumar, and S. S. Xulu, “Energy and momentum of Bianchi type VI h universes,” *Advances in High Energy Physics*, vol. 2015, Article ID 705262, 8 pages, 2015.
- [20] M. Saleh, B. B. Thomas, and T. C. Kofane, “Energy distribution and thermodynamics of the quantum-corrected Schwarzschild black hole,” *Chinese Physics Letters*, vol. 34, no. 8, Article ID 080401, 2017.
- [21] P. K. Sahoo, K. L. Mahanta, D. Goit et al., “Einstein energy-momentum complex for a phantom black hole metric,” *Chinese Physics Letters*, vol. 32, no. 2, Article ID 020402, 2015.
- [22] I.-C. Yang, “Some characters of the energy distribution for a charged wormhole,” *Chinese Journal of Physics*, vol. 53, no. 6, Article ID 110108, pp. 1–4, 2015.
- [23] I. Radinschi and T. Grammenos, “Møller’s energy-momentum complex for a spacetime geometry on a noncommutative curved D3-brane,” *International Journal of Theoretical Physics*, vol. 47, no. 5, pp. 1363–1372, 2008.
- [24] I.-C. Yang, C.-L. Lin, and I. Radinschi, “The energy of regular black hole in general relativity coupled to nonlinear electrodynamics,” *International Journal of Theoretical Physics*, vol. 48, no. 1, pp. 248–255, 2009.
- [25] E. C. Vagenas, “Energy distribution in 2D stringy black hole backgrounds,” *International Journal of Modern Physics A*, vol. 18, no. 31, pp. 5781–5794, 2003.

- [26] I. Radinschi, F. Rahaman, and A. Banerjee, "On the energy of Hořava-Lifshitz black holes," *International Journal of Theoretical Physics*, vol. 50, no. 9, pp. 2906–2916, 2011.
- [27] I. Radinschi, F. Rahaman, T. Grammenos, and S. Islam, "Einstein and Møller Energy-Momentum Complexes for a New Regular Black Hole Solution with a Nonlinear Electrodynamics Source," *Advances in High Energy Physics*, vol. 2016, Article ID 9049308, 2016.
- [28] I. Radinschi, T. Grammenos, F. Rahaman et al., "Energy-Momentum for a Charged Nonsingular Black Hole Solution with a Nonlinear Mass Function," *Advances in High Energy Physics*, vol. 2017, Article ID 7656389, 10 pages, 2017.
- [29] M. Abdel-Megied and R. M. Gad, "Møller's Energy in the Kantowski-Sachs Space-Time," *Advances in High Energy Physics*, vol. 2010, Article ID 379473, 6 pages, 2010.
- [30] M. Sharif and M. Azam, "Energy-momentum distribution: some examples," *International Journal of Modern Physics A*, vol. 22, no. 10, pp. 1935–1951, 2007.
- [31] T. Multamäki, A. Putaja, E. C. Vagenas, and I. Vilja, "Energy-momentum complexes in $f(R)$ theories of gravity," *Classical and Quantum Gravity*, vol. 25, no. 7, Article ID 075017, 2008.
- [32] L. Balart, "Energy distribution of (2+1)-dimensional black holes with nonlinear electrodynamics," *Modern Physics Letters A*, vol. 24, no. 34, pp. 2777–2785, 2009.
- [33] A. M. Abbassi, S. Mirshekari, and A. H. Abbassi, "Energy-momentum distribution in static and nonstatic cosmic string space-times," *Physical Review D: Particles, Fields, Gravitation and Cosmology*, vol. 78, no. 6, Article ID 064053, 9 pages, 2008.
- [34] J. Matyjasek, "Some remarks on the Einstein and Møller pseudotensors for static and spherically-symmetric configurations," *Modern Physics Letters A*, vol. 23, no. 8, pp. 591–601, 2008.
- [35] J. W. Maluf, "The teleparallel equivalent of general relativity," *Annalen der Physik*, vol. 525, no. 5, pp. 339–357, 2013.
- [36] R. M. Gad, "On teleparallel version of stationary axisymmetric solutions and their energy contents," *Astrophysics and Space Science*, vol. 346, no. 2, pp. 553–557, 2013.
- [37] G. G. Nashed, "Energy and momentum of a spherically symmetric dilaton frame as regularized by teleparallel gravity," *Annalen der Physik*, vol. 523, no. 6, pp. 450–458, 2011.
- [38] G. G. L. Nashed, "Braneworld black holes in teleparallel theory equivalent to general relativity and their Killing vectors, energy, momentum and angular momentum," *Chinese Physics B*, vol. 19, no. 2, p. 020401, 2010.
- [39] M. Sharif and A. Jawad, "Energy contents of some well-known solutions in teleparallel gravity," *Astrophysics and Space Science*, vol. 331, no. 1, pp. 257–263, 2010.
- [40] J. G. da Silva and S. C. Ulhoa, "On gravitational energy in conformal teleparallel gravity," *Modern Physics Letters A*, vol. 32, no. 21, 1750113, 10 pages, 2017.
- [41] R. Penrose, "Quasilocal mass and angular momentum in general relativity," *Proceedings of the Royal Society A Mathematical, Physical and Engineering Sciences*, vol. 381, no. 1780, pp. 53–63, 1982.
- [42] K. P. Tod, "Some examples of Penrose's quasi-local mass construction," *Proceedings of the Royal Society A Mathematical, Physical and Engineering Sciences*, vol. 388, no. 1795, pp. 457–477, 1983.
- [43] J. M. Aguirregabiria, A. Chamorro, and K. S. Virbhadra, "Energy and angular momentum of charged rotating black holes," *General Relativity and Gravitation*, vol. 28, no. 11, pp. 1393–1400, 1996.
- [44] S. S. Xulu, "Bergmann-Thomson energy-momentum complex for solutions more general than the Kerr-Schild class," *International Journal of Theoretical Physics*, vol. 46, no. 11, pp. 2915–2922, 2007.
- [45] K. S. Virbhadra, "Naked singularities and Seifert's conjecture," *Physical Review D: Particles, Fields, Gravitation and Cosmology*, vol. 60, no. 10, Article ID 104041, 6 pages, 1999.
- [46] G. Sun, C.-M. Chen, J.-L. Liu, and J. M. Nester, "An optimal choice of reference for the quasi-local gravitational energy and angular momentum," *Chinese Journal of Physics*, vol. 52, no. 1, part 1, pp. 111–125, 2014.
- [47] C.-M. Chen and J. M. Nester, "A symplectic Hamiltonian derivation of the quasilocal energy-momentum for general relativity," *Gravitation & Cosmology*, vol. 6, no. 4, pp. 257–270, 2000.
- [48] C.-M. Chen, J. M. Nester, and R.-S. Tung, "Gravitational energy for GR and Poincaré gauge theories: a covariant Hamiltonian approach," *International Journal of Modern Physics D: Gravitation, Astrophysics, Cosmology*, vol. 24, no. 11, 1530026, 73 pages, 2015.
- [49] J. M. Nester, C. M. Chen, J.-L. Liu, and G. Sun, "A reference for the covariant Hamiltonian boundary term," in *Relativity and Gravitation-100 years after Einstein in Prague*, J. Bicák and T. Ledvinka, Eds., pp. 177–184, Springer, 2014.
- [50] P. Bargueño and E. C. Vagenas, "Black holes with constant topological Euler density," *European Physics Letters*, vol. 115, no. 6, p. 60002, 2016.
- [51] P. Gilkey, J. H. Park, and R. Vázquez-Lorenzo, *Aspects of Differential Geometry I*, chapter 3, Morgan & Claypool Publishers, 2015.
- [52] M. Ammon and J. Erdmenger, *Gauge/Gravity Duality – Foundations and Applications*, Cambridge University Press, 2015.
- [53] A. Strominger, "Massless black holes and conifolds in string theory," *Nuclear Physics. B. Theoretical, Phenomenological, and Experimental High Energy Physics. Quantum Field Theory and Statistical Systems*, vol. 451, no. 1-2, pp. 96–108, 1995.
- [54] K. Behrndt, "About a class of exact string backgrounds," *Nuclear Physics. B. Theoretical, Phenomenological, and Experimental High Energy Physics. Quantum Field Theory and Statistical Systems*, vol. 455, no. 1-2, pp. 188–210, 1995.
- [55] R. Emparan, "Massless black hole pairs in string theory," *Physics Letters. B. Particle Physics, Nuclear Physics and Cosmology*, vol. 387, no. 4, pp. 721–726, 1996.
- [56] U. Nucamendi and D. Sudarsky, "Black holes with zero mass," *Classical and Quantum Gravity*, vol. 17, no. 19, pp. 4051–4058, 2000.
- [57] P. Goulart, "Massless black holes and charged wormholes in string theory," 2016, <https://arxiv.org/abs/1611.03164>.

Research Article

Revisiting the Black Hole Entropy and the Information Paradox

Ovidiu Cristinel Stoica 

Department of Theoretical Physics, National Institute of Physics and Nuclear Engineering – Horia Hulubei, Bucharest, Romania

Correspondence should be addressed to Ovidiu Cristinel Stoica; holotronix@gmail.com

Received 12 July 2018; Revised 13 September 2018; Accepted 20 September 2018; Published 10 October 2018

Academic Editor: Theophanes Grammenos

Copyright © 2018 Ovidiu Cristinel Stoica. This is an open access article distributed under the Creative Commons Attribution License, which permits unrestricted use, distribution, and reproduction in any medium, provided the original work is properly cited. The publication of this article was funded by SCOAP³.

The black hole information paradox and the black hole entropy are currently extensively researched. The consensus about the solution of the information paradox is not yet reached, and it is not yet clear what can we learn about quantum gravity from these and the related research. It seems that the apparently irreducible paradoxes force us to give up on at least one well-established principle or another. Since we are talking about a choice between the principle of equivalence from general relativity and some essential principles from quantum theory, both being the most reliable theories we have, it is recommended to proceed with caution and search more conservative solutions. These paradoxes are revisited here, as well as the black hole complementarity and the firewall proposals, with an emphasis on the less obvious assumptions. Some arguments from the literature are reviewed, and new counterarguments are presented. Some less considered less radical possibilities are discussed, and a conservative solution, which is more consistent with both the principle of equivalence from general relativity and the unitarity from quantum theory, is discussed.

1. Introduction

By applying general relativity and quantum field theory on curved spacetime, Hawking arrives at the conclusion that the information is lost in the black holes, and this breaks the predictability [1]. Apparently, no matter how was formed and what information was contained in the matter falling in a black hole, the only degrees of freedom characterizing it are its mass, angular momentum, and electric charge, so black holes are “hairless” [2–5]. This means that the information describing the matter crossing the event horizon is lost, because nothing outside the black hole reminds us of it. In general relativity, this information loss is irreversible, not only because we cannot extract it from beyond the event horizon, but also because in a finite time the infalling matter reaches the singularity of the black hole. And the occurrence of singularities is unavoidable, according to the singularity theorems [6–8]. This already seemed to be a problem, but it would not be so severe if we at least know that the information is still there, censored behind the horizon [9, 10]. But we are not even left with this possibility, since Hawking proved that quantum effects make the black holes evaporate [11]. It was already expected that black holes should radiate, after the

realization that they have entropy and temperature [11, 12], and these should be part of an extension of thermodynamics which includes matter as well. This evaporation is thermal, and after the black hole reaches a planckian size, it explodes and reveals to the exterior world that the information is indeed lost. In addition, if the quantum state prior to the formation of the black hole was pure, the final state is mixed, increasing the drama even more. Moreover, a problem seems to occur long before the complete evaporation, since the black hole entropy seems to increase during evaporation, until the Page time is reached [13]. Some consider this to be the real black hole information paradox [14].

Mainly for general relativists the information loss seemed to be definitive and yet not a big problem [15], position initially endorsed by Hawking too. On the other hand, for high energy physicists, loss of unitarity was considered a problem, and various proposals to fix it appeared (see, e.g., [16–18] and references therein). For example, *remnants* were proposed, containing the information remaining in the black hole after evaporation. The remnant is in a mixed state but together with the Hawking radiation forms a pure state. A possible cause for remnants is the yet unknown quantum corrections expected to occur when the black hole becomes

too small, comparable to the Planck scale, and the usual analysis of Hawking radiation no longer applies [19–21]. There are other possibilities, some being discussed in the above-mentioned reviews. For example, it was proposed that the information leaks out of the black hole through evaporation, including by quantum tunneling, that it escapes at the final explosion or that it leaks out of the universe in a baby universe [22, 23]. Another possibility is that the information escapes as Hawking radiation by *quantum teleportation* [24], which actually happens as if the particle zig-zags forward and backward in time to escape without exceeding the speed of light. This is not so unnatural, if we assume that the final boundary condition at the future singularity of the black hole forces the maximally entangled particles to be in a singlet state. There are also *bounce scenarios* [25] or by using local scale invariance to avoid singularities [26]. Some bounce scenarios are based on *loop quantum gravity*, like [27, 28], as well as *black hole to white hole tunneling scenarios* in which quantum tunneling is supposed to break the Einstein equation, and the apparent horizon is prevented to evolve into an event horizon [29, 30]. It would take a long review to do justice to the various proposals, and this is beyond the scope of this article.

The dominating proposed solution was, for two decades, *black hole complementarity* [31–33]. This was later challenged by the *firewall paradox* [34]. The debate is not settled down yet, but the dominant opinion seems to be that we have to give up at least one principle considered fundamental so far, and the unlucky one is most likely the principle of equivalence from general relativity. One of the objectives of the present article is to show that we can avoid this radical solution while keeping unitarity.

The problems related to the black hole information loss are considered important, being seen as a benchmark for the candidate theories of quantum gravity, which are expected to solve these problems.

The main purpose of this discussion is to identify the main assumptions and see if it is possible to solve the problem in a less radical way. I argue that some of the usually made assumptions are unnecessary, that there are less radical possibilities, and that the black hole information problem is not a decisive test for candidate theories of quantum gravity. New counterarguments to some popular models proposed in relation to the black hole information problem are the following. Black hole complementarity is discussed in Section 3, in particular the fact that an argument by Susskind, aiming to prove that no-cloning is satisfied by the black hole complementarity, does not apply to most black holes (Section 3.1), the fact that its main argument, the “no-omniscience” proposal, does not really hold for black holes in general (Section 3.3), and the fact that black hole complementarity is also at odds with the principle of equivalence (Section 3.2). As for the firewall proposal, in Section 4.1, I explain why the tacit assumption that unitarity should apply only to the exterior of the black hole, and that we should ignore the interior, is not justified, and anyway if taken as true, it imposes boundary conditions to the field, which is why the firewall seems to emerge. Section 5 is dedicated to black hole entropy. In Section 5.1, I present an argument based

on time symmetry that the true entropy is not necessarily proportional to the area of the event horizon and at best in the usual cases is bounded. This has negative implications to the various proposals that the event horizon would contain some bits representing the microstates of the black hole, discussed in Section 5.4. This may also explain the so-called “real black hole information paradox,” discussed in Section 6. Section 5.2 contains an explanation of the fact that if the laws of black hole mechanics should be connected with those of thermodynamics, this happens already at the classical level, so they are not necessarily indications of quantum gravity or tests of such approaches. Section 5.3 contains arguments that one should not read too much in the so-called no-hair theorems; in particular they do not constrain, contrary to a widespread belief, neither the horizon nor the interior of a black hole. A major motivation invoked for the theoretical research of the black hole information and entropy is that these may provide a benchmark to test approaches to quantum gravity, but in Section 5.5 I argue that these features appear merely by considering quantum fields on spacetime. Consequently, any approach to quantum gravity which includes both quantum field theory and the curved spacetime of general relativity, as a minimal requirement, will also satisfy the consequences derived from them.

To my knowledge, the above-mentioned arguments, presented in more detail in the following, are new, and in the cases when I was aware of other results seeming to point in the same direction, I gave the relevant references. While most part of the article may look like a review of the literature, it is a critical review, aiming to point out some assumptions which, in my opinion, drove us too far from the starting point, which is just the most straightforward and conservative combination of quantum field theory with the curved background of general relativity. The entire structure of arguments converges therefore towards a more conservative picture than that suggested by the more popular proposals. The counterarguments are meant to build up the willingness to consider the less radical proposal that I made, which follows naturally from my work on singularities in standard general relativity ([35] and references therein) and is discussed in Section 7. The background theory is presented in Section 7.1, and a new, enhanced version of the proposal is made in Section 7.2.

2. Black Hole Evaporation

Hawking’s derivation of the black hole evaporation [1, 11] has been disputed and checked many times and redone in different settings, and it turned valid, at most allowing some improvements of the unavoidable approximations, as well as mild generalizations. But the result is correct; the radiation is as predicted and thermal in the Kubo-Martin-Schwinger sense [36, 37]. Moreover, it is corroborated via the principle of equivalence with the Unruh radiation, which takes place in the Minkowski spacetime for accelerated observers [38]. Hawking’s derivation is obtained in the framework of quantum field theory on curved spacetime, but since the black hole is considered large and the time scale is also large, the spacetime curvature induced by the radiation is ignored.

The derivation, as well as the discussion surrounding black hole information, requires the framework of quantum field theory on curved spacetime [39–41]. Quantum field theory on curved spacetime is a good effective limit of the true but yet unknown theory of quantum gravity. On curved background, there is no Poincaré symmetry to select a preferred vacuum, so there is no canonical Fock space construction of the Hilbert space. The stress-energy expectation value of the quantum fields, $\langle \hat{T}_{ab}(x) \rangle$, is connected with the spacetime geometry via Einstein's equation,

$$R_{ab} - \frac{1}{2}Rg_{ab} + \Lambda g_{ab} = \frac{8\pi G}{c^4} \langle \hat{T}_{ab}(x) \rangle, \quad (1)$$

where R_{ab} is the *Ricci tensor*, R is the *scalar curvature*, g_{ab} is the *metric tensor*, Λ is the *cosmological constant*, G is Newton's gravitational constant, and c is the speed of light constant.

But in the calculations of the Hawking radiation, the gravitational backreaction is ignored, being very small. To have well behaved solutions, the spacetime slicing is such that the intrinsic and extrinsic curvatures of the spacelike slices are considered small compared to the Planck length; the curvature in a neighborhood of the spacelike surface is also taken to be small. The wavelengths of particles are considered large compared to the Planck length. The energy and momentum densities are assumed small compared to the Planck density. The stress-energy tensor satisfies the positive energy conditions. The solution evolves smoothly into future slices that also satisfy these conditions.

The canonical (anti)commutation relations at distinct points of the slice are imposed. A decomposition into positive and negative frequency solutions is assumed to which the Fock construction is applied to obtain the Hilbert space. The renormalizability of the stress-energy expectation value $\langle \hat{T}_{ab}(x) \rangle$ and the uniqueness of the n -point function $\langle \hat{\phi}(x_1) \dots \hat{\phi}(x_n) \rangle$ are ensured by imposing the *Hadamard condition* to the quantum states [41]. This condition is needed because when two of the n -points coincide, there is no invariant way to define the n -point function on curved spacetime. The Hadamard condition is imposed on the *Wightman function* $G(x, y) = \langle \hat{\phi}(x)\hat{\phi}(y) \rangle$, and it is preserved under time evolution. This condition is naturally satisfied in the usual quantum field theory in Minkowski spacetime. It ensures the possibility to renormalize the stress-energy tensor and to prevent it from diverging.

The Fock space construction of the Hilbert space can be made in many different ways in curved spacetime, since the decomposition into positive and negative frequency solutions depends on the choice of the slicing of spacetime into spacelike hypersurfaces.

Suppose that a basis of annihilation operators is (\hat{a}_ν) , and they satisfy the canonical commutation relations if they are bosons and the canonical anticommutation relations if they are fermions. Another observer has a different basis of annihilation operators (\hat{b}_ω) , assuming that the spacetime is curved or that one observer accelerates with respect to

the other. The two bases are related by the *Bogoliubov transformations*,

$$\hat{b}_\omega = \frac{1}{2\pi} \int_0^\infty (\alpha_{\omega\nu} \hat{a}_\nu + \beta_{\omega\nu} \hat{a}_\nu^\dagger) d\nu, \quad (2)$$

where $\alpha_{\omega\nu}$ and $\beta_{\omega\nu}$ are the *Bogoliubov coefficients*.

The Bogoliubov transformation preserves the canonical (anti)commutation relations and expresses the change of basis of the Fock space, allowing us to move from one construction to another. The Bogoliubov transformations are linear but not unitary. They are symplectic for bosons and orthogonal for fermions though. The number of particles is not preserved, so there is no invariant notion of particles.

This is in fact the reason for both the Unruh effect near a Rindler horizon and the Hawking evaporation near a black hole event horizon. Because of the nonunitarity of the Bogoliubov transformation relating the Fock space representations of two distinct observers, particles can be produced [38–40], including for black holes [11]. This means that what is a vacuum state for an inertial observer is a state with many particles for an accelerated one. This is true in the Minkowski spacetime, if one observer is accelerated with respect to the other, but also for two inertial observers, if the curvature is relevant, as in the case of infalling and escaping observers near a black hole. Moreover, the many-particle state in which the vacuum of one observer appears to the other is thermal. The particle and the antiparticle created in pair during the evaporation are maximally entangled.

3. Black Hole Complementarity

While Hawking's derivation of the black hole evaporation is rigorous and the result is correct, the implication that the information is definitively lost can be challenged. In fact, most of the literature on this problem is trying to find a workaround to restore the lost information and the unitarity. The most popular proposals like black hole complementarity and firewalls do not actually dispute the calculations, but rather they add the requirement that the Hawking radiation should contain the complete information.

Additional motivation for unitarity comes from the AdS/CFT correspondence [43]. The AdS/CFT is not yet rigorously proven, and it is in fact against the current cosmological observations that the cosmological constant is positive [44, 45], but it is widely considered true or standing for a correct gauge-gravity duality, and it is likely that it convinced Hawking to change his mind about information loss [46].

The favorite scenario among high-energy physicists was, for two decades, the idea of *black hole complementarity* [31–33], which supposedly resolves the conflict between unitarity, essential for quantum theory, and the principle of equivalence from general relativity. Susskind and collaborators framed the black hole information paradox as implying a contradiction between unitarity and the principle of equivalence. They proposed a radical solution of this apparent conflict by admitting two distinct Hilbert space descriptions for the infalling matter and the escaping radiation [31].

Assuming that unitarity is to be restored by evaporation alone, the infalling information should be found in the Hawking radiation or should somehow remain above the black hole event horizon, forming the *stretched horizon* [31], similar to the *membrane paradigm* [47]. But since this information falls in the black hole, it would violate the *no-cloning theorem* of quantum mechanics [48–50]. If the cloning does not happen, either the information is not recovered (and unitarity is violated) or no information can cross the horizon, which would violate the principle of equivalence from general relativity, which implies that nothing dramatic should happen at the event horizon, assuming that the black hole is large enough. The black hole complementarity assumes that both unitarity and the principle of equivalence hold true, by allowing cloning, but the cloning cannot be observed, because each observer sees only one copy. The infalling copy of the information is accessible to an infalling observer only (usually named Alice) and the escaping one to an escaping observer (Bob). Susskind and collaborators conjectured that Alice and Bob can never meet to confirm that the infalling quantum information was cloned and the copy escaped the black hole.

At first sight, it may seem that the black hole complementarity solves the contradiction by allowing it to exist, as long as no experiment is able to prove it. Alice and Bob's lightcones intersect, but none of them is included in the other, and they cannot be made so. This means that whatever slicing of spacetime they choose in their reference frames, the Hilbert space constructions they make will be different. So it would be impossible to compare quantum information from the interior of the black hole with the copy of quantum information escaping it. And it is impossible to conceive an observer able to see both copies of information—this would be the so-called *omniscience condition*, which is rejected by Susskind and collaborator to save both unitarity and the principle of equivalence.

3.1. No-Cloning and Timelike Singularities. An early objection to the proposal that Alice and Bob can never compare the two copies of quantum information was that the escaping observer Bob can collect the escaping copy of the information and jump into the black hole to collect the infalling copy. This objection was rejected because, in order to collect a single bit of infalling information from the Hawking radiation, Bob should wait until the black hole loses half of its initial mass by evaporation—the time needed for this to happen is called the *Page time* [13]. So if Bob decides to jump in the black hole to compare the escaping information with the infalling one, it would be too late, because the infalling information will have just enough time to reach the singularity.

The argument based on the Page time works well, but it applies only to black holes of the Schwarzschild type (more precisely this is an Oppenheimer-Snyder black hole [51]), whose singularity is a spacelike hypersurface. For rotating or electrically charged black holes, the singularity is a timelike curve or cylinder. In this case, Alice can carry the infalling information around the singularity for an indefinitely long time, without reaching the singularity. So Bob will be able to reach Alice and confirm that the quantum information was cloned.

This objection is relevant, because for the black hole to be of Schwarzschild type, two of the three parameters defining the black hole, the angular momentum and the electric charge, have to vanish, which is very unlikely. The things are even more complicated if we take into account the fact that, during evaporation or any additional particle falling in the black hole, the type of the black hole changes. Usually particles have nonvanishing electric charges and spin, and even if an infalling particle is electrically neutral and has the spin equal to 0, most likely it will not collide with the black hole radially. This continuous change of the type of the black hole may result in changes of type of the singularity, rendering the argument based on the Page time invalid.

In Section 3.3, we will see that even if the black hole somehow manages to remain of Schwarzschild type, the cloning can be made manifest to a single observer.

3.2. No-Cloning and the Principle of Equivalence. Because of the principle of equivalence, Susskind's argument should also hold for Rindler horizons in Minkowski spacetime. The equivalence implies that Bob is an accelerated observer, and Alice is an inertial observer, who crosses Bob's Rindler horizon. Because of the Unruh effect, Bob will perceive the vacuum state as thermal radiation, while for Alice it would be just vacuum. Bob can see Alice being burned at the Rindler horizon by the thermal radiation, but Alice will experience nothing of this sort. But since they are now in the Minkowski spacetime, Bob can stop and go back to check the situation with Alice, and he will find that she did not experience the thermal bath he saw her experiencing. While we can just say that the complementarity should be applied only to black holes, to rule it out for the Rindler horizon and still maintain the idea of stretched horizon only for black holes, this would be at odds with the principle of equivalence which black hole complementarity is supposed to rescue.

3.3. The “No-Omniscience” Proposal. The resolution proposed by black hole complementarity appeals to the fact that the Hilbert spaces constructed by Alice and Bob are distinct, which would allow quantum cloning, as long as the two copies belong to distinct Hilbert spaces and there is no observer to see the violation of the no-cloning theorem. This means that the patches of spacetime covered by Alice and Bob are distinct, such that apparently no observer can cover both of them. If there was such an “omniscient” observer, he or she would see the cloning of quantum information and see that the laws of quantum theory are violated.

Yet, there is such an observer, albeit moving backwards in time (see Figure 1). Remember that the whole point of trying to restore the lost information and unitarity is because quantum theory should be unitary. This means not only deterministic, but also that the time evolution laws have to be time symmetric, as quantum theory normally is, so that we can recover the lost information. So everything quantum evolution does forward in time should be accessible by backwards in time evolution. An observer going backwards in time, Charlie, can then in principle be able to perceive both copies of the information carried by Alice and Bob, so he is “omniscient.”

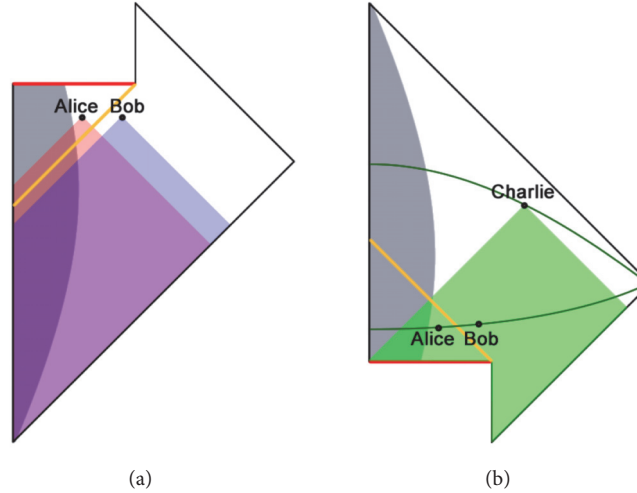


FIGURE 1: (a) The Penrose diagram of black hole evaporation, depicting Alice and Bob and their past lightcones. (b) The Penrose diagram of a backwards in time observer Charlie, depicting how he observes Alice and Bob, and the quantum information each of them carries, even if this information is cloned, therefore disclosing a violation of quantum theory.

One can try to rule Charlie out, on the grounds that he violates causality or more precisely the second law of thermodynamics [52]. But from the point of view of quantum theory, the von Neumann entropy is preserved by unitary evolution, and the quantum evolution is reversible anyway, so it is irrelevant that if in our real universe there is a thermodynamic arrow of time, this does not invalidate a principal thought experiment like this one.

4. The Firewall Paradox

After two decades since the proposal of black hole complementarity, this solution was disputed by the *firewall paradox* [34], which suggested that the equivalence principle should be violated at the event horizon, where a highly energetic curtain or a singularity should form to prevent the information falling inside the black hole.

The firewall argument takes place in the same settings as the black hole complementarity proposal, but this time it involves the *monogamy of entanglement*. More precisely, it is shown that the late radiation has to be maximally entangled with both the early radiation and the infalling counterpart of the late radiation. Since the monogamy of entanglement forbids this, it is proposed that one of the assumptions has to go, most likely the principle of equivalence. The immediate reaction varied from quick acceptance to arguments that the paradox is solved too by the black hole complementarity [53, 54]. After all, we can think of the late radiation as being entangled with the early one in Bob's Hilbert space and with the infalling radiation in Alice's Hilbert space. But it turned out that, unlike the case of the violation of the no-cloning theorem, the violation of monogamy cannot be resolved by Alice and Bob having different Hilbert spaces [55].

One can argue that if the firewall experiment is performed, it creates the firewall, and if it is not performed, Alice

sees no firewall, so black hole complementarity is not completely lost. Susskind and Maldacena proposed the *ER=EPR* solution, which states that if entangled particles are thrown in different black holes, then they become connected by a wormhole [56]; also see [57]. The firewall idea also stimulated various discussions about the relevance of complexity of quantum computation and error correction codes in the black hole evaporation and decoding the information from the Hawking radiation using unitary operations (see [54, 58, 59] and references therein).

Various proposals to rescue both the principle of equivalence and unitarity were made, for example, based on the entropy of entanglement across the event horizon in [60, 61]. Hawking proposed that the black hole horizons are only apparent horizons and never actual event horizons [62]. Later, Hawking proposed that supertranslations allow the preservation of information and further expanded the idea with Perry and Strominger [63–65].

Having to give up the principle of equivalence or unitarity is a serious dilemma, so it is worth revisiting the arguments to find a way to save both.

4.1. The Meaning of “Unitarity”. In the literature about black hole complementarity and firewalls, by the assumption or requirement of “unitarity,” we should understand “unitarity of the Hawking radiation” or, more precisely, “unitarity of the quantum state exterior to the black hole.” Let us call this *exterior unitarity* to emphasize that it ignores the interior of the black hole. It is essential to clarify this, because when we feel that we are forced to choose between unitarity and the principle of equivalence, we are in fact forced to choose between exterior unitarity and the principle of equivalence. This assumption is also at the origin of the firewall proposal. So no choice between unitarity and the principle of equivalence is enforced to us, unless by “unitarity” we understand “exterior unitarity.”

The idea that unitarity should be restored from the Hawking radiation alone, ignoring the interior of the black hole, was reinforced by the holographic principle and the idea of stretched horizon [31, 32, 66], a place just above the event horizon which presumably stores the infalling information until it is restored through evaporation, and it was later reinforced even more by the AdS/CFT conjecture [43]. But it is not excluded to solve the problem by taking into consideration both the exterior and interior of the black hole and the corresponding quantum states. A proposal accounting for the interior in the AdS/CFT correspondence, based on the impossibility to localize the quantum operators in quantum gravity in a background-independent manner, was made in [67]. A variation of the AdS/CFT leading to a regularization was made in [68].

In fact, considering both the exterior and the interior of the black hole is behind proposals like remnants and baby universes. But we will see later that there is a less radical option.

Exterior unitarity, or the proposal that the full information and purity are restored from Hawking radiation alone, simply removes the interior of the black hole from the reference frame of an escaping observer, consequently from his Hilbert space. This type of unitarity imposes a boundary condition to the quantum fields, which is simply the fact that there is no relevant information inside the black hole. So it is natural that, at the boundary of the support of the quantum fields, which is the black hole event horizon, quantum fields behave as if there is a firewall. This is what the various estimates revealing the existence of a highly energetic firewall or horizon singularity confirm. Note that since the boundary condition which aims to rescue the purity of the Hawking radiation is a condition about the final state, sometimes its consequences give the impression of a conspiracy, as sometimes Bousso and Hayden put it [69].

While I have no reason to doubt the validity of the firewall argument [34], I have reservations about assuming unitarity as referring only to quantum fields living only to the exterior of the black hole, while ignoring those from its interior.

4.2. Firewalls versus Complementarity. The initial Hilbert spaces of Alice and Bob are not necessarily distinct. Even if they and their Fock constructions are distinct, each state from one of the spaces may correspond to a state from the other. The reason is that a basis of annihilation operators in Alice's frame, say (\hat{a}_ν) , is related to a basis of annihilation operators in Bob's frame, (\hat{b}_ω) , by a Bogoliubov transformation (2). The Bogoliubov transformation is linear, although not unitary.

Thus, one may hope that the Hilbert spaces of Alice and Bob may be identified, even though through a very scrambled vector space isomorphism, so that black hole complementarity saves the day. However, exterior unitarity imposes that the evolved quantum fields from the Hilbert spaces have different supporting regions in spacetime. While before the creation of the black hole they may have the same support in the spacelike slice, they evolve differently because of the exterior unitarity condition. Bob's system evolves so that his quantum fields are constrained to the

exterior of the black hole, while Alice's quantum fields include the interior too. Bob's Hilbert space is different, because when the condition of exterior unitarity was imposed, it excluded the interior of the black hole. So even if the initial underlying vector space is the same for both the Hilbert space constructed by Alice and that constructed by Bob, their coordinate systems diverged in time, so the way they slice spacetime became different. While normally Alice's vacuum is perceived by Bob as loaded with particles in a thermal state, this time in Bob's frame Alice's vacuum energy becomes singular at the horizon. This makes the firewall paradox a problem for black hole complementarity. A cleaner argument based on purity rather than monogamy is made by Bousso [70].

An interesting issue is that Bob can infer that if the modes he detects passed very close to the event horizon, they were redshifted. So, evolving the modes backwards in time, it must be that the particle passes close to the horizon at a very high frequency, maybe even higher than the Planck frequency. Does this mean that Alice should feel dramatically this radiation? There is the possibility that, for Alice, Bob's high frequency modes are hidden in her vacuum state. This is also confirmed by acoustic black holes [71]. Only if these modes are somehow disclosed, for example, if Bob, being accelerated, performs some temperature detection nearby Alice, these modes may become manifest due to the projection postulate; otherwise, they remain implicit in Alice's vacuum.

It seems that the strength of the firewall proposal comes from rendering black hole complementarity unable to solve the firewall paradox. They are two competing proposals, both aiming to solve the same problem. While one can logically think that proposals that take into account the interior of black holes to restore unitarity are good candidates as well and that they may have the advantage of rescuing the principle of equivalence, sometimes they are dismissed as not addressing the "real" black hole information paradox. I will say more about this in Section 6.

5. Black Hole Entropy

The purposes of this section are to prepare for Section 6 and to discuss the implications of black hole entropy for the black hole information paradox and for quantum gravity.

The entropy bound of a black hole is proportional to the area of the event horizon [12, 72, 73],

$$S_{BH} = \frac{k_B A}{4\ell_P^2}, \quad (3)$$

where k_B is the Boltzmann constant, A is the area of the event horizon, and ℓ_P is the Planck length.

The black hole entropy bound (3) was suggested by Hawking's result that the black hole horizon area never decreases [74], as well as the development of this result into the four laws of black hole mechanics [72].

5.1. The Area of the Event Horizon and the Entropy. It is tempting to think that the true entropy of quantum fields in spacetime should also include the areas of the event horizons.

In fact, there are computational indications that the black hole evaporation leaks the right entropy to compensate the decrease of the area of the black hole event horizon.

But there is a big difference between the entropy of quantum fields and the areas of horizons. First, entropy is associated with the state of the matter (including radiation, of course). If we look at the phase space, we see that the entropy is a property of the state alone, so it is irrelevant if the system evolves in one direction of time or the opposite; the entropy corresponding to the state at a time t is the same. The same is true for quantum entropy, associated with the quantum states, which in fact is preserved by unitary evolution and is the same in either time direction.

On the other hand, the very notion of event horizon in general relativity depends on the direction of time. By looking again at Figure 1(b), this time without being interested in black hole complementarity, we can see that for Charlie there is no event horizon. But the entropy corresponding to matter is the same independently of his time direction. So even if we are able to put the area on the event horizon in the same formula with the entropy of the fields and still have the second law of thermodynamics, the two terms behave completely differently. So if the area of the event horizon is required to compensate for the disappearance of entropy beyond the horizon and for its reemergence as Hawking radiation, for Charlie the things are quite different, because he has full clearance to the interior of the black hole, which for him is white. In other words, he is so omniscient that he knows the true entropy of the matter inside the black hole and not a mere bound given by the event horizon.

This is consistent with the usual understanding of entropy as hidden information; indeed, the true information about the microstates is not accessible (only the macrostate), and this is what entropy stands for. But it is striking, nevertheless, to see that black holes do the same, yet in a completely time-asymmetric manner. This is because the horizon entropy is just a bound for the entropy beyond the horizon; the true entropy is a property of the state.

5.2. Black Hole Mechanics and Thermodynamics: Matter or Geometry? The four laws of black hole mechanics are the following [72, 75]:

- (i) **0th law:** the surface gravity κ is constant over the event horizon
- (ii) **1st law:** for nearby solutions, the differences in mass are equal to differences in area times the surface gravity, plus some additional terms similar to work
- (iii) **2st law:** in any physical process, the area of the event horizon never decreases (assuming positive energy of matter and regularity of spacetime)
- (iv) **3rd law:** there is no procedure, consisting of a finite number of steps, to reduce the surface gravity to zero.

The analogy between the laws of black hole mechanics and thermodynamics is quite impressive [75]. In particular, enthalpy, temperature, entropy, and pressure correspond, respectively, to the mass of the black hole, its surface gravity, its horizon area, and the cosmological constant.

These laws of black hole mechanics are obtained in purely classical general relativity but were interpreted as laws of black hole thermodynamics [11, 76, 77]. Their thermodynamical interpretation occurs when considering quantum field theory on curved spacetime, and it is expected to follow more precisely from the yet to be found quantum gravity.

Interestingly, despite their analogy with the laws of thermodynamics, the laws of black hole mechanics hold in purely classical general relativity. While we expect general relativity to be at least a limit theory of a more complete, quantized one, it is a standalone and perfectly selfconsistent theory. This suggests that it is possible that the laws of black hole mechanics already have thermodynamic interpretation in the geometry of spacetime. And this turns out to be true, since black hole entropy can be shown to be the Noether charge of the diffeomorphism symmetry [78]. This works exactly for general relativity, and it is different for gravity modified so that the action is of higher order in terms of curvature. In addition, we already know that Einstein's equation can be understood from an entropic perspective, which has a geometric interpretation [79, 80].

This is not to say that the interpretations of the laws of black hole mechanics in terms of thermodynamics of quantum fields do not hold, because there are strong indications that they do. My point is rather that there are thermodynamics of the spacetime geometry, which are tied somehow with the thermodynamics of quantum matter and radiation. This connection is probably made via Einstein's equation or whatever equation whose classical limit is Einstein's equation.

5.3. Do Black Holes Have No Hair? Classically, black holes are considered to be completely described by their mass, angular momentum, and electric charge. This idea is based on the *no-hair theorems*. These results were obtained for the Einstein-Maxwell equations, assuming that the solutions are asymptotically flat and stationary. While it is often believed that these results hold universally, they are in fact similar to Birkhoff's theorem [81], which states that any spherically symmetric solution of the vacuum field equations must be static and asymptotically flat; hence the exterior solution must be given by the Schwarzschild metric. Werner Israel establishes that the Schwarzschild solution is the unique asymptotically flat static nonrotating solution of Einstein's equation in vacuum, under certain conditions [2]. This was generalized to the Einstein-Maxwell equations (electrovac) [3–5], the result being the characterization of static asymptotically flat solutions only by mass, electric charge, and angular momentum. It is conjectured that this result is general, but counterexamples are known [82, 83].

In classical general relativity, the black holes radiate gravitational waves and are expected to converge to a no-hair solution very fast. If this is true, it happens asymptotically, and the gravitational waves carry the missing information about the initial shape of the black hole horizon, because classical general relativity is deterministic on regular globally hyperbolic regions of spacetime.

Moreover, it is not known what happens when quantum theory is applied. If the gravitational waves are quantized

(resulting in gravitons), it is plausible to consider the possibility that quantum effects prevent such a radiation, like in the case of the electron in the atom. Therefore, it is not clear that the information about the infalling matter is completely lost in the black hole, even in the absence of Hawking evaporation. So we should expect at most that black holes converge asymptotically to the simple static solutions, but if they would reach them in finite time, there would be no time reversibility in GR.

Nevertheless, this alone is unable to provide a solution to the information loss paradox, especially since spacetime curvature does not contain the complete information about matter fields. But we see that we have to be careful when we use the no-hair conjecture as an assumption in other proofs.

5.4. Counting Bits. While black hole mechanics suggest that the entropy of a black hole is limited by the Bekenstein bound (3), it is known that the usual classical entropy of a system can be expressed in terms of its microstates:

$$S_Q = -k_B \sum_i p_i \ln p_i, \quad (4)$$

where p_i denotes the number of microstates which cannot be distinguished because of the coarse graining, macroscopically appearing as the i -th macrostate. A similar formula gives the quantum von Neumann entropy, in terms of the density matrix ρ :

$$S = -k_B \text{tr}(\rho \ln \rho). \quad (5)$$

Because of the *no-hair theorem* (see Section 5.3), it is considered that classical black holes can be completely characterized by the mass, angular momentum, and electric charge, at least from the outside. This is usually understood as suggesting that quantum black holes have to contain somewhere, most likely on their horizons, some additional degrees of freedom corresponding to their microstates, so that (3) can be interpreted in terms of (4).

It is often suggested that there are some horizon microstates, either floating above the horizon but not falling because of a *brick wall* [84–86] or being horizon gravitational states [87].

Other counting proposals are based on counting string excited microstates [88–90]. There are also proposals of counting microstates in LQG, for example, by using a Chern-Simons field theory on the horizon, as well as choosing a particular Immirzi parameter [91].

Another interesting possible origin of entropy comes from *entropy of entanglement* resulting by the reduced density matrix of an external observer [92, 93]. This is proportional but for short distances requires renormalization.

But, following the arguments in Section 5.1, I think that the most natural explanation of black hole entropy seems to be to consider the internal states of matter and gravity [94]. A model of the internal state of the black hole similar to the atomic model was proposed in [95–97]. Models based on Bose-Einstein condensates can be found in [98–100] and references therein.

Since in Section 5.1 it was explained that the horizons just hide matter, and hence entropy, and are not in fact the carriers of the entropy, it seems more plausible to me that the structure of the matter inside the black hole is just bounded by the Bekenstein bound, and does not point to an unknown microstructure.

5.5. A Benchmark to Test Quantum Gravity Proposals? The interest in the black hole information paradox and black hole entropy is not only due to the necessity of restoring unitarity. This research is also motivated by testing various competing candidate theories of quantum gravity. Quantum gravity seems to be far from our experimental possibilities, because it is believed to become relevant at very small scales. On the other hand, black hole information loss and black hole entropy pose interesting problems, and the competing proposals of quantum gravity are racing to solve them. The motivation is that it is considered that black hole entropy and information loss can be explained by one of these quantum gravity approaches.

On the other hand, it is essential to remember how black hole evaporation and black hole entropy were derived. The mathematical proofs are done within the framework of quantum field theory on curved spacetime, which is considered a good effective limit of the true but yet to be discovered theory of quantum gravity. The calculations are made near the horizon; they do not involve extreme conditions like singularities or planckian scales, where quantum gravity is expected to take the lead. The main assumptions are

- (1) quantum field theory on curved spacetime
- (2) the Einstein equation, with the stress-energy tensor replaced by the stress-energy expectation value $\langle \hat{T}_{ab}(x) \rangle$ (see (1))

For example, when we calculate the Bekenstein entropy bound, we do this by throwing matter in a black hole and see how much the event horizon area increases.

These conditions are expected to hold in the effective limit of any theory of quantum gravity.

But since both the black hole entropy and the Hawking evaporation are obtained from the two conditions mentioned above, this means that any theory in which these conditions are true, at least in the low energy limit, is also able to imply both the black hole entropy and the Hawking evaporation. In other words, if a theory of quantum gravity becomes in some limit the familiar quantum field theory and also describes Einstein's gravity, it should also reproduce the black hole entropy and the Hawking evaporation.

Nevertheless, some candidate theories to quantum gravity do not actually work in a dynamically curved spacetime, being, for example, defined on flat or AdS spacetime, yet they still are able to reproduce a microstructure of black hole entropy. This should not be very surprising, given that, even in nonrelativistic quantum mechanics, quantum systems bounded in a compact region of space have discrete spectrum. So it may be very well possible that these results are due to the fact that even in nonrelativistic quantum mechanics entropy bounds hold [101]. In flat spacetime, we

can think that the number of states in the spectrum is proportional with the volume. However, when we plug in the masses of the particles in the formula for the Schwarzschild radius (which incidentally is the same as Michell's formula in Newtonian gravity [102]), we should obtain a relation similar to (3).

The entropy bound (3) connects the fundamental constants usually considered to be characteristic for general relativity, quantum theory, and thermodynamics. This does not necessarily mean that the entropy of the black hole witnesses about quantum gravity. This should be clear already from the fact that the black hole entropy bound was not derived by assuming quantum gravity but simply from the assumptions mentioned above. It is natural that if we plug the information and the masses of the particles in the formula for the Schwarzschild radius, we obtain a relation between the constants involved in general relativity, quantum theory, and thermodynamics. It is simply a property of the system itself, not a witness of a deeper theory. But, of course, if a candidate theory of quantum gravity fails to pass even this test, this may be a bad sign for it.

6. The Real Black Hole Information Paradox

Sometimes it is said that the true black hole information paradox is the one following from Don Page's article [13]. For example, Marolf considers that here lies the true paradoxical nature of the black hole information, while he calls the mere information loss and loss of purity, "the straw man information problem" [14]. Apparently, the black hole von Neumann entropy should increase with one bit for each emitted photon. At the same time, its area decreases by losing energy, so the black hole entropy should also decrease by the usual Bekenstein-Hawking kind of calculation. So what happens with the entropy of the black hole? Does it increase or decrease? This problem occurs much earlier in the evolution of the black hole, when the black hole area is reduced to half of its initial value (the *Page time*), so we do not have to wait for the complete evaporation to notice this problem. Marolf put it as follows[14]:

This is now a real problem. Evaporation causes the black hole to shrink and thus to reduce its surface area. So S_{BH} decreases at a steady rate. On the other hand, the actual von Neumann entropy of the black hole must increase at a steady rate. But the first must be larger than the second. So some contradiction is reached at a finite time.

I think there are some assumptions hidden in this argument. We compare the von Neumann entropy of the black hole calculated during evaporation with the black hole entropy calculated by Bekenstein and Hawking by throwing particles in the black hole. While the proportionality of the black hole entropy with the area of the event horizon has been confirmed by various calculations for numerous cases, the two types of processes are different, so it is natural that they lead to different states of the black hole and hence to different values for the entropy. This is not a paradox; it is just an evidence that the entropy contained in the black hole

depends on the way it is created, despite the bound given by the horizon. So it seems more natural not to consider that the entropy of the matter inside the black hole reached the maximum bound at the beginning but rather that it reaches its maximum at the Page time, due to the entanglement entropy with the Hawking radiation. Alternatively, we may still want to consider the possibility of having more entropy in the black hole than the Bekenstein bound allows. In fact, Rovelli made another argument pointing in the same direction that the Bekenstein-Bound is violated, by counting the number of states that can be distinguished by local observers (as opposed to external observers) using local algebras of observables [103]. This argument provided grounds for a proposal of a white hole remnant scenario discussed in [104].

7. A More Conservative Solution

We have seen in the previous sections that some important approaches to the black hole information paradox and the related topics assume that the interior of the black hole is irrelevant or does not exist, and the event horizon plays the important role. I also presented arguments that if it is to recover unitarity without losing the principle of equivalence, then the interior of the black hole should be considered as well, and the event horizon should not be endowed with special properties. More precisely, given that the original culprit of the information loss is its supposed disappearance at singularities, then singularities should be closely investigated. The least radical approach is usually considered the avoidance of singularity, by modifying gravity (*i.e.*, the relation between the stress-energy tensor and the spacetime curvature as expressed by the Einstein equation), so that one or more of the three assumptions of the singularity theorems [6–8] no longer hold. In particular, it is hoped that this may be achieved by the quantum effects in a theory of quantum gravity. However, it would be even less radical if the problem could be solved without modifying general relativity, and such an approach is the subject of this section.

But singularities are accompanied by divergences in the very quantities involved in the Einstein equation, in particular the curvature and the stress-energy tensor. So even if it is possible to reformulate the Einstein equation in terms of variables that do not diverge, remaining instead finite at the singularity, the question remains whether the physical fields diverge or break down. In other words, what are in fact the true, fundamental physical fields, the diverging variables, or those that remain finite? This question will be addressed soon.

An earlier mention of the possibility of changing the variables in the Einstein equation was made by Ashtekar, for example, in [105] and references therein, where it is also proposed that the new variables could remain finite at singularities even in the classical theory. However, it turned out that one of his two new variables diverges at singularities (see, *e.g.*, [106]). Eventually this formulation led to loop quantum gravity, where the avoidance is instead achieved on some toy bounce models (see *e.g.*, [28, 29]). But the problem whether standard general relativity can admit a formulation free of infinities at singularities remained open for a while.

7.1. Singular General Relativity. In [107, 108], the author introduced a mathematical formulation of semi-Riemannian geometry which allows a description of a class of singularities free of infinities. The fields that allowed this are invariant, and in the regions without singularities they are equivalent to the standard formulation. To understand what the problem is and how it is solved, recall that in geometry the metric tensor is assumed to be smooth and regular, that is, without infinite components and nondegenerate, which means that its determinant is nonvanishing. If the metric tensor has infinite components or if it is degenerate, the metric is called singular. If the determinant is vanishing, one cannot define the Levi-Civita connection, because the definition relies on the Christoffel symbols of the second kind,

$$\Gamma_{jk}^i := \frac{1}{2} g^{is} (g_{sj,k} + g_{sk,j} - g_{jk,s}), \quad (6)$$

which involve the contraction with g^{is} , which is the inverse of the metric tensor g_{ij} ; hence it assumes it to be nondegenerate. This makes it impossible to define the covariant derivative and the Riemann curvature (hence the Ricci and scalar curvatures as well) at the points where the metric is degenerate. These quantities blow up while approaching the singularities. Therefore, Einstein's equation as well breaks down at singularities.

However, it turns out that, on the space obtained by factoring out the subspace of isotropic vectors, an inverse can be defined in a canonical and invariant way and that there is a simple condition that leads to a finite Riemann tensor, which is defined smoothly over the entire space, including at singularities. This allows the contraction of a certain class of tensors and the definition of all quantities of interest to describe the singularities without running into infinities and is equivalent to the usual, nondegenerate semi-Riemannian geometry outside the singularities [107]. Moreover, it works well for warped products [108], allowing the application for big bang models [109, 110]. This approach also works for black hole singularities [42, 111, 112], allowing the spacetime to be globally hyperbolic even in the presence of singularities [113]. More details can be found in [35, 114] and the references therein. Here I will first describe some of the already published results and continue with new and more general arguments.

An essential difficulty related to singularities is given by the fact that, despite the Riemann tensor being smooth and finite at such singularities, the Ricci tensor $R_{ij} := R^s_{isj}$ usually continues to blow up. The Ricci tensor and its trace, the scalar curvature $R = R^s_s$, are necessary to define the Einstein tensor, $G_{ij} = R_{ij} - (1/2)Rg_{ij}$. Now here is the part where the physical interpretation becomes essential. In the Einstein equation, the Einstein tensor is equated to the stress-energy tensor. So they both seem to blow up, and indeed they do. Physically, the stress-energy tensor represents the density of energy and momentum at a point. However, what is physically measurable is never such a density at a point but its integral over a volume. The energy or momentum in a finite measure volume is obtained by integrating with respect to the volume element. And the quantity to be integrated, for

example, the energy density $T_{00}d_{vol}$, where $T_{00} = T(u, u)$ for a timelike vector u and $d_{vol} := \sqrt{-\det g} dx^0 \wedge dx^1 \wedge dx^2 \wedge dx^3$, is finite, even if $T_{00} \rightarrow \infty$, since $d_{vol} \rightarrow 0$ in the proper way. The mathematical theory of integration on manifolds makes it clear that what we integrate are differential forms, like $T_{00}d_{vol}$, and not scalar functions like T_{00} . So I suggest that we should do in physics the same as in geometry, because it makes more sense to consider the physical quantities to be the differential forms rather than the scalar components of the fields [109]. This is also endorsed by two other mathematical reasons. On one hand, when we define the stress-energy T_{ij} , we do it by functional derivative of the Lagrangian with respect to the metric tensor, and the result contains the volume element, which we then divide out to get T_{ij} . Should we keep it, we would get instead $T_{ij}d_{vol}$. Also, when we derive the Einstein equation from the Lagrangian density R , we in fact vary the integral of the differential form Rd_{vol} and not of the scalar R . And the resulting Einstein equation has again a factor d_{vol} , which we leave out of the equation on the grounds that it is never vanishing. Well, at singularities it vanishes, so we should keep it, because otherwise we divide by 0 and we get infinities. The resulting densitized form of the Einstein equation,

$$G_{ij}d_{vol} + \Lambda g_{ij}d_{vol} = \frac{8\pi G}{c^4} T_{ij}d_{vol}, \quad (7)$$

is equivalent to Einstein's outside singularities, but, as already explained, I submit that it better represents the physical quantities and not only because these quantities remain finite at singularities. I call this *densitized Einstein equation*, but they are in fact tensorial as well; the fields involved are tensors, being the tensor products between other tensors and the volume form, which itself is a completely antisymmetric tensor. Note that Ashtekar's variables are also densities, and they are more different from the usual tensor fields involved in the semi-Riemannian geometry and Einstein's equation, yet they were proposed to be the real variables both for quantization and for eliminating the infinities in the singularities [105]. But the formulation I proposed remains finite even at singularities, and it is closer as interpretation to the original fields.

Another difficulty this approach had to solve was that it applies to a class of degenerate metrics, but the black holes are nastier, since the metric has components that blow up at the singularities. For example, the metric tensor of the Schwarzschild black hole solution, expressed in the Schwarzschild coordinates, is

$$ds^2 = -\left(1 - \frac{2m}{r}\right) dt^2 + \left(1 - \frac{2m}{r}\right)^{-1} dr^2 + r^2 d\sigma^2, \quad (8)$$

where m is the mass of the body, the units were chosen so that $c = 1$ and $G = 1$, and

$$d\sigma^2 = d\theta^2 + \sin^2\theta d\phi^2 \quad (9)$$

is the metric of the unit sphere S^2 .

For the horizon $r = 2m$, the singularity of the metric can be removed by a singular coordinate transformation; see, for

example, [115, 116]. Nothing of this sort could be done for the $r = 0$ singularity, since no coordinate transformation can make the Kretschmann scalar $R^{ijkl}R_{ijkl}$ finite. However, it turns out that it is possible to make the metric at the singularity $r = 0$ into a degenerate and analytic metric by coordinate transformations. In [111], it was shown that this is possible, and an infinite number of solutions were found, which lead to an analytic metric degenerate at $r = 0$. Among these solutions, there is a unique one that satisfies the condition of semiregularity from [107], which ensures the smoothness and analyticity of the solution for the interior of the black hole. This transformation is

$$\begin{aligned} r &= \tau^2 \\ t &= \xi \tau^4 \end{aligned} \quad (10)$$

and the resulting metric describing the interior of the Schwarzschild black hole is

$$\begin{aligned} ds^2 = & -\frac{4\tau^4}{2m - \tau^2} d\tau^2 + (2m - \tau^2) \tau^4 (4\xi d\tau + \tau d\xi)^2 \\ & + \tau^4 d\sigma^2. \end{aligned} \quad (11)$$

This is not to say that physics depend on the coordinates. It is similar to the case of switching from polar to Cartesian coordinates in plane or like the Eddington-Finkelstein coordinates. In all these cases, the transformation is singular at the singularity, so it is not a diffeomorphism. The atlas, the differential structure, is changed, and in the new atlas, with its new differential structure, the diffeomorphisms preserve, of course, the semiregularity of the metric. And just like in the case of the polar or spherical coordinates and the Eddington-Finkelstein coordinates, it is assumed that the atlas in which the singularity is regularized is the real one, and the problems were an artifact of the Schwarzschild coordinates, which themselves were in fact singular.

Similar transformations were found for the other types of black holes (Reissner-Nordström, Kerr, and Kerr-Newman) and for the electrically charged ones the electromagnetic field also no longer blows up [42, 112].

7.2. Beyond the Singularity. Returning to the Schwarzschild black hole in the new coordinates (11), the solution extends analytically through the singularity. If we plug this solution in the Oppenheimer-Snyder black hole solution, we get an analytic extension depicting a black hole which forms and then evaporates, whose Penrose-Carter diagram is represented in Figure 2.

The resulting spacetime does not have Cauchy horizons, being hyperbolic, which allows the partial differential equations describing the fields on spacetime to be well posed and continued through the singularity. Of course, there is still the problem that the differential operators in the field equations of the matter and gauge fields going through the singularity should be replaced with the new ones. Such formulations are introduced in [117], and sufficient conditions are to be satisfied by the fields at the singularities so that their evolution equations work as given, in the case of Maxwell and Yang-Mills equations.

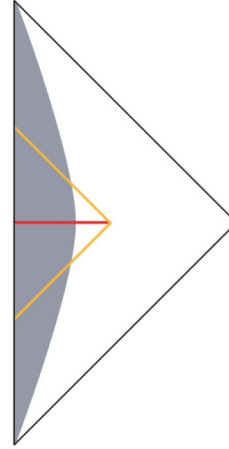


FIGURE 2: An analytic extension of the black hole solution beyond the singularity.

It is an open problem whether the backreaction will make the spacetime to curve automatically so that these conditions are satisfied for all possible initial conditions of the field. This should be researched in the future, including for quantum fields. It is to be expected that the problem is difficult, and what is given here is not the general solution but rather a toy model. Anyway, no one should expect very soon an exact treatment of real case situations, so the whole discussion here is in principle to establish whether this conservative approach is plausible enough.

However, I would like to propose here a different, more general argument, which avoids the difficulties given by the necessity that the field equations should satisfy at the singularities special conditions like the sufficient conditions found in [117] and also the open problem of which are the conditions to be satisfied by the fermionic fields at singularities.

First consider Fermat's principle in optics. A ray of light in geometric optics is straight, but if it passes from one medium to another having a different refraction index, the ray changes its direction and appears to be broken. It is still continuous, but the velocity vector is discontinuous, and it appears that the acceleration blows up at the surface separating the two media. But Fermat's principle still allows us to know exactly what happens with the light ray in geometric optics.

On a similar vein, I think that, in the absence of a proof that the fields satisfy the exact conditions [117] when crossing a singularity, we can argue that the singularities are not a threat to the information contained in the field by using the least action principle instead.

The least action principle involves the integration of the Lagrangian densities of the fields. While the conditions the fields have to satisfy at the singularity in order to behave well are quite restrictive, the Lagrangian formulation is much more general. The reason is that integration can be done over fields with singularities, also on distributions, and the result can still be finite.

Consider first classical, point-like particles falling in the black hole, crossing the singularity, and exiting through the

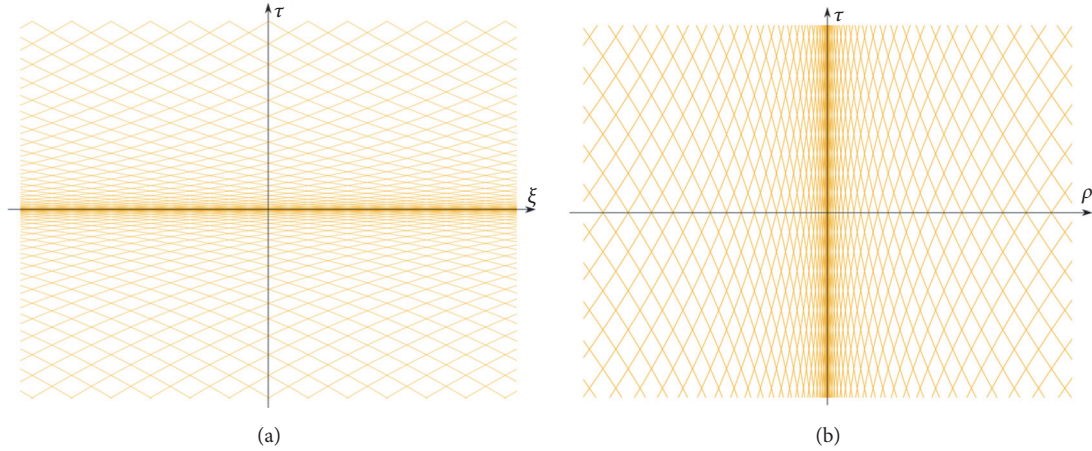


FIGURE 3: (a) The causal structure of the Schwarzschild black hole in coordinates (τ, ξ) from (10). (b) The causal structure of the Reissner-Nordström black hole, in coordinates (τ, ρ) playing a similar role (see [42]).

white hole which appears after the singularity disappears. The history of such a test particle is a geodesic, and to understand the behavior of geodesics, we need to understand first the causal structure. In Figure 3, the causal structures of (a) a Schwarzschild black hole and (b) a Reissner-Nordström black hole are represented in the coordinates which smoothen the singularity (see [118]).

If the test particle is massless, its path is a null geodesic. In [118], I showed that, for the standard black holes, the causal structure at singularities is not destroyed. The lightcones will be squashed, but they will remain lightcones. Therefore, the history of a massless particle like a photon is, if we apply the least action principle, just a null geodesic crossing the singularity and getting out.

If the test particle is massive, its history is a timelike geodesic. In this case, a difficulty arises, because in the new coordinates the lightcones are squashed. This allows for distinct geodesics to intersect the singularity at the same point and to have the same spacetime tangent direction. In the Schwarzschild case, this does not happen for timelike geodesics, but in the Reissner-Nordström case [42] all of the timelike geodesics crossing the singularity at the same point become tangent. Apparently, this seems to imply that a geodesic crossing a timelike singularity can get out of it in any possible direction in a completely undetermined way. To fix this, one may want to also consider the second derivative or to use the local cylindrical symmetry around the timelike singularity.

But the least action principle allows this to be solved regardless of the specific local solution of the problem at the singularity. The timelike geodesics are tangent only at the singularity, which is a zero-measure subset of spacetime. So we can apply the least action principle to obtain the history of a massive particle and obtain a unique solution. The least action principle can be applied for classical test particles because a particle falling in the black hole reaches the singularity in finite proper time, and similarly a finite proper time is needed for it to get out. Moreover, the path integral quantization will consider anyway all possible paths,

so even if there would be an indeterminacy at the classical level, it will be removed by integrating them all.

For classical fields, the same holds as for point-like classical particles; only the paths are much more difficult to visualize. The least action principle is applied in the configuration space even for point-like particles, and the same holds for fields, the only difference being the dimension of the configuration space and the Lagrangian. The points from the singularity form again a zero-measure subset compared to the full configuration space, so finding the least action path is similar to the case of point-like particles. The Lagrangian density is finite at least at the points of the configuration space outside the singularities, which means almost everywhere. But the volume element vanishes at singularities, which improves the situation. So its integral can very well be finite, even if the Lagrangian density would be divergent at the singularities. It may be the case that the fields have singular Lagrangian density at the singularity and that when we integrate them it is not excluded that even the integral may diverge, but in this case the least action principle will force us anyway to choose the paths that have a finite action density at the singularities, and such paths exist, for example, those satisfying the conditions found in [117].

So far we have seen that the principle of least action allows determining the history of classical, point-like particles or fields, from the initial and final conditions, even if they cross the singularity. This is done so far on fixed background, so no backreaction via Einstein's equation is considered, only particles or fields. But the Lagrangian approach extends easily to include the backreaction; we simply add the Hilbert-Einstein Lagrangian to that of the fields or point-like particles. So now we vary not only the path of point-like particles or fields in the configuration space but also the geometry of spacetime in order to find the least action history. This additional variation gives even more freedom to choose the least action path, so even if on fixed background the initial condition of a particular field will not evolve to become, at the singularity, a field satisfying the conditions from [117], because the spacetime geometry is varied as well to include

backreaction; the spacetime adjusts itself to minimize the action, and it is not too wild to conjecture that it adjusts itself to satisfy such conditions.

Now let us consider quantum fields. When moving to quantum fields on curved background, since the proper time of all classical test particles is finite, we can apply the path integral formulation of quantum field theory [119, 120]. Since the proper time is finite along each path φ joining two points, including for the paths crossing a singularity, and since the action $S(\varphi, t)$ is well defined for almost all times t , then $e^{(i/\hbar)S(\varphi, t)}$ is also well defined. So at least on fixed curved background, even with singularities, it seems to exist little difference from special relativistic quantum field theory via path integrals.

Of course the background geometry should also depend on the quantum fields. Can we account for this, in the absence of a theory of quantum gravity? We know that at least the framework of path integrals works on curved classical spacetime (see, e.g., [121]), where the Einstein equation becomes (1). To also include quantized gravity is more difficult because of its nonrenormalizability by perturbative methods. Add to this the fact that at least for the Standard Model we know that in flat background renormalization helps and even on curved background without singularities. But what about singularities? Is not it possible that they make renormalization impossible? In fact, quite the contrary may be true: in [122], it is shown that singularities improve the behavior of the quantum fields, including for gravity, at UV scales. These results are applied to already existing results obtained by various researchers who use various types of dimensional reduction to improve this behavior for quantum fields, including gravity. In fact, some of these approaches improve the renormalizability of quantum fields so well that even the Landau poles disappear even for nonrenormalizable theories [123, 124]. But the various types of dimensional reduction are, in these approaches, postulated somehow *ad hoc*, for no other reason than to improve perturbative renormalizability. On the contrary, if the perturbative expansion is made in terms of point-like particles, these behave like black holes with singularities, and some of the already postulated types of dimensional reduction emerge automatically, with no additional assumption, from the properties of singularities [122]. Thus, the very properties of the singularities lead automatically to improved behavior at the UV scale, even for theories thought to be perturbatively nonrenormalizable.

The proposal I described in this section is still at the beginning, compared to the difficulty of the remaining open problems to be addressed. First, there is obviously no experimental confirmation, and it is hard to imagine that the close future can provide one. The plausibility rests mainly upon making as few new assumptions as possible, in addition to those coming from general relativity and quantum theory, theories well established and confirmed, but not in the regimes where both become relevant. For some simple examples, there are mathematical results, but a truly general proof, with fully developed mathematical steps and no gaps, does not exist yet. And, considering the difficulty of the problem, it is hard to believe that it is easy to have very

soon a completely satisfying proof in this or other approaches. Nevertheless, I think that promising avenues of research are opened by this proposal.

Data Availability

Everything is included; no additional data is needed; it is a hep-th manuscript.

Conflicts of Interest

The author declares that there are no conflicts of interest.

References

- [1] S. W. Hawking, "Breakdown of predictability in gravitational collapse," *Physical Review D: Particles, Fields, Gravitation and Cosmology*, vol. 14, no. 10, pp. 2460–2473, 1976.
- [2] W. Israel, "Event horizons in static vacuum space-times," *Physical Review A: Atomic, Molecular and Optical Physics*, vol. 164, no. 5, pp. 1776–1779, 1967.
- [3] W. Israel, "Event horizons in static electrovac space-times," *Communications in Mathematical Physics*, vol. 8, no. 3, pp. 245–260, 1968.
- [4] B. Carter, "Axisymmetric black hole has only two degrees of freedom," *Physical Review Letters*, vol. 26, no. 6, pp. 331–333, 1971.
- [5] W. K. Misner, S. Thorne, and J. A. Wheeler, *Gravitation*, W. H. Freeman and Company, 1973.
- [6] R. Penrose, "Gravitational collapse and space-time singularities," *Physical Review Letters*, vol. 14, pp. 57–59, 1965.
- [7] S. W. Hawking and R. Penrose, "The singularities of gravitational collapse and cosmology," *Proceedings of the Royal Society of London*, vol. 314, no. 1519, pp. 529–548, 1970.
- [8] S. W. Hawking and G. F. R. Ellis, *The Large Scale Structure of Space-Time*, Cambridge University Press, 1995.
- [9] R. Penrose, "Gravitational Collapse: the Role of General Relativity," *Revista del Nuovo Cimento; Numero speciale 1*, pp. 252–276, 1969.
- [10] R. Penrose, "The Question of Cosmic Censorship," in *Black Holes and Relativistic Stars*, R. M. Wald, Ed., pp. 233–248, University of Chicago Press, Chicago, IL, USA, 1998.
- [11] S. W. Hawking, "Particle creation by black holes," *Communications in Mathematical Physics*, vol. 43, no. 3, pp. 199–220, 1975.
- [12] J. D. Bekenstein, "Black holes and entropy," *Physical Review D: Particles, Fields, Gravitation and Cosmology*, vol. 7, pp. 2333–2346, 1973.
- [13] D. N. Page, "Average entropy of a subsystem," *Physical Review Letters*, vol. 71, no. 9, pp. 1291–1294, 1993.
- [14] D. Marolf, "The black hole information problem: Past, present, and future," *Reports on Progress in Physics*, vol. 80, no. 9, 2017.
- [15] W. G. Unruh and R. M. Wald, "Information loss," *Reports on Progress in Physics*, vol. 80, no. 9, p. 092002, 2017.
- [16] J. Preskill, "Do black holes destroy information?" in *Black Holes, Membranes, Wormholes and Superstrings*, vol. 1, p. 22, World Scientific, River Edge, NJ, USA, 1993.
- [17] S. B. Giddings, "The black hole information paradox," 1995, <https://arxiv.org/abs/hep-th/9508151>.

- [18] S. Hossenfelder and L. Smolin, “Conservative solutions to the black hole information problem,” *Physical Review D: Particles, Fields, Gravitation and Cosmology*, vol. 81, no. 6, Article ID 064009, 13 pages, 2010.
- [19] S. W. Hawking, “The unpredictability of quantum gravity,” *Communications in Mathematical Physics*, vol. 87, no. 3, pp. 395–415, 1982/83.
- [20] S. B. Giddings, “Constraints on black hole remnants,” *Physical Review D: Particles, Fields, Gravitation and Cosmology*, vol. 49, no. 2, pp. 947–957, 1994.
- [21] S. B. Giddings, “Why aren’t black holes infinitely produced?” *Physical Review D: Particles, Fields, Gravitation and Cosmology*, vol. 51, no. 12, pp. 6860–6869, 1995.
- [22] M. A. Markov, “Problems of a perpetually oscillating universe,” *Annals of Physics*, vol. 155, no. 2, pp. 333–357, 1984.
- [23] M. K. Parikh and F. Wilczek, “Hawking radiation as tunneling,” *Physical Review Letters*, vol. 85, no. 24, pp. 5042–5045, 2000.
- [24] S. Lloyd, “Almost certain escape from black holes in final state projection models,” *Physical Review Letters*, vol. 96, no. 6, 061302, 4 pages, 2006.
- [25] V. P. Frolov, “Information loss problem and a ‘black hole’ model with a closed apparent horizon,” *Journal of High Energy Physics*, vol. 2014, no. 5, 2014.
- [26] D. P. Prester, “Curing Black Hole Singularities with Local Scale Invariance,” *Advances in Mathematical Physics*, vol. 2016, Article ID 6095236, 9 pages, 2016.
- [27] A. Ashtekar, V. Taveras, and M. Varadarajan, “Information is not lost in the evaporation of 2D black holes,” *Physical Review Letters*, vol. 100, no. 21, 211302, 4 pages, 2008.
- [28] A. Ashtekar, F. Pretorius, and F. M. Ramazanoglu, “Evaporation of two-dimensional black holes,” *Physical Review D*, vol. 83, no. 4, Article ID 044040, 2011.
- [29] C. Rovelli and F. Vidotto, “Planck stars,” *International Journal of Modern Physics D*, vol. 23, no. 12, Article ID 1442026, 2014.
- [30] H. M. Haggard and C. Rovelli, “Quantum-gravity effects outside the horizon spark black to white hole tunneling,” *Physical Review D: Particles, Fields, Gravitation and Cosmology*, vol. 92, no. 10, 104020, 11 pages, 2015.
- [31] L. Susskind, L. Thorlacius, and J. Uglum, “The stretched horizon and black hole complementarity,” *Physical Review D: Particles, Fields, Gravitation and Cosmology*, vol. 48, no. 8, pp. 3743–3761, 1993.
- [32] C. R. Stephens, G. ’t Hooft, and B. F. Whiting, “Black hole evaporation without information loss,” *Classical and Quantum Gravity*, vol. 11, no. 3, pp. 621–647, 1994.
- [33] S. Leonard and L. James, *The holographic universe – An introduction to black holes, information and the string theory revolution*, World Scientific, 2004.
- [34] A. Almheiri, D. Marolf, J. Polchinski, and J. Sully, “Black holes: Complementarity or firewalls?” *Journal of High Energy Physics*, vol. 2013, no. 2, pp. 1–19, 2013.
- [35] O. C. Stoica, *Singular General Relativity [Ph.D. Thesis]*, Minkowski Institute Press, 2013.
- [36] R. Kubo, “Statistical-mechanical theory of irreversible processes. I. general theory and simple applications to magnetic and conduction problems,” *Journal of the Physical Society of Japan*, vol. 12, no. 6, pp. 570–586, 1957.
- [37] P. C. Martin and J. Schwinger, “Theory of many-particle systems. I,” *Physical Review A: Atomic, Molecular and Optical Physics*, vol. 115, no. 6, pp. 1342–1373, 1959.
- [38] W. G. Unruh, “Notes on black-hole evaporation,” *Physical Review D: Particles, Fields, Gravitation and Cosmology*, vol. 14, no. 4, pp. 870–892, 1976.
- [39] S. A. Fulling, “Nonuniqueness of canonical field quantization in riemannian space-time,” *Physical Review D: Particles, Fields, Gravitation and Cosmology*, vol. 7, no. 10, pp. 2850–2862, 1973.
- [40] P. C. Davies, “Scalar production in Schwarzschild and Rindler metrics,” *Journal of Physics A: Mathematical and General*, vol. 8, no. 4, pp. 609–616, 1975.
- [41] R. M. Wald, *Quantum Field Theory in Curved Space-Time and Black Hole Thermodynamics*, University of Chicago Press, 1994.
- [42] O. Stoica, “Analytic Reissner–Nordström singularity,” *Physica Scripta*, vol. 85, no. 5, p. 055004, 2012.
- [43] M. Maldacena, “The large- N limit of superconformal field theories and supergravity,” *International Journal of Theoretical Physics*, vol. 38, no. 4, pp. 1113–1133, 1999.
- [44] A. G. Riess, A. V. Filippenko, P. Challis et al., “Observational evidence from supernovae for an accelerating universe and a cosmological constant,” *The Astronomical Journal*, vol. 116, no. 3, pp. 1009–1038, 1998.
- [45] S. Perlmutter, G. Aldering, and G. Goldhaber, “Measurements of Ω and Λ from 42 High-Redshift Supernovae,” *The Astrophysical Journal*, vol. 517, no. 2, pp. 565–586, 1999.
- [46] S. W. Hawking, “Information loss in black holes,” *Physical Review D: Particles, Fields, Gravitation and Cosmology*, vol. 72, Article ID 084013, 2005.
- [47] R. H. Price and K. S. Thorne, “Membrane viewpoint on black holes: properties and evolution of the stretched horizon,” *Physical Review D: Particles, Fields, Gravitation and Cosmology*, vol. 33, no. 4, pp. 915–941, 1986.
- [48] J. L. Park, “The concept of transition in quantum mechanics,” *Foundations of Physics*, vol. 1, no. 1, pp. 23–33, 1970.
- [49] W. K. Wootters and W. H. Zurek, “A single quantum cannot be cloned,” *Nature*, vol. 299, no. 5886, pp. 802–803, 1982.
- [50] D. Dieks, “Communication by EPR devices,” *Physics Letters A*, vol. 92, no. 6, pp. 271–272, 1982.
- [51] J. R. Oppenheimer and H. Snyder, “On continued gravitational contraction,” *Physical Review A: Atomic, Molecular and Optical Physics*, vol. 56, no. 5, pp. 455–459, 1939.
- [52] L. S. Schulman, *Time’s arrows and quantum measurement*, Cambridge University Press, 1997.
- [53] R. Bousso, “Observer complementarity upholds the equivalence principle,” 2012, <https://arxiv.org/abs/1207.5192>.
- [54] D. Harlow and P. Hayden, “Quantum computation vs. firewalls,” *Journal of High Energy Physics*, vol. 6, no. 85, 2013.
- [55] R. Bousso, “Complementarity is not enough,” *Physical Review D: Particles, Fields, Gravitation and Cosmology*, vol. 87, no. 12, 2013.
- [56] J. Maldacena and L. Susskind, “Cool horizons for entangled black holes,” *Fortschritte der Physik/Progress of Physics*, vol. 61, no. 9, pp. 781–811, 2013.
- [57] K. L. H. Bryan and A. J. M. Medved, “Black holes and information: a new take on an old paradox,” *Advances in High Energy Physics*, vol. 2017, Article ID 7578462, 8 pages, 2017.
- [58] D. Stanford and L. Susskind, “Complexity and shock wave geometries,” *Physical Review D: Particles, Fields, Gravitation and Cosmology*, vol. 90, no. 12, 2014.
- [59] S. Aaronson, “The complexity of quantum states and transformations: from quantum money to black holes,” 2016, <https://arxiv.org/abs/1607.05256>.

- [60] S. L. Braunstein, S. Pirandola, and K. Życzkowski, “Better late than never: Information retrieval from black holes,” *Physical Review Letters*, vol. 110, no. 10, Article ID 101301, 2013.
- [61] A. Y. Yosifov and L. G. Filipov, “Entropic Entanglement: Information Prison Break,” *Advances in High Energy Physics*, vol. 2017, Article ID 8621513, 7 pages, 2017.
- [62] S. W. Hawking, “Information preservation and weather forecasting for black holes,” 2014, <https://arxiv.org/abs/1401.5761>.
- [63] S. W. Hawking, “The information paradox for black holes,” Tech. Rep. DAMTP-2015-49, 2015.
- [64] S. W. Hawking, M. J. Perry, and A. Strominger, “Soft Hair on Black Holes,” *Physical Review Letters*, vol. 116, no. 23, Article ID 231301, 2016.
- [65] S. W. Hawking, M. J. Perry, and A. Strominger, “Superrotation charge and supertranslation hair on black holes,” *Journal of High Energy Physics*, vol. 5, p. 161, 2017.
- [66] L. Susskind, “The world as a hologram,” *Journal of Mathematical Physics*, vol. 36, no. 11, pp. 6377–6396, 1995.
- [67] K. Papadodimas and S. Raju, “Black Hole Interior in the Holographic Correspondence and the Information Paradox,” *Physical Review Letters*, vol. 112, no. 5, 2014.
- [68] Z.-L. Wang and Y. Yan, “Bulk Local Operators, Conformal Descendants, and Radial Quantization,” *Advances in High Energy Physics*, vol. 2017, Article ID 8185690, 11 pages, 2017.
- [69] A. Geffer, “Complexity on the horizon,” *Nature*, 2014.
- [70] R. Bousso, “Firewalls from double purity,” *Physical Review D: Particles, Fields, Gravitation and Cosmology*, vol. 88, no. 8, 2013.
- [71] S. Weinert, E. W. Tedford, M. C. Penrice, W. G. Unruh, and G. A. Lawrence, “Measurement of Stimulated Hawking Emission in an Analogue System,” *Physical Review Letters*, vol. 106, no. 2, 2011.
- [72] J. M. Bardeen, B. Carter, and S. W. Hawking, “The four laws of black hole mechanics,” *Communications in Mathematical Physics*, vol. 31, pp. 161–170, 1973.
- [73] R. Bousso, “The holographic principle,” *Reviews of Modern Physics*, vol. 74, no. 3, pp. 825–874, 2002.
- [74] S. W. Hawking, “Gravitational radiation from colliding black holes,” *Physical Review Letters*, vol. 26, no. 21, pp. 1344–1346, 1971.
- [75] R. B. Mann, *Black Holes: Thermodynamics, Information, And Firewalls*, Springer, New York, NY, USA, 2015.
- [76] L. Parker, “Quantized fields and particle creation in expanding universes. I,” *Physical Review A: Atomic, Molecular and Optical Physics*, vol. 183, no. 5, pp. 1057–1068, 1969.
- [77] B. P. Dolan, *Where is the pdv term in the first law of black hole thermodynamics?*, 2014.
- [78] R. M. Wald, “Black hole entropy is the Noether charge,” *Physical Review D: Particles, Fields, Gravitation and Cosmology*, vol. 48, no. 8, pp. R3427–R3431, 1993.
- [79] T. Jacobson, “Thermodynamics of spacetime: the Einstein equation of state,” *Physical Review Letters*, vol. 75, p. 1260, 1995.
- [80] E. Verlinde, “On the origin of gravity and the laws of Newton,” *Journal of High Energy Physics*, vol. 4, p. 29, 2011.
- [81] G. D. Birkhoff and R. E. Langer, *Relativity and Modern Physics*, vol. 1, Harvard University Press Cambridge, 1923.
- [82] M. Heusler, “No-hair theorems and black holes with hair,” *Helvetica Physica Acta. Physica Theoretica. Societatis Physicae Helveticae Commentaria Publica*, vol. 69, no. 4, pp. 501–528, 1996.
- [83] N. E. Mavromatos, “Eluding the no-hair conjecture for black holes,” 1996, <https://arxiv.org/abs/gr-qc/9606008>.
- [84] W. H. Zurek and K. S. Thorne, “Statistical mechanical origin of the entropy of a rotating, charged black hole,” *Physical Review Letters*, vol. 54, no. 20, pp. 2171–2175, 1985.
- [85] G. ’t Hooft, “On the quantum structure of a black hole,” *Nuclear Physics B*, vol. 256, no. 4, pp. 727–745, 1985.
- [86] R. B. Mann, L. Tarasov, and A. Zelnikov, “Brick walls for black holes,” *Classical and Quantum Gravity*, vol. 9, no. 6, pp. 1487–1494, 1992.
- [87] S. Carlip, “Entropy from conformal field theory at Killing horizons,” *Classical and Quantum Gravity*, vol. 16, no. 10, pp. 3327–3348, 1999.
- [88] A. Strominger and C. Vafa, “Microscopic origin of the Bekenstein-Hawking entropy,” *Physics Letters B*, vol. 379, no. 1–4, pp. 99–104, 1996.
- [89] G. T. Horowitz and A. Strominger, “Counting States of Near-Extremal Black Holes,” *Physical Review Letters*, vol. 77, no. 12, pp. 2368–2371, 1996.
- [90] A. Dabholkar, “Exact counting of supersymmetric black hole microstates,” *Physical Review Letters*, vol. 94, no. 24, 241301, 4 pages, 2005.
- [91] A. Ashtekar, J. Baez, A. Corichi, and K. Krasnov, “Quantum geometry and black hole entropy,” *Physical Review Letters*, vol. 80, no. 5, pp. 904–907, 1998.
- [92] L. Bombelli, R. K. Koul, J. Lee, and R. D. Sorkin, “Quantum source of entropy for black holes,” *Physical Review D: Particles, Fields, Gravitation and Cosmology*, vol. 34, no. 2, pp. 373–383, 1986.
- [93] M. Srednicki, “Entropy and area,” *Physical Review Letters*, vol. 71, no. 5, pp. 666–669, 1993.
- [94] V. Frolov and I. Novikov, “Dynamical origin of the entropy of a black hole,” *Physical Review D: Particles, Fields, Gravitation and Cosmology*, vol. 48, no. 10, pp. 4545–4551, 1993.
- [95] C. Corda, “Effective temperature, hawking radiation and quasinormal modes,” *International Journal of Modern Physics D*, vol. 21, no. 11, Article ID 1242023, 2012.
- [96] C. Corda, “Black hole quantum spectrum,” *The European Physical Journal C*, vol. 73, p. 2665, 2013.
- [97] C. Corda, “Bohr-like model for black-holes,” *Classical and Quantum Gravity*, vol. 32, no. 19, article 5007, 2015.
- [98] G. Dvali and C. Gomez, “Quantum compositeness of gravity: black holes, AdS and inflation,” *Journal of Cosmology and Astroparticle Physics*, no. 1, 023, front matter+46 pages, 2014.
- [99] R. Casadio, A. Giugno, O. Micu, and A. Orlandi, “Black holes as self-sustained quantum states and Hawking radiation,” *Physical Review D: Particles, Fields, Gravitation and Cosmology*, vol. 90, no. 8, 2014.
- [100] R. Casadio, A. Giugno, O. Micu, and A. Orlandi, “Thermal BEC black holes,” *Entropy*, vol. 17, no. 10, pp. 6893–6924, 2015.
- [101] J. D. Bekenstein, “How does the entropy/information bound work?” *Foundations of Physics. An International Journal Devoted to the Conceptual Bases and Fundamental Theories of Modern Physics*, vol. 35, no. 11, pp. 1805–1823, 2005.
- [102] S. Schaffer, “John michell and black holes,” *Journal for the History of Astronomy*, vol. 10, no. 1, pp. 42–43, 1979.
- [103] C. Rovelli, “Black holes have more states than those giving the Bekenstein-Hawking entropy: a simple argument,” 2017, <https://arxiv.org/abs/1710.00218>.

- [104] E. Bianchi, M. Christodoulou, F. D'Ambrosio, H. M. Haggard, and C. Rovelli, "White holes as remnants: A surprising scenario for the end of a black hole," 2018, <https://arxiv.org/abs/1802.04264>.
- [105] A. Ashtekar, *Lectures on Non-Perturbative Canonical Gravity*, World Scientific, Singapore, 1991.
- [106] G. Yoneda, H.-a. Shinkai, and A. Nakamichi, "Trick for passing degenerate points in the Ashtekar formulation," *Physical Review D: Particles, Fields, Gravitation and Cosmology*, vol. 56, no. 4, pp. 2086–2093, 1997.
- [107] O. C. Stoica, "On singular semi-Riemannian manifolds," *International Journal of Geometric Methods in Modern Physics*, vol. 11, no. 5, 1450041, 40 pages, 2014.
- [108] O. C. Stoica, "The geometry of warped product singularities," *International Journal of Geometric Methods in Modern Physics*, vol. 14, no. 2, 1750024, 16 pages, 2017.
- [109] O. C. Stoica, "The Friedmann-Lemaître-Robertson-Walker Big Bang Singularities are Well Behaved," *International Journal of Theoretical Physics*, vol. 55, no. 1, pp. 71–80, 2016.
- [110] O. C. Stoica, "Beyond the Friedmann-Lemaître-Robertson-Walker Big Bang singularity," *Communications in Theoretical Physics*, vol. 58, pp. 613–616, 2012.
- [111] O. C. Stoica, "Schwarzschild singularity is semi-regularizable," *The European Physical Journal Plus*, vol. 127, no. 83, pp. 1–8, 2012.
- [112] O. C. Stoica, "Kerr-Newman solutions with analytic singularity and no closed timelike curves," *"Politehnica" University of Bucharest. Scientific Bulletin. Series A. Applied Mathematics and Physics*, vol. 77, no. 1, pp. 129–138, 2015.
- [113] O. C. Stoica, "Spacetimes with singularities," *Analele stiintifice ale Universitatii Ovidius Constanta*, vol. 20, no. 2, pp. 213–238, 2012.
- [114] O. C. Stoica, "The geometry of singularities and the black hole information paradox," *Journal of Physics: Conference Series*, vol. 626, Article ID 012028, 2015.
- [115] A. S. Eddington, "A Comparison of Whitehead's and Einstein's Formulæ," *Nature*, vol. 113, no. 2832, p. 192, 1924.
- [116] D. Finkelstein, "Past-future asymmetry of the gravitational field of a point particle," *Physical Review Journals Archive*, vol. 110, p. 965, 1958.
- [117] O. C. Stoica, "Gauge theory at singularities," 2014, <https://arxiv.org/abs/1408.3812>.
- [118] O. C. Stoica, "Causal structure and spacetime singularities," 2015, <https://arxiv.org/abs/1504.07110>.
- [119] PAM Dirac, "The Lagrangian in quantum mechanics," *Physikalische Zeitschrift der Sowjetunion*, vol. 1, no. 3, 1933.
- [120] R. P. Feynman and A. R. Hibbs, *Quantum Mechanics and Path Integrals: Emended Edition*, Dover Publications, Incorporated, 2012.
- [121] H. Kleinert, *Path integrals in quantum mechanics, statistics, polymer physics, and financial markets*, World Scientific, Singapore, 2009.
- [122] O. C. Stoica, "Metric dimensional reduction at singularities with implications to quantum gravity," *Annals of Physics*, vol. 347, pp. 74–91, 2014.
- [123] P. P. Fiziev and D. V. Shirkov, "Solutions of the Klein-Gordon equation on manifolds with variable geometry including dimensional reduction," *Theoretical and Mathematical Physics*, vol. 167, no. 2, pp. 680–691, 2011.
- [124] D. V. Shirkov, "Dream-land with Classic Higgs field, Dimensional Reduction and all that," in *Proceedings of the Steklov Institute of Mathematics*, vol. 272, pp. 216–222, 2011.

Research Article

Hawking Radiation of a Single-Partition Black Hole

Youngsub Yoon 

Department of Physics and Astronomy, Seoul National University, Seoul 08826, Republic of Korea

Correspondence should be addressed to Youngsub Yoon; youngsub@post.harvard.edu

Received 28 March 2018; Revised 20 May 2018; Accepted 26 June 2018; Published 24 September 2018

Academic Editor: Farook Rahaman

Copyright © 2018 Youngsub Yoon. This is an open access article distributed under the Creative Commons Attribution License, which permits unrestricted use, distribution, and reproduction in any medium, provided the original work is properly cited. The publication of this article was funded by SCOAP³.

Brian Kong and the present author recently presented a new area spectrum and showed that the new area spectrum implies that the decay time of a single-partition black hole (i.e., a black hole with the area not big enough to have two or more partitions) is roughly constant. In this article, we show why the decay time of a single-partition black hole is roughly constant.

1. Introduction

It is now very well-known that black hole emits particles thanks to Hawking's semiclassical treatment of black hole [1]. However, as Rovelli and Smolin discovered loop quantum gravity as a possible method to quantize gravity in late 80s [2], it was destined that Hawking's semiclassical treatment of Hawking radiation needed some modification. Soon, it was discovered that area is discrete according to loop quantum gravity [3–5], and Rovelli found the first connection between the Bekenstein-Hawking entropy and loop quantum gravity in his seminal paper in 1996 [6]. Soon, Hawking radiation spectrum was also approached from the loop quantum gravity framework using the discreteness of area [7–9]. In mid-2010s, the present author approached the problem of Hawking radiation spectrum from the discreteness of area as well and found surprising results such as full discreteness of Hawking radiation spectrum [10] and Maxwell-Boltzmann nature of Hawking radiation spectrum [11]. Also, Brian Kong and the present author suggested a new area spectrum in [12], boldly claiming that the conventional area spectrum known in loop quantum gravity community could be wrong, if one considers that, for area two-form, one needs to use Levi-Civita tensor instead of Levi-Civita symbol as conventionally used in loop quantum gravity community. This consideration predicted that the area spectrum was the square root of the conventional one. As for the evidence of this area spectrum, we showed that the Bekenstein-Hawking entropy was approximately satisfied (we conjectured that it would be

exactly satisfied if the effect of extra dimension is considered, which can lead to the prediction of fine structure constant) and found a strange, coincidental numerical relation that implied that the decay time of a single-partition black hole is roughly constant. In this article, we show why the decay time of a single-partition black hole is roughly constant. This new further evidence will give another support the area spectrum proposed by Brian Kong and us. The organization of this paper is as follows. In Section 2, we briefly review loop quantum gravity and its approach to Hawking radiation, particularly focusing on our previous work. In Section 3, we briefly review Brian Kong and the present author's work on new area spectrum focusing on the strange, coincidental numerical relation. In Section 4, we explain our own work on Hawking radiation briefly mentioned in Section 2 in more detail. In Section 5, we explain what is special about single-partition black hole. In Section 6, we derive the constancy of decay time for single-partition black hole. In Section 7, we conclude our paper.

2. Loop Quantum Gravity and Its Approach to Hawking Radiation

According to loop quantum gravity, the eigenvalues of the area operator are quantized [3–5] and the black hole area, as much as any area, is the sum of these eigenvalues. For example, let us say that we have the following area eigenvalues (i.e., the unit areas):

$$A_i = A_1, A_2, A_3, A_4, A_5, A_6, \dots \quad (1)$$

TABLE 1: C(A).

y	A	K(A)	I(A)	C(A)
1	17.8	4	767.4	191.8
2	21.1	14	2740	195.7
3	23.4	32	5552	173.5
4	25.1	50	9276	185.5
5	26.6	72	14000	194.4
6	27.8	110	19814	180.1
7	28.9	154	26817	174.1
8	29.9	204	35109	172.1
9	30.8	262	44797	171.0
10	31.6	326	55990	171.7
11	32.4	388	68803	177.3
12	33.1	474	83353	175.8
13	33.7	584	99761	170.8
14	34.4	684	118155	172.7
15	35.0	804	138664	172.5

Then, the black hole area A must be given by the following formula:

$$A = \sum_i N_i A_i, \quad (2)$$

where N_i s are nonnegative integers. Here, we can regard the black hole as having $\sum N_i$ partitions, each of which has one of the A_i as its area.

In [10], the present author showed that the black hole area decrease upon a single emission of photon during Hawking radiation must be given by the unit area. In other words, we have

$$\Delta A = -A_i \quad (3)$$

As the Bekenstein-Hawking entropy is given by $S = kA/4$, [1, 13] and we know $\Delta Q = T\Delta S$, the energy decrease is given by

$$\Delta Q = -\frac{A_i}{4}kT \quad (4)$$

Since this energy must be equal to the energy of photon emitted (i.e., $\Delta Q = -E_{\text{photon}}$) the energy of the photon emitted during the Hawking radiation is given by

$$E_{\text{photon}} = \frac{A_i}{4}kT \quad (5)$$

In particular, the Hawking radiation spectrum is discrete.

3. Area Spectrum and Single-Partition Black Holes

In [12] (see also [14]), Brian Kong and the present author showed that the area spectrum (i.e., the unit areas) in black hole horizon is given by

$$A = 8\pi \sum_i \sqrt{\frac{1}{2} \sqrt{2j_i^u(j_i^u + 1) + 2j_i^d(j_i^d + 1) - j_i^t(j_i^t + 1)}} \quad (6)$$

with the degeneracy $(2j_i^u + 1) + (2j_i^d + 1)$ where j_i^u , j_i^d , and j_i^t satisfy the triangle inequality (i.e., $j_i^1 + j_i^2 \geq j_i^3$) and j_i^t is an integer, and both j_i^u and j_i^d are integers or half-integers at the same time. We want to remark that (6) is not a conventional one and it has an extra square root compared to [14]. However, Brian Kong and the present author argued in [12] that we arrive at this formula, if we use, in the equation for the area two-form, a Levi-Civita tensor instead of a Levi-Civita symbol as conventionally done in loop quantum gravity community.

Using this, we calculated the degeneracy of area spectrum using Java. This yielded $K(A)$ in Table 1 where $K(A)$ is the number of states for area equal to or below A , and $I(A)$ is given by

$$I(A) = \int_{A_{\text{cut}}}^A \sqrt{A'} (e^{A'/4} - 1) dA' \quad (7)$$

and y is conveniently defined as follows:

$$y = 2j_i^u(j_i^u + 1) + 2j_i^d(j_i^d + 1) - j_i^t(j_i^t + 1) \quad (8)$$

Of course, using y , we have the following relation:

$$A(y) = 8\pi \sqrt{\frac{1}{2} \sqrt{y}} \quad (9)$$

$C(A)$ is given by

$$C(A) = \frac{I(A)}{K(A)} \quad (10)$$

The point of this table is that $C(A)$ is roughly constant. We found this accidentally. Of course $C(A)$ is not exactly but only approximately constant, but the biggest value for $C(A)$ in our result is 195.7, deviating from the “right value” of C , i.e., the value of C for large A by only about 13 percent. As $K(A)$ at this biggest value of $C(A)$ is only 14, it necessarily has a big “statistical” variation. Therefore, 195.7 is not a big deviation.

Then, in Sections X and XI of the same paper, we showed that this constancy can be explained if the decay time of a single-partition black hole is constant. Let us briefly summarize some of the main reasonings.

Let us denote the average number of photons emitted from a black hole during the infinitesimal time Δt by $j_{\Delta t}$. Then, we have

$$j_{\Delta t} = \frac{\Delta t}{\tau} \quad (11)$$

For macroscopic black hole, if dn_{photon} is the number of photons with a frequency between ν and $\nu + d\nu$ emitted during unit time, from Planck's blackbody radiation formula, we have

$$dn_{\text{photon}} = \frac{2\pi\nu^2}{c^2} \frac{A_{BH}d\nu}{e^{h\nu/kT} - 1} \quad (12)$$

where A_{BH} is the area of black hole. Of course, we naturally have

$$\frac{1}{\tau} = \int dn_{\text{photon}} \quad (13)$$

Now let us say that, during the time Δt , the number of emitted photons which correspond to a decrease in the black hole area by amount a is given by $x_{a(y),\Delta t}$. Here, y is given by (8), and $a(y)$ is given by (9).

Then, in section XI, by some calculations we showed

$$x_{a,\Delta t} = \frac{3\sqrt{\pi c}}{2\sqrt{A_{BH}}} \frac{1}{e^{a/4} - 1} \Delta t \quad (14)$$

We proceeded by borrowing the idea from a paper by Bekenstein and Mukhanov [7]. The idea is that $x_{a,\Delta t}/j_{\Delta t}$ is proportional to the degeneracy of the black hole after emission divided by the degeneracy of the black hole before emission. Let us denote the degeneracy of the black hole with area A_{BH} by $W(A_{BH})$. Then, from (11) and (14), we have

$$\frac{W(A_{BH} - a)}{W(A_{BH})} \propto \frac{\tau}{\sqrt{A_{BH}}} \frac{1}{e^{a/4} - 1} \quad (15)$$

Now, if a black hole is a single-partition black hole (a black hole not big enough to have two or more partitions), upon emission of a photon, there is no other value for area decrease than $a = A_{BH}$. Plugging this value to the above formula, we get

$$\frac{W(0)}{W(A_{BH})} \propto \frac{\tau}{\sqrt{A_{BH}}} \frac{1}{e^{A_{BH}/4} - 1} \quad (16)$$

which implies

$$W(A_{BH}) \propto \frac{\sqrt{A_{BH}}}{\tau} (e^{A_{BH}/4} - 1) \quad (17)$$

If τ is constant for single-partition black hole, then it is precisely our earlier relations (7) and (10). Also, one thing very noticeable is that these relations do not hold for

multipartitioned black holes. The minimum area a black hole can have is given by $A(y = 1) = 4\pi\sqrt{2}$. For it to be a single-partition black hole, its area should be smaller than $2A(y = 1) = A(y = 16)$. Our relations suddenly do not hold beginning from $y = 16$ even though it holds very well for $y < 16$. This is the reason why the table is presented up to $y = 15$.

However, we later realized formula (14), which we derived in section XI of [12], is due to an error. Nevertheless, we obtained a strong hint that Table 1 is due to Hawking radiation of single-partition black hole.

4. Quantum Corrections to the Hawking Radiation Spectrum

As mentioned in Section 2, the present author showed in [10] that, upon emission of a single photon during Hawking radiation, only single area quanta can decrease. Let us briefly repeat the main argument in that paper. (In an earlier work [11], the author showed that Hawking radiation should follow Maxwell-Boltzmann statistics rather than Bose-Einstein statistics as considered in [10]. We adjust our presentation here considering this earlier work.)

Consider the following problem [15].

Let us say that the unit areas A_1, A_2, A_3, \dots have degeneracies d_1, d_2, d_3, \dots . Suppose we have a black hole with area A which satisfies $A = \sum_i N_i A_i$ as explained before in (2). For a given configuration ($N_i = N_1, N_2, N_3, \dots$), how many different ways can this be achieved?

According to Rovelli [6], the area quanta are distinguishable, as they have fixed location on the black hole horizon, and, only if they are so, the Bekenstein-Hawking entropy can be satisfied. Using this distinguishability, the answer to the above question is given by

$$Q = N! \prod_{i=1}^{\infty} \frac{d_i^{N_i}}{N_i!} \quad (18)$$

where $N = \sum_i N_i$.

By maximizing Q and using (5), one obtains that the Hawking radiation for macroscopic black hole is given by the following Maxwell-Boltzmann distribution:

$$N_i = N d_i e^{-hf_i/(kT)} = N d_i e^{-A_i/4} \quad (19)$$

(Note that if we do not follow the present author's earlier work [11], this would be the familiar Einstein-Bose distribution of Hawking radiation, namely, $N_i/N = d_i/(\exp(hf_i/kT) - 1)$.)

We can do better than this. We can express the above expression in terms of the black hole horizon area A . By plugging the above formula to (2), we get

$$N = \frac{A}{\sum_i d_i A_i e^{-A_i/4}} \quad (20)$$

By plugging the above formula back to (19), we get

$$N_i = \frac{A d_i e^{-A_i/4}}{\sum_i d_i A_i e^{-A_i/4}} \quad (21)$$

Notice that the above expression is proportional to the black hole horizon area A . Therefore, we conclude that the Hawking radiation for macroscopic black hole is proportional to the area of black hole, as much as Planck's blackbody radiation spectrum is proportional to the area of blackbody.

5. Single-Partition Black Hole

Let us see what happens for (2) for a single-partition black hole. In such a case we have $N = 1$. This implies $N_i = 1$ for the concerned i and 0 for other unconcerned values of i . Now, remember what N_i meant in (19). It is exactly Hawking radiation spectrum of given frequency. As the sum of N_i is N , N is the sum of Hawking radiation of every frequency, namely, total Hawking radiation. Thus, we conclude that the decay time of the single-partition black hole is constant as N , which is 1, is constant. In other words, τ is constant as desired.

6. Derivation

In this section, we derive (7) and (10) using the correct method.

At the end of Section 4, we showed that Hawking radiation is proportional to the black hole area A . However, this is only half correct as this holds true only if the temperature of black hole were fixed constant. In reality, the temperature of black hole depends on the black hole area A .

So, let us consider this dependence. The number of black hole area quanta is given by (20), and the number of photons emitted per a second is given by (12) and (13). That is,

$$\frac{1}{\tau} = A_{BH} \frac{2\pi}{c^2} \int_{\pi\sqrt{2}}^{\infty} \frac{u^2 du}{e^u - 1} \left(\frac{kT}{h} \right)^3 \quad (22)$$

where the integration range is not from 0 but from $\pi\sqrt{2}$ because the minimum unit area satisfies $A(y=1)/4 = \pi\sqrt{2}$ which is nonzero. As $kT = 1/(8\pi M)$ and $A = 16\pi M^2$ (in this article and earlier ones we only consider Schwarzschild black hole for simplicity), we can write

$$\frac{1}{\tau} = N \frac{\alpha_0}{A_{BH}^{3/2}} \quad (23)$$

for some constant α_0 calculable from (20) and (22). Therefore, for macroscopic black hole, we can write

$$\frac{x_{A_i, \Delta t}}{\Delta t} = N_i \frac{\alpha_0}{A_{BH}^{3/2}} \quad (24)$$

which, when plugged in (21), is given by

$$\frac{x_{A_i, \Delta t}}{\Delta t} = \frac{d_i e^{-A_i/4}}{\sqrt{A_{BH}}} \left(\frac{\alpha_0}{\sum_i d_i A_i e^{-A_i/4}} \right) \quad (25)$$

Now, let us assume that this formula holds for single-partition black hole and further assume that the left-hand side of the above equation is constant, which is reasonable as N_i , being 1, is constant. Then, as the factors in the parenthesis in the above equation are merely constant, we immediately see that (7) and (10) are reproduced.

7. Discussions and Conclusions

One may argue that the table is not fitted correctly as it is fitted with Bose-Einstein distribution factor $e^{A/4} - 1$ while the table should be fitted with the Maxwell-Boltzmann distribution factor $e^{A/4}$ if author's earlier work [11] is correct. This is true, but the difference is insignificant as the lowest value for $e^{A/4}$ is about 85, which means that extra “−1” would not significantly affect the fitting.

In this paper, we showed what the thermodynamics of single-partition black hole implies about the degeneracy of area spectrum up from $y = 1$ to $y = 15$. For your information, the number of degeneracies for $A(y)$ up to $y = 65$ is available at (<http://youngsubyoon.com/65.csv>). If you add them up, you get $K(A)$.

In conclusion, we strongly believe that the extremely strange behaviors of Table 1 (the approximate constancy of C and the relation not holding beginning from exactly $y = 16$) are not a mere coincidence, instead they indicate the correctness of the area spectrum presented in [12].

Data Availability

The data are available at youngsubyoon.com/65.csv.

Conflicts of Interest

The authors declare that they have no conflicts of interest.

References

- [1] S. W. Hawking, “Particle creation by black holes,” *Communications in Mathematical Physics*, vol. 43, no. 3, pp. 199–220, 1975.
- [2] C. Rovelli and L. Smolin, “Loop space representation of quantum general relativity,” *Nuclear Physics. B. Theoretical, Phenomenological, and Experimental High Energy Physics. Quantum Field Theory and Statistical Systems*, vol. 331, no. 1, pp. 80–152, 1990.
- [3] C. Rovelli and L. Smolin, “Discreteness of area and volume in quantum gravity,” *Nuclear Physics B*, vol. 442, no. 3, pp. 593–619, 1995.
- [4] S. Frittelli, L. Lehner, and C. Rovelli, “The complete spectrum of the area from recoupling theory in loop quantum gravity,” *Classical and Quantum Gravity*, vol. 13, no. 11, pp. 2921–2931, 1996.
- [5] A. Ashtekar and J. Lewandowski, “Quantum theory of geometry. I. Area operators,” *Classical and Quantum Gravity*, vol. 14, no. 1A, pp. A55–A81, 1997.
- [6] C. Rovelli, “Black hole entropy from loop quantum gravity,” *Physical Review Letters*, vol. 77, no. 16, pp. 3288–3291, 1996.
- [7] J. D. Bekenstein and V. F. Mukhanov, “Spectroscopy of the quantum black hole,” *Physics Letters B*, vol. 360, no. 1-2, pp. 7–12, 1995.
- [8] M. Barreira, M. Carfora, and C. Rovelli, “Physics with non-perturbative quantum gravity: radiation from a quantum black hole,” *General Relativity and Gravitation*, vol. 28, no. 11, pp. 1293–1299, 1996.
- [9] K. V. Krasnov, “Quantum geometry and thermal radiation from black holes,” *Classical and Quantum Gravity*, vol. 16, no. 2, pp. 563–578, 1999.

- [10] Y. Yoon, “Quantum corrections to the Hawking radiation spectrum,” *Journal of the Korean Physical Society*, vol. 68, no. 6, pp. 730–734, 2016.
- [11] Y. Yoon, “Maxwell-Boltzmann type Hawking radiation,” *Modern Physics Letters A*, vol. 32, no. 12, 1750071, 4 pages, 2017.
- [12] B. Kong and Y. Yoon, “Black hole entropy predictions without the Immirzi parameter and Hawking radiation of a single-partition black hole,” *Journal of the Korean Physical Society*, vol. 68, no. 6, pp. 735–751, 2016.
- [13] J. D. Bekenstein, “Black holes and entropy,” *Physical Review D: Particles, Fields, Gravitation and Cosmology*, vol. 7, pp. 2333–2346, 1973.
- [14] T. Tanaka and T. Tamaki, “Black hole entropy for the general area spectrum,” *Journal of Physics: Conference Series*, vol. 229, p. 012080, 2010.
- [15] D. J. Griffiths, *Introduction to quantum mechanics*, Prentice Hall, Upper Saddle River, NJ, 2005.

Research Article

Classical Polymerization of the Schwarzschild Metric

Babak Vakili ^{1,2}

¹Research Institute for Astronomy and Astrophysics of Maragha (RIAAM), Maragha, P.O. Box 55134-441, Iran

²Department of Physics, Central Tehran Branch, Islamic Azad University, Tehran, Iran

Correspondence should be addressed to Babak Vakili; b.vakili@iauctb.ac.ir

Received 31 May 2018; Accepted 5 September 2018; Published 20 September 2018

Guest Editor: Farook Rahaman

Copyright © 2018 Babak Vakili. This is an open access article distributed under the Creative Commons Attribution License, which permits unrestricted use, distribution, and reproduction in any medium, provided the original work is properly cited. The publication of this article was funded by SCOAP³.

We study a spherically symmetric setup consisting of a Schwarzschild metric as the background geometry in the framework of classical polymerization. This process is an extension of the polymeric representation of quantum mechanics in such a way that a transformation maps classical variables to their polymeric counterpart. We show that the usual Schwarzschild metric can be extracted from a Hamiltonian function which in turn gets modifications due to the classical polymerization. Then, the polymer corrected Schwarzschild metric may be obtained by solving the polymer-Hamiltonian equations of motion. It is shown that while the conventional Schwarzschild space-time is a vacuum solution of the Einstein equations, its polymer-corrected version corresponds to an energy-momentum tensor that exhibits the features of dark energy. We also use the resulting metric to investigate some thermodynamical quantities associated with the Schwarzschild black hole, and in comparison with the standard Schwarzschild metric the similarities and differences are discussed.

1. Introduction

One of the most important arenas that show the power of general relativity in describing the gravitational phenomena is the classical theory of black hole physics. However, when we introduce the quantum considerations to study of a gravitational systems, general relativity does not provide a satisfactory description of the physics of the system. The phenomena such as black hole radiation and all kinds of cosmological singularities are among the phenomena in which the use of quantum mechanics in their description is inevitable. This means that although general relativity is a classical theory, in its most important applications, the system under consideration originally obeys the rules of quantum mechanics. Therefore, any hope in the accurate description of gravitational systems in high energies depends on the development of a complete theory of quantum gravity. That is why the quantum gravity is one of the most important challenges in theoretical physics which from its DeWitt's traditional canonical formulation [1] to the more modern viewpoints of string theory and loop quantum gravity (LQG) [2–4] has gone a long way. One of the main features of the space-time proposed in LQG is its granular structure

which in turn, supports the idea of existence of a minimal measurable length. In the absence of a full theory of quantum gravity, effective theories which somehow exhibit quantum effects in gravitational systems play a significant role. These are theories which show some phenomenological aspects of quantum gravity and usually use a certain deformation in their formalism. For example, theories like generalized uncertainty principles and noncommutative geometry are in this category [5–13].

Among the effective theories that also use a minimal length scale in their formalism, we can mention the polymer quantization [14], which uses the methods very similar to the effective theories of LQG [15]. In polymer quantum approach a polymer length scale, λ , which shows the scale of the segments of the granular space, enters into the Hamiltonian of the system to deform its functional form into a so-called polymeric Hamiltonian. This means that, in a polymeric quantized system in addition of a quantum parameter \hbar , which is responsible to canonical quantization of the system, there is also another quantum parameter λ that labels the granular properties of the underlying space. This approach then opened new windows for the theories which are dealing with the quantum gravitational effects in physical systems

such as quantum cosmology and black hole physics; see, for instance [16–31] and the references therein.

To polymerize a dynamical system one usually begins with a classical system described by Hamiltonian H . The canonical quantization of such a system transforms its Hamiltonian to an Hermitian operator, which now contains the parameter \hbar , in such a way that in the limit $\hbar \rightarrow 0$, the quantum Hamiltonian H_\hbar returns to its classical counterpart. By polymerization, the Hamiltonian gets an additional quantum parameter λ , which is rooted in the ideas of granular structure of the space-time. Therefore, by taking the classical limit of the resulting Hamiltonian $H_{\hbar,\lambda}$, we arrive at a semiclassical theory in which the parameter λ is still present. To achieve the initial classical theory, one should once again take the limit $\lambda \rightarrow 0$ from this intermediate theory. It is believed that such effective classical theories H_λ have enough rich structure to exhibit some important features of the system related to the quantum effects without quantization of the system. The process by which the theory H_λ is obtained from the classical theory is called *classical polymerization*. A detailed explanation of this process with some of its cosmological applications can be found in [32].

In this paper, we are going to study how the metric of the Schwarzschild black hole gets modifications due to the classical polymerization. Since the thermodynamical properties of the black hole come from its geometrical structure, the corrections to the black hole's geometry yield naturally modifications to its thermodynamics. To do this, we begin with a general form of a spherically symmetric space-time and then construct a Hamiltonian in such a way that the Schwarzschild metric is resulted from the corresponding Hamiltonian equations of motion. We then follow the procedure described above and by applying it to the mentioned Hamiltonian we get the classical polymerized Hamiltonian, by means of which we expect to obtain the polymer-corrected Schwarzschild metric. The paper is organized as follows. In Section 2 we have presented a brief review of the polymer representation and classical polymerization. Section 3 is devoted to the Hamiltonian formalism of a general spherically symmetric space time. We show in this section that the resulting Hamiltonian equations of motion yield the Schwarzschild solution. In Section 4, we will apply the classical polymerization on the Hamiltonian of the spherically symmetric space-time given in Section 3 to get the polymerized Hamiltonian. We then construct the deformed Hamiltonian equations of motion and solve them to arrive the polymer corrected Schwarzschild metric. The energy-momentum tensor of the matter field corresponding to this metric as well as some of its thermodynamical properties are also presented in this section. The radial geodesics of the light and particles are obtained in Section 5 and, finally, we summarize the results in Section 6.

2. Classical Polymerization: A Brief Review

As is well known, in Schrödinger picture of quantum mechanics, the coordinates and momentum representations are equivalent and may be easily converted to each other

by a Fourier transformation. However, in the presence of the quantum gravitational effects the space-time may take a discrete structure so that such well-defined representations are no longer applicable. As an alternative, polymer quantization provides a suitable framework for studying these situations [14, 15]. The Hilbert space of this representation of quantum mechanics is $\mathcal{H}_{\text{poly}} = L^2(R_d, d\mu_d)$, where $d\mu_d$ is the Haar measure and R_d denotes the real discrete line whose segments are labeled by an extra dimension-full parameter λ such that the standard Schrödinger picture will be recovered in the continuum limit $\lambda \rightarrow 0$. This means that, by a classical limit $\hbar \rightarrow 0$, the polymer quantum mechanics tends to an effective λ -dependent classical theory which is somehow different from the classical theory from which we have started. Such an effective theory may also be obtained directly from the standard classical theory, without referring to the polymer quantization, by using of the Weyl operator [32]. The process is known as *polymerization* with which we will deal with in the rest of this paper.

According to the mentioned above form of the Hilbert space of the polymer representation of quantum mechanics, the position space (with coordinate q) has a discrete structure with discreteness parameter λ . Therefore, the associated momentum operator \hat{p} , which is the generator of the displacement, does not exist [15]. However, the Weyl exponential operator (shift operator) corresponding to the discrete translation along q is well defined and effectively plays the role of momentum associated to q [14]. This allows us to utilize the Weyl operator to find an effective momentum in the semiclassical regime. So, considering a state $f(q)$, its derivative with respect to the discrete position q may be approximated by means of the Weyl operator as [32]

$$\begin{aligned} \partial_q f(q) &\approx \frac{1}{2\lambda} [f(q+\lambda) - f(q-\lambda)] \\ &= \frac{1}{2\lambda} (\widehat{e^{ip\lambda}} - \widehat{e^{-ip\lambda}}) f(q) = \frac{i}{\lambda} \widehat{\sin(\lambda p)} f(q), \end{aligned} \quad (1)$$

and similarly the second derivative approximation will be

$$\begin{aligned} \partial_q^2 f(q) &\approx \frac{1}{\lambda^2} [f(q+\lambda) - 2f(q) + f(q-\lambda)] \\ &= \frac{2}{\lambda^2} (\widehat{\cos(\lambda p)} - 1) f(q). \end{aligned} \quad (2)$$

Having the above approximations at hand, we define the polymerization process for the finite values of the parameter λ as

$$\begin{aligned} \hat{p} &\rightarrow \frac{1}{\lambda} \widehat{\sin(\lambda p)}, \\ \hat{p}^2 &\rightarrow \frac{2}{\lambda^2} (1 - \widehat{\cos(\lambda p)}). \end{aligned} \quad (3)$$

This replacement suggests the idea that a classical theory may be obtained via this process, but now without any attribution

to the Weyl operator. This is what is dubbed usually as *classical Polymerization* in literature [14, 32]:

$$\begin{aligned} q &\longrightarrow q, \\ p &\longrightarrow \frac{\sin(\lambda p)}{\lambda}, \\ p^2 &\longrightarrow \frac{2}{\lambda^2} [1 - \cos(\lambda p)], \end{aligned} \quad (4)$$

where now (q, p) are a pair of classical phase space variables. Hence, by applying the transformation (4) to the Hamiltonian of a classical system we get its classical polymerized counterpart. A glance at (4) shows that the momentum is periodic and varies in a bounded interval as $p \in [-\pi/\lambda, +\pi/\lambda]$. In the limit $\lambda \rightarrow 0$, one recovers the usual range for the canonical momentum $p \in (-\infty, +\infty)$. Therefore, the polymerized momentum is compactified and topology of the momentum sector of the phase space is S^1 rather than the usual R [33]. Our set-up to explain the classical polymerization of a dynamical system is now complete. In Section 4, we will return to this issue by some more explanations and apply it to the Hamiltonian dynamics of a spherically symmetric space-time.

3. Hamiltonian Model of the Spherically Symmetric Space-Time

We start with the general spherically symmetric line element as (it can be shown that, by introducing of new radial and time coordinates as $b(r) \rightarrow r'$ and $I(r)[a(r)dt - B(r)dr] \rightarrow dt'$, this metric takes the standard form of static spherically symmetric line elements: $ds^2 = -A(r)dt^2 + C(r)dr^2 + r^2(d\vartheta^2 + \sin^2\vartheta d\varphi^2)$) [34, 35]

$$\begin{aligned} ds^2 &= -a(r)dt^2 + N(r)dr^2 + 2B(r)dt dr \\ &\quad + b^2(r)(d\vartheta^2 + \sin^2\vartheta d\varphi^2), \end{aligned} \quad (5)$$

where $a(r)$, $B(r)$, $N(r)$, and $b(r)$ are some functions of r . Upon substitution this metric into the Einstein-Hilbert action

$$\mathcal{S} = \frac{1}{16\pi G} \int d^4x \sqrt{-g} \mathcal{R}, \quad (6)$$

the action taking the form

$$\mathcal{S} = \int dt \int dr L(a, b, n), \quad (7)$$

where [34, 35]

$$L = 2\sqrt{n} \left(\frac{a'b'b}{n} + \frac{ab'^2}{n} + 1 \right) \quad (8)$$

is an effective Lagrangian in which the primes denote differentiation with respect to r and the Lagrange multiplier n is given by

$$n(r) = a(r)N(r) + B^2(r). \quad (9)$$

In metric (5) the function $N(r)$ plays the role of a lapse function with respect to the r -slicing in the ADM terminology; see [34–36]. On the other hand, according to the relation (9), the functions N and B are related to the Lagrange multiplier n which means that we can arbitrarily choose them. This is a reflection of this fact that we have freedom in the definition of the coordinates r and t in the metric (5). Hence, the only independent variables that can be determined by the Einstein field equations are the functions $a(r)$ and $b(r)$. In order to write the Hamiltonian the momenta conjugate to these variables should be evaluated, that is,

$$\begin{aligned} p_a &= \frac{\partial L}{\partial a'} = \frac{2bb'}{\sqrt{n}}, \\ p_b &= \frac{\partial L}{\partial b'} = 2 \frac{(2ab' + a'b)}{\sqrt{n}}. \end{aligned} \quad (10)$$

Also, the momentum associated with n vanishes which gives the primary constraint

$$p_n = \frac{\partial L}{\partial n'} = 0. \quad (11)$$

In terms of these conjugate momenta the canonical Hamiltonian is given by its standard definition $H = \sum_{q=a,b,n} q' p_q - L$, leading to

$$H = \sqrt{n} \left(\frac{p_a p_b}{2b} - \frac{a}{2b^2} p_a^2 - 2 \right) + \Lambda p_n, \quad (12)$$

in which due to existence of the constraint (11) we have added the last term that is the primary constraints multiplied by an arbitrary functions $\Lambda(r)$. The Hamiltonian equation for n then reads

$$n' = \{n, H\} = \Lambda. \quad (13)$$

Now, let us restrict ourselves to a certain class of gauges, namely, $n = \text{const.}$, which is equivalent to the choice $\Lambda = 0$. With a constant n we assume $n = 1$ without losing general character of the solutions. By this choice, the Hamiltonian equations of motion for the other variables are as

$$\begin{aligned} a' &= \{a, H\} = \frac{p_b}{2b} - \frac{a}{b^2} p_a, \\ p'_a &= \{p_a, H\} = \frac{p_a^2}{2b^2}, \\ b' &= \{b, H\} = \frac{p_a}{2b}, \\ p'_b &= \{p_b, H\} = \frac{p_a p_b}{2b^2} - \frac{a}{b^3} p_a^2. \end{aligned} \quad (14)$$

From the second and third equations of (14) we obtain

$$p_a = k_1 b, \quad (15)$$

from which one gets

$$\begin{aligned} b(r) &= \frac{k_1}{2} r + k_2, \\ p_a(r) &= \frac{k_1^2}{2} r + k_1 k_2, \end{aligned} \quad (16)$$

where k_1 and k_2 are integration constants. Upon substituting these results into the first and fourth equations of the system (14), we arrive at the following system:

$$\begin{aligned} a' &= \frac{1}{k_1 r + 2k_2} p_b - \frac{2k_1}{k_1 r + 2k_2} a, \\ p_b' &= \frac{k_1}{k_1 r + 2k_2} p_b - \frac{2k_1^2}{k_1 r + 2k_2} a, \end{aligned} \quad (17)$$

which results $p_b' = k_1 a'$ and then $p_b = k_1 a + k_3$. Therefore,

$$a'(r) = -\frac{k_1 a + k_3}{k_1 r + 2k_2}, \quad (18)$$

In which after integration we obtain

$$a(r) = \frac{k_3}{k_1} + \frac{k_1 k_4}{k_1 r + 2k_2}, \quad (19)$$

and

$$p_b(r) = 2k_3 + \frac{k_1^2 k_4}{k_1 r + 2k_2}, \quad (20)$$

with k_3 and k_4 being integration constants. Now, all of the above results should satisfy the constraint equation $H = 0$. Thus, with the help of (12) we get $k_1 k_3 = 4$, where we fix them as $k_1 = k_3 = 2$. Also, k_2 and k_4 remain arbitrary where we take their values as $k_2 = 0$ and $k_4 = -2M$ with M being a constant. Therefore, the metric functions take the form

$$\begin{aligned} a(r) &= 1 - \frac{2M}{r}, \\ b(r) &= r, \end{aligned} \quad (21)$$

and their conjugate momenta are

$$\begin{aligned} p_a(r) &= 2r, \\ p_b(r) &= 4 - \frac{4M}{r}. \end{aligned} \quad (22)$$

Finally, with using these relations in (5) and (9), the metric is obtained as

$$\begin{aligned} ds^2 &= -\left(1 - \frac{2M}{r}\right) dt^2 + N(r) dr^2 \\ &+ 2 \left[1 - \left(1 - \frac{2M}{r}\right) N(r) \right]^{1/2} dt dr \\ &+ r^2 (d\vartheta^2 + \sin^2 \vartheta d\varphi^2). \end{aligned} \quad (23)$$

In the final stage we have to eliminate the function $N(r)$. This function should be interpreted as a Lagrange-multiplier and, thus, cannot be considered as a real dynamical variable. As we mentioned before, one may freely choose it. From the physical point of view the function $N(r)$ corresponds to a gauge freedom in choice of coordinates r and t in the above

metric. If we choose the lapse function as $N(r) = (1 - 2M/r)^{-1}$ this metric takes its canonical form

$$\begin{aligned} ds^2 &= -\left(1 - \frac{2M}{r}\right) dt^2 + \left(1 - \frac{2M}{r}\right)^{-1} dr^2 \\ &+ r^2 (d\vartheta^2 + \sin^2 \vartheta d\varphi^2), \end{aligned} \quad (24)$$

which is nothing but the familiar form for the metric of the Schwarzschild black hole. However, we may identify the line element (23) with the Eddington-Finkelstein metric

$$\begin{aligned} ds^2 &= -\left(1 - \frac{2M}{r}\right) dt^2 + \frac{4M}{r} dt dr + \left(1 + \frac{2M}{r}\right) dr^2 \\ &+ r^2 (d\vartheta^2 + \sin^2 \vartheta d\varphi^2), \end{aligned} \quad (25)$$

for $N(r) = 1 + 2M/r$, or with some other kinds of spherically symmetric metrics for $N = 1$; see [37]. In summary, from physical viewpoint choosing different gauge functions $N(r)$ is actually looking at a space-time from a different perspective. For example, the metric (25) can be obtained from (24) by introducing a new time coordinate $\bar{t} = t + 2M \ln(r - 2M)$ in which the radial null geodesics (see Section 5) become straight lines. In this sense, the two metrics may differ from some aspects. While the Schwarzschild metric is singular at $r = 2M$ the Eddington-Finkelstein metric is regular not only at $r = 2M$ but also for the whole range $0 < r < 2M$. Indeed, the coordinate range is extended from $2M < r < \infty$ to $0 < r < \infty$.

From now on we focus on Schwarzschild black hole metric and to justify the meaning of the constant M , noting that the Newtonian gravitational potential of a point mass m situated at the origin is given by the relation $\phi = -Gm/r$. On the other hand in the weak-field limit the g_{00} component of the metric takes the form $g_{00} = -(1 + 2\phi/c^2)$ [38]. Therefore, comparing this with (24) we see that $M = Gm/c^2$. This means that we may interpret the constant M as due to the mass of the above mentioned point particle in relativistic units.

4. Polymerization of the Model

As explained in the second section the method of polymerization is based on the modification of the Hamiltonian to get a deformed Hamiltonian H_λ , where λ is the deformation parameter. Quantum polymerization of the spherically symmetric space-time is studied in [39, 40] in which the interior of the Schwarzschild black hole as described by a Kantowski-Sachs cosmological model is quantized by loop quantization method. For our system this method will be done by applying the transformation (4) on the Hamiltonian (12). However, since all of the thermodynamical properties of the black hole are encoded in the function $a(r)$, we will polymerize only the $a(r)$ -sector of the Hamiltonian. So, by means of the transformation

$$\begin{aligned} p_a &\longrightarrow \frac{1}{\lambda} \sin(\lambda p_a), \quad a \longrightarrow a, \\ p_b &\longrightarrow p_b, \quad b \longrightarrow b \end{aligned} \quad (26)$$

the Hamiltonian takes the form

$$H_\lambda = -\frac{a}{2b^2} \frac{\sin^2(\lambda p_a)}{\lambda^2} + \frac{p_b}{2b} \frac{\sin(\lambda p_a)}{\lambda} - 2. \quad (27)$$

As we mentioned earlier, by this one-parameter λ -dependent classical theory, we expect to address the quantum features of the system without a direct reference to the quantum mechanics. Indeed, here instead of first dealing with the quantum pictures based on the quantum Hamiltonian operator, one modifies the classical Hamiltonian according to the transformation (4) and then deals with classical dynamics of the system with this deformed Hamiltonian. In the resulting classical system the discreteness parameter λ plays an essential role since it supports the idea that the λ -correction to the classical theory is a signal from quantum gravity. Under these conditions the Hamiltonian equations of motion for the above Hamiltonian are

$$\begin{aligned} a' &= \{a, H_\lambda\} \\ &= \frac{p_b}{2b} \cos(\lambda p_a) - \frac{a}{\lambda b^2} \sin(\lambda p_a) \cos(\lambda p_a), \\ p'_a &= \{p_a, H_\lambda\} = \frac{\sin^2(\lambda p_a)}{2\lambda^2 b^2}, \\ b' &= \{b, H_\lambda\} = \frac{\sin(\lambda p_a)}{2\lambda b}, \\ p'_b &= \{p_b, H_\lambda\} = \frac{p_b}{2\lambda b^2} \sin(\lambda p_a) - \frac{a}{\lambda^2 b^3} \sin^2(\lambda p_a). \end{aligned} \quad (28)$$

The second and the third equations of this system give $dp_a/db = \sin(\lambda p_a)/\lambda b$, integration of which results in $b = C_1 \tan((1/2)\lambda p_a)$, where C_1 is an integration constant. We note that, in the limit $\lambda \rightarrow 0$, this relation should back to $b = (1/2)p_a$, obtained in the previous section. So, taking this limit fixes the integration constant as $C_1 = 1/\lambda$. Therefore,

$$b = \frac{1}{\lambda} \tan\left(\frac{1}{2}\lambda p_a\right). \quad (29)$$

Now, we may use this result in the second equation of (28) to arrive at

$$p'_a = 2 \cos^4\left(\frac{1}{2}\lambda p_a\right), \quad (30)$$

whose integral is

$$\frac{2}{3} \frac{\tan((1/2)\lambda p_a)}{\lambda} + \frac{1}{3} \frac{\tan((1/2)\lambda p_a)}{\lambda \cos^2((1/2)\lambda p_a)} = r. \quad (31)$$

From (29) we get $\cos^2((1/2)\lambda p_a) = (1 + \lambda^2 b^2)^{-1}$. With the help of these relations (31) takes the following algebraic form for the function $b(r)$:

$$\lambda^2 b^3 + 3b - 3r = 0, \quad (32)$$

which admits the exact solution

$$b(r) = \frac{[3\lambda r + \sqrt{4 + 9\lambda^2 r^2}]^{2/3} - 2^{2/3}}{2^{1/3} \lambda [3\lambda r + \sqrt{4 + 9\lambda^2 r^2}]^{1/3}}. \quad (33)$$

Up to second order of λ , we have

$$b(r) = r - \frac{1}{3} \lambda^2 r^3 + \mathcal{O}(\lambda^3). \quad (34)$$

Now, let us go back to the first and the fourth equations of the system (28). Using (29), they take the form

$$a' = \frac{p_b}{2b} \frac{1 - \lambda^2 b^2}{1 + \lambda^2 b^2} - \frac{2a}{b} \frac{1 - \lambda^2 b^2}{(1 + \lambda^2 b^2)^2}, \quad (35)$$

and

$$p'_b = \frac{p_b}{b} \frac{1}{1 + \lambda^2 b^2} - \frac{4a}{b} \frac{1}{(1 + \lambda^2 b^2)^2}, \quad (36)$$

in which we have used the trigonometric relations: $\sin(\lambda p_a) = 2\lambda b/(1 + \lambda^2 b^2)$ and $\cos^2(\lambda p_a) = (1 - \lambda^2 b^2)/(1 + \lambda^2 b^2)$. From these two equations we get

$$p'_b = \frac{2}{1 - \lambda^2 b^2} a', \quad (37)$$

where up to second order of λ , using (34) is

$$p'_b = 2 [1 + \lambda^2 r^2 + \mathcal{O}(\lambda^3)] a', \quad (38)$$

and thus

$$p_b = 2 \int (1 + \lambda^2 r^2) a' dr. \quad (39)$$

We may use this relation in (35) to get a differential equation for $a(r)$. However, since the resulting equation seems to be too complicated to have an exact solution, we rely on an approximation according to which we ignore all powers of λ in the r.h.s. of (35) and so obtain

$$a'(r) = \frac{1}{r} \int (1 + \lambda^2 r^2) a' dr - \frac{2}{r} a, \quad (40)$$

or after differentiation of both sides

$$r a''(r) = (\lambda^2 r^2 - 2) a', \quad (41)$$

with solution

$$a(r) = C_2 + C_3 \left[-\frac{1}{r} e^{\lambda^2 r^2/2} + \lambda \sqrt{\frac{\pi}{2}} \operatorname{erfi}\left(\frac{\lambda r}{\sqrt{2}}\right) \right], \quad (42)$$

where C_2 and C_3 are two integration constant and $\operatorname{erfi}(z)$ is the imaginary error function. Up to second order of λ this expression has the form

$$a(r) = C_2 - \frac{C_3}{r} + \frac{1}{2} C_3 \lambda^2 r, \quad (43)$$

comparison of which with (21) suggests that the integration constants should fix as $C_2 = 1$ and $C_3 = 2M$. So,

$$a(r) = 1 + 2M \left[-\frac{1}{r} e^{\lambda^2 r^2/2} + \lambda \sqrt{\frac{\pi}{2}} \operatorname{erfi} \left(\frac{\lambda r}{\sqrt{2}} \right) \right]. \quad (44)$$

Therefore, by choosing the lapse function in the form $N(r) = a^{-1}(r)$ (see the discussion after (23)), the polymerized metric takes the form

$$ds^2 = -a(r) dt^2 + a^{-1}(r) dr^2 + b^2(r) (d\vartheta^2 + \sin^2 \vartheta d\varphi^2), \quad (45)$$

where $a(r)$ and $b(r)$ are given in (44) and (34), respectively. It is seen that in the limit $\lambda \rightarrow 0$ the line element (45) returns to the usual Schwarzschild metric (24). However, its asymptotic behavior, which comes from the expansion

$$a(r) = 1 - \frac{2M}{r} + M\lambda^2 r \left[1 + \frac{1}{12} (\lambda r)^2 + \frac{1}{120} (\lambda r)^4 + \dots \right], \quad (46)$$

shows that, in spite of the Schwarzschild case, the metric is not flat for large values of r . Later in this section, we attribute such an asymptotic behavior to the matter field that created this metric. In what follows, we will deal with the physical properties, including thermodynamics, of the space-time (45). Since such properties of a black hole can be derived from its geometry, we expect that the deformed forms of these properties return to their ordinary form in the limit $\lambda \rightarrow 0$.

At first, let us take a look at the horizon(s) radius of the metric (45) which may be deduced from the roots of equation $a(r) = 0$. Up to the leading order of parameter λ , the positive root of this equation is

$$r_H \simeq \frac{\sqrt{1 + 8M^2 \lambda^2} - 1}{2M\lambda^2}. \quad (47)$$

On the other hand since $da(r)/dr = 2Me^{\lambda^2 r^2/2}/r^2 > 0$, the function $a(r)$ is monotonically increasing and thus the metric cannot have more than one horizon whose radius is approximately given in (47). To see the behavior of the above metric near the Schwarzschild essential singularity $r = 0$, we may evaluate some scalars associated with the metric such as Ricci scalar R , $R_{\mu\nu}R^{\mu\nu}$, and the Kretschmann scalar $K = R_{\mu\nu\sigma\delta}R^{\mu\nu\sigma\delta}$. A straightforward calculation shows that

$$R = \frac{2\lambda M}{r^2} e^{\lambda^2 r^2/2} \left[\lambda r + 2\sqrt{2}F \left(\frac{\lambda r}{\sqrt{2}} \right) \right], \quad (48)$$

where $F(x) = e^{-x^2} \int_0^x e^{y^2} dy$ is the Dawson function. Near $r = 0$, the above relation behaves as $6M\lambda^2/r$, so given that the value of the parameter λ is also very small we have $\lim_{r \rightarrow 0} R \simeq \mathcal{O}(\lambda)$. Computing of the scalar $R_{\mu\nu}R^{\mu\nu}$ shows the

similar behavior near $r = 0$, while the Kretschmann scalar takes the form

$$K = \frac{4M^2 e^{\lambda^2 r^2}}{r^6} \left[4\lambda^2 r^2 \left(2F \left(\frac{r\lambda}{\sqrt{2}} \right)^2 - 1 \right) - 8\sqrt{2}\lambda r F \left(\frac{r\lambda}{\sqrt{2}} \right) + \lambda^4 r^4 + 12 \right], \quad (49)$$

which behaves as $K \simeq 48M^2/r^6 + 20M^2\lambda^4/3r^2 + \mathcal{O}(\lambda^5)$. Thus near $r = 0$ we have $K \simeq 48M^2/r^6$. This shows that the space-time described by the metric (45) has an essential singularity at $r = 0$, which cannot be removed by a coordinate transformation.

Now, let us investigate the properties of the matter corresponding to the metric (45). Considering the Einstein equations $G_\nu^\mu = R_\nu^\mu - (1/2)R\delta_\nu^\mu \sim T_\nu^\mu$, the components of the energy-momentum tensor become

$$\begin{aligned} T_\nu^\mu &= \operatorname{diag}(-\rho, p_r, p_\perp, p_\perp) \\ &= \operatorname{diag} \left(-\frac{\sqrt{2\pi}\lambda M \operatorname{erfi}(\lambda r/\sqrt{2})}{r^2}, \right. \\ &\quad \left. -\frac{\sqrt{2\pi}\lambda M \operatorname{erfi}(\lambda r/\sqrt{2})}{r^2}, -\frac{\lambda^2 M e^{\lambda^2 r^2/2}}{r}, \right. \\ &\quad \left. -\frac{\lambda^2 M e^{\lambda^2 r^2/2}}{r} \right). \end{aligned} \quad (50)$$

Before going any further, a remark is in order. The usual Schwarzschild metric is often considered a vacuum solution since it solves $R_{\mu\nu} = 0$ which is equivalent to the Einstein vacuum field equations $G_{\mu\nu} = 0$. However, as (50) explicitly shows the polymer corrected metric (45) is not a vacuum solution. Then, a question arises: what mechanism made it possible starting from a vacuum solution we get a nonvacuum solution? To deal with this question note that any vacuum solution must be found in the absence of matter, strictly speaking, only the Minkowski metric can be considered as a vacuum solution. As shown in [41], in the Schwarzschild case there is a source term (energy-momentum tensor) concentrated on the origin, the origin which usually excluded from the space-time manifold. So we are faced with an unacceptable physical situation in which a curved metric is generated by a zero energy-momentum tensor. In [41] with more accurate calculations based on distributional techniques the energy-momentum tensor of the Schwarzschild geometry is obtained and it has been shown that its Ricci scalar is equal to $8\pi M\delta(r)$ which yields an energy-momentum tensor proportional to $M\delta(r)$. Now, what is happening in the effective theories such as noncommutative, see [42], and polymeric counterparts of the Schwarzschild solution is that the concentrated matter on the origin will spread throughout space by the polymer parameter λ (or noncommutative parameter θ in noncommutative theories).

The energy-momentum tensor (50) shows a fluid with radial pressure $p_r = -\rho$ and tangential pressure $p_\perp = -\rho - (r/2)\partial_r \rho$. In comparison with the conventional perfect

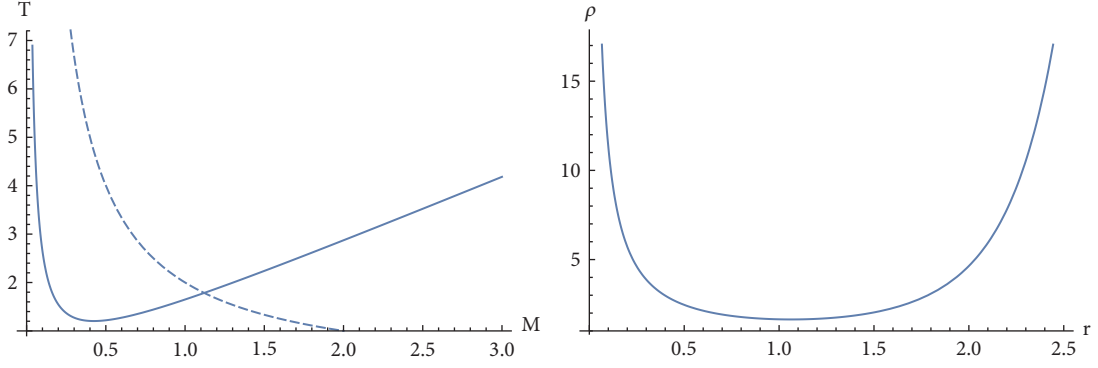


FIGURE 1: Left: Temperature versus mass. The solid line shows the qualitative behavior of the relation (53) while the dashed line refers to the conventional temperature of the Schwarzschild black hole. Right: the density of the matter distribution versus r . The figures are plotted for $\lambda = 0.1$ and $M = 1$.

fluid with isotropic pressure the above energy-momentum tensor shows an unusual behavior since its pressure exhibits an anisotropic behavior. At short distances the difference between p_r and p_\perp is of order λ^2 , which shows that the fluid behaves approximately like a perfect fluid. However, when r grows the anisotropy between the pressure's components increases and the behavior of the fluid is far from the perfect fluid behavior. The nonvanishing radial pressure of the above anisotropic fluid may be interpreted as a result of the quantum fluctuation of given space-time. The large amount of this pressure near the origin prevents the matter collapsing into this point. Such an unusual equation of state for fluids also appeared in the noncommutative theories of black holes [42]. In view of the validity of the energy conditions, we see that

$$\rho + p_r + 2p_\perp = -2 \frac{\lambda^2 M e^{\lambda^2 r^2/2}}{r} < 0, \quad (51)$$

which shows the violation of the strong energy condition for this exotic distribution of matter. On the other hand, in view of the weak energy conditions, while the relation $\rho + p_r \geq 0$ is always satisfied, the condition $\rho + p_\perp \geq 0$ is violated for $r > \mathcal{O}(1/\lambda)$. The violation of the energy conditions shows that the classical description of this type of matter field is not credible and thus the corresponding gravity should be described by an effective quantum theory (here the polymerized theory) rather than the usual general relativity.

Finally, let us take a quick look at thermodynamics of the metric (45). According to the Hawking formulation the black hole's temperature is proportional to the surface gravity at the black hole horizon. It can be shown that for a diagonal metric such as (45) the surface gravity is [43]

$$\kappa = \sqrt{-\frac{1}{4} g^{tt} g^{rr} \left(\frac{\partial g_{tt}}{\partial r} \right)^2} = \frac{M}{r^2} e^{\lambda^2 r^2/2}. \quad (52)$$

Evaluating this expression at the horizon radius (47) gives the temperature as

$$T \propto \frac{4\lambda^4 M^3 e^{(\sqrt{8\lambda^2 M^2 + 1} - 1)^2/8\lambda^2 M^2}}{(\sqrt{8\lambda^2 M^2 + 1} - 1)^2}. \quad (53)$$

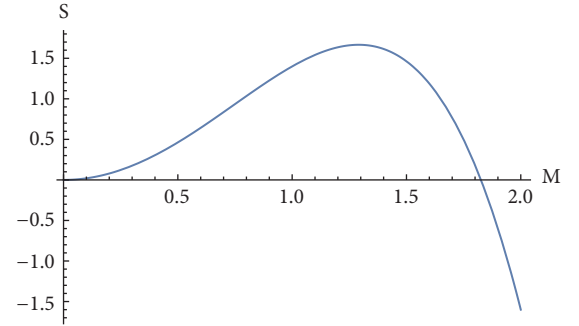


FIGURE 2: The entropy versus mass. The figure is plotted for $\lambda = 0.1$ and $M = 1$.

In Figure 1 we have plotted the qualitative behavior of the above results. As this figure shows near the origin the matter has a dense core like its conventional Schwarzschild counterpart. Thus, the temperature changes like Schwarzschild in this regime. However, in a global look, the exotic properties of the matter cause different behavior for temperature. Unlike the usual Schwarzschild case, by decreasing the mass, the radiation temperature first decreases to a minimum value and then exhibits the normal behavior; i.e., the temperature increases while the mass is decreasing. The reason for this abnormal behavior in the temperature of the radiation may be found in the nature of the dark energy-like of the matter field described by the energy-momentum tensor (50). Now, by the second law of thermodynamics $dS = dM/T$, we may compute the entropy as

$$S = \int \frac{e^{-(\sqrt{8\lambda^2 M^2 + 1} - 1)^2/8\lambda^2 M^2} (\sqrt{8\lambda^2 M^2 + 1} - 1)^2}{4\lambda^4 M^3} dM. \quad (54)$$

We see that this integral cannot be evaluated analytically. In Figure 2, employing numerical methods, we have shown the approximate behavior of the entropy for typical values of the parameters. As the figure shows with decreasing mass, the entropy grows from negative values up to a maximum positive value and then behaves like the Schwarzschild case and decreases to zero.

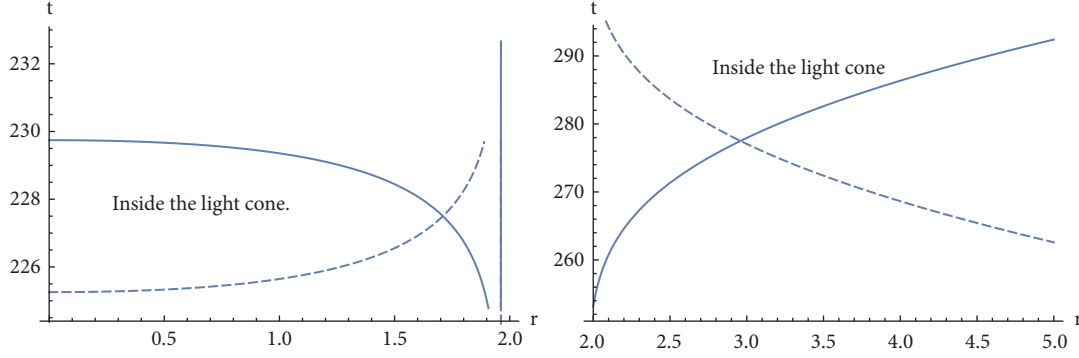


FIGURE 3: Left: the outgoing (dashed line) and incoming (solid line) geodesics for $r < r_H$. Right: The outgoing (solid line) and incoming (dashed line) geodesics for $r > r_H$. The figures are plotted for $\lambda = 0.1$ and $M = 1$.

5. Geodesics of the Polymerized Metric

In this section we are going to study how light and particles will move in the geometrical background given by metric (45). This is important because from the classical trajectories of light or falling particles we understand that the corresponding space-time behaves really like a black hole. First,

consider the radial null geodesics are defined by $ds = 0$ and $d\vartheta = d\varphi = 0$. Therefore, we have

$$-a(r) dt^2 + a^{-1}(r) dr^2 = 0 \implies dt = \pm \frac{dr}{a(r)}. \quad (55)$$

In order to get an analytical solution we use the approximate $a(r) \sim 1 - 2M/r + M\lambda^2 r$, for which we obtain

$$t - t_0 = \pm \frac{2 \left| \tanh^{-1} \left((2Mr\lambda^2 + 1) / \sqrt{8M^2\lambda^2 + 1} \right) \right| / \sqrt{8\lambda^2 M^2 + 1} + \log |Mr^2\lambda^2 - 2M + r|}{2\lambda^2 M}. \quad (56)$$

For $r > r_H$, the above expression with positive (negative) sign shows that r increases (decreases) as t increases and thus the corresponding curve is an *outgoing* (*incoming*) radial null geodesics. For $r < r_H$, the situation is reversed; i.e., the positive and negative signs correspond to the incoming and outgoing curves, respectively; see Figure 3. A glance at this figure makes it clear that none of the null geodesics can pass through the horizon which shows the black hole nature of the underlying space-time. It is clear that in comparison with region $r > r_H$ the local light cones tip over in region $r < r_H$. This is because while the coordinates r and t are space-like and time-like, respectively, in region $r > r_H$ and in region $r < r_H$ they reverse their character. The orientation of the light cones inside the horizon shows that nothing can stay at rest in this region but will be forced to move towards the black hole center.

To complete our geodesics analysis, let us now consider the radial trajectory of a falling free particle. It moves along the time-like geodesics which results the following equations of motion [38]:

$$a(r) \dot{t} = k, \quad (57)$$

$$a(r) \dot{t}^2 - a^{-1}(r) \dot{r}^2 = 1, \quad (58)$$

where a dot denotes differentiation with respect to the proper time τ and k is a constant that depends on the initial

conditions. If we assume that the particle begins to fall with zero initial velocity from a distance r_0 for which $a(r_0) = 1$, then $k = 1$. Also, for the motion around this region we have $\dot{t} \approx 1 \implies t \approx \tau$. Therefore, we may analyse the path of the particle in view of a comoving observer which uses the proper time. Then, (57) and (58) give

$$\frac{d\tau}{dr} = - \left(\frac{r}{2M - M\lambda^2 r^2} \right)^{1/2}, \quad (59)$$

in which we have used the same previous approximation for $a(r)$. Upon integration we get

$$\tau - \tau_0 = -\frac{1}{3} r \sqrt{4 - 2\lambda^2 r^2} {}_2F_1 \left(\frac{1}{2}, \frac{3}{4}; \frac{7}{4}; \frac{r^2 \lambda^2}{2} \right) \cdot \sqrt{\frac{r}{2M - \lambda^2 M r^2}}, \quad (60)$$

where τ_0 is an integration constant and ${}_2F_1(a, b; c; z)$ is a Hypergeometric function. The above equation shows that in view of the proper observer no singular behavior occurs at the horizon radius and the particle falls to the center of the black hole; see Figure 4. If instead one describes the motion in terms of the coordinate time t , the situation becomes like the null geodesics; i.e., in view of a distance observer the particle cannot pass through the horizon and it takes infinite

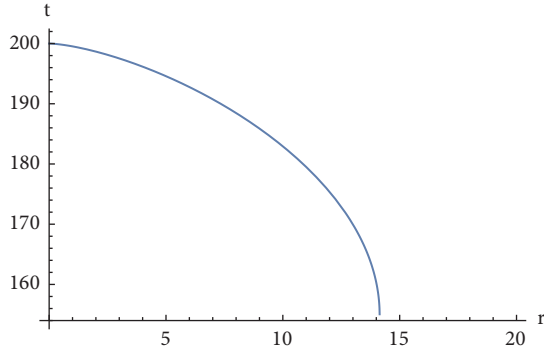


FIGURE 4: The trajectory of an infalling particle in terms of the proper time τ . The particle falls continuously to the singularity $r = 0$ in a finite proper time. The figure is plotted for $\lambda = 0.1$ and $M = 1$.

time for the falling particle to reach the horizon, so that r_H is approached but never passed. All of these results show that in terms of light and particles motion the space-time given by the metric (45) behaves like a black hole as its Schwarzschild counterpart.

6. Summary

In this paper we have studied the classical polymerization procedure applied on the Schwarzschild metric. This procedure is based on a classical transformation under which the momenta are transformed like their polymer quantum mechanical counterpart. After a brief review of the polymer representation of quantum mechanics, we have introduced the classical polymerization by means of which the Hamiltonian of the theory under consideration gets modification in such a way that a parameter λ , coming from polymer quantization, plays the role of a deformation parameter. In order to apply this mechanism on the Schwarzschild black hole, we first presented a Hamiltonian function for a general spherically symmetric space-time and showed that the resulting Hamiltonian equations yield the conventional Schwarzschild metric. Then, we have applied the polymerization on this minisuperspace model and solved the Hamiltonian equations once again to achieve the polymer corrected Schwarzschild metric. We saw that while the usual Schwarzschild metric is a vacuum spherical symmetric solution of the Einstein equations, this is not the case for its polymerized version obtained by the above mentioned method. Interestingly, the energy-momentum tensor of the matter field corresponding to the polymerized metric has anisotropic negative pressure sector with a dark energy-like equation of state. As expected, the unusual behavior of such a matter field resulted in an uncommon behavior for the thermodynamical quantities like temperature and entropy in comparison with the traditional Schwarzschild solution. Finally, to clarify that the polymerized metric has also the black hole nature, we have investigated the null geodesics and verified that the outgoing and incoming geodesics curves can never pass through the horizon. Also, we proved that in view of a comoving observer which uses the proper time an infalling particle continuously falls to the center $r = 0$, without experiencing something

passing through the horizon. All these indicate that the underlying space-time in which the light and particles are traveling is really a black hole.

Data Availability

No data were used to support of the author's study in the manuscript: Classical Polymerization of the Schwarzschild Metric.

Conflicts of Interest

The author declares that they have no conflicts of interest.

Acknowledgments

This work has been supported financially by Research Institute for Astronomy and Astrophysics of Maragha (RIAAM) under research project no. 1/5237-107.

References

- [1] B. S. DeWitt, "Quantum theory of gravity. I. The canonical theory," *Physical Review A: Atomic, Molecular and Optical Physics*, vol. 160, 1967.
- [2] C. Rovelli and L. Smolin, "Discreteness of area and volume in quantum gravity," *Nuclear Physics B*, vol. 442, no. 3, pp. 593–619, 1995.
- [3] A. Ashtekar and J. Lewandowski, "Quantum theory of geometry. I. Area operators," *Classical and Quantum Gravity*, vol. 14, no. 1A, pp. A55–A81, 1997.
- [4] C. Rovelli, "Loop quantum gravity," *Living Reviews*, vol. 1, p. 1, 1998.
- [5] A. Kempf, G. Mangano, and R. B. Mann, "Hilbert space representation of the minimal length uncertainty relation," *Physical Review D: Particles, Fields, Gravitation and Cosmology*, vol. 52, no. 2, pp. 1108–1118, 1995.
- [6] S. Hossenfelder, "Minimal length scale scenarios for quantum gravity," *Living Reviews in Relativity*, vol. 16, no. 2, 2013.
- [7] A. Kempf, "Quantum field theory with nonzero minimal uncertainties in positions and momenta," *High Energy Physics*, vol. 11-12, pp. 1041–1048, 1994.
- [8] A. Kempf and G. Mangano, "Minimal length uncertainty relation and ultraviolet regularization," *Physical Review D: Particles, Fields, Gravitation and Cosmology*, vol. 55, no. 12, 1997.
- [9] S. Hossenfelder, "Interpretation of quantum field theories with a minimal length scale," *Physical Review D: Particles, Fields, Gravitation and Cosmology*, vol. 73, no. 10, 2006.
- [10] J. B. Achour and S. Brahma, "Covariance in self dual inhomogeneous models of effective quantum geometry: Spherical symmetry and Gowdy systems," *Physical Review D: Particles, Fields, Gravitation and Cosmology*, vol. 97, 2018.
- [11] M. Bojowald, S. Brahma, and J. D. Reyes, "Covariance in models of loop quantum gravity: spherical symmetry," *Physical Review D: Covering Particles, Fields, Gravitation, and Cosmology*, vol. 92, no. 4, 2015.
- [12] P. Nicolini, A. Smailagic, and E. Spallucci, "Noncommutative geometry inspired Schwarzschild black hole," *Physics Letters B*, vol. 632, no. 4, pp. 547–551, 2006.

- [13] E. Spallucci, A. Smailagic, and P. Nicolini, "Trace anomaly on a quantum spacetime manifold," *Physical Review D: Particles, Fields, Gravitation and Cosmology*, vol. 73, 2006.
- [14] A. Corichi, T. Vukašinac, and J. A. Zapata, "Polymer quantum mechanics and its continuum limit," *Physical Review D: Particles, Fields, Gravitation and Cosmology*, vol. 76, no. 4, 2007.
- [15] A. Ashtekar, S. Fairhurst, and J. L. Willis, "Quantum gravity, shadow states and quantum mechanics," *Classical and Quantum Gravity*, vol. 20, no. 6, pp. 1031–1061, 2003.
- [16] G. De Risi, R. Maartens, and P. Singh, "Graceful exit via polymerization of pre-big-bang cosmology," *Physical Review D: Particles, Fields, Gravitation and Cosmology*, vol. 76, no. 10, 2007.
- [17] F. Wu and M. Zhong, "TeV scale Lee-Wick fields out of large extra dimensional gravity," *Physical Review D: Particles, Fields, Gravitation and Cosmology*, vol. 78, 2008.
- [18] G. M. Hossain, V. Husain, and S. S. Seahra, "Nonsingular inflationary universe from polymer matter," *Physical Review D: Particles, Fields, Gravitation and Cosmology*, vol. 81, no. 2, 2010.
- [19] A. Corichi and A. Karami, "Loop quantum cosmology of $k = 1$ FRW: A tale of two bounces," *Physical Review D*, vol. 84, 2011.
- [20] S. M. Hassan and V. Husain, "Semiclassical cosmology with polymer matter," *Classical and Quantum Gravity*, vol. 34, no. 8, 2017.
- [21] B. Vakili, K. Nozari, V. Hosseinzadeh, and M. A. Gorji, "Bouncing scalar field cosmology in the polymeric minisuperspace picture," *Modern Physics Letters A*, vol. 29, no. 32, 2014.
- [22] J. B. Achour, F. Lamy, H. Liu, and K. Noui, "Polymer schwarzschild black hole: an effective metric," *Europhysics letters*, vol. 123, 2018.
- [23] C. G. BOehmer and K. Vandersloot, "Loop quantum dynamics of the Schwarzschild interior," *Physical Review D: Particles, Fields, Gravitation and Cosmology*, vol. 76, no. 10, 2007.
- [24] A. Peltola and G. Kunstatter, "Effective polymer dynamics of D -dimensional black hole interiors," *Physical Review D: Particles, Fields, Gravitation and Cosmology*, vol. 80, no. 4, 2009.
- [25] E. Bianchi, "Black hole entropy, loop gravity, and polymer physics," *Classical and Quantum Gravity*, vol. 28, no. 11, 2011.
- [26] E. R. Livine and D. R. Terno, "Entropy in the classical and quantum polymer black hole models," *Classical and Quantum Gravity*, vol. 29, no. 22, 2012.
- [27] G. Chacón-Acosta, E. Manrique, L. Dagdug, and H. A. Morales-Técotl, "Statistical thermodynamics of polymer quantum systems," *Loop Quantum Gravity and Cosmology*, vol. 7, no. 110, p. 23, 2011.
- [28] G. M. Hossain, V. Husain, and S. S. Seahra, "Background-independent quantization and the uncertainty principle," *Classical and Quantum Gravity*, vol. 27, no. 16, 2010.
- [29] M. Gorji, K. Nozari, and B. Vakili, "Polymeric quantization and black hole thermodynamics," *Physics Letters B*, vol. 735, pp. 62–68, 2014.
- [30] M. Gorji, K. Nozari, and B. Vakili, "Thermostatistics of the polymeric ideal gas," *Physical Review D: Particles, Fields, Gravitation and Cosmology*, vol. 90, no. 4, 2014.
- [31] M. A. Gorji, K. Nozari, and B. Vakili, "Polymer quantization versus the Snyder noncommutative space," *Classical and Quantum Gravity*, vol. 32, no. 15, 2015.
- [32] A. Corichi and T. Vukašinac, "Effective constrained polymeric theories and their continuum limit," *Physical Review D: Particles, Fields, Gravitation and Cosmology*, vol. 86, no. 6, 2012.
- [33] K. Nozari, M. A. Gorji, V. Hosseinzadeh, and B. Vakili, "Natural cutoffs via compact symplectic manifolds," *Classical and Quantum Gravity*, vol. 33, no. 2, 2016.
- [34] M. Cavaglia, V. De Alfaro, and A. T. Filippov, "Hamiltonian formalism for black holes and quantization," *International Journal of Modern Physics D*, vol. 4, no. 5, pp. 661–672, 1995.
- [35] M. Cavaglia, V. De Alfaro, and A. T. Filippov, "Quantization of the Schwarzschild black hole," *International Journal of Modern Physics D*, vol. 5, no. 3, pp. 227–250, 1996.
- [36] B. Vakili, "Quantization of the Schwarzschild black hole: a Noether symmetry approach," *International Journal of Theoretical Physics*, vol. 51, no. 1, pp. 133–145, 2012.
- [37] P. Kraus and F. Wilczek, "Some applications of a simple stationary line element for the Schwarzschild geometry," *Modern Physics Letters A*, vol. 9, no. 40, pp. 3713–3719, 1994.
- [38] R. d'Inverno, *Introducing Einstein's Relativity*, Oxford University Press, New York, NY, USA, 1998.
- [39] A. Corichi and P. Singh, "Loop quantization of the Schwarzschild interior revisited," *Classical and Quantum Gravity*, vol. 33, no. 5, 2016.
- [40] J. Olmedo, S. Saini, and P. Singh, "From black holes to white holes: a quantum gravitational, symmetric bounce," *Classical and Quantum Gravity*, vol. 34, no. 22, 2017.
- [41] H. Balasin and H. Nachbagauer, "The energy-momentum tensor of a black hole, or What curves the Schwarzschild geometry?" *Classical and Quantum Gravity*, vol. 10, no. 11, pp. 2271–2278, 1993.
- [42] P. Nicolini, "Noncommutative black holes, the final appeal to quantum gravity: a review," *International Journal of Modern Physics A*, vol. 24, no. 7, 2009.
- [43] Ø. Grøn and S. Hervik, *Einstein's General Theory of Relativity: With Modern Applications in Cosmology*, Springer-Verlag, New York, NY, USA, 2007.

Research Article

Particle Motion around Charged Black Holes in Generalized Dilaton-Axion Gravity

Susmita Sarkar,¹ Farook Rahaman ,¹ Irina Radinschi ,²
Theophanes Grammenos,³ and Joydeep Chakraborty⁴

¹Department of Mathematics, Jadavpur University, Kolkata 700 032, West Bengal, India

²Department of Physics, Gheorghe Asachi Technical University, 700050 Iasi, Romania

³Department of Civil Engineering, University of Thessaly, 383 34 Volos, Greece

⁴Department of Mathematics, Nagar College, P.O. Nagar, Dist. Mursidabad, West Bengal, India

Correspondence should be addressed to Farook Rahaman; rahaman@associates.iucaa.in

Received 14 May 2018; Accepted 8 August 2018; Published 16 September 2018

Academic Editor: Edward Sarkisyan-Grinbaum

Copyright © 2018 Susmita Sarkar et al. This is an open access article distributed under the Creative Commons Attribution License, which permits unrestricted use, distribution, and reproduction in any medium, provided the original work is properly cited. The publication of this article was funded by SCOAP³.

The behaviour of massive and massless test particles around asymptotically flat and spherically symmetric, charged black holes in the context of generalized dilaton-axion gravity in four dimensions is studied. All the possible motions are investigated by calculating and plotting the corresponding effective potential for the massless and massive particles as well. Further, the motion of massive (charged or uncharged) test particles in the gravitational field of charged black holes in generalized dilaton-axion gravity for the cases of static and nonstatic equilibrium is investigated by applying the Hamilton-Jacobi approach.

1. Introduction

Recently, scientists have focused their attention on the black hole solutions in various alternative theories of gravity, particularly theories of gravitation with background scalar and pseudoscalar fields. In the low energy effective action, usually string theory based-models are comprised of two massless scalar fields, the dilaton, and the axion (see, e.g., [1]). Sur, Das, and SenGupta [2] employed the dilaton and axion fields coupled to the electromagnetic field in a more generalized coupling with Einstein and Maxwell theory in four dimensions in the low energy action. Exploiting this new idea, they have found asymptotically flat and nonflat dilaton-axion black hole solutions. The vacuum expectation values of the various moduli of compactification are responsible for these couplings. These black hole solutions have been studied extensively in the literature; e.g., their thermodynamics has been investigated [3], thin-shell wormholes have been constructed from charged black holes in generalized dilaton-axion gravity [4], the energy of charged black holes in generalized dilaton-axion gravity has been calculated [5], the statistical entropy of a charged dilaton-axion black hole has been examined [6], and the superradiant instability of a

dilaton-axion black hole under scalar perturbation has been investigated [7]. Among various properties of such black hole solutions, a subject of great interest is the study of the behaviour of a test particle in the gravitational field of such black holes.

In this paper, we study the behaviour of the time-like and null geodesics in the gravitational field of a charged black hole in generalized dilaton-axion gravity. The solution under study describes an asymptotically flat black hole and the motions of both massless and massive particles are analyzed. The effective potentials are calculated and plotted for various parameters in the cases of circular and radial geodesics. The motion of a charged test particle in the gravitational field of a charged black hole in generalized dilaton-axion gravity is also investigated using the Hamilton-Jacobi approach.

The present paper has the following structure: in Section 2 the charged black hole metric in generalized dilaton-axion gravity is presented. Section 3 focuses on the geodesic equation in the cases of massless particle motion ($L = 0$) and massive particle motion ($L = -1$). In Section 4 the effective potential is studied in both cases of the massless and the massive particle. Section 5 is devoted to the study of the motion of a test particle in static equilibrium as well as in

nonstatic equilibrium. For the latter case, a chargeless ($e = 0$) and a charged test particle are considered. Finally, in Section 6, the results obtained in this paper are discussed.

2. Charged Black Hole Metric in Generalized Dilation-Axion Gravity

Recently, Sur, Das, and SenGupta [2] have discovered a new black hole solution for the Einstein-Maxwell scalar field system inspired by low energy string theory. In fact, they have considered a generalized action in which two scalar fields are minimally coupled to the Einstein-Hilbert-Maxwell field in four dimensions (in the Einstein frame, see, e.g., [8, 9]) having the form

$$I = \frac{1}{2\kappa} \int d^4x \sqrt{-g} \left[R - \frac{1}{2} \partial_\mu \varphi \partial^\mu \varphi - \frac{\omega(\varphi)}{2} \partial_\mu \zeta \partial^\mu \zeta - \alpha(\varphi, \zeta) F_{\mu\nu} F^{\mu\nu} - \beta(\varphi, \zeta) F_{\mu\nu} * F^{\mu\nu} \right], \quad (1)$$

where $\kappa = 8\pi G$, R is the curvature scalar, $F_{\mu\nu}$ describes the Maxwell field strength and φ, ζ are two massless scalar/pseudoscalar fields depending only on the radial coordinate r which are coupled to the Maxwell field through the functions α and β . Here, ζ acquires a nonminimal kinetic term of the form $\omega(\varphi)$ due to its interaction with φ (φ, ζ can be identified with the scalar dilaton field and the pseudoscalar axion field, respectively), while $*F^{\mu\nu} = (1/2)\epsilon^{\mu\nu\kappa\lambda} F_{\kappa\lambda}$ is the Hodge-dual Maxwell field strength.

Indeed, with the action described by (1), a much wider class of black hole solutions has been found, whereby two types of metrics, asymptotically flat and asymptotically non-flat, for the black hole solutions have been obtained.

For our study we use the asymptotically flat solution to analyze the behaviour of massive and massless test particles around a spherically symmetric, charged black hole in generalized dilaton-axion gravity. The asymptotically flat metric considered is given by

$$ds^2 = -f(r) dt^2 + \frac{dr^2}{f(r)} + h(r) d\Omega^2, \quad (2)$$

with

$$f(r) = \frac{(r - r_-)(r - r_+)}{(r - r_0)^{(2-2n)}(r + r_0)^{2n}} \quad (3)$$

and

$$h(r) = \frac{(r + r_0)^{2n}}{(r - r_0)^{(2n-2)}}. \quad (4)$$

In (3) and (4), according to [2], in order to have nontrivial φ and ζ fields, the exponent n is a dimensionless constant strictly greater than 0 and strictly less than 1. The other various parameters are given as follows:

$$r_\pm = m_0 \pm \sqrt{m_0^2 + r_0^2 - \frac{1}{8} \left(\frac{K_1}{n} + \frac{K_2}{1-n} \right)}, \quad (5)$$

$$r_0 = \frac{1}{16m_0} \left(\frac{K_1}{n} - \frac{K_2}{1-n} \right), \quad (6)$$

$$m_0 = m - (2n - 1) r_0, \quad (7)$$

$$K_1 = 4n \left[4r_0^2 + 2r_0(r_+ + r_-) + r_+ r_- \right], \quad (8)$$

$$K_2 = 4(1 - n) r_+ r_-, \quad (9)$$

and

$$m = \frac{1}{16r_0} \left(\frac{K_1}{n} - \frac{K_2}{1-n} \right) + (2n - 1) r_0, \quad (10)$$

where m is the mass of the black hole and $0 < n < 1$. The parameters r_+ and r_- determine the inner and outer event horizons, respectively. Also, for $r = r_0$, there is a curvature singularity and the parameters obey the condition $r_0 < r_- < r_+$.

3. Geodesic Equation

The geodesic equation for the metric (2) describing the motion in the plane $\theta = \pi/2$ is as follows [10]:

$$\left(\frac{dr}{d\tau} \right)^2 = Lf(r) + E^2 - \frac{J^2 f(r)}{h(r)}, \quad (11)$$

$$\frac{d\phi}{d\tau} = \frac{J}{h(r)}, \quad (12)$$

$$\frac{dt}{d\tau} = \frac{E}{f(r)}, \quad (13)$$

where L is known as the Lagrangian having the values 0 for a massless particle and -1 for a massive particle and E, J are constants identified as the energy per unit mass and the angular momentum, respectively.

Now we proceed to discuss the motion of the massless and the massive particle for the radial geodesic.

The radial geodesic equation ($J = 0$) is

$$\left(\frac{dr}{d\tau} \right)^2 = E^2 + Lf(r). \quad (14)$$

Using (13), (14) becomes

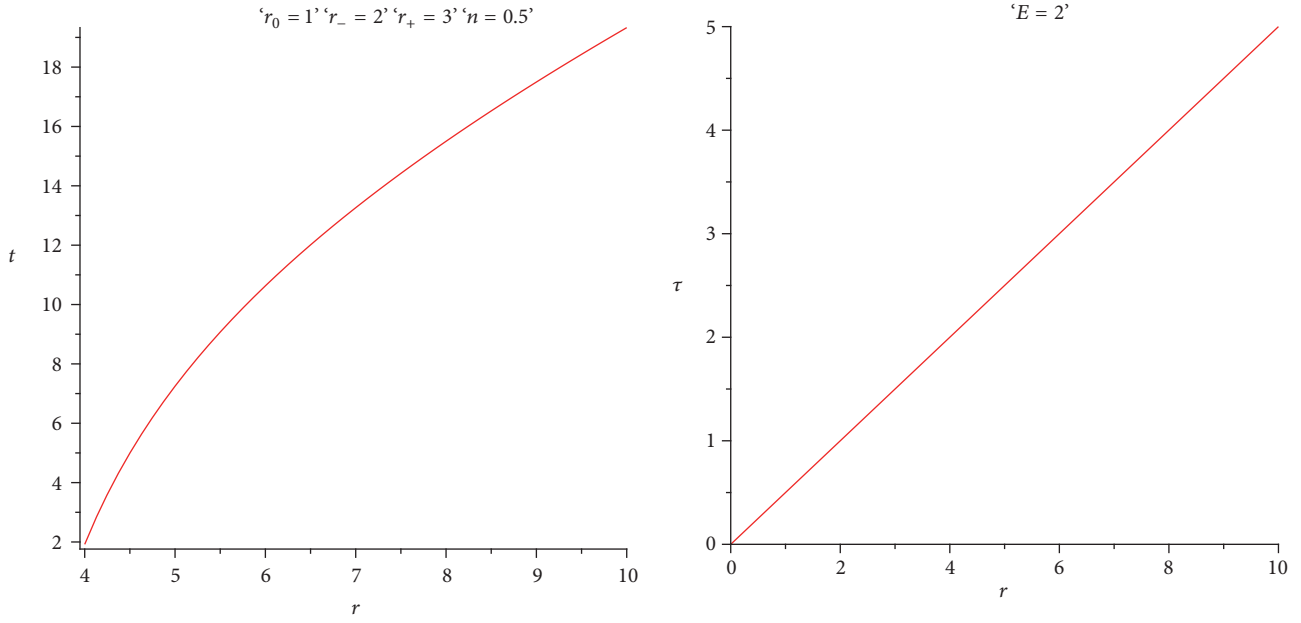
$$\left(\frac{dr}{dt} \right)^2 = (f(r))^2 \left(1 + f(r) \frac{L}{E^2} \right). \quad (15)$$

Then, by inserting $f(r)$ from (3), (15) reads

$$\left(\frac{dr}{dt} \right)^2 = \left(\frac{(r - r_-)(r - r_+)}{(r - r_0)^{(2-2n)}(r + r_0)^{2n}} \right)^2 \cdot \left(1 + \frac{(r - r_-)(r - r_+)}{(r - r_0)^{(2-2n)}(r + r_0)^{2n}} \frac{L}{E^2} \right). \quad (16)$$

3.1. Massless Particle Motion ($L = 0$). For the motion of a massless particle the Lagrangian L vanishes. In this case the equation for the radial geodesic (16) becomes

$$\left(\frac{dr}{dt} \right)^2 = \left(\frac{(r - r_-)(r - r_+)}{(r - r_0)^{(2-2n)}(r + r_0)^{2n}} \right)^2. \quad (17)$$

FIGURE 1: Graphs of $t - r$ (left) and $\tau - r$ (right) for a massless particle.

After integrating we get

$$\begin{aligned} \pm t = r + \frac{\ln(r - r_-) r^2}{r_- - r_+} - \frac{\ln(r - r_-) r_0^2}{r_- - r_+} \\ - \frac{\ln(r - r_+) r_+^2}{r_- - r_+} + \frac{\ln(r - r_+) r_0^2}{r_- - r_+}. \end{aligned} \quad (18)$$

Again from (14) we obtain for $L = 0$

$$\left(\frac{dr}{d\tau} \right)^2 = E^2, \quad (19)$$

from which we have a $\tau - r$ relationship

$$\pm \tau = \frac{r}{E}. \quad (20)$$

In Figure 1 (left) t is plotted with respect to the radial coordinate r and in Figure 1 (right) the proper time (τ) is plotted with respect to radial coordinate r for a massless particle.

3.2. Massive Particle Motion ($L = -1$). For a massive particle the Lagrangian L is -1 and from (14) and (15) we obtain for the motion of a massive particle the relationships between t and r and τ and r , respectively, as

$$\pm t = \int \frac{E dr}{\left((r - r_-)(r - r_+) / (r - r_0)^{(2-2n)} (r + r_0)^{2n} \right) \left(E^2 - (r - r_-)(r - r_+) / (r - r_0)^{(2-2n)} (r + r_0)^{2n} \right)^{1/2}} \quad (21)$$

$$\pm \tau = \int \frac{(r - r_0)^{(1-n)} (r + r_0)^n dr}{\left(E^2 (r - r_0)^{(2-2n)} (r + r_0)^{2n} - (r - r_-)(r - r_+) \right)^{1/2}}. \quad (22)$$

In Figure 2 the graphs of t with respect to the radial coordinate r (left) and of the proper time τ with respect to the radial coordinate r (right) for a massive particle are presented.

4. The Effective Potential

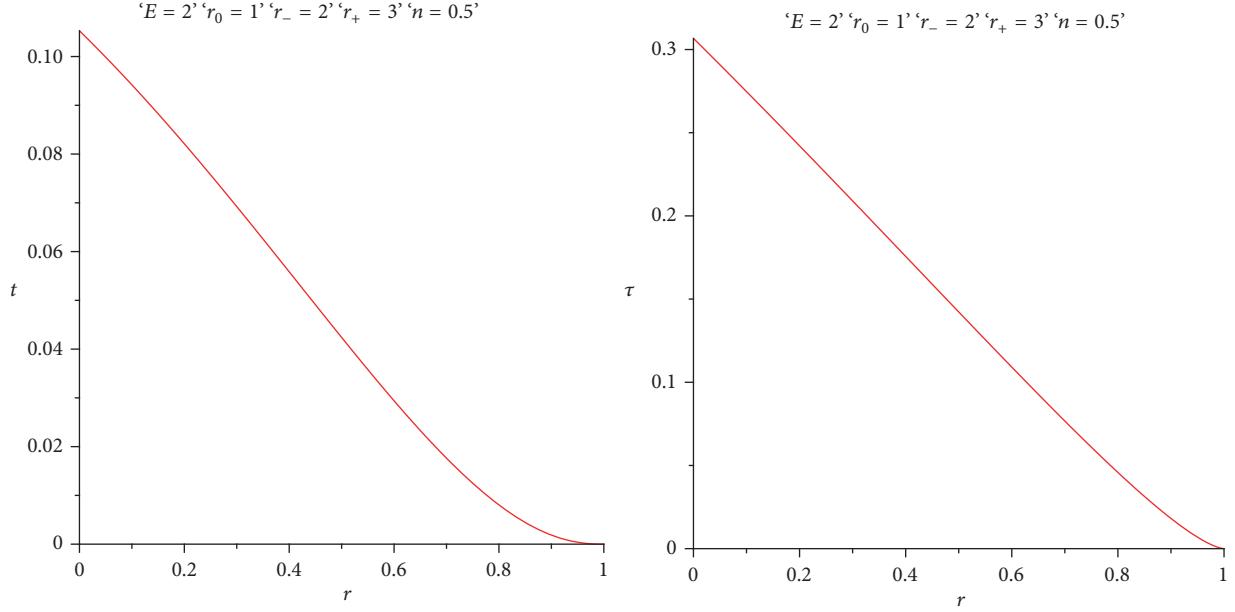
From the geodesic equation (11) we have

$$\frac{1}{2} \left(\frac{dr}{d\tau} \right)^2 = \frac{1}{2} \left[E^2 - f(r) \left(\frac{J^2}{h(r)} - L \right) \right]. \quad (23)$$

After comparing the above equation with the well known equation $(1/2)(dr/d\tau)^2 + V_{\text{eff}} = 0$, we obtain the following expression for the effective potential:

$$V_{\text{eff}} = -\frac{1}{2} \left[E^2 - f(r) \left(\frac{J^2}{h(r)} - L \right) \right]. \quad (24)$$

From (24) one can see that the effective potential depends on the energy per unit mass, E , and the angular momentum, J .

FIGURE 2: Graphs of $t - r$ (left) and $\tau - r$ (right) for a massive particle.

4.1. *Massless Particle Case* ($L = 0$). For the radial geodesics ($J = 0$), (24) yields

$$V_{\text{eff}} = -\frac{E^2}{2} \quad (25)$$

and the particle behaves like a free particle if $E = 0$.

Now we consider the circular geodesics ($J \neq 0$). The corresponding effective potential is given by

$$V_{\text{eff}} = -\frac{E^2}{2} + \frac{J^2}{2} \frac{(r - r_-)(r - r_+)}{(r + r_0)^{4n}}. \quad (26)$$

For $E \neq 0$ and $J = 0$ we infer from (26) that the effective potential does not depend on the charge and the mass of the black hole in generalized dilaton-axion gravity. The shape of the effective potential for $E \neq 0$ is shown in Figure 3 (left) for $J = 6$ (solid curve) and $J = 0$ (dotted line). We notice that for a nonzero value of J , the effective potential acquires a minimum, implying that stable circular orbits might exist. For $J = 0$, there are no stable circular orbits.

Now if we consider $E = 0$ and circular geodesics, i.e., $J \neq 0$, then, from (26), it is clear that the roots of the effective potential are the same as the horizon values. Further, the effective potential is negative between its two roots, i.e., between the horizons. Hence, since the effective potential has a minimum value stable circular orbits must exist, a conclusion that is confirmed in Figure 3 (right).

4.2. *Massive Particle Case* ($L = -1$). The effective potential for the massive particle is obtained from (24) as

$$V_{\text{eff}} = -\frac{1}{2} \left[E^2 - f(r) \left(\frac{J^2}{h(r)} + 1 \right) \right]. \quad (27)$$

Now, for the radial geodesics with $J = 0$, $E = 0$, the above equation yields

$$V_{\text{eff}} = \frac{1}{2} \frac{(r - r_-)(r - r_+)}{(r - r_0)^{(2-2n)}(r + r_0)^{2n}}. \quad (28)$$

From (28) we notice that the solutions for the effective potential coincide with the horizon values for radial geodesics with $E = 0$, which is demonstrated graphically in Figure 4 (left). Further, from Figure 4 (left), one can see that the motion of the particle is bounded in the interior region of the black hole. The behaviour of the effective potential for $E \neq 0$ is depicted in the bottom part of Figure 4 (left). In this case, we also deduce that a bound orbit is possible for the massive particle.

Next we will consider the motion of a test particle with nonzero angular momentum. For $E = 0$, the roots of the effective potential coincide with the horizons (see Figure 4 (right)). Thus the particle is bounded in the interior region of the black hole.

5. Motion of a Test Particle

In this section we study the motion of a test particle of mass M and charge e in the gravitational field of a charged black hole in generalized dilaton-axion gravity. The Hamilton-Jacobi equation [11] is

$$g^{ik} \left(\frac{\partial S}{\partial x^i} + e A_i \right) \left(\frac{\partial S}{\partial x^k} + e A_k \right) + M^2 = 0, \quad (29)$$

where g_{ik} , A_i are the metric potential and the gauge potential, respectively, and S is Hamilton's standard characteristic

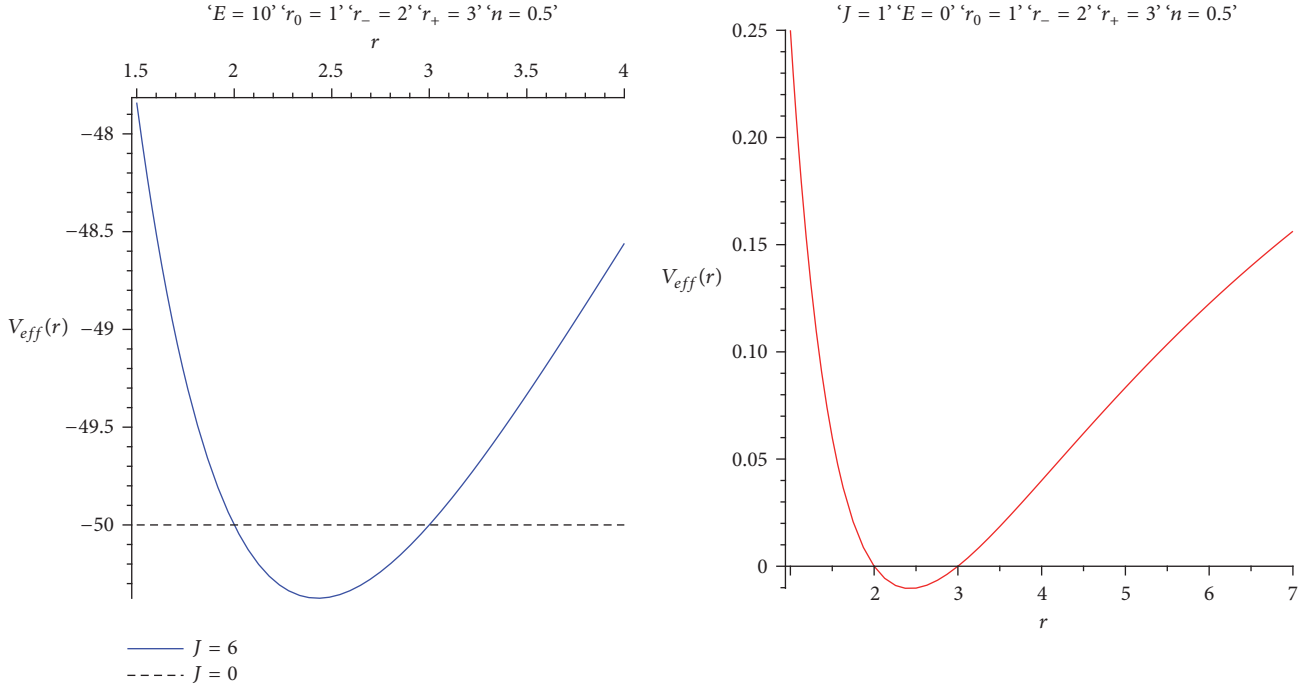


FIGURE 3: Graphs of $V_{\text{eff}} - r$ with $E = 10$, $J = 6$ and $J = 0$ (left) and $V_{\text{eff}} - r$ with $E = 0$ and $J = 1$ (right), for a massless particle.

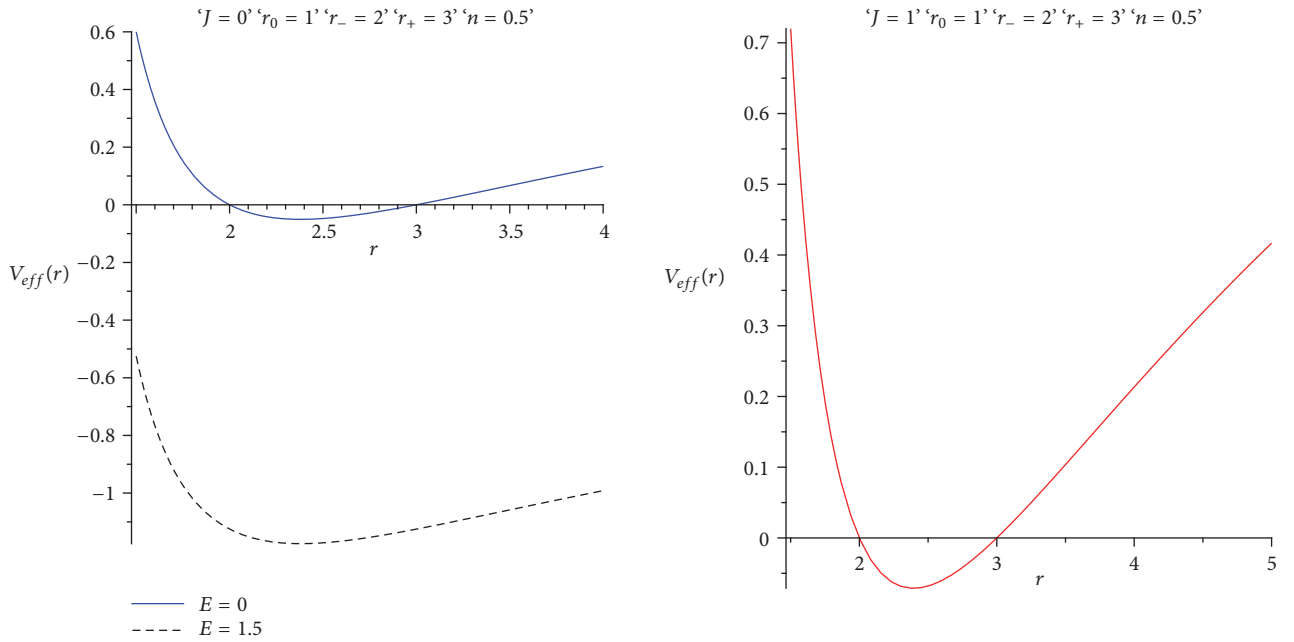


FIGURE 4: Graphs of $V_{\text{eff}} - r$ with $J = 0$, $E = 0$, and $E = 1.5$ (left) and $V_{\text{eff}} - r$ with $J = 1$ and $E = 0$ (right), for a massive particle.

function. The explicit form of the Hamilton-Jacobi equation for the line element (2) is

$$\begin{aligned}
 & -\frac{1}{f(r)} \left(\frac{\partial s}{\partial t} + \frac{eQ}{r} \right)^2 + f(r) \left(\frac{\partial S}{\partial r} \right)^2 + \frac{1}{h(r)} \left(\frac{\partial S}{\partial \theta} \right)^2 \\
 & + \frac{1}{h(r) \sin^2 \theta} \left(\frac{\partial S}{\partial \phi} \right)^2 + M^2 = 0,
 \end{aligned} \tag{30}$$

where Q is the charge of the black hole. To solve the above partial differential equation, let us assume a separable solution in the form

$$S(t, r, \theta, \phi) = -Et + S_1(r) + S_2(\theta) + J\phi, \tag{31}$$

where E and J are the energy and angular momentum of the particle, respectively. After some simplification we obtain

$$S_1(r) = \epsilon \int \left[\frac{(E - eQ/r)^2}{f^2} - \frac{p^2}{fh} - \frac{M^2}{f} \right]^{1/2}, \quad (32)$$

$$S_2(\theta) = \epsilon \int (p^2 - J^2 \operatorname{cosec}^2 \theta)^{1/2}, \quad (33)$$

where $\epsilon = \pm 1$ and p is the separation constant also known as the momentum of the particle.

The radial velocity of the particle is given by

$$\frac{dr}{dt} = f^2 \left(E - \frac{eQ}{r} \right)^{-1} \cdot \left[\frac{1}{f^2} \left(E - \frac{eQ}{r} \right)^2 - \frac{p^2}{fh} - \frac{M^2}{f} \right]^{1/2}. \quad (34)$$

The turning points of the trajectory are obtained by the vanishing of the radial velocity, $dr/dt = 0$, which yields

$$\left(E - \frac{eQ}{r} \right)^2 - \frac{p^2 f}{h} - M^2 f = 0. \quad (35)$$

After solving this equation for E , we get

$$E = \frac{eQ}{r} + \sqrt{f} \left(\frac{p^2}{h} + M^2 \right)^{1/2}. \quad (36)$$

The effective potential is obtained from the relation $V(r) = E/M$ as follows:

$$V = \frac{eQ}{Mr} + \sqrt{f} \left(\frac{p^2}{M^2 h} + 1 \right)^{1/2}. \quad (37)$$

Using (3) and (4) the effective potential becomes

$$V(r) = \frac{eQ}{Mr} + \left(1 + \frac{p^2 (r - r_0)^{2n-2}}{M^2 (r + r_0)^{2n}} \right) \cdot \left(\frac{\sqrt{(r - r_-)(r - r_+)}}{(r - r_0)^{1-n} (r + r_0)^n} \right). \quad (38)$$

In the stationary system ($dV/dr = 0$) we obtain

$$\begin{aligned} & -\frac{eQ}{Mr^2} + \frac{1}{2} \frac{((r - r_-)(r - r_+))^{1/2} (p^2 (r - r_0)^{2n-2} (2n-2)/M^2 (r - r_0)(r + r_0)^{2n} - 2p^2 n (r - r_0)^{2n-2}/M^2 (r + r_0)^{2n+1})}{(1 + p^2 (r - r_0)^{2n-2}/M^2 (r + r_0)^{2n})^{1/2} (r - r_0)^{1-n} (r + r_0)^n} \\ & + \frac{1}{2} \frac{(2r - r_+ - r_-) (1 + p^2 (r - r_0)^{2n-2}/M^2 (r + r_0)^{2n})^{1/2}}{((r - r_-)(r - r_+))^{1/2} (r - r_0)^{1-n} (r + r_0)^n} \\ & - \frac{(1-n) (1 + p^2 (r - r_0)^{2n-2}/M^2 (r + r_0)^{2n})^{1/2} ((r - r_-)(r - r_+))^{1/2}}{(r - r_0)^{2-n} (r + r_0)^n} \\ & - \frac{n (1 + p^2 (r - r_0)^{2n-2}/M^2 (r + r_0)^{2n})^{1/2} ((r - r_-)(r - r_+))^{1/2}}{(r - r_0)^{1-n} (r + r_0)^{n+1}} = 0. \end{aligned} \quad (39)$$

In order to use a more simplified equation and thus be able to visualize it by plotting its graph, one may select some specific value for n . Here we choose $n = 0.5$ (since $0 < n < 1$) and the simplified form of equation (39) is given by

$$\begin{aligned} \alpha(r) & := \frac{2eQ(r^2 - r_0^2)^{1/2}}{Mr^2} \\ & + \frac{2r((r - r_-)(r - r_+))^{1/2}}{(r^2 - r_0^2)} \left(\frac{p^2}{M^2 (r^2 - r_0^2) \beta} + \beta \right) \\ & - \frac{(2r - r_+ - r_-) \beta}{((r - r_-)(r - r_+))^{1/2}} = 0, \end{aligned} \quad (40)$$

where $\beta = (1 + p^2/M^2(r^2 - r_0^2))^{1/2}$.

5.1. Test Particle in Static Equilibrium. The momentum p must be zero in the static equilibrium system; thus from (40) we get

$$\begin{aligned} & (4e^2 Q^2 - M^2 (2r_- r_+ + r_+^2 - r_-^2)) r^8 \\ & + (-4e^2 Q^2 (r_- + r_+)) \\ & + 4M^2 (r_0^2 r_- + r_0^2 r_+ r_-^2 r_+ + r_- r_+^2) r^7 \\ & + (4e^2 Q^2 (r_- r_+ - 3r_0^2)) \\ & - 2M^2 (6r_0^2 r_- r_+ + r_0^2 r_-^2 + r_-^2 r_+^2 + r_0^2 r_+^2 - r_0^4) r^6 \\ & + (12e^2 Q^2 r_0^2 (r_- + r_+)) \\ & + 4M^2 r_0^2 (r_+ r_-^2 + r_+^2 r_- + r_0^2 (r_+ + r_-)) r^5 \end{aligned}$$

$$\begin{aligned}
& + (12e^2 Q^2 r_0^2 (r_0^2 - r_+ r_-) \\
& - M^2 r_0^4 (2r_+ r_- + r_+^2 + r_-^2)) r^4 - 12e^2 Q^2 r_0^4 (r_+ + r_-) \\
& \cdot r^3 + 4e^2 Q^2 r_0^4 (3r_+ r_- - r_0^2) r^2 + 4e^2 Q^2 r_0^6 (r_+ + r_-) \\
& \cdot r - 4e^2 Q^2 r_0^6 r_+ r_- = 0.
\end{aligned} \tag{41}$$

We notice that the last term of the above equation is negative. So, this equation has at least one positive real root. Consequently, a bound orbit is possible for the test particle, i.e., the test particle can be trapped by a charged black hole in generalized dilaton-axion gravity. In other words, a charged black hole in generalized dilaton-axion gravity exerts an attractive gravitational force on matter.

5.2. Test Particle in Nonstatic Equilibrium

5.2.1. *Test Particle without Charge* ($e = 0$). In this case (40) becomes

$$\begin{aligned}
& M^2 (r_- + r_+) r^4 - 2 (r_0^2 M^2 + r_- r_+ M^2 + p^2) r^3 \\
& + 3p^2 (r_+ - r_-) r^2 \\
& + 2 (r^4 M^2 - r_0^2 p^2 + r_0^2 M^2 r_+ r_- - 2p^2 r_+ r_-) r \\
& + r_0^2 (r_+ p^2 + r_- p^2 - M^2 r_0^2 r_+ - M^2 r_0^2 r_-) = 0.
\end{aligned} \tag{42}$$

If $M^2 r_0^2 r_+ + M^2 r_0^2 r_- > r_+ p^2 + r_- p^2$, one can see that the last term of the above equation is negative. Therefore, this equation must have at least one positive real root. Consequently, a bound orbit for the uncharged test particle is possible. If $M^2 r_0^2 r_+ + M^2 r_0^2 r_- = r_+ p^2 + r_- p^2$, then (42) changes to a third-degree equation with two changes of sign. By Descartes's rule of sign, this equation must have either two positive roots or no positive roots at all. Thus, a bound orbit for the uncharged test particle may or may not be possible. For $M^2 r_0^2 r_+ + M^2 r_0^2 r_- < r_+ p^2 + r_- p^2$, (42) has two changes of sign. Here, again a bound orbit for the uncharged test particle may or may not be possible.

5.2.2. *Test Particle with Charge* ($e \neq 0$). For a charged test particle with $n = 0.5$, the stationary system ($dV/dr = 0$) yields the form given in (40). As this equation is algebraically very complicated, we use the graph of $\alpha(r)$ in order to find out whether there exist any real positive roots. From Figure 5 one can see that, for different values of the test particle's charge, $\alpha(r)$ given by (40) does not intersect the r -axis. Hence, no real positive roots are possible. As a result, no bound orbit for the charged test particle is possible.

6. Discussion

In the present investigation, we have analyzed the behaviour of massless and massive particles in the gravitational field of a charged black hole in generalized dilaton-axion gravity in

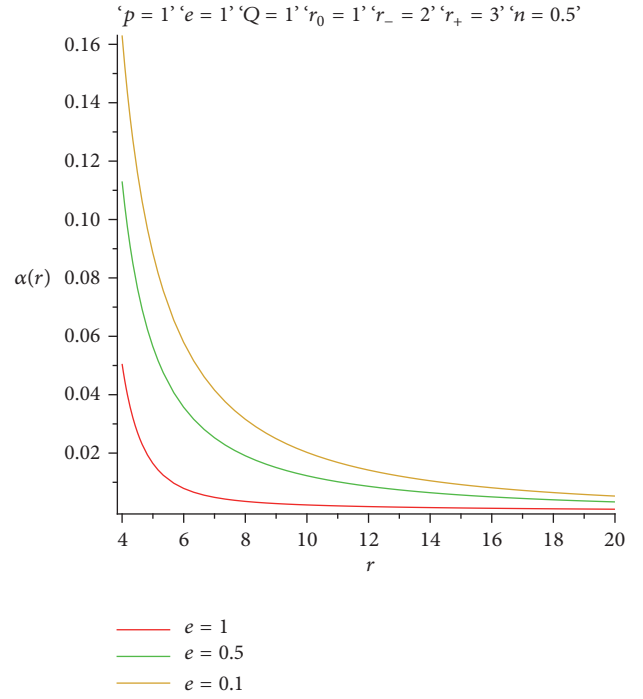


FIGURE 5: Graph of $\alpha(r)$ given in (40) for different values of the test particle's charge.

four dimensions. To this purpose, we have studied the motion of a massless particle ($L = 0$) and a massive particle ($L = -1$). We have plotted the graphs of t and the proper time τ with respect to the radial coordinate r . For the massless particle t increases nonlinearly with r (Figure 1 (left)), while the proper time τ increases linearly with r (Figure 1 (right)). In the case of the massive particle motion both t and τ decrease nonlinearly with r (Figure 2).

Further, studying the effective potential we ended up with (24) from which we conclude that V_{eff} depends on the energy per unit mass E and the angular momentum J . For a massless test particle we found that $V_{\text{eff}} = -E^2/2$ in the case of radial geodesics ($J = 0$), while if $E = 0$ the particle behaves like a free particle. In the case of circular geodesics ($J \neq 0$), V_{eff} is given by (26). In Figure 3 the behaviour of V_{eff} is presented for zero and nonzero E and various values of J . From these graphs it can be inferred that for $E \neq 0$ and $J \neq 0$ the effective potential V_{eff} has a minimum and circular orbits are possible, while for $E \neq 0$ and $J = 0$ no stable circular orbits can exist. In the cases $E = 0$ and $J \neq 0$ the effective potential V_{eff} changes sign two times between the horizons and stable circular orbits must exist.

From the examination of the calculated effective potential, (27) for a massive particle, we have considered the radial geodesics for the cases $J = 0$ and $E = 0$, $J = 0$ and $E \neq 0$, and $J \neq 0$ and $E = 0$. It is seen (Figure 4) that in the first case the roots of the effective potential coincide with the horizons' positions and the particle's orbit is bound in the black hole's interior. In the second case, a bound orbit is also possible. Finally, in the third case, i.e., when the particle's angular momentum does not vanish, the roots of the effective

potential coincide again with the horizons' positions and the particle's orbit is bound again in the black hole's interior.

As a last step we have examined the motion of a massive and charged test particle in the gravitational field of a charged black hole in generalized dilaton-axion gravity by exploiting the Hamilton-Jacobi equation. The latter is set up for the space-time geometry considered and is analytically solved by applying additive separation of variables. As a result, the particle's radial velocity and the effective potential are determined in closed form. Then the case of static equilibrium is examined and it is found that the charged test particle may have a bound orbit; i.e., it can be trapped by a charged black hole in this context or, stated differently, the charged black hole exerts an attractive gravitational force upon the charged particle in generalized dilaton-axion gravity. In the case of nonstatic equilibrium, we have distinguished between an uncharged and a charged test particle. In the former case, conditions have been found for the possibility of existence of the particle's bound orbit. Finally, when the test particle carries a charge, it is seen graphically (Figure 5) that no bound orbit is possible.

An interesting perspective for future work would be the study of the motion of charged or uncharged test particles and the behaviour of geodesics for rotating black hole solutions or for black hole solutions in more than four space-time dimensions in the context of generalized dilaton-axion gravity.

Data Availability

The data used to support the findings of this study are available from the corresponding author upon request.

Conflicts of Interest

The authors declare that they have no conflicts of interest.

Acknowledgments

Farook Rahaman would like to thank the authorities of the Inter-University Centre for Astronomy and Astrophysics, Pune, India, for providing research facilities. Farook Rahaman and Susmita Sarkar are also grateful to DST-SERB (Grant No.: EMR/2016/000193) and UGC (Grant No.: 1162/(sc)(CSIR-UGC NET, DEC 2016)), Govt. of India, for financial support, respectively.

References

[1] T. Ortín, *Gravity and Strings*, Chapter 16, Cambridge University Press, 2004.
 [2] S. Sur, S. Das, and S. SenGupta, "Charged black holes in generalized dilaton-axion gravity," *Journal of High Energy Physics*, vol. 10, article no. 064, 2005.
 [3] T. Ghosh and S. SenGupta, "Thermodynamics of dilation-axion black holes," *Physical Review D*, vol. 78, no. 12, Article ID 124005, 2008.
 [4] A. A. Usmani, Z. Hasan, F. Rahaman, S. A. Rakib, S. Ray, and P. K. Kuhfittig, "Thin-shell wormholes from charged black holes

in generalized dilaton-axion gravity," *General Relativity and Gravitation*, vol. 42, no. 12, pp. 2901–2912, 2010.

- [5] I. Radinschi, F. Rahaman, and A. Ghosh, "On the energy of charged black holes in generalized dilaton-axion gravity," *International Journal of Theoretical Physics*, vol. 49, no. 5, pp. 943–956, 2010.
 [6] Z. M. Yang, X.-L. Li, and Y. Gao, "Entanglement entropy of charged dilaton-axion black hole and quantum isolated horizon," *European Physical Journal Plus*, vol. 131, no. 9, p. 304, 2016.
 [7] T. Ghosh and S. SenGupta, "Tunneling across dilaton-axion black holes," *European Physics Letters*, vol. 120, no. 5, Article ID 50003, 2017.
 [8] A. S. Bhatia and S. Sur, "Dynamical system analysis of dark energy models in scalar coupled metric-torsion theories," *International Journal of Modern Physics D*, vol. 26, no. 13, Article ID 1750149, 2017.
 [9] S. Sur and A. S. Bhatia, "Weakly dynamic dark energy via metric-scalar couplings with torsion," *Journal of Cosmology and Astroparticle Physics*, vol. 2017, no. 7, p. 39, 2017.
 [10] M. Kalam, F. Rahaman, and S. Mondal, "Particle motion around tachyon monopole," *General Relativity and Gravitation*, vol. 40, no. 9, pp. 1849–1861, 2008.
 [11] S. Chakraborty and M. F. Rahaman, "Motion of test particles around gauge monopoles or near cosmic strings considering semiclassical gravitational effects," *International Journal of Modern Physics D*, vol. 9, no. 2, pp. 155–159, 2000.

Research Article

An Alternative Approach to the Static Spherically Symmetric, Vacuum Global Solution to the Einstein Equations

Luis Herrera ¹ and Louis Witten²

¹*Instituto Universitario de Física Fundamental y Matemáticas, Universidad de Salamanca, Salamanca, Spain*

²*Department of Physics, University of Florida, Gainesville, FL 32611, USA*

Correspondence should be addressed to Luis Herrera; lherrera@usal.es

Received 21 June 2018; Accepted 23 August 2018; Published 12 September 2018

Academic Editor: Theophanes Grammenos

Copyright © 2018 Luis Herrera and Louis Witten. This is an open access article distributed under the Creative Commons Attribution License, which permits unrestricted use, distribution, and reproduction in any medium, provided the original work is properly cited. The publication of this article was funded by SCOAP³.

We propose an alternative description of the Schwarzschild black hole based on the requirement that the solution is static not only outside the horizon but also inside it. As a consequence of this assumption, we are led to a change of signature implying a complex transformation of an angle variable. There is a “phase transition” on the surface $R = 2m$, producing a change in the symmetry as we cross this surface. Some consequences of this situation on the motion of test particles are investigated.

1. The Schwarzschild Solution

The Schwarzschild solution of the Einstein gravitational field equations for empty space is the unique static, spherically symmetric, asymptotically flat solution. These statements have a gauge independent meaning.

Indeed, by “static” it is meant that the metric tensor satisfies the Killing equations for the timelike vector field $\chi_{(0)}$

$$\mathcal{L}_{\chi_{(0)}} g_{\alpha\beta} = 0, \quad (1)$$

where \mathcal{L} denotes the Lie derivative with respect to the vector field $\chi_{(0)} = \partial_t$, which, besides being timelike, is also hypersurface orthogonal.

Then, adapting our timelike coordinate to the vector $\chi_{(0)}$, we must demand

$$\frac{\partial g_{\mu\nu}}{\partial t} = g_{0a} = 0, \quad (2)$$

and in the above, Greek indices run from 0 to 3, whereas Latin indices run from 1 to 3.

On the other hand, spherical symmetry implies that the solution admits three additional Killing vectors, describing invariance under rotations; namely,

$$\begin{aligned} \chi_{(1)} &= \partial_\phi, \\ \chi_{(2)} &= -\cos\phi\partial_\theta + \cot\theta\sin\phi\partial_\phi \\ \chi_{(3)} &= \sin\phi\partial_\theta + \cot\theta\cos\phi\partial_\phi. \end{aligned} \quad (3)$$

Then, as is well known, the line element can be written in polar coordinates in the form ($R > 2m$)

$$\begin{aligned} ds^2 &= -\left(1 - \frac{2m}{R}\right)dt^2 + \frac{dR^2}{(1 - 2m/R)} + R^2 d\Omega^2, \\ d\Omega^2 &= d\theta^2 + \sin^2\theta d\phi^2, \end{aligned} \quad (4)$$

where the time coordinate t is adapted to the timelike Killing vector (1). This is a static solution with the (θ, ϕ) curved 2-surface describing a space with a positive Gaussian curvature.

When $R < 2m$, the signature changes from $(-, +, +, +)$ to $(+, -, +, +)$. Although mathematically a solution, this does not describe a physical solution as we wish it to be described.

Since there is no algebraic singularity at the horizon ($R = 2m$) (the physically meaningful components of the Riemann

tensor are regular), there are coordinate transformations that yield acceptable solutions of the Einstein equations with an unchanged signature over the entire resultant space-time. These coordinate transformations yield acceptable solutions of the Einstein equations over the entire manifold but they are not static.

As stressed by Rosen [1], any transformation that maintains the static form of the Schwarzschild metric is unable to remove the singularity in the line element. Indeed, various coordinate transformations have been found that allow the manifold to extend over the whole region $0 < R < \infty$, although all of them necessarily are nonstatic (for $R < 2m$) and require all incoming geodesics (test particles) to end at the central singularity (see, for example, [2–7]).

The point is that, for (4), $R = 2m$ is also a Killing horizon, implying that the timelike Killing vector $\chi_{(0)}$ becomes null on that surface and, still worse, becomes spacelike, inside it.

From a physical point of view, the existence of a static solution would be expected over the whole space-time of a vacuum, as an equilibrium final state of a physical process is expected to be static. Furthermore, we should recall that, in obtaining the Schwarzschild solution, being static is not an additional assumption but follows from the sphericity and the vacuum condition.

In this work we deviate from the classical approach which consists in extending the solution outside the horizon to the interior. We recognize that this is a legitimate possibility but the resultant space-time is necessarily not static. We insist on a static solution everywhere and this will require a radically different description of the significance of the horizon. The resultant static solution describes the space-time as consisting of a complete four-dimensional manifold on the exterior side and a second complete four-dimensional solution in the interior. The two-dimensional R - t submanifold forms a single continuous topological manifold; the addition of a metric requires a change in signature at the horizon. The $\theta - \phi$ submanifolds have a spherical symmetry on the exterior and hyperbolic symmetry in the interior. The two meet only at a single curve, $R = 2m$, $\theta = 0$. Passage of a geodesic from one side of the $R - t$ manifold to the other is possible only on a point on this curve. The horizon has significance as a horizon only for static geodesic observers. A geodesic particle may start at $R = \infty$ and travel a distance to a position R_{min} and remain there or return to $R = \infty$. R_{min} may be interior or exterior to the horizon position $R = 2m$, depending on the energy of the particle; for great enough energy, it will proceed all the way to $R = 0$. The horizon has no significance for such a particle. Similarly a geodesic particle may travel from $R = 0$ to R_{max} and remain there or return to $R = 0$ and R_{max} will be related to the particles energy and not to $R = 2m$. The particles may pass $R = 2m$ as described only at $\theta = 0$. In this paper we do not discuss the motions when θ is not = 0.

2. The Solution inside the Horizon

Our main point is that one should certainly expect that static vacuum should be allowed inside the horizon as well as outside and one should be able to describe a manifold

that permits this. As we shall show in this note, this is in fact the case, although for doing that, we should permit for a change in symmetry, from elliptic (spherical) outside the horizon to hyperbolic inside the horizon. This requires the transformation $d\Omega^2 \rightarrow -d\Omega^2$ which obviously calls for a detour through the complex plane. Doing so, we have a static solution everywhere, but the symmetry of the $R = 2m$ surface is different at both sides of it. Furthermore, as we stated before, we have to consider two different manifolds at both sides of the horizon. Accordingly no match of both solutions at $R = 2m$ surface is needed.

Thus, for $R < 2m$ we have

$$ds^2 = \left(\frac{2m}{R} - 1 \right) dt^2 - \frac{dR^2}{(2m/R - 1)} - R^2 d\Omega^2, \quad (5)$$

$$d\Omega^2 = d\theta^2 + \sinh^2 \theta d\phi^2.$$

Just as when $R > 2m$, this is also a static solution with the (θ, ϕ) space describing a positive Gaussian curvature and with the time coordinate t adapted to the Killing vector (1).

The above metric obviously admits the timelike Killing vector $\chi_{(0)} = \partial_t$ and three additional Killing vectors which are

$$\begin{aligned} \chi_{(1)} &= \partial_\phi, \\ \chi_{(2)} &= -\cos \phi \partial_\theta + \coth \theta \sin \phi \partial_\phi, \\ \chi_{(3)} &= \sin \phi \partial_\theta + \coth \theta \cos \phi \partial_\phi. \end{aligned} \quad (6)$$

The above Killing vectors, of course, differ from the Killing vectors (3) and define a different symmetry in the inner region. Such change of symmetry comes up through the transformation $\theta \rightarrow i\theta$.

The differences in the spatial θ, ϕ subspaces for the external metric ($R > 2m$) and the internal metric ($R < 2m$) become clear when the 2 subspaces are embedded in a flat 3-space.

Thus, for the external metric, we have

$$\begin{aligned} x &= \sin \theta \cos \phi; \\ y &= \sin \theta \sin \phi; \\ z &= \cos \theta, \end{aligned} \quad (7)$$

with a Euclidean metric.

The interior embedding is

$$\begin{aligned} x &= \sinh \theta \cos \phi; \\ y &= \sinh \theta \sin \phi; \\ z &= \cosh \theta, \end{aligned} \quad (8)$$

with $-1 = x^2 + y^2 - z^2$ and $ds^2 = -dx^2 - dy^2 + dz^2$.

The exterior 2-surface is, as expected, a sphere. The interior 2-surface is a hyperboloid of two sheets. At the horizon, they meet only at $R = 2m$, $\theta = 0$. This intersection is not in the space-time 4d manifold because it is not contained in an open set within the manifold. Let us now take a look

at the motion of a test particle as a function of its own proper time. All particles have their proper time differences correlated, although they are free to choose the starting proper time for their clocks. The paths in the two manifolds may be continuous across the horizon as the metric in the $t-R$ plane has a continuous form.

Obviously, motion from the exterior to the interior is possible only when the two manifolds meet at $\theta = 0$. Thus we will assume radial motion. The entire plane is a single mathematical manifold but the change in signature would lead one to expect that, from the standpoint of physical observations, it represents two different manifolds, and it may be called a single manifold with a “phase change” at $R = 2m$.

Of interest then is the path of a geodesic between $R = 0$ and $R = \infty$. Whether we are interested in the path a particle takes in its proper time or in the observers time, we see that the velocity will be given as a square. So wherever a particle went past a point going in one direction, it went past the same point going in the opposite direction at some other time. It was of course always traveling in the positive time direction, so it went past the same point while going in different directions at two different times.

At constant $\theta = 0$ the geodesics may be obtained, and because ∂_t is a Killing vector, there will be a constant of motion

$$\kappa = \left(1 - \frac{2m}{R}\right) \frac{\partial t}{\partial s}. \quad (9)$$

From the metric we get the velocity

$$\left(\frac{dR}{ds}\right)^2 = \kappa^2 - 1 + \frac{2m}{R} \quad (10)$$

Depending on κ there are three possible solutions of (10), stated parametrically:

$$(1) \quad \kappa^2 - 1 = 0.$$

$$R = (2m)^{1/3} \left(\frac{3}{2}\right)^{2/3} s^{2/3}. \quad (11)$$

$$(2) \quad \kappa^2 - 1 > 0.$$

$$R = \frac{m}{\kappa^2 - 1} (\cosh \eta - 1),$$

$$\frac{m}{(\kappa^2 - 1)^{3/2}} (\sinh \eta - \eta) = s - s_0 \quad (12)$$

$$s_0 = \frac{\pi m}{(|\kappa^2 - 1|)^{3/2}}.$$

$$(3) \quad \kappa^2 - 1 < 0.$$

$$R = \frac{m}{|\kappa^2 - 1|} (1 - \cos \eta),$$

$$\frac{m}{(|\kappa^2 - 1|)^{3/2}} (\sin \eta - \eta) = s - s_0, \quad (13)$$

$$s_0 = -\frac{m}{(|\kappa^2 - 1|)^{3/2}} (\sinh \tilde{\eta} - \tilde{\eta}),$$

$$\cos \tilde{\eta} = 3,$$

where for convenience the constants s_0 have been chosen such that particles coming from $R = 0$ and $R = \infty$ meet at $R = 2m/|\kappa^2 - 1|$; at the same time $s = 0$.

The proper time, s , is taken to be 0 when the particle comes to rest at $dR/ds = 0$. As an aid in tracing the paths of geodesics, we see that all three cases have the same limiting behavior when the particle is at rest. All satisfy (10) in this limit, independently of the value of $\kappa^2 - 1$.

We first discuss the motion of a particle with $\kappa^2 - 1 < 0$. We assume it enters at $R = 0$. The behavior there is given by (13), while the behavior of the velocity as given by (10) is $(dR/ds) \sim s^{-1/3}$, so the particle comes into the origin at $\eta = 0$ and immediately curves around, to reemerge at once. At $\eta = \pi$ the particle is at its maximum distance, $R = 2m/|\kappa^2 - 1|$, which may be larger or smaller than $2m$. It comes to rest here, emerges on a cusplike path, and returns along the same path it entered.

In the above, we started out assuming the geodesic begins at $R = 0$. Let us now consider the case when it begins at $R = \infty$.

Then, for the radial geodesic at $\theta = 0$ we may write

$$1 = \left(\frac{2m}{R} - 1\right) \left(\frac{dt}{ds}\right)^2 - \frac{1}{(2m/R - 1)(dR/ds)^2}; \quad (14)$$

denoting now by q the constant of motion (the energy) associated with the timelike Killing vector and feeding it back into (14), we get

$$\left(\frac{dR}{ds}\right)^2 = q^2 + 1 - \frac{2m}{R}. \quad (15)$$

The geodesic comes in from infinity with a velocity $q^2 + 1$, reaches to a minimum zero velocity at $R = 2m/(q^2 + 1)$, and turns around immediately in a cusplike path and returns to infinity with the same speed as it left.

The end goal of starting both at $R = 0$ and $R = \infty$ is to see what happens when two particles meet at the same point at the same time. Unfortunately, Einstein's theory does not tell us if one geodesic bounces back to infinity and the other bounces back to 0 or if each continues forward. In this latter case, the particle must gain energy or lose energy depending on which way it crosses $R = 2m$. They may also meet, interact, and scatter and then return from whence they came.

The particles will meet when $s = 0$ if $\kappa^2 - 1 = 1 - q^2$. If the vacuum level of a zero energy particle in one manifold is -1 , it may be $+1$ on the other side due to the change in signature, so $q^2 = -\kappa^2$, and one may be the antiparticle of the other. If one is the antiparticle of the other, they may annihilate.

Of course a full understanding of the picture described above requires a quantum theory.

On the other hand let us look at the singularity $R = 0$. It is the inverse curvature of a sphere and indicates that the curvature is infinite. However it stays at infinity for zero length of time. It is equivalent to a sphere reducing its radius very rapidly to 0 and immediately, in zero time, expanding again. We would say that this singularity is physically ignorable.

3. Conclusions

In [1] the region $R < 2m$ was considered as nonphysical and thereby excluded. According to Rosen, such an exclusion was justified by two reasons: on the one hand because the coordinates R and t change from spacelike to timelike (R) and inversely (t); on the other hand, he concluded that particles reaching the surface $R = 2m$ from the outside are reflected back.

In this work, we have considered the whole space-time. However, instead of sacrificing the staticity in the region inside the horizon (as in [2–6]), we keep the time independence but change the spatial symmetry.

For doing that we have to consider the whole space-time as consisting of two distinct 4-manifolds, each of which corresponds to a static space-time. Each has the horizon as a boundary; each is a complete manifold. Complete means that a geodesic has a closed path or terminates at a boundary which is singular or infinite. One 4-manifold has the range $2m < R < \infty$ with the signature $(-+++)$ and the second manifold has the range $0 < R < 2m$ with the signature $(+---)$. Proceeding in this way we obtain a global static solution, which presents a “phase transition” on the horizon, being endowed with different symmetry at both sides of it. Both manifolds exclude the $R = 2m$ surface. They meet at $R = 2m$, only when $\theta = 0$. The acceptability of our setup is supported by the fact that from purely physical arguments we should expect a static solution to exist in the “whole space-time” (in the sense above).

Indeed, for $\theta = 0$, as we have seen that the theory permits one geodesic to rebound to infinity and the other to bounce back towards 0. However each may continue in a straight path, one from $R = 0$ to $R = \infty$ and the other in the opposite direction. One would gain two units of energy along the way and the other would lose two units; κ and q refer to two different test particles. They may backscatter with different energies. The times of meeting may have been adjusted so that the two particles meet at the same time, $s = 0$. The zero energy of one vacuum is +1 and because of the change in signature, the zero energy of the other is -1. Since at $s = 0$, $\kappa^2 - 1 = q^2 + 1$, the energy κ is the negative of the energy q and the two may be antiparticles.

If the particles were antiparticles, there would be another level of complexity and uncertainty added to the mix. We have described the particle with the greater energy as falling from infinity and the one with the lesser as rising from $R = 0$. It could just as well be the other way as far as the theory tells us.

On the other hand, $R = 0$ seems to be harmless. As an observable quantity, R is a measure of the curvature of the surface it represents. A particle may, with a probability of measure 0 in a finite proper time, reach a surface of zero curvature with infinite proper velocity and remain there for infinitesimal time. To verify that this statement is valid requires a study of the geodesics including particles with nonzero angular momentum, which we have not done here.

The main lesson to extract from the comments above is that there is no way to understand the complete picture

of the motion of test particles in the neighborhood of the horizon from Einstein's equations alone. A quantum theory is needed to understand it. The two curved surfaces of the metric that meet at the horizon at $\theta = 0$ are continuous with continuous first derivatives but not second derivatives, so a particle cannot cross at the horizon except at this one point. However, it is almost certain that a quantum theory would permit a particle to tunnel across.

It may look strange that we have described a geodesic that comes in from infinity with the metric for $R < 2m$. However this becomes intelligible if we recall that we are dealing only with $\theta = 0$. The behavior is similar coming in from either direction. Either side could have been the starting point if $\kappa = q = 0$.

It should be pointed out that we have not considered the behavior of nonradial geodesics. They need major consideration as the nonradial geodesics will be able to penetrate the horizon only by tunneling.

Also, it is worth noticing that we have not specified a source for the vacuum parameter m , which usually (as measured from the vacuum solution) is associated with a singular (pointlike) source. However, an alternative origin for m might be considered here. Indeed, we have already said that we need quantum mechanics to understand the horizon. Then, if the vacuum has a “mass”, the vacuum mass could come from quantum mechanics. When students first learn about quantum mechanics and its zero point energy, they frequently ask why this does not show up in gravity. We speculate that our m might be a quantum mechanics residue.

Finally we would like to notice that an approach similar to the one presented here could be proposed for the global interpretation of the Kerr metric [8].

To summarize, we have shown that there is a static solution of Einstein's equations with the symmetry of a sphere or of a paraboloid and that the symmetry changes at the horizon. $R > 2m$ is a geodesically complete manifold in that each geodesic may be continued to a singularity or to a boundary. $R < 2m$ is also a geodesically complete manifold. We recognize that our approach represents a radical departure from the standard description. The standard description insists on keeping the curved two surfaces involved (θ, ϕ surface) unchanged but does not describe an everywhere vacuum, static situation. We have no difficulty with this description and furthermore are fully aware of the fact that it had produced an impressive wealth of research work (just as a sample see [9–17] and references therein). However, we do believe that a static vacuum at all times and places should be possible.

Conflicts of Interest

The authors declare that they have no conflicts of interest.

Acknowledgments

This work was partially supported by the Spanish Ministerio de Ciencia e Innovación under Research Project no. FIS2015-65140-P (MINECO/FEDER).

References

- [1] N. Rosen, “The nature of Schwarzschild singularity in “Relativity,”” in *Proceedings of the Relativity Conference in the Midwest*, M. Carmeli, S. I. Fickler, and L. Witten, Eds., Plenum Press, New York, USA, 1970.
- [2] A. S. Eddington, “A comparison of Whitehead’s and Einstein’s formulæ,” *Nature*, vol. 113, 192 pages, 1924.
- [3] G. Lemaître, *Ann. Soc. Sci. Bruxelles*, vol. A 53, p. 51, 1933.
- [4] D. Finkelstein, “Past-future asymmetry of the gravitational field of a point particle,” *Physical Review Journals Archive*, vol. 110, p. 965, 1958.
- [5] M. D. Kruskal, “Maximal Extension of Schwarzschild Metric,” *Physical Review Journals Archive*, vol. 119, no. 5, pp. 1743–1745, 1960.
- [6] W. Israel, “New interpretation of the extended schwarzschild manifold,” *Physical Review Journals Archive*, vol. 143, no. 4, Article ID 1016, 1966.
- [7] R. Gautreau and J. M. Cohen, “Gravitational collapse in a single coordinate system,” *American Journal of Physics*, vol. 63, no. 11, pp. 991–999, 1995.
- [8] R. P. Kerr, “Gravitational field of a spinning mass as an example of algebraically special metrics,” *Physical Review Letters*, vol. 11, pp. 237–238, 1963.
- [9] B. C. Nolan and F. C. Mena, “Geometry and topology of singularities in spherical dust collapse,” *Classical and Quantum Gravity*, vol. 19, no. 10, pp. 2587–2605, 2002.
- [10] O. B. Zaslavskii, “Black Hole as a Supercollider,” *International Journal of Modern Physics A*, vol. 26, pp. 3845–3855, 2011.
- [11] A. Buchel, “Universality of small black hole instability in AdS/CFT,” *International Journal of Modern Physics D: Gravitation, Astrophysics, Cosmology*, vol. 26, no. 13, Article ID 1750140, 2017.
- [12] Y. K. Ha, “Weighing the black holes of GW150914,” *International Journal of Modern Physics D*, vol. 26, no. 12, Article ID 1743018, 2017.
- [13] P. Bueno and P. A. Cano, “Universally stable black holes,” *International Journal of Modern Physics D*, vol. 26, no. 12, Article ID 1743024, 2017.
- [14] T. Nakama, B. Carr, and J. Silk, “Limits on primordial black holes from μ distortions in cosmic microwave background,” *Physical Review D: Particles, Fields, Gravitation and Cosmology*, vol. 97, no. 4, Article ID 043525, 2018.
- [15] G. Antoniou, A. Bakopoulos, and P. Khati, “Black-hole solutions with scalar hair in Einstein-scalar-Gauss-Bonnet theories,” *Physical Review D: Particles, Fields, Gravitation and Cosmology*, vol. 97, Article ID 084037, 2018.
- [16] D. Doneva and S. Yazadjiev, “New gauss-bonnet black holes with curvature-induced scalarization in extended scalar-tensor theories,” *Physical Review Letters*, vol. 120, Article ID 131103, 2018.
- [17] F. Azzurli, N. Bobev, P. Marcos, and V. Min, “A universal counting of black hole microstates in AdS_4 ,” *Journal of High Energy Physics*, vol. 2018, Article ID 54, 2018.

Research Article

λ Phase Transition in Horava Gravity

Wei Xu 

School of Mathematics and Physics, China University of Geosciences, Wuhan 430074, China

Correspondence should be addressed to Wei Xu; xuwei@cug.edu.cn

Received 27 March 2018; Revised 5 July 2018; Accepted 22 July 2018; Published 9 August 2018

Academic Editor: Saibal Ray

Copyright © 2018 Wei Xu. This is an open access article distributed under the Creative Commons Attribution License, which permits unrestricted use, distribution, and reproduction in any medium, provided the original work is properly cited. The publication of this article was funded by SCOAP³.

We present another example of superfluid black hole containing λ phase transition in Horava gravity. After studying the extended thermodynamics of general dimensional Horava-Lifshitz AdS black holes, it is found that only the one with spherical horizon in four and five dimensions has λ phase transition, which is a line of (continuous) second-order phase transitions and was famous in the discussion of superfluidity of liquid ^4He . The “superfluid” black hole phase and “normal” black hole phase are also distinguished. Particularly, six-dimensional Horava-Lifshitz AdS black holes exhibit infinitely many critical points in $P - \nu$ plane and the divergent points for specific heat, for which they only contain the “normal” black hole phase and the “superfluid” black hole phase disappears due to the physical temperature constraint; therefore there is no similar phase transition. In more than six dimensions, there is no $P - \nu$ critical behavior. After choosing the appropriate ordering field, we study the critical phenomena in different planes of thermodynamical phase space. We also calculate the critical exponents, which are the same as the van der Waals fluid.

1. Introduction

Black hole thermodynamics always provides valuable insight into quantum properties of gravity, and it has been studied extensively for quite a long time, especially for the quantum and microscopic interpretation of black hole temperature and entropy (see [1, 2], for example). Besides, thermodynamics and phase transitions of AdS black holes have been of great interest since the Hawking-Page phase transition [3] between stable large black hole and thermal gas is explained as the confinement/deconfinement phase transition of gauge field [4] inspired by the AdS/CFT correspondence [5–7].

After treating the cosmological constant as a pressure with its conjugate quantity being the thermodynamic volume in thermodynamic phase space of charged AdS black holes [8–14], the small/large black hole phase transition is established in [15], which is exactly analogous to the liquid/gas phase transition of the van der Waals fluid. This kind of black hole phase transitions has attracted much attention (see the recent review papers [16, 17]). Besides, this semiclassical method of analogue is generalized to study the microscopic structure of black holes and sheds some light on the black hole molecules [18] and microscopic origin of the

black hole reentrant phase transition [19]. The study is also extended to the quantum statistic viewpoint, as the superfluid black holes are reported recently [20]. In Lovelock gravity with conformally coupled scalar field, the authors present the first example of λ phase transition, which is a line of (continuous) second-order phase transitions and was famous for the successful quantum and microscopic interpretation of superfluidity of liquid ^4He .

In this paper, we present another example of black holes containing λ phase transition in Horava gravity, which is a candidate of quantum gravity in ultrahigh energy [21]. The Horava-Lifshitz (HL) black hole solutions, thermodynamics, and phase transitions have attracted a lot of attention [22–29] (see [30] for a review on the recent development of various areas). The general dimensional HL black hole solutions are also introduced [31]. We will consider the extended thermodynamics of general dimensional HL AdS black holes. It is shown that only the one with spherical horizon in four and five dimensions has λ phase transition. Note that the first example of “superfluid” black holes always has a hyperbolic horizon [20]. Particularly, six-dimensional HL AdS black holes exhibit infinitely many critical points in $P - \nu$ plane and the divergent points for specific heat, for which they only

contain the “normal” black hole phase and the “superfluid” black hole phase disappears due to the physical temperature constraint; therefore there is no similar phase transition. In more than six dimensions, there is no $P - \nu$ critical behavior. After identifying parameter ϵ as the ordering field instead of pressure and temperature, we study the critical phenomena in different planes of thermodynamical phase space. We also obtain the critical exponents, which are the same as the van der Waals fluid.

The paper is structured as follows: in next section, we present the extended thermodynamics of generalized topological HL black holes. Then we study $P - V$ criticality in Section 3. We show the λ phase transition for four and five dimensions and the discussion for six dimensions in Sections 4 and 5, respectively. In Sections 6 and 7, we discuss the critical phenomena and calculate the critical exponents in different planes. In final section, some concluding remarks are given.

2. Extended Thermodynamics of Generalized HL Black Holes

In this section, we present the extended thermodynamics of generalized topological HL black holes in $(d + 1)$ dimensions ($d \geq 3$). We begin with the action of HL gravity at the $z = 3$ UV fixed point, which can be reexpressed as [31]

$$\begin{aligned} S &= \int dt \left[L_0 + (1 - \epsilon^2) L_1 \right], \\ L_0 &\equiv \int d^d x \sqrt{g} N \left[\frac{2}{\kappa^2} (K_{ij} K^{ij} - \lambda K^2) \right. \\ &\quad \left. + \frac{\kappa^2}{8\kappa_W^4} \frac{\Lambda_W}{1 - d\lambda} ((d - 2) R - d\Lambda_W) \right], \\ L_1 &\equiv \int d^d x \sqrt{g} N \frac{\kappa^2}{8\kappa_W^4} \frac{1}{1 - d\lambda} \left[\left(1 - \frac{d}{4} - \lambda \right) R^2 \right. \\ &\quad \left. - (1 - d\lambda) R^{ij} R_{ij} \right], \end{aligned} \quad (1)$$

where the first two terms in the L_0 are the kinetic actions, while the residue corresponds to the potential actions. R_{ij} is the Ricci tensor, R is the Ricci scalar, and K_{ij} is defined by $K_{ij} = (1/2N)(\dot{g}_{ij} - \nabla_i N_j - \nabla_j N_i)$, which are based on the ADM decomposition of the higher dimensional metric, i.e., $ds_{d+1}^2 = -N^2 dt^2 + g_{ij}(dx^i - N^i dt)(dx^j - N^j dt)$. Here the lapse, shift, and d -metric N , N^i , and g_{ij} are all functions of t and x^i , and a dot denotes a derivative with respect to t . There are five constant parameters in the action: Λ_W , λ , ϵ , κ , and κ_W . $\Lambda = (d/2(d - 2))\Lambda_W$ is the cosmological constant. κ and κ_W have their origin as the Newton constant and the speed of light. λ represents a dynamical coupling constant which is susceptible to quantum corrections. We will fix $\lambda = 1$ in the following paper, only for which general relativity can be recovered in the large distance approximation. In addition, we will only consider the general values of ϵ in the region

$0 \leq \epsilon^2 \leq 1$, as $\epsilon = 0$ corresponds to the so-called detailed-balance condition, and HL gravity with $\epsilon = 1$ returns back to general relativity.

Action Eq. (1) admits arbitrary dimensional topological AdS black holes with the metric

$$ds^2 = -f(r) dt^2 + \frac{dr^2}{f(r)} + r^2 d\Omega_{d-1,k}^2 \quad (2)$$

and the horizon function [23, 31]

$$\begin{aligned} f(r) &= k - \frac{2\Lambda_W}{(1 - \epsilon^2)} \frac{r^2}{(d - 1)(d - 2)} \\ &\quad - r^{2-d/2} \sqrt{\frac{c_0}{(1 - \epsilon^2)} + \frac{\epsilon^2}{(1 - \epsilon^2)^2} \frac{4\Lambda_W^2 r^d}{(d - 1)^2 (d - 2)^2}}, \end{aligned} \quad (3)$$

where $d\Omega_{d-1,k}^2$ denotes the line element of a $(d - 1)$ -dimensional manifold with constant scalar curvature $(d - 1)k$, and $k = 0, \pm 1$ indicates different topology of the spatial space. c_0 is integration constant, which is related to the black hole mass

$$M = -\frac{\Omega_{d-1,k}^2 c^3}{16\pi G_N} \frac{1}{(d - 2)\Lambda_W} c_0 = -\frac{c_0}{\Lambda_W}, \quad (4)$$

where we have chosen the natural units and $\Omega_{d-1,k}^2 = 16(d - 2)\pi$.

In AdS space-time, the cosmological constant is introduced as the thermodynamical pressure [15]:

$$P = -\frac{\Lambda}{8\pi} = -\frac{d}{16\pi(d - 2)}\Lambda_W. \quad (5)$$

Then we can rewrite the horizon function as

$$\begin{aligned} f(r) &= k + \frac{32\pi P r^2}{(1 - \epsilon^2)d(d - 1)} \\ &\quad - 4r^{2-d/2} \sqrt{\frac{(d - 2)MP\pi}{d(1 - \epsilon^2)} + \frac{64\epsilon^2 P^2 \pi^2 r^d}{(1 - \epsilon^2)^2 d^2 (d - 1)^2}}, \end{aligned} \quad (6)$$

and the mass is

$$\begin{aligned} M &= \frac{64P\pi r_+^d}{(d - 1)^2 (d - 2)d} + \frac{(1 - \epsilon^2)dk^2 r_+^{d-4}}{16P(d - 2)\pi} \\ &\quad + \frac{4kr_+^{d-2}}{(d - 2)(d - 2)}, \end{aligned} \quad (7)$$

where r_+ denotes the event horizon which is the largest positive root of $f(r) = 0$. The conjugate thermodynamic volume of pressure is

$$V = \frac{64\pi r_+^d}{(d - 1)^2 (d - 2)d} - \frac{(1 - \epsilon^2)dk^2 r_+^{d-4}}{P^2 (d - 2)\pi}. \quad (8)$$

The entropy and temperature are presented in [31] with the following forms:

$$S = \begin{cases} 4\pi r_+^2 \left(1 + \frac{kd(1-\epsilon^2)\ln(r_+)}{8(d-2)P\pi r_+^2} \right) + S_0, & d = 3, \\ \frac{16\pi r_+^{d-1}}{(d-1)^2(d-2)} \left(1 + \frac{kd(d-1)^2(d-2)(1-\epsilon^2)}{32(d-2)(d-3)P\pi r_+^2} \right) + S_0, & d \geq 4, \end{cases} \quad (9)$$

$$T = \frac{1024P^2\pi^2 r_+^4 + 64k(d-1)(d-2)P\pi r_+^2 + k^2d(d-1)^2(d-4)(1-\epsilon^2)}{8(d-1)\pi r_+(32P\pi r_+^2 + kd(d-1)(1-\epsilon^2))}. \quad (10)$$

It is easy to check the first law of thermodynamics:

$$dM = TdS + VdP, \quad (11)$$

while the Smarr relation always fails to exist. This can be easily found because of the existence of S_0 (and logarithmic term for $d = 3$) in black hole entropy, which is not fixed and may be calculated by invoking the quantum theory of gravity as argued in [23]. Note that ϵ scales as $[L]^0$, and there is no other dimensional quantity in extended thermodynamic phase space. In this meaning, the validity of the Smarr relation will bring another physical consideration on the parameter S_0 .

In order to analyze the global thermodynamic stability and phase transition of the HL black hole, it is always to study the Gibbs free energy:

$$G = H - TS = M - TS, \quad (12)$$

as the black hole mass M should be considered as the enthalpy H in the extended thermodynamic phase space. For the local thermodynamic stability, one can turn to the specific heat of black hole

$$C = \frac{dM}{dT} = \frac{dM/dr_+}{dT/dr_+}. \quad (13)$$

We present the above two quantities in the Appendix, as their forms are very complicated.

3. $P - V$ Criticality

According to (10), we can obtain the equation of state (EOS):

$$\begin{aligned} & 1024P^2\pi^2 r_+^4 + 64k(d-1)(d-2)P\pi r_+^2 \\ & + k^2d(d-1)^2(d-4)(1-\epsilon^2) \\ & - 8(d-1)\pi r_+(32P\pi r_+^2 + kd(d-1)(1-\epsilon^2))T \\ & = 0, \end{aligned} \quad (14)$$

which reflects the double-valuedness of the pressure in the extended thermodynamic phase space. On the other hand, we can derive the pressure $P(T, r_+)$ as

$$\begin{aligned} P(T, r_+) = & \frac{(d-1)}{32\pi r_+^2} \left(-kd + 2(k + 2\pi r_+ T) \right. \\ & \left. + \sqrt{4(k + 2\pi r_+ T)^2 - kd\epsilon^2(4k - kd + 8\pi r_+ T)} \right), \end{aligned} \quad (15)$$

while another one is the negative pressure branch. After taking a series expansion, it leads to

$$P = \frac{(d-1)T}{4r_+} - \frac{k(d-1)(d\epsilon^2 + d - 4)}{32\pi r_+^2} + \mathcal{O}(r_+^{-3}). \quad (16)$$

Comparing the above equation with the Van der Waals equation

$$P = \frac{T}{v-b} - \frac{a}{v^2} \approx \frac{T}{v} + \frac{bT}{v^2} - \frac{a}{v^2} + \mathcal{O}(v^{-3}), \quad (17)$$

one can easily find the specific volume $v \propto r_+$. Therefore we will just use the horizon radius r_+ in EOS instead of the specific volume v and study the $P - r_+$ behavior in the following paper.

To consider the $P - V$ criticality, we can focus on

$$\begin{aligned} \frac{\partial P}{\partial r_+} &= 0, \\ \frac{\partial^2 P}{\partial r_+^2} &= 0, \end{aligned} \quad (18)$$

to find the critical points. As the direct differentiation of P (see (15)) is too complicated, we prefer to employ the implicit differentiation on EOS (see (14)) and the above equations, and we can derive two simple conditions:

$$\begin{aligned} & 512P^2\pi r_+^3 + 16(d-1)(k(d-2)r_+ - 6\pi r_+^2 T)P \\ & - kd(d-1)^2(1-\epsilon^2)T = 0, \end{aligned} \quad (19)$$

$$96P\pi r_+^2 - 12(d-1)\pi r_+ T + (d-1)(d-2)k = 0. \quad (20)$$

TABLE 1: The critical points of HL AdS spherical black holes.

Dimensions	P_c	T_c	ϵ_c	critical relation $P_c r_+/T_c$
Four	$\frac{2\sqrt{3}-1}{48\pi r_+^2}$	$\frac{\sqrt{3}}{6\pi r_+}$	$\pm \frac{2}{9}\sqrt{9+6\sqrt{3}}$	$\frac{6-\sqrt{3}}{24} \approx 0.178$
Five	$\frac{1}{8\pi r_+^2}$	$\frac{1}{2\pi r_+}$	$\pm \frac{2}{3}\sqrt{2}$	$\frac{1}{4}$
Six	$\frac{1}{8\pi r_+^2}$	$\frac{1}{2\pi r_+}$	$\pm \frac{2}{5}\sqrt{5}$	$\frac{1}{4}$

They lead to the critical points:

$$P_c = \frac{k(d-1)(12\pi X + 2-d)}{96\pi r_+^2}, \quad (21)$$

$$T_c = \frac{kX}{r_+}, \quad (22)$$

by which, the EOS (see (14)) is simplified as an equation of ϵ and results in the following condition:

$$\epsilon_c = \pm 2\sqrt{\frac{(2(d-5)X\pi + 2d-7)}{3d(d-4)}}, \quad (23)$$

where

$$X = \frac{3(d-3) \pm \sqrt{-3(d-1)(d-5)}}{12\pi}. \quad (24)$$

It is interesting that there is no critical volume or horizon radius, but the critical parameter ϵ . To start the physical discussion, we should firstly calculate the physical critical points with real and positive pressure and temperature, which lead to the constraint

$$1 \leq d \leq 5. \quad (25)$$

Namely, there is $P - V$ criticality only in four, five, and six dimensions. Besides, the physical critical points are simplified as

$$P_c = \frac{k(2\sqrt{3}\gamma - 1)}{48\pi r_+^2},$$

$$T_c = \frac{\sqrt{3}k\gamma}{6\pi r_+},$$

$$\epsilon_c = \pm \frac{2}{9}\sqrt{9+6\sqrt{3}\gamma},$$

$$d = 3;$$

$$P_c = \frac{k}{8\pi r_+^2},$$

$$T_c = \frac{k}{2\pi r_+},$$

$$\epsilon_c = \pm \frac{2}{3}\sqrt{2},$$

$$d = 4;$$

$$P_c = \frac{k}{8\pi r_+^2},$$

$$T_c = \frac{k}{2\pi r_+},$$

$$\epsilon_c = \pm \frac{2}{5}\sqrt{5},$$

$$d = 5,$$

$$(26)$$

where $\gamma = \pm 1$. It is easy to find that positive pressure and temperature require the conditions ($k = 1, \gamma = 1$). In four dimensions ($d = 3$), the critical behavior is studied in [29].

Totally, we conclude that only four-, five-, and six-dimensional HL AdS black holes with spherical horizon have physical critical points, as shown in Table 1.

In next sections, we will give the physical discussion about the critical phenomena, i.e., the infinitely critical points and continuous second-order phase transitions. Especially for four-dimensional case, it is reported in [29], which is called “peculiar critical phenomena”. In Section 4, we will conclude that they are actually the famous λ phase transition after studying the specific heat C_P of HL black holes. We also present the λ phase transition in five dimensions. In Section 5, it is found that six-dimensional HL AdS black holes only contain “normal” black hole phase and thus no similar phase transition. In Sections 6 and 7, we discuss the critical phenomena and calculate the critical exponents in different planes, by identifying parameter ϵ as the ordering field instead of pressure and temperature, respectively.

4. λ Phase Transition in Four and Five Dimensions

In this section, we discuss phase transitions in four and five dimensions. Back to the critical points in Table 1, it is interesting that there is no critical volume or horizon radius, but the critical parameter ϵ . Moreover, the $P - r_+$ oscillatory behavior and the classical “swallow tail” characterizing the first-order phase transition are controlled by the parameter ϵ , instead of the temperature T , which is clearly shown in Figure 1. The $P - r_+$ diagrams are plotted at the same temperature T and $G - T$ diagrams are plotted at the same pressure P . When $\epsilon > \epsilon_c$, there exist the small/large black holes phase transition in both four and five dimensions, which is exactly the same as the liquid/gas phase transition

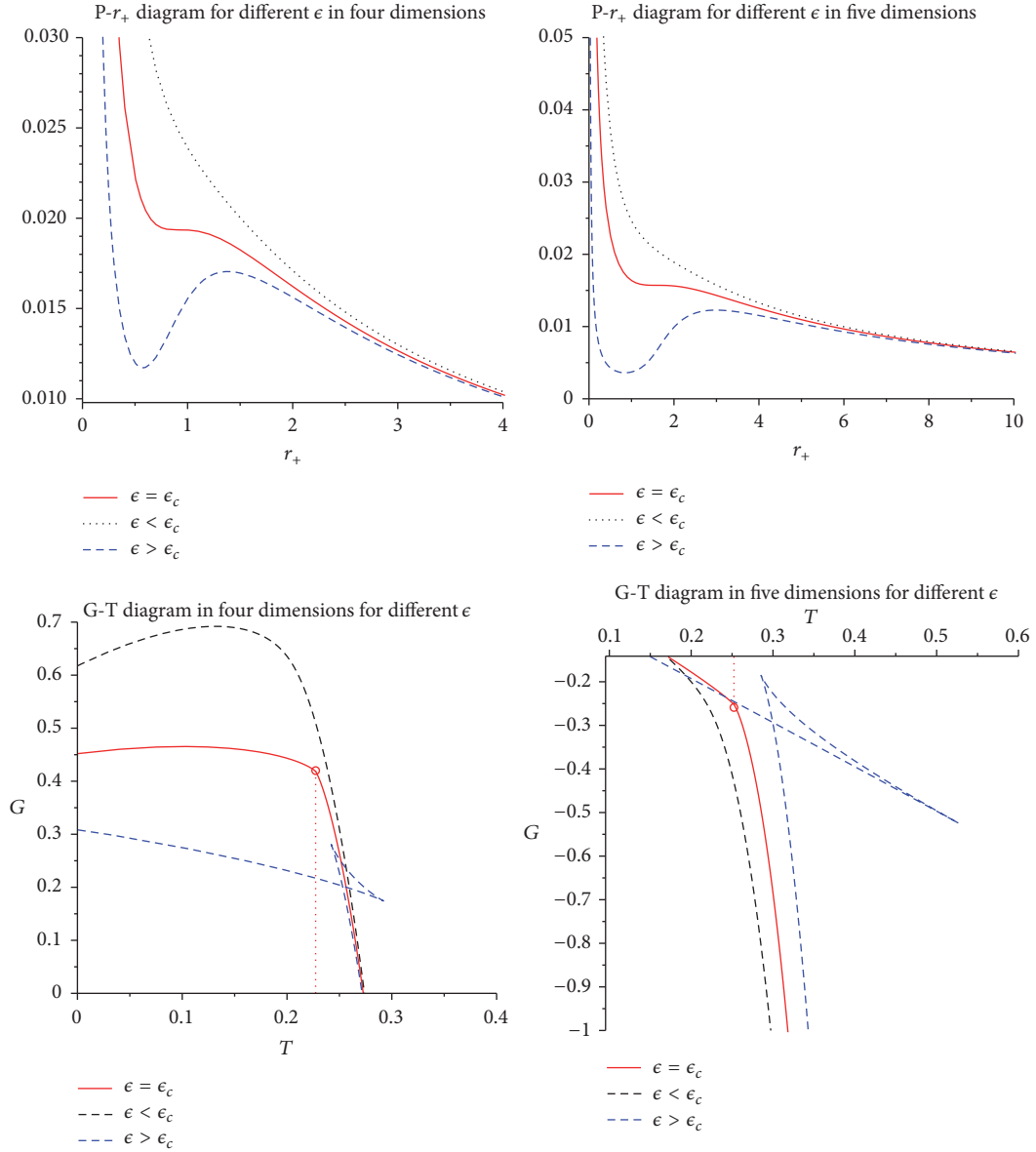


FIGURE 1: Curves of $P-r_+$ at the same temperature $T = 1/10$ and $G-T$ at the same pressure $P = 1/10$ in four and five dimensions for different ϵ . When $\epsilon > \epsilon_c$, there are the $P-r_+$ oscillatory behavior and the classical “swallow tail” characterizing the small/large black holes phase transition. When $\epsilon = \epsilon_c$, the second-order phase transition emerges and the dotted lines highlight the points where the second derivative of the Gibbs free energy G diverges.

of van der Waals fluid. Especially for $\epsilon = \epsilon_c$, the $P-r_+$ curves become a critical isotherm having an inflection point, and the second-order phase transition emerges.

On the other hand, black holes with spherical horizon and arbitrary mass M always have event horizon $r_+ > 0$, which is arbitrary as well. As a result, four and five dimensional HL AdS black holes with $\epsilon = \epsilon_c$ exhibit infinitely many critical points with arbitrary temperature T_c and horizon radius r_+ as

$$P_c = \frac{(2\sqrt{3}-1)\pi}{4} T_c^2,$$

$$T_c = \frac{\sqrt{3}}{6\pi r_+},$$

$$d = 3;$$

$$P_c = \frac{\pi}{2} T_c^2,$$

$$T_c = \frac{1}{2\pi r_+},$$

$$d = 4.$$

(27)

Namely, every isotherm in $P-r_+$ diagrams is a critical isotherm, which has an inflection point at

$$r_+ = \begin{cases} \frac{\sqrt{3}}{6\pi T}, & d = 3; \\ \frac{1}{2\pi T}, & d = 4. \end{cases} \quad (28)$$

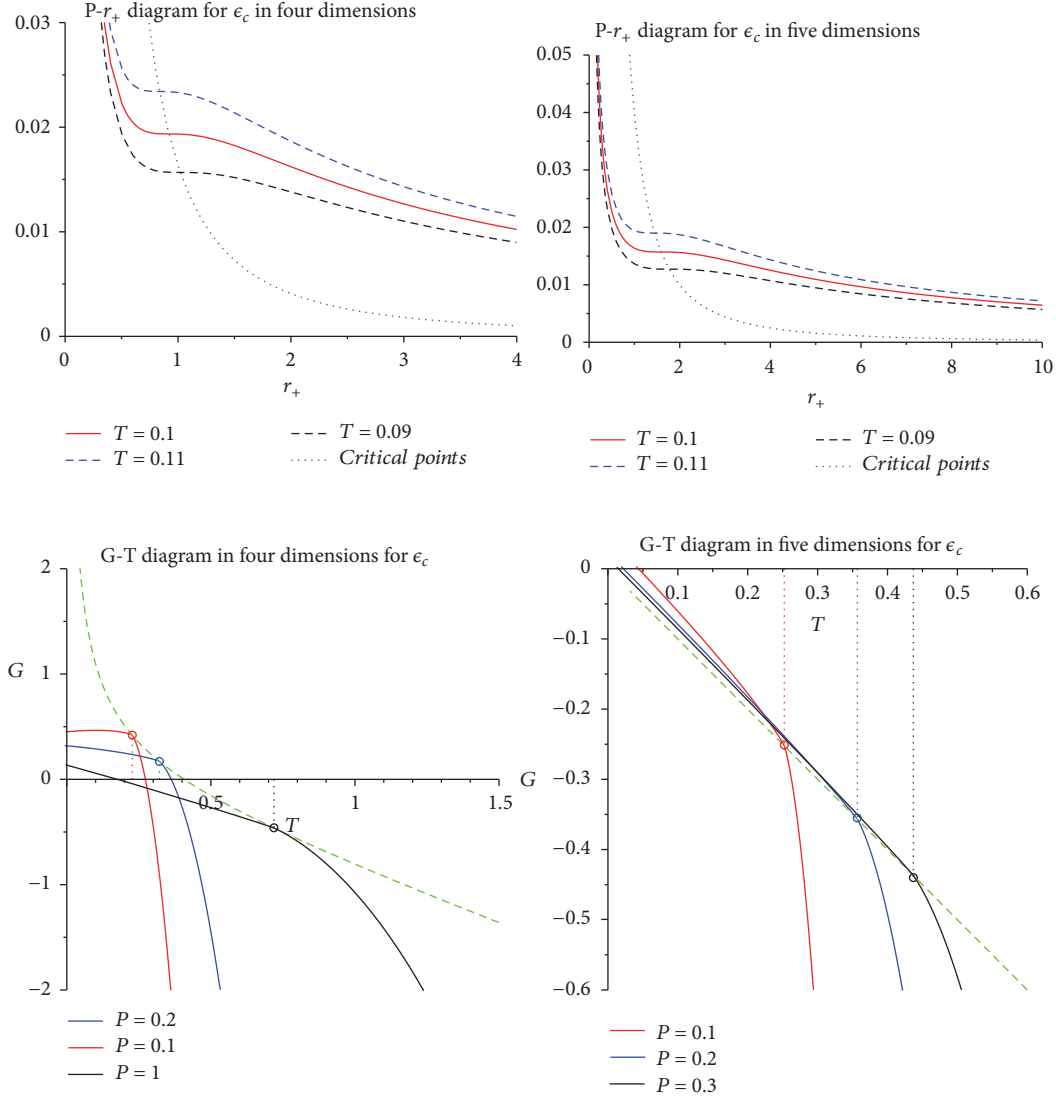


FIGURE 2: Curves of $P - r_+$ at the different temperature T and $G - T$ at the different pressure P in four and five dimensions for $\epsilon = \epsilon_c$. Every isotherm in $P - r_+$ diagrams is a critical isotherm, and the dotted lines describe the position of all critical points. A line of second-order phase transitions is shown in $G - T$ diagrams, and the dashed lines describe the position of all phase transition points.

One can find it easily in Figure 2, and the dotted lines in $P - r_+$ diagrams describe the position of all critical points (see (28)) at arbitrary temperature T . Besides, in $G - T$ diagrams, there is no first-order phase transition but rather a line of second-order phase transitions, for which the phase transition points are highlighted by the dotted lines in Figure 2. The dashed lines in $G - T$ diagrams describe the position of all phase transition points

$$T = \begin{cases} \sqrt{\frac{4P}{(2\sqrt{3}-1)\pi}}, & d = 3; \\ \sqrt{\frac{2P}{\pi}}, & d = 4 \end{cases} \quad (29)$$

at arbitrary pressure P , where the second derivative of the Gibbs free energy G diverges.

To study the continuous second-order phase transitions, we focus on the specific heat C_P of black holes with $\epsilon = \epsilon_c$. From the $C_P - T$ diagrams in Figure 3, one can obtain that the specific heat C_P always diverges at the critical temperature (see (29)). This is the classical λ line, i.e., the line of second-order phase transitions, in $C_P - T$ diagrams, which was famous in the discussion of superfluidity of liquid ^4He . Similarly, in the $P - T$ parameter space (right two plots of Figure 3), a line of critical points, i.e., the λ line, separates the two phases of system, which are the “superfluid” black hole phase and “normal” black hole phase. To determine the two phases, we consider the $S - P$ diagrams, i.e., the middle two plots in Figure 3. The dashed lines highlight the critical pressure (see (27)). One can observe that the entropy of black holes with pressure smaller than the critical pressure is bigger, corresponding to the “normal” black hole phase. Another one is the “superfluid” black hole phase

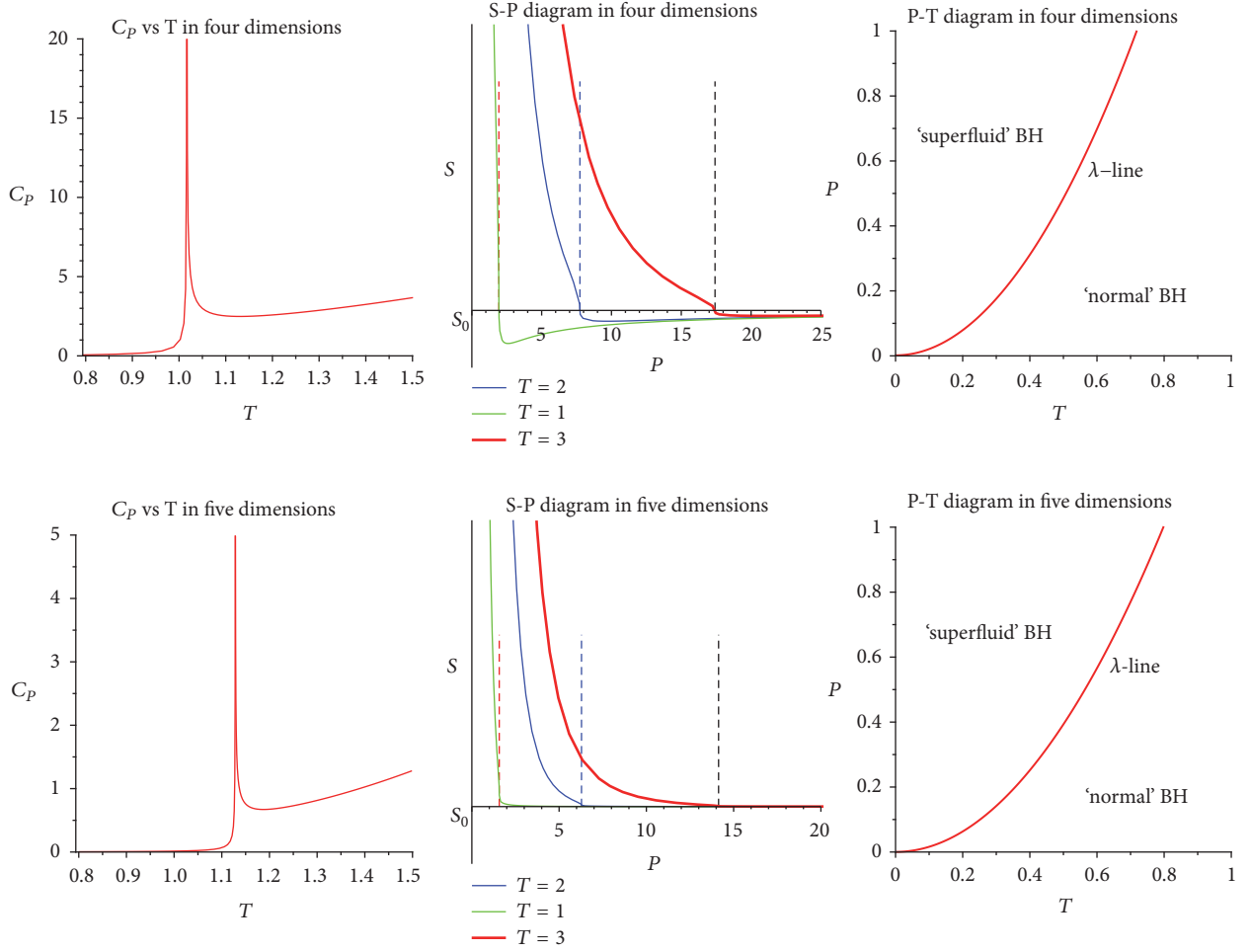


FIGURE 3: Curves of $C_p - T$ and $S - P$ and $P - T$ parameter space of black holes with $\epsilon = \epsilon_c$ in four and five dimensions. The λ line in $C_p - T$ and $P - T$ plots indicates the second-order phase transitions between “superfluid” black hole phase and “normal” black hole phase, which are distinguished in the $S - P$ plots by the dashed lines.

having smaller entropy and corresponding to black holes with pressure larger than the critical pressure. Particularly, the entropy of “superfluid” black hole phase is almost vanishing in five dimensions, while it seems to be negative in four dimensions. Note that the positivity of entropy depends on S_0 , which is not clear and could be fixed by counting microscopic degrees of freedom in quantum theory of gravity as argued in [23].

Finally, we conclude that this continuous second-order phase transition between small/large black holes corresponds to the phase transition between “superfluid” black hole and “normal” black hole, which is firstly reported in Lovelock gravity with conformally coupled scalar field [20].

5. “Normal” Black Hole Phase in Six Dimensions

In six dimensions, there are critical points in $P - r_+$ plane as presented in Table 1. Actually, they describe infinitely many critical points with arbitrary temperature T_c and horizon

radius r_+ for HL black holes with $\epsilon = \epsilon_c = \pm(2/5)\sqrt{5}$; i.e.,

$$\begin{aligned} P_c &= \frac{\pi}{2} T_c^2, \\ T_c &= \frac{1}{2\pi r_+}, \end{aligned} \quad (30)$$

which is exactly the same as the one in five dimensions. However, from Figure 4, it is strange that there is no $P - r_+$ oscillatory behavior and classical “swallow tail” for different ϵ ; especially for $\epsilon = \epsilon_c$, one can never find the second-order phase transitions. This is different from the cases in four and five dimensions, and six-dimensional black holes seem to have no phase transition.

To interpret the strange critical point, we could study the specific heat C_p . One can look at the $C_p - T$ curve in the right plot of Figure 5. The specific heat C_p diverges at the critical point (phase transition point)

$$T = \sqrt{\frac{2P}{\pi}}, \quad (31)$$

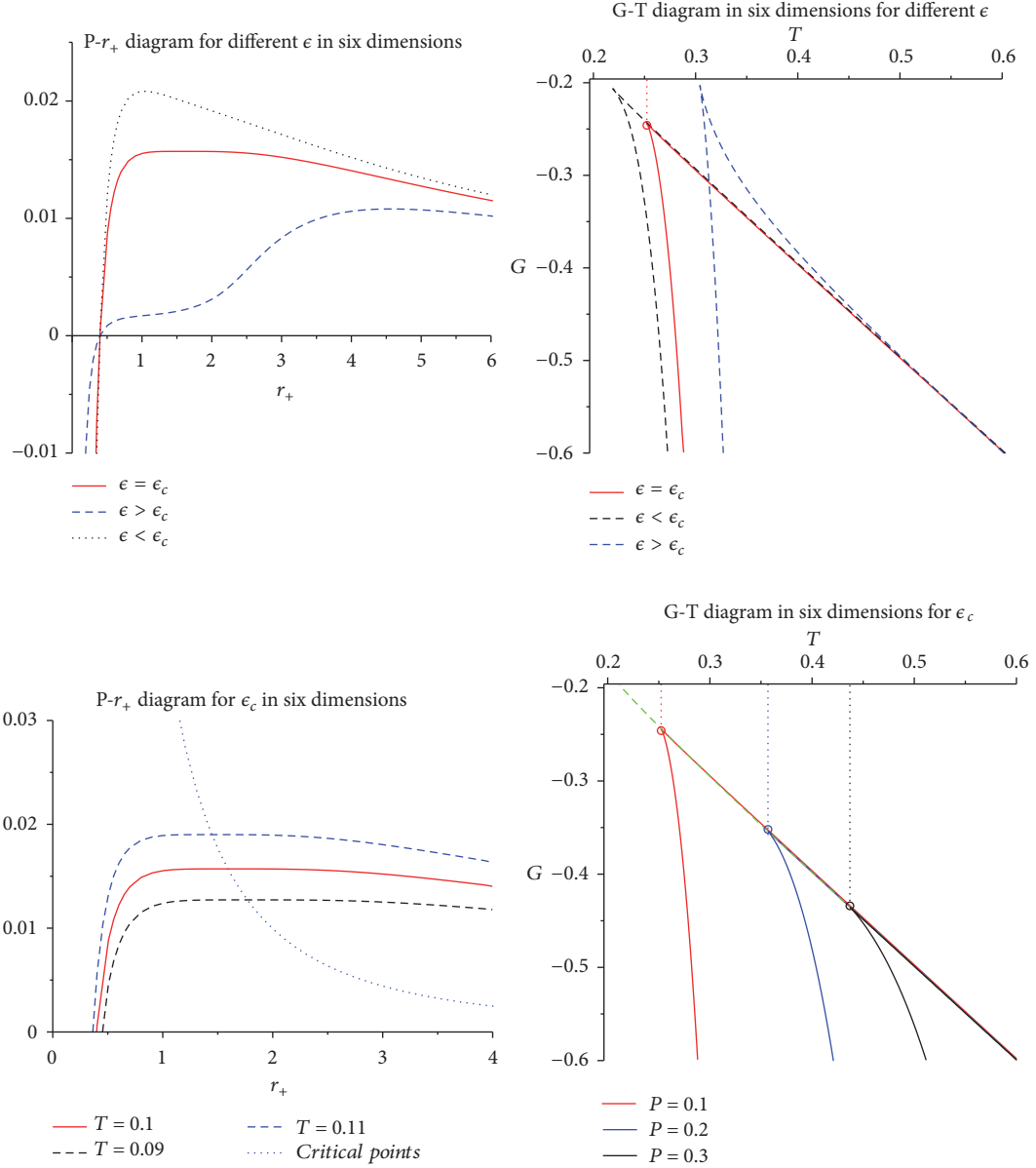


FIGURE 4: Curves of $P - r_+$ and $G - T$ in six dimensions for different ϵ and $\epsilon = \epsilon_c$. There is no $P - r_+$ oscillatory behavior and phase transition.

while the dashed line highlighting a lower bound of temperature destroys the λ line. It is easy to calculate the minimal temperature of six-dimensional HL AdS spherical black holes with $\epsilon = \epsilon_c$, for which the temperature is reduced to

$$T(r_+) = \frac{64P^2\pi^2r_+^4 + 48P\pi r_+^2 + 1}{8\pi r_+(1 + 8P\pi r_+^2)}. \quad (32)$$

Considering the first-order derivative

$$T' = \frac{(8P\pi r_+^2 - 1)^3}{8\pi r_+^2(1 + 8P\pi r_+^2)^2}, \quad (33)$$

it leads to the minima at $r_+ = 1/\sqrt{8\pi P}$; i.e.,

$$T_{min} = \sqrt{\frac{2P}{\pi}}, \quad (34)$$

which is exactly the phase transition point (see (31)). This temperature bound could be treated as a physical temperature constraint, which cancels the “superfluid” black hole phase. This physical temperature constraint is equivalent to an upper bound of pressure, i.e., $P \leq \pi T^2/2$, for arbitrary temperature. Then in the $S - P$ diagram in the middle one of Figure 5, one can also observe that there are no (“superfluid”) black holes for $P > \pi T^2/2$, which correspond to the exact λ line in $P - T$ parameter space as shown in the right plot in Figure 5. Therefore, even six-dimensional HL AdS black holes exhibit infinitely many critical points in $P - \nu$ plane and the

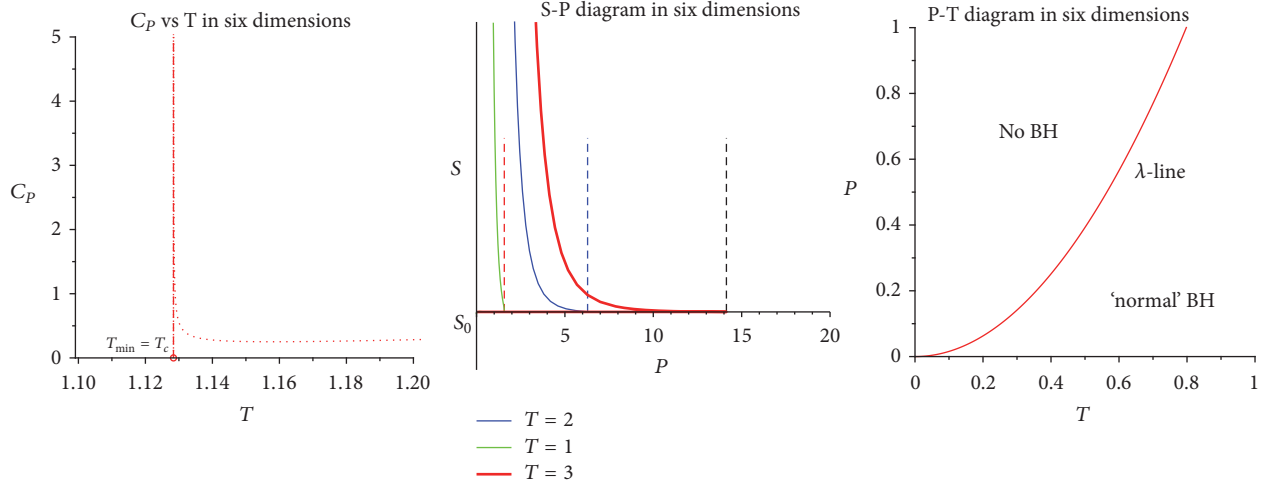


FIGURE 5: Curves of $C_p - T$ and $S - P$ and $P - T$ parameter space of black holes with $\epsilon = \epsilon_c$ in six dimensions. The dashed lines highlight the minimal temperature, which could be treated as a physical temperature constraint and cancel the “superfluid” black hole phase. Therefore there is no λ phase transition in six dimensions even when the specific heat diverges.

divergent points for specific heat; there does not exist λ phase transition, as they only contain the “normal” black hole phase and the “superfluid” black hole phase disappears in the $P - T$ parameter space due to the physical temperature constraint (see (34)).

6. Critical Phenomena in $\epsilon - r_+$ Plane

Because of the existence of infinite critical points, it is not able to calculate the critical exponents. Actually, to study the critical exponents for λ phase transitions of liquid ^4He , thermodynamic pressure is no longer the appropriate ordering field [32]. For the “superfluid” black hole, pressure should be instead of other parameters [20]. As for HL AdS black holes, there is only one option for the appropriate ordering field, i.e., parameter ϵ . Though ϵ is a dimensionless quantity, it does characterize the critical phenomena for four- and five-dimensional HL AdS black holes as shown later.

Firstly, we study the critical points in $\epsilon - r_+$ plane, for which the thermodynamic variables of EOS should be ϵ , r_+ (i.e., r), T . Thus, we should firstly rewrite the EOS by rearranging the expression for temperature Eq. (10) for the chosen ordering field ϵ , which behaves as

$$\epsilon(T, r_+) = \pm \sqrt{\frac{(d(d-1)k + 32\pi Pr_+^2)}{d(d-1)^2 k} \left((d-1) - \frac{32\pi Pr_+^2}{8\pi r_+ T - (d-4)k} \right)}. \quad (35)$$

We follow the conditions

$$\begin{aligned} \frac{\partial \epsilon}{\partial r_+} &= 0, \\ \frac{\partial^2 \epsilon}{\partial r_+^2} &= 0, \end{aligned} \quad (36)$$

to find the critical points. However, the direct differentiation of ϵ is too complicated; we also prefer to employ the implicit

differentiation on EOS (see (14)) and the above equations. After a careful calculation, we obtain the same two conditions (19) and (20). Thus, one can easily get the critical point:

$$\epsilon_c = \pm 2 \sqrt{\frac{(2(d-5)X\pi + 2d-7)}{3d(d-4)}}, \quad (37)$$

$$r_c = \frac{1}{4} \sqrt{\frac{k(d-1)(12\pi X + 2-d)}{6\pi P}}, \quad (38)$$

$$T_c = 4kX \sqrt{\frac{6\pi P}{k(d-1)(12\pi X + 2-d)}}, \quad (39)$$

where X has the value as (24) and P is a positive constant indicating AdS space-time.

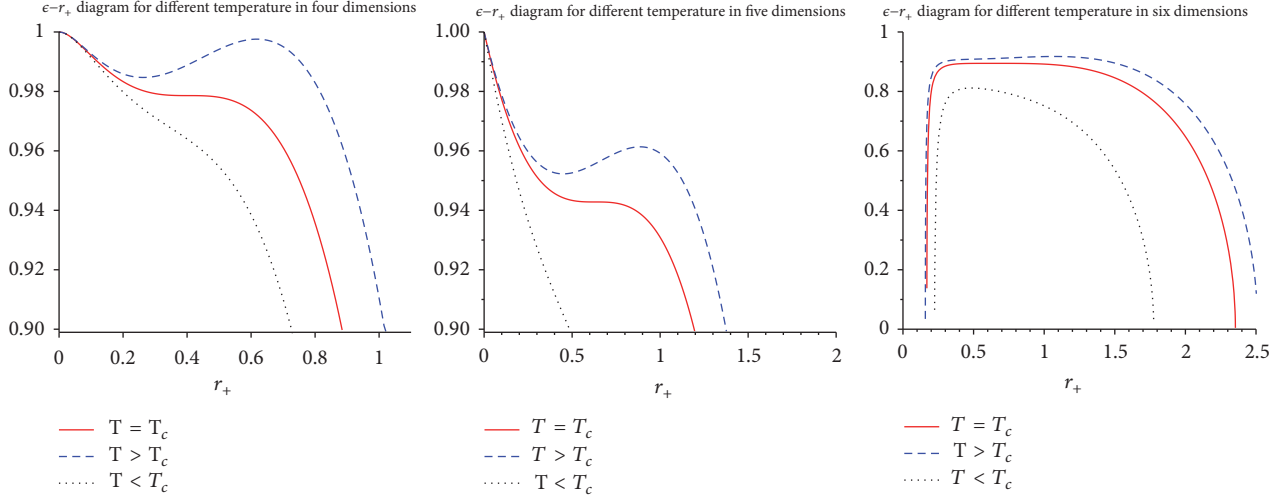
Following the discussions in Section 3, it is shown that only four-, five-, and six-dimensional HL AdS black holes with spherical horizon have physical critical point, as shown in Table 2. Besides, in four and five dimensions, there exist the $\epsilon - r_+$ oscillatory behavior when $T > T_c$ as shown in Figure 6 and the classical “swallow tail” characterizing the small/large black holes phase transition when $\epsilon > \epsilon_c$ as shown in $G - T$ diagrams of Figure 1. In six dimensions, it is easy to check that the critical point leads to $\partial^3 \epsilon / \partial r_+^3 = 0$. As a result, one can never find the $\epsilon - r_+$ oscillatory behavior as shown in Figure 6, and no first-order phase transition exists as shown in $G - T$ diagrams of Figure 4.

Finally, we consider the critical exponents in four and five dimensions. After introducing the dimensionless quantities

$$\begin{aligned} \Xi &= \frac{\epsilon}{\epsilon_c}, \\ \omega &= \frac{r_+}{r_c} - 1, \\ t &= \frac{T}{T_c} - 1, \end{aligned} \quad (40)$$

TABLE 2: The critical point of HL AdS spherical black holes in $\epsilon - r_+$ plane.

Dimensions	ϵ_c	r_c	T_c
Four	$\pm \frac{2}{9} \sqrt{9 + 6\sqrt{3}}$	$\sqrt{\frac{(2\sqrt{3} - 1)}{48\pi P}}$	$\sqrt{\frac{4P}{(2\sqrt{3} - 1)\pi}}$
Five	$\pm \frac{2}{3} \sqrt{2}$	$\sqrt{\frac{1}{8\pi P}}$	$\sqrt{\frac{2P}{\pi}}$
Six	$\pm \frac{2}{5} \sqrt{5}$	$\sqrt{\frac{1}{8\pi P}}$	$\sqrt{\frac{2P}{\pi}}$

FIGURE 6: Curves of $\epsilon - r_+$ with $P = 1/10$ in four, five, and six dimensions for different temperature. In four and five dimensions, one can observe the $\epsilon - r_+$ oscillatory behavior when $T > T_c$, while no oscillatory behavior for six dimensions is observed.

the ordering field can be expanded near the critical point as

$$\Xi = \begin{cases} 1 + 0.115t + 0.234t\omega - 0.042\omega^3 + \mathcal{O}(t\omega^2, \omega^4), & d = 3, \\ 1 + \frac{1}{4}t + \frac{3}{8}t\omega - \frac{1}{16}\omega^3 + \mathcal{O}(t\omega^2, \omega^4), & d = 4, \end{cases} \quad (41)$$

where the coefficients for four-dimensional case all have complicated forms, and their approximate values are given. The above expansions both have the same form as that for the van der Waals fluid and the RN-AdS black hole [15]. As the system can be characterized by the critical exponents

$$\begin{aligned} C_\omega &\propto |t|^{-\alpha}, \\ \omega &\propto |t|^\beta, \\ \kappa_t &= -\omega^{-1} \left(\frac{\partial \omega}{\partial \Xi} \right)_t \propto |t|^{-\gamma}, \\ \Xi &\propto |\omega|^\delta, \end{aligned} \quad (42)$$

one can obtain that

$$\begin{aligned} \alpha &= 0, \\ \beta &= \frac{1}{2}, \\ \gamma &= 1, \\ \delta &= 3. \end{aligned} \quad (43)$$

Particularly, $\omega \propto \sqrt{t}$ indicates that phase transition appears when $T > T_c$. Moreover, it is easy to check that they obey the scaling symmetry like the ordinary thermodynamic systems and in particular coincide with those for a superfluid [32].

7. Critical Phenomena in $P - r_+$ Plane with “Temperature” ϵ

It is interesting to find that the parameter ϵ controls the $P - r_+$ oscillatory behavior instead of the temperature T , other than the pressure P , as shown in $P - r_+$ diagrams of Figure 1. This indicates that there is still a critical phenomenon in $P - r_+$ plane. For this case, pressure could still be treated as the ordering field, while ϵ should be considered as “temperature”. This is different from that for the first “superfluid” black holes [20].

TABLE 3: The critical point of HL AdS spherical black holes in $P - r_+$ plane with “temperature” ϵ .

Dimensions	P_c	r_c	ϵ_c
Four	$\frac{(2\sqrt{3}-1)\pi T^2}{4}$	$\frac{\sqrt{3}}{6\pi T}$	$\pm \frac{2}{9}\sqrt{9+6\sqrt{3}}$
Five	$\frac{\pi T^2}{2}$	$\frac{1}{2\pi T}$	$\pm \frac{2}{3}\sqrt{2}$
Six	$\frac{\pi T^2}{2}$	$\frac{1}{2\pi T}$	$\pm \frac{2}{5}\sqrt{5}$

To study the corresponding critical phenomena, we can still follow the procedure studying $P - r_+$ criticality in Section 3, which leads to the same three critical equations: (14), (19), and (20). As the thermodynamic variables of EOS for this case should be P , r_+ (i.e., ν), ϵ , we can find the following critical point:

$$P_c = \frac{(d-1)(12\pi X + 2-d)}{96\pi k X^2} T^2, \quad (44)$$

$$r_c = \frac{kX}{T}, \quad (45)$$

with the critical “temperature”

$$\epsilon_c = \pm 2\sqrt{\frac{(2(d-5)X\pi + 2d-7)}{3d(d-4)}}, \quad (46)$$

where X takes the value as (24) and T is a positive constant.

As similar as the discussions in Section 3, one can find that only four-, five-, and six-dimensional HL AdS black holes with spherical horizon have physical critical point, as shown in Table 3. In four and five dimensions, when “temperature” $\epsilon > \epsilon_c$, there exist the $P - r_+$ oscillatory behavior (Figure 1)

and the classical “swallow tail” characterizing the small/large black holes phase transition as shown in $G - P$ diagrams of Figure 7. As for the case of six dimensions, it is easy to find that the critical point leads to $\partial^3 P / \partial r_+^3 = 0$. Therefore, one can not observe the $P - r_+$ oscillatory behavior as shown in Figure 4, and no first-order phase transition exists as shown in Figure 7.

Then, we can also calculate the critical exponents in four and five dimensions near the critical point. Similarly, we begin with the following dimensionless quantities:

$$p = \frac{P}{P_c},$$

$$\omega = \frac{r_+}{r_c} - 1, \quad (47)$$

$$\tau = \frac{\epsilon}{\epsilon_c} - 1.$$

The EOS can be reduced to the dimensionless case, for which its Taylor series expansion at the critical point takes the following forms:

$$p = \begin{cases} 1 - \frac{(56\sqrt{3}+94)}{11}\tau + (10\sqrt{3}+18)\tau\omega - (\sqrt{3}-1)\omega^3 + \mathcal{O}(\tau\omega^2, \omega^4), & d=3, \\ 1 - 8\tau + 12\tau\omega - \frac{1}{2}\omega^3 + \mathcal{O}(\tau\omega^2, \omega^4), & d=4. \end{cases} \quad (48)$$

They still both have the same form as that for the van der Waals fluid and the RN-AdS black hole [15]. After introducing the critical exponents

$$\begin{aligned} C_\omega &\propto |\tau|^{-\alpha}, \\ \omega &\propto |\tau|^\beta, \\ \kappa_\tau &= -\omega^{-1} \left(\frac{\partial \omega}{\partial p} \right) \Big|_\tau \propto |\tau|^{-\gamma}, \\ p &\propto |\omega|^\delta, \end{aligned} \quad (49)$$

it is easy to find

$$\begin{aligned} \alpha &= 0, \\ \beta &= \frac{1}{2}, \\ \gamma &= 1, \\ \delta &= 3, \end{aligned} \quad (50)$$

which satisfy the scaling laws of the ordinary thermodynamic systems. Besides, $\omega \propto \sqrt{\tau}$ indicates that phase transition appears when $\epsilon > \epsilon_c$.

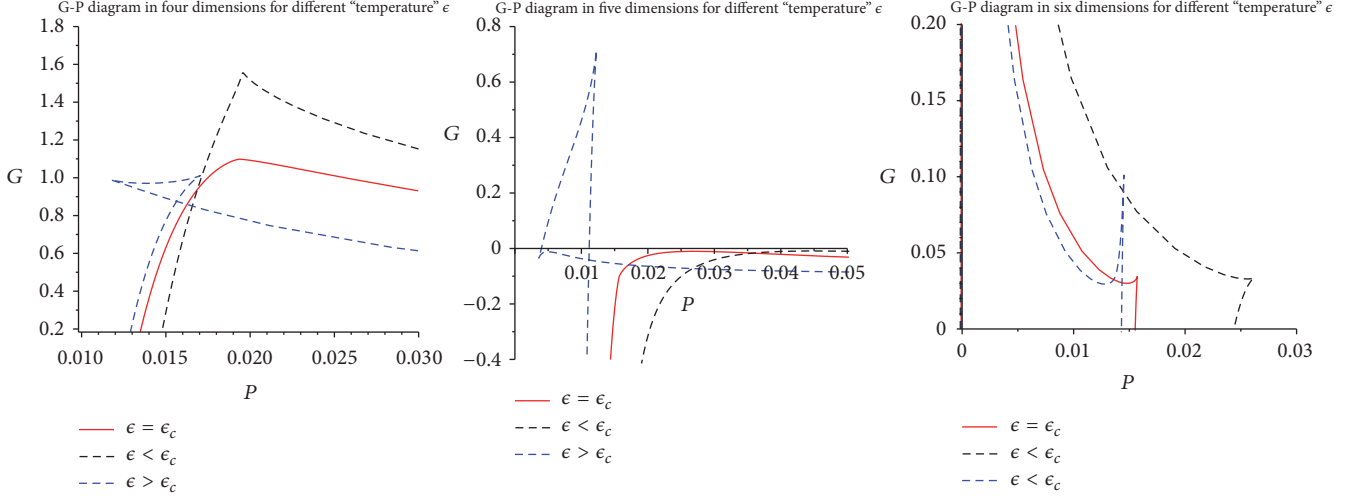


FIGURE 7: Curves of $G - P$ with $T = 1/10$ in four, five, and six dimensions for different “temperature” ϵ . In four and five dimensions, one can observe the classical “swallow tail” characterizing the small/large black holes phase transition when “temperature” $\epsilon > \epsilon_c$, while no “swallow tail” exists for six dimensions.

8. Discussion

In this paper, we study the extended thermodynamics of general dimensional HL AdS black holes and present another example of “superfluid” black holes. It is found that only four- and five-dimensional HL AdS black holes with spherical horizon have the λ phase transition, which correspond to the phase transition between “superfluid” black hole and “normal” black hole. After considering the behavior of entropy, the “superfluid” black hole phase and “normal” black hole phase are distinguished. Particularly, six-dimensional HL AdS black holes exhibit infinitely many critical points in $P - \nu$ plane and the divergent points for specific heat, for which they only contain the “normal” black hole phase and the “superfluid” black hole phase disappears due to the physical temperature constraint; therefore there is no similar phase transition. In more than six dimensions, there is no $P - V$ critical behavior. After identifying parameter ϵ as the ordering field instead of pressure and temperature, we study

the critical phenomena in different planes of thermodynamical phase space. We also obtain the critical exponents in both planes, which are the same as the van der Waals fluid.

The “superfluid” black hole is firstly reported in Lovelock gravity with conformally coupled scalar field [20], which contains at least four free parameters in the action of theory. Comparing with it, the one in Horava gravity has only one free parameter ϵ . It is interesting to consider the necessary and sufficient conditions for general “superfluid” black hole; i.e., a black hole EOS must satisfy to display similar λ phase transition, which is still unclear. Besides, could the “superfluid” black holes appear in Einstein gravity? These are all interesting and left to be the future tasks.

Appendix

Gibbs Free Energy and Capacity

The Gibbs free energy is

$$\begin{aligned}
 G &= \left[\frac{3k^2(1-\epsilon^2)}{16P\pi r_+} + 2kr_+ + \frac{16}{3}P\pi r_+^3 - \frac{(1024P^2\pi^2 r_+^4 + 128kP\pi r_+^2 - 12k^2(1-\epsilon^2))}{16\pi r_+(32P\pi r_+^2 + 6k(1-\epsilon^2))} \right. \\
 &\quad \times \left(4\pi r_+^2 \left(1 + \frac{3k(1-\epsilon^2)\ln(r_+)}{8\pi r_+^2} \right) + S_0 \right), \quad d=3; \quad (\text{A.1}) \\
 &= \left[\frac{k^2 d r_+^{d-4}(1-\epsilon^2)}{16(d-2)P\pi} + \frac{4kr_+^{d-2}}{(d-1)(d-2)} + \frac{64P\pi r_+^6}{d(d-1)^2(d-2)} - \frac{1024P^2\pi^2 r_+^4 + 64k(d-1)(d-2)P\pi r_+^2 + k^2 d(d-1)^2(d-4)(1-\epsilon^2)}{8(d-1)\pi r_+(32P\pi r_+^2 + kd(d-1)(1-\epsilon^2))} \right. \\
 &\quad \times \left(\frac{16\pi r_+^{d-1}}{(d-1)^2(d-2)} \left(1 + \frac{kd(d-1)^2(d-2)(1-\epsilon^2)}{32(d-2)(d-3)P\pi r_+^4} \right) + S_0 \right), \quad d \geq 4.
 \end{aligned}$$

The specific heat is

$$\begin{aligned}
 C_P &= \frac{r_+^{d-3}}{2(d-1)(d-2)P} \left(32P\pi r_+^2 \right. \\
 &\quad \left. + kd(d-1)(1-\epsilon^2) \right)^2 \times (1024P^2\pi^2 r_+^4
 \end{aligned}$$

$$\begin{aligned}
 &+ 64k(d-1)(d-2)P\pi r_+^2 \\
 &+ k^2 d(d-1)^2(d-4)(1-\epsilon^2) \times (32768P^3\pi^3 r_+^6 \\
 &- 1024k(d-1)(3d\epsilon^2 - d - 4)P^2\pi^2 r_+^4
 \end{aligned}$$

$$\begin{aligned}
& -32k^2 d(d-1)^2(d-8)P\pi r_+^2(1-\epsilon^2) \\
& -k^3 d^2(d-1)^3(d-4)(1-\epsilon^2)^{-1}.
\end{aligned}
\tag{A.2}$$

Data Availability

No data were used to support this study.

Conflicts of Interest

The author declares that he has no conflicts of interest.

Acknowledgments

Wei Xu was supported by the National Natural Science Foundation of China (NSFC), under Grants no. 11505065, no. 11374330, and no. 91636111, and the Fundamental Research Funds for the Central Universities, China University of Geosciences (Wuhan).

References

- [1] M. K. Parikh and F. Wilczek, "Hawking radiation as tunneling," *Physical Review Letters*, vol. 85, no. 24, pp. 5042–5045, 2000.
- [2] A. Strominger and C. Vafa, "Microscopic origin of the Bekenstein-Hawking entropy," *Physics Letters B*, vol. 379, no. 1–4, pp. 99–104, 1996.
- [3] S. W. Hawking and D. N. Page, "Thermodynamics of black holes in anti-de Sitter space," *Communications in Mathematical Physics*, vol. 87, no. 4, pp. 577–588, 1982/83.
- [4] E. Witten, "Anti-de Sitter space, thermal phase transition, and confinement in gauge theories," *Advances in Theoretical and Mathematical Physics*, vol. 2, no. 3, pp. 505–532, 1998.
- [5] J. Maldacena, "The large N limit of superconformal field theories and supergravity," *Advances in Theoretical and Mathematical Physics*, vol. 2, no. 2, pp. 231–252, 1998.
- [6] S. S. Gubser, I. R. Klebanov, and A. M. Polyakov, "Gauge theory correlators from non-critical string theory," *Physics Letters B*, vol. 428, no. 1–2, pp. 105–114, 1998.
- [7] E. Witten, "Anti de Sitter space and holography," *Advances in Theoretical and Mathematical Physics*, vol. 2, no. 2, pp. 253–291, 1998.
- [8] D. Kastor, S. Ray, and J. Traschen, "Enthalpy and the mechanics of AdS black holes," *Classical and Quantum Gravity*, vol. 26, no. 19, Article ID 195011, 2009.
- [9] B. P. Dolan, "Pressure and volume in the first law of black hole thermodynamics," *Classical and Quantum Gravity*, vol. 28, no. 23, Article ID 235017, 2011.
- [10] M. Cvetič, G. Gibbons, D. Kubiznak, and C. Pope, "Black hole enthalpy and an entropy inequality for the thermodynamic volume," *Physical Review D: Particles, Fields, Gravitation and Cosmology*, vol. 84, Article ID 024037, 2011.
- [11] B. P. Dolan, D. Kastor, D. Kubizňák, R. B. Mann, and J. Traschen, "Thermodynamic volumes and isoperimetric inequalities for de Sitter black holes," *Physical Review D: Particles, Fields, Gravitation and Cosmology*, vol. 87, no. 10, Article ID 104017, 2013.
- [12] D. Kastor, S. Ray, and J. Traschen, "Smarr formula and an extended first law for Lovelock gravity," *Classical and Quantum Gravity*, vol. 27, no. 23, Article ID 235014, 2010.
- [13] A. Castro, N. Dehmami, G. Giribet, and D. Kastor, "On the universality of inner black hole mechanics and higher curvature gravity," *Journal of High Energy Physics*, vol. 2013, no. 07, 2013.
- [14] B. M. El-Menoufi, B. Ett, D. Kastor, and J. Traschen, "Gravitational tension and thermodynamics of planar AdS spacetimes," *Classical and Quantum Gravity*, vol. 30, no. 15, Article ID 155003, p. 18, 2013.
- [15] D. Kubiznak and R. B. Mann, "P-V criticality of charged AdS black holes," *Journal of High Energy Physics*, vol. 2012, no. 7, article 033, 2012.
- [16] N. Altamirano, D. Kubiznak, R. B. Mann, and Z. Sherkatghanad, "Thermodynamics of rotating black holes and black rings: phase transitions and thermodynamic volume," *Galaxies*, vol. 2, 2014.
- [17] D. Kubiznak, R. B. Mann, and M. Teo, "Black hole chemistry: thermodynamics with lambda," *Classical and Quantum Gravity*, vol. 34, no. 6, 2017.
- [18] S. Wei and Y. Liu, "Insight into the microscopic structure of an AdS black hole from a thermodynamical phase transition," *Physical Review Letters*, vol. 115, no. 11, 2015, Erratum: vol. 116, no. 16, 2016.
- [19] M. K. Zangeneh, A. Dehyadegari, A. Sheykhi, and R. Mann, "Microscopic origin of black hole reentrant phase transitions," *Physical Review D: Particles, Fields, Gravitation and Cosmology*, vol. 97, no. 8, 2018.
- [20] R. A. Hennigar, R. B. Mann, and E. Tjoa, "Superfluid black holes," *Physical Review Letters*, vol. 118, no. 2, Article ID 021301, 2017.
- [21] P. Hořava, "Quantum gravity at a Lifshitz point," *Physical Review D: Particles, Fields, Gravitation and Cosmology*, vol. 79, no. 8, Article ID 084008, 2009.
- [22] H. Lü, J. Mei, and C. N. Pope, "Solutions to Hořava gravity," *Physical Review Letters*, vol. 103, no. 9, Article ID 091301, 2009.
- [23] R. G. Cai, L. M. Caoand, and N. Ohta, "Topological black holes in Horava-Lifshitz gravity," *Physical Review D: Particles, Fields, Gravitation and Cosmology*, vol. 80, no. 2, Article ID 024003, 2009.
- [24] R.-G. Cai, L.-M. Cao, and N. Ohta, "Thermodynamics of black holes in Hořava-Lifshitz gravity," *Physics Letters B*, vol. 679, no. 5, pp. 504–509, 2009.
- [25] Y. S. Myung, "Thermodynamics of black holes in the deformed Horava-Lifshitz gravity," *Physics Letters B: Particle Physics, Nuclear Physics and Cosmology*, vol. 678, no. 1, pp. 127–130, 2009.
- [26] Q. Cao, Y. Chen, and K. Shao, "Black hole phase transitions in Hořava-Lifshitz gravity," *Physical Review D: Particles, Fields, Gravitation and Cosmology*, vol. 83, no. 6, 2011.
- [27] B. R. Majhi and D. Roychowdhury, "Phase transition and scaling behavior of topological charged black holes in Horava-Lifshitz gravity," *Classical and Quantum Gravity*, vol. 29, no. 24, Article ID 245012, 2012.
- [28] J.-X. Mo, X.-X. Zeng, G.-Q. Li, X. Jiang, and W.-B. Liu, "A unified phase transition picture of the charged topological black hole in Hořava-Lifshitz gravity," *Journal of High Energy Physics*, vol. 2013, no. 56, 2013.
- [29] M.-S. Ma and R.-H. Wang, "Peculiar P-V criticality of topological Hořava-Lifshitz black holes," *Physical Review D: Particles, Fields, Gravitation and Cosmology*, vol. 96, no. 2, Article ID 024052, 2017.

- [30] A. Wang, “Horava gravity at a Lifshitz point: a progress report,” *International Journal of Modern Physics D: Gravitation, Astrophysics, Cosmology*, vol. 26, no. 7, Article ID 1730014, 2017.
- [31] T. Li, Y. Qi, Y. Wu, and Y. Zhang, “Topological charged black holes in generalized Hořava-Lifshitz gravity,” *Physical Review D: Particles, Fields, Gravitation and Cosmology*, vol. 90, no. 12, 2014.
- [32] P. B. Weichman, A. W. Harter, and D. L. Goodstein, “Criticality and superfluidity in liquid,” *Reviews of Modern Physics*, vol. 73, no. 1, pp. 1–15, 2001.

Research Article

Tunneling Glashow-Weinberg-Salam Model Particles from Black Hole Solutions in Rastall Theory

Ali Övgün ^{1,2} Wajiha Javed,³ and Riasat Ali³

¹*Instituto de Física, Pontificia Universidad Católica de Valparaíso, Casilla 4950, Valparaíso, Chile*

²*Physics Department, Arts and Sciences Faculty, Eastern Mediterranean University, Famagusta, Northern Cyprus, Mersin 10, Turkey*

³*Division of Science and Technology, University of Education, Township Campus, Lahore, Pakistan*

Correspondence should be addressed to Ali Övgün; ali.ovgun@pucv.cl

Received 17 April 2018; Revised 25 June 2018; Accepted 10 July 2018; Published 18 July 2018

Academic Editor: Saibal Ray

Copyright © 2018 Ali Övgün et al. This is an open access article distributed under the Creative Commons Attribution License, which permits unrestricted use, distribution, and reproduction in any medium, provided the original work is properly cited. The publication of this article was funded by SCOAP³.

Using the semiclassical WKB approximation and Hamilton-Jacobi method, we solve an equation of motion for the Glashow-Weinberg-Salam model, which is important for understanding the unified gauge-theory of weak and electromagnetic interactions. We calculate the tunneling rate of the massive charged W-bosons in a background of electromagnetic field to investigate the Hawking temperature of black holes surrounded by perfect fluid in Rastall theory. Then, we study the quantum gravity effects on the generalized Proca equation with generalized uncertainty principle (GUP) on this background. We show that quantum gravity effects leave the remnants on the Hawking temperature and the Hawking radiation becomes nonthermal.

1. Introduction

General relativity is analogously linked to the thermodynamics and quantum effects which strongly support it [1–3]. Black holes are the strangest objects in the Universe and they arise in general relativity, a classical theory of gravity, but it is needed to include quantum effects to understand the nature of the black holes properly. After Bekenstein found a relation between the surface area and entropy of a black hole [4], Hawking theoretically showed that black holes with the surface gravity κ radiate at temperature $\kappa/2\pi$ [5–7]. On the other hand, Bekenstein-Hawking radiation causes the information loss paradox because of the thermal evaporation. To solve the information paradox, recently soft-hair idea has been proposed by Hawking et al. [8].

Since Bekenstein and Hawking great contribution to the black hole's thermodynamics, the radiation from the black hole gets attention from researchers. There are many different methods to obtain the Bekenstein-Hawking radiation using the quantum field theory or the semiclassical methods. The quantum tunneling method is one of them [9–16]. Nozari and Mehdipour [17] have studied the Hawking

radiation as tunneling phenomenon for Schwarzschild BH in noncommutative space-time. Nozari and Saghafi [18] have investigated the tunneling of massless particles for Schwarzschild BH by considering quantum gravity effects. The semiclassical tunneling method by using the Hamilton-Jacobi ansatz with WKB approximation is another way to obtain the Bekenstein-Hawking temperature and the tunneling rate as $\Gamma \approx \exp[-2ImS]$ [19]. Different kinds of particles such as bosons, fermions, and vector particles are used to study the tunneling of the particles from the black holes and wormholes and obtain their Hawking temperature [20–46]. Nozari and Sefidgar [47] have discussed quantum corrections approach to study BH thermodynamics. Nozari and Etemadi [48] have investigated the KMM seminal work in case of a maximal test particles momentum. They showed that, in the presence of both minimal length and maximal momentum, there is no divergence in energy spectrum of a test particle. Moreover, the uncertainty principle is modified as a generalized uncertainty principle (GUP) [49, 50] to work on the effect of the quantum gravity which is applied to different areas. The important contribution of the GUP is to remove the divergences in physics. On the

other hand, GUP can be used to modify Proca equation and Klein-Gordon equation to obtain the effects of the GUP on the Hawking temperature and check if it leaves remnants [51–54]. Nozari and Mehdipour [55] have discussed BH remnants and their cosmological constraints. Moreover, GUP is used to modify the thermodynamics of N-dimensional Schwarzschild-Tangherlini black hole, speed of graviton, and the Entropic Force. Feng et al. [56] have studied the difference between the propagation speed of gravitons and the speed of light by using GUP. They have also investigated the modified speed of graviton by considering GUP. Rama [57] has studied the consequences of GUP which leads to varying speed of light and modified dispersion relations, which are likely to have implications for cosmology and black hole physics.

Since Maxwell, it was the dream of theoretical physicist to unify the fundamental forces in the nature in a single equation. Glashow, Weinberg, and Salam unified the theory of weak and electromagnetic interactions as an electroweak interaction in the 1960s. They assumed that the symmetry between the two different interactions would be clear at very large momentum transfers. However, at low energy, there is a mass difference between the photon and the W_+ , W_- , and Z_0 bosons which break the symmetry.

This paper is organized as follows: In Section 2, we investigate the Hawking temperature of the black hole solutions surrounded by perfect fluid in Rastall theory using the tunneling of the massive vector particles. For this purpose we solve the equation of the motion of the Glashow-Weinberg-Salam model using the semiclassical WKB approximation with Hamilton-Jacobi method. In Section 3, we use the GUP-corrected Proca equation to investigate the tunneling of massive uncharged vector particles for finding the corrected Hawking temperature of the black hole solutions surrounded by perfect fluid in Rastall theory. In Section 4, we conclude the paper with our results.

2. Tunneling of Charged Massive Vector Bosons

In this section, we study the tunneling of the charged massive bosons from the different types of black holes surrounded by the perfect fluids in Rastall theory.

2.1. The Black Hole Surrounded by the Dust Field in Rastall Theory. First we study the line element of the black hole surrounded by the dust field [58]:

$$ds^2 = - \left(1 - \frac{2M}{r} + \frac{Q^2}{r^2} - \frac{N_d}{r^{(1-6\kappa\lambda)/(1-3\kappa\lambda)}} \right) dt^2 + \frac{dr^2}{1 - 2M/r + Q^2/r^2 - N_d/r^{(1-6\kappa\lambda)/(1-3\kappa\lambda)}} + r^2 (d\theta^2 + \sin^2\theta d\phi^2), \quad (1)$$

where M is a mass of black hole, κ and λ are the Rastall geometric parameters, N_d is the dust field structure parameter,

and Q is a charge of black hole. Now, we can rewrite (1) in the following form:

$$ds^2 = -G(r) dt^2 + B(r) dr^2 + C(r) d\theta^2 + D(r) d\phi^2, \quad (2)$$

where $G(r)$, $B(r)$, $C(r)$, and $D(r)$ are given below:

$$\begin{aligned} G(r) &= 1 - \frac{2M}{r} + \frac{Q^2}{r^2} - \frac{N_d}{r^{(1-6\kappa\lambda)/(1-3\kappa\lambda)}}, \\ C(r) &= r^2, \\ B(r) &= \frac{1}{1 - 2M/r + Q^2/r^2 - N_d/r^{(1-6\kappa\lambda)/(1-3\kappa\lambda)}}, \\ D(r) &= r^2 \sin^2\theta. \end{aligned} \quad (3)$$

The equation of motion for the Glashow-Weinberg-Salam model [59–61] is

$$\begin{aligned} \frac{1}{\sqrt{-g}} \partial_\mu (\sqrt{-g} \Phi^{\nu\mu}) + \frac{m^2}{h^2} \Phi^\nu + \frac{i}{h} e A_\mu \Phi^{\nu\mu} + \frac{i}{h} e F^{\nu\mu} \Phi_\mu \\ = 0, \end{aligned} \quad (4)$$

where $|g|$ is a coefficients matrix, m is particles mass, and $\Phi^{\mu\nu}$ is antisymmetric tensor, since

$$\begin{aligned} \Phi_{\nu\mu} &= \partial_\nu \Phi_\mu - \partial_\mu \Phi_\nu + \frac{i}{h} e A_\nu \Phi_\mu - \frac{i}{h} e A_\mu \Phi_\nu, \\ F^{\mu\nu} &= \Delta^\mu A^\nu - \Delta^\nu A^\mu, \end{aligned} \quad (5)$$

where A_μ is the vector potential of the charged black hole and A_0 and A_3 are the components of A_μ , e is the charge of the particle, and Δ_μ is covariant derivative. The values of Φ^μ and $\Phi^{\nu\mu}$ are given by

$$\begin{aligned} \Phi^0 &= \frac{\Phi_0}{G}, \\ \Phi^1 &= \frac{\Phi_1}{B}, \\ \Phi^2 &= \frac{\Phi_2}{C}, \\ \Phi^3 &= \frac{\Phi_3}{D}, \\ \Phi^{01} &= \frac{\Phi_{01}}{GB}, \\ \Phi^{02} &= \frac{\Phi_{02}}{GC}, \\ \Phi^{03} &= \frac{\Phi_{03}}{GD}, \\ \Phi^{12} &= \frac{\Phi_{12}}{BC}, \\ \Phi^{13} &= \frac{\Phi_{13}}{BD}, \\ \Phi^{23} &= \frac{\Phi_{23}}{CD}. \end{aligned} \quad (6)$$

Using WKB approximation for the wave function ansatz [62], i.e.,

$$\Phi_\nu = c_\nu \exp \left[\frac{i}{\hbar} I_0(t, r, \theta, \phi) + \sum_{\zeta=1}^{\zeta=n} \hbar^\zeta I_\zeta(t, r, \theta, \phi) \right], \quad (7)$$

to the Lagrangian (4) (where I_0 and I_i correspond to particles action, for $i = 1, 2, 3, \dots$) and neglecting the higher order terms, we get the following set of equations given below:

$$\begin{aligned} & \frac{1}{B} [c_1 (\partial_0 I_0) (\partial_1 I_0) + eA_0 c_1 (\partial_1 I_0) - c_0 (\partial_1 I_0)^2] \\ & + \frac{1}{C} [c_2 (\partial_0 I_0) (\partial_2 I_0) - c_0 (\partial_2 I_0)^2 + eA_0 c_2 (\partial_2 I_0)] \\ & + \frac{1}{D} [c_3 (\partial_0 I_0) (\partial_3 I_0) + eA_0 c_3 (\partial_3 I_0) - c_0 (\partial_3 I_0)^2] \\ & + \frac{eA_3}{D} [c_3 (\partial_0 I_0) + eA_0 c_3 - c_0 (\partial_3 I_0)] - m^2 c_0 = 0, \end{aligned} \quad (8)$$

$$\begin{aligned} & \frac{1}{G(r)} [c_0 (\partial_0 I_0) (\partial_1 I_0) - eA_0 c_1 (\partial_0 I_0) - c_1 (\partial_0 I_0)^2] \\ & - \frac{1}{C} [c_2 (\partial_1 I_0) (\partial_2 I_0) - c_1 (\partial_2 I_0)^2] \\ & + \frac{1}{D} [c_3 (\partial_1 I_0) (\partial_3 I_0) - c_1 (\partial_3 I_0) - eA_3 c_1 (\partial_3 I_0)] \\ & + \frac{eA_3}{D} [c_3 ((\partial_1 I_0) - eA_3) c_1 - c_1 (\partial_3 I_0)] - m^2 c_1 \\ & = 0, \end{aligned} \quad (9)$$

$$\begin{aligned} & \frac{1}{G(r)} [c_0 (\partial_0 I_0) (\partial_2 I_0) - c_2 (\partial_0 I_0)^2 - eA_0 (\partial_0 I_0) c_2] \\ & - \frac{1}{B} [c_2 (\partial_1 I_0)^2 - c_1 (\partial_1 I_0) (\partial_2 I_0)] \\ & - \frac{1}{D} [c_3 (\partial_2 I_0) (\partial_3 I_0) - c_2 (\partial_3 I_0)^2 - eA_3 c_2 (\partial_3 I_0)] \\ & + \frac{eA_0}{G(r)} [c_0 (\partial_2 I_0) - c_2 (\partial_0 I_0) - c_2 eA_0] \end{aligned} \quad (10)$$

$$\begin{aligned} & + \frac{eA_3}{D} [c_3 (\partial_2 I_0) - c_2 (\partial_3 I_0) - eA_3 c_2] - m^2 c_2 = 0, \\ & \frac{1}{G(r)} [c_0 (\partial_0 I_0) (\partial_3 I_0) - c_3 (\partial_0 I_0)^2 + eA_3 c_0 (\partial_0 I_0) \\ & - eA_0 c_3 (\partial_0 I_0)] + \frac{1}{B} [c_1 (\partial_1 I_0) (\partial_3 I_0) - c_3 (\partial_1 I_0)^2 \\ & + eA_3 c_1 (\partial_1 I_0)] + \frac{1}{C} [c_2 (\partial_2 I_0) (\partial_3 I_0) - c_3 (\partial_2 I_0)^2 \\ & + eA_3 c_2 (\partial_2 I_0)] + \frac{eA_0}{G(r)} [c_0 (\partial_3 I_0) - c_3 (\partial_0 I_0) \\ & + eA_3 c_0 - eA_0 c_3] - m^2 c_3 = 0. \end{aligned} \quad (11)$$

We can choose I_0 by using separation of variables technique, i.e.,

$$I_0 = - (E - \tilde{\omega} \tilde{\Omega}) t + W(r) + \tilde{\omega} \phi + \nu(\theta), \quad (12)$$

where $\tilde{\Omega}$ is the angular momentum of the BH and E and $\tilde{\omega}$ represent particle energy and angular momentum, respectively. From (8)–(11), we can obtain the following matrix equation:

$$\tilde{K}(c_0, c_1, c_2, c_3)^T = 0, \quad (13)$$

which provides “ \tilde{K} ” as a matrix of order 4×4 and its components are given by

$$\begin{aligned} \tilde{K}_{00} &= -\frac{\dot{W}^2}{B} - \frac{\tilde{\omega}}{C} - \frac{\dot{\nu}}{D} - \nu eA_3 - m^2, \\ \tilde{K}_{01} &= -\frac{\dot{W}(E - \tilde{\omega} \tilde{\Omega})}{B} + \frac{\dot{W} eA_0}{B}, \\ \tilde{K}_{02} &= \frac{\dot{\nu}(E - \tilde{\omega} \tilde{\Omega})}{C}, \\ \tilde{K}_{03} &= \frac{\dot{\nu}(E - \tilde{\omega} \tilde{\Omega})}{D} + eA_0 \dot{\nu} + eA_3 (E - \tilde{\omega} \tilde{\Omega}) + eA_0, \\ \tilde{K}_{10} &= (E - \tilde{\omega} \tilde{\Omega}) \frac{\dot{W}}{G(r)}, \\ \tilde{K}_{11} &= \frac{-(E - \tilde{\omega} \tilde{\Omega})^2}{G(r)} - \frac{(E - \tilde{\omega} \tilde{\Omega}) eA_0}{G(r)} - \frac{\tilde{\omega}^2}{C} - \frac{\dot{\nu}}{D} \\ & \quad - \frac{eA_3 \dot{\nu}}{D} - eA_3 \dot{\nu} - e^2 A_3^2 - m^2, \\ \tilde{K}_{12} &= \frac{\dot{W} \tilde{\omega}}{C}, \\ \tilde{K}_{13} &= \frac{\dot{\nu} \dot{W}}{D} + eA_3 \dot{W}, \\ \tilde{K}_{20} &= \frac{\dot{\nu}(E - \tilde{\omega} \tilde{\Omega})}{A} + eA_0 \frac{\dot{\nu}}{G(r)}, \\ \tilde{K}_{21} &= -\dot{W} \dot{\nu}, \\ \tilde{K}_{22} &= -\frac{1}{G(r)} [(E - \tilde{\omega} \tilde{\Omega})^2 + eA_0 (E - \tilde{\omega} \tilde{\Omega})] + \frac{1}{B} \dot{W} \\ & \quad - \frac{1}{D} [\dot{\nu} - eA_3 \dot{\nu}] - \frac{eA_3}{D} [\dot{\nu} + eA_3] - m^2, \\ \tilde{K}_{23} &= \frac{1}{D} \tilde{\omega} \dot{\nu} + \frac{eA_3 \tilde{\omega}}{D}, \\ \tilde{K}_{30} &= \frac{1}{G(r)} [(E - \tilde{\omega} \tilde{\Omega}) \dot{\nu} + eA_3 (E - \tilde{\omega} \tilde{\Omega})] \\ & \quad + \frac{eA_0}{G(r)} [\dot{\nu} + eA_3], \end{aligned}$$

$$\begin{aligned}
\tilde{K}_{31} &= \frac{1}{B} [\dot{W}\dot{v} + eA_3\dot{W}], \\
\tilde{K}_{32} &= \frac{1}{C} [\tilde{\omega}\dot{v} + eA_3\dot{v}], \\
\tilde{K}_{33} &= -\frac{1}{G(r)} \left[(E - \tilde{\omega}\tilde{\Omega})^2 + (E - \tilde{\omega}\tilde{\Omega})eA_0 \right] - \frac{1}{B}\dot{W}^2 \\
&\quad - \frac{\dot{v}^2}{C} - \frac{eA_0}{G(r)} [(E - \tilde{\omega}\tilde{\Omega}) + eA_0] - m^2,
\end{aligned} \tag{14}$$

where $\dot{W} = \partial_r I_0$, $\dot{v} = \partial_\theta I_0$, and $\tilde{\omega} = \partial_\phi I_0$. For the nontrivial solution $|\tilde{K}| = 0$ and solving above equations one can yield

$$\text{Im}W^\pm = \pm \int \sqrt{\frac{(E - eA_0 - \tilde{\omega}\tilde{\Omega} - eA_3)^2 + X}{G(r)B^{-1}}} dr, \tag{15}$$

where + and – represent the outgoing and incoming particles, respectively, whereas, “X” is the function which can be defined as

$$\begin{aligned}
X &= -\frac{G(r)}{C}\dot{v}^2 - m^2G(r) + 2eA_3(E - \tilde{\omega}\tilde{\Omega}) \\
&\quad + 2e^2A_0A_3 - e^2A_3^2
\end{aligned} \tag{16}$$

and $\tilde{\omega}$ is the angular velocity at event horizon. By integrating (15) around the pole, we get

$$\text{Im}W^\pm = \pm i\pi \frac{(E - eA_0 - \tilde{\omega}\tilde{\Omega} - eA_3)}{2\rho(r_+)}, \tag{17}$$

where the surface gravity $\kappa(r_+)$ of the charged black hole is given by

$$\kappa(r_+) = \left[\frac{2M}{r^2} - \frac{2Q^2}{r^3} + \frac{1 - 6\kappa\lambda}{1 - 3\kappa\lambda} N_d r^{3\kappa\lambda/(3\kappa\lambda-1)} \right]_{r=r_+}^2. \tag{18}$$

The tunneling probability Γ for outgoing charged vector particles can be obtained by

$$\begin{aligned}
\Gamma(\text{Im}W^+) &= \frac{\text{Prob}[\text{emission}]}{\text{Prob}[\text{absorption}]} = \frac{\exp[-2(\text{Im}W^+ + \text{Im}\Phi)]}{\exp[-2(\text{Im}W^- - \text{Im}\Phi)]} = \exp[-4\text{Im}W^+] \\
&= \exp \left[-\frac{2\pi(E - eA_0 - \tilde{\omega}\tilde{\Omega} - eA_3)}{(2M/r^2 - 2Q^2/r^3 + ((1 - 6\kappa\lambda)/(1 - 3\kappa\lambda)) N_d r^{3\kappa\lambda/(3\kappa\lambda-1)})^2} \right].
\end{aligned} \tag{19}$$

Now, we can calculate the $\tilde{T}_H(\text{Im}W^+)$ by comparing the $\tilde{\Gamma}(\text{Im}W^+)$ with the Boltzmann formula $\tilde{\Gamma}_B(\text{Im}W^+) \approx e^{-(E - eA_0 - \tilde{\omega}\tilde{\Omega} - eA_3)/\tilde{T}_H(\text{Im}W^+)}$, and we get

$$\begin{aligned}
T_H(\text{Im}W^+) \\
= \left[\frac{M}{\pi r^2} - \frac{Q^2}{\pi r^3} + \frac{1 - 6\kappa\lambda}{2\pi(1 - 3\kappa\lambda)} N_d r^{3\kappa\lambda/(3\kappa\lambda-1)} \right]_{r=r_+}^2.
\end{aligned} \tag{20}$$

The result shows that the $\tilde{\Gamma}(\text{Im}W^+)$ is dependent on r , the vector potential components (A_0 and A_3), energy E , angular momentum $\tilde{\Omega}$, and mass of black hole M ; κ and λ are the Rastall geometric parameters; and N_d and Q are dust field structure parameter and charge of black hole, respectively.

2.2. The Black Hole Surrounded by the Radiation Field. Second example of the line element of black hole surrounded by the radiation field [58] is given below:

$$\begin{aligned}
ds^2 &= -\left(1 - \frac{2M}{r} + \frac{Q^2 - N_r}{r^2}\right) dt^2 \\
&\quad + \frac{dr^2}{(1 - 2M/r + (Q^2 - N_r)/r^2)} \\
&\quad + r^2(d\theta^2 + \sin^2\theta d\phi^2),
\end{aligned} \tag{21}$$

where M is a mass of black hole, N_r is the negative radiation structure parameter, and Q is a charge of black hole.

Following the procedure given in Section 2.1 for this line element, we can obtain the surface gravity $\kappa(r_+)$ of this charged black hole surrounded by the radiation field in the following form:

$$\kappa(r_+) = \left[\frac{2M}{r^2} - \frac{2Q^2}{r^3} - \frac{r^2\dot{N}_r - 2rN_r}{r^4} \right]_{r=r_+}^2, \tag{22}$$

where $\dot{N}_r = \partial N_r / \partial r$. The tunneling rate of particles can be calculated as

$$\tilde{\Gamma}(\text{Im}W^+) = \exp \left[-\frac{4\pi(E - eA_\mu - \tilde{\omega}\tilde{\Omega})r^6}{[2Mr - 2Q^2 - r\dot{N}_r + 2N_r]^2} \right] \tag{23}$$

and the corresponding Hawking temperature at horizon can be obtained as

$$\tilde{T}(r_+) = \frac{1}{4\pi r_+^6} [2Mr - 2Q^2 - r\dot{N}_r + 2N_r]^2 \Big|_{r=r_+}. \tag{24}$$

This temperature depends on radiation structure parameter N_r , mass M , and black hole charge Q .

2.3. *The Black Hole Surrounded by the Quintessence Field.* Third example of the line element of the black hole surrounded by the quintessence field [58] is given below:

$$ds^2 = - \left(1 - \frac{2M}{r} + \frac{Q^2}{r^2} - \frac{N_q}{r^{(-1-2\kappa\lambda)/(1-\kappa\lambda)}} \right) dt^2 + \frac{dr^2}{\left(1 - 2M/r + Q^2/r^2 - N_q/r^{(-1-2\kappa\lambda)/(1-\kappa\lambda)} \right)} + r^2 (d\theta^2 + \sin^2\theta d\phi^2), \quad (25)$$

where N_q is a quintessence field structure parameter. By following the same process and using the vector potential for this black hole, the surface gravity can be derived as

$$\kappa(r_+) = \left[\frac{2M}{r^2} - \frac{2Q^2}{r^3} - \left(\frac{1+2\kappa\lambda}{1-\kappa\lambda} \right) N_q r^{3\kappa\lambda/(1-\kappa\lambda)} \right]_{r=r_+}^2. \quad (26)$$

The corresponding tunneling probability

$$\bar{\Gamma} = \exp \left[\frac{-4\pi (E - eA_\mu - \tilde{\omega}\tilde{\Omega})}{\left[2M/r^2 - 2Q^2/r^3 + ((1-6\kappa\lambda)/(1-3\kappa\lambda)) N_d r^{3\kappa\lambda/(3\kappa\lambda-1)} \right]^2} \right] \quad (27)$$

and Hawking temperature

$$\bar{T} = \left[\frac{\left(2M/r^2 - 2Q^2/r^3 - ((1+2\kappa\lambda)/(1-\kappa\lambda)) N_q r^{3\kappa\lambda/(1-\kappa\lambda)} \right)^2}{4\pi} \right]_{r=r_+} \quad (28)$$

are derived and given in the above expressions. The Hawking temperature depends on M , Q , and N_q , i.e., quintessence field structure parameter, mass, and charge of black hole, respectively.

2.4. *The Black Hole Surrounded by the Cosmological Constant Field.* Fourth example of the line element of black hole surrounded by the cosmological constant field is given below [58]:

$$ds^2 = - \left(1 - \frac{2M}{r} + \frac{Q^2}{r^2} - N_c r^2 \right) dt^2 + \frac{dr^2}{\left(1 - 2M/r + Q^2/r^2 - N_c r^2 \right)} + r^2 (d\theta^2 + \sin^2\theta d\phi^2), \quad (29)$$

where N_c is a cosmological constant field structure parameter. For this black hole, the surface gravity at outer horizon is obtained by following the above-mentioned similar procedure; i.e.,

$$\kappa(r_+) = \left[\frac{2M}{r^2} - \frac{2Q^2}{r^3} - 2N_c r \right]_{r=r_+}^2. \quad (30)$$

Moreover, the required tunneling probability of particles

$$\hat{\Gamma} = \exp \left[\frac{-4\pi (E - eA_\mu - \tilde{\omega}\tilde{\Omega})}{(2M/r^2 - 2Q^2/r^3 - 2N_c r)^2} \right], \quad (31)$$

and their corresponding Hawking temperature is calculated in the following expression:

$$\hat{T} = \left[\frac{\left(2M/r^2 - 2Q^2/r^3 - 2N_c r \right)^2}{4\pi} \right]_{r=r_+}. \quad (32)$$

This temperature depends on N_c , M , and Q , i.e., cosmological constant field structure parameter, mass, and charge of black hole, respectively.

2.5. *The Black Hole Surrounded by the Phantom Field.* Last example of the line element of black hole surrounded by the phantom field is [58]

$$ds^2 = - \left(1 - \frac{2M}{r} + \frac{Q^2}{r^2} - \frac{N_p}{r^{(-3+2\kappa\lambda)/(1+\kappa\lambda)}} \right) dt^2 + \frac{dr^2}{\left(1 - 2M/r + Q^2/r^2 - N_p/r^{(-3+2\kappa\lambda)/(1+\kappa\lambda)} \right)} + r^2 (d\theta^2 + \sin^2\theta d\phi^2), \quad (33)$$

where N_p is a phantom field structure parameter. For vector potential A_μ of this black hole, the surface gravity can be derived as

$$\kappa(r_+) = \left[\frac{2M}{r^2} - \frac{2Q^2}{r^3} - \left(\frac{3-2\kappa\lambda}{1+\kappa\lambda} \right) N_p r^{(2-3\kappa\lambda)/(1+\kappa\lambda)} \right]_{r=r_+}^2. \quad (34)$$

The tunneling probability of particles

$$\tilde{\Gamma} = \exp \left[\frac{-4\pi (E - eA_\mu - \tilde{\omega}\tilde{\Omega})}{(2M/r^2 - 2Q^2/r^3 - ((3 - 2\kappa\lambda)/(1 + \kappa\lambda)) N_p r^{(2-3\kappa\lambda)/(1+\kappa\lambda)})^2} \right] \quad (35)$$

and the required Hawking temperature of particles can be obtained as given below:

$$\tilde{T} = \left[\frac{(2M/r^2 - 2Q^2/r^3 - ((3 - 2\kappa\lambda)/(1 + \kappa\lambda)) N_p r^{(2-3\kappa\lambda)/(1+\kappa\lambda)})^2}{4\pi} \right]_{r=r_+}. \quad (36)$$

The Hawking temperature depends on M , Q , and N_p ; these are phantom field structure parameter, mass, and charge of black hole, respectively.

3. GUP-Corrected Proca Equation and the Corrected Hawking Temperature

In this section, we focus on the effect of the GUP on the tunneling of massive uncharged vector particles from the black hole solutions surrounded by perfect fluid in Rastall theory. Firstly we use the GUP-corrected Lagrangian for the massive uncharged vector field ψ_μ given by [63]

$$L_{GUP} = -\frac{1}{2} (D_\mu \psi_\nu - D_\nu \psi_\mu) (D^\mu \psi^\nu - D^\nu \psi^\mu) - \frac{m_W^2}{\hbar^2} \psi_\mu \psi^\mu. \quad (37)$$

One can derive the equation of the motion for the GUP-corrected Lagrangian of massive uncharged vector field as follows [63]:

$$\begin{aligned} \partial_\mu (\sqrt{-g} \psi^{\mu\nu}) - \sqrt{-g} \frac{m_W^2}{\hbar^2} \psi^\nu \\ + \beta \hbar^2 \partial_0 \partial_0 \partial_0 (\sqrt{-g} g^{00} \psi^{0\nu}) \\ - \beta \hbar^2 \partial_i \partial_i \partial_i (\sqrt{-g} g^{ii} \psi^{i\nu}) = 0, \end{aligned} \quad (38)$$

with

$$\psi_{\mu\nu} = (1 - \beta \hbar^2 \partial_\mu^2) \partial_\mu \psi_\nu - (1 - \beta \hbar^2 \partial_\nu^2) \partial_\nu \psi_\mu. \quad (39)$$

It is noted that we use the Latin indices for the modified tensor $\psi_{i\mu}$ as follows: $i = 1, 2, 3$; on the other hand, for $\psi_{0\mu}$, we use the 0 for the time coordinate. Moreover, we note that $\beta = 1/(3M_f^2)$, where M_f is the Planck mass and m_W stands for the mass of the particle.

3.1. The Black Hole Surrounded by the Dust Field in Rastall Theory. The metric is given by

$$ds^2 = -G(r) dt^2 + B(r) dr^2 + C(r) d\theta^2 + D(r) d\phi^2, \quad (40)$$

where $G(r)$, $B(r)$, $C(r)$, and $D(r)$ are given below:

$$G(r) = 1 - \frac{2M}{r} + \frac{Q^2}{r^2} - \frac{N_d}{r^{(1-6\kappa\lambda)/(1-3\kappa\lambda)}}, \quad (41)$$

$$C(r) = r^2,$$

$$\begin{aligned} B(r) &= \frac{1}{G(r)} \\ &= \frac{1}{1 - 2M/r + Q^2/r^2 - N_d/r^{(1-6\kappa\lambda)/(1-3\kappa\lambda)}}, \end{aligned} \quad (42)$$

$$D(r) = r^2 \sin^2 \theta.$$

Using the WKB method, we define the ψ_μ as follows:

$$\Psi_\mu = c_\mu(t, r, \theta, \phi) \exp \left[\frac{i}{\hbar} I(t, r, \theta, \phi) \right], \quad (43)$$

where I is defined as

$$\begin{aligned} I(t, r, \theta, \phi) &= I_0(t, r, \theta, \phi) + \hbar I_1(t, r, \theta, \phi) \\ &\quad + \hbar^2 I_2(t, r, \theta, \phi) + \dots \end{aligned} \quad (44)$$

We use (43), (44), and the metric (40) into (38), and then we only consider the lowest order terms in \hbar to calculate the equations with the corresponding coefficients c_μ :

$$\begin{aligned} G(r) [c_0 (\partial_r I_0)^2 \mathcal{A}_1^2 - c_1 (\partial_r I_0) (\partial_t I_0) \mathcal{A}_1 \mathcal{A}_0] \\ + \frac{1}{C(r)} [c_0 (\partial_\theta I_0)^2 \mathcal{A}_2^2 - c_2 (\partial_\theta I_0) (\partial_t I_0) \mathcal{A}_2 \mathcal{A}_0] \\ + \frac{1}{D(r)} [c_0 (\partial_\phi I_0)^2 \mathcal{A}_3^2 - c_3 (\partial_\phi I_0) (\partial_t I_0) \mathcal{A}_3 \mathcal{A}_0] \\ + c_0 m_W^2 = 0, \end{aligned} \quad (45)$$

$$\begin{aligned}
& -\frac{1}{G(r)} \left[c_1 (\partial_t I_0)^2 \mathcal{A}_0^2 - c_0 (\partial_t I_0) (\partial_r I_0) \mathcal{A}_0 \mathcal{A}_1 \right] \\
& + \frac{1}{C(r)} \left[c_1 (\partial_\theta I_0)^2 \mathcal{A}_2^2 - c_2 (\partial_\theta I_0) (\partial_r I_0) \mathcal{A}_2 \mathcal{A}_1 \right] \\
& + \frac{1}{D(r)} \left[c_1 (\partial_\phi I_0)^2 \mathcal{A}_3^2 - c_3 (\partial_\phi I_0) (\partial_r I_0) \mathcal{A}_3 \mathcal{A}_1 \right] \\
& + c_1 m_W^2 = 0,
\end{aligned} \tag{46}$$

$$\begin{aligned}
& -\frac{1}{G(r)} \left[c_2 (\partial_t I_0)^2 \mathcal{A}_0^2 - c_0 (\partial_t I_0) (\partial_\theta I_0) \mathcal{A}_0 \mathcal{A}_2 \right] \\
& + G(r) \left[c_2 (\partial_r I_0)^2 \mathcal{A}_1^2 - c_1 (\partial_r I_0) (\partial_\theta I_0) \mathcal{A}_1 \mathcal{A}_2 \right] \\
& + \frac{1}{D(r)} \left[c_2 (\partial_\phi I_0)^2 \mathcal{A}_3^2 - c_3 (\partial_\phi I_0) (\partial_\theta I_0) \mathcal{A}_3 \mathcal{A}_2 \right] \\
& + c_2 m_W^2 = 0,
\end{aligned} \tag{47}$$

$$\begin{aligned}
& -\frac{1}{G(r)} \left[c_3 (\partial_t I_0)^2 \mathcal{A}_0^2 - c_0 (\partial_t I_0) (\partial_\phi I_0) \mathcal{A}_0 \mathcal{A}_3 \right] \\
& + G(r) \left[c_3 (\partial_r I_0)^2 \mathcal{A}_1^2 - c_1 (\partial_r I_0) (\partial_\phi I_0) \mathcal{A}_1 \mathcal{A}_3 \right] \\
& + \frac{1}{C(r)} \left[c_3 (\partial_\theta I_0)^2 \mathcal{A}_2^2 - c_2 (\partial_\theta I_0) (\partial_\phi I_0) \mathcal{A}_2 \mathcal{A}_3 \right] \\
& + c_3 m_W^2 = 0,
\end{aligned} \tag{48}$$

where the \mathcal{A}_μ s are defined as

$$\begin{aligned}
\mathcal{A}_0 &= 1 + \beta \frac{1}{G(r)} (\partial_t S_0)^2, \\
\mathcal{A}_1 &= 1 + \beta G(r) (\partial_r S_0)^2, \\
\mathcal{A}_2 &= 1 + \beta \frac{1}{C(r)} (\partial_\theta S_0)^2, \\
\mathcal{A}_3 &= 1 + \beta \frac{1}{D(r)} (\partial_\phi S_0)^2.
\end{aligned} \tag{49}$$

Using the semiclassical Hamilton-Jacobi method with WKB ansatz, we separate the variables as follows:

$$I_0 = -Et + R(r) + \Theta(\theta, \phi) + k. \tag{50}$$

Note that the energy of the radiated particle is defined with E . Afterwards, we obtain a matrix equation as follows:

$$\mathbb{U} (c_0, c_1, c_2, c_3)^T = 0, \tag{51}$$

where \mathbb{U} is a 4×4 matrix, the elements of which are

$$\mathbb{U}_{11} = G(r) R'^2 \mathcal{A}_1^2 + \frac{J_\theta^2}{C(r)} \mathcal{A}_2^2 + \frac{J_\phi^2}{D(r)} \mathcal{A}_3^2 + m_W^2,$$

$$\mathbb{U}_{12} = -G(r) R' (-E) \mathcal{A}_1 \mathcal{A}_0,$$

$$\mathbb{U}_{13} = -\frac{J_\theta (-E)}{C(r)} \mathcal{A}_2 \mathcal{A}_0,$$

$$\mathbb{U}_{14} = -\frac{J_\phi (-E)}{D(r)} \mathcal{A}_3 \mathcal{A}_0,$$

$$\mathbb{U}_{21} = \frac{(-E) R'}{G(r)} \mathcal{A}_0 \mathcal{A}_1,$$

$$\mathbb{U}_{22} = -\frac{(-E)^2}{G(r)} \mathcal{A}_0^2 + \frac{J_\theta^2}{C(r)} \mathcal{A}_2^2 + \frac{J_\phi^2}{D(r)} \mathcal{A}_3^2 + m_W^2,$$

$$\mathbb{U}_{23} = -\frac{J_\theta R'}{C(r)} \mathcal{A}_2 \mathcal{A}_1,$$

$$\mathbb{U}_{24} = -\frac{J_\phi R'}{D(r)} \mathcal{A}_3 \mathcal{A}_1,$$

$$\mathbb{U}_{31} = \frac{-E J_\theta}{G(r)} \mathcal{A}_0 \mathcal{A}_2,$$

$$\mathbb{U}_{32} = -G(r) R' J_\theta \mathcal{A}_1 \mathcal{A}_2,$$

$$\mathbb{U}_{33} = -\frac{(-E)^2}{G(r)} \mathcal{A}_0^2 + G(r) R'^2 \mathcal{A}_1^2 + \frac{J_\phi^2}{D(r)} \mathcal{A}_3^2 + m_W^2,$$

$$\mathbb{U}_{34} = -\frac{J_\theta J_\phi}{D(r)} \mathcal{A}_3 \mathcal{A}_2,$$

$$\mathbb{U}_{41} = \frac{(-E) J_\phi}{G(r)} \mathcal{A}_0 \mathcal{A}_3,$$

$$\mathbb{U}_{42} = -G(r) R' J_\phi \mathcal{A}_1 \mathcal{A}_3,$$

$$\mathbb{U}_{43} = -\frac{J_\theta J_\phi}{C(r)} \mathcal{A}_2 \mathcal{A}_3,$$

$$\mathbb{U}_{44} = -\frac{(-E)^2}{G(r)} \mathcal{A}_0^2 + G(r) R'^2 \mathcal{A}_1^2 + \frac{J_\theta^2}{C(r)} \mathcal{A}_2^2 + m_W^2,$$

(52)

where $R' = \partial_r R$, $J_\theta = \partial_\theta \Theta$, and $J_\phi = \partial_\phi \Theta$.

It is noted that, for the condition of $\det \mathbb{U} = 0$, we find the nontrivial solution of (51). First, we consider only the lowest order terms of β and then calculate the $\det \mathbb{U} = 0$. Our main aim is to obtain the radial part of the equation so that we integrate it using the complex integral method around the event horizon as follows:

$$\begin{aligned}
& \text{Im} R_\pm(r) \\
&= \pm \text{Im} \int dr \sqrt{-\frac{m^2}{G(r)} + \frac{E^2}{G(r)^2} - \frac{J_\theta^2 + J_\phi^2}{G(r) D(r)}} \left(1 + \frac{\mathcal{T}_1}{\mathcal{T}_2} \beta \right),
\end{aligned} \tag{53}$$

where

$$\begin{aligned}
\mathcal{T}_1 &= -3G(r) m^4 C(r) + 6m^2 C(r) (E)^2 \\
&\quad - 6G(r) m^2 \left(J_\theta^2 + \frac{J_\phi^2}{D(r)} \right) - \frac{6G(r) J_\theta^4}{C(r)}
\end{aligned}$$

$$\begin{aligned}
& + 6(E)^2 \left(J_\theta^2 + \frac{J_\phi^2}{D(r)} \right) - \frac{7G(r)J_\theta^2J_\phi^2}{D(r)} \\
& - \frac{3G(r)J_\theta^4J_\phi^2}{2m^2D(r)^2} - \frac{5G(r)J_\phi^4\csc^4\theta}{C(r)} \\
& + \frac{3G(r)J_\theta^2J_\phi^4}{2m^2D(r)^2}, \quad (54)
\end{aligned}$$

$$\mathcal{T}_2 = -G(r)m^2r^2 + r^2(E)^2 - G(r) \left(J_\theta^2 + \frac{J_\phi^2}{D(r)} \right). \quad (55)$$

We rewrite the metric close to the event horizon to obtain solution for the integral:

$$G(r_h) \approx \frac{\Delta_{,r}(r_h)}{r_h^2} (r - r_h). \quad (56)$$

Afterwards we manage to obtain the solution of the integral (53) for the radial part as follows:

$$\text{Im}R_\pm(r) = \pm i\pi \frac{r_h^2}{\Delta_{,r}(r_h)} (E) \times (1 + \beta\Xi), \quad (57)$$

where $\Xi = 6m^2 + (6/r_h^2)(J_\theta^2 + J_\phi^2\csc^2\theta)$.

It is quite clear that $\Xi > 0$. We note that R_+ represents the radial function for the outgoing particles and R_- is for the ingoing particles. Thus, the tunneling rate of W bosons near the event horizon is

$$\begin{aligned}
\Gamma &= \frac{P_{\text{outgoing}}}{P_{\text{ingoing}}} = \frac{\exp[-(2/\hbar)(\text{Im}R_+ + \text{Im}\Theta)]}{\exp[-(2/\hbar)(\text{Im}R_- + \text{Im}\Theta)]} \\
&= \exp\left[-\frac{4}{\hbar}\text{Im}R_+\right] \\
&= \exp\left[-\frac{4\pi}{\hbar} \frac{r_h^2}{\Delta_{,r}(r_h)} (E) \times (1 + \beta\Xi)\right]. \quad (58)
\end{aligned}$$

derived and given in above expressions. The Hawking temperature depends on M , Q , and N_q , i.e., quintessence field structure parameter, mass, and charge of black hole, respectively. Naturally, black hole remnants will be left.

3.4. The Black Hole Surrounded by the Cosmological Constant Field. One can repeat the process just for this black hole to calculate the corresponding corrected Hawking temperature with the quantum gravity effects as follows:

If we set $\hbar = 1$, we find the corrected Hawking temperature as follows:

$$T_{e-H} = \frac{\Delta_{,r}(r_h)}{4\pi r_h^2(1 + \beta\Xi)} = T_0(1 - \beta\Xi), \quad (59)$$

where $T_0 = [M/\pi r^2 - Q^2/\pi r^3 + ((1 - 6\kappa\lambda)/2\pi(1 - 3\kappa\lambda)) N_q r^{3\kappa\lambda/(3\kappa\lambda-1)}]_{r=r_+}^2$ is the original Hawking temperature of a corresponding black hole. We find the corrected Hawking temperature with the effect of quantum gravity. In addition, the Hawking temperature is increased if one uses the quantum gravity effects, but then these effects are canceled in some point and black hole remnants occur.

3.2. The Black Hole Surrounded by the Radiation Field. Following the procedure given in Section 2.1 for this line element, we obtain the corrected Hawking temperature with the effect of quantum gravity for this charged black hole surrounded by the radiation field in the following form:

$$T_{e-H} = \frac{\Delta_{,r}(r_h)}{4\pi r_h^2(1 + \beta\Xi)} = T_0(1 - \beta\Xi), \quad (60)$$

where original Hawking temperature is

$$T_0 = \frac{1}{4\pi r^6} [2Mr - 2Q^2 - r\dot{N}_r + 2N_r]^2 \Big|_{r=r_+}. \quad (61)$$

This temperature depends on radiation structure parameter N_r , mass M , and black hole charge Q . Moreover, the quantum effects explicitly counteract the temperature increases during evaporation, which will cancel it out at some point. Naturally, black hole remnants will be left.

3.3. The Black Hole Surrounded by the Quintessence Field. By following the same process, we calculate the corrected Hawking temperature under the effect of quantum gravity as follows:

$$T_{e-H} = \frac{\Delta_{,r}(r_h)}{4\pi r_h^2(1 + \beta\Xi)} = T_0(1 - \beta\Xi), \quad (62)$$

with the original Hawking temperature

$$T_0 = \left[\frac{(2M/r^2 - 2Q^2/r^3 - ((1 + 2\kappa\lambda)/(1 - \kappa\lambda)) N_q r^{3\kappa\lambda/(1-\kappa\lambda)})^2}{4\pi} \right]_{r=r_+}, \quad (63)$$

$$T_{e-H} = \frac{\Delta_{,r}(r_h)}{4\pi r_h^2(1 + \beta\Xi)} = T_0(1 - \beta\Xi), \quad (64)$$

with

$$T_0 = \left[\frac{(2M/r^2 - 2Q^2/r^3 - 2N_c r)^2}{4\pi} \right]_{r=r_+}. \quad (65)$$

This temperature depends on N_c , M , and Q , i.e., cosmological constant field structure parameter, mass, and charge of black hole, respectively. Again here, remnants are left.

3.5. *The Black Hole Surrounded by the Phantom Field.* Last example is the line element of black hole surrounded by the

phantom field. Now we again repeat the same process to obtain the following corrected Hawking temperature:

$$T_{e-H} = \frac{\Delta_{,r}(r_h)}{4\pi r_h^2 (1 + \beta\Xi)} = T_0 (1 - \beta\Xi), \quad (66)$$

with

$$\ddot{T} = \left[\frac{(2M/r^2 - 2Q^2/r^3 - ((3 - 2\kappa\lambda)/(1 + \kappa\lambda)) N_p r^{(2-3\kappa\lambda)/(1+\kappa\lambda)})^2}{4\pi} \right]_{r=r_+}. \quad (67)$$

The Hawking temperature depends on M , Q , and N_p ; these are phantom field structure parameter, mass, and charge of black hole, respectively.

4. Conclusions

In this research paper, we have successfully analyzed the GUP-corrected Hawking temperature of W^\pm boson vector particles using the equation of motion for the Glashow-Weinberg-Salam model. First of all, we analyzed the modified Hamilton-Jacobi equation by resolving the modified Lagrangian equation utilized for the magnetized particles in the space-time. We have analyzed the GUP effect on the radiation of black holes surrounded by perfect fluid in Rastall theory.

As the original Hawking radiation, the Hawking temperature T_H of the black holes is associated with its mass M and charged Q . However, these results indicated that the effect of quantum gravity is counted and the behavior of the tunneling boson vector particle on the event horizon is observed from the original event. The Hawking temperature T_H and tunneling probability Γ quantities are not just sensitively dependent on the mass M and charged Q of the black hole. The Hawking temperature T_H , tunneling probability Γ , and surface gravity κ are only dependent on the geometry (structure parameter) of black hole. Moreover, the corrected Hawking temperature $T_{e-H} = T_0(1 - \beta\Xi)$ has been calculated with the effect of quantum gravity. The Hawking temperature is increased if one uses the quantum gravity effects, but then these effects are canceled in some point and black hole remnants occur.

Data Availability

No data were used to support this study.

Conflicts of Interest

The authors declare that there are no conflicts of interest regarding the publication of this paper.

Acknowledgments

This work is supported by Comisión Nacional de Ciencias y Tecnología de Chile (CONICYT) through FONDECYT Grant N° 3170035 (Ali Övgün).

References

- [1] D. Kubizňák and R. B. Mann, “ $P - V$ criticality of charged AdS black holes,” *Journal of High Energy Physics*, vol. 33, 2012.
- [2] D. Kubizňák and R. B. Mann, “Black hole chemistry,” *Canadian Journal of Physics*, vol. 93, no. 9, pp. 999–1002, 2015.
- [3] D. Kubiznak, R. B. Mann, and M. Teo, “Black hole chemistry: thermodynamics with lambda,” *Classical and Quantum Gravity*, vol. 34, no. 6, Article ID 063001, 2017.
- [4] J. D. Bekenstein, “Generalized second law of thermodynamics in black-hole physics,” *Physical Review D: Particles, Fields, Gravitation and Cosmology*, vol. 9, no. 12, pp. 3292–3300, 1974.
- [5] S. W. Hawking, “Black hole explosions?” *Nature*, vol. 248, no. 5443, pp. 30–31, 1974.
- [6] S. W. Hawking, “Particle creation by black holes,” *Communications in Mathematical Physics*, vol. 43, no. 3, pp. 199–220, 1975.
- [7] S. W. Hawking, “Erratum: ‘Particle creation by black holes,’” *Communications in Mathematical Physics*, vol. 46, no. 2, p. 206, 1976.
- [8] S. W. Hawking, M. J. Perry, and A. Strominger, “Soft Hair on Black Holes,” *Physical Review Letters*, vol. 116, no. 23, Article ID 231301, 2016.
- [9] M. K. Parikh and F. Wilczek, “Hawking radiation as tunneling,” *Physical Review Letters*, vol. 85, no. 24, pp. 5042–5045, 2000.
- [10] R. Kerner and R. B. Mann, “Tunnelling, temperature, and Taub-NUT black holes,” *Physical Review D: Particles, Fields, Gravitation and Cosmology*, vol. 73, no. 10, Article ID 104010, 2006.
- [11] R. Kerner and R. B. Mann, “Tunnelling from Gödel black holes,” *Physical Review D: Particles, Fields, Gravitation and Cosmology*, vol. 75, no. 8, Article ID 084022, 2007.
- [12] R. Banerjee and B. R. Majhi, “Quantum tunneling beyond semiclassical approximation,” *Journal of High Energy Physics*, vol. 2008, article 095, 2008.
- [13] E. T. Akhmedov, V. Akhmedova, and D. Singleton, “Hawking temperature in the tunneling picture,” *Physics Letters B*, vol. 642, no. 1–2, pp. 124–128, 2006.
- [14] E. T. Akhmedov, V. Akhmedova, D. Singleton, and T. Pilling, “Thermal radiation of various gravitational backgrounds,” *International Journal of Modern Physics A*, vol. 22, no. 8–9, pp. 1705–1715, 2007.
- [15] V. E. Akhmedova, T. Pilling, A. de Gill, and D. Singleton, “Tunneling/WKB and anomaly methods for Rindler and de sitter space-times,” *Theoretical and Mathematical Physics*, vol. 163, no. 3, pp. 774–781, 2010.

- [16] V. Akhmedova, T. Pilling, A. de Gill, and D. Singleton, "Temporal contribution to gravitational WKB-like calculations," *Physics Letters B*, vol. 666, no. 3, pp. 269–271, 2008.
- [17] K. Nozari and S. H. Mehdipour, "Hawking radiation as quantum tunneling from a noncommutative Schwarzschild black hole," *Classical and Quantum Gravity*, vol. 25, no. 17, Article ID 175015, 2008.
- [18] K. Nozari and S. Saghafi, "Natural cutoffs and quantum tunneling from black hole horizon," *Journal of High Energy Physics*, vol. 2012, article 005, 2012.
- [19] M. Angheben, M. Nadalini, L. Vanzo, and S. Zerbini, "Hawking radiation as tunneling for extremal and rotating black holes," *Journal of High Energy Physics*, vol. 2005, no. 5, article 014, 2005.
- [20] S. I. Kruglov, "Black hole emission of vector particles in (1+1) dimensions," *International Journal of Modern Physics A*, vol. 29, no. 22, Article ID 1450118, 2014.
- [21] S. I. Kruglov, "Black hole radiation of spin-1 particles in (1+2) dimensions," *International Journal of Modern Physics A*, vol. 29, no. 39, Article ID 1450203, 2014.
- [22] X. M. Kuang, J. Saavedra, and A. Övgün, "The effect of the Gauss–Bonnet term on Hawking radiation from arbitrary dimensional black brane," *The European Physical Journal C*, vol. 77, article 613, 2017.
- [23] I. Sakalli, A. Ovgun, and Lett. Europhys, "Hawking radiation and deflection of light from Rindler modified Schwarzschild black hole," *EPL (Europhysics Letters)*, vol. 118, no. 6, Article ID 60006, 2017.
- [24] K. Jusufi, İ. Sakallı, and A. Övgün, "Quantum tunneling and quasinormal modes in the spacetime of the Alcubierre warp drive," *General Relativity and Gravitation*, vol. 50, article 10, 2018.
- [25] I. Sakalli, A. Övgün, and K. Jusufi, "GUP assisted Hawking radiation of rotating acoustic black holes," *Astrophysics and Space Science. An International Journal of Astronomy, Astrophysics and Space Science*, vol. 361, no. 10, article 330, 2016.
- [26] A. Caliskan, S. O. Kara, and A. Ozansoy, "The Bekenstein–Hawking corpuscular cascading from the back-reacted black hole," *Advances in High Energy Physics*, vol. 2017, Article ID 1573904, pp. 1–9, 2017.
- [27] I. Sakalli and A. Övgün, "Black hole radiation of massive spin-2 particles in (3+1) dimensions," *The European Physical Journal Plus*, vol. 131, no. 6, article 184, 2016.
- [28] A. Övgün and K. Jusufi, "Massive vector particles tunneling from noncommutative charged black holes and its gup-corrected thermodynamics," *The European Physical Journal Plus*, vol. 131, no. 5, article 177, 2016.
- [29] I. Sakalli and A. Ovgun, "Quantum tunneling of massive spin-1 particles from non-stationary metrics," *General Relativity and Gravitation*, vol. 48, article 1, 2016.
- [30] I. Sakalli and A. Ovgun, "Tunnelling of vector particles from Lorentzian wormholes in 3+1 dimensions," *The European Physical Journal Plus*, vol. 130, article 110, 2015.
- [31] A. Övgün, I. Sakalli, and J. Saavedra, "Quasinormal modes of a schwarzschild black hole immersed in an electromagnetic universe," 2017, <https://arxiv.org/abs/1708.08331>.
- [32] I. Sakalli, "Analytical solutions in rotating linear dilaton black holes: resonant frequencies, quantization, greybody factor, and Hawking radiation," *Physical Review D: Particles, Fields, Gravitation and Cosmology*, vol. 94, no. 8, Article ID 084040, 2016.
- [33] T. I. Singh, I. A. Meitei, and K. Y. Singh, "Quantum gravity effects on hawking radiation of schwarzschild-de sitter black holes," *International Journal of Theoretical Physics*, vol. 56, no. 8, pp. 2640–2650, 2017.
- [34] J. Pu and Y. Han, "On Hawking radiation via tunneling from the Reissner–Nordström–de Sitter black hole with a global monopole," *International Journal of Theoretical Physics*, vol. 56, no. 7, pp. 2061–2070, 2017.
- [35] M. H. Ali and K. Sultana, "Particles' tunneling from cosmic string black holes surrounded by quintessence," *International Journal of Theoretical Physics*, vol. 56, no. 7, pp. 2279–2292, 2017.
- [36] W. Javed, R. Ali, and G. Abbas, "Charged vector particles tunneling from 5D black hole and black ring," 2017, <https://arxiv.org/abs/1705.05702>.
- [37] W. Javed, G. Abbas, and R. Ali, "Charged vector particle tunneling from a pair of accelerating and rotating and 5D gauged super-gravity black holes," *The European Physical Journal C*, vol. 77, no. 5, 2017.
- [38] K. Jusufi, "Quantum tunneling of spin-1 particles from a 5D Einstein–Yang–Mills–Gauss–Bonnet black hole beyond semiclassical approximation," *EPL (Europhysics Letters)*, vol. 116, no. 6, Article ID 60013, 2016.
- [39] K. Jusufi and G. Apostolovska, "Hawking radiation of Dirac monopoles from the global monopole black hole with quantum gravity effects," *Astrophysics and Space Science*, vol. 361, no. 12, article 374, 2016.
- [40] M. H. Ali and K. Sultana, "Charged particles' Hawking radiation via tunneling of both horizons from Reissner–Nordström–Taub–NUT black holes," *International Journal of Theoretical Physics*, vol. 52, no. 8, pp. 2802–2817, 2013.
- [41] M. H. Ali, "Charged particles' tunneling from Hot-NUT–Kerr–Newman–Kasuya spacetime," *International Journal of Theoretical Physics*, vol. 47, no. 9, pp. 2203–2217, 2008.
- [42] M. H. Ali, "Hawking radiation via tunneling from hot NUT–Kerr–Newman–KASuya spacetime," *Classical and Quantum Gravity*, vol. 24, no. 23, pp. 5849–5860, 2007.
- [43] I. Sakalli, M. Halilsoy, and H. Pasaoglu, "Erratum to: Fading Hawking radiation," *Astrophysics and Space Science*, vol. 340, no. 1, pp. 155–160, 2012.
- [44] I. Sakalli, M. Halilsoy, and H. Pasaoglu, "Entropy conservation of linear dilaton black holes in quantum corrected Hawking radiation," *International Journal of Theoretical Physics*, vol. 50, no. 10, pp. 3212–3224, 2011.
- [45] H. Pasaoglu and I. Sakalli, "Hawking radiation of linear dilaton black holes in various theories," *International Journal of Theoretical Physics*, vol. 48, no. 12, pp. 3517–3525, 2009.
- [46] I. Sakalli and A. Ovgun, "Hawking radiation of spin-1 particles from a three-dimensional rotating hairy black hole," *Journal of Experimental and Theoretical Physics*, vol. 121, no. 3, pp. 404–407, 2015.
- [47] K. Nozari and A. S. Sefiedgar, "Comparison of approaches to quantum correction of black hole thermodynamics," *Physics Letters B*, vol. 635, no. 2–3, pp. 156–160, 2006.
- [48] K. Nozari and A. Etemadi, "Minimal length, maximal momentum, and Hilbert space representation of quantum mechanics," *Physical Review D: Particles, Fields, Gravitation and Cosmology*, vol. 85, Article ID 104029, 2012.
- [49] A. Kempf, G. Mangano, and R. B. Mann, "Hilbert space representation of the minimal length uncertainty relation," *Physical Review D: Covering Particles, Fields, Gravitation, and Cosmology*, vol. 52, article 1108, 1995.
- [50] S. Hossenfelder, M. Bleicher, S. Hofmann, J. Ruppert, S. Scherer, and H. Stöcker, "Signatures in the Planck regime," *Physics Letters B*, vol. 575, no. 1–2, pp. 85–99, 2003.

- [51] A. N. Tawfik and E. A. El Dahab, "Corrections to entropy and thermodynamics of charged black hole using generalized uncertainty principle," *International Journal of Modern Physics A*, vol. 30, no. 9, Article ID 1550030, 2015.
- [52] M. A. Anacleto, F. A. Brito, and E. Passos, "Quantum-corrected self-dual black hole entropy in tunneling formalism with GUP," *Physics Letters B*, vol. 749, pp. 181–186, 2015.
- [53] M. Dehghani, "Corrections to the Hawking tunneling radiation in extra dimensions," *Physics Letters B*, vol. 749, pp. 125–129, 2015.
- [54] A. Farag Ali, M. M. Khalil, and E. C. Vagenas, "Minimal Length in quantum gravity and gravitational measurements," *EPL (Europhysics Letters)*, vol. 112, no. 2, Article ID 20005, 2015.
- [55] K. Nozari and S. H. Mehdipour, "Gravitational uncertainty and black hole remnants," *Modern Physics Letters A*, vol. 20, no. 38, pp. 2937–2948, 2005.
- [56] Z. W. Feng, S. Z. Yang, H. L. Li, and X. T. Zu, "Constraining the generalized uncertainty principle with the gravitational wave event GW150914," *Physics Letters B*, vol. 768, pp. 81–85, 2017.
- [57] S. K. Rama, "Some consequences of the generalised uncertainty principle: statistical mechanical, cosmological, and varying speed of light," *Physics Letters B*, vol. 519, no. 1-2, pp. 103–110, 2001.
- [58] Y. Heydarzade and F. Darabi, "Black hole solutions surrounded by perfect fluid in Rastall theory," *Physics Letters B*, vol. 771, pp. 365–373, 2017.
- [59] Y. Yang, J. Sun, Y. Guo, Q. Li, J. Huang, and Q. Chang, "Study of $\Upsilon(nS) \rightarrow B_c P$ decays with perturbative QCD approach," *Physics Letters B*, vol. 751, pp. 171–176, 2015.
- [60] D. W. Ebner, "Equations of motion of Glashow-Salam-Weinberg theory after spontaneous symmetry breaking," *Annalen der Physik*, vol. 498, no. 1-2, pp. 119–133, 1986.
- [61] E. D. Commins and P. H. Bucksbaum, *Weak Interactions of Leptons and Quarks*, Cambridge University Press, Cambridge, UK, 1983.
- [62] T. Shivalingaswamy and B. A. Kagali, "Eigenenergies of a relativistic particle in an infinite range linear potential using WKB method," *European Journal of Physics Education*, vol. 2, no. 2, 2011.
- [63] X.-Q. Li and G.-R. Chen, "Massive vector particles tunneling from Kerr and Kerr-Newman black holes," *Physics Letters B*, vol. 751, pp. 34–38, 2015.

Research Article

Spectroscopy of $z = 0$ Lifshitz Black Hole

Gulnihal Tokgoz  and Izzet Sakalli 

Physics Department, Eastern Mediterranean University, Famagusta, Northern Cyprus, Mersin 10, Turkey

Correspondence should be addressed to Gulnihal Tokgoz; gulnihal.tokgoz@emu.edu.tr

Received 22 May 2018; Accepted 8 July 2018; Published 17 July 2018

Academic Editor: Farook Rahaman

Copyright © 2018 Gulnihal Tokgoz and Izzet Sakalli. This is an open access article distributed under the Creative Commons Attribution License, which permits unrestricted use, distribution, and reproduction in any medium, provided the original work is properly cited. The publication of this article was funded by SCOAP³.

We studied the thermodynamics and spectroscopy of a 4-dimensional, $z = 0$ Lifshitz black hole (Z0LBH). Using Wald's entropy formula and the Hawking temperature, we derived the quasi-local mass of the Z0LBH. Based on the exact solution to the near-horizon Schrödinger-like equation (SLE) of the massive scalar waves, we computed the quasi-normal modes of the Z0LBH via employing the adiabatic invariant quantity for the Z0LBH. This study shows that the entropy and area spectra of the Z0LBH are equally spaced.

1. Introduction

Ever since the publication of the seminal papers of Bekenstein and Hawking [1–3], it has been known that black hole (BH) entropy (S_{BH}) should be quantized in discrete levels as discussed in detail by Bekenstein [4–7]. The proportionality between S_{BH} and BH area (\mathcal{A}_{BH}) is justified from the adiabatic invariance [8] properties of area, that is, $S_{BH} = \mathcal{A}_{BH}/4$. Therefore, \mathcal{A}_{BH} should also be quantized in equidistant levels to account for the discrete S_{BH} . Bekenstein [5, 6] proposed that, for the family of Schwarzschild BHs, \mathcal{A}_{BH} should have the following discrete, equidistant spectrum:

$$\mathcal{A}_{BH} = \epsilon \hbar n, \quad n = 0, 1, 2, \dots, \quad (1)$$

where ϵ is known as the undetermined dimensionless constant. According to (1), the minimum increase in the horizon area becomes $\Delta \mathcal{A}_{\min} = 8\pi \hbar$ for the Schwarzschild BH ($\epsilon = 8\pi$) [9–11]. Following the seminal works of Bekenstein, new methods have been developed to derive the entropy/area spectra of the numerous BHs (see [12] and references therein). Among them, Maggiore's method (MM) [9] fully supports Bekenstein's result (1). In fact, MM [9] was based on Kunstatter's study [13], in which the adiabatic invariant quantity (I_{adb}) is expressed as follows:

$$I_{adb} = \int \frac{dM}{\Delta\omega}, \quad (2)$$

where $\Delta\omega = \omega_{n-1} - \omega_n$ denotes the transition frequency between the successive levels of a BH having mass M . Further, (2) was generalized to the hairy BHs (massive, charged, and rotating ones) as follows (see [14] and references therein):

$$I_{adb} = \int \frac{\mathcal{T}_{\mathcal{H}} dS_{BH}}{\Delta\omega}, \quad (3)$$

where $\mathcal{T}_{\mathcal{H}}$ is the temperature of the BH. Bohr-Sommerfeld quantization rule [15] states that I_{adb} acts as a quantized quantity ($I_{adb} \simeq n\hbar$) when the highly excited modes ($n \rightarrow \infty$) are considered. In such a case, the imaginary part of the frequency dominates the real part of the frequency ($\omega_I \gg \omega_R$), implying that $\Delta\omega \simeq \Delta\omega_I$. Meanwhile, for the first time, Hod [16, 17] argued that the quasi-normal modes (QNMs) [18, 19] can be used for computing transition frequency. Hod's arguments inspired Maggiore who considered the Schwarzschild BH as a highly damped harmonic oscillator (i.e., $\Delta\omega \simeq \Delta\omega_I$) and managed to rederive Bekenstein's original result (1) using a different method. Today, there are numerous studies in the literature in which MM has been employed for various BHs (see, e.g., [20–25]).

This study mainly explores the entropy/area spectra of a four-dimensional Lifshitz BH [26] possessing a particular dynamical exponent $z = 0$. To analyze the physical features of the $z = 0$ Lifshitz BH (Z0LBH) geometry, we first calculate its quasi-local mass M_{QL} [27] and temperature via Wald's entropy [28] and statistical Hawking temperature formula

[29, 30], respectively. QNM calculations of the Z0LBH must be performed in order to implement the MM successfully. To this end, we consider the Klein-Gordon equation (KGE) for a massless scalar field in the Z0LBH background. Separation of the angular and the radial equations yields a Schrödinger-like wave equation (SLE) [31]. Asymptotic limits of the potential (36) show that the effective potential may diverge beyond the BH horizon for the massive scalar particle; thus, in the far region, the QNMs might not be perceived by the observer. Hence, following a particular method [23, 32–35], we focus our analysis on the near-horizon (NH) region and impose the boundary conditions (45): ingoing waves at the event horizon and no wave at spatial infinity (since at infinity the effective potential of Schrödinger-like wave equation is divergent). After getting NH form of the SLE, we show that the radial equation is reduced to a confluent hypergeometric (CH) differential equation [36]. Performing some manipulations on the NH solution and using the pole structure of the Gamma functions [36], we show how one finds out the QNMs as in [32, 33, 37–40]. The imaginary part of the QNMs is used in (3), and the quantum spectra of entropy and area of the Z0LBH are obtained.

The following statements elaborate on the organization of this study. In Section 2, we briefly introduce the Z0LBH metric. In addition, we present the derivation of M_{QL} of the Z0LBH based on Wald's entropy formula. Section 3 is devoted to the separation of the KGE and finding the effective potential $V_{eff}(r)$. Next, we solve the NH SLE and show how QNMs are calculated. Then, we compute the entropy/area spectra of the Z0LBH. Finally, we draw our conclusions in Section 4 (throughout this work, the geometrized unit system is used: $G = c = k_B = 1$ and $\ell_P^2 = \hbar$).

2. Z0LBH Spacetime

In this section, we introduce the four-dimensional Lifshitz spacetime and its special case, that is, Z0LBH [26]. Conformal gravity (CG) covers gravity theories that are invariant under Weyl transformations. CG, which is adapted to static and asymptotically Lifshitz BH solutions, has received intensive attention from the researchers studying condensed matter and quantum field theories [41]. The Lifshitz BHs are invariant under anisotropic scale and characterize the gravitational dual of strange metals [42].

The action of the Einstein-Weyl gravity [26] is given by

$$\mathcal{S} = \frac{1}{2\bar{\kappa}^2} \int \sqrt{-g} d^4x \left(R - 2\Lambda + \frac{1}{2}\alpha |Weyl|^2 \right), \quad (4)$$

where $\bar{\kappa}^2 = 8\pi G$, $|Weyl|^2 = R^{\mu\nu\rho\sigma}R_{\mu\nu\rho\sigma} - 2R^{\mu\nu}R_{\mu\nu} + (1/3)R^2$, and $\alpha = (z^2 + 2z + 3)/4z(z - 4)$ (constant), which diverges ($\alpha = \infty$) with $z = 0$ and/or $z = 4$. The Lifshitz BH solutions exist in the CG theory for both $z = 4$ and $z = 0$ [26, 43]; however, when $z = 3$ and $z = 4$, Lifshitz BHs appear in the Horava-Lifshitz gravity [26, 44, 45].

Now, we focus on the Z0LBH of the CG theory whose metric is given by [26]:

$$ds^2 = -f dt^2 + \frac{4dr^2}{r^2 f} + r^2 d\Omega_{2,k}^2, \quad (5)$$

where the metric function f is defined by

$$f = 1 + \frac{c}{r^2} + \frac{c^2 - k^2}{3r^4}. \quad (6)$$

In the above metric, which is conformal to (A)dS (AdS if $c + 2k < 1$ and dS if $c + 2k > 1$) [26], $k = 0$, $k = 1$, and $k = -1$ stand for 2-torus ($d\theta^2 + d\phi^2$), unit 2-sphere ($d\theta^2 + \sin^2 \theta d\phi^2$), and unit hyperbolic plane ($d\theta^2 + \sinh^2 \theta d\phi^2$), respectively [45]. The metric solution has a curvature singularity at $r = 0$, which becomes naked for $k = 0$. There is an event horizon for $k = \pm 1$ solution expressed as follows [26, 45]:

$$r_h^2 = \frac{1}{6} \left(\sqrt{3(4 - c^2)} - 3c \right). \quad (7)$$

Note that the requirement of $r_h^2 \geq 0$ is conditional on this inequality: $-2 \leq c < 1$. When $c = -2$, the solution becomes extremal. Throughout this study, for simplicity, we consider the choice of $c^2 = k^2 = 1$ for which the solution corresponds to a dS BH. Thus, the metric function f becomes

$$f = 1 - \frac{r_h^2}{r^2}. \quad (8)$$

Thus, at spatial infinity, the Ricci and Kretschmann scalars of the Z0LBH can be found as follows:

$$R = R_\lambda^\lambda \sim \frac{5(c^4 - 2c^2 + 1)}{12r^8}, \quad (9)$$

$$K = R^{\mu\nu\rho\sigma}R_{\mu\nu\rho\sigma} \sim \frac{25(c^4 - 2c^2 + 1)}{12r^8}.$$

By performing the surface gravity calculation [1, 2, 30], we obtain

$$\kappa = \frac{1}{2}. \quad (10)$$

Therefore, the Hawking or BH temperature [30] of the Z0LBH reads

$$\mathcal{T}_H = \frac{\kappa}{2\pi} = \frac{1}{4\pi}. \quad (11)$$

2.1. Mass Computation of Z0LBH via Wald's Entropy Formula. The GR unifies space, time, and gravitation and the gravitational force is represented by the curvature of the spacetime. Energy conservation is a sine qua non in GR as well. Because the metric (5) of Z0LBH represents a non-asymptotically-flat geometry, one should consider the quasi-local mass M_{QL} [27], which measures the density of matter/energy of the spacetime. In this section, we shall employ Wald's entropy calculation [29, 30] and derive M_{QL} using Wald's entropy

formula. To this end, we follow the study of Eune and Kim [28].

Starting with the time-like Killing vector ξ^μ , which describes the symmetry of time translation in a spacetime, Wald's entropy is expressed by [29, 30] as

$$S_{BH} = \frac{2\pi}{\kappa} \int_{\Sigma} d^2x \sqrt{h} \beta, \quad (12)$$

where

$$\begin{aligned} \beta &= \epsilon_{\mu\nu} J^{\mu\nu}, \\ \epsilon_{\mu\nu} &= \frac{1}{2} (n_\mu u_\nu - n_\nu u_\mu). \end{aligned} \quad (13)$$

Here, κ and h are the surface gravity and the induced metric on a hypersurface Σ of the horizon (here 2-sphere with $\sqrt{h} = r_h^2 \sin \theta$), respectively. u_μ is the four-vector velocity defined as the proper velocity of a fiducial observer moving along the orbit of $\xi^\mu = \gamma(\partial/\partial t)$ (where γ is a normalization constant), which must satisfy $g_{\mu\nu} \xi^\mu \xi^\nu = -1$ at spatial infinity. Thus, one can immediately see that $\gamma = 1$. $J^{\mu\nu}$ is called the Noether potential [46, 47], which is given by

$$J^{\mu\nu} = -2\Theta^{\mu\nu\rho\sigma} (\nabla_\rho \xi_\sigma) + 4 (\nabla_\rho \Theta^{\mu\nu\rho\sigma}) \xi_\sigma, \quad (14)$$

with

$$\Theta^{\mu\nu\rho\sigma} = \frac{1}{32} (g^{\mu\rho} g^{\nu\sigma} - g^{\mu\sigma} g^{\nu\rho}). \quad (15)$$

The surface gravity κ can be calculated by [30]

$$\kappa = \lim_{r \rightarrow r_h} \sqrt{\frac{\xi^\mu \nabla_\mu \xi_\nu \xi^\rho \nabla_\rho \xi^\nu}{-\xi^2}} = \frac{1}{2}. \quad (16)$$

To have an outward unit vector n_μ on Σ , the equality $n_\mu n^\mu = 1$ must also be satisfied. Hence, one can get

$$n_r = \frac{1}{n^r} = \frac{2}{\sqrt{(r^2 - r_h^2)}}. \quad (17)$$

On the contrary, u_μ is the four-vector velocity and is given by

$$u^\mu = \frac{1}{\alpha} \xi^\mu, \quad (18)$$

with

$$\alpha = \sqrt{-\xi^\mu \xi_\mu}. \quad (19)$$

Therefore, the nonzero components of $\epsilon_{\mu\nu}$ are found to be

$$\epsilon_{tr} = -\epsilon_{rt} = -\frac{1}{r}. \quad (20)$$

In sequel, the four-vector velocity reads

$$u^t = \frac{r}{\sqrt{r^2 - r_h^2}}. \quad (21)$$

The nonzero components of $\Theta^{\mu\nu\rho\sigma}$ (15) are obtained as follows:

$$\begin{aligned} \Theta^{trtr} &= \Theta^{trrt} = -\Theta^{trrt} = -\Theta^{rttr} = \frac{-r^2}{128\pi}, \\ \Theta^{\theta r \theta r} &= \Theta^{r \theta r \theta} = -\Theta^{\theta r r \theta} = -\Theta^{r \theta \theta r} = \frac{r^2 - r_h^2}{128\pi r^2}, \\ \Theta^{\phi r \phi r} &= \Theta^{r \phi r \phi} = -\Theta^{\phi r r \phi} = -\Theta^{r \phi \phi r} = \frac{r^2 - r_h^2}{128\pi r^2 \sin^2 \theta}, \\ \Theta^{\theta \phi \theta \phi} &= \Theta^{\phi \theta \phi \theta} = -\Theta^{\theta \phi \phi \theta} = -\Theta^{\phi \theta \theta \phi} = \frac{1}{32\pi r^4 \sin^2 \theta}, \\ \Theta^{t \phi t \phi} &= \Theta^{\phi t \phi t} = -\Theta^{t \phi t \phi} = -\Theta^{\phi t t \phi} \\ &= \frac{-1}{32\pi (r^2 - r_h^2) \sin^2 \theta}, \\ \Theta^{t \theta t \theta} &= \Theta^{\theta t \theta t} = -\Theta^{t \theta t \theta} = -\Theta^{\theta t t \theta} = \frac{-1}{32\pi (r^2 - r_h^2)}. \end{aligned} \quad (22)$$

One can verify that $\nabla_\rho \Theta^{\mu\nu\rho\sigma} = 0$. The latter result yields that the second term of the Noether potential vanishes. Therefore, we have

$$J^{\mu\nu} = -2\Theta^{\mu\nu\rho\sigma} (\nabla_\rho \xi_\sigma) = -2\Theta^{\mu\nu\rho\sigma} C_{\rho\sigma}, \quad (23)$$

The nonzero components of $C_{\rho\sigma} = \nabla_\rho \xi_\sigma$ are as follows:

$$C_{tr} = -C_{rt} = -\frac{r_h^2}{r^3}. \quad (24)$$

After substituting those findings into (14), we find the nonzero components of the Noether potential:

$$J^{tr} = -J^{rt} = \frac{-r_h^2}{32\pi}. \quad (25)$$

Thus, from (20) and (25), β is found as

$$\beta = \frac{r_h^2}{16r^2\pi}, \quad (26)$$

and, in sequel computing the entropy through the integral formulation (12), we obtain

$$\mathcal{S} = \pi r_h^2 = \frac{\mathcal{A}_h}{4}. \quad (27)$$

The above result is fully consistent with the Bekenstein-Hawking entropy. The quasi-local mass M_{QL} can be derived from this entropy by integrating the first law of thermodynamics $dM_{QL} = \mathcal{T}_{\mathcal{H}} dS_{BH}$. After some manipulation, one easily finds the following result:

$$M_{QL} = \frac{r_h^2}{4}, \quad (28)$$

which matches with the quasi-local mass computation of Brown and York [27].

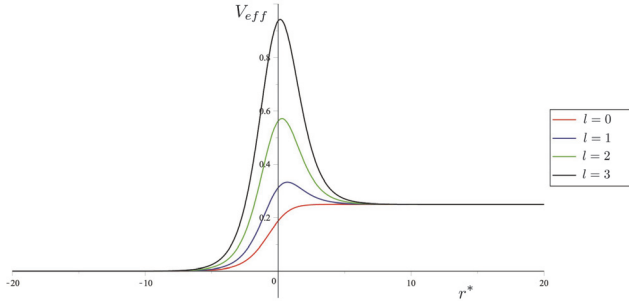


FIGURE 1: Effective potential versus tortoise coordinate graph for various orbital quantum numbers.

3. QNMs and Spectroscopy of ZOLBH

In this section, we shall study the QNMs and the entropy of a perturbed ZOLBH via MM [9]. QNMs of a considered BH can be derived by solving the eigenvalue problem of the KGE with the proper boundary conditions. The boundary condition at the horizon implies that there are no outgoing waves at the event horizon (i.e., only ingoing waves carry the QNMs at the event horizon) and the boundary condition at spatial infinity imposes that only outgoing waves are allowed to survive at spatial infinity. The second boundary condition is appropriate for bumpy shape effective potential that dies off at the two ends. Yet, as seen in (36) and shown in Figure 1, the potential never terminates at spatial infinity; instead it diverges for very massive ($m \rightarrow \infty$) scalar particles. Thus, the potential blocks the waves that come off from the BH and prevents them from reaching spatial infinity. Hence, in this section, we will consider the very massive scalar particles and employ the particular method of [23, 32–35], in which only the QNMs are defined to be those for which one has purely ingoing plane wave at the horizon and no wave at spatial infinity (see (44)). Namely, we will find the QNMs of the ZOLBH using their NH boundary condition. For this purpose, we first consider the massive KGE:

$$\frac{1}{\sqrt{-g}} \partial_\mu (\sqrt{-g} g^{\mu\nu} \partial_\nu) \Psi - m^2 \Psi = 0, \quad (29)$$

where Ψ adopts the ansatz for the above wave equation chosen as

$$\Psi = \frac{1}{r} F(r) e^{i\omega t} Y_{lm}(\theta, \phi), \quad (30)$$

in which $F(r)$ is the function of r and $Y_{lm}(\theta, \phi)$ represents the spherical harmonics with the eigenvalues $-l(l+1)$ and m . After performing some straightforward calculations, the radial part of the KGE reduces to a SLE [31]:

$$\left[-\frac{d}{dr^{*2}} + V_{eff} \right] F(r) = \omega^2 F(r), \quad (31)$$

where V_{eff} and r^* are called the effective potential and the tortoise coordinate, respectively. The tortoise coordinate r^* can be found by the following integral:

$$r^* = 2 \int \frac{dr}{rf}, \quad (32)$$

which results in

$$r^* = \ln \left(\frac{r^2}{r_h^2} - 1 \right). \quad (33)$$

One may check that the limits of r^* admit the following:

$$\begin{aligned} \lim_{r \rightarrow r_h} r^* &= -\infty, \\ \lim_{r \rightarrow \infty} r^* &= \infty. \end{aligned} \quad (34)$$

The effective potential seen in (33) is obtained as

$$V_{eff} = f \left\{ \frac{l(l+1)}{r^2} + \frac{1}{4} \left[f + r \frac{df}{dr} \right] + m^2 \right\}, \quad (35)$$

which admits these limits:

$$\begin{aligned} \lim_{r \rightarrow r_h} V_{eff}(r) &= 0, \\ \lim_{r \rightarrow \infty} V_{eff}(r) &= m^2 + \frac{1}{4}. \end{aligned} \quad (36)$$

It is clear that, for any constant m , the potential is finite at infinite radius (see Figure 1). The potential diverges when the scalar particle is very massive. In other words, the waves tend to cease as $m \rightarrow \infty$.

3.1. Entropy/Area Spectra of ZOLBH. In this section, we shall nudge (perturb) the ZOLBH by the massive scalar fields propagating near the event horizon and read their corresponding QNM frequencies.

We can expand ZOLBH's metric function f to a series around r_h and express it in terms of the surface gravity κ as

$$f = f(r_h) + f'(r_h)(r - r_h) + O[(r - r_h)^2] \approx 2\kappa y, \quad (37)$$

where $y = r - r_h$ and prime ($'$) denotes the derivative with respect to r . After substituting (37) into (35) and performing Taylor expansion, the NH form of the effective potential is obtained as

$$\begin{aligned} V &= 4\kappa G y \left[G^2 (1 - 2Gy) l(l+1) + \kappa (1 + 2Gy) + m^2 \right], \end{aligned} \quad (38)$$

with the parameter $G = 1/r_h$. The tortoise coordinate in the NH region becomes $r^* \approx (1/2\kappa) \ln y$, which enables us to find the NH form of the one-dimensional SLE:

$$\left[-4\kappa^2 y \left(y \frac{d^2}{dy^2} + \frac{d}{dy} \right) + V - \omega^2 \right] F(y) = 0. \quad (39)$$

The solutions to the above equation can be expressed in terms of the CH functions of the first and second kinds [36] as follows:

$$F(y) = y^{i\omega/2\kappa} e^{-z/2} [C_1 M(a, b, z) + C_2 U(a, b, z)], \quad (40)$$

with the parameters

$$\begin{aligned} a &= \frac{\lambda}{\sqrt{\delta}} + \frac{b}{2}, \\ b &= 1 + i\frac{\omega}{\kappa}, \\ z &= 2iG\sqrt{\delta}y, \end{aligned} \quad (41)$$

where

$$\begin{aligned} \lambda &= \frac{1}{2} \left\{ 1 + \frac{1}{\kappa} \left[l(l+1)G^2 + m^2 \right] \right\}, \\ \delta &= 2 \left[l(l+1) \frac{G^2}{\kappa} - 1 \right]. \end{aligned} \quad (42)$$

With the aid of the limiting forms of the CH functions [36], one can find the NH limit of solution (40) as

$$\begin{aligned} F(y) &\sim \left[C_1 + C_2 \frac{\Gamma(1-b)}{\Gamma(1+a-b)} \right] y^{i\omega/2\kappa} \\ &\quad + C_2 \frac{\Gamma(b-1)}{\Gamma(a)} y^{-i\omega/2\kappa}. \end{aligned} \quad (43)$$

We can alternatively represent (43) in terms of r^* ($y \approx e^{2\kappa r^*}$). Thus, the NH ingoing and outgoing waves are distinguished:

$$\begin{aligned} \Psi &\sim \left[C_1 + C_2 \frac{\Gamma(1-b)}{\Gamma(1+a-b)} \right] e^{i\omega(t+r^*)} \\ &\quad + C_2 \frac{\Gamma(b-1)}{\Gamma(a)} e^{i\omega(t-r^*)}. \end{aligned} \quad (44)$$

For QNMs, imposing the boundary conditions that the outgoing waves must vanish at the horizon and no wave at the spatial infinity, that is,

$$F(r^*)_{QNM} \sim \begin{cases} e^{i\omega r^*} & \text{at } r^* \rightarrow -\infty \\ 0 & \text{at } r^* \rightarrow \infty, \end{cases} \quad (45)$$

the solution having coefficient C_2 should be terminated. By using the pole structure of the Gamma function for the denominator of the second term, the outgoing waves vanish for $a = -n$ ($n = 0, 1, 2, \dots$). The latter remark yields the frequencies of the QNMs of the ZOLBH as

$$\omega_n = 2\kappa \left[\left(n + \frac{1}{2} \right) i + \frac{\lambda}{\sqrt{\delta}} \right], \quad (46)$$

where n is known as the overtone quantum number [48]. Accordingly, the transition frequency between two highly excited subsequent states ($\omega_I \gg \omega_R$) is easily obtained as follows:

$$\Delta\omega \approx \Delta\omega_I = 2\kappa = \frac{4\pi\mathcal{T}_{\mathcal{H}}}{\hbar}. \quad (47)$$

Subsequently, using the adiabatic invariant quantity (3) and Bohr-Sommerfeld quantization rule,

$$I_{adb} = \frac{\hbar}{4\pi} \int \frac{dM}{\mathcal{T}_{\mathcal{H}}} = \frac{\hbar}{4\pi} S_{BH} = \hbar n, \quad (48)$$

we can read the entropy/area spectra of the ZOLBH as follows:

$$S_{BHn} = \frac{\mathcal{A}_n}{4\hbar} = 4\pi n, \quad \mathcal{A}_n = 16\pi\hbar n. \quad (49)$$

Therefore, the minimum spacing of the BH area becomes

$$\Delta\mathcal{A}_{\min} = 16\pi\hbar. \quad (50)$$

Our finding is in agreement with Bekenstein's conjecture [7], and the equispacing of the entropy/area spectra of the ZOLBH supports Kothawala et al.'s hypothesis [21], which states that BHs should have equally spaced area spectrum in Einstein's gravity theory.

4. Conclusions

In this work, the quantum spectra of the ZOLBH were studied using the MM, which is based on the adiabatic invariant quantity (3). After separating the radial and angular parts of the massive KGE on the ZOLBH background, we have found the SLE (31) and its corresponding effective potential (35). We have checked the behaviors of the potential around horizon and at the spatial infinity [see (36)]. In addition, we have depicted the effective potential for different values and have shown that the potential never terminates at the spatial infinity. The SLE associated with the ZOLBH is approximated to a CH differential equation. We have derived QNMs of the ZOLBH using the pole feature of the Gamma functions. The MM is applied for the highly excited modes ($n \rightarrow \infty$) and the entropy/area spectra are calculated. Both spectra are evenly spaced and independent of the parameters of the BH as expected. On the contrary, we obtained different area equispacing with dimensionless constant $\epsilon = 16\pi$ in comparison to the usual value ($\epsilon = 8\pi$ [9–11]). However, as shown by Hod [17], the spacing between two adjacent levels might be different depending on which method is applied for studying the BH quantization. Besides, our findings are in agreement with both Bekenstein's conjecture [7] and Wei et al. and Kothawala et al.'s studies [21, 49].

In addition, M_{QL} of the ZOLBH is also investigated via Wald's entropy formula (12) by integrating the total energy (mass). The result obtained is in agreement with the BH thermodynamics [50]. Our next target is to study the Dirac QNMs of the 4-dimensional ZOLBH and analyze the spin effect on the area/entropy quantization.

Data Availability

No data were used to support this study.

Conflicts of Interest

The authors declare that they have no conflicts of interest.

References

- [1] S. W. Hawking, "Black hole explosions?" *Nature*, vol. 248, no. 5443, pp. 30–31, 1974.
- [2] S. W. Hawking, "Particle creation by black holes," *Communications in Mathematical Physics*, vol. 46, no. 2, 206 pages, 1976.
- [3] J. D. Bekenstein, "Black holes and the second law," *Lettere Al Nuovo Cimento Series 2*, vol. 4, no. 15, pp. 737–740, 1972.
- [4] J. D. Bekenstein, "Black holes and entropy," *Physical Review D: Particles, Fields, Gravitation and Cosmology*, vol. 7, pp. 2333–2346, 1973.
- [5] J. D. Bekenstein, "The quantum mass spectrum of the Kerr black hole," *Lettere Al Nuovo Cimento Series 2*, vol. 11, no. 9, pp. 467–470, 1974.
- [6] J. D. Bekenstein, "Quantum Black Holes as Atoms," in *Proceedings of the Eight Marcel Grossmann Meeting*, T. Piran and R. Ruffini, Eds., pp. 92–111, World Scientific Singapore, 1999.
- [7] J. D. Bekenstein, *Cosmology and Gravitation*, M. Novello, Ed., Atlantisciences, France, 2000.
- [8] P. Ehrenfest, "A mechanical theorem of Boltzmann and its relation to the theory of energy quanta," in *Proceedings of the Amsterdam Academy*, vol. 16, p. 591, 1913.
- [9] M. Maggiore, "Physical interpretation of the spectrum of black hole quasinormal modes," *Physical Review Letters*, vol. 100, no. 14, Article ID 141301, 4 pages, 2008.
- [10] E. C. Vagenas, "Area spectrum of rotating black holes via the new interpretation of quasinormal modes," *Journal of High Energy Physics*, vol. 0811, no. 073, 2008.
- [11] A. J. M. Medved, "On the Kerr quantum area spectrum," *Classical and Quantum Gravity*, vol. 25, no. 20, Article ID 205014, 2008.
- [12] G. Gua, "Area spectra of extreme Kerr and nearly extreme Kerr-Newmann black holes from quasinormal modes," *General Relativity and Gravitation*, vol. 45, no. 9, pp. 1711–1721, 2013.
- [13] G. Kunstatter, " d -dimensional black hole entropy spectrum from quasinormal modes," *Physical Review Letters*, vol. 90, Article ID 161301, 2003.
- [14] Y. Kwon and S. Nam, "Quantization of entropy spectra of black holes," *International Journal of Modern Physics D: Gravitation, Astrophysics, Cosmology*, vol. 22, no. 2, Article ID 1330001, 19 pages, 2013.
- [15] L. D. Landau and E. M. Lifshitz, *Course of Theoretical Physics Quantum Mechanics*, Oxford Press, 1972.
- [16] S. Hod, "Bohr's correspondence principle and the area spectrum of quantum black holes," *Physical Review Letters*, vol. 81, no. 20, pp. 4293–4296, 1998.
- [17] S. Hod, "Rotating traversable wormholes," *Physical Review D*, vol. 59, Article ID 024014, 1998.
- [18] R. M. Corless, G. H. Gonnet, D. E. G. Hare, and D. E. Knuth, "On the Lambert W function," *Advances in Computational Mathematics*, vol. 5, no. 1, pp. 329–359, 1996.
- [19] S. Fernando, "Null geodesics of charged black holes in string theory," *Physical Review D: Particles, Fields, Gravitation and Cosmology*, vol. 85, Article ID 024033, 2012.
- [20] W. Li, L. Xu, and J. Lu, "Area spectrum of near-extremal sds black holes via the new interpretation of quasinormal modes," *Physics Letters B*, vol. 676, p. 177, 2009, <http://arxiv.org/abs/1004.2606>.
- [21] D. Kothawala, T. Padmanabhan, and S. Sarkar, "Is gravitational entropy quantized?" *Physical Review D: Particles, Fields, Gravitation and Cosmology*, vol. 78, no. 10, Article ID 104018, 5 pages, 2008.
- [22] A. López-Ortega, "Area spectrum of the D-dimensional de Sitter spacetime," *Physics Letters B*, vol. 682, no. 1, pp. 85–88, 2009.
- [23] I. Sakalli, "Quantization of higher-dimensional linear dilation black hole area/entropy from quasinormal modes," *International Journal of Modern Physics A*, vol. 26, no. 13, pp. 2263–2269, 2011.
- [24] I. Sakalli, "Quasinormal modes of charged dilaton black holes and their entropy spectra," *Modern Physics Letters A*, vol. 28, no. 27, Article ID 1350109, 10 pages, 2013.
- [25] I. Sakalli and G. Tokgoz, "Spectroscopy of rotating linear dilaton black holes from boxed quasinormal modes," *Annals of Physics*, vol. 528, p. 612, 2016.
- [26] H. Lü, Y. Pang, C. N. Pope, and J. F. Vázquez-Poritz, "AdS and Lifshitz black holes in conformal and Einstein-Weyl gravities," *Physical Review D: Particles, Fields, Gravitation and Cosmology*, vol. 86, no. 4, Article ID 044011, 2012.
- [27] J. D. Brown and J. W. York Jr., "Quasilocal energy and conserved charges derived from the gravitational action," *Physical Review D: Particles, Fields, Gravitation and Cosmology*, vol. 47, no. 4, pp. 1407–1419, 1993.
- [28] M. Eune and W. Kim, "Entropy and temperatures of Nariai black hole," *Physics Letters. B. Particle Physics, Nuclear Physics and Cosmology*, vol. 723, no. 1–3, pp. 177–181, 2013.
- [29] R. M. Wald, "Black hole entropy is the Noether charge," *Physical Review D: Particles, Fields, Gravitation and Cosmology*, vol. 48, no. 8, pp. R3427–R3431, 1993.
- [30] R. M. Wald, *General Relativity*, University of Chicago Press, 1984.
- [31] S. Chandrasekhar, *The Mathematical Theory of Black Holes*, The Clarendon Press, New York, NY, USA, 1983.
- [32] B. R. Majhi, "Hawking radiation and black hole spectroscopy in Hořava–Lifshitz gravity," *Physics Letters B*, vol. 686, no. 1, pp. 49–54, 2010.
- [33] M. R. Setare and D. Momeni, "Spacing of the entropy spectrum for KS black hole in Hořava-Lifshitz gravity," *Modern Physics Letters A*, vol. 26, no. 2, pp. 151–159, 2011.
- [34] A. J. Medved, D. Martin, and M. Visser, "Dirty black holes: quasinormal modes for squeezed horizons," *Classical and Quantum Gravity*, vol. 21, no. 9, pp. 2393–2405, 2004.
- [35] T. Padmanabhan, "Quasi-normal modes: a simple derivation of the level spacing of the frequencies," *Classical and Quantum Gravity*, vol. 21, no. 1, pp. L1–L6, 2004.
- [36] M. Abramowitz and I. A. Stegun, *Handbook of Mathematical Functions, with Formulas, Graphs, and Mathematical Tables*, Dover, New York, NY, USA, 1972.
- [37] H. M. Murad and N. Pant, "A class of exact isotropic solutions of Einstein's equations and relativistic stellar models in general relativity," *Astrophysics and Space Science*, vol. 350, no. 1, pp. 349–359, 2014.
- [38] I. Sakalli, "Analytical solutions in rotating linear dilaton black holes: resonant frequencies, quantization, greybody factor, and Hawking radiation," *Physical Review D: Particles, Fields, Gravitation and Cosmology*, vol. 94, no. 8, 084040, 12 pages, 2016.
- [39] A. Lopez-Ortega, "Entropy spectra of single horizon black holes in two dimensions," *International Journal of Modern Physics D: Gravitation, Astrophysics, Cosmology*, vol. 20, no. 13, pp. 2525–2542, 2011.
- [40] B. Cuadros-Melgar, J. de Oliveira, and C. E. Pellicer, "Stability analysis and area spectrum of three-dimensional Lifshitz black holes," *Physical Review D: Particles, Fields, Gravitation and Cosmology*, vol. 85, no. 2, 2012.

- [41] S. Kachru, X. Liu, and M. Mulligan, "Gravity duals of Lifshitz-like fixed points," *Physical Review D: Particles, Fields, Gravitation and Cosmology*, vol. 78, no. 10, Article ID 106005, 8 pages, 2008.
- [42] S. A. Hartnoll, J. Polchinski, E. Silverstein, and D. Tong, "Towards strange metallic holography," *Journal of High Energy Physics*, vol. 2010, no. 4, 2010.
- [43] R. G. Cai, Y. Liu, and Y. W. Sun, "On the $z=4$ Horava-Lifshitz Gravity," *High Energy Physics - Theory*, 2009.
- [44] M. Catalan, E. Cisternas, P. A. Gonzalez, and Y. Vasquez, "Quasinormal modes and greybody factors of a four-dimensional Lifshitz black hole with $z=0$," *General Relativity and Quantum Cosmology*, 2014.
- [45] F. Herrera and Y. Vásquez, "AdS and Lifshitz black hole solutions in conformal gravity sourced with a scalar field," *Physics Letters B*, 2017, arXiv.
- [46] G. L. Cardoso, B. de Wit, and T. Mohaupt, "Deviations from the area law for supersymmetric black holes," *Fortschritte der Physik*, vol. 48, no. 1-3, pp. 49–64, 2000.
- [47] M. K. Parikh and S. Sarkar, "Beyond the Einstein Equation of State: Wald Entropy and Thermodynamical Gravity," *High Energy Physics - Theory*, 2009, High Energy Physics - Theory.
- [48] S. Hod, "Kerr-Newman black holes with stationary charged scalar clouds," *Physical Review D: Particles, Fields, Gravitation and Cosmology*, vol. 90, Article ID 024051, 2014.
- [49] S.-W. Wei, Y.-X. Liu, K. Yang, and Y. Zhong, "Entropy/area spectra of the charged black hole from quasinormal modes," *Physical Review D: Particles, Fields, Gravitation and Cosmology*, vol. 81, Article ID 104042, 2010.
- [50] R. B. Mann, *Black holes: thermodynamics, information, and firewalls*, SpringerBriefs in Physics, Springer, Cham, 2015.

Research Article

Thermodynamic Volume Product in Spherically Symmetric and Axisymmetric Spacetime

Parthapratim Pradhan 

Department of Physics, Hiralal Mazumdar Memorial College for Women, Dakshineswar, Kolkata 700035, India

Correspondence should be addressed to Parthapratim Pradhan; pppradhan77@gmail.com

Received 6 March 2018; Revised 14 May 2018; Accepted 21 May 2018; Published 13 June 2018

Academic Editor: Farook Rahaman

Copyright © 2018 Parthapratim Pradhan. This is an open access article distributed under the Creative Commons Attribution License, which permits unrestricted use, distribution, and reproduction in any medium, provided the original work is properly cited. The publication of this article was funded by SCOAP³.

We have examined the thermodynamic volume products for spherically symmetric and axisymmetric spacetime in the framework of *extended phase space*. Such volume products are usually formulated in terms of the outer horizon (\mathcal{H}^+) and the inner horizon (\mathcal{H}^-) of black hole (BH) spacetime. Besides volume product, the other thermodynamic formulations like *volume sum*, *volume minus*, and *volume division* are considered for a wide variety of spherically symmetric spacetime and axisymmetric spacetime. Like area (or entropy) product of multihorizons, the mass-independent (universal) features of volume products sometimes also *fail*. In particular, for a spherically symmetric AdS spacetime, the simple thermodynamic volume product of \mathcal{H}^\pm is not mass-independent. In this case, more complicated combinations of outer and inner horizon volume products are indeed mass-independent. For a particular class of spherically symmetric cases, i.e., Reissner Nordström BH of Einstein gravity and Kehagias-Sfetsos BH of Hořava Lifshitz gravity, the thermodynamic volume products of \mathcal{H}^\pm are indeed *universal*. For axisymmetric class of BH spacetime in Einstein gravity, all the combinations are *mass-dependent*. There has been no chance to formulate any combinations of volume product relation to be mass-independent. Interestingly, *only the rotating BTZ black hole* in 3D provides that the volume product formula is mass-independent, i.e., *universal*, and hence it is quantized.

1. Introduction

It has been examined by a number of researchers that the area (or entropy) product of various spherically symmetric and axisymmetric BHs are mass-independent (universal) [1–9]. For instance, Ansorg and Hennig [1] demonstrated that for a stationary and axisymmetric class of Einstein-Maxwell gravity the area product formula satisfied the universal relation as

$$\mathcal{A}_h \mathcal{A}_c = (8\pi J)^2 + (4\pi Q^2)^2. \quad (1)$$

\mathcal{A}_h and \mathcal{A}_c are area of outer horizon (OH) or event horizon (EH) and inner horizon (IH) or Cauchy horizon (CH). The parameters, J and Q , are denoted as the angular momentum and charge of the black hole (BH), respectively.

On the other hand, Cvetič et al. [2] extended this work for a higher dimensions spacetime and showed that

for multihorizon BHs the area product formula should be quantized by satisfying the following relation:

$$\mathcal{A}_h \mathcal{A}_c = (8\pi \ell_{pl}^2)^2 N, \quad N \in \mathbb{N}. \quad (2)$$

ℓ_{pl} is the Planck length. This relation indicates that the product relation is indeed universal in nature. This is a very fascinating topic of research since 2009.

Aspects of BH thermodynamic properties have started by the seminal work of Hawking and Page [10]; they first proposed that certain type of phase transition occurs between small and large BHs in case of Schwarzschild-AdS BH. This phase transition is now called the famous Hawking-Page phase transition. For a charged AdS BH, the study of thermodynamic properties is initiated by Chamblin et al. [11, 12], where the authors demonstrated the critical behaviour of Van der Waal like liquid-gas phase transitions. This has

been brought into a new form by Kubizňák and Mann [13] by examining the thermodynamic properties, i.e., $P - V$ criticality of Reissner Nordström AdS BH in the extended phase space. They determined the BH equation of state and computed the critical exponent by using the mean field theory and also computed the other thermodynamic features.

Motivated by the above-mentioned work and our previous investigation [14] in which we have considered the *extended phase space* framework for a wide variety of spherically symmetric AdS spacetime. In the present work, we would like to extend our study for various classes of spherically symmetric BHs and axisymmetric BHs. In the extended phase formalism, the cosmological constant is treated as thermodynamic pressure P and its conjugate variable as thermodynamic volume \mathcal{V} [13, 15–17]. They are defined as

$$P = -\frac{\Lambda}{8\pi} = \frac{3}{8\pi\ell^2}. \quad (3)$$

and

$$\mathcal{V} = \left(\frac{\partial M}{\partial P} \right)_{S,Q,J} \quad (4)$$

The extended phase space is more meaningful than conventional phase space due to the following reasons. The conventional phase space allows the physical parameters like temperature, entropy, charge, and potential, whereas the extended phase space allows the parameters like pressure, volume, and enthalpy (rather than internal energy). In addition to that, the mass parameter should be considered there as enthalpy of the system, which is useful to study the critical behaviour of the thermodynamic system. The BH equation of state could be used to study for comparisons with the classical thermodynamic equation of state (Van der-Waal equation). Once the BH thermodynamic equation of state is in hand, then one may compute different thermodynamic quantities like isothermal compressibility, specific heat at constant pressure, and so forth.

This thermodynamic volume (there are different types of definitions regarding the volume of a BH in the literature; the idea regarding the BH volume was first introduced by Parikh [18]; for other types of definition like dynamical volume and vector volume, see [19–21]; here we are particularly interested regarding the thermodynamic volume [22]) of a spherically symmetric BH and for OH should read

$$\mathcal{V}_h = \frac{4}{3}\pi r_h^3 = \frac{\mathcal{A}_h r_h}{3}. \quad (5)$$

r_h is OH radius. Similarly, this volume for IH should be

$$\mathcal{V}_c = \frac{4}{3}\pi r_c^3 = \frac{\mathcal{A}_c r_c}{3}. \quad (6)$$

It should be noted that the thermodynamic volume of CH can be obtained by using the symmetric properties [14] of OH radius r_h and IH radius r_c , i.e.,

$$\mathcal{V}_c = \mathcal{V}_h|_{r_h \leftrightarrow r_c}. \quad (7)$$

Another important point in the extended phase space is that the ADM mass should be treated as the total enthalpy of the thermodynamic system, i.e., $M = H = U + P\mathcal{V}$, where U is thermal energy of the system [15]. Therefore the first law of BH thermodynamics in this phase space for any spherically symmetric spacetime and for OH should be

$$dH = T_h dS_h + \mathcal{V}_h dP + \Phi_h dQ. \quad (8)$$

The quantities T_h , S_h , and Φ_h are denoted as the BH temperature, entropy, and electric potential of OH. The parameter Q is denoted as the charge of a BH.

Analogously, the first law of BH mechanics for IH should be

$$dH = -T_c dS_c + \mathcal{V}_c dP + \Phi_c dQ. \quad (9)$$

The quantities T_c , S_c , and Φ_c are denoted as the corresponding BH temperature, entropy, and electric potential which could be defined on the IH.

When we add the rotation parameter, the first law of BH thermodynamics in the extended phase space (for axisymmetric spacetime and for OH) becomes

$$dH = T_h dS_h + \mathcal{V}_h dP + \Phi_h dQ + \Omega_h dJ. \quad (10)$$

Ω_h and J are the angular velocity defined on the OH and the angular momentum of BH. For IH, the first law becomes

$$dH = -T_c dS_c + \mathcal{V}_c dP + \Phi_c dQ + \Omega_c dJ. \quad (11)$$

Ω_c is the angular velocity defined on the IH. Using symmetric features of r_h and r_c , one can determine the following thermodynamic relations for IH:

$$\begin{aligned} \mathcal{A}_c &= \mathcal{A}_h|_{r_h \leftrightarrow r_c}, \\ \mathcal{S}_c &= \mathcal{S}_h|_{r_h \leftrightarrow r_c}, \\ \Omega_c &= \Omega_h|_{r_h \leftrightarrow r_c}, \\ \Phi_c &= \Phi_h|_{r_h \leftrightarrow r_c}, \\ T_c &= -T_h|_{r_h \leftrightarrow r_c}, \\ \mathcal{V}_c &= \mathcal{V}_h|_{r_h \leftrightarrow r_c}. \end{aligned} \quad (12)$$

However in this work, we wish to extend our study by computing the volume product, volume sum, volume minus, and volume division in the *extended phase space* for various spherically symmetric BHs and axisymmetric BHs (including the various AdS spacetime). By evaluating these quantities we prove that for a spherically symmetric AdS spacetime the simple volume product is *not* mass-independent. In this case, somewhat complicated combination of volume functional relations of OH and IH are indeed mass-independent. For instance, we have derived the mass-independence volume functional relation for RN-AdS BH as

$$f(\mathcal{V}_h, \mathcal{V}_c) = \ell^2, \quad (13)$$

where

$$f(\mathcal{V}_h, \mathcal{V}_c) = \left(\frac{3}{32\pi}\right)^{1/3} \frac{(8\pi\ell^2 Q^2/3)}{(\mathcal{V}_h \mathcal{V}_c)^{1/3}} - \left(\frac{3}{4\pi}\right)^{2/3} \left[\mathcal{V}_h^{2/3} + \mathcal{V}_c^{2/3} + (\mathcal{V}_h \mathcal{V}_c)^{1/3}\right]. \quad (14)$$

For simple Reissner Nordström BH (which is a spherically symmetric solution of Einstein equation) of Einstein gravity and Kehagias-Sfetsos BH of Hořava Lifshitz gravity, the thermodynamic volume products of \mathcal{H}^\pm are mass-independent. Therefore they behave as a universal character by its own features. Moreover, we have derived the thermodynamic volume functional relation for Hořava Lifshitz-AdS BH and phantom AdS BH. The phantom fields are exotic because they were produced via negative energy density. Furthermore we have derived volume functional relation for regular BH. Regular BH is a kind of BH which is free from a curvature singularity.

Whereas for axisymmetric class of BHs including AdS spacetime there has been no chance to formulate any possible combinations of thermodynamic volume product to be mass-independent, it should be noted that, for a KN-AdS BH, there may be a possibility of formulating the area (or entropy) product relations to be mass-independent. The reason is that, for a simple Kerr BH, the area (or entropy) product is universal, i.e., mass-independent, while the *volume product* is not! This is because the thermodynamic volume is proportional to the spin parameter. That is why *there has been no chance to produce any combinations of volume product of \mathcal{H}^\pm to be mass-independent*. Therefore the axisymmetric BHs show *no* universal behaviour for volume products. Interestingly, only rotating BTZ BH shows the mass-independent feature. Thus *only* axisymmetric BHs in 3D provided the universal character of thermodynamic volume product.

In our previous investigation [8, 9], we computed the BH area (or entropy) products, BH temperature products, Komar energy products, and specific heat products for various classes of BHs. Besides the area (or entropy) product, it should be important to study whether the thermodynamic *volume product, volume sum, volume minus, and volume division* for all the horizons are universal or not and whether they should be quantized or not. This is the main motivation behind this work.

The structure of the paper is as follows. In Section 2, we shall compute the various thermodynamic volume products for spherically symmetric BHs and conclude that the product is mass-independent. In Section 3, we compute various thermodynamic volume products for axisymmetric spacetime and conclude that the product is mass-dependent. Interestingly, for the spinning BTZ BH, the said volume product is *mass-independent*.

2. Spherically Symmetric BH

In this section, we would consider various spherically symmetric BHs.

2.1. Reissner Nordström BH. We begin with charged BH with zero cosmological constant which is a solution of Einstein equation. The metric form is given by

$$ds^2 = -\mathcal{Z}(r) dt^2 + \frac{dr^2}{\mathcal{Z}(r)} + r^2 d\Omega_2^2, \quad (15)$$

where

$$\mathcal{Z}(r) = 1 - \frac{2M}{r} + \frac{Q^2}{r^2}, \quad (16)$$

and $d\Omega_2^2$ is metric on the unit sphere in two dimensions.

The OH (there are several definitions of horizons for a static spherically symmetric spacetime; we have used Killing horizons for computations of thermodynamic volume) radius and IH radius read

$$r_h = M + \sqrt{M^2 - Q^2} \quad (17)$$

$$r_c = M - \sqrt{M^2 - Q^2}. \quad (18)$$

M and Q denote the mass and charge of BH, respectively. When $M^2 > Q^2$, it describes a BH; otherwise it has a naked singularity. The thermodynamic volume for OH and IH should read

$$\mathcal{V}_h = \frac{4}{3}\pi r_h^3 \quad (19)$$

$$\mathcal{V}_c = \frac{4}{3}\pi r_c^3. \quad (20)$$

The thermodynamic volume (in the limit $Q = 0$, one obtains the thermodynamic volume for Schwarzschild BH; since in this case the BH has only OH located at $r_h = 2M$, therefore the volume should be $\mathcal{V}_h = (32/3)\pi M^3$; thus for an isolated Schwarzschild BH, the thermodynamic volume should be mass-dependent; therefore it is not universal and not quantized in nature by its own character) product for OH and IH should be

$$\mathcal{V}_h \mathcal{V}_c = \frac{16}{9}\pi^2 Q^6. \quad (21)$$

It is indeed mass-independent; thus it is universal in character and it is also quantized.

The volume sum for OH and IH is calculated to be

$$\mathcal{V}_h + \mathcal{V}_c = \frac{32}{3}\pi M^3 \left(1 - \frac{3}{4} \frac{Q^2}{M^2}\right). \quad (22)$$

Similarly, one can compute the volume minus for OH and IH as

$$\mathcal{V}_h - \mathcal{V}_c = \frac{32}{3}\pi M^2 \sqrt{M^2 - Q^2} \left(1 - \frac{Q^2}{4M^2}\right), \quad (23)$$

and the volume division should be

$$\frac{\mathcal{V}_h}{\mathcal{V}_c} = \left(\frac{M + \sqrt{M^2 - Q^2}}{M - \sqrt{M^2 - Q^2}}\right)^3. \quad (24)$$

It follows from the calculation that all these quantities are mass-dependent so they are not universal in nature by its own right. From (23) and (24), we can easily see that, in the extremal limit $M^2 = Q^2$, one obtains $\mathcal{V}_h = \mathcal{V}_c$. This is a new condition of extreme limit in spherically symmetric cases.

2.2. Hořava Lifshitz BH. In this section, we would briefly review the UV complete theory of gravity which is a nonrelativistic renormalizable theory of gravity known as Hořava Lifshitz [23–25] gravity. It reduces to Einstein's gravity at large scales for the value of dynamical coupling constant $\lambda = 1$. Using ADM formalism, one could write the metric as

$$ds^2 = -N^2 dt^2 + g_{ij} (dx^i - N^i dt) (dx^j - N^j dt). \quad (25)$$

In addition for a spacelike hypersurface with a fixed time the extrinsic curvature K_{ij} is given by

$$K_{ij} = \frac{1}{2N} (\dot{g}_{ij} - \nabla_i N_j - \nabla_j N_i). \quad (26)$$

A dot represents a derivative with respect to t . The generalized action for Hořava Lifshitz could be written as

$$\begin{aligned} S = \int dt d^3x \sqrt{g} N \left[\frac{2}{\kappa^2} (K_{ij} K^{ij} - \lambda K^2) \right. \\ \left. + \frac{\kappa^2 \mu^2 (\Lambda_w R - 3\Lambda_w^2)}{8(1-3\lambda)} + \frac{\kappa^2 \mu^2 (1-4\lambda)}{32(1-3\lambda)} R^2 \right. \\ \left. - \frac{\kappa^2}{2w^4} \left(C_{ij} - \frac{\mu w^2}{2} R_{ij} \right) \left(C^{ij} - \frac{\mu w^2}{2} R^{ij} \right) + \mu^4 R \right]. \end{aligned} \quad (27)$$

Here κ^2 , λ , μ , w , and Λ are the constant parameters and the cotton tensor, C_{ij} , is defined to be

$$C^{ij} = \epsilon^{ikl} \nabla_k \left(R_l^j - \frac{1}{4} \epsilon^{ikj} \partial_k R \right). \quad (28)$$

As compared with Einstein's general relativity, one could obtain the speed of light, Newtonian constant, and the cosmological constant as

$$c = \frac{\kappa^2 \mu}{4} \sqrt{\frac{\Lambda_w}{1-3\lambda}} \quad (29)$$

$$G = \frac{\kappa^2}{32\pi c} \quad (30)$$

$$\Lambda = \frac{3}{2} \Lambda_w, \quad (31)$$

respectively. It should be mentioned here that when $\lambda = 1$, the first three terms in (27) reduce to that one obtains as in Einstein's gravity. It must also be noted that λ is a dynamic coupling constant and for $\lambda > 1/3$, the cosmological constant should be a negative one. However, it could be made a positive one if one could give a following transformation like $\mu \rightarrow i\mu$ and $w^2 \rightarrow -iw^2$. Here we restrict ourselves that the BH

solution is in the limit of $\Lambda_w \rightarrow 0$. That is why, we have to set $N^i = 0$ and to get the spherically symmetric solution we have to choose the metric ansatz as

$$ds^2 = -N^2(r) dt^2 + \frac{dr^2}{g(r)} + r^2 (d\theta^2 + \sin^2\theta d\phi^2). \quad (32)$$

In order to get the spherically symmetric solution, substitute the metric ansatz 32 into the action and one obtains reduced Lagrangian as

$$\begin{aligned} \mathcal{L} = \frac{\kappa^2 \mu^2 N}{8(1-3\lambda)\sqrt{g}} \left[(2\lambda-1) \frac{(g-1)^2}{r^2} - 2\lambda \frac{g-1}{r} g' \right. \\ \left. + \frac{g-1}{2} g'^2 - 2\omega(1-g-r g') \right], \end{aligned} \quad (33)$$

where $\omega = 8\mu^2(3\lambda-1)/\kappa^2$. Here we are interested to investigate the situation $\lambda = 1$, i.e., $\omega = 16\mu^2/\kappa^2$. Then one finds the solution of the metric [26] as

$$N^2(r) = g = 1 - \sqrt{4M\omega r + \omega^2 r^4} + \omega r^2, \quad (34)$$

where M is an integration constant related to the mass parameter. Thus the static, spherically symmetric solution is given by

$$ds^2 = -g(r) dt^2 + \frac{dr^2}{g(r)} + r^2 (d\theta^2 + \sin^2\theta d\phi^2). \quad (35)$$

For $r \gg (M/\omega)^{1/3}$, one gets the usual behaviour of a Schwarzschild BH. The BH horizons correspond to $g(r) = 0$. The OH radius and IH radius should read

$$r_h = M + \sqrt{M^2 - \frac{1}{2\omega}} \quad (36)$$

$$r_c = M - \sqrt{M^2 - \frac{1}{2\omega}}, \quad (37)$$

where M and ω denote the mass and coupling constant of BH, respectively. When $M^2 > 1/2\omega$, it describes a BH and when $M^2 < 1/2\omega$, it describes a naked singularity.

The thermodynamic volume product for KS BH should be

$$\mathcal{V}_h \mathcal{V}_c = \frac{2\pi^2}{9\omega^3}. \quad (38)$$

It indicates that it is mass-independent; therefore it is universal in nature and it also be quantized. We do not calculate other possible combinations because it is clear that these combinations are surely mass-dependent as we have seen in case of RN BH. It should be mentioned that the Smarr formula is satisfied in case of Einstein-Aether theory and some variants of infrared HL gravity [27]. It would be interesting if one could examine what the status of HL gravity is when the extended phase space formalism is applied. It could be found elsewhere.

2.3. Nonrotating BTZ BH. The nonrotating BTZ BH is a solution of Einstein-Maxwell gravity in three spacetime dimensions. The metric form is given by

$$ds^2 = -\left(\frac{r^2}{\ell^2} - M\right)dt^2 + \frac{dr^2}{(r^2/\ell^2 - M)} + r^2 d\phi^2. \quad (39)$$

M is the ADM mass of the BH and $-\Lambda = 1/\ell^2 = 8\pi PG_3$ denotes the cosmological constant. Here we have set $c = \hbar = k = 1$. The BH OH is located at $r_h = \sqrt{8G_3 M \ell}$ (we have already mentioned that in the extended phase space $\ell = \sqrt{3/8\pi P}$; in the subsequent expression, we have to put this condition to obtain the results in terms of thermodynamic pressure). G_3 is 3D Newtonian constant. Interestingly, the thermodynamic volume for 3D static BTZ BH is computed in [17]

$$\mathcal{V}_h = \pi r_h^2 = 8\pi G_3 M \ell^2 \quad (40)$$

This is an isolated case and the thermodynamic volume is mass-dependent; thus it is not quantized as well as it is not universal. $\Lambda = -1/\ell^2$ is cosmological constant.

2.4. Schwarzschild-AdS BH. This BH is a solution of Einstein equation. The form of the metric function is given by

$$\mathcal{Z}(r) = 1 - \frac{2M}{r} + \frac{r^2}{\ell^2}, \quad (41)$$

where $\Lambda = -3/\ell^2$ is cosmological constant. The horizon radii could be calculated from the following equation:

$$r^3 + \ell^2 r - 2M\ell^2 = 0. \quad (42)$$

Among the three roots, only one root is real. Therefore the BH possesses only one physical horizon which is located at

$$r_{h,c} = \frac{1}{2} \sqrt{\frac{1}{3} \left(\frac{x}{2}\right)^{1/3} + \left(\frac{2}{x}\right)^{1/3} \frac{\ell^2 (\ell^2 + 12Q^2)}{3} - \frac{2\ell^2}{3}} \pm \frac{1}{2} \cdot \sqrt{\frac{4M\ell^2}{\sqrt{(1/3)(x/2)^{1/3} + (2/x)^{1/3} \ell^2 (\ell^2 + 12Q^2)/3 - 2\ell^2/3}} - \frac{1}{3} \left(\frac{x}{2}\right)^{1/3} - \left(\frac{2}{x}\right)^{1/3} \frac{\ell^2 (\ell^2 + 12Q^2)}{3} - \frac{4\ell^2}{3}}, \quad (47)$$

where

$$x = 2\ell^6 + 108M^2\ell^4 - 72\ell^4 Q^2 + \sqrt{(2\ell^6 + 108M^2\ell^4 - 72\ell^4 Q^2)^2 - 4\ell^6 (\ell^2 + 12Q^2)^3} \quad (48)$$

The thermodynamic volume product of RN-AdS BH for OH and IH is computed to be

$$r_h = \left(\frac{\ell}{3}\right)^{2/3} \left(9M + \sqrt{3}\sqrt{\ell^2 + 27M^2}\right)^{1/3} - \left(\frac{\ell^4}{3}\right)^{1/3} \frac{1}{(9M + \sqrt{3}\sqrt{\ell^2 + 27M^2})^{1/3}}. \quad (43)$$

The thermodynamic volume is computed to be

$$\mathcal{V}_h = \frac{4}{3} \pi r_h^3 = \frac{4}{3} \cdot \pi \left[\left(\frac{\ell}{3}\right)^{2/3} \left(9M + \sqrt{3}\sqrt{\ell^2 + 27M^2}\right)^{1/3} - \left(\frac{\ell^4}{3}\right)^{1/3} \frac{1}{(9M + \sqrt{3}\sqrt{\ell^2 + 27M^2})^{1/3}} \right]^3. \quad (44)$$

Since it is an isolated case and the thermodynamic volume is mass-dependent, therefore it is not universal nor does it quantized. We do not consider the other AdS spacetime because it has already been discussed in [14].

2.5. RN-AdS BH. For this BH, the metric function is given by

$$\mathcal{Z}(r) = 1 - \frac{2M}{r} + \frac{Q^2}{r^2} + \frac{r^2}{\ell^2}. \quad (45)$$

The horizon radii could be found from the following equation:

$$r^4 + \ell^2 r^2 - 2M\ell^2 r + \ell^2 Q^2 = 0. \quad (46)$$

Among the four roots, two roots are real and two roots are imaginary. Thus the OH and IH radii become

$$\mathcal{V}_h \mathcal{V}_c = \frac{\pi^2}{36} \left[\frac{2}{3} \left(\frac{x}{2}\right)^{1/3} + \left(\frac{2}{x}\right)^{1/3} \frac{2\ell^2 (\ell^2 + 12Q^2)}{3} + \frac{2\ell^2}{3} - \frac{4M\ell^2}{\sqrt{(1/3)(x/2)^{1/3} + (2/x)^{1/3} \ell^2 (\ell^2 + 12Q^2)/3 - 2\ell^2/3}} \right]^3. \quad (49)$$

It is clearly evident from the above expression that the product is strictly mass-dependent. Thus the product is not universal. But below we would like to determine that somewhat complicated function of inner and outer horizon

volume is indeed mass-independent. To proceed it we would like to use Vieta's theorem. Therefore from (46), we get

$$\sum_{i=1}^4 r_i = 0. \quad (50)$$

$$\sum_{1 \leq i < j \leq 4} r_i r_j = \ell^2. \quad (51)$$

$$\sum_{1 \leq i < j < k \leq 4} r_i r_j r_k = 2M\ell^2. \quad (52)$$

$$\prod_{i=1}^4 r_i = \ell^2 Q^2. \quad (53)$$

Hence the mass-independent *volume sum* and *volume product* relations are

$$\sum_{i=1}^4 \mathcal{V}_i^{1/3} = 0. \quad (54)$$

$$\sum_{1 \leq i < j \leq 4} (\mathcal{V}_i \mathcal{V}_j)^{1/3} = \left(\frac{3}{32\pi} \right)^{1/3} \frac{8\pi\ell^2}{3}. \quad (55)$$

$$\prod_{i=1}^4 (\mathcal{V}_i)^{1/3} = \left(\frac{\pi}{6} \right)^{1/3} \frac{8\pi\ell^2 Q^2}{3}. \quad (56)$$

The mass-independent volume functional relations in terms of two horizons are

$$f(\mathcal{V}_h, \mathcal{V}_c) = \ell^2, \quad (57)$$

where

$$\begin{aligned} f(\mathcal{V}_h, \mathcal{V}_c) &= \left(\frac{3}{32\pi} \right)^{1/3} \frac{(8\pi\ell^2 Q^2/3)}{(\mathcal{V}_h \mathcal{V}_c)^{1/3}} \\ &\quad - \left(\frac{3}{4\pi} \right)^{2/3} \left[\mathcal{V}_h^{2/3} + \mathcal{V}_c^{2/3} + (\mathcal{V}_h \mathcal{V}_c)^{1/3} \right]. \end{aligned} \quad (58)$$

These are explicitly mass-independent volume functional relations in the extended phase space.

2.6. Hořava Lifshitz-AdS BH. The metric function for Hořava Lifshitz BH in AdS space [28, 29] is given by

$$\mathcal{Z}(r) = 1 + \left(1 - \frac{2\Lambda}{3\omega} \right) \omega r^2 - \omega r^2 \sqrt{1 - \frac{4\Lambda}{3\omega} + \frac{4M}{\omega r^3}}. \quad (59)$$

The horizon radii could be calculated from the following equation:

$$4r^4 + 2(\omega\ell^2 + 2)\ell^2 r^2 - 4M\omega\ell^4 r + \ell^4 = 0. \quad (60)$$

Similarly, among the four roots, two roots are real and two roots are imaginary. Thus the OH and IH radii become

$$\begin{aligned} r_h &= \frac{(a+b)}{2}, \\ r_c &= \frac{(a-b)}{2}, \end{aligned} \quad (61)$$

where

$$a = \sqrt{\frac{2^{1/3}(\omega^2\ell^8 + 4\omega\ell^6 + 16\ell^4) - (\ell^2/3)(\omega\ell^2 + 2)}{3y^{1/3}}} + \frac{1}{12} \left(\frac{y}{2} \right)^{1/3} \quad (62)$$

$$b = \sqrt{\frac{2M\omega\ell^4}{a} - \frac{1}{12} \left(\frac{y}{2} \right)^{1/3} - \frac{[2^{1/3}(\omega^2\ell^8 + 4\omega\ell^6 + 16\ell^4) + (2/3)\ell^2(\omega\ell^2 + 2)]}{3y^{1/3}}} \quad (63)$$

and

$$\begin{aligned} y &= 1728M^2\omega^2\ell^8 - 576\ell^6(\omega\ell^2 + 2) + 16\ell^6(\omega\ell^2 + 2)^3 \\ &\quad + \sqrt{[1728M^2\omega^2\ell^8 - 576\ell^6(\omega\ell^2 + 2) + 16\ell^6(\omega\ell^2 + 2)^3]^2 - 256\ell^{12}(\omega^2\ell^4 + 4\omega\ell^2 + 16)^3}. \end{aligned} \quad (64)$$

The thermodynamic volume for this BH is quite different from RN-AdS spacetime and it has been calculated in [29]:

$$\mathcal{V}_h = \frac{4}{3}\pi r_h^3 \left[\frac{4}{\ell^2} + \frac{2}{\omega r_h^2} \right] \quad (65)$$

and

$$\mathcal{V}_c = \frac{4}{3}\pi r_c^3 \left[\frac{4}{\ell^2} + \frac{2}{\omega r_c^2} \right]. \quad (66)$$

The volume product is calculated to be

$$\begin{aligned} \mathcal{V}_h \mathcal{V}_c &= \frac{16\pi^2}{9} \left[\frac{2^{4/3} (\omega^2 \ell^8 + 4\omega \ell^6 + 16\ell^4) + (\ell^2/3) (\omega \ell^2 + 2)}{3y^{1/3}} \right. \\ &\quad \left. + \frac{1}{6} \left(\frac{y}{2} \right)^{1/3} - \frac{2M\omega \ell^4}{a} \right] \\ &\times \left[\frac{1}{4\ell^4} \left\{ \frac{2^{4/3} (\omega^2 \ell^8 + 4\omega \ell^6 + 16\ell^4) + (\ell^2/3) (\omega \ell^2 + 2)}{3y^{1/3}} \right. \right. \\ &\quad \left. \left. + \frac{1}{6} \left(\frac{y}{2} \right)^{1/3} - \frac{2M\omega \ell^4}{a} \right\}^2 + \frac{1}{\omega^2} + \frac{1}{\omega \ell^2} \left\{ \frac{2M\omega \ell^4}{a} \right. \right. \\ &\quad \left. \left. - \frac{\ell^2 (\omega \ell^2 + 2)}{3y^{1/3}} \right\} \right]. \quad (67) \end{aligned}$$

From the above expression, we can conclude that the volume product for Hořava Lifshitz BH in AdS space is strictly mass-dependent. Thus this product is not a universal quantity. Below we will derive *more complicated function of inner and outer horizon volume* that is indeed mass-independent. To compute it, we should apply Vieta's theorem. Thus from (60), we find

$$\sum_{i=1}^4 r_i = 0. \quad (68)$$

$$\sum_{1 \leq i < j \leq 4} r_i r_j = \frac{\omega \ell^4}{2} \left(1 + \frac{2}{\omega \ell^2} \right). \quad (69)$$

$$\sum_{1 \leq i < j < k \leq 4} r_i r_j r_k = M\omega \ell^4. \quad (70)$$

$$\sum_{1 \leq i < j < k < l \leq 4} r_i r_j r_k r_l = \frac{\ell^4}{4}. \quad (71)$$

Eliminating the mass parameter in terms of two horizons, one could obtain the following mass-independent volume functional relation:

$$g(\mathcal{V}_h, \mathcal{V}_c) = \frac{\omega \ell^4}{2} \left(1 + \frac{2}{\omega \ell^2} \right), \quad (72)$$

where

$$g(\mathcal{V}_h, \mathcal{V}_c) = \frac{(\ell^4/4)}{r_h r_c} - (r_h^2 + r_c^2 + r_h r_c), \quad (73)$$

where the parameters r_h and r_c could be obtained by solving (65) and (66) in terms of thermodynamic volume as

$$r_h = \frac{1}{2} \left[\left(\frac{u_h}{9} \right)^{1/3} \frac{1}{\omega} - \frac{2\ell^2}{(3u_h)^{1/3}} \right], \quad (74)$$

$$r_c = \frac{1}{2} \left[\left(\frac{u_c}{9} \right)^{1/3} \frac{1}{\omega} - \frac{2\ell^2}{(3u_c)^{1/3}} \right], \quad (75)$$

and

$$\begin{aligned} u_h &= \sqrt{3} \sqrt{8\omega^3 \ell^6 + 27\ell^4 \omega^6 + 27\ell^4 \omega^6 \left(\frac{3V_h}{4\pi} \right)^3} \\ &\quad - 9\ell^2 \omega^3 \left(\frac{3V_h}{4\pi} \right), \end{aligned} \quad (76)$$

$$\begin{aligned} u_c &= \sqrt{3} \sqrt{8\omega^3 \ell^6 + 27\ell^4 \omega^6 + 27\ell^4 \omega^6 \left(\frac{3V_c}{4\pi} \right)^3} \\ &\quad - 9\ell^2 \omega^3 \left(\frac{3V_c}{4\pi} \right). \end{aligned} \quad (77)$$

Now (72) is completely mass-independent volume functional relation.

2.7. Thermodynamic Volume Products for Phantom BHs. In this section, we would like to discuss the thermodynamic volume products for phantom AdS BH [30]. The phantom fields are exotic fields in BH physics. They could be generated via negative energy density. They could explain the acceleration of our universe. Thus one could expect that these exotic fields might have an important role in BH thermodynamics. We want to study here what is the key role of these phantom fields in thermodynamic volume functional relation? This is the main motivation behind this work. For phantom BH, the metric function is given by

$$\mathcal{Z}(r) = 1 - \frac{2M}{r} - \frac{\Lambda}{3} r^2 + \eta \frac{Q^2}{r^2}, \quad (78)$$

where the parameter η determines the nature of electromagnetic (EM) field. For $\eta = 1$, one obtains the classical EM theory but when $\eta = -1$, one obtains the Maxwell field which is *phantom*.

Therefore for phantom BH, the horizon radii could be found from the following equation:

$$r^4 + \ell^2 r^2 - 2M\ell^2 r - \ell^2 Q^2 = 0. \quad (79)$$

The above equation has four roots; among them the two roots are real and other two roots are imaginary. Thus the OH and IH radii are

$$r_{h,c} = \frac{1}{2} \sqrt{\frac{1}{3} \left(\frac{z}{2}\right)^{1/3} + \left(\frac{2}{z}\right)^{1/3} \frac{\ell^2 (\ell^2 - 12Q^2)}{3} - \frac{2\ell^2}{3} \pm \frac{1}{2} \sqrt{\frac{4M\ell^2}{\sqrt{(1/3)(z/2)^{1/3} + (2/z)^{1/3} \ell^2 (\ell^2 - 12Q^2)/3 - 2\ell^2/3}} - \frac{1}{3} \left(\frac{z}{2}\right)^{1/3} - \left(\frac{2}{z}\right)^{1/3} \frac{\ell^2 (\ell^2 - 12Q^2)}{3} - \frac{4\ell^2}{3}},} \quad (80)$$

where

$$z = 2\ell^6 + 108M^2\ell^4 + 72\ell^4Q^2 + \sqrt{(2\ell^6 + 108M^2\ell^4 + 72\ell^4Q^2)^2 - 4\ell^6(\ell^2 - 12Q^2)^3} \quad (81)$$

Now we compute the thermodynamic volume product which turns out to be

$$\mathcal{V}_h \mathcal{V}_c = \frac{\pi^2}{36} \left[\frac{2}{3} \left(\frac{z}{2}\right)^{1/3} + \left(\frac{2}{z}\right)^{1/3} \frac{2\ell^2 (\ell^2 - 12Q^2)}{3} + \frac{2\ell^2}{3} - \frac{4M\ell^2}{\sqrt{(1/3)(z/2)^{1/3} + (2/z)^{1/3} \ell^2 (\ell^2 - 12Q^2)/3 - 2\ell^2/3}} \right]^3 \quad (82)$$

The above product indicates that it is strictly mass-dependent. Therefore the product is not universal. Below we would like to prove that *more complicated function of inner and outer horizon volume* is indeed mass-independent.

To do this we would like to use Vieta's theorem. Thus from (79), we find

$$\sum_{i=1}^4 r_i = 0. \quad (83)$$

$$\sum_{1 \leq i < j \leq 4} r_i r_j = \ell^2. \quad (84)$$

$$\sum_{1 \leq i < j < k \leq 4} r_i r_j r_k = 2M\ell^2. \quad (85)$$

$$\prod_{i=1}^4 r_i = -\ell^2 Q^2. \quad (86)$$

Thus the mass-independent *volume sum* and *volume product* relations should read

$$\sum_{i=1}^4 \mathcal{V}_i^{1/3} = 0. \quad (87)$$

$$\sum_{1 \leq i < j \leq 4} (\mathcal{V}_i \mathcal{V}_j)^{1/3} = \left(\frac{3}{32\pi}\right)^{1/3} \frac{8\pi\ell^2}{3}. \quad (88)$$

$$\prod_{i=1}^4 (\mathcal{V}_i)^{1/3} = \left(\frac{\pi}{6}\right)^{1/3} \frac{8\pi\ell^2 Q^2}{3}. \quad (89)$$

Therefore the mass-independent volume functional relations in terms of two horizons are

$$f(\mathcal{V}_h, \mathcal{V}_c) = -\ell^2, \quad (90)$$

where

$$\begin{aligned} f(\mathcal{V}_h, \mathcal{V}_c) &= \left(\frac{3}{32\pi}\right)^{1/3} \frac{(8\pi\ell^2 Q^2/3)}{(\mathcal{V}_h \mathcal{V}_c)^{1/3}} \\ &+ \left(\frac{3}{4\pi}\right)^{2/3} [\mathcal{V}_h^{2/3} + \mathcal{V}_c^{2/3} + (\mathcal{V}_h \mathcal{V}_c)^{1/3}]. \end{aligned} \quad (91)$$

These are explicitly mass-independent volume functional relations in the extended phase space.

2.8. Thermodynamic Volume Products for AdS BH in $f(R)$ Gravity. In this section, we are interested in deriving the thermodynamic volume products for a static, spherically symmetric AdS BH in $f(R)$ gravity. To some extent, it is called modified gravity. It is a very crucial tool for explaining the current and future status of the accelerating universe. Thus it is very important to investigate the thermodynamic volume products for this gravity. The metric [14, 31] function for this kind of gravity can be written as

$$\mathcal{L}(r) = 1 - \frac{2m}{r} + \frac{q^2}{\alpha r^2} - \frac{R_0}{12} r^2, \quad (92)$$

where $\alpha = 1 + f'(R_0)$. The parameters m and q are related to the ADM mass, M , and electric charge, Q , by the following expression:

$$\begin{aligned} m &= \frac{M}{\alpha}, \\ q &= \sqrt{\alpha} Q. \end{aligned} \quad (93)$$

In this gravity, the thermodynamic pressure could be written as $P = -(\Lambda/8\pi)\alpha = 3/8\pi\ell^2$ and the scalar curvature constant as $R_0 = -12/\ell^2 = 4\Lambda$. Thus the horizon equation for $f(R)$ gravity becomes

$$r^4 + \ell^2 r^2 - 2m\ell^2 r + \frac{\ell^2 q^2}{\alpha} = 0. \quad (94)$$

The EH radius and CH radius are

$$\begin{aligned} r_h &= \frac{(a+b)}{2}, \\ r_c &= \frac{(a-b)}{2}, \end{aligned} \quad (95)$$

where

$$a = \sqrt{\frac{1}{3\alpha} \left(\frac{\mu}{2}\right)^{1/3} + \left(\frac{2}{\mu}\right)^{1/3} \frac{\ell^2 (\alpha\ell^2 + 12q^2)}{3} - \frac{2\ell^2}{3}} \quad (96)$$

and

$$b = \sqrt{\frac{4m\ell^2}{a} - \frac{1}{3\alpha} \left(\frac{\mu}{2}\right)^{1/3} - \left(\frac{2}{\mu}\right)^{1/3} \frac{\ell^2 (\alpha\ell^2 + 12q^2)}{3} - \frac{4\ell^2}{3}}, \quad (97)$$

where

$$\begin{aligned} \mu &= 2\alpha^3 \ell^6 + 108\alpha^3 m^2 \ell^4 - 72\alpha^2 \ell^4 q^2 \\ &+ \sqrt{(2\alpha^3 \ell^6 + 108\alpha^3 m^2 \ell^4 - 72\alpha^2 \ell^4 q^2)^2 - 4\ell^6 (\alpha^2 \ell^2 + 12\alpha q^2)^3} \end{aligned} \quad (98)$$

The volume products for $f(R)$ gravity are derived to be

$$\begin{aligned} \mathcal{V}_h \mathcal{V}_c &= \frac{\pi^2}{36} \left[\frac{2}{3\alpha} \left(\frac{\mu}{2}\right)^{1/3} \right. \\ &\left. + \left(\frac{2}{\mu}\right)^{1/3} \frac{2\ell^2 (\alpha\ell^2 + 12q^2)}{3} + \frac{2\ell^2}{3} - \frac{4m\ell^2}{a} \right]^3. \end{aligned} \quad (99)$$

It indicates that the volume product is not mass-independent. Now we shall give an alternative approach where we would see that more complicated function of volume functional relation is quite mass-independent. To derive it, we should use Vieta's theorem; then one could find

$$\sum_{i=1}^4 r_i = 0. \quad (100)$$

$$\sum_{1 \leq i < j \leq 4} r_i r_j = \ell^2. \quad (101)$$

$$\sum_{1 \leq i < j < k \leq 4} r_i r_j r_k = 2m\ell^2. \quad (102)$$

$$\prod_{i=1}^4 r_i = \frac{q^2 \ell^2}{\alpha}. \quad (103)$$

Eliminating third and fourth roots, the mass-independent volume functional relation is derived as

$$f(\mathcal{V}_h, \mathcal{V}_c) = \ell^2, \quad (104)$$

where

$$\begin{aligned} f(\mathcal{V}_h, \mathcal{V}_c) &= \left(\frac{3}{32\pi}\right)^{1/3} \frac{(8\pi\ell^2 q^2/3)}{\alpha(\mathcal{V}_h \mathcal{V}_c)^{1/3}} \\ &- \left(\frac{3}{4\pi}\right)^{2/3} \left[\mathcal{V}_h^{2/3} + \mathcal{V}_c^{2/3} + (\mathcal{V}_h \mathcal{V}_c)^{1/3} \right]. \end{aligned} \quad (105)$$

This equation is explicitly mass-independent.

2.9. Thermodynamic Volume Products for Regular BH. In this section, we compute the thermodynamic volume products for a regular BH derived by Ayón-Beato and García (ABG) [32, 33]. It is a spherically symmetric solution of Einstein's general relativity and it is a curvature singularity free solution. The metric function form of ABG BH is given by

$$\mathcal{L}(r) = 1 - \frac{2mr^2}{(r^2 + q^2)^{3/2}} + \frac{q^2 r^2}{(r^2 + q^2)^2}. \quad (106)$$

m is the mass of the BH and q is the monopole charge. The horizon radii could be found from the following equation:

$$\begin{aligned} r^8 + (6q^2 - 4m^2)r^6 + (11q^4 - 4m^2 q^2)r^4 + 6q^6 r^2 \\ + q^8 = 0. \end{aligned} \quad (107)$$

This is a polynomial equation of order 8^{th} . This could be reduced to fourth-order polynomial equation by putting $r^2 = z$; then one obtains [33]

$$\begin{aligned} z^4 + (6q^2 - 4m^2)z^3 + (11q^4 - 4m^2 q^2)z^2 + 6q^6 z \\ + q^8 = 0. \end{aligned} \quad (108)$$

The EH and CH are located at

$$r_h = \sqrt{\frac{(2m^2 - 3q^2)}{2} + \frac{a}{2} + \frac{b}{2}} \quad (109)$$

$$r_c = \sqrt{\frac{(2m^2 - 3q^2)}{2} - \frac{a}{2} - \frac{b}{2}} \quad (110)$$

and the other horizons (we have considered only here EH and CH; the other horizons are discarded) are located at

$$r_{hc} = \sqrt{\frac{(2m^2 - 3q^2)}{2} + \frac{a}{2} - \frac{b}{2}} \quad (111)$$

$$r_{ch} = \sqrt{\frac{(2m^2 - 3q^2)}{2} - \frac{a}{2} + \frac{b}{2}} \quad (112)$$

where

$$a = \sqrt{4m^2q^2 - 11q^4 + (2m^2 - 3q^2)^2 + \frac{(11q^4 - 4m^2q^2)}{3} + \left(\frac{2}{\delta}\right)^{1/3} \frac{(16m^4q^4 - 16m^2q^6 + 25q^8)}{3} + \frac{1}{3} \left(\frac{\delta}{2}\right)^{1/3}} \quad (113)$$

and

$$b = \sqrt{c} \quad (114)$$

where

$$c = 4m^2q^2 - 11q^4 + 2(2m^2 - 3q^2)^2 + \frac{(4m^2q^2 - 11q^4)}{3}$$

and

$$\begin{aligned} & - \left(\frac{2}{\delta}\right)^{1/3} \frac{(16m^4q^4 - 16m^2q^6 + 25q^8)}{3} - \frac{1}{3} \left(\frac{\delta}{2}\right)^{1/3} \\ & + \frac{\{48q^6 - 8(2m^2 - 3q^2)^3 + 8(2m^2 - 3q^2)(11q^4 - 4m^2q^2)\}}{4a} \end{aligned} \quad (115)$$

$$\delta = 624m^4q^8 - 128m^6q^6 - 240m^2q^{10} + 250q^{12} + \sqrt{324864m^8q^{16} - 110592m^{10}q^{14} - 193536m^6q^{18} + 172800m^4q^{20}}. \quad (116)$$

The volume product of \mathcal{H}^\pm is evaluated to be

$$\mathcal{V}_h \mathcal{V}_c = \frac{\pi^2}{36} \left[(2m^2 - 3q^2)^2 - (a + b)^2 \right]. \quad (117)$$

As usual, the volume product is not mass-independent. Now we would see below that *somewhat more complicated function of inner and outer horizon volume* is indeed mass-independent. To derive it, we have to apply Vieta's theorem in (108); thus one obtains

$$\sum_{i=1}^4 z_i = 4m^2 - 6q^2. \quad (118)$$

$$\sum_{1 \leq i < j \leq 4} z_i z_j = 11q^4 - 4m^2q^2. \quad (119)$$

$$\sum_{1 \leq i < j < k \leq 4} z_i z_j z_k = -6q^2. \quad (120)$$

$$\prod_{i=1}^4 z_i = q^8. \quad (121)$$

Eliminating the mass parameter, one obtains the mass-independent equation in terms of two horizons

$$\begin{aligned} & z_1 z_2 (z_1 + z_2) + 6q^2 z_1 z_2 - q^8 \frac{(z_1 + z_2)}{z_1 z_2} \\ & - \frac{1}{z_1 + z_2 + q^2} \left[(z_1 + z_2)^2 + 6q^2 (z_1 + z_2) - z_1 z_2 \right. \\ & \left. - \frac{q^8}{z_1 z_2} + 11q^4 \right] = 6q^6. \end{aligned} \quad (122)$$

It should be noted that the symbols (h, c) and $(1, 2)$ both have the same meaning. Now in terms of volume of \mathcal{H}^\pm the mass-independent volume functional relation becomes

$$f(\mathcal{V}_h, \mathcal{V}_c) = 6q^6, \quad (123)$$

where

$$\begin{aligned} f(\mathcal{V}_h, \mathcal{V}_c) &= \left(\frac{3}{4\pi}\right)^2 (\mathcal{V}_h \mathcal{V}_c)^{2/3} \{ \mathcal{V}_h^{2/3} + \mathcal{V}_c^{2/3} \} \\ &+ 6q^2 \left(\frac{3}{4\pi}\right)^{4/3} (\mathcal{V}_h \mathcal{V}_c)^{2/3} - q^8 \left(\frac{4\pi}{3}\right)^{2/3} \\ &\cdot \frac{(\mathcal{V}_h^{2/3} + \mathcal{V}_c^{2/3})}{(\mathcal{V}_h \mathcal{V}_c)^{2/3}} - \left(\frac{3}{4\pi}\right)^{2/3} \\ &\cdot \frac{(\mathcal{V}_h \mathcal{V}_c)^{2/3}}{\left\{ \mathcal{V}_h^{2/3} + \mathcal{V}_c^{2/3} + \left(\frac{4\pi}{3}\right)^{2/3} q^2 \right\}} \\ &\times \left[\left(\frac{3}{4\pi}\right)^{4/3} (\mathcal{V}_h^{2/3} + \mathcal{V}_c^{2/3})^2 \right. \\ &+ 6q^2 \left(\frac{3}{4\pi}\right)^{2/3} (\mathcal{V}_h^{2/3} + \mathcal{V}_c^{2/3}) \\ &- \left(\frac{3}{4\pi}\right)^{4/3} (\mathcal{V}_h \mathcal{V}_c)^{2/3} - \left(\frac{4\pi}{3}\right)^{2/3} \frac{q^8}{(\mathcal{V}_h \mathcal{V}_c)^{2/3}} \\ &\left. + 11q^4 \right] \end{aligned} \quad (124)$$

Now we are moving to axisymmetric spacetime, to see what happens there?

3. Axisymmetric Spacetime

In this section, we have considered only the various axisymmetric BHs. It is easy to compute volume products for spherically symmetric cases because of $\mathcal{V}_h \propto \mathcal{A}_h r_h$ for OH and $\mathcal{V}_c \propto \mathcal{A}_c r_c$ for IH. For axisymmetric spacetime,

this proportionality is quite different because here the spin parameter is present. Now see what happens in this case by starting with Kerr BH.

3.1. Kerr BH. The Kerr BH is a solution of Einstein equation. The OH radius and IH radius for this BH should read

$$r_h = M + \sqrt{M^2 - a^2} \quad (125)$$

$$r_c = M - \sqrt{M^2 - a^2}, \quad (126)$$

where $a = J/M$. J is angular momentum of the BH. When $M^2 > a^2$, it describes a BH; when $M^2 < a^2$, it describes a naked singularity. The thermodynamic volume for OH [34] and IH [14] becomes

$$\mathcal{V}_h = \frac{\mathcal{A}_h r_h}{3} \left[1 + \frac{a^2}{2r_h^2} \right] \quad (127)$$

$$\mathcal{V}_c = \frac{\mathcal{A}_c r_c}{3} \left[1 + \frac{a^2}{2r_c^2} \right]. \quad (128)$$

The thermodynamic volume product of Kerr BH for OH and IH is calculated to be

$$\mathcal{V}_h \mathcal{V}_c = \frac{128}{9} \pi^2 J^2 M^2 \left(1 + \frac{a^2}{8M^2} \right). \quad (129)$$

The volume sum for OH and IH is

$$\mathcal{V}_h + \mathcal{V}_c = \frac{32}{3} \pi M^3 \left(1 - \frac{a^2}{4M^2} \right). \quad (130)$$

Similarly, the volume minus for OH and IH is

$$\mathcal{V}_h - \mathcal{V}_c = \frac{32}{3} \pi M^2 \sqrt{M^2 - a^2}. \quad (131)$$

The volume division is

$$\frac{\mathcal{V}_h}{\mathcal{V}_c} = \left(\frac{4M^2 - a^2 + 4M\sqrt{M^2 - a^2}}{4M^2 - a^2 - 4M\sqrt{M^2 - a^2}} \right). \quad (132)$$

It indicates that the volume product, volume sum, volume minus, and volume division for Kerr BH are mass-dependent. Therefore the product, the sum, the minus, and the division all are *not* universal.

3.2. Kerr-AdS BH. The horizon function for Kerr-AdS BH [35] is given by

$$\Delta_r = (r^2 + a^2) \left(1 + \frac{r^2}{\ell^2} \right) - 2Mr = 0, \quad (133)$$

which gives the quartic order of horizon equation

$$\frac{r^4}{\ell^2} + \left(1 + \frac{a^2}{\ell^2} \right) r^2 - 2mr + a^2 = 0. \quad (134)$$

The quantities m and a are related to the parameters mass M and angular momentum J as follows:

$$m = M\Xi^2, \quad (135)$$

$$a = \frac{J}{m}\Xi^2$$

where $\Xi = 1 - a^2/\ell^2$. To obtain the roots of (134), we apply Vieta's theorem, and we find

$$\sum_{i=1}^4 r_i = 0. \quad (136)$$

$$\sum_{1 \leq i < j \leq 4} r_i r_j = \ell^2 \left(1 + \frac{a^2}{\ell^2} \right). \quad (137)$$

$$\sum_{1 \leq i < j < k \leq 4} r_i r_j r_k = 2m\ell^2. \quad (138)$$

$$\prod_{i=1}^4 r_i = a^2 \ell^2. \quad (139)$$

There are at least two real zeros of (134) which is OH radius and IH radius. After some algebraic computation, we have

$$r_h + r_c = \frac{2m\ell^2}{a^2 + \ell^2 + r_h^2 + r_c^2}, \quad (140)$$

$$r_h r_c = \frac{a^2 \ell^2 - (r_h r_c)^2}{a^2 + \ell^2 + r_h^2 + r_c^2}. \quad (141)$$

The area of the BH for OH is

$$\mathcal{A}_h = \frac{4\pi (r_h^2 + a^2)}{\Xi}, \quad (142)$$

and for IH is

$$\mathcal{A}_c = \frac{4\pi (r_c^2 + a^2)}{\Xi}. \quad (143)$$

The thermodynamic volume for OH [17, 22] becomes

$$\mathcal{V}_h = \frac{2\pi [(r_h^2 + a^2)(2r_h^2 \ell^2 + a^2 \ell^2 - r_h^2 a^2)]}{3r_h \ell^2 \Xi^2}. \quad (144)$$

And we derive that the thermodynamic volume for IH becomes

$$\mathcal{V}_c = \frac{2\pi [(r_c^2 + a^2)(2r_c^2 \ell^2 + a^2 \ell^2 - r_c^2 a^2)]}{3r_c \ell^2 \Xi^2}. \quad (145)$$

The thermodynamic volume product for Kerr-AdS BH is calculated in

$$\mathcal{V}_h \mathcal{V}_c = \frac{4\pi^2 \{r_h^2 r_c^2 + a^2 (r_h^2 + r_c^2) + a^4\}}{9\Xi^4 r_h r_c} \times [3r_h^2 r_c^2 + 2a^2 (r_h^2 + r_c^2) + \Xi^2 r_h^2 r_c^2]. \quad (146)$$

Using (140), (141), (142), and (143), we observe that there is no way to eliminate the mass parameter from (146); therefore the volume product for Kerr-AdS BH is not mass-independent; thus it is not universal and not quantized.

3.3. Kerr-Newman BH. It is an axisymmetric solution of Einstein-Maxwell equations. The OH radius and IH radius for this BH become

$$r_h = M + \sqrt{M^2 - a^2 - Q^2} \quad (147)$$

$$r_c = M - \sqrt{M^2 - a^2 - Q^2}. \quad (148)$$

The thermodynamic volume for OH [17] is

$$\mathcal{V}_h = \frac{2\pi \left[(r_h^2 + a^2)(2r_h^2 + a^2) + a^2 Q^2 \right]}{3r_h}. \quad (149)$$

And we derive that the thermodynamic volume for IH is

$$\mathcal{V}_c = \frac{2\pi \left[(r_c^2 + a^2)(2r_c^2 + a^2) + a^2 Q^2 \right]}{3r_c}. \quad (150)$$

The thermodynamic volume product for KN BH is computed to be

$$\begin{aligned} \mathcal{V}_h \mathcal{V}_c &= \frac{16\pi^2}{9} \\ &\times \frac{\left[J^2 (8J^2 + a^4 - a^2 Q^2 - 2Q^4 + 8M^2 Q^2) + Q^4 (a^2 + Q^2)^2 \right]}{a^2 + Q^2}. \end{aligned} \quad (151)$$

It also indicates that the thermodynamic volume for KN BH is mass-dependent. Thus the volume product is not universal for any axisymmetric spacetime. In the appropriate limit, i.e., when $a = J = 0$, one obtains the thermodynamic volume product for Reissner Nordström BH and when $Q = 0$, one obtains the volume product for Kerr BH.

3.4. Kerr-Newman-AdS BH. The horizon function for Kerr-Newman-AdS BH [36] reads

$$\Delta_r = (r^2 + a^2) \left(1 + \frac{r^2}{\ell^2} \right) - 2Mr + q^2 = 0, \quad (152)$$

which has the quartic order of horizon equation

$$\frac{r^4}{\ell^2} + \left(1 + \frac{a^2}{\ell^2} \right) r^2 - 2mr + a^2 + q^2 = 0. \quad (153)$$

The quantity q is related to the charge parameter Q as

$$q = Q\Xi \quad (154)$$

To determine the roots of (153) again we apply Vieta's rule; then one obtains

$$\sum_{i=1}^4 r_i = 0. \quad (155)$$

$$\sum_{1 \leq i < j \leq 4} r_i r_j = \ell^2 \left(1 + \frac{a^2}{\ell^2} \right). \quad (156)$$

$$\sum_{1 \leq i < j < k \leq 4} r_i r_j r_k = 2m\ell^2. \quad (157)$$

$$\prod_{i=1}^4 r_i = (a^2 + q^2) \ell^2. \quad (158)$$

Similarly, there are at least two real zeros of (153) which is OH radius and IH radius. After some algebraic derivation, one gets

$$r_h + r_c = \frac{2m\ell^2}{a^2 + \ell^2 + r_h^2 + r_c^2}, \quad (159)$$

$$r_h r_c = \frac{(a^2 + q^2) \ell^2 - (r_h r_c)^2}{a^2 + \ell^2 + r_h^2 + r_c^2}. \quad (160)$$

The area of this BH for OH is

$$\mathcal{A}_h = \frac{4\pi (r_h^2 + a^2)}{\Xi} \quad (161)$$

and for IH is

$$\mathcal{A}_c = \frac{4\pi (r_c^2 + a^2)}{\Xi}. \quad (162)$$

The thermodynamic volume for OH [17, 22] becomes

$$\begin{aligned} \mathcal{V}_h &= \frac{2\pi \left[(r_h^2 + a^2)(2r_h^2 \ell^2 + a^2 \ell^2 - r_h^2 a^2) + \ell^2 q^2 a^2 \right]}{3r_h \ell^2 \Xi^2}. \end{aligned} \quad (163)$$

And we derive that the thermodynamic volume for IH becomes

$$\mathcal{V}_c = \frac{2\pi \left[(r_c^2 + a^2)(2r_c^2 \ell^2 + a^2 \ell^2 - r_c^2 a^2) + \ell^2 q^2 a^2 \right]}{3r_c \ell^2 \Xi^2}. \quad (164)$$

The thermodynamic volume product for Kerr-Newman-AdS BH is computed in

$$\begin{aligned}
\mathcal{V}_h \mathcal{V}_c = & \frac{4\pi^2}{9\Xi^4 r_h r_c} \times \left[\left\{ r_h^2 r_c^2 + a^2 (r_h^2 + r_c^2) + a^4 \right\}^2 + \left\{ r_h^2 r_c^2 + a^2 (r_h^2 + r_c^2) + a^4 \right\} \left\{ 2r_h^2 r_c^2 + a^2 (r_h^2 + r_c^2) \right\} \right] \\
& + \frac{4\pi^2 \left[a^2 q^2 \left\{ r_h^4 + r_c^4 + 2a^2 (r_h^2 + r_c^2) + 2a^4 \right\} + \Xi^2 r_h^2 r_c^2 \left\{ r_h^2 r_c^2 + a^2 (r_h^2 + r_c^2) + a^4 \right\} \right]}{9\Xi^4 r_h r_c} \\
& + \frac{4\pi^2 \left[a^2 q^2 \Xi \left\{ r_h^4 + r_c^4 + a^2 (r_h^2 + r_c^2) \right\} + a^4 q^4 \right]}{9\Xi^4 r_h r_c}.
\end{aligned} \tag{165}$$

Again using (159), (160), (161), and (162), we speculate that there has been no chance to eliminate the mass parameter from (165); thus the volume product for Kerr-Newman-AdS BH is not mass-independent; therefore it is not universal and not quantized.

3.5. Spinning BTZ BH. The metric for rotating BTZ BH [37] in 2 + 1 dimension is given by

$$\begin{aligned}
ds^2 = & - \left(\frac{r^2}{\ell^2} + \frac{J^2}{4r^2} - M \right) dt^2 \\
& + \frac{dr^2}{(r^2/\ell^2 + J^2/4r^2 - M)} \\
& + r^2 \left(-\frac{J}{2r^2} dt + d\phi \right)^2.
\end{aligned} \tag{166}$$

M and J represent the ADM mass and the angular momentum of the BH. $-\Lambda = 1/\ell^2 = 8\pi G_3$ denotes the cosmological constant. Here we have set $8G_3 = 1 = c = \hbar = k$. When $J = 0$, one obtains the static BTZ BH.

The BH OH radius and IH radius are [37, 38]

$$r_h = \sqrt{\frac{M\ell^2}{2} \left(1 + \sqrt{1 - \frac{J^2}{M^2\ell^2}} \right)}. \tag{167}$$

$$r_c = \sqrt{\frac{M\ell^2}{2} \left(1 - \sqrt{1 - \frac{J^2}{M^2\ell^2}} \right)}. \tag{168}$$

The thermodynamic volume for 3D spinning BTZ BH for OH and IH is

$$\mathcal{V}_h = \left(\frac{\partial M}{\partial P} \right)_J = \pi r_h^2 \tag{169}$$

$$\mathcal{V}_c = \left(\frac{\partial M}{\partial P} \right)_J = \pi r_c^2 \tag{170}$$

The thermodynamic volume product is computed to be

$$\mathcal{V}_h \mathcal{V}_c = \frac{\pi^2 J^2 \ell^2}{4}. \tag{171}$$

Interestingly, the thermodynamic volume product for rotating BTZ BH is *mass-independent*, i.e., *universal*, and it is also

quantized. This is the only example for *rotating* cases; the volume product is universal. This is an interesting result of this work.

4. Discussion

In this work, we have demonstrated the thermodynamic products, in particular thermodynamic volume products, of spherically symmetric spacetime and axisymmetric spacetime by incorporating the extended phase space formalism. In this formalism, the cosmological constant should be considered as a thermodynamic pressure and its conjugate parameter as thermodynamic volume. In addition to that, the mass parameter should be treated as enthalpy of the system rather than internal energy. Then in this phase space the first law of BH thermodynamics should be satisfied for both the OH and IH.

We explicitly computed the thermodynamic volume products both for OH and IH of several classes of spherically symmetric and axisymmetric BHs including the AdS spacetime. In this case, the simple volume product of \mathcal{H}^\pm is not mass-independent. Rather slightly more complicated volume functional relations are indeed mass-independent. We have proved that, for simple Reissner Nordström BH of Einstein gravity and Kehagias-Sfetsos BH of Hořava Lifshitz gravity, the thermodynamic volume product of \mathcal{H}^\pm is indeed *universal*. Such products are *mass-independent* for spherically symmetric cases because of $\mathcal{V}_h \propto \mathcal{A}_h r_h$ for OH and $\mathcal{V}_c \propto \mathcal{A}_c r_c$ for IH.

Axisymmetric spacetime does not satisfy this proportionality due to presence of the spin parameter; thus such spacetime shows *no* mass-independent features except the rotating BTZ BH; the only axisymmetric spacetime in 3D showed *universal* features; thus it has been quantized in this sense. We also computed thermodynamic volume sum but they are always mass-dependent so they are not universal as well as they are not quantized.

Like area (or entropy) products, the simple thermodynamic volume product of \mathcal{H}^\pm is not mass-independent; rather more complicated function of volume functional relation is indeed mass-independent. This is often true for spherically symmetric BHs including AdS spacetime. This scenario for axisymmetric spacetime (except 3D BTZ BH) is quite different. In this case, the area functional relation becomes mass-independent whereas the volume functional relation is not mass-independent. For volume products, this

is the main difference between spherically symmetric space-time and axisymmetric spacetime. To sum up, the volume functional relation that we have studied in this work in spherically symmetric cases (but not for axisymmetric cases) further provides some universal properties of the BH which gives some insight into microscopic origin of BH entropy of both outer and inner horizons.

Data Availability

The data used to support the findings of this study are available from the corresponding author upon request.

Conflicts of Interest

The author declares that there are no conflicts of interest.


References

- [1] M. Ansorg and J. Hennig, "Inner Cauchy Horizon of Axisymmetric and Stationary Black Holes with Surrounding Matter in Einstein-Maxwell Theory," *Physical Review Letters*, vol. 102, no. 22, Article ID 221102, 2009.
- [2] M. Cvetič, G. W. Gibbons, and C. N. Pope, "Universal Area Product Formulas for Rotating and Charged Black Holes in Four and Higher Dimensions," *Physical Review Letters*, vol. 106, no. 12, Article ID 121301, 2011.
- [3] A. Castro and M. J. Rodriguez, "Universal properties and the first law of black hole inner mechanics," *Physical Review D: Particles, Fields, Gravitation and Cosmology*, vol. 86, no. 2, Article ID 024008, 5 pages, 2012.
- [4] A. Castro, "Holographic entanglement entropy and gravitational anomalies," *Journal of High Energy Physics*, vol. 07, no. 164, 2013.
- [5] A. Bagchi, S. Detournay, and D. Grumiller, "Flat-Space Chiral Gravity," *Physical Review Letters*, vol. 109, no. 15, 2012.
- [6] M. Visser, "Area products for stationary black hole horizons," *Physical Review D: Particles, Fields, Gravitation and Cosmology*, vol. 88, no. 4, Article ID 044014, 2013.
- [7] J. Hennig, "Geometric relations for rotating and charged AdS black holes," *Classical and Quantum Gravity*, vol. 31, no. 13, Article ID 135005, 9 pages, 2014.
- [8] P. Pradhan, "Black hole interior mass formula," *The European Physical Journal C*, vol. 74, article 2887, 2014.
- [9] P. Pradhan, "Thermodynamic product formula for Hořava-Lifshitz black hole," *Physics Letters B*, vol. 747, pp. 64–67, 2015.
- [10] S. W. Hawking and D. N. Page, "Thermodynamics of black holes in anti-de Sitter space," *Communications in Mathematical Physics*, vol. 87, no. 4, pp. 577–588, 1983.
- [11] A. Chamblin, R. Emparan, C. V. Johnson, and R. C. Myers, "Charged AdS black holes and catastrophic holography," *Physical Review D: Covering Particles, Fields, Gravitation and Cosmology*, vol. 60, no. 6, Article ID 064018, 1999.
- [12] A. Chamblin, R. Emparan, C. V. Johnson, and R. C. Myers, "Holography, thermodynamics, and fluctuations of charged AdS black holes," *Physical Review D: Particles, Fields, Gravitation and Cosmology*, vol. 60, no. 10, Article ID 104026, 1999.
- [13] D. Kubiznak and R. B. Mann, "P-V criticality of charged AdS black holes," *High Energy Physics - Theory*, vol. 1207, no. 033, 2012.
- [14] P. Pradhan, "Thermodynamic products in extended phase-space," *International Journal of Modern Physics D*, vol. 26, Article ID 1750010, 2017.
- [15] D. Kastor, S. Ray, and J. Traschen, "Enthalpy and the Mechanics of AdS Black Holes," *Classical and Quantum Gravity*, vol. 26, Article ID 195011, 2009.
- [16] B. P. Dolan, "The cosmological constant and black-hole thermodynamic potentials," *Classical and Quantum Gravity*, vol. 28, no. 12, Article ID 125020, 2011.
- [17] B. P. Dolan, "Pressure and volume in the first law of black hole thermodynamics," *Classical and Quantum Gravity*, vol. 28, no. 23, Article ID 235017, 2011.
- [18] M. K. Parikh, "Volume of black holes," *Physical Review D: Particles, Fields, Gravitation and Cosmology*, vol. 73, no. 12, Article ID 124021, 5 pages, 2006.
- [19] M. Christodoulou and C. Rovelli, "How big is a black hole?" *Physical Review D: Particles, Fields, Gravitation, and Cosmology*, vol. 91, no. 6, Article ID 064046, 2015.
- [20] W. Ballik and K. Lake, "Vector volume and black holes," *Physical Review D: Particles, Fields, Gravitation and Cosmology*, vol. 88, no. 10, Article ID 104038, 2013.
- [21] B. S. DiNunno and R. A. Matzner, "The Volume Inside a Black Hole," *General Relativity and Quantum Cosmology*, vol. 42, pp. 63–76, 2010.
- [22] M. Cvetič, G. W. Gibbons, D. Kubiznak, and C. N. Pope, "Black hole enthalpy and an entropy inequality for the thermodynamic volume," *Physical Review D: Particles, Fields, Gravitation and Cosmology*, vol. 84, no. 2, 2011.
- [23] P. Hořava, "Spectral dimension of the universe in quantum gravity at a Lifshitz point," *Physical Review Letters*, vol. 102, no. 16, Article ID 161301, 2009.
- [24] P. Hořava, "Quantum gravity at a Lifshitz point," *Physical Review D: Particles, Fields, Gravitation and Cosmology*, vol. 79, no. 8, p. 084008, 2009.
- [25] P. Hořava, "Membranes at quantum criticality," *Journal of High Energy Physics*, vol. 2009, article 020, 2009.
- [26] A. F. Ali, S. Das, and E. C. Vagenas, "Discreteness of space from the generalized uncertainty principle," *Physics Letters B*, vol. 678, no. 5, pp. 497–499, 2009.
- [27] C. Pacilio and S. Liberati, "Improved derivation of the Smarr formula for Lorentz-breaking gravity," *Physical Review D: Particles, Fields, Gravitation, And Cosmology*, vol. 95, no. 12, Article ID 124010, 2017.
- [28] M.-i. Park, "The Black Hole and Cosmological Solutions in IR modified Horava Gravity," *High Energy Physics - Theory*, vol. 0909, no. 123, 2009.
- [29] P. Pradhan, "Area Products for H^\pm in AdS Space," *Galaxies*, vol. 5, p. 10, 2017.
- [30] H. Quevedo, M. N. Quevedo, and A. Sánchez, "Geometrothermodynamics of phantom AdS black holes," *The European Physical Journal C*, vol. 76, no. 110, 2016.
- [31] T. Moon, Y. Myung, and E. J. Son, " $f(R)$ black holes," *General Relativity and Gravitation*, vol. 34, no. 3079, 2011.
- [32] E. Ayón-Beato and A. García, "Regular black hole in general relativity coupled to nonlinear electrodynamics," *Physical Review Letters*, vol. 80, no. 23, pp. 5056–5059, 1998.
- [33] P. Pradhan, "Area functional relation for 5D-Gauss-Bonnet-AdS black hole," *General Relativity and Gravitation*, vol. 48, no. 8, article 116, 2016.

- [34] N. Altamirano, D. Kubizňák, R. Mann, and Z. Sherkatghanad, “Thermodynamics of rotating black holes and black rings: phase transitions and thermodynamic volume,” *Galaxies*, vol. 2, no. 1, pp. 89–159, 2014.
- [35] B. Carter, “Hamilton-Jacobi and Schrodinger separable solutions of Einstein’s equations,” *Communications in Mathematical Physics*, vol. 10, pp. 280–310, 1968.
- [36] M. M. Caldarelli, G. Cognola, and D. Klemm, “Thermodynamics of Kerr-Newman-AdS black holes and conformal field theories,” *Classical and Quantum Gravity*, vol. 17, no. 2, 2000.
- [37] M. Banados, C. Teitelboim, and J. Zanelli, “Black hole in three-dimensional spacetime,” *Physical Review Letters*, vol. 69, no. 13, pp. 1849–1851, 1992.
- [38] P. Pradhan, “Entropy product formula for a spinning BTZ black hole,” *JETP Letters*, vol. 102, no. 7, article 427, 2015.

Research Article

Interactions in an Acoustic World: Dumb Hole

Ion Simaciu ¹, Gheorghe Dumitrescu,² Zoltan Borsos,¹ and Mariana Brădac¹

¹*Petroleum-Gas University of Ploiesti, Ploiesti 100680, Romania*

²*High School Toma N. Socolescu, Ploiesti, Romania*

Correspondence should be addressed to Ion Simaciu; isimaciu@yahoo.com

Received 26 February 2018; Accepted 5 April 2018; Published 23 May 2018

Academic Editor: Farook Rahaman

Copyright © 2018 Ion Simaciu et al. This is an open access article distributed under the Creative Commons Attribution License, which permits unrestricted use, distribution, and reproduction in any medium, provided the original work is properly cited. The publication of this article was funded by SCOAP³.

The present paper aims to complete an earlier paper where the acoustic world was introduced. This is accomplished by analyzing the interactions which occur between the inhomogeneities of the acoustic medium, which are induced by the acoustic vibrations travelling in the medium. When a wave packet travels in a medium, the medium becomes inhomogeneous. The spherical wave packet behaves like an acoustic spherical lens for the acoustic plane waves. According to the principle of causality, there is an interaction between the wave and plane wave packet. In specific conditions, the wave packet behaves as an acoustic black hole.

1. Introduction

Acoustic waves carry energy, momentum, angular momentum, and also physical information regarding the source and the medium through which they propagate. Therefore one can say that the acoustic waves intermediate interactions occurring within the medium. Nowadays extended theoretical [1–18] and experimental [19–26] research work is being carried out to study the interactions induced by acoustic waves.

One can distinguish two types of interactions induced by acoustic waves. The former type are those which are the interactions between solids, liquids, and gases (cavities, bubbles, and drops) immersed into fluid and contained into a solid.

The latter are those interactions which occur between the inhomogeneities of the medium and which are induced by acoustic waves.

The first type of interactions mentioned above were early studied by Basset [1] and substantiated by Bjerknes [2, 3].

In what follows we will assume that the acoustic processes are similar to the processes occurring into vacuum. That is why we will study those processes occurring within a medium, produced by acoustic perturbations. When waves interfere they generate wave packets. These wave packets behave like the inhomogeneities of the medium. Also these

inhomogeneities induce new inhomogeneities due to the combined process diffraction-interference-absorption.

Cavities may appear in the core of the wave packets [8] when the energy of the oscillations is of the same order as the binding energy of the particles of the liquid. All these extended inhomogeneities behave as sources for oscillations and as diffracting objects.

The container where the fluid is, or the boundaries of the solid, plays an important role for these processes. The container behaves like a cavity which reflects the acoustic waves inwards. We name an acoustic world the finite volume of the fluid or of the solid together with the processes occurring within [27]. Within the acoustic world the microscopic parameters of the inhomogeneities and the container parameters are related. For this reason, the microscopic parameters of the inhomogeneities and of the enclosure are dependent on each other. Their relationship is similar to the one between the parameters of the elementary particles and those of the universe [28], according to the present approaches.

In this paper we aim to study which features of the interactions may be generated by an inhomogeneity which is induced by a wave or a wave packet.

In the second section of the paper we infer the expression of the wave propagation velocity in a fluid when the density

and the pressure vary adiabatically. Using this expression, we infer the acoustic expression of the refractive index.

In the third section we deduce the expression of the acoustic index of refraction of a fluid perturbed by a propagating wave and a standing wave.

In the fourth section we achieve the expression of the acoustic index of refraction of a fluid perturbed by a stationary wave packet. The averaged refractive index depends on the position related to the centre of the wave packet.

In the fifth section we argue that a wave which propagates into a fluid, whose properties were changed by a wave packet, deviates from its initial direction of propagation. Also we analyze the possible existence of the acoustic black hole. The radius of the acoustic black hole depends on the wavelength and of the oscillation amplitude of the acoustic wave packet.

Sixth section is dedicated to conclusions.

2. Phase Velocity in the Presence of an Inhomogeneity

2.1. Phase Velocity. In prior papers [27, 29, 30] we have studied the issue of the dual behaviour of matter related to the longitudinal waves. In what follows we will study how these waves may change the density of the medium through which they travel. According to Landau and Lifchitz [31, Ch. 8, § 63], the propagation of a mechanical wave through a medium changes the local density $\rho = \rho_0 + \delta\rho$, the pressure $p = p_0 + \delta p$, and the temperature $T = T_0 + \delta T$.

The phase velocity in a fluid is

$$u = \sqrt{\left(\frac{\partial p}{\partial \rho}\right)_s}. \quad (1)$$

In the case of an ideal gas, the process of the wave propagation is adiabatic and the pressure is related to the density according to the relation

$$p = p_0 \left(\frac{\rho}{\rho_0}\right)^\gamma, \quad (2a)$$

$$\rho = \rho_0 \left(\frac{p}{p_0}\right)^{1/\gamma}. \quad (2b)$$

Using (2a) and (2b) into (1) we can find the velocity of a wave travelling in modified medium, due to the presence of an adiabatic perturbation, as

$$u = u_0 \sqrt{\left(\frac{\rho}{\rho_0}\right)^{\gamma-1}} = u_0 \left(1 + \frac{\delta\rho}{\rho_0}\right)^{(\gamma-1)/2} \quad (3a)$$

or

$$u = u_0 \sqrt{\left(\frac{p}{p_0}\right)^{(\gamma-1)/\gamma}} = u_0 \left(1 + \frac{\delta p}{p_0}\right)^{(\gamma-1)/2\gamma}. \quad (3b)$$

For a compressible liquid [32, p. 44] the dependency between the phase velocity and the density is

$$u = u_0 \left(\frac{\rho}{\rho_0}\right)^{(\beta-1)/2} = u_0 \left(1 + \frac{\delta\rho}{\rho_0}\right)^{(\beta-1)/2} \quad (4a)$$

or

$$u = u_0 \left(\frac{p}{p_0}\right)^{(\beta-1)/2\beta} = u_0 \left(1 + \frac{\delta p}{p_0}\right)^{(\beta-1)/2\beta}, \quad (4b)$$

with β , constant which depends on the liquid type.

One notices the difference between these two expressions of velocities, (3a), (3b), (4a), and (4b), due to the difference $\beta \neq \gamma$. One can generalize the phase velocity of a longitudinal wave for all states of the matter

$$u = u_0 \left(1 + \frac{\delta\rho}{\rho_0}\right)^\zeta \quad (5a)$$

or

$$u = u_0 \left(1 + \frac{\delta p}{p_0}\right)^{\zeta/(2\zeta+1)}. \quad (5b)$$

For a gaseous state of the matter $\zeta = (\gamma - 1)/2$ is subunitary and for a liquid state of the matter, it is greater than 1 (e.g., for water $\beta \cong 7$ and hence $\zeta = (\beta - 1)/2 \cong 3$ [32, p. 44]).

According to relations (3a)–(5b), for every state of the matter, the increasing of the density ($\delta\rho > 0$), due to the deformation, implies a growth of the velocity. Conversely, the decreasing of the density ($\delta\rho < 0$) leads to a decrease in velocity.

2.2. The Acoustic Index of Refraction. We will assign an acoustic index of refraction to the perturbed medium as

$$n_a = \frac{u_0}{u}. \quad (6)$$

According to (5a) and with $\delta\rho \ll \rho_0$, the above definition leads to

$$n_a(\rho) = \left(1 + \frac{\delta\rho}{\rho_0}\right)^{-\zeta} \cong 1 - \zeta \frac{\delta\rho}{\rho_0} + \frac{\zeta(\zeta+1)}{2} \left(\frac{\delta\rho}{\rho_0}\right)^2 \quad (7a)$$

and, according to (5b), with $\delta p \ll p_0$,

$$\begin{aligned} n_a(p) &= \left(1 + \frac{\delta p}{p_0}\right)^{-\zeta/(2\zeta+1)} \\ &\cong 1 - \frac{\zeta}{2\zeta+1} \frac{\delta p}{p_0} + \frac{\zeta(3\zeta+1)}{2(2\zeta+1)^2} \left(\frac{\delta p}{p_0}\right)^2. \end{aligned} \quad (7b)$$

The averaged expressions of the acoustic index of refraction are

$$\langle n_a(\rho) \rangle \cong 1 - \zeta \frac{\langle \delta\rho \rangle}{\rho_0} + \frac{\zeta(\zeta+1)}{2} \frac{\langle (\delta\rho)^2 \rangle}{\rho_0^2}, \quad (8a)$$

$$\langle n_a(p) \rangle \cong 1 - \frac{\zeta}{2\zeta+1} \frac{\langle \delta p \rangle}{p_0} + \frac{\zeta(3\zeta+1)}{2(2\zeta+1)^2} \frac{\langle (\delta p)^2 \rangle}{p_0^2}. \quad (8b)$$

According to the results of [31, Ch. 8, § 64], there are the relations

$$\langle \delta \rho \rangle = \frac{\langle (\delta \rho)^2 \rangle}{2} \left(\frac{\partial^2 \rho}{\partial p^2} \right)_{s, p=p_0} = -\zeta \rho_0 \frac{\langle v^2 \rangle}{u_0^2}, \quad (9a)$$

$$\langle \delta p \rangle = 0, \quad (9b)$$

$$\langle (\delta \rho)^2 \rangle = \rho_0^2 \frac{\langle v^2 \rangle}{c_0^2}, \quad (9c)$$

$$\langle (\delta p)^2 \rangle = \rho_0^2 c_0^2 \langle v^2 \rangle. \quad (9d)$$

By replacing relations (9a), (9b), (9c), and (9d) in the expression of the averaged acoustic index of refraction (8b), it yields

$$\langle n_a(\rho) \rangle \cong 1 + \frac{\zeta(3\zeta + 1)}{2} \frac{\langle v^2 \rangle}{u_0^2}. \quad (10a)$$

The same result is obtained by replacing relations (9a), (9b), (9c), and (9d) in the expression of the averaged acoustic index of refraction (8a)

$$\langle n_a(p) \rangle \cong 1 + \frac{\zeta(3\zeta + 1)}{2(2\zeta + 1)^2} \frac{\langle (\delta p)^2 \rangle}{p_0^2} = \langle n_a(\rho) \rangle. \quad (10b)$$

Hence, we find that the index of refraction is a measure of the inhomogeneity of the medium.

3. The Inhomogeneity Induced by a Wave

According to [31, Ch. 8, § 63], the relative variance of the density, in the presence of a wave, is the ratio between the velocity of the vibration $\dot{q}(x, t)$ and the phase velocity u_0

$$\frac{\delta \rho}{\rho} = \frac{v}{u_0} = \frac{\dot{q}}{u_0} \ll 1. \quad (11)$$

Substituting (11) in (10a), with $\gamma p_0 = (2\zeta + 1)p_0 = \rho_0 u_0^2$, the expression of the index of refraction becomes

$$\langle n_a \rangle \cong 1 + \frac{\zeta(3\zeta + 1)}{2} \frac{\langle \dot{q}^2 \rangle}{u_0^2}. \quad (12)$$

For a plane wave $\Psi(z, t) = q_z = q_{0z} \sin(\omega t - kz)$, the velocity of the oscillation is

$$\dot{q}_z = q_{0z} \omega \cos(\omega t - kz). \quad (13)$$

Averaging, in time, the square velocity, one obtains

$$\langle \dot{q}_z^2 \rangle_t = \frac{q_{0z}^2 \omega^2}{T} \int_0^T \cos^2(\omega t - kz) d(\omega t) = \frac{q_{0z}^2 \omega^2}{2}, \quad (14a)$$

$$\frac{\langle \dot{q}_z^2 \rangle_t}{u_0^2} = \frac{q_{0z}^2 \omega^2}{2u_0^2} = \frac{2\pi^2 q_{0z}^2}{\lambda^2} \ll 1 \text{ or } q_{0z} \ll \lambda. \quad (14b)$$

Substituting (14a) and (14b) in (12), the expression of the index of refraction becomes

$$\langle n_a \rangle_t \cong \left[1 + \frac{\zeta(3\zeta + 1)}{2} \left(\frac{q_{0z} \omega}{u_0} \right)^2 \right] > 1. \quad (15)$$

Hence for a standing wave, $\Psi_s(z, t) = q_{zs} = q_{0zs} \sin(kz) \sin(\omega t)$ [33], with the velocity of oscillation

$$\dot{q}_{zs} = q_{0zs} \omega \sin(kz) \cos(\omega t). \quad (16)$$

The averaged velocity of oscillation through time is zero, but the averaged square velocity of oscillation through time is not zero.

$$\begin{aligned} \langle \dot{q}_{zs}^2 \rangle_t &= \frac{q_{0zs}^2 \omega^2 \sin^2 kz}{T} \int_0^T \cos^2(\omega t) d(\omega t) \\ &= \frac{q_{0zs}^2 \omega^2}{2} \sin^2 kz. \end{aligned} \quad (17)$$

Now, according to (15), the following expressions occur:

$$\langle n_a \rangle_t \cong \left[1 + \frac{\zeta(3\zeta + 1)}{4} \left(\frac{q_{0zs} \omega}{u_0} \sin kz \right)^2 \right] \quad (18)$$

which depicts the dependence of the index to the position z . Also the process mentioned above involves the change of the optical index, due to the changes of the mass density of the medium. This phenomenon is used as a diffraction grating [34, 35].

Performing a spatial average $\langle \sin^2 kz \rangle_z = 1/2$, it yields

$$\begin{aligned} \langle n_a \rangle_{ts} &\cong 1 + \frac{\zeta(3\zeta + 1)}{8} \left(\frac{q_{0zs} \omega}{u_0} \right)^2 \\ &= 1 + \frac{\zeta(3\zeta + 1)}{2} \left(\frac{q_{0z} \omega}{u_0} \right)^2, \end{aligned} \quad (19)$$

since the amplitude of the standing wave is double of the amplitude of the nonstanding wave $q_{0zs} = 2q_{0z}$. Relations (15), (18), and (19) display how a longitudinal wave changes the acoustic index of a medium.

4. Inhomogeneity Induced by a Wave Packet

4.1. The Acoustic Index of Refraction in the Presence of a Wave Packet. If we assume a three-dimensional standing wave packet, $\Psi_p(r, t) = q_p = q_{0p} [\sin(k_0 r)/k_0 r] \cdot \sin(\omega_0 t)$. Its velocity of oscillation is

$$\begin{aligned} \dot{q}_p &= q_{0p} \omega_0 \frac{\sin(k_0 r)}{k_0 r} \cos(\omega_0 t) \\ &= u_0 q_{0p} \frac{\sin(k_0 r)}{r} \cos(\omega_0 t). \end{aligned} \quad (20)$$

We will assume that the medium becomes spatially and temporally inhomogeneous. Its temporal averaged velocity of oscillation is null. But its averaged square velocity is not

$$\begin{aligned} \langle \dot{q}_p^2 \rangle_t &= \frac{q_{0p}^2 \omega_0 \sin^2 k_0 r}{(k_0 r)^2 T_0} \int_0^{T_0} \cos^2(\omega_0 t) d(\omega_0 t) \\ &= \frac{q_{0p}^2 \omega_0^2 \sin^2 k_0 r}{2 (k_0 r)^2}. \end{aligned} \quad (21)$$

Now we can express the temporal averaged acoustic index as

$$\langle n_a \rangle_t \cong \left[1 + \frac{\zeta (3\zeta + 1)}{4} \left(q_{0p} \frac{\sin k_0 r}{r} \right)^2 \right] > 1. \quad (22)$$

Hence, according to (22), the index of refraction depends on the position (r).

5. Acoustic Dumb Hole

5.1. The Deflection of the Acoustic Waves. Using the above index of refraction one can infer the deflection of a wave which travels through a medium, when the medium is modified by the wave packet. A simple calculus [36, 37] can be performed if one assumes an analogy between the medium with variable index and a spherical lens, with radius of curvature $R_1 = -R_2 = r$ and the index of refraction from (22).

The focal length of the acoustic lens is [38, Ch. 27.3]

$$\frac{1}{f} = \frac{2}{r} (\langle n_a \rangle_t - 1) = \frac{\zeta (3\zeta + 1)}{2r} \left(q_{0p} \frac{\sin k_0 r}{r} \right)^2 > 0. \quad (23)$$

Hence, the lens is a converging lens. For small angles, the deflection of the wave (which far away from the lens is null and where r is the impact parameter) is

$$\begin{aligned} \varphi &\cong \tan \varphi = \frac{r}{f} = 2 (\langle n \rangle_{trm} - 1) \\ &= \frac{\zeta (3\zeta + 1)}{2} \left(q_{0p} \frac{\sin k_0 r}{r} \right)^2. \end{aligned} \quad (24)$$

From (22) one can see that the wave deviates from initial direction and this deflection can be interpreted as an attraction of the wave by the wave packet. This interaction is similar to the interaction between light and a body with gravitational mass.

5.2. The Radius of Acoustic Horizon. The wave packet behaves like a dumb hole (acoustic black hole, sonic black hole) where the focal length of the lens is equal to the acoustic impact parameter

$$f = r = r_a. \quad (25)$$

The acoustic hole corresponding to the acoustic wave packet is static. This hole is different from the acoustic black hole or acoustic wormhole generated by fluid flow [39–41].

Replacing the focal length (25) into expression (23), we obtain the equation for the radius of the acoustic black hole or the radius of the acoustic horizon

$$\frac{\sin k_0 r_a}{k_0 r_a} = \frac{1}{k_0 q_{0p}} \sqrt{\frac{2}{\zeta (3\zeta + 1)}}. \quad (26)$$

For small angles $k_0 r_a < \pi/36$, with the approximation $\sin k_0 r_a \cong k_0 r_a [1 - (k_0 r_a)^2/6]$, the physical solution is

$$\begin{aligned} r_a &= \frac{6}{k_0} \sqrt{1 - \frac{1}{k_0 q_{0p}} \sqrt{\frac{2}{\zeta (3\zeta + 1)}}} \\ &= \frac{3\lambda_0}{\pi} \sqrt{1 - \frac{\lambda_0}{q_{0p} \pi \sqrt{2\zeta (3\zeta + 1)}}}. \end{aligned} \quad (27)$$

The solution given by (27) is real if

$$\frac{\lambda_0}{q_{0p}} < \pi \sqrt{2\zeta (3\zeta + 1)}. \quad (28)$$

For the liquid, with $\zeta \cong 3$, it yields

$$\frac{\lambda_0}{q_{0p}} < \sqrt{60}\pi. \quad (29)$$

If we take into account the relationship between the wave packet parameters and the fluid parameters [27, § 3.1] and [29, § 5.3]

$$\begin{aligned} q_{0p} &< a, \\ \lambda_0 &\geq 2a, \end{aligned} \quad (30)$$

it follows that

$$\frac{a}{\pi \sqrt{15}} < q_{0p} < a. \quad (31)$$

Those restrictive requirements addressed to the oscillation amplitude and the wavelength are related to the binding energy of the liquid particles (molecules). When the wavelength and the amplitude meet the boundaries one generates a bubble in the centre of the wave packet. It follows that the acoustic black hole (dumb hole) is associated with the generation of a bubble. The bubbles are able to interact each other in the presence of the acoustic waves and therefore in the presence of the waves background of the acoustics world. Then a further development of the papers [1–26] can be done starting from this issue.

The restrictive requirement (14b) is in contradiction with the requirement (29). In order to achieve an appropriate study of the existence of the acoustic black hole we have to address the issue of the acoustic refractive index related to high density variation (i.e., $\delta\rho \leq \rho_0$).

6. Conclusions

We have proved that a fluid becomes inhomogeneous in interaction with a wave or a wave packet. The inhomogeneity

involves the change of the propagation velocity of a plane wave. The change of the speed of propagation of a wave is similar to the existence of an acoustic refractive index.

For a spherical wave packet, the refractive index depends on the position from the centre of the wave packet. The spherical wave packet induces a change in the trajectory of the acoustic plane wave. Following the approach of the gravitational deviation of the light we computed the deviation of a plane wave in the presence of the wave packet. According to the principle of causality, an interaction may obey between the wave and the plane wave packet.

The deviation depends on the wave packet parameters: the wavelength and the amplitude of oscillations and the position relative to the centre of the wave packet. The existence of the deviation of the plane wave travelling in the fluid (modified for spherical wave packet) suggests that, for certain values of the impact parameter, the plane wave has a circular trajectory. This is an acoustic black hole.

In our approach we have adopted the same frequency for the plane wave as for the waves of the wave packets which disturb the fluid. In a forthcoming paper we will analyze the consequences which can arise from the assumption that the plane wave has another angular frequency and therefore the average is done for a period corresponding to this angular frequency.

Data Availability

No data were used to support this study.

Conflicts of Interest

The authors declare that they have no conflicts of interest.

References

- [1] A. B. Basset, "On the motion of two spheres in a liquid, and allied problems," *Proceedings of the London Mathematical Society*, vol. 18, pp. 369–377, 1887.
- [2] C. A. Bjerknes, *Hydrodynamische Fernkraft*, Engelmann, Leipzig, Germany, 1915.
- [3] V. F. K. Bjerknes, *Fields of Force*, Columbia University Press, New York, NY, USA, 1906.
- [4] H. Lamb, *Hydrodynamics*, Cambridge Mathematical Library, Cambridge University Press, Cambridge, UK, 6th edition, 1932.
- [5] M. Minnaert, "On the musical air bubbles and the sound of running water," *Philosophical Magazine*, vol. 16, pp. 235–248, 1933.
- [6] M. S. Plesset and A. Prosperetti, "Bubble dynamics and cavitation," *Annual Review of Fluid Mechanics*, vol. 9, pp. 145–185, 1977.
- [7] E. A. Zabolotskaya, "Interaction of gas bubbles in a sound field," *Soviet Physics—Acoustics*, vol. 30, no. 5, pp. 365–368, 1983.
- [8] T. G. Leighton, *The Acoustic Bubble*, London Academic Press, 1994.
- [9] A. A. Doinikov and S. T. Zavtrak, "On the mutual interaction of two gas bubbles in a sound field," *Physics of Fluids*, vol. 7, no. 8, pp. 1923–1930, 1995.
- [10] A. A. Doinikov, "Dissipative effects on Bjerknes forces between two bubbles," *The Journal of the Acoustical Society of America*, vol. 102, no. 2, pp. 747–751, 1997.
- [11] A. A. Doinikov, "Acoustic radiation force on a spherical particle in a viscous heat-conducting fluid. I. General formula," *The Journal of the Acoustical Society of America*, vol. 101, no. 2, pp. 713–721, 1997.
- [12] A. A. Doinikov and S. T. Zavtrak, "Radiation forces between two bubbles in a compressible liquid," *The Journal of the Acoustical Society of America*, vol. 102, no. 3, pp. 1424–1431, 1997.
- [13] R. Mettin, I. Akhatov, U. Parlitz, C. D. Ohl, and W. Lauterborn, "Bjerknes forces between small cavitation bubbles in a strong acoustic field," *Physical Review E: Statistical Physics, Plasmas, Fluids, and Related Interdisciplinary Topics*, vol. 56, no. 3, pp. 2924–2931, 1997.
- [14] A. Harkin, T. J. Kaper, and A. Nadim, "Coupled pulsation and translation of two gas bubbles in a liquid," *Journal of Fluid Mechanics*, vol. 445, pp. 377–411, 2001.
- [15] Y. Zhang, Y. Zhang, and S. Li, "The secondary Bjerknes force between two gas bubbles under dual-frequency acoustic excitation," *Ultrasonics Sonochemistry*, vol. 29, Article ID 2982, pp. 129–145, 2016.
- [16] A. O. Maksimov and T. G. Leighton, "Acoustic radiation force on a parametrically distorted bubble," *The Journal of the Acoustical Society of America*, vol. 143, no. 1, pp. 296–305, 2018.
- [17] M. Parmar, S. Annamalai, S. Balachandar, and A. Prosperetti, "Differential formulation of the viscous history force on a particle for efficient and accurate computation," *Journal of Fluid Mechanics*, vol. 844, pp. 970–993, 2018.
- [18] A. A. Doinikov and P. Marmottant, "Natural oscillations of a gas bubble in a liquid-filled cavity located in a viscoelastic medium," *Journal of Sound and Vibration*, vol. 420, pp. 61–72, 2018.
- [19] L. A. Crum, "Bjerknes forces on bubbles in a stationary sound field," *The Journal of the Acoustical Society of America*, vol. 57, no. 6, pp. 1363–1370, 1975.
- [20] S. T. Zavtrak, "On the experimental verification of the theory of the long range radiative forces," *Pis'ma v Zhurnal Tekhnicheskoi Fiziki (Soviet Technical Physics Letters)*, vol. 17, p. 34, 1991.
- [21] T. Barbat, N. Ashgriz, and C.-S. Liu, "Dynamics of two interacting bubbles in an acoustic field," *Journal of Fluid Mechanics*, vol. 389, pp. 137–168, 1999.
- [22] L. Wang, D. Sharp, J. Masliyah, and Z. Xu, "Measurement of interactions between solid particles, liquid droplets, and/or gas bubbles in a liquid using an integrated thin film drainage apparatus," *Langmuir*, vol. 29, no. 11, pp. 3594–3603, 2013.
- [23] J. Jiao, Y. He, S. E. Kentish, M. Ashokkumar, R. Manasseh, and J. Lee, "Experimental and theoretical analysis of secondary Bjerknes forces between two bubbles in a standing wave," *Ultrasonics*, vol. 58, pp. 35–42, 2015.
- [24] X. Ma, T. Xing, B. Huang, Q. Li, and Y. Yang, "Combined experimental and theoretical investigation of the gas bubble motion in an acoustic field," *Ultrasonics Sonochemistry*, vol. 40, pp. 480–487, 2018.
- [25] K. Rajamanickam and S. Basu, "On the dynamics of vortex-droplet interactions, dispersion and breakup in a coaxial swirling flow," *Journal of Fluid Mechanics*, vol. 827, pp. 572–613, 2017.
- [26] Z. Wang, M. Zhao, J. Jiang et al., "Measurement of interaction between water droplets and curved super-hydrophobic substrates in the air," *AIP Advances*, vol. 8, no. 4, p. 045009, 2018.

- [27] I. Simaciu, Z. Borsos, G. Dumitrescu, and A. Baci, "Planck-Einstein-de Broglie type relations for the acoustic waves," *General Physics*, 11 pages, 2016, <https://arxiv.org/abs/1610.05611>.
- [28] Y. Ryazantsev, "The large numbers in a quantized universe," *Journal of Modern Physics*, vol. 04, no. 12, pp. 1647–1653, 2013.
- [29] I. Simaciu, Z. Borsos, G. Dumitrescu, and G. Nan, "Planck-Einstein-de Broglie relations for wave packet: the acoustic world," *Classical Physics*, 18 pages, 2015, <https://arxiv.org/abs/1511.01049>.
- [30] I. Simaciu, Z. Borsos, A. Baci, and G. Nan, "The acoustic world: mechanical inertia of waves," *Buletinul Institutului Politehnic din Iași, Sec. Matematică. Mecanică Teoretică. Fizică*, vol. 62, no. 4, pp. 51–63, 2016.
- [31] L. Landau and E. Lifchitz, *Mécanique des fluides*, Moscou, Mir edition, 1971.
- [32] R. H. Cole, *Underwater Explosions*, Princeton University Press, Princeton, NJ, USA, 1948.
- [33] E. I. Butikov, "Peculiarities in the energy transfer by waves on strained strings," *Physica Scripta*, vol. 88, no. 6, Article ID 065402, 2013.
- [34] P. M. Morse, "Light scattering by a sound beam," in *Theoretical Acoustics*, pp. 809–816, Princeton University Press, 1986.
- [35] C. F. Quate, C. D. W. Wilkinson, and D. K. Winslow, "Interaction of light and microwave sound," *Proceedings of the IEEE*, vol. 53, no. 10, pp. 1604–1623, 1965.
- [36] I. Simaciu, "An easy estimation of the light deviation in the gravitational field," in *3rd General Physics Conference of the Balkan Physics Union (BPU 3)*, Babes-Bolyai University, Cluj-Napoca, Romania, 1997.
- [37] M. Meneghetti, *Introduction to Gravitational Lensing - Lecture scripts*, 2016, https://www.researchgate.net/publication/310620466_Introduction_to_Gravitational_Lensing_-_Lecture_scripts.
- [38] R. P. Feynman, R. B. Leighton, and M. Sands, *The Feynman Lectures on Physics*, vol. 1, Massachusetts: Addison-Wesley, 1964.
- [39] M. Visser, "Acoustic black holes: horizons, ergospheres and Hawking radiation," *Classical and Quantum Gravity*, vol. 15, no. 6, pp. 1767–1791, 1998.
- [40] K. K. Nandi, Y. Z. Zhang, and R. G. Cai, "Acoustic wormholes," *General Relativity and Quantum Cosmology*, 14 pages, 2004, <https://arxiv.org/abs/gr-qc/0409085>.
- [41] O. Lahav, A. Itah, A. Blumkin et al., "Realization of a sonic black hole analog in a Bose-Einstein condensate," *Physical Review Letters*, vol. 105, no. 24, Article ID 240401, 4 pages, 2010.

Research Article

Rainbow Gravity Corrections to the Entropic Force

Zhong-Wen Feng ^{1,2} and Shu-Zheng Yang^{1,2}

¹Physics and Space Science College, China West Normal University, Nanchong 637009, China

²Department of Astronomy, China West Normal University, Nanchong 637009, China

Correspondence should be addressed to Zhong-Wen Feng; zwfengphy@163.com

Received 9 February 2018; Revised 3 April 2018; Accepted 8 April 2018; Published 15 May 2018

Academic Editor: Saibal Ray

Copyright © 2018 Zhong-Wen Feng and Shu-Zheng Yang. This is an open access article distributed under the Creative Commons Attribution License, which permits unrestricted use, distribution, and reproduction in any medium, provided the original work is properly cited. The publication of this article was funded by SCOAP³.

The entropic force attracts a lot of interest for its multifunctional properties. For instance, Einstein's field equation, Newton's law of gravitation, and the Friedmann equation can be derived from the entropic force. In this paper, utilizing a new kind of rainbow gravity model that was proposed by Magueijo and Smolin, we explore the quantum gravity corrections to the entropic force. First, we derive the modified thermodynamics of a rainbow black hole via its surface gravity. Then, according to Verlinde's theory, the quantum corrections to the entropic force are obtained. The result shows that the modified entropic force is related not only to the properties of the black hole but also to the Planck length ℓ_p and the rainbow parameter γ . Furthermore, based on the rainbow gravity corrected entropic force, the modified Einstein field equation and the modified Friedmann equation are also derived.

1. Introduction

Prior research generally confirms that black holes have thermal properties [1–4]. This idea started out with an analogy connecting the laws of thermodynamics and those of gravity. In 1973, Bekenstein proved that the entropy of a black hole S is proportional to its horizon area A ; that is, $S = Ak_B c^3 / 4\hbar^2 G$, where \hbar is the Planck constant, k_B is the Boltzmann constant, and G is the Newton's gravitational constant, respectively [1, 2]. Subsequently, inspired by Bekenstein's theory of entropy, Hawking first showed that the temperature of Schwarzschild black hole is $T = \kappa / 2\pi$ with surface gravity κ [3]. After years of continuous efforts, the authors in [5] established the laws of black hole thermodynamics, which imply that the thermodynamics of black holes have profound connections with gravity.

In the past twenty years, several theories have been proposed to study the deeper-seated relation between gravity and thermodynamics [6–11]. Among these perspectives, the entropic force approach, which was introduced by Verlinde, has attracted a lot of attention. In [11], Verlinde claimed that gravity is not a fundamental force; instead, it would be explained as an entropic force, which arises from changes in the information associated with the positions of material

bodies. This idea turns out to be very powerful. First, with the help of the entropic force approach and the Unruh temperature, one can obtain Newton's second law. Second, Newton's law of gravitation can be derived by incorporating the entropic force approach together with the holographic principle and the equipartition law of energy. Third, and most importantly, the entropic force approach results in Einstein's equation. Subsequently, according to this new proposal of gravity, many relevant works appeared. In [12–16], the authors derived the Friedmann equation of a Friedmann-Robertson-Walker (FRW) universe via the entropic force approach. In [17], the holographic dark energy has been investigated in the context of the entropic force approach. Nozari et al. used the entropic force approach to study the Hamiltonians of the quantum systems in quasi-space [18]. Shi et al. noted that entanglement entropy in loop quantum gravity can be used to derive an entropic force [19]. Moreover, it should be noted that the effect of quantum gravity can influence the entropic force. Based on the entropic force approach, Aragão and Silva obtained Newtonian gravity in loop quantum gravity [20]. In addition, the generalized uncertainty principle (GUP) corrected entropic force has been investigated in [21–23].

On the other hand, it is well known that rainbow gravity (RG) is also motivated by quantum gravity [24]. RG

originates from the modified dispersion relation (MDR). In many quantum gravity theories, it is found that the Planck length is variable, which conflicts with previous conclusions [25–27]. To resolve this contradiction, the standard energy-momentum dispersion relation must be changed to a MDR. Interestingly, the MDR can modify special relativity. Currently, special relativity is called double special relativity (DSR) since it has two invariants: the velocity of light and the Planck length [28]. In 2004, Magueijo and Smolin generalized DSR to curved space-time and obtained RG. In RG, the space-time background is related to the energy of a test particle. Therefore, the background of this space-time can be described by a family of metrics (rainbow metrics) parameterized by $E\ell_p$. In [29, 30], Hendi et al. studied the RG-corrected thermodynamics of black holes. Sefiedgar used the RG model that was introduced by Amelino-Camelia et al. in [31, 32] to study the modified entropy-area law [33]. His work showed that the modifications are related to the rainbow functions. As a matter of fact, there are many works demonstrating that the RG model is not unique. According to different phenomenological motivations, a series of RG models can be obtained. Based on the varying speed of light theory, which is a model that can explain the cosmological horizon, flatness, and cosmological constant problems of Big-Bang cosmology, Magueijo and Smolin proposed a kind of MDR:

$$\frac{E^2}{(1 - \gamma E\ell_p)^2} - p^2 = m^2, \quad (1)$$

where γ , ℓ_p , and m represent the rainbow parameter, the Planck length, and the mass of the test particle, respectively. Obviously, (1) indicates that space-time has an energy-dependent velocity $c(E) = dE/dp = 1 - E\ell_p$. Comparing it with the general form of MDR, namely, $E^2 f^2(E\ell_p) - p^2 g^2(E\ell_p) = m^2$, one can easily obtain a new model of RG, whose rainbow functions are expressed as follows [34, 35]:

$$\begin{aligned} f(E\ell_p) &= \frac{1}{(1 - \gamma E\ell_p)}, \\ g(E\ell_p) &= 1. \end{aligned} \quad (2)$$

It should be mentioned the rainbow functions are responsible for the modification of the energy-momentum relation in the ultraviolet regime. Besides, (2) satisfies

$$\begin{aligned} \lim_{E\ell_p \rightarrow 0} f(E\ell_p) &= 1, \\ \lim_{E\ell_p \rightarrow 0} g(E\ell_p) &= 1. \end{aligned} \quad (3)$$

Using (2), Zhao and Liu calculated the modified thermodynamics of black objects [36]. The results showed that the effect of rainbow gravity leads to new mass-entropy relations. In addition to that, we showed that (2) can influence the phase transition of black holes [37]. Inspired by those works, it is interesting to investigate the RG-corrected entropic force.

Therefore, in this paper, using the rainbow functions that were introduced by Magueijo and Smolin, we calculate the modified Hawking temperature and entropy of a black hole. Then, extending the work of Verlinde, the RG-corrected entropic force is yielded. Furthermore, according to the modified entropic force, the deformed Einstein field equation and the deformed Friedmann equation are derived.

The organization of the paper is as follows. In Section 2, we calculate the modified Hawking temperature and entropy via the surface gravity from RG. In Section 3, the modified entropic force is derived. Sections 4 and 5 are devoted to the derivation of the deformed Einstein field equation and the deformed Friedmann equation, respectively. Finally, the results are briefly discussed in Section 6.

Throughout the paper, the natural units of $k_B = c = \hbar = 1$ are used.

2. The Impact of Rainbow Gravity on Black Hole Thermodynamics

Generally, in order to obtain the modified metric of black holes in rainbow gravity, one can simply make the replacements $dt \rightarrow dt/f(E\ell_p)$ for time coordinates and $dx^i \rightarrow dx^i/g(E\ell_p)$ for all spatial coordinates. Therefore, the metric of a static spherically symmetric black hole without charge in the framework of RG is

$$\begin{aligned} ds^2 &= -\frac{1 - (2GM/r)}{f^2(E\ell_p)} dt^2 + \frac{dr^2}{[1 - (2GM/r)] g^2(E\ell_p)} \\ &\quad + \frac{r^2}{g^2(E\ell_p)} d\Omega^2, \end{aligned} \quad (4)$$

where M , G , and $d\Omega^2$ are the mass of a static spherically symmetric black hole, Newton's gravitational constant, and line elements of hypersurfaces, respectively [24]. The vanishing of $[1 - (2GM/r)]/f^2(E\ell_p)$ at point $r_H = 2GM$ indicates the presence of an event horizon. Equation (4) reproduces the standard static spherically symmetric black hole if (3) holds. According to (4), surface gravity on the event horizon is given by

$$\kappa = -\frac{1}{2} \lim_{r \rightarrow r_H} \sqrt{-\frac{g^{11}}{g^{00}}} (g^{00})' = \frac{g(E\ell_p)}{f(E\ell_p)} \frac{1}{4GM}, \quad (5)$$

where $(g^{00})' = \partial_t(g^{00})$. The above equation indicates that the surface gravity is modified by RG. It is well known that the Hawking temperature is defined in terms of surface gravity; that is, $T_H = \kappa/2\pi$. Using the Hawking temperature-surface gravity relation, the RG-corrected Hawking temperature can be expressed as

$$T_H = \frac{g(E\ell_p)}{f(E\ell_p)} \frac{1}{8\pi GM} = \frac{1}{8\pi GM} (1 - \gamma E\ell_p). \quad (6)$$

According to [38–41], in the vicinity of the Schwarzschild surface, there is a relationship between the minimum value

of position uncertainty Δx of emitted particles and the Schwarzschild radius r_H ; namely, $\Delta x \approx r_H$. Then, by considering that the Heisenberg uncertainty principle $\Delta p \Delta x \geq 1$ still holds in RG, the energy uncertainty can be expressed as $\Delta E = 1/\Delta x$. Therefore, one can obtain the following relation:

$$E \geq \frac{1}{\Delta x} \approx \frac{1}{r_H} = \frac{1}{2GM}, \quad (7)$$

where E is a lower bound on the energy of emitted particles. With the help of (7), the RG-corrected Hawking temperature can be rewritten as

$$T_H = T_0 \left(1 - \frac{\gamma \ell_p}{2GM} \right) = \frac{1}{8\pi GM} \left(1 - \frac{\gamma \ell_p}{2GM} \right), \quad (8)$$

where $T_0 = 1/8\pi GM$ is the original Hawking temperature. Using the first law of black hole thermodynamics, the modified entropy is given by

$$\begin{aligned} S &= \int T_H^{-1} dM \\ &= 4\pi GM^2 + 4\pi\gamma M \ell_p + 2 \frac{\pi\gamma^2 \ell_p^2}{G} \ln(2GM - \gamma \ell_p) \\ &= \frac{A}{4\ell_p^2} \left[1 + 4\gamma \ell_p \sqrt{\frac{\pi}{A}} + \frac{8\pi\gamma^2 \ell_p^2}{A} \ln \left(\sqrt{\frac{\pi}{4A}} - \gamma \ell_p \right) \right]. \end{aligned} \quad (9)$$

In the above expression, we use the area of horizon $A = 16\pi G^2 M^2$. It is clear that the modified entropy is related to the area of horizon A , Planck length ℓ_p , and rainbow parameter γ . Furthermore, there is a logarithmic correction term in (9), which is coincident with those results achieved in previous works (e.g., [42, 43]). When $\gamma = 0$, (9) reduces to the original entropy; namely, $S = A/4\ell_p^2$.

3. The Modified Newton Law of Gravitation due to the Rainbow Gravity

In the framework of quantum gravity, it is believed that information can be stored on a volume of space. This viewpoint is known as the holographic principle, which is supported by black hole physics and the anti-de Sitter/conformal field theory (AdS/CFT) correspondence. Now, following the idea of Verlinde, one can assume there is a screen in space and it can separate points. When the particles move from one side of the screen to the other side, the information is stored on the screen. In [11], this screen is called a holographic screen. Therefore, according to the holographic principle and the second law of thermodynamics, when a test particle approaches a holographic screen, the entropic force of a gravitational system obeys the following relation:

$$F \Delta x = T \Delta S, \quad (10)$$

where F , T , ΔS , and Δr represent the entropic force, the temperature, the change of entropy on holographic screen, and the displacement of the particle from the holographic screen, respectively. Equation (10) means that a nonzero force

leads to a nonzero temperature. Motivated by an argument in [1], which posits that the change in entropy is related to the information on the boundary, that is, $\Delta S = 2\pi m \Delta r$ with the mass of particle m , hence, a linear relation between the ΔS and Δr is given by

$$\Delta S = 2\pi m \Delta r, \quad (11)$$

where $\Delta r = 1/m$ with the mass of the elementary component. In [44], Hooft demonstrated that the horizon of black holes can be considered as a storage device for information. Assuming that the amount of information is N bits, and combining the equipartition law of energy with the holographic principle, the number of bits N and area of horizon A obey the following relation:

$$N = \frac{A}{G}. \quad (12)$$

Substituting the entropy-area law $S = A/4G$ and modified entropy (9) into (12), the relation between N and A can be rewritten as

$$\begin{aligned} N &= 4S \\ &= \frac{A}{\ell_p^2} \left[1 + 4\gamma \ell_p \sqrt{\frac{\pi}{A}} + \frac{8\pi\gamma^2 \ell_p^2}{A} \ln \left(\sqrt{\frac{\pi}{4A}} - \gamma \ell_p \right) \right]. \end{aligned} \quad (13)$$

In the above equation, we utilize the natural units, which says $G = \ell_p^2$. Next, by adopting the equipartition law of energy, the total energy of the holographic system can be written as

$$E = \frac{NT}{2}. \quad (14)$$

Now, substituting the relations $E = M$ and $A = 4\pi r^2$, and (10)–(13) into (14), the entropic force becomes

$$\begin{aligned} F &= 4\pi \frac{Mm}{N} \\ &= F_0 \left[1 - \frac{2\gamma}{r} \ell_p - \frac{2\gamma^2}{r^2} \ln \left(\frac{1}{4r} - \gamma \ell_p \right) \ell_p^2 \right] \\ &= \frac{GMm}{r^2} \left[1 - \frac{2\gamma}{r} \ell_p - \frac{2\gamma^2}{r^2} \ln \left(\frac{1}{4r} - \gamma \ell_p \right) \ell_p^2 \right]. \end{aligned} \quad (15)$$

Obviously, (15) is the modified Newton law of gravitation, and $F_0 = GMm/r^2$ is the original Newton law of gravitation. One can find that the modification is dependent not only on the mass of two bodies M and m , the distances between the two bodies r , and Newton's gravitational constant G but also on the Planck length ℓ_p and the rainbow parameter γ . It illustrates that the modified Newton law of gravitation is valid at small scales due to the effect of rainbow gravity (or the effect of quantum gravity). Moreover, when $\gamma = 0$, (15) reduces to the conventional one.

4. The Modified Einstein Field Equation due to the Rainbow Gravity

In previous work, people found that Einstein's field equation can be derived from the entropic force approach. Therefore,

in this section, we derive the modified Einstein field equation via the RG-corrected entropic force. Taking into account (13), one can generalize the entropy-corrected relation to the following form:

$$dN = \frac{dA}{G} \left[1 + 2\gamma \sqrt{\frac{\pi G}{A}} - \frac{4G\pi^{3/2}\gamma^2}{A(\sqrt{\pi} - 2\gamma\sqrt{AG})} \right], \quad (16)$$

which is the bit density on a holographic screen. Next, consider a certain static mass configuration with total mass M enclosed in the holographic screen \mathcal{S} , and take the energy associated with it divided over N bits. It is easy to find that each bit carries a mass equal to $T/2$. Hence, the total mass can be expressed as

$$M = \frac{1}{2} \int_{\mathcal{S}} T dN, \quad (17)$$

and the local temperature on the screen is

$$T = \frac{e^\phi n^b \nabla_b \phi}{2\pi}, \quad (18)$$

where e^ϕ is the redshift factor as the local temperature T is measured by an observer at infinity [45]. Inserting the identifications for dN and T , (17) can be rewritten as

$$M = \frac{1}{4\pi G} \int_{\mathcal{S}} e^\phi \cdot \nabla \phi \left[1 + 2\gamma \sqrt{\frac{\pi G}{A}} - \frac{4G\pi^{3/2}\gamma^2}{A(\sqrt{\pi} - 2\gamma\sqrt{AG})} \right] \cdot dA, \quad (19)$$

where the right hand side (RHS) of (19) is the modified Komar mass while the original Komar mass is $M_K = 1/4\pi G \int_{\mathcal{S}} e^\phi \nabla \phi dA$ [11]. Now, combining the Stokes theorem with the killing equation $\nabla^a \nabla_a = -R^b_a \xi^a$, one can express the original Komar mass in terms of the Ricci tensor R_{ab} and the killing vector ξ^a [12, 13]:

$$M_K = \frac{1}{4\pi G} \int_{\Sigma} R_{ab} n^a \xi^b dV. \quad (20)$$

Equating (19) and (20), one obtains

$$M = \frac{1}{4\pi G} \int_{\Sigma} R_{ab} n^a \xi^b dV + \frac{1}{4\pi G} e^\phi \cdot \nabla \phi \int_{\mathcal{S}} \left[2\gamma \sqrt{\frac{\pi G}{A}} - \frac{4G\pi^{3/2}\gamma^2}{A(\sqrt{\pi} - 2\gamma\sqrt{AG})} \right] \cdot dA. \quad (21)$$

In the above equation, Σ represents the three-dimensional volume bounded by the holographic screen and n^a is the volume's normal. On the other hand, following the viewpoint that was proposed by Sefiedgar, the total mass M can be expressed as the stress-energy $T_{\mu\nu}$ [33]; that is,

$$M = 2 \int_{\Sigma} dV \left(T_{\mu\nu} - \frac{1}{2} T g_{\mu\nu} \right) n^a \xi^b. \quad (22)$$

Putting (22) into (21), one can obtain the following expression:

$$\begin{aligned} & \int_{\Sigma} \left[R_{ab} - 8\pi G \left(T_{ab} - \frac{1}{2} T g_{ab} \right) \right] n^a \xi^b dV \\ &= - \int_{\mathcal{S}} e^\phi \nabla \phi \left[2\gamma \sqrt{\frac{\pi G}{A}} - \frac{4G\pi^{3/2}\gamma^2}{A(\sqrt{\pi} - 2\gamma\sqrt{AG})} \right] \cdot dA. \end{aligned} \quad (23)$$

The RHS of (23) is a correction term, which is caused by quantum gravity. In order to obtain Einstein's field equation, the RHS should be rewritten as [46]

$$\begin{aligned} & - \int_{\mathcal{S}} e^\phi \nabla \phi \left[2\gamma \sqrt{\frac{\pi G}{A}} - \frac{4G\pi^{3/2}\gamma^2}{A(\sqrt{\pi} - 2\gamma\sqrt{AG})} \right] \cdot dA \\ &= -GM \left[2\gamma \sqrt{\frac{\pi G}{A}} - \frac{4G\pi^{3/2}\gamma^2}{A(\sqrt{\pi} - 2\gamma\sqrt{AG})} \right]. \end{aligned} \quad (24)$$

Substituting (22) and (24) into (23), one has

$$\begin{aligned} & \int_{\Sigma} \left\{ R_{ab} - 8\pi G \left(T_{ab} - \frac{1}{2} T g_{ab} \right) \right. \\ & \quad \left. + 2G \left[2\gamma \sqrt{\frac{\pi G}{A}} - \frac{4G\pi^{3/2}\gamma^2}{A(\sqrt{\pi} - 2\gamma\sqrt{AG})} \right] \right. \\ & \quad \left. \cdot \left(T_{ab} - \frac{1}{2} T g_{ab} \right) \right\} n^a \xi^b dV = 0. \end{aligned} \quad (25)$$

Finally, the deformed Einstein field equation is

$$\begin{aligned} R_{ab} &= 8\pi G \left(T_{ab} - \frac{1}{2} T g_{ab} \right) \\ & \cdot \left[1 + \frac{\gamma}{2} \sqrt{\frac{G}{\pi A}} - \frac{G\pi^{1/2}\gamma^2}{A(\sqrt{\pi} - 2\gamma\sqrt{AG})} \right]. \end{aligned} \quad (26)$$

It is obvious that this field equation is affected by the geometry of space-time, the energy-momentum tensor, and the rainbow parameter γ . If γ vanishes or the horizon area becomes too large, (26) reduces to the original Einstein field equation.

5. The Modified Friedmann Equation due to Rainbow Gravity

In this section, according to the methods which were proposed in [12–16, 23, 29, 30], the RG-corrected Friedmann equation is derived via the modified entropic force approach. First, let us consider a 4-dimensional rainbow FRW universe, whose linear element is given by

$$ds^2 = -\frac{dt^2}{f^2(El_p)} + \frac{a(t)^2}{g^2(El_p)} \left(\frac{dr^2}{1-kr^2} + r^2 d\Omega^2 \right), \quad (27)$$

where $d\Omega^2 = d\theta^2 + \sin^2\theta d\varphi^2$ represents the metric of a two-dimensional unit sphere, a is scale factor of the universe, and

k is the spatial curvature constant. According to [47, 48], it is suitable to use the notion $\tilde{r} = f(E\ell_p)a(t)r/g(E\ell_p)$ and relation $h^{\mu\nu}\partial_\mu\tilde{r}\partial_\nu\tilde{r} = 0$; the modified dynamical apparent horizon of FRW space-time becomes

$$\tilde{r}_a = \frac{1}{\sqrt{H^2 + (f(E\ell_p)k/g(E\ell_p)a^2)}}, \quad (28)$$

where $H = \dot{a}/a$ is the Hubble parameter with $\dot{a} = \partial_t a$. Significantly, (28) recovers the original apparent horizon of FRW space-time when $f(E\ell_p) = 1$ and $g(E\ell_p) = 1$. If one assumes that the matter source in the FRW universe is a perfect fluid, the stress-energy tensor of this fluid can be expressed as

$$T_{\mu\nu} = (\rho + p)u_\mu u_\nu + pg_{\mu\nu}. \quad (29)$$

Hence, the following continuity equation can be derived from the conservation law of energy-momentum:

$$\dot{\rho} + 3H(\rho + p) = 0. \quad (30)$$

For obtaining the modified Friedmann equation, we need to consider a compact spatial region with volume $V = (4/3)\pi\tilde{r}^3$. By incorporating the Newton second law with the gravitational force, one has

$$F = m\frac{\partial^2\tilde{r}}{\partial t^2} = m\ddot{a}\tilde{r} = \frac{f(E\ell_p)}{g(E\ell_p)} = -G\frac{Mm}{\tilde{r}^2}\chi(\ell_p, \gamma), \quad (31)$$

where $\chi(\ell_p, \gamma) = 1 - 2\gamma\ell_p/\tilde{r} - 2\gamma^2\ln(1/4\tilde{r} - \gamma\ell_p)\ell_p^2/\tilde{r}^2$. Substituting (31) into (30), one can obtain the following acceleration equation with some manipulations:

$$\frac{\ddot{a}}{a} = -\frac{4}{3}\pi G\rho\chi(\ell_p, \gamma). \quad (32)$$

Furthermore, the total physical M can be defined as

$$M = \int_{\mathcal{V}} dV (T_{\mu\nu}u^\mu u^\nu) = \frac{4}{3}\pi\tilde{r}^3\rho, \quad (33)$$

with energy density of the matter $\rho = M/V$, and the volume becomes $V = 4\pi[\text{arf}(E\ell_p)]^3/3g^3(E\ell_p)$. However, in order to get the Friedmann equation, one should use the active gravitational mass $\mathcal{M} = 4\pi\rho[\text{arf}(E\ell_p)]^3/3g^3(E\ell_p)$ to replace the total mass M . Then, following the agreement of [13, 16], the active gravitational mass is given by

$$\begin{aligned} \mathcal{M} &= 2 \int_{\mathcal{V}} \left(T_{\mu\nu} - \frac{1}{2}Tg_{\mu\nu} \right) u^\mu u^\nu dV \\ &= \frac{4}{3} \left[\frac{\pi\tilde{r}f(E\ell_p)}{g(E\ell_p)} \right]^3 (\rho + 3p). \end{aligned} \quad (34)$$

Next, using the active gravitational mass instead of the total mass in (33), the modified acceleration equation for the dynamical evolution of the FRW universe becomes

$$\frac{\ddot{a}}{a} = -\frac{4}{3}\pi G(\rho + 3p)\chi(\ell_p, \gamma). \quad (35)$$

It should be noted that the effect of correction terms in (35) is too small to detect because the apparent horizon radius \tilde{r} is very large. However, according to the viewpoint in [16], the rainbow gravity parameter γ can be investigated by using the modified acceleration equation for the dynamical evolution of the FRW universe.

As we know, prior research and observational data substantiates that our universe is accelerating [49, 50]. One of the possible explanations for this fact is that our universe is dominated by dark energy. Therefore, we can constrain the rainbow parameter γ with the modified acceleration equation at the late time. When assuming our universe is dominated by the dark energy, the modified acceleration equation at the late time satisfies the following expression:

$$\frac{\ddot{a}}{a} = -\frac{4}{3}\pi G(\rho + 3p)\left(1 - \frac{2\gamma\ell_p}{\tilde{r}}\right), \quad (36)$$

where $p = w\rho$. For the sake of discussion, we only retain the terms up to $\mathcal{O}(\gamma)$. Since dark energy has negative pressure, one has the relationship $1 + 3w < 0$. Hence, the upper bound of γ is given by

$$\gamma < \frac{\tilde{r}\ell_p}{2}. \quad (37)$$

Furthermore, when considering a universe dominated by dust, the modified acceleration equation at the late time is given by

$$\frac{\ddot{a}}{a} = -\frac{4}{3}\pi G\rho\left(1 - \frac{2\gamma\ell_p}{\tilde{r}}\right). \quad (38)$$

In the equation above, we ignore the higher order terms of $\mathcal{O}(\gamma^2)$. For obtaining an accelerating universe, it is required that $\ddot{a}/a > 0$. Therefore, the lower bound of the rainbow parameter turns out to be

$$\gamma > \frac{\tilde{r}\ell_p}{2}. \quad (39)$$

Next, substituting the continuity equation (30) into the modified acceleration equation (35), and multiplying both sides with $\dot{a}a$, then integrating, one yields [51, 52]

$$\frac{d(\dot{a}^2)}{dt} = \frac{8\pi G}{3} \frac{d(\rho a^2)}{dt} \chi(\ell_p, \gamma). \quad (40)$$

Integrating both sides for each term of (40), the result is

$$\begin{aligned} H^2 + \frac{k}{a^2} &= \frac{8\pi G}{3} \rho \left\{ 1 + \frac{1}{\rho a^2} \right. \\ &\cdot \int \left[-\frac{2\gamma}{ra}\ell_p - \frac{2\gamma^2}{(ra)^2} \times \ln\left(\frac{1}{4ra} - \gamma\ell_p\right) \right] \\ &\cdot \ell_p^2 d(\rho a^2) \Big\}, \end{aligned} \quad (41)$$

where H means the Hubble parameter and k is the spatial curvature. For $k = 1$, $k = -1$, and $k = 0$, one

has a hyperspherical, hyperbolic, and flat FRW universe, respectively. According to the time-independent constant (or equation of state parameter) $w = p/\rho$, the continuity equation (33) is integrated to give

$$\rho = \rho_0 a^{-3(1+w)}, \quad (42)$$

where ρ_0 is an integration constant. By incorporating (42) with (41), then integrating, one has

$$\begin{aligned} H^2 + \frac{k}{a^2} = \frac{8\pi G}{3} \rho \left\{ 1 + (1+3w) \left\{ -\frac{2\gamma}{\tilde{r}(2+3w)} \ell_p \right. \right. \\ \left. \left. + \frac{2\gamma^2}{9\tilde{r}^2(1+w)^2} \left[1 - 3(1+2) \ln \left(\frac{1}{4\tilde{r}} - \ell_p \gamma \right) \right] \right. \right. \\ \left. \left. \cdot \ell_p^2 \right\} \right\}, \end{aligned} \quad (43)$$

where $\mathcal{O}(\gamma^3, \ell_p^3)$ is the higher order correction terms. With the help of the expression of dynamical apparent horizon \tilde{r}_a , (43) can be rewritten as

$$\begin{aligned} \left(H^2 + \frac{k}{a^2} \right) \left\{ 1 - (1+3w) \left\{ -\frac{2\gamma}{(2+3w)} \sqrt{H^2 + \frac{k^2}{a^2}} \ell_p \right. \right. \\ \left. \left. + \frac{2\gamma^2}{9(1+w)^2} \left(H^2 + \frac{k^2}{a^2} \right) \left[1 - 3(1+w) \right. \right. \right. \\ \left. \left. \times \ln \left(\frac{1}{4} \sqrt{H^2 + \frac{k^2}{a^2}} - \ell_p \gamma \right) \ell_p^2 \right] \right\} \right\} = \frac{8\pi G}{3} \rho. \end{aligned} \quad (44)$$

Finally, we derive the modified Friedmann equation from the RG-corrected entropic force. Equation (44) shows that the deformed Friedmann equation is related not only to the spatial curvature k , Hubble parameter H , scale factor of the universe a , and equation of state parameter ω but also to the rainbow parameter γ and Planck length ℓ_p . It means that the Friedmann equation is observer-dependent. Due to the effect of rainbow gravity, the deformed Friedmann equation (44) becomes susceptible when the apparent horizon approaches the order of Planck scale. Therefore, our result can be used to analyze the early stage of the universe. In addition, when the apparent horizon radius becomes too large or $\gamma = 0$, (44) recovers the original Friedmann equation.

6. Conclusions

In the paper, we studied the RG-corrected entropic force. First, we investigated the RG-corrected thermodynamics and found that RG leads to a new mass-entropy relation. Then, following Verlinde's new perspective on the relation between gravity and thermodynamics, the quantum corrections to the entropic force and Newton's law of gravitation are obtained. Moreover, we further extended our study to the relativistic case as well as cosmological case; hence, we derived the modified Einstein field equation and the modified Friedmann

equation via the RG-corrected entropic force. Our results reveal that the modified Newton law of gravitation, modified Einstein's field equation, and the modified Friedmann equation are influenced by the effect of rainbow gravity (rainbow parameter γ). In other words, the results are observer-dependent. Meanwhile, it has been found that the results are sensitive to a scale that is comparable to the Planck energy scale. However, when rainbow parameter γ vanishes or the scale becomes too large, the modifications reduce to the original cases. Therefore, one can use the modified Newton law of gravitation and Einstein's field equation to investigate the gravitational interaction between objects at the sub- μm scale and analyze the properties of the early universe by using the modified Friedmann equation. Moreover, according to the observational data of today's astronomy, one can also constrain the rainbow parameter γ by various energy combinations of the universe. Furthermore, it is easily found that our results are different from those in [16] since we adopt a new RG model, which was proposed by Magueijo and Smolin. Recently, the authors in [50] show that velocity of light in the early universe was faster than it is now, and RG model we used in this paper just fits their view point. Therefore, we think our results are more suitable for the study of the physical properties of the early universe.

Conflicts of Interest

The authors declare that they have no conflicts of interest.

Acknowledgments

This work was supported by the National Natural Science Foundation of China (Grant nos. 11573022 and 11703018) and the Fundamental Research Funds of China West Normal University (Grant nos. 17E093 and 17YC518).

References

- [1] J. D. Bekenstein, "Black holes and entropy," *Physical Review D*, vol. 7, p. 2333, 1973.
- [2] J. D. Bekenstein, "Generalized second law of thermodynamics in black-hole physics," *Physical Review D*, vol. 9, p. 3292, 1974.
- [3] S. W. Hawking, "Particle creation by black holes," *Communications in Mathematical Physics*, vol. 46, no. 2, p. 206, 1976.
- [4] W. G. Unruh, "Notes on black-hole evaporation," *Physical Review D*, vol. 14, no. 4, p. 870, 1976.
- [5] J. M. Bardeen, B. Carter, and S. W. Hawking, "The four laws of black hole mechanics," *Communications in Mathematical Physics*, vol. 31, no. 2, pp. 161–170, 1973.
- [6] T. Jacobson, "Thermodynamics of spacetime: the Einstein equation of state," *Physical Review Letters*, vol. 75, p. 1260, 1995.
- [7] A. D. Sakharov, "Vacuum quantum fluctuations in curved space and the theory of gravitation," *General Relativity and Gravitation*, vol. 32, no. 2, pp. 365–367, 2000.
- [8] C. Eling, R. Guedens, and T. Jacobson, "Non-equilibrium Thermodynamics of Spacetime," *Physical Review Letters*, vol. 96, no. 12, Article ID 121301, 2006.
- [9] T. Padmanabhan, "Classical and Quantum Thermodynamics of horizons in spherically symmetric spacetimes," *General*

- Relativity and Quantum Cosmology*, vol. 19, Article ID 0204019, p. 5387, 2002, <https://arxiv.org/abs/gr-qc/arXiv:gr-qc/>.
- [10] T. Padmanabhan, "Thermodynamical aspects of gravity: new insights," *Reports on Progress in Physics*, vol. 73, no. 4, Article ID 046901, 2010.
 - [11] E. Verlinde, "On the Origin of Gravity and the Laws of Newton," *Journal of High Energy Physics*, vol. 2011, no. 29, 2011.
 - [12] R. G. Cai and S. P. Kim, "First Law of Thermodynamics and Friedmann Equations of Friedmann-Robertson-Walker Universe," *Journal of High Energy Physics*, vol. 2, p. 50, 2005.
 - [13] R.-G. Cai, L.-M. Cao, and N. Ohta, "Friedmann equations from entropic force," *Physical Review D: Particles and Fields*, vol. 81, no. 6, Article ID 061501, 2010.
 - [14] A. Sheykhi, "Entropic Corrections to Friedmann Equations," *Physical Review D: Particles and Fields*, vol. 81, no. 10, Article ID 104011, 2010.
 - [15] Y. F. Cai, J. Liu, and H. Li, "Entropic cosmology: A unified model of inflation and late-time acceleration," *Physics Letters B*, vol. 690, no. 3, pp. 213–219, 2010.
 - [16] A. S. Sefiedgar, "From the entropic force to the Friedmann equation in rainbow gravity," *Europhysics Letters*, vol. 117, no. 6, p. 69001, 2017.
 - [17] M. Li and Y. Wang, "Quantum UV/IR relations and holographic dark energy from entropic force," *Physics Letters B*, vol. 687, no. 2-3, pp. 243–247, 2010.
 - [18] K. Nozari, P. Pedram, and M. Molkara, "Minimal length, maximal momentum and the entropic force law," *International Journal of Theoretical Physics*, vol. 51, no. 4, pp. 1268–1275, 2012.
 - [19] J. Shi, S. Hu, and R. Zhao, "Entanglement entropy of a black hole and isolated horizon," *Astrophysics and Space Science*, vol. 55, no. 2, pp. 555–558, 2012.
 - [20] R. G. L. Aragão and C. A. S. Silva, "Entropic corrected Newton's law of gravitation and the loop quantum black hole gravitational atom," *General Relativity and Gravitation*, vol. 48, no. 83, 2016.
 - [21] A. Awad and A. F. Ali, "Minimal length, Friedmann equations and maximum density," *Journal of High Energy Physics*, vol. 2014, no. 93, 2014.
 - [22] A. Awad and A. F. Ali, "Planck-Scale Corrections to Friedmann Equation," *General Relativity and Quantum Cosmology*, vol. 12, p. 245, 2014.
 - [23] Z.-W. Feng, S.-Z. Yang, H.-L. Li, and X.-T. Zu, "The Effects of Minimal Length, Maximal Momentum, and Minimal Momentum in Entropic Force," *Advances in High Energy Physics*, vol. 2014, Article ID 2341879, 9 pages, 2014.
 - [24] J. Magueijo and L. Smolin, "Gravity's Rainbow," *General Relativity and Quantum Cosmology*, vol. 21, Article ID 0305055, p. 1725, 2004.
 - [25] D. Amati, M. Ciafaloni, and G. Veneziano, "Can spacetime be probed below the string size?" *Physics Letters B*, vol. 216, no. 1-2, pp. 41–47, 1989.
 - [26] R. Gambini and J. Pullin, "Nonstandard optics from quantum space-time," *Physical Review D*, vol. 59, Article ID 124021, 1999.
 - [27] F. Girelli, E. R. Livine, and D. Oriti, "Deformed special relativity as an effective flat limit of quantum gravity," *Nuclear Physics B*, vol. 708, no. 1-2, pp. 411–433, 2005.
 - [28] G. Amelino-Camelia, "Relativity in Spacetimes with Short-Distance Structure Governed by An Observer-Independent (Planckian) Length Scale," *International Journal of Modern Physics D*, vol. 11, no. 1, pp. 35–59, 2002.
 - [29] S. H. Hendi, M. Momennia, B. E. Panah, and M. Faizal, "Nonsingular universes in gauss-bonnet gravity's rainbow," *The Astrophysical Journal*, vol. 827, no. 2, p. 153, 2016.
 - [30] S. H. Hendi, M. Momennia, B. E. Panah, and S. Panahiyan, "Nonsingular universe in massive gravity's rainbow," *General Relativity and Quantum Cosmology*, vol. 16, p. 13, 2017.
 - [31] G. Amelino-Camelia, J. Ellis, N. E. Mavromatos, and D. V. Nanopoulos, "Distance measurement and wave dispersion in a Liouville-string approach to quantum gravity," *International Journal of Modern Physics A*, vol. 12, no. 3, p. 607, 1997.
 - [32] G. Amelino-Camelia, "Distance Measurement and Wave Dispersion in a Liouville-String Approach to Quantum Gravity," *International Journal of Modern Physics A*, vol. 16, no. 5, 2012.
 - [33] A. S. Sefiedgar, "How can rainbow gravity affect gravitational force?" *International Journal of Modern Physics D*, vol. 25, no. 14, 1650101, 11 pages, 2016.
 - [34] J. Magueijo and L. Smolin, "Lorentz invariance with an invariant energy scale," *Physical Review Letters*, vol. 88, 19, p. 190403, 2002, <http://arxiv.org/abs/1606.06285>.
 - [35] J. Magueijo and L. Smolin, "Generalized Lorentz invariance with an invariant energy scale," *Physical Review D: Particles and Fields*, vol. 67, no. 4, Article ID 044017, 2003.
 - [36] Y.-J. Zhao and X. Liu, "Remnants of black holes from rainbow gravity in terms of a new VSL theory," *General Relativity and Quantum Cosmology*, 2016.
 - [37] Z.-W. Feng and S.-Z. Yang, "Thermodynamic phase transition of a black hole in rainbow gravity," *Physics Letters B*, vol. 772, pp. 737–742, 2017.
 - [38] R. J. Adler, P. Chen, and D. I. Santiago, "The Generalized Uncertainty Principle and Black Hole Remnants," *General Relativity and Gravitation*, vol. 33, no. 12, Article ID 0106080, pp. 2101–2108, 2001.
 - [39] G. Amelino-Camelia, M. Arzano, and A. Procaccini, "Severe constraints on Loop-Quantum-Gravity energy-momentum dispersion relation from black-hole area-entropy law," *Physical Review D: Particles and Fields*, vol. 70, no. 10, Article ID 107501, 2004.
 - [40] B. Majumder, "Black hole entropy and the modified uncertainty principle: A heuristic analysis," *Physics Letters B*, vol. 703, no. 4, pp. 402–405, 2011.
 - [41] E. M. Lifshitz, L. P. Pitaevskii, and V. B. Berestetskii, *Landau-Lifshitz Course of Theoretical Physics*, vol. 4 of *Quantum Electrodynamics*, Reed Educational and Professional Publishing, 1982.
 - [42] R. Banerjee and B. R. Majhi, "Quantum tunneling beyond semiclassical approximation," *Journal of High Energy Physics*, vol. 2008, no. 6, pp. 95–208, 2008.
 - [43] P. Bargueño and E. C. Vagenas, "Semiclassical corrections to black hole entropy and the generalized uncertainty principle," *Physics Letters B*, vol. 742, pp. 15–18, 2015.
 - [44] G. T. Hooft, "Dimensional Reduction in Quantum Gravity," in *Proceedings of the AIP Conference Proceedings*, vol. 116, 1984.
 - [45] B. Majumder, "The Effects of Minimal Length in Entropic Force Approach," *Advances in High Energy Physics*, vol. 2013, Article ID 296836, 8 pages, 2013.
 - [46] H. S. Hendi and A. Sheykhi, "Entropic Corrections to Einstein Equations," *High Energy Physics - Theory*, vol. 83, Article ID 084012, 2011.
 - [47] K. Lin and S. Z. Yang, "Quantum tunneling from apparent horizon of rainbow-FRW universe," *International Journal of Theoretical Physics*, vol. 48, no. 7, pp. 2061–2067, 2009.

- [48] A. S. Sefiedgar and M. Daghigh, “Thermodynamics of the FRW universe in rainbow gravity,” *International Journal of Modern Physics D*, vol. 48, no. 13, 2017.
- [49] A. G. Riess, L. Strolger et al., “New Hubble Space Telescope Discoveries of Type Ia Supernovae at $z \geq 1$: Narrowing Constraints on the Early Behavior of Dark Energy,” *The Astrophysical Journal*, vol. 198, no. 1, Article ID 0611572, p. 659, 2007.
- [50] J. Yoo and Y. Watanabe, “Theoretical Models of Dark Energy,” *Cosmology and Nongalactic Astrophysics*, vol. 21, Article ID 1230002, 2012.
- [51] Y.-F. Cai and E. N. Saridakis, “Inflation in entropic cosmology: Primordial perturbations and non-Gaussianities,” *Physics Letters B*, vol. 697, no. 4, pp. 280–287, 2011.
- [52] P. Jizba, H. Kleinert, and F. Scardigli, “Inflationary cosmology from quantum conformal gravity,” *The European Physical Journal C*, vol. 75, p. 245, 2015.